The Structure of Quantum Chromodynamics at the Symmetric point

Thesis submitted in accordance with the requirements of
the University of Liverpool for the degree of Doctor in Philosophy
by

Miss Jaclyn Bell
Supervisors: Prof. John Gracey and Dr. Thomas Teubner

September 2015

Abstract

This thesis contains a study on the structure of the vertex functions of Quantum Chromodynamics (QCD) in both linear and non-linear gauges. In particular we show results for the arbitrary linear covariant gauge at two loops as well as renormalizing the one loop non-linear Curci-Ferrari gauge and maximal abelian gauge (MAG). The full minimal subtraction $\overline{\text{MS}}$ and momentum subtraction (MOM) scheme renormalization of QCD is performed in all three gauges. This is carried out for an arbitrary colour group at one loop for the maximal abelian gauge and at two loops for the arbitrary linear covariant and Curci-Ferrari gauges. From the n loop $\overline{\text{MS}}$ results the $(n+1)$ loop β-functions and anomalous dimensions can be constructed in the respective gauges for each MOM scheme. This is demonstrated in all of the gauges considered. In addition to analysing the vertex functions at the symmetric subtraction point for both the $\overline{\text{MS}}$ and MOM schemes, we also consider an operator insertion into the quark 2-point function at the asymmetric point with an interpolating parameter. This requires a new configuration setup and introduces new master integrals which we determine. The scalar, vector and tensor operators are considered along with W_2 and ∂W_2, the twist-2 Wilson operators for moment $n = 2$. The operator renormalization is performed at two loops in the $\overline{\text{MS}}$ and modified regularization invariant (RI$'$) scheme, both of which are preferred schemes of the lattice. Following the construction of the conversion function for the scalar operator for checking purposes, the amplitudes are presented for all other operators in the $\overline{\text{MS}}$ scheme.

Declaration

I hereby declare that all work described in this thesis is the result of my own research activities unless reference to others is given. None of this material has been previously submitted to this or any other university. All work was carried out in the Theoretical Physics division of the Department of Mathematical Sciences during the period of September 2011 to September 2015.

Contributions from this work have been published in the following:
J.M. Bell & J.A. Gracey, Phys. Rev. **D88** (2013), 085027.
J.M. Bell & J.A. Gracey, Phys. Rev. **D92** (2015), 125001.
J.M. Bell & J.A. Gracey, Phys. Rev. **D93** (2016), 065031.

Acknowledgements

Firstly I would like to thank STFC, The University of Liverpool and Yoko Ono for supporting me through my PhD financially with a stipend and John Lennon memorial scholarship. I thank my supervisors Prof. John Gracey and Dr. Thomas Teubner for all of their support and patience throughout my time at The University of Liverpool, in particular John who I have had the pleasure of knowing since my first year as an undergraduate and has grown to become a very dear friend of mine. He has helped me to become the person I am today.

The Mathematical Physics Group at Humboldt University, Berlin, is also thanked for its hospitality. I would particularly like to thank Dirk Kreimer and his wife Susan for their hospitality, kindness and generosity. Sylvia and Isabella, also for their kindness and hospitality as well as Dirk's students, particularly Henry, Marko, Lutz and Mattias for making me feel welcome and for useful discussions during my time in Berlin. I would like to also thank David Broadhurst for his continued interest in our work, useful discussions and stories. It has been a pleasure to know you all.

I would like to thank my family for standing by me and always supporting me with whatever choices I made in life, especially my little brother who knows how much of a struggle it can be. My colleagues and also closest friends, Stephen, Paul, Viraf and Will for helping me when times seemed at their worst. My thanks also go out to Alan at Daresbury Lab for persuading me to keep going when I was almost about to give up. All the girls of Liverpool Foxes who are like a family to me, especially Kimi, Adaora and Nadine for keeping me sane and knowing exactly what to say to cheer me up and believe in myself again. My second cheer family at Eclipse, especially Natalie and my friends and colleagues at Walton Youth Project for always being supportive of my limited availability by juggling University, cheerleading and work! I thank everyone who has supported my choices, despite how crazy they may have seemed at the time, I love you all

so much and you have made my time at Liverpool University something I will always cherish. Finally I thank Ian for putting up with me being a student for way too long and not getting a "proper job" haha. I love you.

Contents

Part I

Renormalization of Linear and Non-linear Gauges in Symmetric Momentum Subtraction

Chapter 1

Introduction

Upon the successes of quantum electrodynamics (QED) in the 1940's as a field theory, it was Yang whose interest in the strong interaction led him, in partnership with Mills, to construct a prototype quantum field theory of the strong interaction modelled closely on QED and its symmetries. Unable to define a suitable set of Feynman rules for their theory, which only satisfied $SU(2)$ gauge invariance if self interactions were allowed, the gauge theory was put on hold with findings published in 1954. It was not until the discovery of asymptotic freedom of Yang-Mills theories, [1, 2], via the counter-intuitive result for the one loop β-function that non-abelian gauge theory became a strong candidate theory of the strong interaction. At high momenta the gauge theory behaved like a "free" theory, therefore gauge theory was asymptotically free.

The discovery that gauge theory was asymptotically free was a key advancement in physics, with its importance first remarked upon in June 1972, [3]. In the years following, gauge theory was shown to be renormalizable. The theory became known as quantum chromodynamics (QCD), first referred to as QCD in [4] with credit for the name given to Gell-Mann. QCD is a renormalizable quantum field theory describing the quanta of the strong interaction; quarks and gluons. These elementary constituents of hadrons were first independently proposed by Gell-Mann and Zweig with the name quark accredited to Gell-Mann, [5]. Gell-Manns Eightfold Way in 1961, [6], was the first time baryons and mesons had been classified, and paved the way in some sense for the standard model. In 1964 a triangular "Eightfold Way" pattern was proposed, known as the quark model and was put forward by both Gell-Mann and Zweig. This model consisted of three quarks which were all that was needed at the time to describe all known particles that were not leptons. These quarks were called *up*, *down* and *strange*.

Although mathematically sound, the problem with the model was that no individual quark had ever been seen in nature, a problem which still exists today. At that moment in time QCD did not have a solid set of Feynman rules, nor had the predicted quarks or gluons been observed as free particles. It was not until the late 1960's that experiments led by Friedman, Kendall and Taylor at the Stanford Linear Accelerator Centre (SLAC) produced evidence that quarks did exist. The experiments were similar to those by Geiger and Marsden in 1908 which had detected that the nucleus contained protons and neutrons, [7]. At around the same time a similar experiment was being carried out at the European Organization for Nuclear Research (CERN), also investigating the the structure of the proton. Instead of firing electrons at the proton, which was the technique at SLAC, neutrinos were used. This experiment confirmed the results at SLAC; protons contained smaller constituents. The experimental evidence that quarks existed was coming together. Friedman, Kendall and Taylor were awarded the Nobel prize in 1990 for their contributions to the discovery of these quanta of the strong force.

With the discovery of more particles came the need to introduce more quarks. The three new quarks predicted were much heavier than the others and were not discovered until several years after the up, down and strange quarks had been confirmed. The fourth in the family, the *charm* quark, was found in 1974 with the discovery of the J/ψ particle. Finally the *top* quark was spotted in 1995 at Fermilab [8, 9] with a mass of 175GeV. There were now six *flavours* of quark; up, down, strange, charm, bottom and top, which completed the quark model, [7]. In 1979, gluons, which were predicted in QCD to be the carrier of the strong force, the force that binds quarks so tightly together was discovered via electron-positron annihilation at the Deutsches Elektronen-Synchrotron (DESY), [10]. These gluons played the same role as the photon in QED, where the photon is the carrier of the electromagnetic force.

In QCD, where calculations have been possible overall there has been good agreement between theory and observation. For this reason it is generally accepted that QCD is the best and most realistic quantum field theory describing the strong nuclear force at both the microscopic (quarks and gluons) and macroscopic (hadronic) level. Despite the problem that quarks are thought to be absolutely confined. QCD and the electroweak theory form what is called the Standard Model, which is the basis of all physics except for gravity. With the existence

of the Higgs boson confirmed, this only strengthens the model which has so far never been disproved.

The name given to the phenomenom that quarks and gluons are particles that are never seen in nature was confinement, [4]. Confinement prevents coloured quarks and gluons from being experimentally detected since in our world we can only observe particles in colourless states; colour is permanently confined. The confinement problem and its underlying mechanism is still very much unsolved. As QCD has prospered in phenomenological applications the proof of confinement has become one of the biggest and most important problems in theoretical physics, [12]. The infrared region is the area of interest for studying confinement and since standard perturbative calculational techniques do not suffice in the infrared region this makes the problem of confinement very difficult to probe. To properly study the infrared region requires the development of non-perturbative approaches. Focusing on the confinement problem lies outside the scope of our research and computational ability, however we have chosen to study and compute results for gauges we believe to be important in understanding some of the hypothesised mechanisms of confinement.

Lattice studies of vertex functions have improved in recent years with strong focus on ideas for testing gluon confinement, [13]. The lattice measures vertex functions non-perturbatively and requires matching to the high energy limit. To aid investigation, the perturbative structure of the 3-point vertices of QCD have been computed [14], mainly at two loops in linear covariant gauges following intense activity in understanding the propagators. Higher loop order results for the QCD Green's functions computed perturbatively can be used to assist in Schwinger-Dyson analysis, [4, 15, 16, 17], as well as reducing error estimates on infrared measurements computed non-perturbatively. As well as linear gauges, multiloop information for non-linear gauges is also of importance. The interest in understanding the low energy properties of Yang Mills theories may in fact be best described using gauges non-linear in nature. There is research [18, 19, 20, 21, 22] looking in to gluon effective mass effects in QCD and it has been argued that if mass was dynamically generated for the gluon then this may lead to a better understanding of confinement. 't Hooft suggested that some components of the gluon field may acquire dynamically generated masses due to the condensation of abelian monopoles originating from the diagonal elements of the group algebra. This implies that low energies may be best described by an abelian theory.

This is where our motivation in studying the maximal abelian gauge lies. Lattice activity to persue this hypothesis will be interested in results computed in the maximal abelian gauge as in this gauge the gluon and ghost fields are split into their diagonal and off-diagonal counterparts. Studying this gauge may give us an insight in to any strange behaviour exhibited in either sector. Exact details of how the gauge group is decomposed are presented in chapter 5.

The aim of this thesis is to coherently demonstrate how we performed the full $\overline{\text{MS}}$ and MOM renormalization of massless QCD in the Maximal Abelian Gauge (MAG) for an arbitrary colour group at one loop. As a preliminary to this in-depth and technically difficult calculation we first consider the arbitrary linear covariant gauge. By considering a linear covariant gauge one can develop the necessary skills and computational techniques needed to renormalize and compute in a much simpler gauge fixing before moving to a more complicated non-linear gauge choice, such as the MAG. Although we do not compute the two loop explicit calculation of the MAG within this thesis due to the technical difficulty in developing the correct and consistent colour algebra at higher loop orders, we do however consider calculations in preliminary gauges at two loops. This includes our second calculation prior to tackling the MAG, namely the (non-linear) Curci-Ferrari gauge, which we encounter in chapter 4.

The structure of Part 1 of the thesis is as follows. We review the QCD Lagrangian and how it is formulated including the Lie algebra, properties of QCD and gauge fixing for multiple gauge choices. We discuss renormalization, in particular the techniques used and the schemes chosen after regularization. After discussing the $\overline{\text{MS}}$ and MOM schemes in depth we then follow this with a summary of results where we explicitly show the renormalization constants and amplitudes in both schemes. The mappings which define the coupling constant in one scheme in terms of a coupling constant in another scheme are constructed and the formulation of the three loop β-functions and anomalous dimensions in all MOMi schemes are given. Unlike the $\overline{\text{MS}}$ scheme the MOMi schemes are defined at the vertex functions where $i \in \{A^a_\mu A^b_\nu A^c_\sigma,\, \psi\bar{\psi}A^a_\mu,\, c^a\bar{c}^b A^c_\mu\}$ as discussed in chapter 2, see (2.1.62). This results in three different MOM schemes for the three vertices we consider at the symmetric subtraction point. For convenience we call these schemes MOMg, MOMq and MOMh respectively. Studying these vertex functions at the symmetric subtraction point means that all of the external momenta individually squared are set equal to each other. This greatly simplifies our inte-

gral reduction.

Since the MAG is non-linear in nature it is useful to consider another preparatory non-linear gauge, which is of interest in its own right. Closely related to the MAG is the Curci-Ferrari gauge which we consider in chapter 4. We repeat the process in chapter 4 for this non-linear gauge and present our results. Although it is not necessary to study both the arbitrary linear covariant gauge and the Curci-Ferrari gauge in as much detail as we have done prior to the MAG it is extremely useful for background and insight, as well as a safe method in ensuring computational technique and programming is correct before tackling a more complicated problem. Errors could occur may these tedious preliminary steps not be taken to prevent such an oversight, and so we proceed with the Curci-Ferrari gauge in the section following the analysis of the arbitrary linear covariant gauge, discussing its properties and a summary of results. The Curci-Ferrari gauge is of particular interest because of its strong relation to the MAG, where in the abelian sector the MAG and Curci-Ferrari results agree. The maximal abelian gauge will be described in depth in the section following, where we construct the MAG Lagrangian and any new group theory results required for the one loop renormalization. We then present the mappings for the MAG between the $\overline{\text{MS}}$ and MOMi schemes and also our calculation of the 2-loop β-function and anomalous dimensions for all MOMi schemes. We summarize with a discussion on all three gauges, their similarities and importance within the study of QCD.

Due to the page limit imposed on this document it is only possible to present analytic results for one of the three vertex functions. We choose to display results analytically for the ghost-gluon vertex since this has the simplest structure. This vertex also differs between schemes, with results in the Curci-Ferrari gauge different in this vertex to that of the linear covariant gauge, even for the case when the Landau limit is taken. This is not the case for the other two vertices where they agree in this limit. Their results are presented numerically.

In Part 2 we consider an operator insertion in a massless quark 2-point function for an interpolating momentum configuration, away from the symmetric subtraction point, and its direct application in lattice gauge theory. This extends work carried out in Part 1 where only the symmetric point was considered. The asymmetric point is a much more desired computational setup by lattice theorists since there is more flexibility in results which will therefore enable lattice specialists

to achieve better precision results on the lattice. Computing the amplitudes for the scalar, vector and tensor operators in the $\overline{\text{MS}}$ scheme, we construct the conversion function for the scalar operator for the RI′ scheme. Both $\overline{\text{MS}}$ and RI′ are schemes commonly associated with lattice calculations when renormalizing operators. Reproducing the results of [133] for the scalar conversion function at the asymmetric point we then display the amplitudes for the remaining operators renormalized in the $\overline{\text{MS}}$ scheme only. This is also carried out for the deep inelastic scattering (DIS) operators. Moving away from the symmetric point means more complicated master integrals appear within the calculation. The introduction of new masters along with a new configuration setup is the reason we dedicate a separate section of our thesis to this work.

Chapter 2

Background

2.1 Notation and conventions

The standard model is a renormalizable quantum field theory comprising of the electromagnetic, weak and the strong nuclear forces. It consists of three gauge groups, each representing one of the three forces, with an overall gauge symmetry of $SU(3) \times SU(2) \times U(1)$. These unitary groups provide the basis for all gauge theories of the standard model. The combination of the electromagnetic and weak forces, aptly named the electroweak force covers the $SU(2) \times U(1)$ symmetries with the remaining $SU(3)$ sector of the Standard Model corresponds to the theory best describing all particle physics. This quantum field theory is called Quantum Chromodynamics (QCD) and is based on a Yang Mills theory [12] with an $SU(3)$ gauge group. This special unitary group is represented as a set of unitary 3×3 traceless hermitian matrices, each with determinant 1. The word *special* meaning that all $N_c \times N_c$ matrices U in the group $SU(N_c)$ must have $\det U = +1$ compared to a unitary group satisfying $|\det U| = 1$. Since the dimension of $SU(N_c)$ is determined by $N_c^2 - 1$ the result, in the case of $SU(3)$ is a basis of eight matrices satisfying

$$\mathrm{Tr}\left(\lambda^A \lambda^B\right) \;=\; 2\delta^{AB} \;. \tag{2.1.1}$$

Although unconventional, we define our colour indices a, b, c as upper case A, B, C. This is to ease notation later on when we consider the maximal abelian gauge where the colour group is split. Above we have introduced the Gell-Mann λ-matrices specific to $SU(3)$, [23]. This set of matrices play a role that is equivalent to that of the Pauli matrices of $SU(2)$. For completeness the conventional

representation of the Gell-Mann λ-matrices are

$$\begin{aligned}
\lambda^1 &= \begin{pmatrix} 0 & 1 & 0 \\ 1 & 0 & 0 \\ 0 & 0 & 0 \end{pmatrix} , \quad \lambda^2 = \begin{pmatrix} 0 & -i & 0 \\ i & 0 & 0 \\ 0 & 0 & 0 \end{pmatrix} , \quad \lambda^3 = \begin{pmatrix} 1 & 0 & 0 \\ 0 & -1 & 0 \\ 0 & 0 & 0 \end{pmatrix} , \\
\lambda^4 &= \begin{pmatrix} 0 & 0 & 1 \\ 0 & 0 & 0 \\ 1 & 0 & 0 \end{pmatrix} , \quad \lambda^5 = \begin{pmatrix} 0 & 0 & -i \\ 0 & 0 & 0 \\ i & 0 & 0 \end{pmatrix} , \quad \lambda^6 = \begin{pmatrix} 0 & 0 & 0 \\ 0 & 0 & 1 \\ 0 & 1 & 0 \end{pmatrix} , \\
\lambda^7 &= \begin{pmatrix} 0 & 0 & 0 \\ 0 & 0 & -i \\ 0 & i & 0 \end{pmatrix} , \quad \lambda^8 = \frac{1}{\sqrt{3}} \begin{pmatrix} 1 & 0 & 0 \\ 0 & 1 & 0 \\ 0 & 0 & -2 \end{pmatrix} .
\end{aligned} \tag{2.1.2}$$

Although the most popular to use, the Gell-Mann λ-matrices are only one of several possible representations of the infinitesimal generators of $SU(3)$. With the property of unitarity this set of matrices is called the fundamental representation, [24]. The commutators of these λ-matrices define the $SU(3)$ structure constants

$$\left[\lambda^A, \lambda^B\right] = 2if^{ABC}\lambda^C \tag{2.1.3}$$

where it is understood that the repeated index implies the sum over all eight gluon colour states, as is consistent with Einstein's summation convention. The objects f^{ABC} are the colour group structure constants and are anti-symmetric under the exchange of any two indices for all $SU(N_c)$. For $SU(3)$ where the colour indices run from $1, \ldots, 8$ this implies, [24],

$$\begin{aligned}
f^{123} &= 1 , \quad f^{147} = f^{246} = f^{257} = f^{345} = \frac{1}{2} , \\
f^{156} &= f^{367} = -\frac{1}{2} , \quad f^{458} = f^{678} = \frac{\sqrt{3}}{2}
\end{aligned} \tag{2.1.4}$$

with all other $f^{ABC} = 0$. In the fundamental representation, which is the most basic irreducible representation, it is traditional to define the generators of the gauge group by

$$T^A = \frac{1}{2}\lambda^A , \qquad (A = 1, \ldots, 8) \tag{2.1.5}$$

where T^A are Hermitian operators. By irreducible we mean that a matrix or set of matrices cannot be decomposed into block diagonal form. These infinitesimal operators of the group form a Lie Algebra defined by the commutation relation

similar to (2.1.3)

$$\left[T^A, T^B\right] \;=\; if^{ABC}T^C \tag{2.1.6}$$

in which the Jacobi identity can be determined using the general result for the commutators

$$\begin{aligned}
[T^A,[T^B,T^C]]+[T^B,[T^C,T^A]]+[T^C,[T^A,T^B]] &= 0\\
if^{BCE}[T^A,T^E]+if^{CAE}[T^B,T^E]+if^{ABE}[T^C,T^E] &= 0\\
i^2f^{BCE}f^{AED}T^D+i^2f^{CAE}f^{BED}T^D+i^2f^{ABE}f^{CED}T^D &= 0\\
-\left(f^{BCE}f^{AED}+f^{CAE}f^{BED}+f^{ABE}f^{CED}\right)T^D &= 0\\
\Rightarrow\; f^{ADE}f^{BCE}+f^{ACE}f^{DBE}+f^{ABE}f^{CDE} &= 0
\end{aligned} \tag{2.1.7}$$

which all structure constants satisfy. It is important to emphasise that throughout our work we use both the adjoint and fundamental representations when dealing with gluons and fermions respectively. The elementary Casimirs that commute with all generators of the group are defined as

$$\begin{aligned}
\mathrm{Tr}\left(T^AT^B\right) &= T_F\delta^{AB}\\
T^AT^A &= C_F\mathbb{I}\\
f^{ACD}f^{BCD} &= C_A\delta^{AB}
\end{aligned} \tag{2.1.8}$$

where A and F in the subscript represent the adjoint and fundamental representations respectively. Using these definitions of the Casimirs we are able to simplify expressions and are free to calculate in a general $SU(N_c)$ gauge group. Again we have used Einstein's summation convention which can be seen explicitly where we have dropped the indices when writing $T^AT^A = C_F\mathbb{I}$ instead of $\Sigma_A T^A_{IJ}T^A_{JK} = C_F\delta_{IK}$ where I, J run over $1 \leq I \leq N_F$ where N_F is the dimension of the fundamental representation. This is to be understood throughout.

Although it is preferable to compute in an arbitrary gauge for an arbitrary colour group where the same set of analytic results can be analysed for several gauge groups and colour structures simultaneously, there are occasions where we present our results numerically in terms of the true QCD special unitary group $SU(3)$. This is mainly due to the sheer size of expressions and our choice in presentation.

In $SU(3)$ the Casimirs take the following values

$$C_F \;=\; \frac{4}{3}\,, \qquad T_F \;=\; \frac{1}{2}\,, \qquad C_A \;=\; N_c \;=\; 3\,. \tag{2.1.9}$$

Now that we have discussed the basic properties of the group algebra of QCD it is necessary to determine the QCD Lagrangian. When constructing a Lagrangian for a new gauge theory it is useful to first consider the basic Dirac Lagrangian describing the free fermion field

$$\mathcal{L} \;=\; i\bar{\psi}(x)\partial\!\!\!/\psi(x) - m\bar{\psi}(x)\psi(x) \tag{2.1.10}$$

with the convention $c = \hbar = \frac{h}{2\pi} = 1$ and m represents the mass of the quark. Although we have included a mass term here for illustrative purposes, we note that throughout our work we do not consider a mass term for the quark lagrangian, choosing to explore only massless QCD. By choosing a massless regime chiral symmetry is naturally preserved. Here the notation $\partial\!\!\!/$ is shorthand for the contraction of the partial derivative with the Dirac γ-matrices. The same shorthand can be used when contracting momenta with γ^μ, i.e.

$$p\!\!\!/ \;=\; \gamma^\mu p_\mu \tag{2.1.11}$$

where γ^μ is a Dirac matrix, with μ as its Lorentz vector index, considered in d-dimensions and satisfying the Clifford algebra

$$\{\gamma_\mu, \gamma_\nu\} \;=\; \gamma_\mu\gamma_\nu + \gamma_\nu\gamma_\mu \;=\; 2\mathbb{I}_4\eta_{\mu\nu} \tag{2.1.12}$$

where $\eta_{\mu\nu}$ is the metric tensor in d-dimensional Euclidean space satisfying $\eta_\mu{}^\mu = d$ and $\mathbb{I}$ is the 4×4 identity matrix defined as

$$\mathbb{I}_4 \;=\; \begin{pmatrix} 1 & 0 & 0 & 0 \\ 0 & 1 & 0 & 0 \\ 0 & 0 & 1 & 0 \\ 0 & 0 & 0 & 1 \end{pmatrix}\,. \tag{2.1.13}$$

Throughout this thesis μ, ν are our Lorentz indices. Since we are working in d-dimensions we must develop the γ-algebra for $1 \leq \mu \leq d$. We want the γ-algebra in d-dimensions as we will be using dimensional regularization later when we renormalize the theory. In dimensional regularization this requires calculating in

$d = 4 - 2\epsilon$ dimensions. Assuming $\gamma_\mu \gamma^\mu = d$ it follows that

$$\begin{aligned} \gamma_\mu \gamma_\nu \gamma^\mu &= \left(-\gamma_\nu \gamma_\mu + 2\eta_{\mu\nu}\right) \gamma^\mu \\ &= -\gamma_\nu \gamma_\mu \gamma^\mu + 2\gamma_\nu \\ &= (2-d)\, \gamma_\nu \ . \end{aligned} \tag{2.1.14}$$

We assume the basic trace rules in d-dimensions hold:

$$\begin{aligned} \mathrm{Tr}\left[\gamma_\mu \gamma_\nu \gamma_\sigma\right] &= 0 \ \text{ for any odd number of } \gamma\text{'s} \\ \mathrm{Tr}\left[\gamma_\mu \gamma_\nu\right] &= 4\eta_{\mu\nu} \\ \mathrm{Tr}\left[\gamma_\mu \gamma_\nu \gamma_\sigma \gamma_\rho\right] &= 4\left[\eta_{\mu\nu}\eta_{\sigma\rho} - \eta_{\mu\sigma}\eta_{\nu\rho} + \eta_{\mu\rho}\eta_{\nu\sigma}\right] \ . \end{aligned} \tag{2.1.15}$$

We encounter γ-matrices and their traces when evaluating Feynman diagrams containing fermion loops. The matrix γ^5 is not considered in any of our calculations since it does not generalise to d-dimensions and we are always in the chiral limit where the quarks are massless and so we never encounter them in practice. However for completeness we briefly show the basic properties of γ^5 where it exists strictly in 4-dimensions

$$(\gamma^5)^\dagger \ = \ \gamma^5 \quad , \quad \{\gamma^5, \gamma^\mu\} \ = \ \gamma^5\gamma^\mu + \gamma^\mu\gamma^5 \ = \ 0 \tag{2.1.16}$$

where $\mu = 0, 1, 2, 3$ in four dimensional spacetime and $\gamma^0, \gamma^1, \gamma^2, \gamma^3$ are all 3×3 matrices such that

$$\gamma^5 \ = \ \gamma_5 \ = \ \frac{i}{4}\varepsilon_{\mu\nu\rho\sigma}\gamma^\mu\gamma^\nu\gamma^\rho\gamma^\sigma \ = \ \begin{pmatrix} 0 & \mathbb{I}_2 \\ \mathbb{I}_2 & 0 \end{pmatrix} \tag{2.1.17}$$

where ε is the Levi-Civita symbol specific to $d = 4$ and $\mathbb{I}_2$ is the 2×2 identity matrix. Since we are only interested in massless QCD the Lagrangian reduces to

$$\mathcal{L} \ = \ i\bar{\psi}(x)\partial\!\!\!/\psi(x) \tag{2.1.18}$$

where ψ is a three-vector representing the quarks. Here each three-component represents a *colour* charge, the same charge carried by the gluons (the mediators of the strong force). There are three different quark colours

$$\psi(x) \ = \ \begin{pmatrix} \psi_{\mathrm{red}}(x) \\ \psi_{\mathrm{blue}}(x) \\ \psi_{\mathrm{green}}(x) \end{pmatrix} \quad , \quad \bar{\psi}(x) \ = \ \begin{pmatrix} \bar{\psi}_{\mathrm{red}}(x) \ , \ \bar{\psi}_{\mathrm{blue}}(x) \ , \ \bar{\psi}_{\mathrm{green}}(x) \end{pmatrix} \tag{2.1.19}$$

for each flavour, where we recall that there are six known flavours to date; up, down, strange, charm, bottom and top. This colour charge was introduced by Greenberg as a way of solving the problem that the quark model violated the Pauli exclusion principle, [25], which says that no two electrons can occupy the same state, [26]. Since the quarks have half integer spin this rule also applies to them. Although in nature there exist six flavours we have chosen to work with an arbitrary number of flavours. The flavour of a quark is distinguished by the index i on $\psi^i(x)$ where $1 \leq i \leq N_f$. In QCD the flavour index has no dynamical role. We do note however that in nature we are only allowed colourless states; another reason to support why we do not see quarks and gluons as isolated particles in nature.

An important property of the Lagrangian for any theory is that it must be invariant under local gauge transformations. It is straightforward to see that the Dirac Lagrangian (2.1.18) is invariant under global transformations of the form

$$\psi(x) \to U\psi(x) \quad \text{and} \quad \bar{\psi} \to \bar{\psi}(x)U^\dagger \quad \text{with} \quad U = e^{i\Lambda} \tag{2.1.20}$$

where Λ is a 3×3 unitary ($\Lambda^\dagger\Lambda = 1$) Hermitian ($\Lambda = \Lambda^\dagger$) matrix, independent of spacetime variable x. However imposing this transformation locally, i.e. by setting Λ to be a function of x,

$$\psi(x) \to U(x)\psi(x) \quad , \quad \bar{\psi} \to \bar{\psi}(x)U^\dagger(x) \tag{2.1.21}$$

we see that local gauge invariance is not satisfied,

$$i\bar{\psi}(x)\gamma^\mu\partial_\mu\psi(x) \to i\bar{\psi}(x)\gamma^\mu\partial_\mu\psi(x) + i\bar{\psi}(x)U^\dagger(x)\gamma^\mu(\partial_\mu U(x))\psi(x) \ . \tag{2.1.22}$$

Instead we are left with an extra term that appears as a result of the partial derivative acting on U which now depends on x and therefore does not commute past the partial derivative as easily as before (2.1.20). In order to rectify this problem we require a derivative that transforms covariantly. By introducing a covariant derivative, D_μ, to replace the partial derivative, ∂_μ, appearing in the Lagrangian (2.1.18) local gauge invariance is restored. The covariant derivative is defined to be

$$D_\mu \ = \ \partial_\mu + igA_\mu(x) \ . \tag{2.1.23}$$

Note that some authors choose to define the covariant derivative with a minus sign in front of g, where g is the coupling constant. Above A_μ is the group-valued ($A_\mu(x) = A^A_\mu(x)T^A$) gauge potential or gluon field transforming as an adjoint representation of $SU(3)$ with colour index A running from $1, \ldots, 8$. This gauge field transforms locally as

$$A_\mu(x) \to U(x)A_\mu(x)U^\dagger(x) + \frac{i}{g}\left(\partial_\mu U(x)\right)U^\dagger(x) \quad . \tag{2.1.24}$$

Acting on the quark fields the covariant derivative transforms like

$$\begin{aligned} D_\mu\psi(x) &\to U(x)D_\mu\psi(x) \\ D_\mu\psi(x) &= \left(\partial_\mu + igA_\mu(x)\right)\psi(x) \\ D_\mu\psi(x) &= \partial_\mu\psi(x) + igA^A_\mu(x)T^A\psi(x) \end{aligned} \tag{2.1.25}$$

where T^A are the generators of the group, (2.1.5), and $A^A_\mu(x)$ is the vector potential. The covariant derivative of a group valued object, X, satisfies, [27]

$$D_\mu X = \partial_\mu X + ig\left[A_\mu, X\right] \tag{2.1.26}$$

such that the covariant derivative acting on the gauge field A_μ is given by

$$\begin{aligned} D_\mu A_\nu &= \partial_\mu A_\nu + ig\left[A_\mu, A_\nu\right] \\ \left(D_\mu A_\nu(x)\right)^A T^A &= \left(\partial_\mu A^A_\nu(x) - gf^{ABC}A^B_\mu(x)A^C_\nu(x)\right)T^A \\ \left(D_\mu A_\nu(x)\right)^A &= \partial_\mu A^A_\nu(x) - gf^{ABC}A^B_\mu(x)A^C_\nu(x) \end{aligned} \tag{2.1.27}$$

where we have applied (2.1.6) since the A_μ fields commute. To be consistent when comparing results between gauges we have chosen to define the covariant derivative acting on the fields using equation (2.1.26) throughout our work. The Curci-Ferrari gauge which is considered in Chapter 4 shares the same definitions as the linear covariant gauge. However, additional definitions need to be introduced when considering the MAG due to the unique nature of the gauge fixing. We derive these definitions in Chapter 5.

A commutation relation exists between the covariant derivatives giving

$$\left[D_\mu, D_\nu\right] = ig\left(\partial_\mu A_\nu - \partial_\nu A_\mu + ig\left[A_\mu, A_\nu\right]\right) \tag{2.1.28}$$

from which we define the field strength tensor by

$$\mathrm{G}_{\mu\nu} = \partial_\mu A_\nu - \partial_\nu A_\mu + ig\left[A_\mu, A_\nu\right] \tag{2.1.29}$$

and its group valued definition

$$\mathrm{G}^A_{\mu\nu} = \partial_\mu A^A_\nu - \partial_\nu A^A_\mu - g f^{ABC} A^B_\mu A^C_\nu \ . \tag{2.1.30}$$

The field strength tensor is what distinguishes QCD from QED, essentially giving rise to asymptotic freedom due to the gluon self-interactions. Incorporating this gauge invariant term in to the Lagrangian we now have the complete QCD Lagrangian expressed in terms of bare parameters, where the subscript, $_o$, indicates the bare parameter, given by

$$\mathcal{L} = -\frac{1}{4}\left(\mathrm{G}^A_{o\,\mu\nu}\right)^2 + i\bar{\psi}_o \not{D}_o \psi_o + L_{\mathrm{gf}} \tag{2.1.31}$$

where the $\left(\mathrm{G}^A_{o\,\mu\nu}\right)^2$ term contains the cubic and quartic gluon self-interactions. By definition $\left(\mathrm{G}^A_{o\,\mu\nu}\right)^2$ is gauge invariant under the transformation

$$\mathrm{G}_{\mu\nu} \to U \mathrm{G}_{\mu\nu} U^\dagger \ . \tag{2.1.32}$$

Recall that we are only interested in massless QCD and so our Lagrangian does not contain an explicit mass term for any field.

The importance of the Lagrangian is that it tells us what interactions we can have in our theory. We have seen that it must be constructed using local gauge symmetries. Our Lagrangian as it stands is invariant under local $SU(3)$ gauge transformations, but it is more appropriate to consider a general Lie group, to which we can specify a gauge group later on. The extra parameters introduced by unspecifying a gauge group will allow us to cross check results.

2.1.1 Gauge fixing

Before we can define and calculate the Feynman diagrams that encode the interactions between fields originating from the interacting terms in the Lagrangian we must first fix the gauge. It is not possible to do any perturbative calculations until the gauge is fixed for two important reasons. Firstly the degrees of freedom in the original theory are incorrect. This must be dealt with before any meaningful calculations can take place otherwise results obtained will be unphysical and

therefore have no relation to nature. The second of our problems comes when we try to determine the gluon propagator. To successfully construct the propagator we need to be able to invert the gluon Lagrangian (the quadratic in A_μ piece). This is not possible without first including additional terms which allow us to invert the matrix.

An appropriate gauge choice can greatly simplify calculations. We do this by introducing gauge fixing terms to the original Lagrangian. The role played by the gauge fixing terms is to reduce the number of degrees of freedom in the theory, eliminating the unphysical degrees of freedom in the gauge field A^A_μ. Faddeev and Popov, [28], proposed a condition in the form

$$\mathrm{F}^A\left[A_\mu\right] \;=\; 0 \tag{2.1.33}$$

which must be satisfied, where F^A is some function on the gauge field A_μ, [29]. The standard gauge fixing condition for an arbitrary (linear) covariant gauge is the Landau gauge fixing condition

$$\mathrm{F}^A\left[A_\mu\right] \;=\; \partial^\mu A^a_\mu \;=\; 0 \tag{2.1.34}$$

commonly referred to in the literature as the Lorentz condition or Lorentz gauge. This condition reduces the number of independent components of A_μ from four to three, [30], as

$$\partial^0 A_0 + \partial^1 A_1 + \partial^2 A_2 + \partial^3 A_3 \;=\; 0\;. \tag{2.1.35}$$

In other words one component is dependent on the other three. However, the Faddeev-Popov construction (2.1.34) was originally presented for Landau type gauges and was found only to be valid for covariant gauges. Once gauge invariance had been broken by introducing these non gauge invariant ghost terms via the Faddeev-Popov gauge fixing procedure a new symmetry needed to be introduced to guarantee unitarity and ensure gauge independent results emerged for physical quantities. Although 't Hooft was working on this at the same time, Slavnov and Taylor were first to generalise a set of offshell identities extending the Ward-Takahashi identities of QED, [31, 32], that must be fullfilled. We discuss these identities and their practical purpose in depth in section 2.1.2. For a non-linear gauge fixing such as the MAG the definition of (2.1.33) is more involved. A more general, and in many ways easier way of gauge fixing was discovered by Becchi,

Rouet, Stora and Tyutin, [33, 34, 35], who proposed a way of using symmetry arguments, in particular global symmetries to define a set of gauge fixing terms which satisfied the global gauge symmetries

$$\begin{aligned}
\delta A^A_\mu &= -D_\mu c^A && (2.1.36)\\
\delta c^A &= -\frac{g}{2} f^{ABC} c^B c^C && (2.1.37)\\
\delta \bar{c}^A &= b^A && (2.1.38)\\
\delta b^A &= 0 && (2.1.39)
\end{aligned}$$

where δ is the BRST transform that anticommutes with the ghost fields c^A and $\bar{c}^A$, where $\bar{c}^A$ is the *anti*-ghost. These ghost particles are unphysical fields which can mathematically be included in a theory but which never directly contribute to the physics. They restore unitarity, which without ghosts was found to be violated at the one loop level. The role of the ghost degrees of freedom is to cancel the longitudinal component of the gluon propagator, leaving it fully transverse and physical in the quantum theory, [28, 36, 37, 38]. The quarks and anti-quarks also transform in a BRST way as

$$\begin{aligned}
\delta \psi^{iI} &= igc^A \left(T^A\right)_{IJ} \psi^{iJ} && (2.1.40)\\
\delta \bar{\psi}^{iI} &= -igc^A \left(T^A\right)_{IJ} \bar{\psi}^{iJ} && (2.1.41)
\end{aligned}$$

where lower case i here corresponds to the flavour index and upper case I is the group spinor index on a quark. Valid in the gauge fixed theory this BRST invariance, which can be applied to both linear and non-linear gauges effectively replaces gauge invariance. Since we consider multiple gauge fixings within this thesis we define the gauge fixing conditions, [39, 41], in the form of (2.1.33) below

$$\begin{aligned}
\mathrm{F}^A_{\mathrm{Landau}}[A_\mu] &= \partial^\mu A^A_\mu \\
\mathrm{F}^A_{\mathrm{CF}}[A_\mu, \bar{c}, c, b] &= \left\{ \partial^\mu A^a_\mu + \tfrac{\alpha}{2} b^a_{\mathrm{CF}} - \tfrac{\alpha}{4} g f^{abc} \bar{c}^b c^c \quad \text{for } A \in \{a,b,c\} \right. \\
\mathrm{F}^A_{\mathrm{MAG}}[A_\mu, \bar{c}, c, b] &= \begin{cases} \partial^\mu A^i_\mu + \frac{\alpha_p}{2} b^i_{\mathrm{MAG}} & \text{for } A \in \{i,j,k\} \\ \left(D^\mu A_\mu\right)^a + \frac{\alpha_p}{2} b^a_{\mathrm{MAG}} - \frac{\alpha}{2} g f^{abi} \bar{c}^b c^i - \frac{\alpha}{4} g f^{abc} \bar{c}^b c^c & \\ & \text{for } A \in \{a,b,c\} \end{cases}
\end{aligned} \qquad (2.1.42)$$

where, in the case of the MAG gauge fixing $A \in \{i,j,k\}$ denotes the diagonal and $A \in \{a,b,c\}$ the off-diagonal generators of the Lie algebra. This splitting of the

gauge group is discussed in more depth in chapter 5. Here b^A are the commuting auxiliary Nakanishi-Lautrup fields, [40, 42] coming directly from imposing BRST symmetry. For a full derivation of the BRST transforms in the arbitrary linear covariant and non-linear Curci-Ferrari and maximal abelian gauges refer to Appendix A.

Returning to (2.1.31) and imposing the method of Faddeev and Popov (2.1.34) we get the full QCD gauge fixed Lagrangian for an arbitrary (linear) covariant gauge

$$\mathcal{L}_{\text{total}} = \mathcal{L}_{\text{gauge invariant}} + \mathcal{L}_{\text{gf}} + \mathcal{L}_{\text{ghost}} \tag{2.1.43}$$

$$\mathcal{L} = -\frac{1}{4}\left(\mathrm{G}^{a}_{\mu\nu}\right)^2 + i\bar{\psi}\not{D}\psi - \frac{1}{2\alpha}\left(\partial^{\mu}A^{a}_{\mu}\right)^2 - \bar{c}^{a}\partial_{\mu}D^{\mu}c^{a}\ . \tag{2.1.44}$$

It is natural to combine both $\mathcal{L}_{\text{gf}}$ and $\mathcal{L}_{\text{ghost}}$ such that

$$\mathcal{L}_{\text{GF}} = \mathcal{L}_{\text{gf}} + \mathcal{L}_{\text{ghost}} \tag{2.1.45}$$

since when gauge fixing the Curci-Ferrari and maximal abelian gauges the ghosts couple to physical fields. The textbook approach of (2.1.43) is inapplicable in non-linear gauges since the gauge fixing term, $\mathcal{L}_{\text{gf}}$, and ghost term, $\mathcal{L}_{\text{ghost}}$, are not treated separately. Throughout this thesis when we refer to the gauge fixing term it will be of the combined form (2.1.45), i.e. $\mathcal{L}_{\text{GF}}$.

Introduced via gauge fixing is the arbitrary gauge parameter α, and $c^a, \bar{c}^a$ represent the interacting scalar particles called ghosts. To reiterate, these Grassmann variables are unphysical particles which are inserted on a purely mathematical level and do not contibute to the overall physics. Since they are Grassmann variables they anti-commute with

$$c^{a}\bar{c}^{b} = -\bar{c}^{b}c^{a}\ . \tag{2.1.46}$$

This above method of fixing the gauge is not unique and our overall result should always be independent of our gauge choice. This corresponds to choosing a coordinate system in order to perform a calculation, [44]. No matter what set of coordinates one uses the result should always be consistent. On introducing the ghost fields it is appropriate to give the definition of the covariant derivative

acting on this particular field, based on (2.1.26) as

$$D_\mu c^a \;=\; \partial_\mu c^a - g f^{abc} A^b_\mu c^c \;. \tag{2.1.47}$$

It may seem non-trivial that these ghost fields should then couple to A_μ for certain gauge fixings, however the ghosts only occur in the internal part of the diagram, i.e. in closed loops and never as incoming or outgoing physical particles, leaving the physics intact. Without the addition of ghost fields unitarity would be violated.

In the step prior to obtaining (2.1.44) it is possible to write (2.1.45) of the form

$$\mathcal{L}_{\rm GF} \;=\; -\frac{\left(\mathrm{F}^A\left[A_\mu\right]\right)^2}{2\alpha} - \bar{c}^a \left(\frac{\delta \mathrm{F}^A\left[A_\mu\right]}{\delta \Lambda^b}\right) c^b \tag{2.1.48}$$

where Λ was defined in (2.1.20). In the case of the arbitrary (linear) covariant gauge a clear choice can be made for $\mathrm{F}^A\left[A_\mu\right]$ to obtain (2.1.44). For $\mathrm{F}^A_{\rm CF}$ and $\mathrm{F}^A_{\rm MAG}$, the gauge fixed part of the Lagrangian for the Curci-Ferrari gauge and MAG respectively, we can introduce the more appropriate BRST symmetry to define the gauge fixing terms. Transforming our definition of $\mathcal{L}_{\rm GF}$ in (2.1.48) to be

$$\mathcal{L}_{\rm GF} \;=\; \delta\left[\bar{c}^a\left(F^A\left[A_\mu, c, \bar{c}, b\right]\right)\right] \tag{2.1.49}$$

which accommodates all three gauge fixings defined in (2.1.42) and performing a BRST transformation on each of the fields the following can be obtained, [67],

$$\mathcal{L}^{\rm Linear}_{\rm GF} \;=\; -\frac{1}{2\alpha}(\partial^\mu A^a_\mu)^2 \;-\; \bar{c}^a \partial^\mu D_\mu c^a \;, \tag{2.1.50}$$

$$\begin{aligned}\mathcal{L}^{\rm CF}_{\rm GF} \;=\;& -\frac{1}{2\alpha}(\partial^\mu A^a_\mu)^2 \;-\; \bar{c}^a \partial^\mu D_\mu c^a \\ &+ \frac{g}{2} f^{abc} \partial^\mu A^a_\mu \bar{c}^b c^c \;+\; \frac{\alpha g^2}{8} f^{eab} f^{ecd} \bar{c}^a c^b \bar{c}^c c^d \;,\end{aligned} \tag{2.1.51}$$

$$\begin{aligned}\mathcal{L}^{\rm MAG}_{\rm GF} \;=\;& -\frac{1}{2\alpha}\left(\partial^\mu A^a_\mu\right)^2 - \frac{1}{2\alpha_p}\left(\partial^\mu A^i_\mu\right)^2 + \bar{c}^a \partial^\mu \partial_\mu c^a + \bar{c}^i \partial^\mu \partial_\mu c^i \\ &+ g\left[f^{abk} A^a_\mu \bar{c}^k \partial^\mu c^b - f^{abc} A^a_\mu \bar{c}^b \partial^\mu c^c - \frac{1}{\alpha} f^{abk} \partial^\mu A^a_\mu A^b_\nu A^{k\,\nu}\right. \\ &\quad - f^{abk} \partial^\mu A^a_\mu c^b \bar{c}^k - \frac{1}{2} f^{abc} \partial^\mu A^a_\mu \bar{c}^b c^c - 2 f^{abk} A^k_\mu \bar{c}^a \partial^\mu \bar{c}^b \\ &\quad \left. - f^{abk} \partial^\mu A^k_\mu \bar{c}^b c^c\right]\end{aligned}$$

$$
\begin{aligned}
&+ g^2 \Big[f_d^{acbd} A_\mu^a A^{b\,\mu} \bar{c}^c c^d - \frac{1}{2\alpha} f_o^{akbl} A_\mu^a A^{b\,\mu} A_\nu^k A^{l\,\nu} + f_o^{adcj} A_\mu^a A^{j\,\mu} \bar{c}^c c^d \\
&- \frac{1}{2} f_o^{ajcd} A_\mu^a A^{j\,\mu} \bar{c}^c c^d + f_o^{ajcl} A_\mu^a A^{j\,\mu} \bar{c}^c c^l + f_o^{alcj} A_\mu^a A^{j\,\mu} \bar{c}^c c^l \\
&- f_o^{cjdi} A_\mu^i A^{j\,\mu} \bar{c}^c c^d - \frac{\alpha}{4} f_d^{abcd} \bar{c}^a \bar{c}^b c^c c^d - \frac{\alpha}{8} f_o^{abcd} \bar{c}^a \bar{c}^b c^c c^d \\
&+ \frac{\alpha}{8} f_o^{acbd} \bar{c}^a \bar{c}^b c^c c^d - \frac{\alpha}{4} f_o^{abcl} \bar{c}^a \bar{c}^b c^c c^l + \frac{\alpha}{4} f_o^{acbl} \bar{c}^a \bar{c}^b c^c c^l \\
&- \frac{\alpha}{4} f_o^{albc} \bar{c}^a \bar{c}^b c^c c^l + \frac{\alpha}{2} f_o^{akbl} \bar{c}^a \bar{c}^b c^k c^l \Big] \, . \qquad (2.1.52)
\end{aligned}
$$

The gauge fixing terms for the linear covariant and Curci-Ferrari gauges have been checked and verified explicitly with [79, 104, 126]
The properties and construction of the MAG gives rise to two independent arbitrary gauge fixing parameters, α and α_p. Adding an above gauge fixing term to the Lagrangian forces gauge invariance to break, since the gauge fixing terms are gauge dependent. BRST symmetry preserves some remnant of this lost gauge symmetry. It is taken for granted that the original terms in each Lagrangian are BRST invariant since gauge invariance implies BRST invariance and the gauge fixing term in each Lagrangian ensures that any extra terms added will not affect the original terms in (2.1.31). We construct and display the BRST transformations and their relations, in particular the b-fields, for both the CF gauge and MAG, whilst discussing this technique in more detail in Appendix A. Once the gauge is fixed, ensuring all additional terms satisfy $\mathrm{F}^A\left[A_\mu\right] = 0$ we can proceed to calculating with this now complete Lagrangian.

2.1.2 Renormalization

An important property of QCD is that it is a renormalizable theory. Let us explain what this means by considering the complete QCD Lagrangian for an arbitrary (linear) covariant gauge fixing, (2.1.44). If one were to naively start computing quantum corrections to the Green's functions with this Lagrangian as their starting point they would encounter Feynman diagrams that are infinite in four dimensions. This is problematic since it would be impossible to obtain meaningful physical results due to the infinities appearing within the calculation. These infinities are a result of divergent Feynman integrals contained within certain Feynman diagrams. Generally there are two types of divergence; these are known as infrared (IR) and ultraviolet (UV). Ultraviolet behaviour occurs at high energies whereas infrared occurs at low energies. A procedure called renormalization was introduced to tackle such infinities. Renormalization theory is based

on the UV divergences, as these can be handled systematically. Renormalization is a systematic and mathematically consistent method of redefining the variables of a theory in a way that removes these infinities. It simply means re-expressing results of the theory via physical (measurable) quantities. There are a number of ways in which one can renormalize massless QCD and there are several regulators which can be used. The three most popular regulators are cut-off, lattice regularization and dimensional regularization, each with their own advantages and disadvantages. As QCD is a real world gauge theory we must ensure gauge symmetry is preserved, as mentioned in the previous section. This automatically excludes the use of cut-off renormalization since this technique breaks gauge symmetry. Lattice regularization preserves this gauge symmetry but does not preserve Lorentz symmetry which is necessary for obtaining measurable results independent of coordinate system and/or direction i.e. the results have the same value in all frames. Lattice also requires super computers and is costly to implement. In order to ensure gauge symmetry and Lorentz symmetry are conserved we use dimensional regularization developed by 't Hooft and Veltman in [45] and also [46, 47]. This type of regularization is the most popular approach used in practical calculations with the basic idea behind it being to reduce the number of dimensions over which one integrates, resulting in the divergences disappearing, [48]. But how do we know what dimension to work in?

Consider an integral commonly encountered in one loop calculations. When mass m is small and negligible, then

$$\int \frac{\mathrm{d}^4k}{(k^2-m^2)^2} \to \int_{\varepsilon}^{\Lambda} \frac{\mathrm{d}^4k}{(k^2)^2} \quad = \quad \ln\Lambda - \ln\varepsilon \tag{2.1.53}$$

which tends to infinity when $\varepsilon \to 0$ or $\Lambda \to \infty$, where the integral is considered in 4-dimensional Minkowski space. We see that the integral will diverge at large momenta k^2. To avoid our integral diverging we can choose a regulator to transform the ill-defined integral into a well-defined one. This means considering the same integral integrated over d^dk where d is some arbitrary number of dimensions. For $d = 4$ we have a divergence. For $d > 4$ our integral will continue to diverge, and so this leaves us with the choice $d < 4$. For this value of d we see that the integral is now convergent and can be calculated explicitly, [49]. Hence for $d < 4$ logarithmic divergences which are encountered in quantum field theories vanish.

In other words when using dimensional regularization we have the following

$$\int d^d k \frac{\partial}{\partial k^\mu} f(k^2) \;=\; 0 \;. \tag{2.1.54}$$

In dimensional regularization the space-time dimension d becomes a complex variable and can be written as $d = 4 - 2\epsilon$ where ϵ is the regularizing parameter. Singularities manifest themselves as poles in ϵ where the physical limit $\epsilon \to 0$ brings us to our real-world 4-dimensional space-time after renormalization, [50].

When renormalizing a theory we introduce renormalization constants, or scaling factors, Z_i, that cancel the divergences in the theory. How one removes the divergences is known as the renormalization scheme. These schemes can vary in their definitions, from absorbing only the divergences, which when using dimensional regularization manifest themselves as poles in ϵ, to the renormalization constants also absorbing a finite piece in addition to the divergences. Let us demonstrate how these renormalization constants look in practice. Recall for example the QCD Lagrangian for an arbitrary (linear) covariant gauge (2.1.44). We can redefine the theory with

$$A^\mu_o = \sqrt{Z_A} A^\mu \,,\; g_o = \mu^\epsilon Z_g g \,,\; \psi_o = \sqrt{Z_\psi}\psi \,,\; c^a_o = \sqrt{Z_c} c^a \,,\; \alpha_o = \frac{Z_A}{Z_\alpha}\alpha \;. \tag{2.1.55}$$

In renormalization Z_i is the quantity we want to fix in order for it to cancel out the divergences in the theory. The way in which we define this set of renormalization constants is simply a matter of convention, since our overall results will ultimately be independent of the scheme. If it was possible to calculate all orders of perturbation theory physical results would be independent of the renormalization scheme chosen. The specifics of scheme definitions will be discussed later. In gauge theories, such as QCD, there are relations between the renormalization constants in consequence of the Slavnov-Taylor identities. In our work [51] and the work of [14] the renormalization constants have been constructed such that the Slavnov-Taylor identities [31, 32] are automatically satisfied. Let us demonstrate this. In [52] the Slavnov-Taylor identities are defined to be

$$\frac{Z_1^{F(\mathrm{qqg})}}{Z_2} \;=\; \frac{\tilde{Z}_1^{(\mathrm{ccg})}}{\tilde{Z}_3} \;=\; \frac{Z_1^{(\mathrm{ggg})}}{Z_3} \quad , \quad \frac{Z_4^{(\mathrm{gggg})}}{Z_3} \;=\; \left(\frac{Z_1^{(\mathrm{ggg})}}{Z_3}\right)^2 \tag{2.1.56}$$

where there is a renormalization constant corresponding to each interaction term in the Lagrangian. Particularly Z_1^F, $\tilde{Z}_1$ and Z_1 are the renormalization constants

for the quark-gluon, ghost-gluon and triple-gluon vertices respectively and Z_3, $\tilde{Z}_3$ and Z_2 are the gluon, ghost and quark wave function renormalization constants. On defining a renormalization constant per field, as we have done in (2.1.55), one can directly relate Celmaster and Gonsalves' definitions to ours such that

$$Z_3 \;=\; Z_A \;\;,\;\; \tilde{Z}_3 \;=\; Z_c \;\;,\;\; Z_2 \;=\; Z_\psi \tag{2.1.57}$$

and those corresponding to the vertices

$$\begin{aligned} Z_1^{F(\mathrm{qqg})} \;&=\; Z_g^{(\mathrm{qqg})} Z_\psi \sqrt{Z_A} \;\;,\;\; \tilde{Z}_1^{(\mathrm{ccg})} \;=\; Z_g^{(\mathrm{ccg})} Z_c \sqrt{Z_A} \;\;, \\ Z_1^{(\mathrm{ggg})} \;&=\; Z_g^{(\mathrm{ggg})} Z_A \sqrt{Z_A} \end{aligned} \tag{2.1.58}$$

where our definition of the renormalization constants are on the right hand side of the equals sign while the Slavnov-Taylor definitions are on the left. Defining our renormalization constants this way ensures that the Slavnov-Taylor identities (2.1.56) are naturally satisfied, since they imply that

$$Z_g^{(\mathrm{ggg})} \sqrt{Z_A}\,\Big|_{\overline{\mathrm{MS}}} = Z_g^{(\mathrm{qqg})} \sqrt{Z_A}\,\Big|_{\overline{\mathrm{MS}}} = Z_g^{(\mathrm{ccg})} \sqrt{Z_A}\,\Big|_{\overline{\mathrm{MS}}} \tag{2.1.59}$$

for all three vertices in the $\overline{\mathrm{MS}}$ scheme. Celmaster and Gonsalves, [52], also define a relation between the 3- and 4-point gluon functions in (2.1.56) with, in terms of our definition of the renormalization constants, $Z_4^{(\mathrm{gggg})} = Z_g^{2(\mathrm{ggg})} Z_A^2$ which must be satisfied for the theory to be consistent. This ratio between the $(n+1)$ and n-point functions must hold for all n. Therefore with our redefinition of the renormalization constants the Slavnov-Taylor identities are naturally satisfied via this construction and so proving that $Z_g\sqrt{Z_A}$ is equivalent for all 3-point functions is enough to prove that the Slavnov-Taylor identities hold. Although the way in which the renormalization constants are defined should be independent of the physics, our way of defining the Z's builds the above identities into the definitions which in turn saves us the trouble of separately checking the identities again later on. When renormalizing the fields it is vital to take into account the renormalization of the arbitrary gauge parameter α, as just like the coupling constant g, the renormalization of the gauge parameter can be different in different schemes. This becomes apparent in the next chapter where we relate the coupling constants in two schemes to one another. The renormalized Lagrangian is now given in terms of renormalized parameters

$$\mathcal{L} = -\frac{1}{4} Z_A \left(\mathrm{G}^a_{\mu\nu}\right)^2 - \frac{Z_\alpha}{2\alpha}\left(\partial^\mu \mathrm{A}^a_\mu\right)^2 + i Z_\psi \bar{\psi} \not{D} \psi - Z_c \bar{c}^a \partial_\mu \mathrm{D}^\mu c^a \tag{2.1.60}$$

where the renormalized coupling constant is embedded in the covariant derivatives and field strength tensor. Notice how in (2.1.55) the renormalized coupling constant comes with a pre-factor of μ^ϵ. When using a regularization scheme we must include an associated mass scale. For dimensional regularization this mass scale is μ which is introduced in order to ensure the coupling constant is dimensionless in d-dimensions, [14]. After re-expressing the results for physical quantities via renormalized parameters we can remove the regularization, [53]. In d-dimensional regularization, removing the regularization simply means taking the limit $\epsilon \to 0$ since dimensional regularization is something of a mathematical procedure. We note that physical expressions only make sense in this limit, [54].

Now that we have chosen the gauge in which we are calculating in, and dimensional regularization as our regulator, we next have the task of choosing which scheme to work in. The most popular scheme choice in QCD is the modified minimal subtraction ($\overline{\text{MS}}$) scheme. This is a modification of the MS scheme, [55, 56], first formulated by 't Hooft. Both the MS and $\overline{\text{MS}}$ schemes fall into the class of mass independent renormalization schemes. Rather than using the MS prescription of $\frac{1}{\epsilon}$ being absorbed into the renormalization constants, $\overline{\text{MS}}$ requires that $\frac{1}{\epsilon} - \gamma_{\text{E}} + \ln(4\pi)$ is absorbed, [57], where γ_{E} is the Euler-Mascheroni constant. This keeps the expressions for the renormalized Green's functions much simpler, and hence the reason this scheme has been adopted as the most popular to use in practical calculations. With high order multiloop results previously calculated and readily available in this scheme, $\overline{\text{MS}}$ has become the standard reference scheme. However, at one loop it is possible to map between the MS and $\overline{\text{MS}}$ schemes by taking the limit $\frac{1}{\epsilon} \to \frac{1}{\epsilon} - \gamma_{\text{E}} + \ln(4\pi)$ and vice-versa, [57]. At higher loop orders however this mapping is less trivial. In the $\overline{\text{MS}}$ scheme at two loops the renormalization constants have the form

$$Z_i(a_{\overline{\text{MS}}}) = 1 + \frac{z_{i_1}}{\epsilon} a_{\overline{\text{MS}}} + \left(\frac{z_{i_{22}}}{\epsilon^2} + \frac{z_{i_{21}}}{\epsilon} \right) a^2_{\overline{\text{MS}}} + \mathcal{O}(a^3_{\overline{\text{MS}}}) \tag{2.1.61}$$

where we have chosen to define our coupling constant a, in relation to the gauge coupling constant as $a = \frac{g^2}{16\pi^2}$ and use this definition throughout.

An additional scheme to consider is the momentum subtraction (MOM) scheme. Although fewer results exist to the same multiloop precision in this scheme, the MOM scheme is an improvement on the $\overline{\text{MS}}$ scheme in that it is a physical scheme choice. The MOM scheme is based upon the 3-point vertices of the Lagrangian,

where the determination of the renormalized coupling constant requires calculating the vertex corrections at the symmetric subtraction point. Original MOM schemes were developed by Celmaster and Gonsalves in 1979, [52]. Only recently in [14, 58] have results been obtained for the renormalization of the triple gluon, quark-gluon and ghost-gluon vertices for the MOMi schemes at two loops. The i here refers to the vertex at which the renormalization has been applied. Within this thesis $i \in \{A^a_\mu A^b_\nu A^c_\sigma,\, \psi\bar{\psi}A^a_\mu,\, c^a\bar{c}^b A^c_\mu\}$ where no other 3-point vertices are considered. We define the MOMi schemes explicitly in further detail in section 2.1.5. This large gap between developing the MOMi schemes and computations being able to take place in these schemes illustrates the technical difficulty of moving to this scheme at higher orders. In the thirty years between [52] and [14, 58] came the development of the Laporta algorithm, [60], which greatly sped up algebraic operations, and many master integrals which were unknown in 1979 were now solved, enabling computations in the momentum subtraction schemes to continue.

2.1.3 Feynman rules

Next we require the Feynman rules. The Feynman rules allow us to translate a Feynman diagram into a set of mathematical instructions which we then solve using integration. Each Lagrangian determines a particular set of Feynman rules specific to that gauge, [29, 26]. It is not to be assumed that the Feynman rules in one gauge are identical to those in another. A perfect example of this is the addition of a Feynman rule to describe the quartic ghost interaction which exists in a non-linear gauge fixing such as Curci-Ferrari but not in the Landau gauge. The Feynman rules are directly derived from the Lagrangian. In essence the free Lagrangian determines the propagator whilst the interaction terms define the vertex rules. We define our set of Feynman rules for each setup in Appendix C. Note that we never consider individual diagrams, only the overall sum of all contributing diagrams. In massless theories dimensional regularization regularizes both types of infinities so it is never clear where the poles in ϵ originate from. In calculating the sum of all diagrams we are able to compute the amplitudes and by the nature of these diagrams some divergences will naturally cancel.

2.1.4 Momentum configuration and technical aspects

Having discussed the method of renormalization in depth we now move on to detailing the techniques used within our calculations. Unlike past computations in

this area that have been studied for the exceptional case, where the linear combination of the external momentum is zero, in our setup for the three point vertices we choose not to nullify any external momenta, instead using a non-exceptional momentum configuration. We choose this setup since despite nullification of an external leg simplifying a calculation, this nullification can create spurious IR divergences of which there is no consistent way of dealing with these mathematically. It is also a more desired setup for those wishing to analyse the results. The three Green's functions we consider throughout Part 1 of this thesis in each gauge are

$$\langle A^A_\mu(p)A^B_\nu(q)A^C_\sigma(r)\rangle \ , \ \langle(\psi^{iI}(p))_\alpha(\bar{\psi}^{jJ}(q))^\beta A^C_\sigma(r)\rangle \text{ and } \langle c^A(p)\bar{c}^B(q)A^C_\sigma(r)\rangle \quad (2.1.62)$$

representing the triple-gluon, quark-gluon and ghost-gluon vertices respectively with momentum conservation along $p+q+r=0$. Although many authors choose not to explicitly show spinor indices on the quark fields we include them here to help ease our explaination of choosing a tensor basis later on. The vertices are considered at the symmetric subtraction point in which the sum of the squares of the three external momenta are set equal to each other i.e.

$$p^2 \ = \ q^2 \ = \ r^2 \ = \ (p+q)^2 \ = \ -\,\mu^2 \ , \quad (2.1.63)$$

where μ is the same associated mass scale defined earlier to ensure the coupling constant is dimensionless in d-dimensions. In (2.1.63) one could regard this as a kinematical variable different from the scale which makes the coupling constant dimensionless in d-dimensions. In this case when the variables are different one would have additional terms involving logarithms of ratios of these scales throughout all of our amplitudes. We choose to keep the scales the same throughout as they can readily be restored by a coupling constant rescaling. We will assume this throughout the thesis. Note here that we have only two independent external momenta, p and q, with $r=-p-q$, again reiterating the fact that we do not nullify any external momenta. The diagrams are set up with the momentum defined in Figure 2.1 where we always choose the top leg to be the gluon. We can write each of our three vertices as follows, [14],

$$\begin{aligned}
\langle A^A_\mu(p)A^B_\nu(q)A^C_\sigma(-p-q)\rangle|_{p^2=q^2=-\mu^2} &= f^{ABC}\,\Sigma^{\mathrm{ggg}}_{\mu\nu\sigma}(p,q)|_{p^2=q^2=-\mu^2} \\
\langle(\psi^{Ii}(p))_\alpha(\bar{\psi}^{Jj}(q))^\beta A^C_\sigma(-p-q)\rangle|_{p^2=q^2=-\mu^2} &= \delta^{ij}T^C_{IJ}\left(\Sigma^{\mathrm{qqg}}_\sigma(p,q)\right)_\alpha^{\ \beta}|_{p^2=q^2=-\mu^2} \\
\langle c^A(p)\bar{c}^B(q)A^C_\sigma(-p-q)\rangle|_{p^2=q^2=-\mu^2} &= f^{ABC}\,\Sigma^{\mathrm{ccg}}_\sigma(p,q)|_{p^2=q^2=-\mu^2} \ ,
\end{aligned}$$

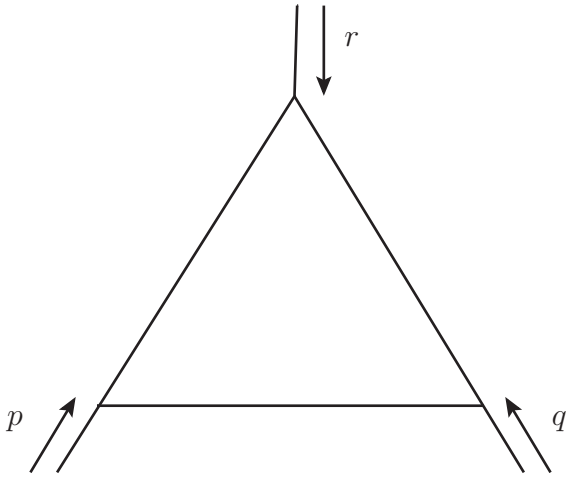

Figure 2.1: Incoming external momenta for the one loop triangle graph.

(2.1.64)

where ggg, qqg and ccg represent the triple-gluon, quark-gluon and ghost-gluon vertex functions respectively. We note that (2.1.64) is used for calculations in all three gauges, considered in the subsequent chapters. The colour group tensors associated with each vertex naturally factor out at leading order and next-to-leading order (NLO), i.e. the diagrams considered at the symmetric point which contribute to the triple-gluon vertex are directly proportional to f^{abc} and so this can be factored out. Whether this is true for all orders is not yet known. Similarly with the quark- and ghost-gluon vertices. This factorization of the colour tensors is a property of symmetric point calculations for 3-point vertices which allows us to purely focus on the Lorentz component. $\Sigma^{V}_{\mu_1\ldots\mu_n}(p,q)$ are the Lorentz amplitudes for the vertex V, where $V \in \{\mathrm{ggg}, \mathrm{ccg}, \mathrm{qqg}\}$. This decomposes further into scalar amplitudes

$$\begin{aligned}
\Sigma^{\mathrm{ggg}}_{\mu\nu\sigma}(p,q)|_{p^2=q^2=-\mu^2} &= \sum_{k=1}^{14} \mathcal{P}^{\mathrm{ggg}}_{(k)\mu\nu\sigma}(p,q)\Sigma^{\mathrm{ggg}}_{(k)}(p,q) \\
\left(\Sigma^{\mathrm{qqg}}_{\sigma}(p,q)\right)_{\alpha}^{\ \beta}|_{p^2=q^2=-\mu^2} &= \sum_{k=1}^{6} \left(\mathcal{P}^{\mathrm{qqg}}_{(k)\sigma}(p,q)\right)_{\alpha}^{\ \beta}\Sigma^{\mathrm{qqg}}_{(k)}(p,q) \\
\Sigma^{\mathrm{ccg}}_{\sigma}(p,q)|_{p^2=q^2=-\mu^2} &= \sum_{k=1}^{2} \mathcal{P}^{\mathrm{ccg}}_{(k)\sigma}(p,q)\Sigma^{\mathrm{ccg}}_{(k)}(p,q)\ . \qquad (2.1.65)
\end{aligned}$$

where $\mathcal{P}^{V}_{(k)\ \mu_1\ldots\nu_n}(p,q)$ are the basic tensors for each vertex, V, and $\Sigma^{V}_{(k)}(p,q)$ are the scalar amplitudes. For the triple-gluon vertex we have $\mathcal{P}^{\mathrm{ggg}}_{(k)\mu\nu\sigma}(p,q)$ with

$1 \leq k \leq 14$, where k can be called the *channel* of the amplitude. For example channel 1 would be when $k = 1$, where it is our convention to choose channel 1 to correspond to the tree level vertex. A prescription for choosing the tensor basis is explicitly shown in Appendix B where we note that the tensor basis is dependent on the Green's functions and not on the gauge choice. Once we have the tensor basis we project out the amplitudes for each individual channel k using the projection technique of [61]. For the triple-gluon vertex there are 14 channels, since $1 \leq k \leq 14$. This is achieved using the projection matrices presented in Appendix B. The amplitudes play an important role in the construction of the renormalization constants and we present the results for the amplitudes in all chapters for each scheme.

As previously mentioned it is appropriate within this thesis to present the majority of our results numerically, particularly those of chapters 3 and 4 where results are calculated up to NNNLO and these results displayed analytically are of considerable length. For this reason we present the numerical values for the various functions that arise in the master integrals of [62, 63, 64, 65]. These are

$$\begin{aligned} \zeta_3 &= 1.20205690 \;,\; \zeta_2 = \tfrac{\pi}{6}^2 = 1.64493407 \;,\; \psi'\left(\tfrac{1}{3}\right) = 10.09559713 \;, \\ \psi'''\left(\tfrac{1}{3}\right) &= 488.1838167 \;,\; s_2\left(\tfrac{\pi}{2}\right) = 0.32225882 \;,\; s_2\left(\tfrac{\pi}{6}\right) = 0.22459602 \;, \\ s_3\left(\tfrac{\pi}{2}\right) &= 0.32948320 \;,\; s_3\left(\tfrac{\pi}{6}\right) = 0.19259341 \;, \end{aligned} \tag{2.1.66}$$

where $\psi(z)$ is the derivative of the logarithm of the Euler Γ-function and ζ_n is the Riemann zeta function. The Euler Γ-function $\Gamma(z)$ is a special function defined for $\Re(z) > 0$ by

$$\Gamma(z) = \int_0^\infty e^{-t} t^{z-1} \mathrm{d}t \tag{2.1.67}$$

satisfying the functional equation

$$z\Gamma(z) = \Gamma(z+1) \tag{2.1.68}$$

such that for any integer z we have $\Gamma(z) = (z-1)\Gamma(z-1)$ and it follows that $\Gamma(z+1) = z!$ for all positive integer z. In dimensional regularization we have the following definition

$$\Gamma(\epsilon) = \frac{1}{\epsilon}(1 + \gamma_{\mathrm{E}}\epsilon + \mathcal{O}(\epsilon)) \tag{2.1.69}$$

where

$$\gamma_{\rm E} \;=\; \lim_{n\to\infty}\left[\sum_{i=1}^{n}\frac{1}{i}-\ln(n)\right] \;=\; 0.5772156649\ldots \tag{2.1.70}$$

is the Euler-Masceroni constant.

At the symmetric point the following functions arise for various arguments,

$$s_n(z) \;=\; \frac{1}{\sqrt{3}}\Im\left[\mathrm{Li}_n\left(\frac{e^{iz}}{\sqrt{3}}\right)\right] \tag{2.1.71}$$

where $\mathrm{Li}_n(z)$ is the polylogarithm function and n defines the loop order. As a result of computing 3-point and, in the case of non-linear gauge fixings, 4-point functions at one loop in a non-exceptional momentum configuration dilogarithms appear. The dilogarithm [66] is defined by the integral

$$\mathrm{Li}_2(z) \;=\; -\int_0^z \mathrm{d}t\frac{\ln(1-t)}{t} \tag{2.1.72}$$

or the sum

$$\mathrm{Li}_2(z) \;=\; \sum_{n=1}^{\infty}\frac{z^n}{n^2} \tag{2.1.73}$$

for $|z|\leq 1$. Similarly $\mathrm{Li}_3(z)$ would be

$$\mathrm{Li}_3(z) \;=\; \sum_{n=1}^{\infty}\frac{z^n}{n^3}\;. \tag{2.1.74}$$

A combination of harmonic polylogarithms appear in our results, which have been presented in published work, [14, 67], as

$$\Sigma \;=\; \mathcal{H}^{(2)}_{31} \;+\; \mathcal{H}^{(2)}_{43}\;. \tag{2.1.75}$$

This combination is specific to a symmetric point computation. As explained in [67] we now record this combination of harmonic polylogarithms within our thesis as

$$\Sigma \;=\; \mathcal{H}^{(2)}_{31} \;+\; \mathcal{H}^{(2)}_{43} \;=\; \frac{1}{36}\psi'''\left(\tfrac{1}{3}\right)-\frac{2\pi^4}{27} \tag{2.1.76}$$

rather than leaving results in terms of Σ.

2.1.5 Definition of renormalization schemes

Following the thorough definition of the $\overline{\text{MS}}$ scheme in section 2.1.2 we now focus on the explicit definition of the MOM renormalization schemes. Let us first discuss the similarities between both non-physical and physical schemes. When renormalizing, the Lagrangian has the same form as in (2.1.60). However in the MOM schemes the renormalization constants contain both the divergent and finite parts, compared to just the divergences being removed in the $\overline{\text{MS}}$ scheme. However, there is a second aspect of renormalization which is to define the point where the Green's function is renormalized. In the MOM schemes of Celmaster and Gonsalves, [52], for both the 2-point and 3-point functions this is the point where the external momenta squared is $-\mu^2$. In particular for the 3-point functions this corresponds to the completely symmetric point (2.1.63). When one evaluates the 3-point function at this particular symmetric point then the renormalization constant is defined so that after renormalization there are no $\mathcal{O}(a)$ corrections at the symmetric point. In other words the renormalization constant has a finite part removed, unlike $\overline{\text{MS}}$. The 2-point functions are treated in the same way for the MOM schemes of Celmaster and Gonsalves.

Our renormalization constants therefore take the form of (2.1.61) where now at one loop $z_{i_1}(a_{\text{MOMi}}) = A + B\epsilon$ such that

$$Z_i^{\text{MOMi}}(a_{\text{MOMi}}) = 1 + \left(\frac{A}{\epsilon} + B \right) a_{\text{MOMi}} + \ldots \tag{2.1.77}$$

where B represents the finite contribution, in comparison to

$$Z_i^{\overline{\text{MS}}}(a_{\overline{\text{MS}}}) = 1 + \frac{A}{\epsilon} a_{\text{MOMi}} + \ldots \tag{2.1.78}$$

in the $\overline{\text{MS}}$ scheme. Unfortunately there are infinitely many ways to define a momentum subtraction renormalization, [58], i.e. we have the freedom to select which finite parts we absorb into the counterterms subject to respecting the Slavnov-Taylor identities. In the MOMi schemes we absorb both $\mathcal{O}(\frac{1}{\epsilon})$ and $\mathcal{O}(1)$ pieces in to the renormalization constants as shown above such that no $\mathcal{O}(a)$ pieces remain in the amplitudes at the subtraction point. The benefit of calculating in this scheme rather than $\overline{\text{MS}}$ is that the scheme is based on the physical properties of the particles.

Another mass dependent renormalization scheme popular with lattice studies is

the modified regularization invariant (RI′) scheme which we consider in Chapter 7. The coupling constant depends directly on the characteristic external momenta, [49]. We consider all three renormalization schemes ($\overline{\text{MS}}$, MOM and RI′) within our work, constructing results in several gauges for analysis and comparison which we comment on in the subsequent chapters.

2.2 Reduction of scalar 3-point integrals

The reduction of scalar 3-point integrals are handled by using the computer package REDUZE. As we will mention in the following section, when outlining our computational approach, REDUZE implements the Laporta algorithm to systematically reduce scalar integrals to a set of basic master integrals using a technique known as integration by parts. REDUZE works by starting with a topology and using integration by parts and Lorentz invariance relations to generate relations involving this topology and lower ones which it can get by *pinching* certain propagators, [66]. In graph theory this simply means removing an internal propagator. Any integrals that cannot be ultimately simplified in this way are called master integrals. Let us consider an l loop diagram with e independent external momenta. An auxilliary topology (or integral family) for any diagram must contain exactly $l\left[\frac{1}{2}(l+1)+e\right]$ propagators, otherwise a reduction cannot happen. An auxilliary topology is an ordered set of all propagators where all scalar products containing at least one loop momenta k_i can be expressed as a linear combination of propagators from this set, [68]. This means that, for example, in the case of the two loop ladder topology one must "add" an extra propagator in the form of a scalar product of the momenta. It is important to understand what REDUZE is doing internally when performing the integral reduction. For this reason we can illustrate the procedure by hand, in particular applying the Laporta algorithm to the two loop triangle at the symmetric point. Let us first, as a preliminary to the two loop 3-point function, consider a simple one loop diagram. A general definition of a one loop integral containing three propagators is

$$\text{I}_1(\alpha,\beta,\gamma) \;=\; \int_k \frac{\text{d}^d k}{(2\pi)^d} \frac{1}{(k^2)^\alpha ((k-p)^2)^\beta ((k+q)^2)^\gamma} \tag{2.2.79}$$

where α,β,γ take any integer value. Our integral is of the form $\frac{1}{abc}$ where a,b,c are the product of propagators. This integral is represented diagramatically in Figure 2.2 with internal loop momenta k. Recall that the symmetric point is defined by the condition (2.1.63) where $pq = \frac{1}{2}\mu^2$. With each external leg now

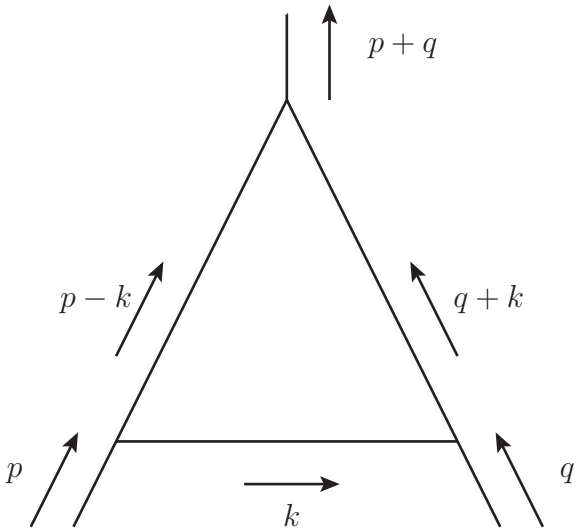

Figure 2.2: Momentum routing around the one loop triangle graph.

having the same incoming/outgoing momenta this implies that

$$\mathrm{I}_1(\alpha,\beta,\gamma) \;=\; \mathrm{I}_1(\alpha,\gamma,\beta) \;=\; \mathrm{I}_1(\beta,\gamma,\alpha) \;=\; \ldots \tag{2.2.80}$$

i.e the 3-point function is completely symmetric. Using this symmetry rule we can represent other integrals in the form $I(\alpha,\beta,\gamma)$, for example let us take

$$\mathrm{I}_1(2,1,1) \;=\; \int_k \frac{\mathrm{d}^d k}{(2\pi)^d} \frac{1}{(k^2)^2(k-p)^2(k+q)^2} \;. \tag{2.2.81}$$

Using the symmetry rule we see that $\mathrm{I}_1(2,1,1) = \mathrm{I}_1(1,2,1) = \mathrm{I}_1(1,1,2)$ such that

$$\begin{aligned}
\mathrm{I}_1(2,1,1) &= \int_k \frac{\mathrm{d}^d k}{(2\pi)^d} \frac{1}{(k^2)^2(k-p)^2(k+q)^2} \\
&= \int_k \frac{\mathrm{d}^d k}{(2\pi)^d} \frac{1}{k^2((k-p)^2)^2(k+q)^2} \\
&= \int_k \frac{\mathrm{d}^d k}{(2\pi)^d} \frac{1}{k^2(k-p)^2((k+q)^2)^2} \;.
\end{aligned} \tag{2.2.82}$$

Applying the rule (2.1.54), performing the explicit differentiation and taking all terms over to the right-hand side we obtain

$$\begin{aligned}
0 \;=\; & \int \frac{\mathrm{d}^d k}{(2\pi)^d} \frac{d}{(k^2)^\alpha((k-p)^2)^\beta((k+q)^2)^\gamma} \\
& -2\alpha \int \frac{\mathrm{d}^d k}{(2\pi)^d} \frac{1}{(k^2)^\alpha((k-p)^2)^\beta((k+q)^2)^\gamma}
\end{aligned}$$

$$
\begin{aligned}
&-2\beta \int \frac{\mathrm{d}^d k}{(2\pi)^d} \frac{k(k-p)}{(k^2)^\alpha ((k-p)^2)^{\beta+1} ((k+q)^2)^\gamma} \\
&-2\gamma \int \frac{\mathrm{d}^d k}{(2\pi)^d} \frac{k(k+q)}{(k^2)^\alpha ((k-p)^2)^{\beta} ((k+q)^2)^{\gamma+1}}
\end{aligned} \tag{2.2.83}
$$

where we have used $\frac{\partial k^\mu}{\partial k^\mu} = d$. The above expression can be rewritten as

$$
\begin{aligned}
0 \;=\; & \int \frac{\mathrm{d}^d k}{(2\pi)^d} \frac{d}{(k^2)^\alpha ((k-p)^2)^\beta ((k+q)^2)^\gamma} \\
& -2\alpha \int \frac{\mathrm{d}^d k}{(2\pi)^d} \frac{1}{(k^2)^\alpha ((k-p)^2)^\beta ((k+q)^2)^\gamma} \\
& -\beta \int \frac{\mathrm{d}^d k}{(2\pi)^d} \frac{k^2 + (k-p)^2 - p^2}{(k^2)^\alpha ((k-p)^2)^{\beta+1} ((k+q)^2)^\gamma} \\
& -\gamma \int \frac{\mathrm{d}^d k}{(2\pi)^d} \frac{k^2 + (k+q)^2 - q^2}{(k^2)^\alpha ((k-p)^2)^{\beta} ((k+q)^2)^{\gamma+1}} \; .
\end{aligned} \tag{2.2.84}
$$

Writing the integrals in terms of $\mathrm{I}_1(\alpha, \beta, \gamma)$ and rearranging we have

$$
\begin{aligned}
0 \;=\; & (d - 2\alpha - \beta - \gamma) \mathrm{I}_1(\alpha, \beta, \gamma) \\
& -\beta \left[\mathrm{I}_1(\alpha - 1, \beta + 1, \gamma) - p^2 \mathrm{I}_1(\alpha, \beta + 1, \gamma) \right] \\
& -\gamma \left[\mathrm{I}_1(\alpha - 1, \beta, \gamma + 1) - q^2 \mathrm{I}_1(\alpha, \beta, \gamma + 1) \right] \; .
\end{aligned} \tag{2.2.85}
$$

Taking the most general case by setting $\alpha = \beta = \gamma = 1$ gives

$$
\mathrm{I}_1(1,2,1) \;=\; \frac{1}{\mu^2} \left[\frac{1}{2}(d-4) \mathrm{I}_1(1,1,1) - \mathrm{I}_1(0,2,1) \right] \tag{2.2.86}
$$

where $\mathrm{I}_1(0,2,1)$ and $\mathrm{I}_1(1,1,1)$ are the 2- and 3-point master integrals respectively. This explicitly shows that one can write any integral in terms of the set of master integrals for that theory as $I_1(0,2,1)$ is proportional to $I_1(1,1,0)$. For completeness

$$
I_1(1,2,1) \;=\; \frac{1}{2p^2} \left[\frac{2\Gamma\left(3 - \frac{d}{2}\right) \Gamma\left(\frac{d}{2} - 2\right) \Gamma\left(\frac{d}{2} - 1\right) (p^2)^{\frac{d}{2} - 3}}{(4\pi)^{\frac{d}{2}} \Gamma(d-3)} - (d-4) I_1(1,1,1) \right] \; . \tag{2.2.87}
$$

Now that we have a basic understanding of the Laporta algorithm at one loop let us consider a two loop 3-point diagram, also at the symmetric point. Most

generally this can be written as

$$\mathrm{I}_2(\alpha,\beta,\gamma,\delta,\rho) \;=\; \int_k \frac{\mathrm{d}^d k}{(2\pi)^d} \frac{1}{(k^2)^\alpha((k-p)^2)^\beta((k-l)^2)^\gamma(l^2)^\delta((l+q)^2)^\rho} \tag{2.2.88}$$

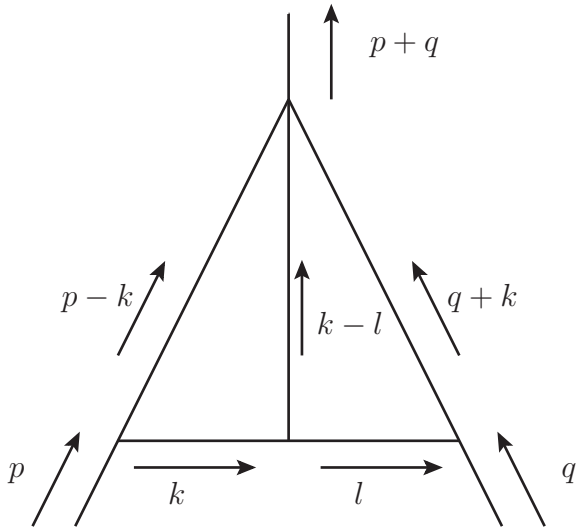

Figure 2.3: Momentum routing around a two loop triangle graph.

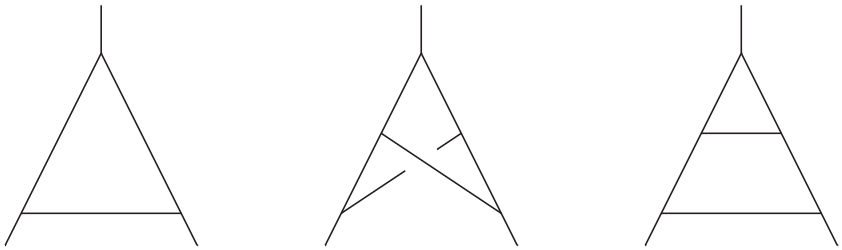

Figure 2.4: Integral families at one and two loops for the symmetric point.

which we present diagramatically in Figure 2.3. Here we have two internal loop momenta, k and l. Unlike the one loop case which was symmetric about α, β and γ, we now do not have as much freedom since there are three basic topologies at two loops, see Figure 2.4 compared to just one topology for the 3-point function at one loop level. Shifting the momenta in Figure 2.3 such that

$$\begin{aligned} -l &\to q \\ k-l &\to k+q \end{aligned} \tag{2.2.89}$$

we obtain a triangle subgraph whose internal loop momenta is k. By rerouting the momenta the external legs of this one loop subgraph are of the form of Figure 2.2. Considering only this subgraph we can apply the Laporta algorithm to the integral

$$\mathrm{I}_2(\alpha,\beta,\gamma,\delta,\rho) \;=\; \int_k \frac{\mathrm{d}^d k}{(2\pi)^d} \frac{1}{(k^2)^\alpha((k-p)^2)^\beta((k+q)^2)^\gamma(q^2)^\delta((l+q)^2)^\rho} \quad (2.2.90)$$

to obtain

$$\begin{aligned} 0 \;=\; & (d-2\alpha-\beta-\gamma-\delta-\rho)\mathrm{I}_2(\alpha,\beta,\gamma,\delta,\rho) \\ & -\beta\left[\mathrm{I}_2(\alpha-1,\beta+1,\gamma,\delta,\rho) - p^2\mathrm{I}_2(\alpha,\beta+1,\gamma,\delta,\rho)\right] \\ & -\gamma\left[\mathrm{I}_2(\alpha-1,\beta,\gamma+1,\delta,\rho) - q^2\mathrm{I}_2(\alpha,\beta,\gamma+1,\delta,\rho)\right] \;. \end{aligned} \quad (2.2.91)$$

Setting $\alpha=\beta=\gamma=\delta=\rho=1$ the above becomes

$$\begin{aligned} 0 \;=\; & (d-6)\mathrm{I}_2(1,1,1,1,1) - \left[\mathrm{I}_2(0,2,1,1,1) - p^2\mathrm{I}_2(1,2,1,1,1)\right] \\ & -\left[\mathrm{I}_2(0,1,2,1,1) - \mathrm{I}_2(1,1,2,0,1)\right] \;. \end{aligned} \quad (2.2.92)$$

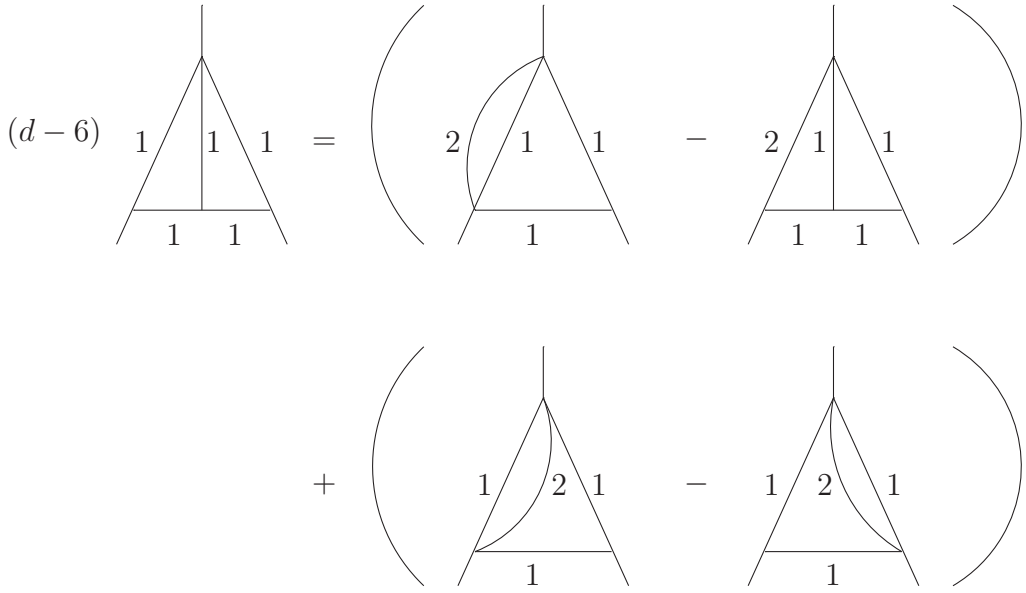

Figure 2.5: Integral Reduction.

Expressed diagramatically in Figure 2.5 we see that there appears only one integral that is not a master integral, i.e. the diagram can be expressed in terms of other topologies. Rearranging (2.2.92) in terms of the unknown integral we obtain

$$\mathrm{I}_2(1,2,1,1,1) \;=\; -\frac{1}{\mu^2}\left[(d-6)\mathrm{I}_2(1,1,1,1,1) - \mathrm{I}_2(0,2,1,1,1)\right] \;. \qquad (2.2.93)$$

Re-expressing all integrals in terms of masters dramatically simplifies expressions and reduces the number of integrals one needs to explicitly solve. At higher loop orders one can apply the same algorithm as for the one loop case by considering a subgraph as we have done at two loops. This is how Reduze works internally.

2.3 Computational setup

Here we discuss the computational setup we have used throughout our work. In order to compute the renormalization of QCD up to and including two loops in a variety of gauges and schemes we use a combination of programs, [68, 69, 70,

71]. A computation of this size would be near impossible without using these tools. We begin by using the QGRAF package [69] to electronically generate all Feynman diagrams corresponding to each of our Green's functions. This is done by specifying the number of loops we wish to calculate to, the loop momenta, incoming particles and the interactions our theory allows. In our setup we choose to have all particles incoming, as is consistent with our momentum routing, and specify no tadpoles, no snails and only graphs that are 1-particle irreducible (1PI). We call a diagram irreducible if it cannot be split in to two disconnected graphs by cutting only one internal line. A tadpole diagram is a diagram with one external leg (or line). We choose not to include tadpoles since graphs of this type are redundant when considering 1PI graphs only. Since we are in a massless regime we also have no need to consider snail diagrams due to them vanishing when applying dimensional regularization. We display both graphs in Figure 2.6 for the benefit of the reader. Tables 2.1 through 2.3 show the total number of diagrams calculated at one, two and three loops for each gauge.

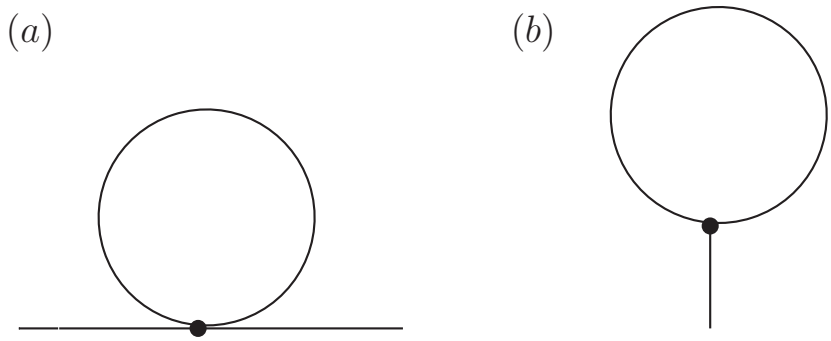

Figure 2.6: (a) Snail Feynman diagram, (b) Tadpole Feynman diagram.

The need for such computing tools can be gauged by the sheer number of Feynman diagrams considered, increasing tenfold when one increases the loop order. Once the diagrams have been generated for each setup, we identify and order the graphs into their basic topologies, applying Lorentz and colour indices to the diagrams automatically. Finally we integrate each diagram using a MINCER, [72], routine implemented in FORM, [70]. Applying the MINCER algorithm to 3-point vertex functions requires one external momenta of the Green's function to be nullified. This is provided that when we nullify an external leg we do not inadvertently introduce infrared singularities. Note that the potential infrared singularities that arise are only a problem if one considers diagrams on an individual level. By us-

Green's Function	One loop	Two loop	Three loop
$A^A_\mu A^B_\nu$	3	18	254
$c^A \bar{c}^B$	1	6	78
$\psi\bar{\psi}$	1	6	78
$A^A_\mu A^B_\nu A^C_\sigma$	8	106	2382
$c^A \bar{c}^B A^C_\sigma$	2	33	688
$\psi^A \bar{\psi}^B A^C_\sigma$	2	33	688
Total:	17	202	4168

Table 2.1: Number of Feynman diagrams computed for each 2- and 3-point function in the arbitrary linear covariant gauge

Green's Function	One loop	Two loop	Three loop
$A^A_\mu A^B_\nu$	3	19	282
$c^A \bar{c}^B$	1	9	124
$\psi\bar{\psi}$	1	6	79
$A^A_\mu A^B_\nu A^C_\sigma$	8	112	2616
$c^A \bar{c}^B A^C_\sigma$	3	49	1097
$\psi^A \bar{\psi}^B A^C_\sigma$	2	33	697
Total:	18	228	4895

Table 2.2: Number of Feynman diagrams computed for each 2- and 3-point function in the Curci-Ferrari gauge

ing our method of summing all the diagrams these infrared singularities naturally cancel, and so do not pose as a problem for the QCD Lagrangian. For QCD this nullification is possible and has allowed for the computation of renormalization group functions to three loops, for example, [73]. MINCER does not currently have the capacity to compute 3-point vertices with a non-exceptional momentum configuration and so cannot be applied directly to a 3-point vertex symmetric point analysis. The MINCER package can only be applied to at most massless three loop 2-point functions when considering a non-exceptional setup and works by implementing a star-triangle relation to recursively reduce topologies of a certain type into a combination of other more simple topologies. In MINCER this is done by implementing a separate routine for each topology, therefore optimizing the programs run time. By reducing the powers of the propagators recursively the routine stops when it hits the simplest topology, this leaves us with a set of basic master integrals. REDUZE, [68], which was written in GINAC, [74], in most ways supersedes MINCER and works by using a C^{++} implementation of the Laporta algorithm, [60]. The Laporta algorithm, in contrast to the MINCER package creates all possible relations between the scalar integrals, thus resulting in a

Green's Function	One loop	Two loop	Three loop
$A^A_\mu A^B_\nu$	6	131	6590
$c^A \bar{c}^B$	3	81	4006
$\psi\bar{\psi}$	2	27	979
$A^A_\mu A^B_\nu A^C_\sigma$	23	1291	103548
$c^A \bar{c}^B A^C_\sigma$	16	867	66256
$\psi^A \bar{\psi}^B A^C_\sigma$	5	217	13108
Total:	55	2614	194487

Table 2.3: Number of Feynman diagrams computed for each 2- and 3-point function in the maximal abelian gauge

large degree of redundancy in reducing the graphs. As with MINCER, REDUZE will always give a reduction to a set of basic master integrals. However REDUZE requires more computing time since the algorithm systematically constructs all integration by parts relations before rewriting the scalar integrals in terms of only master integrals, as we have seen when implementing the procedure by hand in the previous section. There is no separate routine for each topology internally programmed like there is in MINCER. One benefit of using REDUZE over MINCER is that it is not limited. With the Laporta algorithm it is possible to compute any l-loop and n-point function provided one has a big enough computer and disk capacity. REDUZE constructs a database of all the relations between integrals which is then used to lift out the integrals we require for our computation. An advantage to computing at the symmetric point becomes apparent (2.2.80) since the vertex diagrams are symmetric under rotation, resulting in a minimal set of integrals for a minimal set of topologies.

To clarify, the 2-point functions are evaluated using MINCER whilst all 3-point vertices are evaluated using REDUZE. For the benefit of the reader we present our systematic approach which is repeated for all calculations set out in this thesis. Firstly, as discussed above we use QGRAF to generate all diagrams electronically. We then identify topologies and map the diagrams to the corresponding MINCER topology as well as including the Lorentz, colour and spinor indices. We do this so that they are picked up by our next program which rewrites the momentum flow in a language compatible with MINCER and REDUZE. Following this the Feynman rules for the propagators and vertices are substituted and after this we multiply by the projection tensors. We rewrite the numerators of the integrals by stringing the γ-algebra together and evaluate the group algebra. The scalar products are rewritten in terms of propagators including the irreducible propagators

required for the integral families of REDUZE. Once in this form we can apply the REDUZE algorithm to determine the integral reductions. For the 2-point functions the method runs parallel to this, where one would apply the MINCER algorithm instead of REDUZE. The irreducible numerators are automatically handled within MINCER. To finish, all master inegrals are substituted, and the remainder of algebra manipulation is done using FORM, its threaded version TFORM and REDUCE.

After applying the Laporta algorithm all that remains is to evaluate the master integrals and apply our chosen method of renormalization, which is carried out last. In the case of our research these master integrals have been previously determined directly in [62, 63, 64, 65] and summarized in [75]. We map back to FORM notation where FORM and its threaded version TFORM [71] carry out any remainding algebraic manipulation. All vertex functions are computed in terms of bare parameters, following from the technique of [73]. Once all the graphs/Green's functions have been computed as functions of bare parameters and summed, FORM is used as a tool to determine the associated counterterms by rescaling the Green's functions at the end via the definition of the renormalization constants, i.e. $g_o = Z_g g$. Once the counterterms have been implemented the divergence remaining at that particular loop order is absorbed in to the renormalization constant of the associated Green's function, [73]. Finally we use REDUCE, [76], alongside FORM to manipulate our results into an output we desire. Of course, without such programs computations at high loop order would be virtually impossible to do, and to such accuracy, by hand. It is appropriate here to also note that any Feynman diagrams visually presented within this thesis have been drawn using JAXODRAW, [77, 78].

Chapter 3

The QCD arbitrary (linear) covariant gauge

As part of the development process it is important to first check the known results of a preliminary calculation or simpler model before proceeding on to our desired calculation. Reproducing these known results serves three purposes: 1) to ensure our computational method is correct before extending to a more difficult, yet similar model; 2) to learn and develop the techniques needed to be able to tackle such problems and 3) to check that current results by other authors, for example [52, 14] are consistent.

In this chapter we show how the triple-gluon, quark-gluon and ghost-gluon vertices of QCD are computed at the symmetric subtraction point explicitly at two loops in both the modified minimal subtraction ($\overline{\text{MS}}$) scheme and the momentum subtraction (MOM) schemes. Applying the techniques and computational method disussed in Chapter 2 we determine the conversion functions for the coupling constant, gauge parameter and each wave function, as well as the mappings between the coupling constants and arbitrary gauge parameters in each scheme. Using these two loop results along with known three loop $\overline{\text{MS}}$ results, [79], for the β-function and wave function anomalous dimensions, we are able to construct the three loop anomalous dimensions for the gluon, quark, ghost and gauge parameter, in addition to the three loop β-functions in an arbitrary linear covariant gauge for each MOMi scheme. We note that although results within this chapter have already been published in [14] the renormalization constants are given here explicitly for the first time. We do note however that these results can be reconstructed via the details published in [14].

3.1 Renormalization constants

Although we have described our renormalization procedure in the previous chapter we take this opportunity to describe the technical details of the calculation in fine detail. So far we have formulated the QCD Lagrangian for an arbitrary (linear) covariant gauge. We have added our gauge fixing terms and checked that the full Lagrangian is BRST invariant. We have generated our Feynman diagrams using QGRAF and computed the integral reduction using a combination of MINCER and REDUZE to determine the needed master integrals. See Appendix C for a full list of integrals needed at two loops as well as a discussion on more general configurations. From this we have then inserted the master integrals and used FORM to renormalize the theory and generate the amplitudes for each channel. From the amplitudes we have constructed the renormalization constants in both the $\overline{\text{MS}}$ and MOMi schemes. In all of our calculations we determine the renormalization constants by following the technique of [73], by first computing the Green's functions in terms of bare parameters and then rescaling them at the end via the definition of the renormalization constants (2.1.55). To determine each of the renormalization constants to two loops the gluon, ghost and quark 2-point functions are computed first. These determine the one loop contributions to the renormalization constants Z_A, Z_c, Z_ψ and Z_α where Z_α is the renormalization constant for the arbitrary gauge-fixing parameter α. We determine Z_g, the renormalization constant for the $\overline{\text{MS}}$ coupling constant directly from the triple-gluon vertex. However, as a special feature of the $\overline{\text{MS}}$ scheme the renormalization constant for the coupling constant can be determined using any one of the vertex functions. This is due to each vertex, once all diagrams have been added together, being multiplied by a pre-factor. For instance the ghost-gluon vertex has the pre-factor $Z_g^{(\text{ccg})}\sqrt{Z_A}Z_c$ and the quark-gluon vertex $Z_g^{(\text{qqg})}\sqrt{Z_A}Z_\psi$. Since Z_A, Z_c and Z_ψ have been fixed at one loop by our wave function renormalization we can determine Z_g using either vertex since

$$Z_g^{(\text{ggg})}\big|_{\overline{\text{MS}}} = Z_g^{(\text{qqg})}\big|_{\overline{\text{MS}}} = Z_g^{(\text{ccg})}\big|_{\overline{\text{MS}}} \tag{3.1.1}$$

i.e. a finite solution which implies that the theory is renormalizable. The Slavnov-Taylor identity is automatically satisfied, [80], as we have already visited in section 2.1.2. After determining Z_g at one loop from one of the 3-point vertices and checking that it holds for the other two vertex functions, we can obtain the two loop renormalization constants by substituting our one loop result for Z_g into the 2-point wave function amplitudes. Only once the one loop renormalization con-

stants are known can they allow for the computation of the subsequent two loop expressions. Doing so we obtain the two loop contributions to the Z's, i.e. the $z*_{21}$ and $z*_{22}$ terms in (2.1.61). In particular we obtain the two loop piece for Z_A from the gluon 2-point function, Z_ψ from the quark 2-point function and Z_c from the ghost 2-point function, with the two loop contribution to Z_g finally coming from the vertices. Again, the value of Z_g should be consistent across all three vertices in the $\overline{\text{MS}}$ scheme. This is a property specific to non-physical gauges and is consistent with our scheme definitions (see section 2.1.5). A table summarizing from which Green's functions the respective renormalization constants have been obtained is included below where (Z_*) have already been, or can be obtained

Green's Function	Ren. constants obtained
ghost 2pt function	Z_c , Z_α
gluon 2pt function	Z_A (Z_α)
quark 2pt function	Z_ψ
ghost-gluon vertex	$Z_g^{(\text{ccg})}$
triple-gluon vertex	$(Z_g^{(\text{ggg})})$
quark-gluon vertex	$(Z_g^{(\text{qqg})})$

Table 3.1: Construction of the renormalization constants

via either function. This is useful in $\overline{\text{MS}}$ as a check on the consistency of our renormalization constants.

Since we have discussed how the renormalization constants were determined we now present the results below to the order of two loops for arbitrary $SU(N_c)$ for generality starting with the wave function renormalization constants

$$
\begin{aligned}
Z_A(a,\alpha)\Big|_{\overline{\text{MS}}} &= 1 + \left[C_A\left(\frac{13}{6} - \frac{\alpha}{2}\right) - \frac{4}{3}T_F N_f\right]\frac{a}{\epsilon} \\
&\quad + \left[\frac{1}{\epsilon^2}\left[C_A^2\left(-\frac{17}{24}\alpha + \frac{\alpha^2}{4} - \frac{13}{8}\right) + C_A T_F N_f\left(\frac{2}{3}\alpha + 1\right)\right]\right. \\
&\quad \left. + \frac{1}{\epsilon}\left[C_A^2\left(-\frac{11}{16}\alpha - \frac{\alpha^2}{8} + \frac{59}{16}\right) + C_A T_F N_f\left(-\frac{5}{2}\right)\right.\right. \\
&\quad \left.\left. - 2C_F T_F N_f\right]\right] a^2 + \mathcal{O}\left(a^3\right) \\
Z_\alpha(a,\alpha)\Big|_{\overline{\text{MS}}} &= 1 + \mathcal{O}\left(a^3\right) \\
Z_c(a,\alpha)\Big|_{\overline{\text{MS}}} &= 1 + \left[C_A\left(\frac{3}{4} - \frac{\alpha}{4}\right)\right]\frac{a}{\epsilon}
\end{aligned}
$$

$$
\begin{aligned}
&+ \left[\frac{1}{\epsilon^2} \left[C_A^2 \left(-\frac{35}{32} + \frac{3}{32}\alpha^2 \right) + C_A T_F N_f \left(\frac{1}{2} \right) \right] \right. \\
&\left. + \frac{1}{\epsilon} \left[C_A^2 \left(\frac{95}{96} + \frac{\alpha}{32} \right) + C_A T_F N_f \left(-\frac{5}{12} \right) \right] \right] a^2 + \mathcal{O}\left(a^3\right) \\
Z_\psi(a,\alpha)\Big|_{\overline{\text{MS}}} &= 1 - \frac{\alpha C_F a}{\epsilon} + \left[\frac{1}{\epsilon^2} \left[C_F C_A \left(\frac{3}{4}\alpha + \frac{\alpha^2}{4} \right) + C_F^2 \left(\frac{\alpha^2}{2} \right) \right] \right. \\
&\quad + \frac{1}{\epsilon} \left[C_F C_A \left(-\frac{25}{8} - \alpha - \frac{\alpha^2}{8} \right) + T_F N_f C_F \right. \\
&\quad \left. \left. + C_F^2 \left(\frac{3}{4} \right) \right] \right] a^2 + \mathcal{O}\left(a^3\right) \qquad (3.1.2)
\end{aligned}
$$

and finally for the coupling constant renormalization constant

$$
\begin{aligned}
Z_g^{(\text{ggg})}(a,\alpha)\Big|_{\overline{\text{MS}}} &\equiv Z_g^{(\text{ccg})}(a,\alpha)\Big|_{\overline{\text{MS}}} \equiv Z_g^{(\text{qqg})}(a,\alpha)\Big|_{\overline{\text{MS}}} \\
&= 1 + \left[C_A \left(-\frac{11}{6} \right) + \frac{2}{3} T_F N_f \right] \frac{a}{\epsilon} \\
&\quad + \left[\frac{1}{\epsilon^2} \left[C_A^2 \left(\frac{121}{24} \right) + T_F^2 N_f^2 \left(\frac{2}{3} \right) + T_F N_f C_A \left(-\frac{11}{3} \right) \right] \right. \\
&\quad \left. + \frac{1}{\epsilon} \left[C_A^2 \left(-\frac{17}{6} \right) + T_F N_f C_F + T_F N_f C_A \left(\frac{5}{3} \right) \right] \right] a^2 \\
&\quad + \mathcal{O}\left(a^3\right) \ . \qquad (3.1.3)
\end{aligned}
$$

Note that we have chosen not to label the variables a and α here to save on space when presenting results. When variables are not labelled it is understood that they correspond to the scheme defined on the function on the left hand side of the equals sign. For example $Z_A(a,\alpha)\big|_{\overline{\text{MS}}}$ implies $a = a_{\overline{\text{MS}}}$ and $\alpha = \alpha_{\overline{\text{MS}}}$, where $a_{\overline{\text{MS}}}$ is the coupling constant specific to the $\overline{\text{MS}}$ scheme. Since the coupling constant gets renormalized it becomes scheme dependent, as with the gauge parameter. Again in the $\overline{\text{MS}}$ scheme, Z_g is independent of the vertex and so can be determined using either the ghost-gluon, quark-gluon or triple-gluon vertex. For the momentum subtraction schemes this is not the case. For the MOMi schemes, where MOMi indicates one of the three MOM schemes as defined in section 2.1.5, the renormalization is done in a similar way. However, recall that our renormalization constants must now include both the $\mathcal{O}\left(\frac{1}{\epsilon}\right)$ and finite $\mathcal{O}(1)$ pieces. Based on this condition alone we can see that this will cause problems when constructing the renormalization constants for the vertices, namely the two loop contributions to the Z's and the renormalization of the coupling constant, g. Unlike in the $\overline{\text{MS}}$ scheme where Z_g was the same for each vertex, the renormalization constants now depend upon the vertex at which they are constructed. This means there

will be three different renormalization constants for the coupling constant which we label $Z_g^{\rm MOMg}\Big|_{\overline{\rm MS}}$, $Z_g^{\rm MOMq}\Big|_{\overline{\rm MS}}$ and $Z_g^{\rm MOMh}\Big|_{\overline{\rm MS}}$, the labels corresponding to the scheme defined via the triple-gluon, quark-gluon and ghost-gluon vertices respectively. We begin with the scheme corresponding to the ghost-gluon vertex. For the MOMh scheme the renormalization constants are

$$
\begin{aligned}
Z_g^{(\rm ccg)}\big|_{\rm MOMh} \;=\; & 1 + \Big[3\psi'\big(\tfrac{1}{3}\big)\,\alpha^2 C_A + 24\psi'\big(\tfrac{1}{3}\big)\,\alpha C_A - 15\psi'\big(\tfrac{1}{3}\big)\,C_A - 2\alpha^2 C_A\pi^2 \\
& \quad -27\alpha^2 C_A - 16\alpha C_A\pi^2 - 162\alpha C_A + 10 C_A\pi^2 - 615 C_A \\
& \quad +240 N_f T_F + 36(-11 C_A + 4 N_f T_F)\frac{1}{\epsilon}\Big]\,\frac{a}{216} \\
& + \Bigg[(121 C_A^2 - 88 C_A N_f T_F + 16 N_f^2 T_F^2)\frac{1}{24\epsilon^2} \\
& \quad + \Big(36\sqrt{3}\psi'\big(\tfrac{1}{3}\big)^2\,\alpha^4 C_A^2 + 576\sqrt{3}\psi'\big(\tfrac{1}{3}\big)^2\,\alpha^3 C_A^2 \\
& \qquad +1944\sqrt{3}\psi'\big(\tfrac{1}{3}\big)^2\,\alpha^2 C_A^2 - 2880\sqrt{3}\psi'\big(\tfrac{1}{3}\big)^2\,\alpha C_A^2 \\
& \qquad +900\sqrt{3}\psi'\big(\tfrac{1}{3}\big)^2\,C_A^2 - 48\sqrt{3}\psi'\big(\tfrac{1}{3}\big)\,\alpha^4 C_A^2\pi^2 \\
& \qquad -324\sqrt{3}\psi'\big(\tfrac{1}{3}\big)\,\alpha^4 C_A^2 - 768\sqrt{3}\psi'\big(\tfrac{1}{3}\big)\,\alpha^3 C_A^2\pi^2 \\
& \qquad -2808\sqrt{3}\psi'\big(\tfrac{1}{3}\big)\,\alpha^3 C_A^2 - 2592\sqrt{3}\psi'\big(\tfrac{1}{3}\big)\,\alpha^2 C_A^2\pi^2 \\
& \qquad -40536\sqrt{3}\psi'\big(\tfrac{1}{3}\big)\,\alpha^2 C_A^2 + 2880\sqrt{3}\psi'\big(\tfrac{1}{3}\big)\,\alpha^2 C_A N_f T_F \\
& \qquad +3840\sqrt{3}\psi'\big(\tfrac{1}{3}\big)\,\alpha C_A^2\pi^2 - 45504\sqrt{3}\psi'\big(\tfrac{1}{3}\big)\,\alpha C_A^2 \\
& \qquad +25344\sqrt{3}\psi'\big(\tfrac{1}{3}\big)\,\alpha C_A N_f T_F - 1200\sqrt{3}\psi'\big(\tfrac{1}{3}\big)\,C_A^2\pi^2 \\
& \qquad +239076\sqrt{3}\psi'\big(\tfrac{1}{3}\big)\,C_A^2 - 102528\sqrt{3}\psi'\big(\tfrac{1}{3}\big)\,C_A N_f T_F \\
& \qquad +9\sqrt{3}\psi'''\big(\tfrac{1}{3}\big)\,\alpha^3 C_A^2 - 171\sqrt{3}\psi'''\big(\tfrac{1}{3}\big)\,\alpha^2 C_A^2 \\
& \qquad +279\sqrt{3}\psi'''\big(\tfrac{1}{3}\big)\,\alpha C_A^2 + 999\sqrt{3}\psi'''\big(\tfrac{1}{3}\big)\,C_A^2 \\
& \qquad +19440\sqrt{3}s_2\big(\tfrac{\pi}{6}\big)\,\alpha^3 C_A^2 - 124416\sqrt{3}s_2\big(\tfrac{\pi}{6}\big)\,\alpha^2 C_A^2 \\
& \qquad +136080\sqrt{3}s_2\big(\tfrac{\pi}{6}\big)\,\alpha C_A^2 + 1275264\sqrt{3}s_2\big(\tfrac{\pi}{6}\big)\,C_A^2 \\
& \qquad -497664\sqrt{3}s_2\big(\tfrac{\pi}{6}\big)\,C_A N_f T_F - 38880\sqrt{3}s_2\big(\tfrac{\pi}{2}\big)\,\alpha^3 C_A^2 \\
& \qquad +248832\sqrt{3}s_2\big(\tfrac{\pi}{2}\big)\,\alpha^2 C_A^2 - 272160\sqrt{3}s_2\big(\tfrac{\pi}{2}\big)\,\alpha C_A^2 \\
& \qquad -2550528\sqrt{3}s_2\big(\tfrac{\pi}{2}\big)\,C_A^2 + 995328\sqrt{3}s_2\big(\tfrac{\pi}{2}\big)\,C_A N_f T_F \\
& \qquad -32400\sqrt{3}s_3\big(\tfrac{\pi}{6}\big)\,\alpha^3 C_A^2 + 207360\sqrt{3}s_3\big(\tfrac{\pi}{6}\big)\,\alpha^2 C_A^2 \\
& \qquad -226800\sqrt{3}s_3\big(\tfrac{\pi}{6}\big)\,\alpha C_A^2 - 2125440\sqrt{3}s_3\big(\tfrac{\pi}{6}\big)\,C_A^2 \\
& \qquad +829440\sqrt{3}s_3\big(\tfrac{\pi}{6}\big)\,C_A N_f T_F + 25920\sqrt{3}s_3\big(\tfrac{\pi}{2}\big)\,\alpha^3 C_A^2 \\
& \qquad -165888\sqrt{3}s_3\big(\tfrac{\pi}{2}\big)\,\alpha^2 C_A^2 + 181440\sqrt{3}s_3\big(\tfrac{\pi}{2}\big)\,\alpha C_A^2 \\
& \qquad +1700352\sqrt{3}s_3\big(\tfrac{\pi}{2}\big)\,C_A^2 - 663552\sqrt{3}s_3\big(\tfrac{\pi}{2}\big)\,C_A N_f T_F \\
& \qquad +16\sqrt{3}\alpha^4 C_A^2\pi^4 + 216\sqrt{3}\alpha^4 C_A^2\pi^2 - 486\sqrt{3}\alpha^4 C_A^2
\end{aligned}
$$

$$
\begin{aligned}
&+232\sqrt{3}\alpha^3 C_A^2\pi^4 + 1872\sqrt{3}\alpha^3 C_A^2\pi^2 - 324\sqrt{3}\alpha^3 C_A^2\zeta_3 \\
&+3888\sqrt{3}\alpha^3 C_A^2 + 1320\sqrt{3}\alpha^2 C_A^2\pi^4 + 27024\sqrt{3}\alpha^2 C_A^2\pi^2 \\
&+11016\sqrt{3}\alpha^2 C_A^2\zeta_3 + 96228\sqrt{3}\alpha^2 C_A^2 \\
&-1920\sqrt{3}\alpha^2 C_A N_f\pi^2 T_F - 25920\sqrt{3}\alpha^2 C_A N_f T_F \\
&-2024\sqrt{3}\alpha C_A^2\pi^4 + 30336\sqrt{3}\alpha C_A^2\pi^2 - 45036\sqrt{3}\alpha C_A^2\zeta_3 \\
&+353160\sqrt{3}\alpha C_A^2 - 16896\sqrt{3}\alpha C_A N_f\pi^2 T_F \\
&-145152\sqrt{3}\alpha C_A N_f T_F - 2264\sqrt{3}C_A^2\pi^4 - 159384\sqrt{3}C_A^2\pi^2 \\
&-51192\sqrt{3}C_A^2\zeta_3 - 408870\sqrt{3}C_A^2 + 68352\sqrt{3}C_A N_f\pi^2 T_F \\
&+331776\sqrt{3}C_A N_f T_F\zeta_3 - 39168\sqrt{3}C_A N_f T_F \\
&-497664\sqrt{3}C_F N_f T_F\zeta_3 + 570240\sqrt{3}C_F N_f T_F \\
&+115200\sqrt{3}N_f^2 T_F^2 + 135\ln(3)^2\alpha^3 C_A^2\pi - 864\ln(3)^2\alpha^2 C_A^2\pi \\
&+945\ln(3)^2\alpha C_A^2\pi + 8856\ln(3)^2 C_A^2\pi \\
&-3456\ln(3)^2 C_A N_f\pi T_F - 1620\ln(3)\alpha^3 C_A^2\pi \\
&+10368\ln(3)\alpha^2 C_A^2\pi - 11340\ln(3)\alpha C_A^2\pi \\
&-106272\ln(3)C_A^2\pi + 41472\ln(3)C_A N_f\pi T_F - 145\alpha^3 C_A^2\pi^3 \\
&+928\alpha^2 C_A^2\pi^3 - 1015\alpha C_A^2\pi^3 - 9512 C_A^2\pi^3 \\
&+3712 C_A N_f\pi^3 T_F + 144\sqrt{3}\left(-33\psi'\left(\tfrac{1}{3}\right)\alpha^2 C_A^2\right. \\
&+12\psi'\left(\tfrac{1}{3}\right)\alpha^2 C_A N_f T_F - 264\psi'\left(\tfrac{1}{3}\right)\alpha C_A^2 \\
&+96\psi'\left(\tfrac{1}{3}\right)\alpha C_A N_f T_F + 165\psi'\left(\tfrac{1}{3}\right)C_A^2 - 60\psi'\left(\tfrac{1}{3}\right)C_A N_f T_F \\
&+22\alpha^2 C_A^2\pi^2 + 297\alpha^2 C_A^2 - 8\alpha^2 C_A N_f\pi^2 T_F \\
&-108\alpha^2 C_A N_f T_F + 176\alpha C_A^2\pi^2 + 1782\alpha C_A^2 \\
&-64\alpha C_A N_f\pi^2 T_F - 648\alpha C_A N_f T_F - 110 C_A^2\pi^2 \\
&+5541 C_A^2 + 40 C_A N_f\pi^2 T_F - 4380 C_A N_f T_F \\
&\left.+432 C_F N_f T_F + 960 N_f^2 T_F^2\right)\frac{1}{\epsilon}\Bigg)\frac{1}{62208\sqrt{3}}\Bigg] a^2 \;+\; \mathcal{O}(a^3)\;.
\end{aligned}
\tag{3.1.4}
$$

Recall that we are using the same scale μ for the coupling constant as the kinematic scale, see (2.1.63). Numerically for the wave function and gauge parameter renormalization we have

$$
\begin{aligned}
Z_A^{(\mathrm{ccg})}\Big|_{\mathrm{MOMh}} \;=\; 1 + \Bigg[&(-1.5\alpha - 0.666667 N_f + 6.5)\frac{1}{\epsilon} \\
&+0.75\alpha^2 + 1.5\alpha - 1.111111 N_f + 8.083333\Bigg] a
\end{aligned}
$$

$$
\begin{aligned}
&+\Bigg[(2.25\alpha^2+\alpha N_f-6.375\alpha+1.5N_f-14.625)\frac{1}{\epsilon^2}\\
&\quad+(-1.564483\alpha^3-0.195326\alpha^2N_f-0.486436\alpha^2\\
&\quad+2.104062\alpha N_f-6.879690\alpha+1.893295N_f\\
&\quad-34.834623)\frac{1}{\epsilon}+0.782241303913\alpha^4+3.884913\alpha^3\\
&\quad-0.325543\alpha^2N_f+1.972977\alpha^2+0.728992\alpha N_f-1.707555\alpha\\
&\quad-24.322251N_f+106.171599\Bigg]a^2\;+\;\mathcal{O}(a^3)\\
Z_\alpha^{(\mathrm{ccg})}\big|_{\mathrm{MOMh}} &= 1+\mathcal{O}(a^3)\\
Z_c^{(\mathrm{ccg})}\big|_{\mathrm{MOMh}} &= 1+\left[(-0.75\alpha+2.25)\frac{1}{\epsilon}+3.0\right]a\\
&\quad+\Bigg[(0.84375\alpha^2+0.75N_f-9.84375)\frac{1}{\epsilon^2}+(-0.219741\alpha^3\\
&\quad-0.536207\alpha^2+1.028748\alpha+1.875N_f-26.077370)\frac{1}{\epsilon}\\
&\quad-0.024506\alpha^2-3.395711\alpha-2.604167N_f+25.290944\Bigg]a^2\\
&\quad+\mathcal{O}(a^3)\\
Z_\psi^{(\mathrm{ccg})}\Big|_{\mathrm{MOMh}} &= 1-1.333333\alpha\left(1+\frac{1}{\epsilon}\right)a\\
&\quad+\Bigg[\alpha(1.888889\alpha+3.0)\frac{1}{\epsilon^2}+(-0.390651\alpha^3+2.152568\alpha^2\\
&\quad+9.953256\alpha+0.666667N_f-11.166667)\frac{1}{\epsilon}-0.390651\alpha^3\\
&\quad-1.847432\alpha^2+2.377939\alpha+2.333333N_f-25.464206\Bigg]a^2\\
&\quad+\mathcal{O}(a^3)\;. \qquad (3.1.5)
\end{aligned}
$$

Notice how the two loop contribution to the wave function renormalization constants are now dependent on a particular MOMi scheme compared to the $\overline{\mathrm{MS}}$ scheme where the Z's were independent of the 3-point Green's functions used to determine them. At one loop, $Z_a, Z_\alpha, Z_c, Z_\psi$ remain scheme independent. It is only by increasing the loop order that this scheme dependence becomes apparent. Above, a and α depend on the MOMh scheme, and we have suppressed the argument $(a_{\mathrm{MOMh}}, \alpha_{\mathrm{MOMh}})$ on the renormalization constants. The renormalization constants for each of the MOMg and MOMq schemes were constructed using the same techniques and are presented below for completeness. Starting with the MOMg scheme

$$
Z_g^{(\mathrm{ggg})}\big|_{\mathrm{MOMg}} = 1+\left[-36\psi'\left(\tfrac{1}{3}\right)\alpha^2C_A+162\psi'\left(\tfrac{1}{3}\right)\alpha C_A-138\psi'\left(\tfrac{1}{3}\right)C_A\right.
$$

$$
\begin{aligned}
&+384\psi'\left(\tfrac{1}{3}\right) N_f T_F - 27\alpha^3 C_A + 24\alpha^2 C_A \pi^2 + 162\alpha^2 C_A \\
&-108\alpha C_A \pi^2 - 243\alpha C_A + 92 C_A \pi^2 - 2376 C_A - 256 N_f \pi^2 T_F \\
&+864 N_f T_F + 108\left(-11 C_A + 4 N_f T_F\right) \frac{1}{\epsilon}\Bigg] \frac{a}{648} \\
&+(121 C_A^2 - 88 C_A N_f T_F + 16 N_f^2 T_F^2) \frac{a^2}{24\epsilon^2} \\
&+\Bigg[2592\sqrt{3}\psi'\left(\tfrac{1}{3}\right)^2 \alpha^4 C_A^2 - 23328\sqrt{3}\psi'\left(\tfrac{1}{3}\right)^2 \alpha^3 C_A^2 \\
&+72360\sqrt{3}\psi'\left(\tfrac{1}{3}\right)^2 \alpha^2 C_A^2 - 55296\sqrt{3}\psi'\left(\tfrac{1}{3}\right)^2 \alpha^2 C_A N_f T_F \\
&-89424\sqrt{3}\psi'\left(\tfrac{1}{3}\right)^2 \alpha C_A^2 + 248832\sqrt{3}\psi'\left(\tfrac{1}{3}\right)^2 \alpha C_A N_f T_F \\
&+38088\sqrt{3}\psi'\left(\tfrac{1}{3}\right)^2 C_A^2 - 211968\sqrt{3}\psi'\left(\tfrac{1}{3}\right)^2 C_A N_f T_F \\
&+294912\sqrt{3}\psi'\left(\tfrac{1}{3}\right)^2 N_f^2 T_F^2 + 3888\sqrt{3}\psi'\left(\tfrac{1}{3}\right) \alpha^5 C_A^2 \\
&-3456\sqrt{3}\psi'\left(\tfrac{1}{3}\right) \alpha^4 C_A^2 \pi^2 - 46656\sqrt{3}\psi'\left(\tfrac{1}{3}\right) \alpha^4 C_A^2 \\
&+31104\sqrt{3}\psi'\left(\tfrac{1}{3}\right) \alpha^3 C_A^2 \pi^2 + 74196\sqrt{3}\psi'\left(\tfrac{1}{3}\right) \alpha^3 C_A^2 \\
&-41472\sqrt{3}\psi'\left(\tfrac{1}{3}\right) \alpha^3 C_A N_f T_F - 96480\sqrt{3}\psi'\left(\tfrac{1}{3}\right) \alpha^2 C_A^2 \pi^2 \\
&-119880\sqrt{3}\psi'\left(\tfrac{1}{3}\right) \alpha^2 C_A^2 + 73728\sqrt{3}\psi'\left(\tfrac{1}{3}\right) \alpha^2 C_A N_f \pi^2 T_F \\
&+134784\sqrt{3}\psi'\left(\tfrac{1}{3}\right) \alpha^2 C_A N_f T_F + 119232\sqrt{3}\psi'\left(\tfrac{1}{3}\right) \alpha C_A^2 \pi^2 \\
&-1107756\sqrt{3}\psi'\left(\tfrac{1}{3}\right) \alpha C_A^2 - 331776\sqrt{3}\psi'\left(\tfrac{1}{3}\right) \alpha C_A N_f \pi^2 T_F \\
&-119232\sqrt{3}\psi'\left(\tfrac{1}{3}\right) \alpha C_A N_f T_F - 50784\sqrt{3}\psi'\left(\tfrac{1}{3}\right) C_A^2 \pi^2 \\
&+3843072\sqrt{3}\psi'\left(\tfrac{1}{3}\right) C_A^2 + 282624\sqrt{3}\psi'\left(\tfrac{1}{3}\right) C_A N_f \pi^2 T_F \\
&-3827520\sqrt{3}\psi'\left(\tfrac{1}{3}\right) C_A N_f T_F + 497664\sqrt{3}\psi'\left(\tfrac{1}{3}\right) C_F N_f T_F \\
&-393216\sqrt{3}\psi'\left(\tfrac{1}{3}\right) N_f^2 \pi^2 T_F^2 + 774144\sqrt{3}\psi'\left(\tfrac{1}{3}\right) N_f^2 T_F^2 \\
&+81\sqrt{3}\psi'''\left(\tfrac{1}{3}\right) \alpha^3 C_A^2 + 1134\sqrt{3}\psi'''\left(\tfrac{1}{3}\right) \alpha^2 C_A^2 \\
&-11664\sqrt{3}\psi'''\left(\tfrac{1}{3}\right) \alpha C_A^2 + 34587\sqrt{3}\psi'''\left(\tfrac{1}{3}\right) C_A^2 \\
&-20736\sqrt{3}\psi'''\left(\tfrac{1}{3}\right) C_A N_f T_F - 139968\sqrt{3} s_2\left(\tfrac{\pi}{6}\right) \alpha^3 C_A^2 \\
&-69984\sqrt{3} s_2\left(\tfrac{\pi}{6}\right) \alpha^2 C_A^2 - 4408992\sqrt{3} s_2\left(\tfrac{\pi}{6}\right) \alpha C_A^2 \\
&+24214464\sqrt{3} s_2\left(\tfrac{\pi}{6}\right) C_A^2 - 11197440\sqrt{3} s_2\left(\tfrac{\pi}{6}\right) C_A N_f T_F \\
&+279936\sqrt{3} s_2\left(\tfrac{\pi}{2}\right) \alpha^3 C_A^2 + 139968\sqrt{3} s_2\left(\tfrac{\pi}{2}\right) \alpha^2 C_A^2 \\
&+8817984\sqrt{3} s_2\left(\tfrac{\pi}{2}\right) \alpha C_A^2 - 48428928\sqrt{3} s_2\left(\tfrac{\pi}{2}\right) C_A^2 \\
&+22394880\sqrt{3} s_2\left(\tfrac{\pi}{2}\right) C_A N_f T_F + 233280\sqrt{3} s_3\left(\tfrac{\pi}{6}\right) \alpha^3 C_A^2 \\
&+116640\sqrt{3} s_3\left(\tfrac{\pi}{6}\right) \alpha^2 C_A^2 + 7348320\sqrt{3} s_3\left(\tfrac{\pi}{6}\right) \alpha C_A^2 \\
&-40357440\sqrt{3} s_3\left(\tfrac{\pi}{6}\right) C_A^2 + 18662400\sqrt{3} s_3\left(\tfrac{\pi}{6}\right) C_A N_f T_F \\
&-186624\sqrt{3} s_3\left(\tfrac{\pi}{2}\right) \alpha^3 C_A^2 - 93312\sqrt{3} s_3\left(\tfrac{\pi}{2}\right) \alpha^2 C_A^2 \\
&-5878656\sqrt{3} s_3\left(\tfrac{\pi}{2}\right) \alpha C_A^2 + 32285952\sqrt{3} s_3\left(\tfrac{\pi}{2}\right) C_A^2
\end{aligned}
$$

$$
\begin{aligned}
&-14929920\sqrt{3}s_3\left(\tfrac{\pi}{2}\right)C_AN_fT_F + 1458\sqrt{3}\alpha^6C_A^2 \\
&-2592\sqrt{3}\alpha^5C_A^2\pi^2 - 21870\sqrt{3}\alpha^5C_A^2 + 1152\sqrt{3}\alpha^4C_A^2\pi^4 \\
&+31104\sqrt{3}\alpha^4C_A^2\pi^2 + 67797\sqrt{3}\alpha^4C_A^2 - 10584\sqrt{3}\alpha^3C_A^2\pi^4 \\
&-49464\sqrt{3}\alpha^3C_A^2\pi^2 - 11664\sqrt{3}\alpha^3C_A^2\zeta_3 + 170100\sqrt{3}\alpha^3C_A^2 \\
&+27648\sqrt{3}\alpha^3C_AN_f\pi^2T_F - 54432\sqrt{3}\alpha^3C_AN_fT_F \\
&+29136\sqrt{3}\alpha^2C_A^2\pi^4 + 79920\sqrt{3}\alpha^2C_A^2\pi^2 + 2916\sqrt{3}\alpha^2C_A^2\zeta_3 \\
&-971028\sqrt{3}\alpha^2C_A^2 - 24576\sqrt{3}\alpha^2C_AN_f\pi^4T_F \\
&-89856\sqrt{3}\alpha^2C_AN_f\pi^2T_F + 349920\sqrt{3}\alpha^2C_AN_fT_F \\
&-8640\sqrt{3}\alpha C_A^2\pi^4 + 738504\sqrt{3}\alpha C_A^2\pi^2 + 664848\sqrt{3}\alpha C_A^2\zeta_3 \\
&+1027890\sqrt{3}\alpha C_A^2 + 110592\sqrt{3}\alpha C_AN_f\pi^4T_F \\
&+79488\sqrt{3}\alpha C_AN_f\pi^2T_F - 349920\sqrt{3}\alpha C_AN_fT_F \\
&-75304\sqrt{3}C_A^2\pi^4 - 2562048\sqrt{3}C_A^2\pi^2 - 2767284\sqrt{3}C_A^2\zeta_3 \\
&-203067\sqrt{3}C_A^2 - 38912\sqrt{3}C_AN_f\pi^4T_F \\
&+2551680\sqrt{3}C_AN_f\pi^2T_F + 2985984\sqrt{3}C_AN_fT_F\zeta_3 \\
&-681696\sqrt{3}C_AN_fT_F - 331776\sqrt{3}C_FN_f\pi^2T_F \\
&-2239488\sqrt{3}C_FN_fT_F\zeta_3 + 2379456\sqrt{3}C_FN_fT_F \\
&+131072\sqrt{3}N_f^2\pi^4T_F^2 - 516096\sqrt{3}N_f^2\pi^2T_F^2 \\
&+767232\sqrt{3}N_f^2T_F^2 - 972\ln(3)^2\alpha^3C_A^2\pi - 486\ln(3)^2\alpha^2C_A^2\pi \\
&-30618\ln(3)^2\alpha C_A^2\pi + 168156\ln(3)^2C_A^2\pi \\
&-77760\ln(3)^2C_AN_f\pi T_F + 11664\ln(3)\alpha^3C_A^2\pi \\
&+5832\ln(3)\alpha^2C_A^2\pi + 367416\ln(3)\alpha C_A^2\pi \\
&-2017872\ln(3)C_A^2\pi + 933120\ln(3)C_AN_f\pi T_F \\
&+1044\alpha^3C_A^2\pi^3 + 522\alpha^2C_A^2\pi^3 + 32886\alpha C_A^2\pi^3 \\
&-180612C_A^2\pi^3 + 83520C_AN_f\pi^3T_F \\
&+216\sqrt{3}\left(396\psi'\left(\tfrac{1}{3}\right)\alpha^2C_A^2 - 144\psi'\left(\tfrac{1}{3}\right)\alpha^2C_AN_fT_F\right. \\
&-1782\psi'\left(\tfrac{1}{3}\right)\alpha C_A^2 + 648\psi'\left(\tfrac{1}{3}\right)\alpha C_AN_fT_F + 1518\psi'\left(\tfrac{1}{3}\right)C_A^2 \\
&\left.-4776\psi'\left(\tfrac{1}{3}\right)C_AN_fT_F + 1536\psi'\left(\tfrac{1}{3}\right)N_f^2T_F^2 + 297\alpha^3C_A^2\right. \\
&-108\alpha^3C_AN_fT_F - 264\alpha^2C_A^2\pi^2 - 1782\alpha^2C_A^2 \\
&+96\alpha^2C_AN_f\pi^2T_F + 648\alpha^2C_AN_fT_F + 1188\alpha C_A^2\pi^2 \\
&+2673\alpha C_A^2 - 432\alpha C_AN_f\pi^2T_F - 972\alpha C_AN_fT_F - 1012C_A^2\pi^2 \\
&+22464C_A^2 + 3184C_AN_f\pi^2T_F - 16848C_AN_fT_F \\
&+1296C_FN_fT_F - 1024N_f^2\pi^2T_F^2
\end{aligned}
$$

$$+3456N_f^2T_F^2\Big)\,\frac{1}{\epsilon}\Big]\,\frac{a^2}{279936\sqrt{3}}\;+\;\mathcal{O}(a^3)\;. \tag{3.1.6}$$

Numerically the renormalization constants for the wave functions and gauge parameter are given as

$$\begin{aligned}
Z_A^{(\mathrm{ggg})}\Big|_{\mathrm{MOMg}} &= 1+\Big[0.75\alpha^2+1.5\alpha-1.111111N_f+8.083333\\
&\quad +(-1.5\alpha-0.666667N_f+6.5)\frac{1}{\epsilon}\Big]\,a\\
&\quad +\Bigg[\Big(2.25\alpha^2+\alpha N_f-6.375000\alpha+1.5N_f-14.625000\Big)\,\frac{1}{\epsilon^2}\\
&\quad -0.187500\alpha^5+0.996035\alpha^4+0.277778\alpha^3N_f+6.926580\alpha^3\\
&\quad +0.531442\alpha^2N_f+10.130529\alpha^2-1.567892\alpha N_f\\
&\quad +28.246854\alpha-2.561884N_f^2+3.142356N_f+41.955873\\
&\quad +\Big(0.375000\alpha^4+0.166667\alpha^3N_f-4.367070\alpha^3\\
&\quad -0.718698\alpha^2N_f-3.153385\alpha^2-4.807737\alpha N_f\\
&\quad +38.705877\alpha-1.537130N_f^2+22.176457N_f\\
&\quad -86.472011\Big)\,\frac{1}{\epsilon}\Bigg]\,a^2\;+\;\mathcal{O}(a^3)\\
Z_\alpha^{(\mathrm{ggg})}\big|_{\mathrm{MOMg}} &= 1\;+\;\mathcal{O}(a^3)\\
Z_c^{(\mathrm{ggg})}\big|_{\mathrm{MOMg}} &= 1+\left[3.0+(-0.75\alpha+2.25)\,\frac{1}{\epsilon}\right]a\\
&\quad +\Bigg[\Big(0.843750\alpha^2+0.75N_f-9.843750\Big)\,\frac{1}{\epsilon^2}-0.75\alpha^3\\
&\quad +2.330668\alpha^2+12.143941\alpha+4.312919N_f+1.458303\\
&\quad +\Big(0.187500\alpha^4-1.371035\alpha^3-2.654739\alpha^2\\
&\quad -1.729271\alpha N_f+18.641647\alpha+7.062814N_f\\
&\quad -43.951850\Big)\,\frac{1}{\epsilon}\Bigg]\,a^2\;+\;\mathcal{O}(a^3)\\
Z_\psi^{(\mathrm{ggg})}\Big|_{\mathrm{MOMg}} &= 1+\left[-1.333333\alpha-1.333333\frac{\alpha}{\epsilon}\right]a\\
&\quad +\Bigg[\alpha\,(1.888889\alpha+3.0)\,\frac{1}{\epsilon^2}+0.333333\alpha^4-1.437395\alpha^3\\
&\quad -8.753944\alpha^2-3.074260\alpha N_f+12.970224\alpha+2.333333N_f\\
&\quad -25.464206+\Big(0.333333\alpha^4-1.437395\alpha^3-4.753944\alpha^2\\
&\quad -3.074260\alpha N_f+20.545541\alpha+0.666667N_f\\
&\quad -11.166667\Big)\,\frac{1}{\epsilon}\Bigg]\,a^2\;+\;\mathcal{O}(a^3)\;.
\end{aligned} \tag{3.1.7}$$

Finally for the momentum subtraction scheme corresponding to the quark-gluon vertex we have

$$
\begin{aligned}
Z_g^{(\mathrm{qqg})}\big|_{\mathrm{MOMq}} \;=\; & 1 + \big[-6\psi'\left(\tfrac{1}{3}\right)\alpha^2 C_A + 24\psi'\left(\tfrac{1}{3}\right)\alpha C_A + 96\psi'\left(\tfrac{1}{3}\right)\alpha C_F \\
& +78\psi'\left(\tfrac{1}{3}\right) C_A - 48\psi'\left(\tfrac{1}{3}\right) C_F + 4\alpha^2 C_A\pi^2 + 27\alpha^2 C_A \\
& -16\alpha C_A\pi^2 - 54\alpha C_A - 64\alpha C_F\pi^2 - 216\alpha C_F - 52 C_A\pi^2 \\
& -993 C_A + 32 C_F\pi^2 + 432 C_F + 240 N_f T_F \\
& +36(-11 C_A + 4 N_f T_F)\frac{1}{\epsilon}\Big]\,\frac{a}{216} \\
& + \Bigg[(121 C_A^2 - 88 C_A N_f T_F + 16 N_f^2 T_F^2)\frac{1}{24\epsilon} \\
& \quad + \Big(72\sqrt{3}\psi'\left(\tfrac{1}{3}\right)^2\alpha^4 C_A^2 - 576\sqrt{3}\psi'\left(\tfrac{1}{3}\right)^2\alpha^3 C_A^2 \\
& \qquad -2304\sqrt{3}\psi'\left(\tfrac{1}{3}\right)^2\alpha^3 C_A C_F \\
& \qquad -720\sqrt{3}\psi'\left(\tfrac{1}{3}\right)^2\alpha^2 C_A^2 + 10368\sqrt{3}\psi'\left(\tfrac{1}{3}\right)^2\alpha^2 C_A C_F \\
& \qquad +18432\sqrt{3}\psi'\left(\tfrac{1}{3}\right)^2\alpha^2 C_F^2 + 7488\sqrt{3}\psi'\left(\tfrac{1}{3}\right)^2\alpha C_A^2 \\
& \qquad +25344\sqrt{3}\psi'\left(\tfrac{1}{3}\right)^2\alpha C_A C_F - 18432\sqrt{3}\psi'\left(\tfrac{1}{3}\right)^2\alpha C_F^2 \\
& \qquad +19080\sqrt{3}\psi'\left(\tfrac{1}{3}\right)^2 C_A^2 - 35712\sqrt{3}\psi'\left(\tfrac{1}{3}\right)^2 C_A C_F \\
& \qquad +18432\sqrt{3}\psi'\left(\tfrac{1}{3}\right)^2 C_F^2 - 96\sqrt{3}\psi'\left(\tfrac{1}{3}\right)\alpha^4 C_A^2\pi^2 \\
& \qquad -972\sqrt{3}\psi'\left(\tfrac{1}{3}\right)\alpha^4 C_A^2 + 768\sqrt{3}\psi'\left(\tfrac{1}{3}\right)\alpha^3 C_A^2\pi^2 \\
& \qquad +2160\sqrt{3}\psi'\left(\tfrac{1}{3}\right)\alpha^3 C_A^2 + 3072\sqrt{3}\psi'\left(\tfrac{1}{3}\right)\alpha^3 C_A C_F\pi^2 \\
& \qquad +17280\sqrt{3}\psi'\left(\tfrac{1}{3}\right)\alpha^3 C_A C_F + 960\sqrt{3}\psi'\left(\tfrac{1}{3}\right)\alpha^2 C_A^2\pi^2 \\
& \qquad +26820\sqrt{3}\psi'\left(\tfrac{1}{3}\right)\alpha^2 C_A^2 - 13824\sqrt{3}\psi'\left(\tfrac{1}{3}\right)\alpha^2 C_A C_F\pi^2 \\
& \qquad -55296\sqrt{3}\psi'\left(\tfrac{1}{3}\right)\alpha^2 C_A C_F - 2880\sqrt{3}\psi'\left(\tfrac{1}{3}\right)\alpha^2 C_A N_f T_F \\
& \qquad -24576\sqrt{3}\psi'\left(\tfrac{1}{3}\right)\alpha^2 C_F^2\pi^2 - 82944\sqrt{3}\psi'\left(\tfrac{1}{3}\right)\alpha^2 C_F^2 \\
& \qquad -9984\sqrt{3}\psi'\left(\tfrac{1}{3}\right)\alpha C_A^2\pi^2 - 65232\sqrt{3}\psi'\left(\tfrac{1}{3}\right)\alpha C_A^2 \\
& \qquad -33792\sqrt{3}\psi'\left(\tfrac{1}{3}\right)\alpha C_A C_F\pi^2 - 379872\sqrt{3}\psi'\left(\tfrac{1}{3}\right)\alpha C_A C_F \\
& \qquad +17280\sqrt{3}\psi'\left(\tfrac{1}{3}\right)\alpha C_A N_f T_F + 24576\sqrt{3}\psi'\left(\tfrac{1}{3}\right)\alpha C_F^2\pi^2 \\
& \qquad +324864\sqrt{3}\psi'\left(\tfrac{1}{3}\right)\alpha C_F^2 + 46080\sqrt{3}\psi'\left(\tfrac{1}{3}\right)\alpha C_F N_f T_F \\
& \qquad -25440\sqrt{3}\psi'\left(\tfrac{1}{3}\right) C_A^2\pi^2 - 127512\sqrt{3}\psi'\left(\tfrac{1}{3}\right) C_A^2 \\
& \qquad +47616\sqrt{3}\psi'\left(\tfrac{1}{3}\right) C_A C_F\pi^2 + 496224\sqrt{3}\psi'\left(\tfrac{1}{3}\right) C_A C_F \\
& \qquad -44352\sqrt{3}\psi'\left(\tfrac{1}{3}\right) C_A N_f T_F - 24576\sqrt{3}\psi'\left(\tfrac{1}{3}\right) C_F^2\pi^2 \\
& \qquad -293760\sqrt{3}\psi'\left(\tfrac{1}{3}\right) C_F^2 - 9216\sqrt{3}\psi'\left(\tfrac{1}{3}\right) C_F N_f T_F \\
& \qquad +108\sqrt{3}\psi'''\left(\tfrac{1}{3}\right)\alpha^2 C_A^2 - 144\sqrt{3}\psi'''\left(\tfrac{1}{3}\right)\alpha^2 C_A C_F
\end{aligned}
$$

$$
\begin{aligned}
&-198\sqrt{3}\psi'''\left(\tfrac{1}{3}\right)\alpha C_A^2 - 720\sqrt{3}\psi'''\left(\tfrac{1}{3}\right)\alpha C_A C_F \\
&-1152\sqrt{3}\psi'''\left(\tfrac{1}{3}\right)\alpha C_F^2 - 414\sqrt{3}\psi'''\left(\tfrac{1}{3}\right) C_A^2 \\
&-864\sqrt{3}\psi'''\left(\tfrac{1}{3}\right) C_A C_F + 576\sqrt{3}\psi'''\left(\tfrac{1}{3}\right) C_A N_f T_F \\
&+4608\sqrt{3}\psi'''\left(\tfrac{1}{3}\right) C_F^2 + 69984\sqrt{3}s_2\left(\tfrac{\pi}{6}\right)\alpha^2 C_A^2 \\
&-124416\sqrt{3}s_2\left(\tfrac{\pi}{6}\right)\alpha^2 C_A C_F + 108864\sqrt{3}s_2\left(\tfrac{\pi}{6}\right)\alpha C_A^2 \\
&-995328\sqrt{3}s_2\left(\tfrac{\pi}{6}\right)\alpha C_A C_F + 497664\sqrt{3}s_2\left(\tfrac{\pi}{6}\right)\alpha C_F^2 \\
&-443232\sqrt{3}s_2\left(\tfrac{\pi}{6}\right) C_A^2 + 1306368\sqrt{3}s_2\left(\tfrac{\pi}{6}\right) C_A C_F \\
&-124416\sqrt{3}s_2\left(\tfrac{\pi}{6}\right) C_A N_f T_F + 248832\sqrt{3}s_2\left(\tfrac{\pi}{6}\right) C_F^2 \\
&-139968\sqrt{3}s_2\left(\tfrac{\pi}{2}\right)\alpha^2 C_A^2 + 248832\sqrt{3}s_2\left(\tfrac{\pi}{2}\right)\alpha^2 C_A C_F \\
&-217728\sqrt{3}s_2\left(\tfrac{\pi}{2}\right)\alpha C_A^2 + 1990656\sqrt{3}s_2\left(\tfrac{\pi}{2}\right)\alpha C_A C_F \\
&-995328\sqrt{3}s_2\left(\tfrac{\pi}{2}\right)\alpha C_F^2 + 886464\sqrt{3}s_2\left(\tfrac{\pi}{2}\right) C_A^2 \\
&-2612736\sqrt{3}s_2\left(\tfrac{\pi}{2}\right) C_A C_F + 248832\sqrt{3}s_2\left(\tfrac{\pi}{2}\right) C_A N_f T_F \\
&-497664\sqrt{3}s_2\left(\tfrac{\pi}{2}\right) C_F^2 - 116640\sqrt{3}s_3\left(\tfrac{\pi}{6}\right)\alpha^2 C_A^2 \\
&+207360\sqrt{3}s_3\left(\tfrac{\pi}{6}\right)\alpha^2 C_A C_F - 181440\sqrt{3}s_3\left(\tfrac{\pi}{6}\right)\alpha C_A^2 \\
&+1658880\sqrt{3}s_3\left(\tfrac{\pi}{6}\right)\alpha C_A C_F - 829440\sqrt{3}s_3\left(\tfrac{\pi}{6}\right)\alpha C_F^2 \\
&+738720\sqrt{3}s_3\left(\tfrac{\pi}{6}\right) C_A^2 - 2177280\sqrt{3}s_3\left(\tfrac{\pi}{6}\right) C_A C_F \\
&+207360\sqrt{3}s_3\left(\tfrac{\pi}{6}\right) C_A N_f T_F - 414720\sqrt{3}s_3\left(\tfrac{\pi}{6}\right) C_F^2 \\
&+93312\sqrt{3}s_3\left(\tfrac{\pi}{2}\right)\alpha^2 C_A^2 - 165888\sqrt{3}s_3\left(\tfrac{\pi}{2}\right)\alpha^2 C_A C_F \\
&+145152\sqrt{3}s_3\left(\tfrac{\pi}{2}\right)\alpha C_A^2 - 1327104\sqrt{3}s_3\left(\tfrac{\pi}{2}\right)\alpha C_A C_F \\
&+663552\sqrt{3}s_3\left(\tfrac{\pi}{2}\right)\alpha C_F^2 - 590976\sqrt{3}s_3\left(\tfrac{\pi}{2}\right) C_A^2 \\
&+1741824\sqrt{3}s_3\left(\tfrac{\pi}{2}\right) C_A C_F - 165888\sqrt{3}s_3\left(\tfrac{\pi}{2}\right) C_A N_f T_F \\
&+331776\sqrt{3}s_3\left(\tfrac{\pi}{2}\right) C_F^2 + 32\sqrt{3}\alpha^4 C_A^2\pi^4 + 648\sqrt{3}\alpha^4 C_A^2\pi^2 \\
&+2673\sqrt{3}\alpha^4 C_A^2 - 256\sqrt{3}\alpha^3 C_A^2\pi^4 - 1440\sqrt{3}\alpha^3 C_A^2\pi^2 \\
&-1024\sqrt{3}\alpha^3 C_A C_F\pi^4 - 11520\sqrt{3}\alpha^3 C_A C_F\pi^2 \\
&-27216\sqrt{3}\alpha^3 C_A C_F - 608\sqrt{3}\alpha^2 C_A^2\pi^4 - 17880\sqrt{3}\alpha^2 C_A^2\pi^2 \\
&-4860\sqrt{3}\alpha^2 C_A^2\zeta_3 - 73710\sqrt{3}\alpha^2 C_A^2 + 4992\sqrt{3}\alpha^2 C_A C_F\pi^4 \\
&+36864\sqrt{3}\alpha^2 C_A C_F\pi^2 + 20736\sqrt{3}\alpha^2 C_A C_F\zeta_3 \\
&+38880\sqrt{3}\alpha^2 C_A C_F + 1920\sqrt{3}\alpha^2 C_A N_f\pi^2 T_F \\
&+12960\sqrt{3}\alpha^2 C_A N_f T_F + 8192\sqrt{3}\alpha^2 C_F^2\pi^4 \\
&+55296\sqrt{3}\alpha^2 C_F^2\pi^2 + 93312\sqrt{3}\alpha^2 C_F^2 + 3856\sqrt{3}\alpha C_A^2\pi^4 \\
&+43488\sqrt{3}\alpha C_A^2\pi^2 + 20736\sqrt{3}\alpha C_A^2\zeta_3 + 136728\sqrt{3}\alpha C_A^2 \\
&+13184\sqrt{3}\alpha C_A C_F\pi^4 + 253248\sqrt{3}\alpha C_A C_F\pi^2
\end{aligned}
$$

$$
\begin{aligned}
&+10368\sqrt{3}\alpha C_A C_F\zeta_3 + 444528\sqrt{3}\alpha C_A C_F \\
&-11520\sqrt{3}\alpha C_A N_f\pi^2 T_F - 25920\sqrt{3}\alpha C_A N_f T_F \\
&-5120\sqrt{3}\alpha C_F^2\pi^4 - 216576\sqrt{3}\alpha C_F^2\pi^2 + 41472\sqrt{3}\alpha C_F^2\zeta_3 \\
&-311040\sqrt{3}\alpha C_F^2 - 30720\sqrt{3}\alpha C_F N_f\pi^2 T_F \\
&-103680\sqrt{3}\alpha C_F N_f T_F + 9584\sqrt{3}C_A^2\pi^4 + 85008\sqrt{3}C_A^2\pi^2 \\
&+109836\sqrt{3}C_A^2\zeta_3 + 115029\sqrt{3}C_A^2 - 13568\sqrt{3}C_A C_F\pi^4 \\
&-330816\sqrt{3}C_A C_F\pi^2 - 31104\sqrt{3}C_A C_F\zeta_3 \\
&-694656\sqrt{3}C_A C_F - 1536\sqrt{3}C_A N_f\pi^4 T_F \\
&+29568\sqrt{3}C_A N_f\pi^2 T_F + 145152\sqrt{3}C_A N_f T_F\zeta_3 \\
&-79200\sqrt{3}C_A N_f T_F - 4096\sqrt{3}C_F^2\pi^4 + 195840\sqrt{3}C_F^2\pi^2 \\
&-290304\sqrt{3}C_F^2\zeta_3 + 264384\sqrt{3}C_F^2 + 6144\sqrt{3}C_F N_f\pi^2 T_F \\
&-248832\sqrt{3}C_F N_f T_F\zeta_3 + 430272\sqrt{3}C_F N_f T_F \\
&+57600\sqrt{3}N_f^2 T_F^2 + 486\ln(3)^2\alpha^2 C_A^2\pi \\
&-864\ln(3)^2\alpha^2 C_A C_F\pi + 756\ln(3)^2\alpha C_A^2\pi \\
&-6912\ln(3)^2\alpha C_A C_F\pi + 3456\ln(3)^2\alpha C_F^2\pi \\
&-3078\ln(3)^2 C_A^2\pi + 9072\ln(3)^2 C_A C_F\pi \\
&-864\ln(3)^2 C_A N_f\pi T_F + 1728\ln(3)^2 C_F^2\pi \\
&-5832\ln(3)\alpha^2 C_A^2\pi + 10368\ln(3)\alpha^2 C_A C_F\pi \\
&-9072\ln(3)\alpha C_A^2\pi + 82944\ln(3)\alpha C_A C_F\pi \\
&-41472\ln(3)\alpha C_F^2\pi + 36936\ln(3)C_A^2\pi \\
&-108864\ln(3)C_A C_F\pi + 10368\ln(3)C_A N_f\pi T_F \\
&-20736\ln(3)C_F^2\pi - 522\alpha^2 C_A^2\pi^3 + 928\alpha^2 C_A C_F\pi^3 \\
&-812\alpha C_A^2\pi^3 + 7424\alpha C_A C_F\pi^3 - 3712\alpha C_F^2\pi^3 \\
&+3306 C_A^2\pi^3 - 9744 C_A C_F\pi^3 + 928 C_A N_f\pi^3 T_F - 1856 C_F^2\pi^3 \\
&+72\sqrt{3}\left(66\psi'\left(\tfrac{1}{3}\right)\alpha^2 C_A^2 - 24\psi'\left(\tfrac{1}{3}\right)\alpha^2 C_A N_f T_F\right. \\
&-264\psi'\left(\tfrac{1}{3}\right)\alpha C_A^2 - 1056\psi'\left(\tfrac{1}{3}\right)\alpha C_A C_F \\
&+96\psi'\left(\tfrac{1}{3}\right)\alpha C_A N_f T_F + 384\psi'\left(\tfrac{1}{3}\right)\alpha C_F N_f T_F \\
&-858\psi'\left(\tfrac{1}{3}\right) C_A^2 + 528\psi'\left(\tfrac{1}{3}\right) C_A C_F + 312\psi'\left(\tfrac{1}{3}\right) C_A N_f T_F \\
&\left.-192\psi'\left(\tfrac{1}{3}\right) C_F N_f T_F - 44\alpha^2 C_A^2\pi^2 - 297\alpha^2 C_A^2\right. \\
&+16\alpha^2 C_A N_f\pi^2 T_F + 108\alpha^2 C_A N_f T_F + 176\alpha C_A^2\pi^2 \\
&+594\alpha C_A^2 + 704\alpha C_A C_F\pi^2 + 2376\alpha C_A C_F \\
&-64\alpha C_A N_f\pi^2 T_F - 216\alpha C_A N_f T_F - 256\alpha C_F N_f\pi^2 T_F
\end{aligned}
$$

$$
\begin{aligned}
&-864\alpha C_F N_f T_F + 572 C_A^2 \pi^2 + 9699 C_A^2 - 352 C_A C_F \pi^2 \\
&-4752 C_A C_F - 208 C_A N_f \pi^2 T_F - 5892 C_A N_f T_F \\
&+128 C_F N_f \pi^2 T_F + 2160 C_F N_f T_F \\
&+960 N_f^2 T_F^2 \Big) \frac{1}{\epsilon} \Bigg) \frac{1}{31104\sqrt{3}} \Bigg] a^2 \; + \; \mathcal{O}(a^3)
\end{aligned} \tag{3.1.8}
$$

for the coupling constant renormalization constant, with

$$
\begin{aligned}
Z_A^{(\mathrm{qqg})}\Big|_{\mathrm{MOMq}} &= 1 + \Bigg[(-1.5\alpha - 0.666667 N_f + 6.5) \frac{1}{\epsilon} \\
&\quad + 0.75\alpha^2 + 1.5\alpha - 1.111111 N_f + 8.083333 \Big] a \\
&\quad + \Bigg[(2.25\alpha^2 + \alpha N_f - 6.375\alpha + 1.5 N_f - 14.625) \frac{1}{\epsilon^2} \\
&\quad + (-2.496035\alpha^3 - 0.609349\alpha^2 N_f - 3.200129\alpha^2 \\
&\quad - 0.896125\alpha N_f + 19.623376\alpha + 0.671627 N_f \\
&\quad - 22.923368) \frac{1}{\epsilon} \\
&\quad + 1.248017\alpha^4 + 8.191675\alpha^3 - 1.015581\alpha^2 N_f \\
&\quad + 15.117803\alpha^2 - 4.271319\alpha N_f + 37.418456\alpha \\
&\quad - 26.358363 N_f + 120.984314 \Big] a^2 \; + \; \mathcal{O}(a^3) \\
Z_\alpha^{(\mathrm{qqg})}\Big|_{\mathrm{MOMq}} &= 1 + \mathcal{O}(a^3) \\
Z_c^{(\mathrm{qqg})}\Big|_{\mathrm{MOMq}} &= 1 + \left[(-0.75\alpha + 2.25) \frac{1}{\epsilon} + 3.0 \right] a \\
&\quad + \Bigg[(0.84375\alpha^2 + 0.75 N_f - 9.84375) \frac{1}{\epsilon^2} + (-0.685518\alpha^3 \\
&\quad - 2.514088\alpha^2 + 9.780001\alpha + 1.875 N_f - 21.954243) \frac{1}{\epsilon} \\
&\quad + 1.838599\alpha^2 + 10.105127\alpha - 2.604167 N_f + 30.788446 \Big] a^2 \\
&\quad + \mathcal{O}(a^3) \\
Z_\psi^{(\mathrm{qqg})}\Big|_{\mathrm{MOMq}} &= 1 - 1.333333\alpha \left(1 + \frac{1}{\epsilon} \right) a \\
&\quad + \Bigg[\alpha (1.888889\alpha + 3.0) \frac{1}{\epsilon^2} + (-1.218698\alpha^3 - 3.847805\alpha^2 \\
&\quad + 7.509922\alpha + 0.666667 N_f - 11.166667) \frac{1}{\epsilon} - 1.218698\alpha^3 \\
&\quad - 7.847805\alpha^2 - 0.065396\alpha + 2.333333 N_f - 25.464206 \Big] a^2 \\
&\quad + \mathcal{O}(a^3)
\end{aligned} \tag{3.1.9}
$$

numerically. Again we make the important remark that the above three vertex

functions were all calculated at the symmetric subtraction point. The renormalization constants, by definition, already satisfy the Slavnov-Taylor identities. Therefore it is not necessary to check these again since by construction they are automatically satisfied.

3.2 Results for the vertex functions

Once the renormalization constants are fixed up to our desired loop order (in the case of the linear covariant gauge fixing this is up to and including two loops), we can construct the amplitudes. We recall that the amplitudes are the complete set of terms resulting from the sum of all contributing Feynman diagrams for each wave function or vertex function. In this section we record our results for the amplitudes, separately for each channel in both the $\overline{\text{MS}}$ and MOMi schemes. To reiterate all results computed in this gauge have been done so independently as a comparison and a check on our computer code prior to considering other more technical gauges. The results have been published in [14] and are presented numerically for all three vertices in both schemes. For this reason, and for comparison later on in Chapters 4 and 5, we present the amplitudes analytically for only one vertex in both schemes with all other results presented numerically.

3.2.1 The ghost-gluon vertex

We begin by recording the $\overline{\text{MS}}$ amplitudes and relations analytically at two loops for the ghost-gluon vertex. Despite the ghost-gluon vertex having the same number of diagrams as the quark-gluon vertex, the ghost-gluon vertex is chosen to be the vertex we represent results analytically in for two reasons. Firstly this vertex is the simplest of the two, with only two channels to consider, i.e. $\Sigma^{\text{ccg}}_{(1)}(p,q)$ and $\Sigma^{\text{ccg}}_{(2)}(p,q)$. Secondly the ghost-gluon vertex provides the smallest set of analytic results for all three vertices since the ghosts are scalars, whereas the quarks are fermions which involve extra spinor indices and γ-matrices by construction. It is also the case that in the Curci-Ferrari gauge it is this vertex which is different from the arbitrary (linear) covariant gauge, as briefly mentioned in our introduction. For the $\overline{\text{MS}}$ scheme the two independent amplitudes for the ghost-gluon

vertex are

$$
\begin{aligned}
\Sigma^{\rm ccg}_{(1)}(p,q)\Big|_{\overline{\rm MS}} \;=\; 1 + \Big(&288\sqrt{3}C_A\left[3\psi'\left(\tfrac{1}{3}\right)\alpha^2 + 24\psi'\left(\tfrac{1}{3}\right)\alpha - 15\psi'\left(\tfrac{1}{3}\right) - 2\alpha^2\pi^2\right.\\
&\left.-16\alpha\pi^2 - 108\alpha + 10\pi^2 - 108\right]a\\
&+C_A\left[-216\sqrt{3}\psi'\left(\tfrac{1}{3}\right)\alpha^4 C_A + 2592\sqrt{3}\psi'\left(\tfrac{1}{3}\right)\alpha^3 C_A\right.\\
&-9240\sqrt{3}\psi'\left(\tfrac{1}{3}\right)\alpha^2 C_A + 1920\sqrt{3}\psi'\left(\tfrac{1}{3}\right)\alpha^2 N_f T_F\\
&+19368\sqrt{3}\psi'\left(\tfrac{1}{3}\right)\alpha C_A + 2304\sqrt{3}\psi'\left(\tfrac{1}{3}\right)\alpha N_f T_F\\
&+175416\sqrt{3}\psi'\left(\tfrac{1}{3}\right) C_A - 78528\sqrt{3}\psi'\left(\tfrac{1}{3}\right) N_f T_F\\
&+9\sqrt{3}\psi'''\left(\tfrac{1}{3}\right)\alpha^3 C_A - 171\sqrt{3}\psi'''\left(\tfrac{1}{3}\right)\alpha^2 C_A\\
&+279\sqrt{3}\psi'''\left(\tfrac{1}{3}\right)\alpha C_A + 999\sqrt{3}\psi'''\left(\tfrac{1}{3}\right) C_A\\
&+19440\sqrt{3}s_2\left(\tfrac{\pi}{6}\right)\alpha^3 C_A - 124416\sqrt{3}s_2\left(\tfrac{\pi}{6}\right)\alpha^2 C_A\\
&+136080\sqrt{3}s_2\left(\tfrac{\pi}{6}\right)\alpha C_A + 1275264\sqrt{3}s_2\left(\tfrac{\pi}{6}\right) C_A\\
&-497664\sqrt{3}s_2\left(\tfrac{\pi}{6}\right) N_f T_F - 38880\sqrt{3}s_2\left(\tfrac{\pi}{2}\right)\alpha^3 C_A\\
&+248832\sqrt{3}s_2\left(\tfrac{\pi}{2}\right)\alpha^2 C_A - 272160\sqrt{3}s_2\left(\tfrac{\pi}{2}\right)\alpha C_A\\
&-2550528\sqrt{3}s_2\left(\tfrac{\pi}{2}\right) C_A + 995328\sqrt{3}s_2\left(\tfrac{\pi}{2}\right) N_f T_F\\
&-32400\sqrt{3}s_3\left(\tfrac{\pi}{6}\right)\alpha^3 C_A + 207360\sqrt{3}s_3\left(\tfrac{\pi}{6}\right)\alpha^2 C_A\\
&-226800\sqrt{3}s_3\left(\tfrac{\pi}{6}\right)\alpha C_A - 2125440\sqrt{3}s_3\left(\tfrac{\pi}{6}\right) C_A\\
&+829440\sqrt{3}s_3\left(\tfrac{\pi}{6}\right) N_f T_F + 25920\sqrt{3}s_3\left(\tfrac{\pi}{2}\right)\alpha^3 C_A\\
&-165888\sqrt{3}s_3\left(\tfrac{\pi}{2}\right)\alpha^2 C_A + 181440\sqrt{3}s_3\left(\tfrac{\pi}{2}\right)\alpha C_A\\
&+1700352\sqrt{3}s_3\left(\tfrac{\pi}{2}\right) C_A - 663552\sqrt{3}s_3\left(\tfrac{\pi}{2}\right) N_f T_F\\
&+144\sqrt{3}\alpha^4 C_A\pi^2 - 24\sqrt{3}\alpha^3 C_A\pi^4 - 1728\sqrt{3}\alpha^3 C_A\pi^2\\
&-324\sqrt{3}\alpha^3 C_A\zeta_3 + 456\sqrt{3}\alpha^2 C_A\pi^4 + 6160\sqrt{3}\alpha^2 C_A\pi^2\\
&-648\sqrt{3}\alpha^2 C_A\zeta_3 - 16848\sqrt{3}\alpha^2 C_A\\
&-1280\sqrt{3}\alpha^2 N_f\pi^2 T_F - 744\sqrt{3}\alpha C_A\pi^4\\
&-12912\sqrt{3}\alpha C_A\pi^2 + 40500\sqrt{3}\alpha C_A\zeta_3\\
&-215784\sqrt{3}\alpha C_A - 1536\sqrt{3}\alpha N_f\pi^2 T_F\\
&+10368\sqrt{3}\alpha N_f T_F - 2664\sqrt{3}C_A\pi^4\\
&-116944\sqrt{3}C_A\pi^2 - 202824\sqrt{3}C_A\zeta_3\\
&-194616\sqrt{3}C_A + 52352\sqrt{3}N_f\pi^2 T_F\\
&+82944\sqrt{3}N_f T_F\zeta_3 + 53568\sqrt{3}N_f T_F\\
&+135\ln(3)^2\alpha^3 C_A\pi - 864\ln(3)^2\alpha^2 C_A\pi\\
&+945\ln(3)^2\alpha C_A\pi + 8856\ln(3)^2 C_A\pi
\end{aligned}
$$

$$
\begin{aligned}
&-3456\ln(3)^2 N_f\pi T_F - 1620\ln(3)\alpha^3 C_A\pi \\
&+10368\ln(3)\alpha^2 C_A\pi - 11340\ln(3)\alpha C_A\pi \\
&-106272\ln(3)C_A\pi + 41472\ln(3)N_f\pi T_F \\
&-145\alpha^3 C_A\pi^3 + 928\alpha^2 C_A\pi^3 - 1015\alpha C_A\pi^3 \\
&-9512 C_A\pi^3 + 3712 N_f\pi^3 T_F\big]\, a^2\Big)\,\frac{1}{62208\sqrt{3}} \;+\; \mathcal{O}(a^3)
\end{aligned}
$$

$$
\begin{aligned}
\Sigma^{\rm ccg}_{(2)}(p,q)\Big|_{\overline{\rm MS}} \;=\; &\Big(288\sqrt{3}C_A\left[-3\psi'\left(\tfrac{1}{3}\right)\alpha^2 + 12\psi'\left(\tfrac{1}{3}\right)\alpha + 15\psi'\left(\tfrac{1}{3}\right) + 2\alpha^2\pi^2\right. \\
&\left.-8\alpha\pi^2 - 54\alpha - 10\pi^2 + 54\right] a \\
&+C_A\Big[216\sqrt{3}\psi'\left(\tfrac{1}{3}\right)\alpha^4 C_A - 2592\sqrt{3}\psi'\left(\tfrac{1}{3}\right)\alpha^3 C_A \\
&+19608\sqrt{3}\psi'\left(\tfrac{1}{3}\right)\alpha^2 C_A - 1920\sqrt{3}\psi'\left(\tfrac{1}{3}\right)\alpha^2 N_f T_F \\
&+25992\sqrt{3}\psi'\left(\tfrac{1}{3}\right)\alpha C_A - 2304\sqrt{3}\psi'\left(\tfrac{1}{3}\right)\alpha N_f T_F \\
&-91176\sqrt{3}\psi'\left(\tfrac{1}{3}\right) C_A + 78528\sqrt{3}\psi'\left(\tfrac{1}{3}\right) N_f T_F \\
&-9\sqrt{3}\psi'''\left(\tfrac{1}{3}\right)\alpha^3 C_A - 45\sqrt{3}\psi'''\left(\tfrac{1}{3}\right)\alpha^2 C_A \\
&-171\sqrt{3}\psi'''\left(\tfrac{1}{3}\right)\alpha C_A - 999\sqrt{3}\psi'''\left(\tfrac{1}{3}\right) C_A \\
&-19440\sqrt{3}s_2\left(\tfrac{\pi}{6}\right)\alpha^3 C_A + 54432\sqrt{3}s_2\left(\tfrac{\pi}{6}\right)\alpha^2 C_A \\
&+3888\sqrt{3}s_2\left(\tfrac{\pi}{6}\right)\alpha C_A - 878688\sqrt{3}s_2\left(\tfrac{\pi}{6}\right) C_A \\
&+497664\sqrt{3}s_2\left(\tfrac{\pi}{6}\right) N_f T_F + 38880\sqrt{3}s_2\left(\tfrac{\pi}{2}\right)\alpha^3 C_A \\
&-108864\sqrt{3}s_2\left(\tfrac{\pi}{2}\right)\alpha^2 C_A - 7776\sqrt{3}s_2\left(\tfrac{\pi}{2}\right)\alpha C_A \\
&+1757376\sqrt{3}s_2\left(\tfrac{\pi}{2}\right) C_A - 995328\sqrt{3}s_2\left(\tfrac{\pi}{2}\right) N_f T_F \\
&+32400\sqrt{3}s_3\left(\tfrac{\pi}{6}\right)\alpha^3 C_A - 90720\sqrt{3}s_3\left(\tfrac{\pi}{6}\right)\alpha^2 C_A \\
&-6480\sqrt{3}s_3\left(\tfrac{\pi}{6}\right)\alpha C_A + 1464480\sqrt{3}s_3\left(\tfrac{\pi}{6}\right) C_A \\
&-829440\sqrt{3}s_3\left(\tfrac{\pi}{6}\right) N_f T_F - 25920\sqrt{3}s_3\left(\tfrac{\pi}{2}\right)\alpha^3 C_A \\
&+72576\sqrt{3}s_3\left(\tfrac{\pi}{2}\right)\alpha^2 C_A + 5184\sqrt{3}s_3\left(\tfrac{\pi}{2}\right)\alpha C_A \\
&-1171584\sqrt{3}s_3\left(\tfrac{\pi}{2}\right) C_A + 663552\sqrt{3}s_3\left(\tfrac{\pi}{2}\right) N_f T_F \\
&-144\sqrt{3}\alpha^4 C_A\pi^2 + 24\sqrt{3}\alpha^3 C_A\pi^4 + 1728\sqrt{3}\alpha^3 C_A\pi^2 \\
&+324\sqrt{3}\alpha^3 C_A\zeta_3 + 120\sqrt{3}\alpha^2 C_A\pi^4 - 13072\sqrt{3}\alpha^2 C_A\pi^2 \\
&+648\sqrt{3}\alpha^2 C_A\zeta_3 - 29808\sqrt{3}\alpha^2 C_A + 1280\sqrt{3}\alpha^2 N_f\pi^2 T_F \\
&+456\sqrt{3}\alpha C_A\pi^4 - 17328\sqrt{3}\alpha C_A\pi^2 - 17172\sqrt{3}\alpha C_A\zeta_3 \\
&-13608\sqrt{3}\alpha C_A + 1536\sqrt{3}\alpha N_f\pi^2 T_F - 10368\sqrt{3}\alpha N_f T_F \\
&+2664\sqrt{3}C_A\pi^4 + 60784\sqrt{3}C_A\pi^2 + 148392\sqrt{3}C_A\zeta_3 \\
&+98280\sqrt{3}C_A - 52352\sqrt{3}N_f\pi^2 T_F - 82944\sqrt{3}N_f T_F\zeta_3 \\
&-19008\sqrt{3}N_f T_F - 135\ln(3)^2\alpha^3 C_A\pi + 378\ln(3)^2\alpha^2 C_A\pi
\end{aligned}
$$

$$
\begin{aligned}
&+27\ln(3)^2\alpha C_A\pi - 6102\ln(3)^2 C_A\pi + 3456\ln(3)^2 N_f\pi T_F \\
&+1620\ln(3)\alpha^3 C_A\pi - 4536\ln(3)\alpha^2 C_A\pi - 324\ln(3)\alpha C_A\pi \\
&+73224\ln(3) C_A\pi - 41472\ln(3) N_f\pi T_F + 145\alpha^3 C_A\pi^3 \\
&-406\alpha^2 C_A\pi^3 - 29\alpha C_A\pi^3 + 6554 C_A\pi^3 \\
&-3712 N_f\pi^3 T_F\big]\, a^2\Big)\,\frac{1}{62208\sqrt{3}} \;+\; \mathcal{O}(a^3)\;. \qquad (3.2.10)
\end{aligned}
$$

The same amplitudes considered in the MOMh scheme are

$$
\begin{aligned}
\Sigma^{\rm ccg}_{(1)}(p,q)\Big|_{\rm MOMh} &= -\,1\,+\,\mathcal{O}(a^3) \\
\Sigma^{\rm ccg}_{(2)}(p,q)\Big|_{\rm MOMh} &= \Big(288\sqrt{3}C_A\left[-3\psi'\left(\tfrac{1}{3}\right)\alpha^2 + 12\psi'\left(\tfrac{1}{3}\right)\alpha + 15\psi'\left(\tfrac{1}{3}\right) + 2\alpha^2\pi^2\right. \\
&\qquad \left. -8\alpha\pi^2 - 54\alpha - 10\pi^2 + 54\right] a \\
&\quad +C_A\left[-36\sqrt{3}\psi'\left(\tfrac{1}{3}\right)^2\alpha^4 C_A - 144\sqrt{3}\psi'\left(\tfrac{1}{3}\right)^2\alpha^3 C_A\right. \\
&\qquad +1512\sqrt{3}\psi'\left(\tfrac{1}{3}\right)^2\alpha^2 C_A + 720\sqrt{3}\psi'\left(\tfrac{1}{3}\right)^2\alpha C_A \\
&\qquad -900\sqrt{3}\psi'\left(\tfrac{1}{3}\right)^2 C_A + 48\sqrt{3}\psi'\left(\tfrac{1}{3}\right)\alpha^4 C_A\pi^2 \\
&\qquad +192\sqrt{3}\psi'\left(\tfrac{1}{3}\right)\alpha^3 C_A\pi^2 - 2376\sqrt{3}\psi'\left(\tfrac{1}{3}\right)\alpha^3 C_A \\
&\qquad -2016\sqrt{3}\psi'\left(\tfrac{1}{3}\right)\alpha^2 C_A\pi^2 + 9504\sqrt{3}\psi'\left(\tfrac{1}{3}\right)\alpha^2 C_A \\
&\qquad -960\sqrt{3}\psi'\left(\tfrac{1}{3}\right)\alpha C_A\pi^2 + 13680\sqrt{3}\psi'\left(\tfrac{1}{3}\right)\alpha C_A \\
&\qquad -2304\sqrt{3}\psi'\left(\tfrac{1}{3}\right)\alpha N_f T_F + 1200\sqrt{3}\psi'\left(\tfrac{1}{3}\right) C_A\pi^2 \\
&\qquad -121176\sqrt{3}\psi'\left(\tfrac{1}{3}\right) C_A + 88128\sqrt{3}\psi'\left(\tfrac{1}{3}\right) N_f T_F \\
&\qquad -9\sqrt{3}\psi'''\left(\tfrac{1}{3}\right)\alpha^3 C_A - 45\sqrt{3}\psi'''\left(\tfrac{1}{3}\right)\alpha^2 C_A \\
&\qquad -171\sqrt{3}\psi'''\left(\tfrac{1}{3}\right)\alpha C_A - 999\sqrt{3}\psi'''\left(\tfrac{1}{3}\right) C_A \\
&\qquad -19440\sqrt{3}s_2\left(\tfrac{\pi}{6}\right)\alpha^3 C_A + 54432\sqrt{3}s_2\left(\tfrac{\pi}{6}\right)\alpha^2 C_A \\
&\qquad +3888\sqrt{3}s_2\left(\tfrac{\pi}{6}\right)\alpha C_A - 878688\sqrt{3}s_2\left(\tfrac{\pi}{6}\right) C_A \\
&\qquad +497664\sqrt{3}s_2\left(\tfrac{\pi}{6}\right) N_f T_F + 38880\sqrt{3}s_2\left(\tfrac{\pi}{2}\right)\alpha^3 C_A \\
&\qquad -108864\sqrt{3}s_2\left(\tfrac{\pi}{2}\right)\alpha^2 C_A - 7776\sqrt{3}s_2\left(\tfrac{\pi}{2}\right)\alpha C_A \\
&\qquad +1757376\sqrt{3}s_2\left(\tfrac{\pi}{2}\right) C_A - 995328\sqrt{3}s_2\left(\tfrac{\pi}{2}\right) N_f T_F \\
&\qquad +32400\sqrt{3}s_3\left(\tfrac{\pi}{6}\right)\alpha^3 C_A - 90720\sqrt{3}s_3\left(\tfrac{\pi}{6}\right)\alpha^2 C_A \\
&\qquad -6480\sqrt{3}s_3\left(\tfrac{\pi}{6}\right)\alpha C_A + 1464480\sqrt{3}s_3\left(\tfrac{\pi}{6}\right) C_A \\
&\qquad -829440\sqrt{3}s_3\left(\tfrac{\pi}{6}\right) N_f T_F - 25920\sqrt{3}s_3\left(\tfrac{\pi}{2}\right)\alpha^3 C_A \\
&\qquad +72576\sqrt{3}s_3\left(\tfrac{\pi}{2}\right)\alpha^2 C_A + 5184\sqrt{3}s_3\left(\tfrac{\pi}{2}\right)\alpha C_A \\
&\qquad -1171584\sqrt{3}s_3\left(\tfrac{\pi}{2}\right) C_A + 663552\sqrt{3}s_3\left(\tfrac{\pi}{2}\right) N_f T_F \\
&\qquad -16\sqrt{3}\alpha^4 C_A\pi^4 - 40\sqrt{3}\alpha^3 C_A\pi^4 + 1584\sqrt{3}\alpha^3 C_A\pi^2
\end{aligned}
$$

$$
\begin{aligned}
&+324\sqrt{3}\alpha^3 C_A\zeta_3 + 792\sqrt{3}\alpha^2 C_A\pi^4 - 6336\sqrt{3}\alpha^2 C_A\pi^2 \\
&+648\sqrt{3}\alpha^2 C_A\zeta_3 - 10368\sqrt{3}\alpha^2 C_A + 776\sqrt{3}\alpha C_A\pi^4 \\
&-9120\sqrt{3}\alpha C_A\pi^2 - 17172\sqrt{3}\alpha C_A\zeta_3 + 9720\sqrt{3}\alpha C_A \\
&+1536\sqrt{3}\alpha N_f\pi^2 T_F - 10368\sqrt{3}\alpha N_f T_F + 2264\sqrt{3}C_A\pi^4 \\
&+80784\sqrt{3}C_A\pi^2 + 148392\sqrt{3}C_A\zeta_3 + 1944\sqrt{3}C_A \\
&-58752\sqrt{3}N_f\pi^2 T_F - 82944\sqrt{3}N_f T_F\zeta_3 \\
&+15552\sqrt{3}N_f T_F - 135\ln(3)^2\alpha^3 C_A\pi \\
&+378\ln(3)^2\alpha^2 C_A\pi + 27\ln(3)^2\alpha C_A\pi - 6102\ln(3)^2 C_A\pi \\
&+3456\ln(3)^2 N_f\pi T_F + 1620\ln(3)\alpha^3 C_A\pi \\
&-4536\ln(3)\alpha^2 C_A\pi - 324\ln(3)\alpha C_A\pi \\
&+73224\ln(3)C_A\pi - 41472\ln(3)N_f\pi T_F + 145\alpha^3 C_A\pi^3 \\
&-406\alpha^2 C_A\pi^3 - 29\alpha C_A\pi^3 + 6554 C_A\pi^3 \\
&-3712 N_f\pi^3 T_F\big]\, a^2\big)\,\frac{1}{62208\sqrt{3}} \;+\; \mathcal{O}(a^3)
\end{aligned}
\tag{3.2.11}
$$

where we recognise that in this scheme there is only one independent amplitude. Since channel 1 contained the poles in ϵ before MOMh renormalization, there exist no corrections at the symmetric subtraction point for this scheme. Recall that channel 1 corresponds to the tree level vertex structure and thus defines the renormalization condition. An important point to note, which we revisit in section 3.3, is that $\Sigma\big|_{\text{MOMh}}$ corresponds to the amplitudes in the MOMh scheme with MOMh scheme-dependent variables. i.e. $\alpha \to \alpha_{\text{MOMh}}$ and $a \to a_{\text{MOMh}}$. The same goes for all schemes where results in the MOMg scheme are dependent on the MOMg scheme variables, etc.

3.2.2 The triple-gluon vertex

Presenting the amplitudes for the triple-gluon vertex numerically we begin with those computed in the $\overline{\text{MS}}$ scheme

$$
\begin{aligned}
\Sigma^{\text{ggg}}_{(1)}(p,q)\Big|_{\overline{\text{MS}}} &= \Sigma^{\text{ggg}}_{(2)}(p,q)\Big|_{\overline{\text{MS}}} = -\frac{1}{2}\,\Sigma^{\text{ggg}}_{(3)}(p,q)\Big|_{\overline{\text{MS}}} = -\Sigma^{\text{ggg}}_{(4)}(p,q)\Big|_{\overline{\text{MS}}} \\
&= \frac{1}{2}\,\Sigma^{\text{ggg}}_{(5)}(p,q)\Big|_{\overline{\text{MS}}} = -\Sigma^{\text{ggg}}_{(6)}(p,q)\Big|_{\overline{\text{MS}}} \\
&= -1 - \big[1.121244 - 3.761896\alpha - 1.289023\alpha^2 + 0.1250000\alpha^3 \\
&\qquad -0.041737 N_f\big]\, a \\
&\quad + \big[29.753068 + 16.460077\alpha - 9.779430\alpha^2 - 3.206081\alpha^3
\end{aligned}
$$

$$
\begin{aligned}
& -1.652285\alpha^4 + 0.281250\alpha^5 - [11.567720 - 0.968698\alpha \\
& -0.911240\alpha^2 + 0.416667\alpha^3]N_f\big]\, a^2 \;+\; \mathcal{O}(a^3) \\
\Sigma^{\rm ggg}_{(7)}(p,q)\Big|_{\overline{\rm MS}} &= 2\,\Sigma^{\rm ggg}_{(9)}(p,q)\Big|_{\overline{\rm MS}} \;=\; -\,2\,\Sigma^{\rm ggg}_{(11)}(p,q)\Big|_{\overline{\rm MS}} \;=\; -\;\Sigma^{\rm ggg}_{(14)}(p,q)\Big|_{\overline{\rm MS}} \\
&= \big[7.056716 - 3.328046\alpha - 0.507930\alpha^2 + 0.057318\alpha^3 \\
& -1.092686N_f\big]\, a \\
& + \big[116.078964 - 13.683082\alpha + 0.348413\alpha^2 + 4.776312\alpha^3 \\
& +0.890861\alpha^4 - 0.128965\alpha^5 - [20.271011 + 1.015302\alpha \\
& -0.574522\alpha^2 - 0.191060\alpha^3]N_f\big]\, a^2 \;+\; \mathcal{O}(a^3) \\
\Sigma^{\rm ggg}_{(8)}(p,q)\Big|_{\overline{\rm MS}} &= -\;\Sigma^{\rm ggg}_{(13)}(p,q)\Big|_{\overline{\rm MS}} \\
&= \big[7.368300 - 3.351838\alpha - 0.570116\alpha^2 + 0.192682\alpha^3 \\
& -1.213010N_f\big]\, a \\
& + \big[126.004871 - 11.804885\alpha + 3.779569\alpha^2 + 4.377919\alpha^3 \\
& +1.288709\alpha^4 - 0.433535\alpha^5 - [23.589819 - 0.015581\alpha \\
& -0.936332\alpha^2 - 0.642274\alpha^3]N_f\big]\, a^2 \;+\; \mathcal{O}(a^3) \\
\Sigma^{\rm ggg}_{(10)}(p,q)\Big|_{\overline{\rm MS}} &= -\;\Sigma^{\rm ggg}_{(12)}(p,q)\Big|_{\overline{\rm MS}} \\
&= -\big[0.311584 - 0.023791\alpha - 0.062186\alpha^2 + 0.135364\alpha^3 \\
& -0.120324N_f]a \\
& - \big[9.925907 + 1.878196\alpha + 3.431156\alpha^2 - 0.398393\alpha^3 \\
& +0.397848\alpha^4 - 0.304570\alpha^5 - [3.318808 - 1.030883\alpha \\
& -0.361810\alpha^2 - 0.451214\alpha^3]N_f\big]\, a^2 \;+\; \mathcal{O}(a^3)\;. \qquad (3.2.12)
\end{aligned}
$$

The relations between amplitudes of the various projection tensor channels have been detailed above. These are consistent with the expectations for the structure of the vertex from symmetry, given that we have evaluated the vertex function at the symmetric point, [14]. A relationship also holds between $\Sigma^{\rm ggg}_{(7)}(p,q)$, $\Sigma^{\rm ggg}_{(8)}(p,q)$ and $\Sigma^{\rm ggg}_{(10)}(p,q)$ in the MOMg scheme, which was commented on in [14]. However, following a misprint in [14] we present the correct relation as

$$
\Sigma^{\rm ggg}_{(7)}(p,q)\Big|_{\overline{\rm MS}} \;=\; \Sigma^{\rm ggg}_{(8)}(p,q)\Big|_{\overline{\rm MS}} \;+\; \Sigma^{\rm ggg}_{(10)}(p,q)\Big|_{\overline{\rm MS}} \qquad (3.2.13)
$$

which holds in the linear covariant gauge for arbitrary α to two loops. The MOMg scheme amplitudes satisfy the same relations. In particular we have

$$
\Sigma^{\rm ggg}_{(1)}(p,q)\Big|_{\rm MOMg} \;=\; \Sigma^{\rm ggg}_{(2)}(p,q)\Big|_{\rm MOMg} \;=\; -\;\frac{1}{2}\,\Sigma^{\rm ggg}_{(3)}(p,q)\Big|_{\rm MOMg}
$$

$$
\begin{aligned}
&= \; - \; \Sigma^{ggg}_{(4)}(p,q)\Big|_{\rm MOMg} \; = \; \frac{1}{2}\,\Sigma^{ggg}_{(5)}(p,q)\Big|_{\rm MOMg} \\
&= \; - \; \Sigma^{ggg}_{(6)}(p,q)\Big|_{\rm MOMg} \; = \; -\,1 \; + \; \mathcal{O}(a^3) \\
\Sigma^{ggg}_{(7)}(p,q)\Big|_{\rm MOMg} &= \; 2\,\Sigma^{ggg}_{(9)}(p,q)\Big|_{\rm MOMg} \; = \; -\,2\,\Sigma^{ggg}_{(11)}(p,q)\Big|_{\rm MOMg} \\
&= \; - \; \Sigma^{ggg}_{(14)}(p,q)\Big|_{\rm MOMg} \\
&= \; \big[7.056716 - 3.328046\alpha - 0.507930\alpha^2 + 0.057318\alpha^3 \\
&\quad -1.092686N_f\big]\,a \\
&\quad - \big[78.783317 - 99.199663\alpha + 10.001223\alpha^2 + 10.910924\alpha^3 \\
&\quad -1.202495\alpha^4 - 0.283161\alpha^5 + 0.021494\alpha^6 \\
&\quad -[34.308079 - 16.242288\alpha - 1.820392\alpha^2 \\
&\quad +0.607994\alpha^3]N_f + 3.779101N_f^2\big]\,a^2 \; + \; \mathcal{O}(a^3) \\
\Sigma^{ggg}_{(8)}(p,q)\Big|_{\rm MOMg} &= \; - \; \Sigma^{ggg}_{(13)}(p,q)\Big|_{\rm MOMg} \\
&= \; \big[7.368300 - 3.351838\alpha - 0.570116\alpha^2 + 0.192682\alpha^3 \\
&\quad -1.213010N_f\big]\,a \\
&\quad - \big[77.461404 - 103.656823\alpha + 5.551499\alpha^2 + 12.546334\alpha^3 \\
&\quad -2.943107\alpha^4 - 0.525374\alpha^5 + 0.0722558\alpha^6 \\
&\quad -[35.389486 - 16.083732\alpha - 1.730035\alpha^2 \\
&\quad +1.121278\alpha^3]N_f + 4.195246N_f^2\big]\,a^2 \; + \; \mathcal{O}(a^3) \\
\Sigma^{ggg}_{(10)}(p,q)\Big|_{\rm MOMg} &= \; - \; \Sigma^{ggg}_{(12)}(p,q)\Big|_{\rm MOMg} \\
&= \; - \big[0.311584 - 0.023791\alpha - 0.062186\alpha^2 + 0.135364\alpha^3 \\
&\quad -0.120324N_f\big]\,a \\
&\quad - \big[1.321912 + 4.457161\alpha + 4.4497230\alpha^2 - 1.635410\alpha^3 \\
&\quad +1.740612\alpha^4 + 0.242213\alpha^5 - 0.050762\alpha^6 \\
&\quad +[1.081407 + 0.158552\alpha + 0.090357\alpha^2 + 0.513285\alpha^3]N_f \\
&\quad -0.416150N_f^2\big]\,a^2 \; + \; \mathcal{O}(a^3)
\end{aligned}
\tag{3.2.14}
$$

with the corresponding relation

$$
\Sigma^{ggg}_{(7)}(p,q)\Big|_{\rm MOMg} \; = \; \Sigma^{ggg}_{(8)}(p,q)\Big|_{\rm MOMg} \; + \; \Sigma^{ggg}_{(10)}(p,q)\Big|_{\rm MOMg} \tag{3.2.15}
$$

for the MOMg scheme also holding true to two loops. Given the nature of the MOMg scheme the relations for the amplitudes of channels 1 to 6 demonstrate

that our renormalization is consistent and that our projection has been implemented consistently within our FORM programmes. The recovery of this relation also serves as a check on our REDUZE database.

3.2.3 The quark-gluon vertex

Finally, we complete our presentation of results for the amplitudes with the quark-gluon vertex and the MOMq scheme expressions. Firstly the $\overline{\rm MS}$ amplitudes are

$$\begin{aligned}
\Sigma^{\rm qqg}_{(1)}(p,q)\Big|_{\overline{\rm MS}} &= 1 + \left[4.316221 - 0.588760\alpha - 0.457012\alpha^2\right] a \\
&\quad + \left[89.287678 - 2.548866\alpha + 0.795946\alpha^2 + 0.234428\alpha^3\right. \\
&\quad \left. +0.342759\alpha^4 - (12.136677 + 0.976628\alpha \right. \\
&\quad \left. +0.507791\alpha^2)N_f\right] a^2 + \mathcal{O}(a^3) \\
\Sigma^{\rm qqg}_{(2)}(p,q)\Big|_{\overline{\rm MS}} &= \Sigma^{\rm qqg}_{(5)}(p,q)\Big|_{\overline{\rm MS}} \\
&= \left[2.598034 - 2.305695\alpha - 0.414023\alpha^2\right] a \\
&\quad + \left[26.481247 - 21.748851\alpha - 5.398494\alpha^2 + 0.454787\alpha^3\right. \\
&\quad \left. +0.310517\alpha^4 - (6.271894 + 1.033946\alpha \right. \\
&\quad \left. +0.460026\alpha^2)N_f\right] a^2 + \mathcal{O}(a^3) \\
\Sigma^{\rm qqg}_{(3)}(p,q)\Big|_{\overline{\rm MS}} &= \Sigma^{\rm qqg}_{(4)}(p,q)\Big|_{\overline{\rm MS}} \\
&= \left[2.050269 - 2.522631\alpha - 0.5\alpha^2\right] a \\
&\quad + \left[12.735294 - 25.229976\alpha - 6.681979\alpha^2 + 0.032068\alpha^3\right. \\
&\quad \left. +0.375\alpha^4 - (4.871593 + 0.919310\alpha + 0.555556\alpha^2)N_f\right] a^2 \\
&\quad + \mathcal{O}(a^3) \\
\Sigma^{\rm qqg}_{(6)}(p,q)\Big|_{\overline{\rm MS}} &= - \left[4.362272 + 2.343907\alpha + 0.585977\alpha^2\right] a \\
&\quad - \left[131.991115 + 45.467503\alpha + 4.857352\alpha^2 + 1.220785\alpha^3\right. \\
&\quad \left. -0.439483\alpha^4 - (10.922850 + 1.953256\alpha \right. \\
&\quad \left. -0.651085\alpha^2)N_f\right] a^2 + \mathcal{O}(a^3)
\end{aligned} \tag{3.2.16}$$

where all the above expressions are dependent on $\overline{\rm MS}$ variables $a_{\overline{\rm MS}}$ and $\alpha_{\overline{\rm MS}}$ and the symmetry of the exchange of the two external quark legs is manifest. This was not imposed but emerges naturally from the computation. The corresponding MOMq scheme expressions are

$$\Sigma^{\rm qqg}_{(1)}(p,q)\Big|_{\rm MOMq} = 1 + \mathcal{O}(a^3)$$

$$
\begin{aligned}
\Sigma^{\mathrm{qqg}}_{(2)}(p,q)\Big|_{\mathrm{MOMq}} &= \Sigma^{\mathrm{qqg}}_{(5)}(p,q)\Big|_{\mathrm{MOMq}} \\
&= \left[2.598034 - 2.305695\alpha - 0.414023\alpha^2\right] a \\
&\quad - \left[28.160581 - 15.726713\alpha + 11.991691\alpha^2 + 5.162779\alpha^3 \right. \\
&\quad \left. + 0.567640\alpha^4 + (3.385190 + 1.033946\alpha)N_f\right] a^2 \; + \; \mathcal{O}(a^3) \\
\Sigma^{\mathrm{qqg}}_{(3)}(p,q)\Big|_{\mathrm{MOMq}} &= \Sigma^{\mathrm{qqg}}_{(4)}(p,q)\Big|_{\mathrm{MOMq}} \\
&= \left[2.050269 - 2.522631\alpha - 0.5\alpha^2\right] a \\
&\quad - \left[30.385945 - 13.448043\alpha + 14.158714\alpha^2 + 6.393020\alpha^3 \right. \\
&\quad \left. + 0.685517\alpha^4 + (2.593517 + 0.919310\alpha)N_f\right] a^2 \; + \; \mathcal{O}(a^3) \\
\Sigma^{\mathrm{qqg}}_{(6)}(p,q)\Big|_{\mathrm{MOMq}} &= - \left[4.362272 + 2.343907\alpha + 0.585977\alpha^2\right] a \\
&\quad - \left[40.243836 + 27.911352\alpha + 15.105921\alpha^2 + 7.910933\alpha^3 \right. \\
&\quad \left. + 0.803395\alpha^4 - (6.075881 + 1.953256\alpha)N_f\right] a^2 \\
&\quad + \mathcal{O}(a^3)
\end{aligned}
\tag{3.2.17}
$$

where clearly channel 1 correctly corresponds to the MOMq scheme definition as it is the only channel to contain the divergences in ϵ. The quark external leg interchange which is manifest in the $\overline{\mathrm{MS}}$ scheme results for the amplitudes also correctly emerges here.

In order to demonstrate the impact that increasing the loop order has on the amplitudes we graphically present the ghost-gluon vertex at the symmetric point. We plot the one and two loop amplitudes for various values of α and N_f with respect to the partial coupling constants $a_l(\mu, \Lambda)$. Here l is the loop order and Λ is the QCD scale defined in (3.2.20), not to be confused with that defined in (2.1.20), where we define and compute the ratio of Λ parameters in all gauges in different renormalization schemes for comparison later. To plot this vertex function we have determined the channel 1 amplitude, the amplitude corresponding to the Feynman rule for this vertex, numerically for $SU(3)$. The partial coupling constants are given by solving the β-function as a differential equation for the coupling constant. The β-function is given by

$$
\beta(a) = \frac{\partial a}{\partial \ln \mu} \; . \tag{3.2.18}
$$

The β-function is a formal power series in a. If we denote the solution to the truncated β-function at l loops by $a_l(\mu, \Lambda)$ then we can write the one loop β-

function as

$$\beta(a_1) = -\beta_0 a_1^2 \tag{3.2.19}$$

for instance. Combining (3.2.18) and (3.2.19) and rearranging for a_1 we obtain

$$\begin{aligned} -\frac{1}{a_1^2}\frac{\partial a_1}{\partial \ln \mu} &= \beta_0 \\ \frac{1}{a_1} &= \beta_0 \ln\left(\frac{\mu^2}{\Lambda^2}\right) \\ a_1 &= \frac{1}{\beta_0 \ln\left(\frac{\mu^2}{\Lambda^2}\right)} \,. \end{aligned} \tag{3.2.20}$$

Here (3.2.20) implicitly defines Λ Thus

$$a_1(\mu, \Lambda) = \frac{1}{\beta_0 L} \tag{3.2.21}$$

where $L = \ln\left(\frac{\mu^2}{\Lambda^2}\right)$. Based on the two loop result, $a_2(\mu, \Lambda)$ is determined a similar way with

$$\beta(a_2) = -\beta_0 a_2^2 - \beta_1 a_2^3 \tag{3.2.22}$$

such that

$$a_2(\mu, \Lambda) = \frac{1}{\beta_0 L}\left[1 - \frac{\beta_1 \ln(L)}{\beta_0^2 L}\right] \,. \tag{3.2.23}$$

These are all we need since we only plot the one and two loop ghost-gluon vertex function amplitudes. If the three loop $\overline{\text{MS}}$ results were computed we would need to introduce a third partial coupling constant, namely

$$a_3(\mu, \Lambda) = \frac{1}{\beta_0 L}\left[1 - \frac{\beta_1 \ln(L)}{\beta_0^2 L} + \left[\beta_1^2\left(\ln^2 L - \ln L - 1\right) + \beta_0\beta_2\right]\frac{1}{\beta_0^4 L^2}\right] \tag{3.2.24}$$

with

$$\begin{aligned} \beta_0 &= \frac{1}{3}\left[-11C_A + 4N_f T_F\right] \quad , \quad \beta_1 = \frac{2}{3}\left[-17C_A^2 + 10C_A N_f T_F + 6C_F N_f T_F\right] \\ \beta_2 &= \frac{1}{54}\left[-2857C_A^3 + 2830C_A^2 N_f T_F + 1230C_A C_F N_f T_F - 316C_A N_f^2 T_F^2\right. \\ &\qquad \left. -108C_F^2 N_f T_F - 264C_F N_f^2 T_F^2\right] \,. \end{aligned} \tag{3.2.25}$$

Note that we are using the three loop solution from [1, 2, 81, 82, 83]. We also choose this point to define the anomalous dimension of the arbitrary gauge parameter, γ_α. We define this here for convenience as it appears in our definition of the β-function (3.3.29) later,

$$\begin{aligned}\gamma_A(a,\alpha) &= \beta(a,\alpha)\frac{\partial}{\partial a}\ln Z_A \;+\; \alpha\gamma_\alpha(a,\alpha)\frac{\partial}{\partial\alpha}\ln Z_A \\ \gamma_\alpha(a,\alpha) &= \left[\beta(a,\alpha)\frac{\partial}{\partial a}\ln Z_\alpha \;-\; \gamma_A(a,\alpha)\right]\left[1 \;-\; \alpha\frac{\partial}{\partial\alpha}\ln Z_\alpha\right]^{-1} . \end{aligned} \tag{3.2.26}$$

Note that we have shown a general definition of γ_α which will be applicable in all gauges. However, in the linear coavariant gauge the anomalous dimensions for the arbitrary gauge parameter and gluon field are equivalent, as we will see in (3.4.60).

In order to plot the one and two loop amplitudes on the same graph we need to truncate the vertex function so that the one loop amplitude is a function of $a_1(\mu,\Lambda)$ and the two loop amplitude consists of both the one and two loop contributions multiplying $a_2(\mu,\Lambda)$ and $a_2(\mu,\Lambda)^2$ respectively. This truncated vertex function is defined by, [67],

$$\mathrm{T}^{\mathrm{ccg}}_{k,l} \;=\; \sum_{n=0}^{l} \Sigma^{\mathrm{ccg}}_{(k)n} \left(a_l(\mu,\Lambda)\right)^n \tag{3.2.27}$$

where k defines the channel and n defines the loop order. Here a_l is the solution to the nth order β-function differential equation. The amplitudes then become

$$\Sigma^{\mathrm{ccg}}_{(k)}(p,q)\Big|_{p^2=q^2=-\mu^2} \;=\; \sum_{n=0}^{\infty} \Sigma^{\mathrm{ccg}}_{(k)n} a^n \;. \tag{3.2.28}$$

These are valid for all three vertex functions, although we only consider the ghost-gluon vertex as this behaves differently in linear and non-linear gauge fixings. We present similar plots for a Curci-Ferrari and MAG analysis in chapters 4 and 5 for comparison. The plots are given for $l = 1, 2$ in the $\overline{\mathrm{MS}}$ scheme at the symmetric point in Figure 3.1. The reason we do not present the MOMi scheme amplitudes graphically for the same channels is because they are constant at the renormalization point. Due to the renormalization prescription imposed the amplitudes corresponding to channel 1 are finite (i.e. fixed to ± 1), which provides no useful comparison between loop orders. Note that in Figure 3.1 and in all later figures the label x on the x-axis is defined by $x = s/\Lambda$, where s is the centre of mass energy and Λ is in the $\overline{\mathrm{MS}}$ scheme, [52, 91, 97]. By studying the plots it

can be seen that there is only a difference of around 1% between the one and two loop amplitudes.

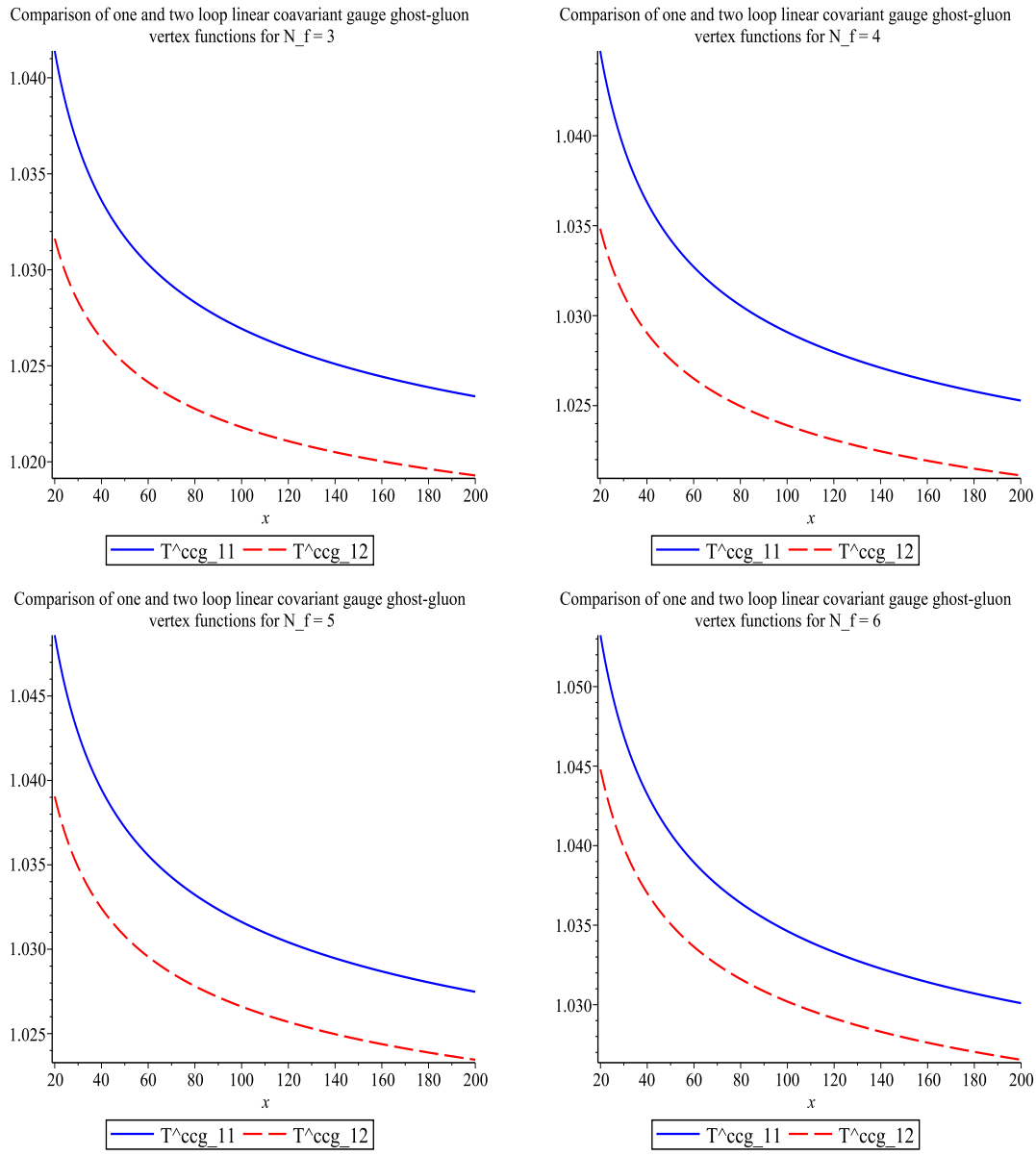

Figure 3.1: Comparison of the one and two loop $\overline{\text{MS}}$ linear covariant gauge ghost-gluon vertex functions for different values of N_f.

3.3 Conversion Functions and Mappings

The aim of our complete calculation is to determine the β-functions and anomalous dimensions for each MOMi scheme at three loops. A similar preliminary evaluation in the $\overline{\text{MS}}$ scheme has already been carried out in [14] of whose work we base our own upon. The renormalization group (RG) equations are used to de-

termine the three loop RG functions without having to complete an explicit three loop calculation. The idea of the renormalization group was originally developed by Gell-Mann and others [84, 85, 86] whilst investigating Quantum Electrodynamics (QED) in the 1950's. Wilson, who was supervised by Gell-Mann at the time, later developed the idea of the renormalization group analysis of strongly coupled field theory, [87]. The RG equation needed in constructing the β-function is

$$\beta^{\mathrm{MOMi}}(a,\alpha) = \left[\beta^{\overline{\mathrm{MS}}}(a_{\overline{\mathrm{MS}}}) \frac{\partial a_{\mathrm{MOMi}}}{\partial a_{\overline{\mathrm{MS}}}} \; + \; \alpha_{\overline{\mathrm{MS}}} \gamma_\alpha^{\overline{\mathrm{MS}}}(a_{\overline{\mathrm{MS}}}, \alpha_{\overline{\mathrm{MS}}}) \frac{\partial a_{\mathrm{MOMi}}}{\partial \alpha_{\overline{\mathrm{MS}}}} \right]_{\overline{\mathrm{MS}} \to \mathrm{MOMi}} \tag{3.3.29}$$

where a and α are the MOMi coupling constant and gauge parameter after a mapping is made of the evaluation of the quantity in square brackets from $\overline{\mathrm{MS}}$ to MOMi. The anomalous dimension of the gauge parameter α has been previously defined (3.2.26) and

$$\beta^{\overline{\mathrm{MS}}}(a_{\overline{\mathrm{MS}}}) = \left(-\frac{11}{3} C_A + \frac{2}{3} N_f \right) a^2_{\overline{\mathrm{MS}}} + \mathcal{O}(a^4_{\overline{\mathrm{MS}}}) \; . \tag{3.3.30}$$

The β-function determines the behaviour of the coupling constant, and was what led [1, 2] to determine that gauge theory is asymptotically free. It is immediately apparent that a mapping is needed between the $\overline{\mathrm{MS}}$ and MOM scheme parameters in order to present the MOMi scheme β-functions in terms of the MOMi scheme gauge parameters and coupling constants only.

In this section we show how this mapping was achieved. We diverge from the construction of the β-function for now, concentrating on the coupling constant and gauge parameter mappings and the construction of the conversion functions. Knowing the conversion functions allows one to transform between schemes, relating physical quantities in one scheme to the same quantities in another. Since we defined our coupling constant renormalization as $g_o = \mu^\epsilon Z_g g$ we define our conversion functions by

$$\begin{aligned} C_g^{\mathrm{MOMi}}(a_{\overline{\mathrm{MS}}}, \alpha_{\overline{\mathrm{MS}}}) &= \left. \frac{Z_g^{\mathrm{MOMi}}}{Z_g^{\overline{\mathrm{MS}}}} \right|_{\mathrm{MOMi} \to \overline{\mathrm{MS}}} \\ C_\phi^{\mathrm{MOMi}}(a_{\overline{\mathrm{MS}}}, \alpha_{\overline{\mathrm{MS}}}) &= \left. \frac{Z_\phi^{\mathrm{MOMi}}}{Z_\phi^{\overline{\mathrm{MS}}}} \right|_{\mathrm{MOMi} \to \overline{\mathrm{MS}}} \end{aligned}$$

$$C_\alpha^{\rm MOMi}(a_{\overline{\rm MS}},\alpha_{\overline{\rm MS}}) \;=\; \left.\frac{Z_\alpha^{\rm MOMi} Z_A^{\overline{\rm MS}}}{Z_\alpha^{\overline{\rm MS}} Z_A^{\rm MOMi}}\right|_{\rm MOMi\to\overline{\rm MS}} \tag{3.3.31}$$

where the conversion functions are always in terms of $\overline{\rm MS}$ variables, as is our convention, and $\phi \in \{A,\psi,c\}$. For each renormalization group function there is an associated conversion function that allows us to transform between schemes.

A problem arises however when one tries to compute the conversion functions in this way, since the renormalization constants, say for example $Z_\phi^{\rm MOMi}$ depend on parameters specific to that of the MOMi scheme, whereas $Z_\phi^{\overline{\rm MS}}$ depends on $a_{\overline{\rm MS}}$ and $\alpha_{\overline{\rm MS}}$. This is partly because we have chosen to use a mass dependent renormalization scheme which results in $a_{\rm MOMi}$ and $\alpha_{\rm MOMi}$ being gauge dependent. Therefore, before attempting to compute the conversion functions it is necessary to first construct mappings for the gauge parameter and coupling constant in the $\overline{\rm MS}$ scheme to that of the MOMi schemes. Let us first consider the mapping of the gauge parameter, α, by recalling its definition

$$\alpha_o = \frac{Z_A}{Z_\alpha}\alpha \tag{3.3.32}$$

where Z_A is the gluon wave function renormalization constant and Z_α is the renormalization constant corresponding to the gauge parameter itself. If we assume the same relation is true in another scheme, say

$$\alpha_o = \frac{\bar{Z}_A}{\bar{Z}_\alpha}\bar{\alpha} \tag{3.3.33}$$

and assume both of these equations are valid such that they can be set equal to each other, then we get a relation between the gauge parameter in one scheme and the gauge parameter in another, such that

$$\begin{aligned} \frac{Z_A}{Z_\alpha}\alpha \;&\equiv\; \frac{\bar{Z}_A}{\bar{Z}_\alpha}\bar{\alpha} \\ \Rightarrow\quad \bar{\alpha} \;&=\; \left(\frac{\bar{Z}_\alpha}{Z_\alpha}\frac{Z_A}{\bar{Z}_A}\right)\alpha\ . \end{aligned} \tag{3.3.34}$$

By taking the barred variables to represent the MOMi scheme variables and the unbarred variables to represent the $\overline{\rm MS}$ scheme we find our mapping can be

constructed using the following formula, [89, 14],

$$\alpha_{\rm MOMi}(\mu) \;=\; \frac{Z_A^{\overline{\rm MS}} Z_\alpha^{\rm MOMi}}{Z_A^{\rm MOMi} Z_\alpha^{\overline{\rm MS}}} \; \alpha_{\overline{\rm MS}}(\mu) \;. \tag{3.3.35}$$

While in our conventions for an arbitrary linear covariant gauge $Z_\alpha = 1$, we include the full definition of the mapping here so as to be formally correct. We will apply this full definition of the gauge parameter mapping when considering non-linear gauges later. Similarly for the coupling constant mapping we have

$$a_o = (\mu^\epsilon)^2 Z_g^2 a \;\;\text{and}\;\; a_o = (\mu^\epsilon)^2 \bar{Z}_g^2 \bar{a} \tag{3.3.36}$$

which by rearrangement, as we have shown with the gauge parameter, gives

$$a_{\rm MOMi}(\mu) \;=\; \left(\frac{Z_g^{\overline{\rm MS}}}{Z_g^{\rm MOMi}} \right)^2 a_{\overline{\rm MS}}(\mu) \tag{3.3.37}$$

where any results in terms of $a_{\rm MOMi}$ can be written as an expansion of $a_{\overline{\rm MS}}$. To get $a_{\overline{\rm MS}}, \alpha_{\overline{\rm MS}}$ in terms of $a_{\rm MOMi}, \alpha_{\rm MOMi}$, which is of a more practical use in our calculations since we require an $\overline{\rm MS} \to$ MOM mapping for the MOMi scheme renormalization group functions, we simply invert the power series of (3.3.35) and (3.3.37) which give

$$\bar{a} \;=\; a + f_1(\alpha) a^2 + f_2(\alpha) a^3 + \mathcal{O}(a^4) \tag{3.3.38}$$

$$\bar{\alpha} \;=\; \alpha + g_1(\alpha) a + g_2(\alpha) a^2 + \mathcal{O}(a^3) \tag{3.3.39}$$

to get

$$a \;=\; \bar{a} - f_1(\bar{\alpha}) \bar{a}^2 + \left(2 f_1(\bar{\alpha})^2 - f_2(\bar{\alpha}) + f_1'(\bar{\alpha}) g_1(\bar{\alpha}) \right) \bar{a}^3 + \mathcal{O}(\bar{a}^4) \tag{3.3.40}$$

$$\alpha \;=\; \bar{\alpha} - g_1(\bar{\alpha}) \bar{a} + \left(-g_2(\bar{\alpha}) + g_1(\bar{\alpha}) f_1(\bar{\alpha}) + g_1'(\bar{\alpha}) g_1(\bar{\alpha}) \right) \bar{a}^2 + \mathcal{O}(\bar{a}^3) \;. \tag{3.3.41}$$

To first order a simple change in sign is enough to invert both the coupling constant and gauge parameter mappings. However as seen above, at higher loop orders the inverted mappings become more involved.

We now record our results for the mappings of both parameters for each MOMi scheme. It was found that the gauge parameter mapping was the same in all

three MOMi schemes,

$$\begin{aligned}
\alpha_{\text{MOMi}} &= \Big[1 + C_A\left[80T_FN_f - 9\alpha^2 - 18\alpha - 97\right]\frac{a}{36} \\
&\quad + \Big[\left[18\alpha^4 - 18\alpha^3 + 190\alpha^2 - 576\zeta(3)\alpha + 463\alpha + 864\zeta(3) - 7143\right]C_A^2 \\
&\quad\quad - \left[320\alpha^2 + 320\alpha - 2304\zeta(3) - 4248\right]C_AT_FN_f \\
&\quad\quad - \left[4608\zeta(3) - 5280\right]C_FT_FN_f\Big]\frac{a^2}{288}\Big]\alpha + \mathcal{O}(a^3)\ . \qquad (3.3.42)
\end{aligned}$$

As expected, the coupling constant mappings are dependent on the vertex functions above one loop order. The coupling constant mapping for the ghost-gluon vertex is given analytically as

$$\begin{aligned}
a_{\text{MOMh}} &= a + \left[3\psi'\left(\tfrac{1}{3}\right)\alpha^2C_A + 24\psi'\left(\tfrac{1}{3}\right)\alpha C_A - 15\psi'\left(\tfrac{1}{3}\right)C_A - 2\alpha^2C_A\pi^2\right. \\
&\quad\quad -27\alpha^2C_A - 16\alpha C_A\pi^2 - 162\alpha C_A + 10C_A\pi^2 - 615C_A \\
&\quad\quad \left.+240N_fT_F\right]\frac{a^2}{108} \\
&\quad + \Big[126\sqrt{3}\psi'\left(\tfrac{1}{3}\right)^2\alpha^4C_A^2 + 2016\sqrt{3}\psi'\left(\tfrac{1}{3}\right)^2\alpha^3C_A^2 + 6804\sqrt{3}\psi'\left(\tfrac{1}{3}\right)^2\alpha^2C_A^2 \\
&\quad\quad -10080\sqrt{3}\psi'\left(\tfrac{1}{3}\right)^2\alpha C_A^2 + 3150\sqrt{3}\psi'\left(\tfrac{1}{3}\right)^2C_A^2 \\
&\quad\quad -168\sqrt{3}\psi'\left(\tfrac{1}{3}\right)\alpha^4C_A^2\pi^2 - 1296\sqrt{3}\psi'\left(\tfrac{1}{3}\right)\alpha^4C_A^2 \\
&\quad\quad -2688\sqrt{3}\psi'\left(\tfrac{1}{3}\right)\alpha^3C_A^2\pi^2 - 12960\sqrt{3}\psi'\left(\tfrac{1}{3}\right)\alpha^3C_A^2 \\
&\quad\quad -9072\sqrt{3}\psi'\left(\tfrac{1}{3}\right)\alpha^2C_A^2\pi^2 - 142920\sqrt{3}\psi'\left(\tfrac{1}{3}\right)\alpha^2C_A^2 \\
&\quad\quad +11520\sqrt{3}\psi'\left(\tfrac{1}{3}\right)\alpha^2C_AN_fT_F + 13440\sqrt{3}\psi'\left(\tfrac{1}{3}\right)\alpha C_A^2\pi^2 \\
&\quad\quad -185832\sqrt{3}\psi'\left(\tfrac{1}{3}\right)\alpha C_A^2 + 99072\sqrt{3}\psi'\left(\tfrac{1}{3}\right)\alpha C_AN_fT_F \\
&\quad\quad -4200\sqrt{3}\psi'\left(\tfrac{1}{3}\right)C_A^2\pi^2 + 754128\sqrt{3}\psi'\left(\tfrac{1}{3}\right)C_A^2 \\
&\quad\quad -321984\sqrt{3}\psi'\left(\tfrac{1}{3}\right)C_AN_fT_F + 27\sqrt{3}\psi'''\left(\tfrac{1}{3}\right)\alpha^3C_A^2 \\
&\quad\quad -513\sqrt{3}\psi'''\left(\tfrac{1}{3}\right)\alpha^2C_A^2 + 837\sqrt{3}\psi'''\left(\tfrac{1}{3}\right)\alpha C_A^2 + 2997\sqrt{3}\psi'''\left(\tfrac{1}{3}\right)C_A^2 \\
&\quad\quad +58320\sqrt{3}s_2\left(\tfrac{\pi}{6}\right)\alpha^3C_A^2 - 373248\sqrt{3}s_2\left(\tfrac{\pi}{6}\right)\alpha^2C_A^2 \\
&\quad\quad +408240\sqrt{3}s_2\left(\tfrac{\pi}{6}\right)\alpha C_A^2 + 3825792\sqrt{3}s_2\left(\tfrac{\pi}{6}\right)C_A^2 \\
&\quad\quad -1492992\sqrt{3}s_2\left(\tfrac{\pi}{6}\right)C_AN_fT_F - 116640\sqrt{3}s_2\left(\tfrac{\pi}{2}\right)\alpha^3C_A^2 \\
&\quad\quad +746496\sqrt{3}s_2\left(\tfrac{\pi}{2}\right)\alpha^2C_A^2 - 816480\sqrt{3}s_2\left(\tfrac{\pi}{2}\right)\alpha C_A^2 \\
&\quad\quad -7651584\sqrt{3}s_2\left(\tfrac{\pi}{2}\right)C_A^2 + 2985984\sqrt{3}s_2\left(\tfrac{\pi}{2}\right)C_AN_fT_F \\
&\quad\quad -97200\sqrt{3}s_3\left(\tfrac{\pi}{6}\right)\alpha^3C_A^2 + 622080\sqrt{3}s_3\left(\tfrac{\pi}{6}\right)\alpha^2C_A^2 \\
&\quad\quad -680400\sqrt{3}s_3\left(\tfrac{\pi}{6}\right)\alpha C_A^2 - 6376320\sqrt{3}s_3\left(\tfrac{\pi}{6}\right)C_A^2 \\
&\quad\quad +2488320\sqrt{3}s_3\left(\tfrac{\pi}{6}\right)C_AN_fT_F + 77760\sqrt{3}s_3\left(\tfrac{\pi}{2}\right)\alpha^3C_A^2
\end{aligned}$$

$$
\begin{aligned}
&-497664\sqrt{3}s_3\left(\tfrac{\pi}{2}\right)\alpha^2C_A^2+544320\sqrt{3}s_3\left(\tfrac{\pi}{2}\right)\alpha C_A^2\\
&+5101056\sqrt{3}s_3\left(\tfrac{\pi}{2}\right)C_A^2-1990656\sqrt{3}s_3\left(\tfrac{\pi}{2}\right)C_AN_fT_F\\
&+56\sqrt{3}\alpha^4C_A^2\pi^4+864\sqrt{3}\alpha^4C_A^2\pi^2+824\sqrt{3}\alpha^3C_A^2\pi^4\\
&+8640\sqrt{3}\alpha^3C_A^2\pi^2-972\sqrt{3}\alpha^3C_A^2\zeta_3+29160\sqrt{3}\alpha^3C_A^2\\
&+4392\sqrt{3}\alpha^2C_A^2\pi^4+95280\sqrt{3}\alpha^2C_A^2\pi^2+33048\sqrt{3}\alpha^2C_A^2\zeta_3\\
&+407592\sqrt{3}\alpha^2C_A^2-7680\sqrt{3}\alpha^2C_AN_f\pi^2T_F\\
&-103680\sqrt{3}\alpha^2C_AN_fT_F-6712\sqrt{3}\alpha C_A^2\pi^4+123888\sqrt{3}\alpha C_A^2\pi^2\\
&-135108\sqrt{3}\alpha C_A^2\zeta_3+1458000\sqrt{3}\alpha C_A^2-66048\sqrt{3}\alpha C_AN_f\pi^2T_F\\
&-590976\sqrt{3}\alpha C_AN_fT_F-6592\sqrt{3}C_A^2\pi^4-502752\sqrt{3}C_A^2\pi^2\\
&-153576\sqrt{3}C_A^2\zeta_3-470160\sqrt{3}C_A^2+214656\sqrt{3}C_AN_f\pi^2T_F\\
&+995328\sqrt{3}C_AN_fT_F\zeta_3-707904\sqrt{3}C_AN_fT_F\\
&-1492992\sqrt{3}C_FN_fT_F\zeta_3+1710720\sqrt{3}C_FN_fT_F\\
&+460800\sqrt{3}N_f^2T_F^2+405\ln(3)^2\alpha^3C_A^2\pi-2592\ln(3)^2\alpha^2C_A^2\pi\\
&+2835\ln(3)^2\alpha C_A^2\pi+26568\ln(3)^2C_A^2\pi-10368\ln(3)^2C_AN_f\pi T_F\\
&-4860\ln(3)\alpha^3C_A^2\pi+31104\ln(3)\alpha^2C_A^2\pi-34020\ln(3)\alpha C_A^2\pi\\
&-318816\ln(3)C_A^2\pi+124416\ln(3)C_AN_f\pi T_F-435\alpha^3C_A^2\pi^3\\
&+2784\alpha^2C_A^2\pi^3-3045\alpha C_A^2\pi^3-28536C_A^2\pi^3\\
&+11136C_AN_f\pi^3T_F\big]\frac{a^3}{93312\sqrt{3}}\;+\;\mathcal{O}(a^4)\;. \qquad (3.3.43)
\end{aligned}
$$

The numerical mapping for the triple-gluon vertex is

$$
\begin{aligned}
a_{\rm MOMg} \;=\;& a+\big[26.492489-3.023791\alpha-0.328046\alpha^2+0.25\alpha^3\\
&\quad -3.416806N_f\big]a^2\\
&+\big[960.462717-46.712079\alpha+7.928513\alpha^2+9.111075\alpha^3\\
&\quad +1.037572\alpha^4-0.322256\alpha^5+0.015625\alpha^6-[202.085012\\
&\quad -8.080297\alpha-1.690792\alpha^2+0.010434\alpha^3\big]N_f\\
&\quad +7.687393N_f^2\big]a^3\;+\;\mathcal{O}(a^4)\;. \qquad (3.3.44)
\end{aligned}
$$

Similarly for the quark-gluon vertex the coupling constant mapping is

$$
\begin{aligned}
a_{\rm MOMq} \;=\;& a\;+\;\big[16.715775-2.344187\alpha-0.164023\alpha^2-1.111111N_f\big]a^2\\
&+\big[472.159095-43.057553\alpha-0.776012\alpha^2+2.020716\alpha^3\\
&\quad +0.208860\alpha^4-[83.111217-0.651396\alpha]N_f+1.234568N_f^2\big]a^3
\end{aligned}
$$

$$+ \mathcal{O}(a^4) \ . \tag{3.3.45}$$

Notice that we are required to compute the a_{MOMi} mapping to an order greater than that of the α_{MOMi} mapping since it is needed to this order to construct the anomalous dimensions and β-functions for each MOMi scheme, as can be understood from (3.3.29). Celmaster and Gonsalves also construct similar mappings in [52] which we have checked our results against, along with [14]. One of the first to consider a mapping between scheme-dependent coupling constants, in particular between the MS scheme and original MOM scheme, Celmaster and Gonsalves define a relation between the MS and MOM scheme coupling constants for the triple-gluon vertex by

$$a_{\text{MOM}} = a_{\text{MS}} \left[1 + a_{\text{MS}} A(\alpha, \, N_f) + \mathcal{O}(a_{\text{MS}}^2)\right] \tag{3.3.46}$$

where $A(\alpha, \, N_f)$ is the finite contribution to the MOM renormalized triple-gluon vertex at one loop. Our results for the MOM renormalization of the triple-gluon vertex at one loop agree with [52] up to a factor of $\frac{1}{2\pi}$. This comes from the way in which we have chosen to define the coupling constant, notably by $a = \frac{g^2}{16\pi^2}$. With the relation

$$\bar{A}(\alpha, \, N_f) = 2\pi A(\alpha, \, N_f) \tag{3.3.47}$$

we can write (3.3.46) in terms of our finite contribution as

$$a_{\text{MOMg}} = a_{\overline{\text{MS}}} \left[1 + \frac{a_{\overline{\text{MS}}}}{2} \bar{A}(\alpha, \, N_f) + \mathcal{O}(a_{\overline{\text{MS}}}^2)\right] \ . \tag{3.3.48}$$

As in [52] we choose various values of α and N_f, using REDUCE as our main data processor to compare with the findings of [52]. Table 3.2 shows the comparison between values.

Another analysis we can make using results for the coupling constant mappings is the Λ-ratio. We define the Λ-ratio as in [52] through

$$\frac{\Lambda_{\text{MOMi}}}{\Lambda_{\overline{\text{MS}}}} = \exp\left[\frac{\Theta^{\text{MOMi}}(\alpha, \, N_f)}{\tilde{\beta}_0}\right] \tag{3.3.49}$$

with $\tilde{\beta}_0$ originating from the one-loop β-function such that, [51],

$$\tilde{\beta}_0 = \frac{22}{3} C_A - \frac{8}{3} T_F N_f \ . \tag{3.3.50}$$

α	N_f	$A(\alpha,\, N_f)_{\mathrm{C+G[52]}}$	$\bar{A}(\alpha,\, N_f)_{\mathrm{Bell}}$
0	0	3.818	2.108
0	1	3.443	1.836
0	2	3.067	1.545
0	3	2.692	1.293
0	4	2.316	1.021
0	5	1.941	0.749
1	0	3.572	1.861
1	3	2.445	1.046
1	4	2.070	0.774
1	5	1.694	0.502

Table 3.2: Comparison between Celmaster and Gonsalves' results for the contribution of the finite piece for the one loop MOM renormalization of the triple-gluon vertex of [52] with my results for the same Green's function also renormalized in the MOM scheme.

The Λ-parameter sets the fundamental scale in QCD. However its actual value depends on the renormalization scheme one is considering. A remarkable feature of this quantity is that the ratio between Λ parameters in different schemes can be determined from a one loop computation. For each MOMi scheme we have

$$\begin{aligned}
\Theta^{\mathrm{MOMh}}(\alpha, N_f) &= \frac{1}{108}\left[3\psi'\left(\tfrac{1}{3}\right)\alpha^2 C_A + 24\psi'\left(\tfrac{1}{3}\right)\alpha C_A - 15\psi'\left(\tfrac{1}{3}\right)C_A - 2\alpha^2 C_A\pi^2\right. \\
&\quad -27\alpha^2 C_A - 16\alpha C_A\pi^2 - 162\alpha C_A + 10 C_A\pi^2 - 615 C_A \\
&\quad \left.+240 N_f T_F\right] \\
\Theta^{\mathrm{MOMg}}(\alpha, N_f) &= \frac{1}{324}\left[36\psi'\left(\tfrac{1}{3}\right)\alpha^2 C_A - 162\psi'\left(\tfrac{1}{3}\right)\alpha C_A + 138\psi'\left(\tfrac{1}{3}\right)C_A\right. \\
&\quad -384\psi'\left(\tfrac{1}{3}\right)N_f T_F + 27\alpha^3 C_A - 24\alpha^2 C_A\pi^2 - 162\alpha^2 C_A \\
&\quad +108\alpha C_A\pi^2 + 243\alpha C_A - 92 C_A\pi^2 + 2376 C_A \\
&\quad \left.+256 N_f\pi^2 T_F - 864 N_f T_F\right] \\
\Theta^{\mathrm{MOMq}}(\alpha, N_f) &= \frac{1}{108}\left[6\psi'\left(\tfrac{1}{3}\right)\alpha^2 C_A - 24\psi'\left(\tfrac{1}{3}\right)\alpha C_A - 96\psi'\left(\tfrac{1}{3}\right)\alpha C_F\right. \\
&\quad -78\psi'\left(\tfrac{1}{3}\right)C_A + 48\psi'\left(\tfrac{1}{3}\right)C_F - 4\alpha^2 C_A\pi^2 - 27\alpha^2 C_A \\
&\quad +16\alpha C_A\pi^2 + 54\alpha C_A + 64\alpha C_F\pi^2 + 216\alpha C_F + 52 C_A\pi^2 \\
&\quad \left.+993 C_A - 32 C_F\pi^2 - 432 C_F - 240 N_f T_F\right] \qquad (3.3.51)
\end{aligned}$$

where $\Theta^{\mathrm{MOMg}}(\alpha, N_f)$ is a variation of $\bar{A}(\alpha, N_f)$. The same goes for $\Theta^{\mathrm{MOMh}}(\alpha, N_f)$ and $\Theta^{\mathrm{MOMq}}(\alpha, N_f)$ which come directly from the coupling constant mappings for the ghost-gluon and quark-gluon vertex functions, (3.3.43) - (3.3.45). For example $\Theta^{\mathrm{MOMh}}(\alpha, N_f)$ is defined by the one loop contribution of a_{MOMh} in (3.3.43),

where a direct comparison of terms can be made. We note that within this thesis $\Theta^{\rm MOMi}(\alpha, N_f)$ is always defined to be the one loop contribution of $a_{\rm MOMi}$. Table 3.3 displays the Λ parameters in each MOMi scheme. The difference between

α	N_f	MOMg [52]	MOMg	MOMh	MOMq
0	0	8.86	3.3341	2.3236	2.1379
0	1	8.113	3.0543	2.3250	2.1277
0	2	7.343	2.7644	2.3267	2.1163
0	3	6.55	2.4654	2.3286	2.1032
0	4	5.73	2.1587	2.3308	2.0881
0	5	4.91	1.8471	2.3335	2.0706
1	0	7.69	2.8957	2.6166	1.9075
1	3	5.51	2.0751	2.6924	1.8296
1	4	4.76	1.7921	2.7265	1.7964
1	5	4.01	1.5088	2.7670	1.7581
3	3	4.89	1.8392	4.1918	1.3110
3	4	4.18	1.5732	4.3978	1.2533
-2	4	6.76	2.5437	2.0081	2.6597

Table 3.3: Values of $\frac{\Lambda_{\rm MOMi}}{\Lambda_{\overline{\rm MS}}}$ for the arbitrary linear covariant gauge in $SU(3)$.

the MS and $\overline{\rm MS}$ results should be 2.65622061617, [52]. This comes from the extra factor of $e^{\frac{1}{2}(\log(4\pi)-\gamma_E)}$ appearing in the MS scheme. By dividing Celmaster and Gonsalves' ratio by ours in Table 3.3, we indeed get 2.65622061617, confirming their results and agreeing with [90]. To understand what we have done is correct we make contact with the old, but still very much relevant work carried out in this area in the 70's. By comparing with MS results the factor of $2.65\ldots$ obtained is confirmation that our work is consistent. With our gauge parameter and coupling constant mappings found, and returning to (3.3.31) we can now compute the two loop conversion functions. The results are presented below for each MOMi scheme. Starting with the conversion functions for the wave functions we find that, along with the gauge parameter, these conversion functions are the same for all MOMi schemes in the arbitrary linear covariant gauge at two loops. These are

$$\begin{aligned} C_A^{\rm MOMi}(a,\alpha) &= 1 + \left[9\alpha^2 C_A + 18\alpha C_A + 97 C_A - 80 N_f T_F\right] \frac{a}{36} \\ &\quad + \left[810\alpha^3 C_A^2 + 2430\alpha^2 C_A^2 + 5184\alpha C_A^2\zeta_3 + 2817\alpha C_A^2 \right. \\ &\quad -2880\alpha C_A N_f T_F - 7776 C_A^2\zeta_3 + 83105 C_A^2 - 20736 C_A N_f T_F \zeta_3 \\ &\quad \left. -69272 C_A N_f T_F + 41472 C_F N_f T_F \zeta_3 - 47520 C_F N_f T_F \right. \end{aligned}$$

$$
\begin{aligned}
&+12800N_f^2T_F^2\big]\,\frac{a^2}{2592} \;+\; \mathcal{O}(a^3)\\
C_\alpha^{\rm MOMi}(a,\alpha) &= 1+\left[-9\alpha^2C_A-18\alpha C_A-97C_A+80N_fT_F\right]\frac{a}{36}\\
&+\big[18\alpha^4C_A^2-18\alpha^3C_A^2+190\alpha^2C_A^2-320\alpha^2C_AN_fT_F-576\alpha C_A^2\zeta_3\\
&\quad+463\alpha C_A^2-320\alpha C_AN_fT_F+864C_A^2\zeta_3-7143C_A^2\\
&\quad+2304C_AN_fT_F\zeta_3+4248C_AN_fT_F-4608C_FN_fT_F\zeta_3\\
&\quad+5280C_FN_fT_F\big]\,\frac{a^2}{288} \;+\; \mathcal{O}(a^3)\\
C_c^{\rm MOMi}(a,\alpha) &= 1+C_Aa+C_A\left[-36\alpha^2C_A\zeta_3+72\alpha^2C_A+72\alpha C_A\zeta_3-21\alpha C_A\right.\\
&\qquad\left.-180C_A\zeta_3+1943C_A-760N_fT_F\right]\frac{a^2}{192} \;+\; \mathcal{O}(a^3)\\
C_\psi^{\rm MOMi}(a,\alpha) &= 1-\alpha C_Fa\\
&+C_F\left[-9\alpha^2C_A+8\alpha^2C_F+24\alpha C_A\zeta_3-52\alpha C_A+24C_A\zeta_3-82C_A\right.\\
&\qquad\left.+5C_F+28N_fT_F\right]\frac{a^2}{8} \;+\; \mathcal{O}(a^3) \qquad (3.3.52)
\end{aligned}
$$

where a and α are $\overline{\rm MS}$ variables. The only conversion functions that are scheme dependent are those that directly contribute to the coupling constant mappings. The vertex-dependent conversion functions are given below for each scheme, with an analytical analysis given for the ghost-gluon vertex first

$$
\begin{aligned}
C_g^{\rm MOMh}(a,\alpha) &= 1 \;+\; \left[3\psi'\left(\tfrac{1}{3}\right)\alpha^2C_A+24\psi'\left(\tfrac{1}{3}\right)\alpha C_A-15\psi'\left(\tfrac{1}{3}\right)C_A-2\alpha^2C_A\pi^2\right.\\
&\qquad-27\alpha^2C_A-16\alpha C_A\pi^2-162\alpha C_A+10C_A\pi^2-615C_A\\
&\qquad\left.+240N_fT_F\right]\frac{a}{216}\\
&+\Big[36\sqrt{3}\psi'\left(\tfrac{1}{3}\right)^2\alpha^4C_A^2+576\sqrt{3}\psi'\left(\tfrac{1}{3}\right)^2\alpha^3C_A^2\\
&\quad+1944\sqrt{3}\psi'\left(\tfrac{1}{3}\right)^2\alpha^2C_A^2-2880\sqrt{3}\psi'\left(\tfrac{1}{3}\right)^2\alpha C_A^2\\
&\quad+900\sqrt{3}\psi'\left(\tfrac{1}{3}\right)^2C_A^2-48\sqrt{3}\psi'\left(\tfrac{1}{3}\right)\alpha^4C_A^2\pi^2\\
&\quad-972\sqrt{3}\psi'\left(\tfrac{1}{3}\right)\alpha^4C_A^2-768\sqrt{3}\psi'\left(\tfrac{1}{3}\right)\alpha^3C_A^2\pi^2\\
&\quad+1944\sqrt{3}\psi'\left(\tfrac{1}{3}\right)\alpha^3C_A^2-2592\sqrt{3}\psi'\left(\tfrac{1}{3}\right)\alpha^2C_A^2\pi^2\\
&\quad-60696\sqrt{3}\psi'\left(\tfrac{1}{3}\right)\alpha^2C_A^2+8640\sqrt{3}\psi'\left(\tfrac{1}{3}\right)\alpha^2C_AN_fT_F\\
&\quad+3840\sqrt{3}\psi'\left(\tfrac{1}{3}\right)\alpha C_A^2\pi^2+4896\sqrt{3}\psi'\left(\tfrac{1}{3}\right)\alpha C_A^2\\
&\quad+29952\sqrt{3}\psi'\left(\tfrac{1}{3}\right)\alpha C_AN_fT_F-1200\sqrt{3}\psi'\left(\tfrac{1}{3}\right)C_A^2\pi^2\\
&\quad+569628\sqrt{3}\psi'\left(\tfrac{1}{3}\right)C_A^2-249984\sqrt{3}\psi'\left(\tfrac{1}{3}\right)C_AN_fT_F\\
&\quad+27\sqrt{3}\psi'''\left(\tfrac{1}{3}\right)\alpha^3C_A^2-513\sqrt{3}\psi'''\left(\tfrac{1}{3}\right)\alpha^2C_A^2\\
&\quad+837\sqrt{3}\psi'''\left(\tfrac{1}{3}\right)\alpha C_A^2+2997\sqrt{3}\psi'''\left(\tfrac{1}{3}\right)C_A^2
\end{aligned}
$$

$$
\begin{aligned}
&+58320\sqrt{3}s_2\left(\tfrac{\pi}{6}\right)\alpha^3C_A^2 - 373248\sqrt{3}s_2\left(\tfrac{\pi}{6}\right)\alpha^2C_A^2 \\
&+408240\sqrt{3}s_2\left(\tfrac{\pi}{6}\right)\alpha C_A^2 + 3825792\sqrt{3}s_2\left(\tfrac{\pi}{6}\right)C_A^2 \\
&-1492992\sqrt{3}s_2\left(\tfrac{\pi}{6}\right)C_AN_fT_F - 116640\sqrt{3}s_2\left(\tfrac{\pi}{2}\right)\alpha^3C_A^2 \\
&+746496\sqrt{3}s_2\left(\tfrac{\pi}{2}\right)\alpha^2C_A^2 - 816480\sqrt{3}s_2\left(\tfrac{\pi}{2}\right)\alpha C_A^2 \\
&-7651584\sqrt{3}s_2\left(\tfrac{\pi}{2}\right)C_A^2 + 2985984\sqrt{3}s_2\left(\tfrac{\pi}{2}\right)C_AN_fT_F \\
&-97200\sqrt{3}s_3\left(\tfrac{\pi}{6}\right)\alpha^3C_A^2 + 622080\sqrt{3}s_3\left(\tfrac{\pi}{6}\right)\alpha^2C_A^2 \\
&-680400\sqrt{3}s_3\left(\tfrac{\pi}{6}\right)\alpha C_A^2 - 6376320\sqrt{3}s_3\left(\tfrac{\pi}{6}\right)C_A^2 \\
&+2488320\sqrt{3}s_3\left(\tfrac{\pi}{6}\right)C_AN_fT_F + 77760\sqrt{3}s_3\left(\tfrac{\pi}{2}\right)\alpha^3C_A^2 \\
&-497664\sqrt{3}s_3\left(\tfrac{\pi}{2}\right)\alpha^2C_A^2 + 544320\sqrt{3}s_3\left(\tfrac{\pi}{2}\right)\alpha C_A^2 \\
&+5101056\sqrt{3}s_3\left(\tfrac{\pi}{2}\right)C_A^2 - 1990656\sqrt{3}s_3\left(\tfrac{\pi}{2}\right)C_AN_fT_F \\
&+16\sqrt{3}\alpha^4C_A^2\pi^4 + 648\sqrt{3}\alpha^4C_A^2\pi^2 + 4374\sqrt{3}\alpha^4C_A^2 \\
&+184\sqrt{3}\alpha^3C_A^2\pi^4 - 1296\sqrt{3}\alpha^3C_A^2\pi^2 - 972\sqrt{3}\alpha^3C_A^2\zeta_3 \\
&+2232\sqrt{3}\alpha^2C_A^2\pi^4 + 40464\sqrt{3}\alpha^2C_A^2\pi^2 + 33048\sqrt{3}\alpha^2C_A^2\zeta_3 \\
&+8748\sqrt{3}\alpha^2C_A^2 - 5760\sqrt{3}\alpha^2C_AN_f\pi^2T_F \\
&-77760\sqrt{3}\alpha^2C_AN_fT_F - 3512\sqrt{3}\alpha C_A^2\pi^4 - 3264\sqrt{3}\alpha C_A^2\pi^2 \\
&-135108\sqrt{3}\alpha C_A^2\zeta_3 - 157464\sqrt{3}\alpha C_A^2 - 19968\sqrt{3}\alpha C_AN_f\pi^2T_F \\
&-124416\sqrt{3}\alpha C_AN_fT_F - 7592\sqrt{3}C_A^2\pi^4 - 379752\sqrt{3}C_A^2\pi^2 \\
&-153576\sqrt{3}C_A^2\zeta_3 - 4252410\sqrt{3}C_A^2 + 166656\sqrt{3}C_AN_f\pi^2T_F \\
&+995328\sqrt{3}C_AN_fT_F\zeta_3 + 2244096\sqrt{3}C_AN_fT_F \\
&-1492992\sqrt{3}C_FN_fT_F\zeta_3 + 1710720\sqrt{3}C_FN_fT_F \\
&-115200\sqrt{3}N_f^2T_F^2 + 405\ln(3)^2\alpha^3C_A^2\pi - 2592\ln(3)^2\alpha^2C_A^2\pi \\
&+2835\ln(3)^2\alpha C_A^2\pi + 26568\ln(3)^2C_A^2\pi \\
&-10368\ln(3)^2C_AN_f\pi T_F - 4860\ln(3)\alpha^3C_A^2\pi \\
&+31104\ln(3)\alpha^2C_A^2\pi - 34020\ln(3)\alpha C_A^2\pi \\
&-318816\ln(3)C_A^2\pi + 124416\ln(3)C_AN_f\pi T_F - 435\alpha^3C_A^2\pi^3 \\
&+2784\alpha^2C_A^2\pi^3 - 3045\alpha C_A^2\pi^3 - 28536C_A^2\pi^3 \\
&+11136C_AN_f\pi^3T_F\big]\,\frac{a^2}{186624\sqrt{3}} \;+\; \mathcal{O}(a^3)\;. \qquad (3.3.53)
\end{aligned}
$$

For the triple-gluon and quark-gluon vertices the conversion functions are presented numerically as

$$
C_g^{\rm MOMg}(a,\alpha) \;=\; 1 \;-\; \big[13.2462444 - 1.5118956\alpha - 0.1640232\alpha^2
$$

$$
\begin{aligned}
&\quad +0.1250000\alpha^3 - 1.7084032N_f\big]\, a \\
&- \big[217.0368707 + 36.7247782\alpha + 7.0535877\alpha^2 - 1.1557619\alpha^3 \\
&\quad +1.0453915\alpha^4 - 0.0996192\alpha^5 - 0.0156250\alpha^6 \\
&\quad -[33.1527255 + 3.7086335\alpha - 0.0047429\alpha^2 \\
&\quad\quad -0.6354341\alpha^3]N_f - 0.5342658N_f^2\big]\, a^2 \;+\; \mathcal{O}(a^3) \\
C_g^{\mathrm{MOMq}}(a,\alpha) \;&=\; 1 \;-\; \big[8.3578873 - 1.1720934\alpha - 0.0820116\alpha^2 \\
&\quad\quad -0.5555556Nf\big]\, a \\
&- \big[131.2981279 + 7.8598968\alpha - 0.3923795\alpha^2 + 0.7219823\alpha^3 \\
&\quad +0.0943409\alpha^4 \;-\; [27.6257962 + 1.6277910\alpha \\
&\quad +0.1366860\alpha^2]N_f + 0.1543230N_f^2\big]\, a^2 \;+\; \mathcal{O}(a^3)\;. \qquad (3.3.54)
\end{aligned}
$$

These conversion functions and parameter mappings are vital in constructing the β-functions for each MOMi scheme, which we visit in the next section.

3.4 β-functions and anomalous dimensions

Now that we have deduced the coupling constant mappings, gauge parameter mapping and conversion functions we can begin constructing the β-functions and anomalous dimensions to *three* loops for each MOMi scheme. This is carried out using the formula (3.3.29), [14, 58]. It has been shown, and confirmed in [1, 2] that the one loop β-function (3.3.30) is both gauge and scheme independent. This can be seen through the absence of α terms at this loop order. We note however that in momentum subtraction schemes gauge dependence appears in the β-function at higher loop orders and that it no longer remains gauge parameter independent, instead depending very much on the scheme used to calculate it. This is not the case for the $\overline{\mathrm{MS}}$ β-function where it remains gauge invariant to all known orders. This is a special property of $\overline{\mathrm{MS}}$. Since there are three MOMi schemes, this means there will be three separate β-functions compared to just one in $\overline{\mathrm{MS}}$, since there are three distinct couplings. The anomalous dimensions can be computed in a similar way using the formula

$$
\begin{aligned}
\gamma_\phi^{\mathrm{MOMi}}(a,\alpha) \;=\; \Bigg[&\gamma_\phi^{\overline{\mathrm{MS}}}\big(a_{\overline{\mathrm{MS}}}\big) + \beta^{\overline{\mathrm{MS}}}\big(a_{\overline{\mathrm{MS}}}\big)\,\frac{\partial}{\partial a_{\overline{\mathrm{MS}}}}\ln C_\phi^{\mathrm{MOMi}}\left(a_{\overline{\mathrm{MS}}},\alpha_{\overline{\mathrm{MS}}}\right) \\
&+ \alpha_{\overline{\mathrm{MS}}}\,\gamma_\alpha^{\overline{\mathrm{MS}}}\big(a_{\overline{\mathrm{MS}}},\alpha_{\overline{\mathrm{MS}}}\big)\,\frac{\partial}{\partial \alpha_{\overline{\mathrm{MS}}}}\ln C_\phi^{\mathrm{MOMi}}\left(a_{\overline{\mathrm{MS}}},\alpha_{\overline{\mathrm{MS}}}\right)\Bigg]_{\overline{\mathrm{MS}}\to\mathrm{MOMi}}
\end{aligned}
\qquad (3.4.55)
$$

with $\phi \in \{A, \psi, c, \alpha\}$. In order to use these formulae we require the $\overline{\rm MS}$ β-function and anomalous dimensions at *three* loops. Since we did not directly carry out a three loop calculation we pull these results from [1, 2, 92, 93, 94, 14], and display them below for the benefit of the reader

$$\begin{aligned}
\beta^{\overline{\rm MS}}(a,\alpha) &= \left[-11C_A + 4N_f T_F\right]\frac{a^2}{3} + 2\left[-17C_A^2 + 10C_A N_f T_F + 6C_F N_f T_F\right]\frac{a^3}{3} \\
&+ \left[-2857C_A^3 + 2830C_A^2 N_f T_F + 1230 C_A C_F N_f T_F - 316 C_A N_f^2 T_F^2\right. \\
&\left. -108 C_F^2 N_f T_F - 264 C_F N_f^2 T_F^2\right]\frac{a^4}{54} \;+\; \mathcal{O}(a^5) \qquad (3.4.56) \\
\gamma_A^{\overline{\rm MS}}(a,\alpha) &= \left[3\alpha C_A - 13 C_A + 8 N_f T_F\right]\frac{a}{6} \\
&+ \left[2\alpha^2 C_A^2 + 11\alpha C_A^2 - 59 C_A^2 + 40 C_A N_f T_F + 32 C_F N_f T_F\right]\frac{a^2}{8} \\
&+ \left[63\alpha^3 C_A^3 + 54\alpha^2 C_A^3\zeta_3 + 297\alpha^2 C_A^3 + 216\alpha C_A^3\zeta_3 + 1503\alpha C_A^3\right. \\
&\quad -576\alpha C_A^2 N_f T_F + 162 C_A^3\zeta_3 - 9965 C_A^3 - 5184 C_A^2 N_f T_F\zeta_3 \\
&\quad +14576 C_A^2 N_f T_F + 6912 C_A C_F N_f T_F\zeta_3 + 80 C_A C_F N_f T_F \\
&\quad \left.-2432 C_A N_f^2 T_F^2 - 576 C_F^2 N_f T_F - 1408 C_F N_f^2 T_F^2\right]\frac{a^3}{288} \;+\; \mathcal{O}(a^4) \\
\gamma_\alpha^{\overline{\rm MS}}(a,\alpha) &= \left[-3\alpha C_A + 13 C_A - 8 N_f T_F\right]\frac{a}{6} \\
&+ \left[-2\alpha^2 C_A^2 - 11\alpha C_A^2 + 59 C_A^2 - 40 C_A N_f T_F - 32 C_F N_f T_F\right]\frac{a^2}{8} \\
&+ \left[-63\alpha^3 C_A^3 - 54\alpha^2 C_A^3\zeta_3 - 297\alpha^2 C_A^3 - 216\alpha C_A^3\zeta_3 - 1503\alpha C_A^3\right. \\
&\quad +576\alpha C_A^2 N_f T_F - 162 C_A^3\zeta_3 + 9965 C_A^3 + 5184 C_A^2 N_f T_F\zeta_3 \\
&\quad -14576 C_A^2 N_f T_F - 6912 C_A C_F N_f T_F\zeta_3 - 80 C_A C_F N_f T_F \\
&\quad \left.+2432 C_A N_f^2 T_F^2 + 576 C_F^2 N_f T_F + 1408 C_F N_f^2 T_F^2\right]\frac{a^3}{288} \;+\; \mathcal{O}(a^4) \\
\gamma_c^{\overline{\rm MS}}(a,\alpha) &= C_A(\alpha - 3)\frac{a}{4} + C_A\left[-3\alpha C_A - 95 C_A + 40 N_f T_F\right]\frac{a^2}{48} \\
&+ C_A\left[81\alpha^3 C_A^2 - 162\alpha^2 C_A^2\zeta_3 + 162\alpha^2 C_A^2 - 648\alpha C_A^2\zeta_3 + 918\alpha C_A^2\right. \\
&\quad -1512\alpha C_A N_f T_F - 486 C_A^2\zeta_3 - 15817 C_A^2 + 15552 C_A N_f T_F\zeta_3 \\
&\quad +1552 C_A N_f T_F - 20736 C_F N_f T_F\zeta_3 + 19440 C_F N_f T_F \\
&\quad \left.+2240 N_f^2 T_F^2\right]\frac{a^2}{1728} \;+\; \mathcal{O}(a^4) \\
\gamma_\psi^{\overline{\rm MS}}(a,\alpha) &= \alpha C_F a + C_F\left[\alpha^2 C_A + 8\alpha C_A + 25 C_A - 6 C_F - 8 N_f T_F\right]\frac{a^2}{4} \\
&+ C_F\left[90\alpha^3 C_A^2 + 108\alpha^2 C_A^2\zeta_3 + 351\alpha^2 C_A^2 + 216\alpha C_A^2\zeta_3 + 2367\alpha C_A^2\right. \\
&\quad -1224\alpha C_A N_f T_F - 2484 C_A^2\zeta_3 + 18310 C_A^2 + 3456 C_A C_F\zeta_3 \\
&\quad \left.-10296 C_A C_F - 9184 C_A N_f T_F + 432 C_F^2 + 864 C_F N_f T_F\right.
\end{aligned}$$

$$+640N_f^2T_F^2\big]\,\frac{a^3}{288} \;+\; \mathcal{O}(a^4) \tag{3.4.57}$$

where the gauge invariance of the $\overline{\rm MS}$ β-function can be explicitly seen here. We now have everything we need to compute the MOMi scheme renormalization group functions. Starting with the MOMh scheme the scheme dependent β-function is

$$\begin{aligned}
\beta^{\rm MOMh}(a,\alpha) \;=\; & \left[-11C_A+4N_fT_F\right]\frac{a^2}{3} \\
& + \Big[9\psi'\left(\tfrac{1}{3}\right)\alpha^3C_A^2 - 3\psi'\left(\tfrac{1}{3}\right)\alpha^2C_A^2 + 24\psi'\left(\tfrac{1}{3}\right)\alpha^2C_AN_fT_F \\
& \quad -156\psi'\left(\tfrac{1}{3}\right)\alpha C_A^2 + 96\psi'\left(\tfrac{1}{3}\right)\alpha C_AN_fT_F - 6\alpha^3C_A^2\pi^2 - 81\alpha^3C_A^2 \\
& \quad +2\alpha^2C_A^2\pi^2 + 108\alpha^2C_A^2 - 16\alpha^2C_AN_f\pi^2T_F - 216\alpha^2C_AN_fT_F \\
& \quad +104\alpha C_A^2\pi^2 + 1053\alpha C_A^2 - 64\alpha C_AN_f\pi^2T_F - 648\alpha C_AN_fT_F \\
& \quad -3672C_A^2 + 2160C_AN_fT_F + 1296C_FN_fT_F\Big]\,\frac{a^3}{324} \\
& + \Big[1080\sqrt{3}\psi'\left(\tfrac{1}{3}\right)^2\alpha^5C_A^3 + 9468\sqrt{3}\psi'\left(\tfrac{1}{3}\right)^2\alpha^4C_A^3 \\
& \quad +2448\sqrt{3}\psi'\left(\tfrac{1}{3}\right)^2\alpha^4C_A^2N_fT_F - 7992\sqrt{3}\psi'\left(\tfrac{1}{3}\right)^2\alpha^3C_A^3 \\
& \quad +27648\sqrt{3}\psi'\left(\tfrac{1}{3}\right)^2\alpha^3C_A^2N_fT_F - 83808\sqrt{3}\psi'\left(\tfrac{1}{3}\right)^2\alpha^2C_A^3 \\
& \quad +54432\sqrt{3}\psi'\left(\tfrac{1}{3}\right)^2\alpha^2C_A^2N_fT_F - 1440\sqrt{3}\psi'\left(\tfrac{1}{3}\right)^2\alpha C_A^3 \\
& \quad -23040\sqrt{3}\psi'\left(\tfrac{1}{3}\right)^2\alpha C_A^2N_fT_F + 29700\sqrt{3}\psi'\left(\tfrac{1}{3}\right)^2C_A^3 \\
& \quad -10800\sqrt{3}\psi'\left(\tfrac{1}{3}\right)^2C_A^2N_fT_F - 1440\sqrt{3}\psi'\left(\tfrac{1}{3}\right)\alpha^5C_A^3\pi^2 \\
& \quad -11664\sqrt{3}\psi'\left(\tfrac{1}{3}\right)\alpha^5C_A^3 - 12624\sqrt{3}\psi'\left(\tfrac{1}{3}\right)\alpha^4C_A^3\pi^2 \\
& \quad -3888\sqrt{3}\psi'\left(\tfrac{1}{3}\right)\alpha^4C_A^3 - 3264\sqrt{3}\psi'\left(\tfrac{1}{3}\right)\alpha^4C_A^2N_f\pi^2T_F \\
& \quad -31104\sqrt{3}\psi'\left(\tfrac{1}{3}\right)\alpha^4C_A^2N_fT_F + 10656\sqrt{3}\psi'\left(\tfrac{1}{3}\right)\alpha^3C_A^3\pi^2 \\
& \quad -222912\sqrt{3}\psi'\left(\tfrac{1}{3}\right)\alpha^3C_A^3 - 36864\sqrt{3}\psi'\left(\tfrac{1}{3}\right)\alpha^3C_A^2N_f\pi^2T_F \\
& \quad -176256\sqrt{3}\psi'\left(\tfrac{1}{3}\right)\alpha^3C_A^2N_fT_F + 111744\sqrt{3}\psi'\left(\tfrac{1}{3}\right)\alpha^2C_A^3\pi^2 \\
& \quad +609768\sqrt{3}\psi'\left(\tfrac{1}{3}\right)\alpha^2C_A^3 - 72576\sqrt{3}\psi'\left(\tfrac{1}{3}\right)\alpha^2C_A^2N_f\pi^2T_F \\
& \quad -648000\sqrt{3}\psi'\left(\tfrac{1}{3}\right)\alpha^2C_A^2N_fT_F + 186624\sqrt{3}\psi'\left(\tfrac{1}{3}\right)\alpha^2C_AC_FN_fT_F \\
& \quad +1920\sqrt{3}\psi'\left(\tfrac{1}{3}\right)\alpha C_A^3\pi^2 - 2171448\sqrt{3}\psi'\left(\tfrac{1}{3}\right)\alpha C_A^3 \\
& \quad +30720\sqrt{3}\psi'\left(\tfrac{1}{3}\right)\alpha C_A^2N_f\pi^2T_F + 1586304\sqrt{3}\psi'\left(\tfrac{1}{3}\right)\alpha C_A^2N_fT_F \\
& \quad +995328\sqrt{3}\psi'\left(\tfrac{1}{3}\right)\alpha C_AC_FN_fT_F - 39600\sqrt{3}\psi'\left(\tfrac{1}{3}\right)C_A^3\pi^2 \\
& \quad +14224896\sqrt{3}\psi'\left(\tfrac{1}{3}\right)C_A^3 + 14400\sqrt{3}\psi'\left(\tfrac{1}{3}\right)C_A^2N_f\pi^2T_F \\
& \quad -11187072\sqrt{3}\psi'\left(\tfrac{1}{3}\right)C_A^2N_fT_F - 311040\sqrt{3}\psi'\left(\tfrac{1}{3}\right)C_AC_FN_fT_F \\
& \quad +2115072\sqrt{3}\psi'\left(\tfrac{1}{3}\right)C_AN_f^2T_F^2 + 243\sqrt{3}\psi'''\left(\tfrac{1}{3}\right)\alpha^4C_A^3
\end{aligned}$$

$$
\begin{aligned}
&-3537\sqrt{3}\psi'''\left(\tfrac{1}{3}\right)\alpha^3C_A^3+432\sqrt{3}\psi'''\left(\tfrac{1}{3}\right)\alpha^3C_A^2N_fT_F\\
&+4563\sqrt{3}\psi'''\left(\tfrac{1}{3}\right)\alpha^2C_A^3-4104\sqrt{3}\psi'''\left(\tfrac{1}{3}\right)\alpha^2C_A^2N_fT_F\\
&+7533\sqrt{3}\psi'''\left(\tfrac{1}{3}\right)\alpha C_A^3+65934\sqrt{3}\psi'''\left(\tfrac{1}{3}\right)C_A^3\\
&-23976\sqrt{3}\psi'''\left(\tfrac{1}{3}\right)C_A^2N_fT_F+524880\sqrt{3}s_2\left(\tfrac{\pi}{6}\right)\alpha^4C_A^3\\
&-3230928\sqrt{3}s_2\left(\tfrac{\pi}{6}\right)\alpha^3C_A^3+933120\sqrt{3}s_2\left(\tfrac{\pi}{6}\right)\alpha^3C_A^2N_fT_F\\
&+2717712\sqrt{3}s_2\left(\tfrac{\pi}{6}\right)\alpha^2C_A^3-2985984\sqrt{3}s_2\left(\tfrac{\pi}{6}\right)\alpha^2C_A^2N_fT_F\\
&+3674160\sqrt{3}s_2\left(\tfrac{\pi}{6}\right)\alpha C_A^3+84167424\sqrt{3}s_2\left(\tfrac{\pi}{6}\right)C_A^3\\
&-63452160\sqrt{3}s_2\left(\tfrac{\pi}{6}\right)C_A^2N_fT_F+11943936\sqrt{3}s_2\left(\tfrac{\pi}{6}\right)C_AN_f^2T_F^2\\
&-1049760\sqrt{3}s_2\left(\tfrac{\pi}{2}\right)\alpha^4C_A^3+6461856\sqrt{3}s_2\left(\tfrac{\pi}{2}\right)\alpha^3C_A^3\\
&-1866240\sqrt{3}s_2\left(\tfrac{\pi}{2}\right)\alpha^3C_A^2N_fT_F-5435424\sqrt{3}s_2\left(\tfrac{\pi}{2}\right)\alpha^2C_A^3\\
&+5971968\sqrt{3}s_2\left(\tfrac{\pi}{2}\right)\alpha^2C_A^2N_fT_F-7348320\sqrt{3}s_2\left(\tfrac{\pi}{2}\right)\alpha C_A^3\\
&-168334848\sqrt{3}s_2\left(\tfrac{\pi}{2}\right)C_A^3+126904320\sqrt{3}s_2\left(\tfrac{\pi}{2}\right)C_A^2N_fT_F\\
&-23887872\sqrt{3}s_2\left(\tfrac{\pi}{2}\right)C_AN_f^2T_F^2-874800\sqrt{3}s_3\left(\tfrac{\pi}{6}\right)\alpha^4C_A^3\\
&+5384880\sqrt{3}s_3\left(\tfrac{\pi}{6}\right)\alpha^3C_A^3-1555200\sqrt{3}s_3\left(\tfrac{\pi}{6}\right)\alpha^3C_A^2N_fT_F\\
&-4529520\sqrt{3}s_3\left(\tfrac{\pi}{6}\right)\alpha^2C_A^3+4976640\sqrt{3}s_3\left(\tfrac{\pi}{6}\right)\alpha^2C_A^2N_fT_F\\
&-6123600\sqrt{3}s_3\left(\tfrac{\pi}{6}\right)\alpha C_A^3-140279040\sqrt{3}s_3\left(\tfrac{\pi}{6}\right)C_A^3\\
&+105753600\sqrt{3}s_3\left(\tfrac{\pi}{6}\right)C_A^2N_fT_F-19906560\sqrt{3}s_3\left(\tfrac{\pi}{6}\right)C_AN_f^2T_F^2\\
&+699840\sqrt{3}s_3\left(\tfrac{\pi}{2}\right)\alpha^4C_A^3-4307904\sqrt{3}s_3\left(\tfrac{\pi}{2}\right)\alpha^3C_A^3\\
&+1244160\sqrt{3}s_3\left(\tfrac{\pi}{2}\right)\alpha^3C_A^2N_fT_F+3623616\sqrt{3}s_3\left(\tfrac{\pi}{2}\right)\alpha^2C_A^3\\
&-3981312\sqrt{3}s_3\left(\tfrac{\pi}{2}\right)\alpha^2C_A^2N_fT_F+4898880\sqrt{3}s_3\left(\tfrac{\pi}{2}\right)\alpha C_A^3\\
&+112223232\sqrt{3}s_3\left(\tfrac{\pi}{2}\right)C_A^3-84602880\sqrt{3}s_3\left(\tfrac{\pi}{2}\right)C_A^2N_fT_F\\
&+15925248\sqrt{3}s_3\left(\tfrac{\pi}{2}\right)C_AN_f^2T_F^2+480\sqrt{3}\alpha^5C_A^3\pi^4\\
&+7776\sqrt{3}\alpha^5C_A^3\pi^2+3560\sqrt{3}\alpha^4C_A^3\pi^4+2592\sqrt{3}\alpha^4C_A^3\pi^2\\
&-8748\sqrt{3}\alpha^4C_A^3\zeta_3-40824\sqrt{3}\alpha^4C_A^3+1088\sqrt{3}\alpha^4C_A^2N_f\pi^4T_F\\
&+20736\sqrt{3}\alpha^4C_A^2N_f\pi^2T_F+46656\sqrt{3}\alpha^4C_A^2N_fT_F\\
&+5880\sqrt{3}\alpha^3C_A^3\pi^4+148608\sqrt{3}\alpha^3C_A^3\pi^2+214812\sqrt{3}\alpha^3C_A^3\zeta_3\\
&-554040\sqrt{3}\alpha^3C_A^3+11136\sqrt{3}\alpha^3C_A^2N_f\pi^4T_F\\
&+117504\sqrt{3}\alpha^3C_A^2N_f\pi^2T_F-15552\sqrt{3}\alpha^3C_A^2N_fT_F\zeta_3\\
&+466560\sqrt{3}\alpha^3C_A^2N_fT_F-49416\sqrt{3}\alpha^2C_A^3\pi^4\\
&-406512\sqrt{3}\alpha^2C_A^3\pi^2-537516\sqrt{3}\alpha^2C_A^3\zeta_3\\
&+832032\sqrt{3}\alpha^2C_A^3+35136\sqrt{3}\alpha^2C_A^2N_f\pi^4T_F\\
&+432000\sqrt{3}\alpha^2C_A^2N_f\pi^2T_F+264384\sqrt{3}\alpha^2C_A^2N_fT_F\zeta_3
\end{aligned}
$$

$$
\begin{aligned}
&-917568\sqrt{3}\alpha^2 C_A^2 N_f T_F - 124416\sqrt{3}\alpha^2 C_A C_F N_f \pi^2 T_F \\
&-1679616\sqrt{3}\alpha^2 C_A C_F N_f T_F - 20728\sqrt{3}\alpha C_A^3 \pi^4 \\
&+1447632\sqrt{3}\alpha C_A^3 \pi^2 - 1215972\sqrt{3}\alpha C_A^3 \zeta_3 + 12422160\sqrt{3}\alpha C_A^3 \\
&-10240\sqrt{3}\alpha C_A^2 N_f \pi^4 T_F - 1057536\sqrt{3}\alpha C_A^2 N_f \pi^2 T_F \\
&-8957952\sqrt{3}\alpha C_A^2 N_f T_F - 663552\sqrt{3}\alpha C_A C_F N_f \pi^2 T_F \\
&-6718464\sqrt{3}\alpha C_A C_F N_f T_F - 162624\sqrt{3} C_A^3 \pi^4 \\
&-9483264\sqrt{3} C_A^3 \pi^2 - 3378672\sqrt{3} C_A^3 \zeta_3 \\
&-70400016\sqrt{3} C_A^3 + 59136\sqrt{3} C_A^2 N_f \pi^4 T_F \\
&+7458048\sqrt{3} C_A^2 N_f \pi^2 T_F + 23125824\sqrt{3} C_A^2 N_f T_F \zeta_3 \\
&+58335552\sqrt{3} C_A^2 N_f T_F + 207360\sqrt{3} C_A C_F N_f \pi^2 T_F \\
&-32845824\sqrt{3} C_A C_F N_f T_F \zeta_3 + 37635840\sqrt{3} C_A C_F N_f T_F \\
&-1410048\sqrt{3} C_A N_f^2 \pi^2 T_F^2 - 7962624\sqrt{3} C_A N_f^2 T_F^2 \zeta_3 \\
&-8211456\sqrt{3} C_A N_f^2 T_F^2 - 1119744\sqrt{3} C_F^2 N_f T_F \\
&+11943936\sqrt{3} C_F N_f^2 T_F^2 \zeta_3 - 11446272\sqrt{3} C_F N_f^2 T_F^2 \\
&+3645 \ln(3)^2 \alpha^4 C_A^3 \pi - 22437 \ln(3)^2 \alpha^3 C_A^3 \pi \\
&+6480 \ln(3)^2 \alpha^3 C_A^2 N_f \pi T_F + 18873 \ln(3)^2 \alpha^2 C_A^3 \pi \\
&-20736 \ln(3)^2 \alpha^2 C_A^2 N_f \pi T_F + 25515 \ln(3)^2 \alpha C_A^3 \pi \\
&+584496 \ln(3)^2 C_A^3 \pi - 440640 \ln(3)^2 C_A^2 N_f \pi T_F \\
&+82944 \ln(3)^2 C_A N_f^2 \pi T_F^2 - 43740 \ln(3) \alpha^4 C_A^3 \pi \\
&+269244 \ln(3) \alpha^3 C_A^3 \pi - 77760 \ln(3) \alpha^3 C_A^2 N_f \pi T_F \\
&-226476 \ln(3) \alpha^2 C_A^3 \pi + 248832 \ln(3) \alpha^2 C_A^2 N_f \pi T_F \\
&-306180 \ln(3) \alpha C_A^3 \pi - 7013952 \ln(3) C_A^3 \pi \\
&+5287680 \ln(3) C_A^2 N_f \pi T_F - 995328 \ln(3) C_A N_f^2 \pi T_F^2 \\
&-3915 \alpha^4 C_A^3 \pi^3 + 24099 \alpha^3 C_A^3 \pi^3 - 6960 \alpha^3 C_A^2 N_f \pi^3 T_F \\
&-20271 \alpha^2 C_A^3 \pi^3 + 22272 \alpha^2 C_A^2 N_f \pi^3 T_F - 27405 \alpha C_A^3 \pi^3 \\
&-627792 C_A^3 \pi^3 + 473280 C_A^2 N_f \pi^3 T_F \\
&-89088 C_A N_f^2 \pi^3 T_F^2 \big] \frac{a^4}{559872\sqrt{3}} \; + \; \mathcal{O}(a^5)
\end{aligned}
\tag{3.4.58}
$$

where gauge dependence is apparent after one loop. This is expected with mass dependent renormalization schemes. One check on (3.4.58) is that the MOMi and $\overline{\rm MS}$ β-functions agree in the limit $\alpha = 0$ at two loops. At three loops they will not agree as this is where the scheme dependence first appears. This has been

checked in all schemes. The anomalous dimensions for the wave functions and arbitrary gauge parameter, constructed using (3.4.55), in the MOMh scheme are

$$
\begin{aligned}
\gamma_A^{\mathrm{MOMh}}(a,\alpha) &= [3\alpha C_A - 13C_A + 8N_f T_F]\,\frac{a}{6} \\
&+ \left[9\psi'\left(\tfrac{1}{3}\right)\alpha^3 C_A^2 + 33\psi'\left(\tfrac{1}{3}\right)\alpha^2 C_A^2 + 24\psi'\left(\tfrac{1}{3}\right)\alpha^2 C_A N_f T_F\right. \\
&\quad -357\psi'\left(\tfrac{1}{3}\right)\alpha C_A^2 + 192\psi'\left(\tfrac{1}{3}\right)\alpha C_A N_f T_F + 195\psi'\left(\tfrac{1}{3}\right) C_A^2 \\
&\quad -120\psi'\left(\tfrac{1}{3}\right) C_A N_f T_F - 6\alpha^3 C_A^2\pi^2 - 162\alpha^3 C_A^2 - 22\alpha^2 C_A^2\pi^2 \\
&\quad +135\alpha^2 C_A^2 - 16\alpha^2 C_A N_f \pi^2 T_F - 432\alpha^2 C_A N_f T_F + 238\alpha C_A^2\pi^2 \\
&\quad +1539\alpha C_A^2 - 128\alpha C_A N_f \pi^2 T_F - 1296\alpha C_A N_f T_F - 130 C_A^2\pi^2 \\
&\quad -3186 C_A^2 + 80 C_A N_f \pi^2 T_F + 2808 C_A N_f T_F \\
&\quad \left.+2592 C_F N_f T_F\right]\frac{a^2}{648} \\
&+ \left[378\sqrt{3}\psi'\left(\tfrac{1}{3}\right)^2\alpha^5 C_A^3 + 4410\sqrt{3}\psi'\left(\tfrac{1}{3}\right)^2\alpha^4 C_A^3\right. \\
&\quad +1008\sqrt{3}\psi'\left(\tfrac{1}{3}\right)^2\alpha^4 C_A^2 N_f T_F - 5796\sqrt{3}\psi'\left(\tfrac{1}{3}\right)^2\alpha^3 C_A^3 \\
&\quad +16128\sqrt{3}\psi'\left(\tfrac{1}{3}\right)^2\alpha^3 C_A^2 N_f T_F - 118692\sqrt{3}\psi'\left(\tfrac{1}{3}\right)^2\alpha^2 C_A^3 \\
&\quad +54432\sqrt{3}\psi'\left(\tfrac{1}{3}\right)^2\alpha^2 C_A^2 N_f T_F + 140490\sqrt{3}\psi'\left(\tfrac{1}{3}\right)^2\alpha C_A^3 \\
&\quad -80640\sqrt{3}\psi'\left(\tfrac{1}{3}\right)^2\alpha C_A^2 N_f T_F - 40950\sqrt{3}\psi'\left(\tfrac{1}{3}\right)^2 C_A^3 \\
&\quad +25200\sqrt{3}\psi'\left(\tfrac{1}{3}\right)^2 C_A^2 N_f T_F - 504\sqrt{3}\psi'\left(\tfrac{1}{3}\right)\alpha^5 C_A^3\pi^2 \\
&\quad -7776\sqrt{3}\psi'\left(\tfrac{1}{3}\right)\alpha^5 C_A^3 - 5880\sqrt{3}\psi'\left(\tfrac{1}{3}\right)\alpha^4 C_A^3\pi^2 \\
&\quad -40176\sqrt{3}\psi'\left(\tfrac{1}{3}\right)\alpha^4 C_A^3 - 1344\sqrt{3}\psi'\left(\tfrac{1}{3}\right)\alpha^4 C_A^2 N_f \pi^2 T_F \\
&\quad -20736\sqrt{3}\psi'\left(\tfrac{1}{3}\right)\alpha^4 C_A^2 N_f T_F + 7728\sqrt{3}\psi'\left(\tfrac{1}{3}\right)\alpha^3 C_A^3\pi^2 \\
&\quad -75816\sqrt{3}\psi'\left(\tfrac{1}{3}\right)\alpha^3 C_A^3 - 21504\sqrt{3}\psi'\left(\tfrac{1}{3}\right)\alpha^3 C_A^2 N_f \pi^2 T_F \\
&\quad -186624\sqrt{3}\psi'\left(\tfrac{1}{3}\right)\alpha^3 C_A^2 N_f T_F + 158256\sqrt{3}\psi'\left(\tfrac{1}{3}\right)\alpha^2 C_A^3\pi^2 \\
&\quad +1189728\sqrt{3}\psi'\left(\tfrac{1}{3}\right)\alpha^2 C_A^3 - 72576\sqrt{3}\psi'\left(\tfrac{1}{3}\right)\alpha^2 C_A^2 N_f \pi^2 T_F \\
&\quad -699840\sqrt{3}\psi'\left(\tfrac{1}{3}\right)\alpha^2 C_A^2 N_f T_F \\
&\quad +124416\sqrt{3}\psi'\left(\tfrac{1}{3}\right)\alpha^2 C_A C_F N_f T_F \\
&\quad -187320\sqrt{3}\psi'\left(\tfrac{1}{3}\right)\alpha C_A^3\pi^2 + 77976\sqrt{3}\psi'\left(\tfrac{1}{3}\right)\alpha C_A^3 \\
&\quad +107520\sqrt{3}\psi'\left(\tfrac{1}{3}\right)\alpha C_A^2 N_f \pi^2 T_F + 597888\sqrt{3}\psi'\left(\tfrac{1}{3}\right)\alpha C_A^2 N_f T_F \\
&\quad +995328\sqrt{3}\psi'\left(\tfrac{1}{3}\right)\alpha C_A C_F N_f T_F + 55296\sqrt{3}\psi'\left(\tfrac{1}{3}\right)\alpha C_A N_f^2 T_F^2 \\
&\quad +54600\sqrt{3}\psi'\left(\tfrac{1}{3}\right) C_A^3\pi^2 - 7120224\sqrt{3}\psi'\left(\tfrac{1}{3}\right) C_A^3 \\
&\quad -33600\sqrt{3}\psi'\left(\tfrac{1}{3}\right) C_A^2 N_f \pi^2 T_F + 7615296\sqrt{3}\psi'\left(\tfrac{1}{3}\right) C_A^2 N_f T_F \\
&\quad -622080\sqrt{3}\psi'\left(\tfrac{1}{3}\right) C_A C_F N_f T_F - 2115072\sqrt{3}\psi'\left(\tfrac{1}{3}\right) C_A N_f^2 T_F^2 \\
&\quad +81\sqrt{3}\psi'''\left(\tfrac{1}{3}\right)\alpha^4 C_A^3 - 1890\sqrt{3}\psi'''\left(\tfrac{1}{3}\right)\alpha^3 C_A^3
\end{aligned}
$$

$$
\begin{aligned}
&+216\sqrt{3}\psi'''\left(\tfrac{1}{3}\right)\alpha^3C_A^2N_fT_F+9180\sqrt{3}\psi'''\left(\tfrac{1}{3}\right)\alpha^2C_A^3\\
&-4104\sqrt{3}\psi'''\left(\tfrac{1}{3}\right)\alpha^2C_A^2N_fT_F-1890\sqrt{3}\psi'''\left(\tfrac{1}{3}\right)\alpha C_A^3\\
&+6696\sqrt{3}\psi'''\left(\tfrac{1}{3}\right)\alpha C_A^2N_fT_F-38961\sqrt{3}\psi'''\left(\tfrac{1}{3}\right)C_A^3\\
&+23976\sqrt{3}\psi'''\left(\tfrac{1}{3}\right)C_A^2N_fT_F+174960\sqrt{3}s_2\left(\tfrac{\pi}{6}\right)\alpha^4C_A^3\\
&-1877904\sqrt{3}s_2\left(\tfrac{\pi}{6}\right)\alpha^3C_A^3+466560\sqrt{3}s_2\left(\tfrac{\pi}{6}\right)\alpha^3C_A^2N_fT_F\\
&+6076944\sqrt{3}s_2\left(\tfrac{\pi}{6}\right)\alpha^2C_A^3-2985984\sqrt{3}s_2\left(\tfrac{\pi}{6}\right)\alpha^2C_A^2N_fT_F\\
&+6170256\sqrt{3}s_2\left(\tfrac{\pi}{6}\right)\alpha C_A^3-1213056\sqrt{3}s_2\left(\tfrac{\pi}{6}\right)\alpha C_A^2N_fT_F\\
&-49735296\sqrt{3}s_2\left(\tfrac{\pi}{6}\right)C_A^3+50015232\sqrt{3}s_2\left(\tfrac{\pi}{6}\right)C_A^2N_fT_F\\
&-11943936\sqrt{3}s_2\left(\tfrac{\pi}{6}\right)C_AN_f^2T_F^2-349920\sqrt{3}s_2\left(\tfrac{\pi}{2}\right)\alpha^4C_A^3\\
&+3755808\sqrt{3}s_2\left(\tfrac{\pi}{2}\right)\alpha^3C_A^3-933120\sqrt{3}s_2\left(\tfrac{\pi}{2}\right)\alpha^3C_A^2N_fT_F\\
&-12153888\sqrt{3}s_2\left(\tfrac{\pi}{2}\right)\alpha^2C_A^3+5971968\sqrt{3}s_2\left(\tfrac{\pi}{2}\right)\alpha^2C_A^2N_fT_F\\
&-12340512\sqrt{3}s_2\left(\tfrac{\pi}{2}\right)\alpha C_A^3+2426112\sqrt{3}s_2\left(\tfrac{\pi}{2}\right)\alpha C_A^2N_fT_F\\
&+99470592\sqrt{3}s_2\left(\tfrac{\pi}{2}\right)C_A^3-100030464\sqrt{3}s_2\left(\tfrac{\pi}{2}\right)C_A^2N_fT_F\\
&+23887872\sqrt{3}s_2\left(\tfrac{\pi}{2}\right)C_AN_f^2T_F^2-291600\sqrt{3}s_3\left(\tfrac{\pi}{6}\right)\alpha^4C_A^3\\
&+3129840\sqrt{3}s_3\left(\tfrac{\pi}{6}\right)\alpha^3C_A^3-777600\sqrt{3}s_3\left(\tfrac{\pi}{6}\right)\alpha^3C_A^2N_fT_F\\
&-10128240\sqrt{3}s_3\left(\tfrac{\pi}{6}\right)\alpha^2C_A^3+4976640\sqrt{3}s_3\left(\tfrac{\pi}{6}\right)\alpha^2C_A^2N_fT_F\\
&-10283760\sqrt{3}s_3\left(\tfrac{\pi}{6}\right)\alpha C_A^3+2021760\sqrt{3}s_3\left(\tfrac{\pi}{6}\right)\alpha C_A^2N_fT_F\\
&+82892160\sqrt{3}s_3\left(\tfrac{\pi}{6}\right)C_A^3-83358720\sqrt{3}s_3\left(\tfrac{\pi}{6}\right)C_A^2N_fT_F\\
&+19906560\sqrt{3}s_3\left(\tfrac{\pi}{6}\right)C_AN_f^2T_F^2+233280\sqrt{3}s_3\left(\tfrac{\pi}{2}\right)\alpha^4C_A^3\\
&-2503872\sqrt{3}s_3\left(\tfrac{\pi}{2}\right)\alpha^3C_A^3+622080\sqrt{3}s_3\left(\tfrac{\pi}{2}\right)\alpha^3C_A^2N_fT_F\\
&+8102592\sqrt{3}s_3\left(\tfrac{\pi}{2}\right)\alpha^2C_A^3-3981312\sqrt{3}s_3\left(\tfrac{\pi}{2}\right)\alpha^2C_A^2N_fT_F\\
&+8227008\sqrt{3}s_3\left(\tfrac{\pi}{2}\right)\alpha C_A^3-1617408\sqrt{3}s_3\left(\tfrac{\pi}{2}\right)\alpha C_A^2N_fT_F\\
&-66313728\sqrt{3}s_3\left(\tfrac{\pi}{2}\right)C_A^3+66686976\sqrt{3}s_3\left(\tfrac{\pi}{2}\right)C_A^2N_fT_F\\
&-15925248\sqrt{3}s_3\left(\tfrac{\pi}{2}\right)C_AN_f^2T_F^2+168\sqrt{3}\alpha^5C_A^3\pi^4\\
&+5184\sqrt{3}\alpha^5C_A^3\pi^2+1744\sqrt{3}\alpha^4C_A^3\pi^4+26784\sqrt{3}\alpha^4C_A^3\pi^2\\
&-2916\sqrt{3}\alpha^4C_A^3\zeta_3-40824\sqrt{3}\alpha^4C_A^3+448\sqrt{3}\alpha^4C_A^2N_f\pi^4T_F\\
&+13824\sqrt{3}\alpha^4C_A^2N_f\pi^2T_F+46656\sqrt{3}\alpha^4C_A^2N_fT_F\\
&+2464\sqrt{3}\alpha^3C_A^3\pi^4+50544\sqrt{3}\alpha^3C_A^3\pi^2\\
&+111780\sqrt{3}\alpha^3C_A^3\zeta_3-349920\sqrt{3}\alpha^3C_A^3\\
&+6592\sqrt{3}\alpha^3C_A^2N_f\pi^4T_F+124416\sqrt{3}\alpha^3C_A^2N_f\pi^2T_F\\
&-7776\sqrt{3}\alpha^3C_A^2N_fT_F\zeta_3+466560\sqrt{3}\alpha^3C_A^2N_fT_F\\
&-77232\sqrt{3}\alpha^2C_A^3\pi^4-793152\sqrt{3}\alpha^2C_A^3\pi^2
\end{aligned}
$$

$$
\begin{aligned}
&-729972\sqrt{3}\alpha^2 C_A^3\zeta_3 - 194400\sqrt{3}\alpha^2 C_A^3 \\
&+35136\sqrt{3}\alpha^2 C_A^2 N_f \pi^4 T_F + 466560\sqrt{3}\alpha^2 C_A^2 N_f \pi^2 T_F \\
&+264384\sqrt{3}\alpha^2 C_A^2 N_f T_F \zeta_3 - 264384\sqrt{3}\alpha^2 C_A^2 N_f T_F \\
&-82944\sqrt{3}\alpha^2 C_A C_F N_f \pi^2 T_F - 1679616\sqrt{3}\alpha^2 C_A C_F N_f T_F \\
&+67480\sqrt{3}\alpha C_A^3 \pi^4 - 51984\sqrt{3}\alpha C_A^3 \pi^2 \\
&-4909572\sqrt{3}\alpha C_A^3 \zeta_3 + 8526384\sqrt{3}\alpha C_A^3 \\
&-53696\sqrt{3}\alpha C_A^2 N_f \pi^4 T_F - 398592\sqrt{3}\alpha C_A^2 N_f \pi^2 T_F \\
&+1158624\sqrt{3}\alpha C_A^2 N_f T_F \zeta_3 - 8009280\sqrt{3}\alpha C_A^2 N_f T_F \\
&-663552\sqrt{3}\alpha C_A C_F N_f \pi^2 T_F - 6718464\sqrt{3}\alpha C_A C_F N_f T_F \\
&-36864\sqrt{3}\alpha C_A N_f^2 \pi^2 T_F^2 + 248832\sqrt{3}\alpha C_A N_f^2 T_F^2 \\
&+85696\sqrt{3} C_A^3 \pi^4 + 4746816\sqrt{3} C_A^3 \pi^2 \\
&+14628600\sqrt{3} C_A^3 \zeta_3 - 37070136\sqrt{3} C_A^3 - 52736\sqrt{3} C_A^2 N_f \pi^4 T_F \\
&-5076864\sqrt{3} C_A^2 N_f \pi^2 T_F + 4121280\sqrt{3} C_A^2 N_f T_F \zeta_3 \\
&+35847360\sqrt{3} C_A^2 N_f T_F + 414720\sqrt{3} C_A C_F N_f \pi^2 T_F \\
&-32845824\sqrt{3} C_A C_F N_f T_F \zeta_3 + 33716736\sqrt{3} C_A C_F N_f T_F \\
&+1410048\sqrt{3} C_A N_f^2 \pi^2 T_F^2 - 3981312\sqrt{3} C_A N_f^2 T_F^2 \zeta_3 \\
&-5225472\sqrt{3} C_A N_f^2 T_F^2 - 1119744\sqrt{3} C_F^2 N_f T_F \\
&+11943936\sqrt{3} C_F N_f^2 T_F^2 \zeta_3 - 11446272\sqrt{3} C_F N_f^2 T_F^2 \\
&+1215 \ln(3)^2 \alpha^4 C_A^3 \pi - 13041 \ln(3)^2 \alpha^3 C_A^3 \pi \\
&+3240 \ln(3)^2 \alpha^3 C_A^2 N_f \pi T_F + 42201 \ln(3)^2 \alpha^2 C_A^3 \pi \\
&-20736 \ln(3)^2 \alpha^2 C_A^2 N_f \pi T_F + 42849 \ln(3)^2 \alpha C_A^3 \pi \\
&-8424 \ln(3)^2 \alpha C_A^2 N_f \pi T_F - 345384 \ln(3)^2 C_A^3 \pi \\
&+347328 \ln(3)^2 C_A^2 N_f \pi T_F - 82944 \ln(3)^2 C_A N_f^2 \pi T_F^2 \\
&-14580 \ln(3) \alpha^4 C_A^3 \pi + 156492 \ln(3) \alpha^3 C_A^3 \pi \\
&-38880 \ln(3) \alpha^3 C_A^2 N_f \pi T_F - 506412 \ln(3) \alpha^2 C_A^3 \pi \\
&+248832 \ln(3) \alpha^2 C_A^2 N_f \pi T_F - 514188 \ln(3) \alpha C_A^3 \pi \\
&+101088 \ln(3) \alpha C_A^2 N_f \pi T_F + 4144608 \ln(3) C_A^3 \pi \\
&-4167936 \ln(3) C_A^2 N_f \pi T_F + 995328 \ln(3) C_A N_f^2 \pi T_F^2 \\
&-1305 \alpha^4 C_A^3 \pi^3 + 14007 \alpha^3 C_A^3 \pi^3 - 3480 \alpha^3 C_A^2 N_f \pi^3 T_F \\
&-45327 \alpha^2 C_A^3 \pi^3 + 22272 \alpha^2 C_A^2 N_f \pi^3 T_F - 46023 \alpha C_A^3 \pi^3 \\
&+9048 \alpha C_A^2 N_f \pi^3 T_F + 370968 C_A^3 \pi^3 - 373056 C_A^2 N_f \pi^3 T_F
\end{aligned}
$$

$$
\begin{aligned}
&+89088 C_A N_f^2 \pi^3 T_F^2 \big] \frac{a^3}{559872\sqrt{3}} \; + \; \mathcal{O}(a^4) \\
\gamma_\alpha^{\rm MOMh}(a,\alpha) \;=\; & \big[-3\alpha C_A + 13 C_A - 8 N_f T_F \big] \frac{a}{6} \\
&+ \big[-9\psi'\left(\tfrac{1}{3}\right) \alpha^3 C_A^2 - 33\psi'\left(\tfrac{1}{3}\right) \alpha^2 C_A^2 - 24\psi'\left(\tfrac{1}{3}\right) \alpha^2 C_A N_f T_F \\
&+357\psi'\left(\tfrac{1}{3}\right) \alpha C_A^2 - 192\psi'\left(\tfrac{1}{3}\right) \alpha C_A N_f T_F - 195\psi'\left(\tfrac{1}{3}\right) C_A^2 \\
&+120\psi'\left(\tfrac{1}{3}\right) C_A N_f T_F + 6\alpha^3 C_A^2 \pi^2 + 162\alpha^3 C_A^2 + 22\alpha^2 C_A^2 \pi^2 \\
&-135\alpha^2 C_A^2 + 16\alpha^2 C_A N_f \pi^2 T_F + 432\alpha^2 C_A N_f T_F - 238\alpha C_A^2 \pi^2 \\
&-1539\alpha C_A^2 + 128\alpha C_A N_f \pi^2 T_F + 1296\alpha C_A N_f T_F + 130 C_A^2 \pi^2 \\
&+3186 C_A^2 - 80 C_A N_f \pi^2 T_F - 2808 C_A N_f T_F \\
&-2592 C_F N_f T_F \big] \frac{a^2}{648} \\
&+ \Big[-378\sqrt{3}\psi'\left(\tfrac{1}{3}\right)^2 \alpha^5 C_A^3 - 4410\sqrt{3}\psi'\left(\tfrac{1}{3}\right)^2 \alpha^4 C_A^3 \\
&-1008\sqrt{3}\psi'\left(\tfrac{1}{3}\right)^2 \alpha^4 C_A^2 N_f T_F + 5796\sqrt{3}\psi'\left(\tfrac{1}{3}\right)^2 \alpha^3 C_A^3 \\
&-16128\sqrt{3}\psi'\left(\tfrac{1}{3}\right)^2 \alpha^3 C_A^2 N_f T_F + 118692\sqrt{3}\psi'\left(\tfrac{1}{3}\right)^2 \alpha^2 C_A^3 \\
&-54432\sqrt{3}\psi'\left(\tfrac{1}{3}\right)^2 \alpha^2 C_A^2 N_f T_F - 140490\sqrt{3}\psi'\left(\tfrac{1}{3}\right)^2 \alpha C_A^3 \\
&+80640\sqrt{3}\psi'\left(\tfrac{1}{3}\right)^2 \alpha C_A^2 N_f T_F + 40950\sqrt{3}\psi'\left(\tfrac{1}{3}\right)^2 C_A^3 \\
&-25200\sqrt{3}\psi'\left(\tfrac{1}{3}\right)^2 C_A^2 N_f T_F + 504\sqrt{3}\psi'\left(\tfrac{1}{3}\right) \alpha^5 C_A^3 \pi^2 \\
&+7776\sqrt{3}\psi'\left(\tfrac{1}{3}\right) \alpha^5 C_A^3 + 5880\sqrt{3}\psi'\left(\tfrac{1}{3}\right) \alpha^4 C_A^3 \pi^2 \\
&+40176\sqrt{3}\psi'\left(\tfrac{1}{3}\right) \alpha^4 C_A^3 + 1344\sqrt{3}\psi'\left(\tfrac{1}{3}\right) \alpha^4 C_A^2 N_f \pi^2 T_F \\
&+20736\sqrt{3}\psi'\left(\tfrac{1}{3}\right) \alpha^4 C_A^2 N_f T_F - 7728\sqrt{3}\psi'\left(\tfrac{1}{3}\right) \alpha^3 C_A^3 \pi^2 \\
&+75816\sqrt{3}\psi'\left(\tfrac{1}{3}\right) \alpha^3 C_A^3 + 21504\sqrt{3}\psi'\left(\tfrac{1}{3}\right) \alpha^3 C_A^2 N_f \pi^2 T_F \\
&+186624\sqrt{3}\psi'\left(\tfrac{1}{3}\right) \alpha^3 C_A^2 N_f T_F - 158256\sqrt{3}\psi'\left(\tfrac{1}{3}\right) \alpha^2 C_A^3 \pi^2 \\
&-1189728\sqrt{3}\psi'\left(\tfrac{1}{3}\right) \alpha^2 C_A^3 + 72576\sqrt{3}\psi'\left(\tfrac{1}{3}\right) \alpha^2 C_A^2 N_f \pi^2 T_F \\
&+699840\sqrt{3}\psi'\left(\tfrac{1}{3}\right) \alpha^2 C_A^2 N_f T_F \\
&-124416\sqrt{3}\psi'\left(\tfrac{1}{3}\right) \alpha^2 C_A C_F N_f T_F \\
&+187320\sqrt{3}\psi'\left(\tfrac{1}{3}\right) \alpha C_A^3 \pi^2 - 77976\sqrt{3}\psi'\left(\tfrac{1}{3}\right) \alpha C_A^3 \\
&-107520\sqrt{3}\psi'\left(\tfrac{1}{3}\right) \alpha C_A^2 N_f \pi^2 T_F - 597888\sqrt{3}\psi'\left(\tfrac{1}{3}\right) \alpha C_A^2 N_f T_F \\
&-995328\sqrt{3}\psi'\left(\tfrac{1}{3}\right) \alpha C_A C_F N_f T_F - 55296\sqrt{3}\psi'\left(\tfrac{1}{3}\right) \alpha C_A N_f^2 T_F^2 \\
&-54600\sqrt{3}\psi'\left(\tfrac{1}{3}\right) C_A^3 \pi^2 + 7120224\sqrt{3}\psi'\left(\tfrac{1}{3}\right) C_A^3 \\
&+33600\sqrt{3}\psi'\left(\tfrac{1}{3}\right) C_A^2 N_f \pi^2 T_F - 7615296\sqrt{3}\psi'\left(\tfrac{1}{3}\right) C_A^2 N_f T_F \\
&+622080\sqrt{3}\psi'\left(\tfrac{1}{3}\right) C_A C_F N_f T_F + 2115072\sqrt{3}\psi'\left(\tfrac{1}{3}\right) C_A N_f^2 T_F^2 \\
&-81\sqrt{3}\psi'''\left(\tfrac{1}{3}\right) \alpha^4 C_A^3 + 1890\sqrt{3}\psi'''\left(\tfrac{1}{3}\right) \alpha^3 C_A^3 \\
&-216\sqrt{3}\psi'''\left(\tfrac{1}{3}\right) \alpha^3 C_A^2 N_f T_F - 9180\sqrt{3}\psi'''\left(\tfrac{1}{3}\right) \alpha^2 C_A^3
\end{aligned}
$$

$$
\begin{aligned}
&+4104\sqrt{3}\psi'''\left(\tfrac{1}{3}\right)\alpha^2 C_A^2 N_f T_F + 1890\sqrt{3}\psi'''\left(\tfrac{1}{3}\right)\alpha C_A^3 \\
&-6696\sqrt{3}\psi'''\left(\tfrac{1}{3}\right)\alpha C_A^2 N_f T_F + 38961\sqrt{3}\psi'''\left(\tfrac{1}{3}\right) C_A^3 \\
&-23976\sqrt{3}\psi'''\left(\tfrac{1}{3}\right) C_A^2 N_f T_F - 174960\sqrt{3}s_2\left(\tfrac{\pi}{6}\right)\alpha^4 C_A^3 \\
&+1877904\sqrt{3}s_2\left(\tfrac{\pi}{6}\right)\alpha^3 C_A^3 - 466560\sqrt{3}s_2\left(\tfrac{\pi}{6}\right)\alpha^3 C_A^2 N_f T_F \\
&-6076944\sqrt{3}s_2\left(\tfrac{\pi}{6}\right)\alpha^2 C_A^3 + 2985984\sqrt{3}s_2\left(\tfrac{\pi}{6}\right)\alpha^2 C_A^2 N_f T_F \\
&-6170256\sqrt{3}s_2\left(\tfrac{\pi}{6}\right)\alpha C_A^3 + 1213056\sqrt{3}s_2\left(\tfrac{\pi}{6}\right)\alpha C_A^2 N_f T_F \\
&+49735296\sqrt{3}s_2\left(\tfrac{\pi}{6}\right) C_A^3 - 50015232\sqrt{3}s_2\left(\tfrac{\pi}{6}\right) C_A^2 N_f T_F \\
&+11943936\sqrt{3}s_2\left(\tfrac{\pi}{6}\right) C_A N_f^2 T_F^2 + 349920\sqrt{3}s_2\left(\tfrac{\pi}{2}\right)\alpha^4 C_A^3 \\
&-3755808\sqrt{3}s_2\left(\tfrac{\pi}{2}\right)\alpha^3 C_A^3 + 933120\sqrt{3}s_2\left(\tfrac{\pi}{2}\right)\alpha^3 C_A^2 N_f T_F \\
&+12153888\sqrt{3}s_2\left(\tfrac{\pi}{2}\right)\alpha^2 C_A^3 - 5971968\sqrt{3}s_2\left(\tfrac{\pi}{2}\right)\alpha^2 C_A^2 N_f T_F \\
&+12340512\sqrt{3}s_2\left(\tfrac{\pi}{2}\right)\alpha C_A^3 - 2426112\sqrt{3}s_2\left(\tfrac{\pi}{2}\right)\alpha C_A^2 N_f T_F \\
&-99470592\sqrt{3}s_2\left(\tfrac{\pi}{2}\right) C_A^3 + 100030464\sqrt{3}s_2\left(\tfrac{\pi}{2}\right) C_A^2 N_f T_F \\
&-23887872\sqrt{3}s_2\left(\tfrac{\pi}{2}\right) C_A N_f^2 T_F^2 + 291600\sqrt{3}s_3\left(\tfrac{\pi}{6}\right)\alpha^4 C_A^3 \\
&-3129840\sqrt{3}s_3\left(\tfrac{\pi}{6}\right)\alpha^3 C_A^3 + 777600\sqrt{3}s_3\left(\tfrac{\pi}{6}\right)\alpha^3 C_A^2 N_f T_F \\
&+10128240\sqrt{3}s_3\left(\tfrac{\pi}{6}\right)\alpha^2 C_A^3 - 4976640\sqrt{3}s_3\left(\tfrac{\pi}{6}\right)\alpha^2 C_A^2 N_f T_F \\
&+10283760\sqrt{3}s_3\left(\tfrac{\pi}{6}\right)\alpha C_A^3 - 2021760\sqrt{3}s_3\left(\tfrac{\pi}{6}\right)\alpha C_A^2 N_f T_F \\
&-82892160\sqrt{3}s_3\left(\tfrac{\pi}{6}\right) C_A^3 + 83358720\sqrt{3}s_3\left(\tfrac{\pi}{6}\right) C_A^2 N_f T_F \\
&-19906560\sqrt{3}s_3\left(\tfrac{\pi}{6}\right) C_A N_f^2 T_F^2 - 233280\sqrt{3}s_3\left(\tfrac{\pi}{2}\right)\alpha^4 C_A^3 \\
&+2503872\sqrt{3}s_3\left(\tfrac{\pi}{2}\right)\alpha^3 C_A^3 - 622080\sqrt{3}s_3\left(\tfrac{\pi}{2}\right)\alpha^3 C_A^2 N_f T_F \\
&-8102592\sqrt{3}s_3\left(\tfrac{\pi}{2}\right)\alpha^2 C_A^3 + 3981312\sqrt{3}s_3\left(\tfrac{\pi}{2}\right)\alpha^2 C_A^2 N_f T_F \\
&-8227008\sqrt{3}s_3\left(\tfrac{\pi}{2}\right)\alpha C_A^3 + 1617408\sqrt{3}s_3\left(\tfrac{\pi}{2}\right)\alpha C_A^2 N_f T_F \\
&+66313728\sqrt{3}s_3\left(\tfrac{\pi}{2}\right) C_A^3 - 66686976\sqrt{3}s_3\left(\tfrac{\pi}{2}\right) C_A^2 N_f T_F \\
&+15925248\sqrt{3}s_3\left(\tfrac{\pi}{2}\right) C_A N_f^2 T_F^2 - 168\sqrt{3}\alpha^5 C_A^3 \pi^4 \\
&-5184\sqrt{3}\alpha^5 C_A^3 \pi^2 - 1744\sqrt{3}\alpha^4 C_A^3 \pi^4 - 26784\sqrt{3}\alpha^4 C_A^3 \pi^2 \\
&+2916\sqrt{3}\alpha^4 C_A^3 \zeta_3 + 40824\sqrt{3}\alpha^4 C_A^3 - 448\sqrt{3}\alpha^4 C_A^2 N_f \pi^4 T_F \\
&-13824\sqrt{3}\alpha^4 C_A^2 N_f \pi^2 T_F - 46656\sqrt{3}\alpha^4 C_A^2 N_f T_F \\
&-2464\sqrt{3}\alpha^3 C_A^3 \pi^4 - 50544\sqrt{3}\alpha^3 C_A^3 \pi^2 - 111780\sqrt{3}\alpha^3 C_A^3 \zeta_3 \\
&+349920\sqrt{3}\alpha^3 C_A^3 - 6592\sqrt{3}\alpha^3 C_A^2 N_f \pi^4 T_F \\
&-124416\sqrt{3}\alpha^3 C_A^2 N_f \pi^2 T_F + 7776\sqrt{3}\alpha^3 C_A^2 N_f T_F \zeta_3 \\
&-466560\sqrt{3}\alpha^3 C_A^2 N_f T_F + 77232\sqrt{3}\alpha^2 C_A^3 \pi^4 \\
&+793152\sqrt{3}\alpha^2 C_A^3 \pi^2 + 729972\sqrt{3}\alpha^2 C_A^3 \zeta_3 \\
&+194400\sqrt{3}\alpha^2 C_A^3 - 35136\sqrt{3}\alpha^2 C_A^2 N_f \pi^4 T_F
\end{aligned}
$$

$$
\begin{aligned}
&-466560\sqrt{3}\alpha^2 C_A^2 N_f \pi^2 T_F - 264384\sqrt{3}\alpha^2 C_A^2 N_f T_F \zeta_3 \\
&+264384\sqrt{3}\alpha^2 C_A^2 N_f T_F + 82944\sqrt{3}\alpha^2 C_A C_F N_f \pi^2 T_F \\
&+1679616\sqrt{3}\alpha^2 C_A C_F N_f T_F - 67480\sqrt{3}\alpha C_A^3 \pi^4 \\
&+51984\sqrt{3}\alpha C_A^3 \pi^2 + 4909572\sqrt{3}\alpha C_A^3 \zeta_3 \\
&-8526384\sqrt{3}\alpha C_A^3 + 53696\sqrt{3}\alpha C_A^2 N_f \pi^4 T_F \\
&+398592\sqrt{3}\alpha C_A^2 N_f \pi^2 T_F - 1158624\sqrt{3}\alpha C_A^2 N_f T_F \zeta_3 \\
&+8009280\sqrt{3}\alpha C_A^2 N_f T_F + 663552\sqrt{3}\alpha C_A C_F N_f \pi^2 T_F \\
&+6718464\sqrt{3}\alpha C_A C_F N_f T_F + 36864\sqrt{3}\alpha C_A N_f^2 \pi^2 T_F^2 \\
&-248832\sqrt{3}\alpha C_A N_f^2 T_F^2 - 85696\sqrt{3} C_A^3 \pi^4 - 4746816\sqrt{3} C_A^3 \pi^2 \\
&-14628600\sqrt{3} C_A^3 \zeta_3 + 37070136\sqrt{3} C_A^3 + 52736\sqrt{3} C_A^2 N_f \pi^4 T_F \\
&+5076864\sqrt{3} C_A^2 N_f \pi^2 T_F - 4121280\sqrt{3} C_A^2 N_f T_F \zeta_3 \\
&-35847360\sqrt{3} C_A^2 N_f T_F - 414720\sqrt{3} C_A C_F N_f \pi^2 T_F \\
&+32845824\sqrt{3} C_A C_F N_f T_F \zeta_3 - 33716736\sqrt{3} C_A C_F N_f T_F \\
&-1410048\sqrt{3} C_A N_f^2 \pi^2 T_F^2 + 3981312\sqrt{3} C_A N_f^2 T_F^2 \zeta_3 \\
&+5225472\sqrt{3} C_A N_f^2 T_F^2 + 1119744\sqrt{3} C_F^2 N_f T_F \\
&-11943936\sqrt{3} C_F N_f^2 T_F^2 \zeta_3 + 11446272\sqrt{3} C_F N_f^2 T_F^2 \\
&-1215 \ln(3)^2 \alpha^4 C_A^3 \pi + 13041 \ln(3)^2 \alpha^3 C_A^3 \pi \\
&-3240 \ln(3)^2 \alpha^3 C_A^2 N_f \pi T_F - 42201 \ln(3)^2 \alpha^2 C_A^3 \pi \\
&+20736 \ln(3)^2 \alpha^2 C_A^2 N_f \pi T_F - 42849 \ln(3)^2 \alpha C_A^3 \pi \\
&+8424 \ln(3)^2 \alpha C_A^2 N_f \pi T_F + 345384 \ln(3)^2 C_A^3 \pi \\
&-347328 \ln(3)^2 C_A^2 N_f \pi T_F + 82944 \ln(3)^2 C_A N_f^2 \pi T_F^2 \\
&+14580 \ln(3) \alpha^4 C_A^3 \pi - 156492 \ln(3) \alpha^3 C_A^3 \pi \\
&+38880 \ln(3) \alpha^3 C_A^2 N_f \pi T_F + 506412 \ln(3) \alpha^2 C_A^3 \pi \\
&-248832 \ln(3) \alpha^2 C_A^2 N_f \pi T_F + 514188 \ln(3) \alpha C_A^3 \pi \\
&-101088 \ln(3) \alpha C_A^2 N_f \pi T_F - 4144608 \ln(3) C_A^3 \pi \\
&+4167936 \ln(3) C_A^2 N_f \pi T_F - 995328 \ln(3) C_A N_f^2 \pi T_F^2 \\
&+1305 \alpha^4 C_A^3 \pi^3 - 14007 \alpha^3 C_A^3 \pi^3 + 3480 \alpha^3 C_A^2 N_f \pi^3 T_F \\
&+45327 \alpha^2 C_A^3 \pi^3 - 22272 \alpha^2 C_A^2 N_f \pi^3 T_F + 46023 \alpha C_A^3 \pi^3 \\
&-9048 \alpha C_A^2 N_f \pi^3 T_F - 370968 C_A^3 \pi^3 + 373056 C_A^2 N_f \pi^3 T_F \\
&-89088 C_A N_f^2 \pi^3 T_F^2 \Big] \frac{a^3}{559872\sqrt{3}} \; + \; \mathcal{O}(a^4)
\end{aligned}
$$

$$
\gamma_c^{\rm MOMh}(a,\alpha) \;=\; C_A(\alpha - 3)\frac{a}{4}
$$

$$
\begin{aligned}
&+C_A\,\big[3\psi'\left(\tfrac{1}{3}\right)\alpha^3 C_A + 15\psi'\left(\tfrac{1}{3}\right)\alpha^2 C_A - 87\psi'\left(\tfrac{1}{3}\right)\alpha C_A \\
&\quad +45\psi'\left(\tfrac{1}{3}\right) C_A - 2\alpha^3 C_A\pi^2 - 10\alpha^2 C_A\pi^2 - 27\alpha^2 C_A \\
&\quad +58\alpha C_A\pi^2 + 135\alpha C_A - 30 C_A\pi^2 - 594 C_A \\
&\quad +216 N_f T_F\big]\,\frac{a^2}{432} \\
&+C_A\,\Big[126\sqrt{3}\psi'\left(\tfrac{1}{3}\right)^2\alpha^5 C_A^2 + 1638\sqrt{3}\psi'\left(\tfrac{1}{3}\right)^2\alpha^4 C_A^2 \\
&\quad +756\sqrt{3}\psi'\left(\tfrac{1}{3}\right)^2\alpha^3 C_A^2 - 30492\sqrt{3}\psi'\left(\tfrac{1}{3}\right)^2\alpha^2 C_A^2 \\
&\quad +33390\sqrt{3}\psi'\left(\tfrac{1}{3}\right)^2\alpha C_A^2 - 9450\sqrt{3}\psi'\left(\tfrac{1}{3}\right)^2 C_A^2 \\
&\quad -168\sqrt{3}\psi'\left(\tfrac{1}{3}\right)\alpha^5 C_A^2\pi^2 - 2184\sqrt{3}\psi'\left(\tfrac{1}{3}\right)\alpha^4 C_A^2\pi^2 \\
&\quad +3888\sqrt{3}\psi'\left(\tfrac{1}{3}\right)\alpha^4 C_A^2 - 1008\sqrt{3}\psi'\left(\tfrac{1}{3}\right)\alpha^3 C_A^2\pi^2 \\
&\quad -77112\sqrt{3}\psi'\left(\tfrac{1}{3}\right)\alpha^3 C_A^2 + 40656\sqrt{3}\psi'\left(\tfrac{1}{3}\right)\alpha^2 C_A^2\pi^2 \\
&\quad +214272\sqrt{3}\psi'\left(\tfrac{1}{3}\right)\alpha^2 C_A^2 + 17280\sqrt{3}\psi'\left(\tfrac{1}{3}\right)\alpha^2 C_A N_f T_F \\
&\quad -44520\sqrt{3}\psi'\left(\tfrac{1}{3}\right)\alpha C_A^2\pi^2 + 311688\sqrt{3}\psi'\left(\tfrac{1}{3}\right)\alpha C_A^2 \\
&\quad -202176\sqrt{3}\psi'\left(\tfrac{1}{3}\right)\alpha C_A N_f T_F + 12600\sqrt{3}\psi'\left(\tfrac{1}{3}\right) C_A^2\pi^2 \\
&\quad -1677024\sqrt{3}\psi'\left(\tfrac{1}{3}\right) C_A^2 + 741312\sqrt{3}\psi'\left(\tfrac{1}{3}\right) C_A N_f T_F \\
&\quad +27\sqrt{3}\psi'''\left(\tfrac{1}{3}\right)\alpha^4 C_A^2 - 594\sqrt{3}\psi'''\left(\tfrac{1}{3}\right)\alpha^3 C_A^2 \\
&\quad +2376\sqrt{3}\psi'''\left(\tfrac{1}{3}\right)\alpha^2 C_A^2 + 486\sqrt{3}\psi'''\left(\tfrac{1}{3}\right)\alpha C_A^2 \\
&\quad -8991\sqrt{3}\psi'''\left(\tfrac{1}{3}\right) C_A^2 + 58320\sqrt{3}s_2\left(\tfrac{\pi}{6}\right)\alpha^4 C_A^2 \\
&\quad -548208\sqrt{3}s_2\left(\tfrac{\pi}{6}\right)\alpha^3 C_A^2 + 1527984\sqrt{3}s_2\left(\tfrac{\pi}{6}\right)\alpha^2 C_A^2 \\
&\quad +2601072\sqrt{3}s_2\left(\tfrac{\pi}{6}\right)\alpha C_A^2 - 1492992\sqrt{3}s_2\left(\tfrac{\pi}{6}\right)\alpha C_A N_f T_F \\
&\quad -11477376\sqrt{3}s_2\left(\tfrac{\pi}{6}\right) C_A^2 + 4478976\sqrt{3}s_2\left(\tfrac{\pi}{6}\right) C_A N_f T_F \\
&\quad -116640\sqrt{3}s_2\left(\tfrac{\pi}{2}\right)\alpha^4 C_A^2 + 1096416\sqrt{3}s_2\left(\tfrac{\pi}{2}\right)\alpha^3 C_A^2 \\
&\quad -3055968\sqrt{3}s_2\left(\tfrac{\pi}{2}\right)\alpha^2 C_A^2 - 5202144\sqrt{3}s_2\left(\tfrac{\pi}{2}\right)\alpha C_A^2 \\
&\quad +2985984\sqrt{3}s_2\left(\tfrac{\pi}{2}\right)\alpha C_A N_f T_F + 22954752\sqrt{3}s_2\left(\tfrac{\pi}{2}\right) C_A^2 \\
&\quad -8957952\sqrt{3}s_2\left(\tfrac{\pi}{2}\right) C_A N_f T_F - 97200\sqrt{3}s_3\left(\tfrac{\pi}{6}\right)\alpha^4 C_A^2 \\
&\quad +913680\sqrt{3}s_3\left(\tfrac{\pi}{6}\right)\alpha^3 C_A^2 - 2546640\sqrt{3}s_3\left(\tfrac{\pi}{6}\right)\alpha^2 C_A^2 \\
&\quad -4335120\sqrt{3}s_3\left(\tfrac{\pi}{6}\right)\alpha C_A^2 + 2488320\sqrt{3}s_3\left(\tfrac{\pi}{6}\right)\alpha C_A N_f T_F \\
&\quad +19128960\sqrt{3}s_3\left(\tfrac{\pi}{6}\right) C_A^2 - 7464960\sqrt{3}s_3\left(\tfrac{\pi}{6}\right) C_A N_f T_F \\
&\quad +77760\sqrt{3}s_3\left(\tfrac{\pi}{2}\right)\alpha^4 C_A^2 - 730944\sqrt{3}s_3\left(\tfrac{\pi}{2}\right)\alpha^3 C_A^2 \\
&\quad +2037312\sqrt{3}s_3\left(\tfrac{\pi}{2}\right)\alpha^2 C_A^2 + 3468096\sqrt{3}s_3\left(\tfrac{\pi}{2}\right)\alpha C_A^2 \\
&\quad -1990656\sqrt{3}s_3\left(\tfrac{\pi}{2}\right)\alpha C_A N_f T_F - 15303168\sqrt{3}s_3\left(\tfrac{\pi}{2}\right) C_A^2 \\
&\quad +5971968\sqrt{3}s_3\left(\tfrac{\pi}{2}\right) C_A N_f T_F + 56\sqrt{3}\alpha^5 C_A^2\pi^4
\end{aligned}
$$

$$
\begin{aligned}
&+656\sqrt{3}\alpha^4 C_A^2\pi^4 - 2592\sqrt{3}\alpha^4 C_A^2\pi^2 - 972\sqrt{3}\alpha^4 C_A^2\zeta_3 \\
&+1920\sqrt{3}\alpha^3 C_A^2\pi^4 + 51408\sqrt{3}\alpha^3 C_A^2\pi^2 \\
&+105948\sqrt{3}\alpha^3 C_A^2\zeta_3 - 91368\sqrt{3}\alpha^3 C_A^2 \\
&-19888\sqrt{3}\alpha^2 C_A^2\pi^4 - 142848\sqrt{3}\alpha^2 C_A^2\pi^2 \\
&+57348\sqrt{3}\alpha^2 C_A^2\zeta_3 - 75816\sqrt{3}\alpha^2 C_A^2 \\
&-11520\sqrt{3}\alpha^2 C_A N_f\pi^2 T_F - 62208\sqrt{3}\alpha^2 C_A N_f T_F \\
&+13544\sqrt{3}\alpha C_A^2\pi^4 - 207792\sqrt{3}\alpha C_A^2\pi^2 \\
&-891324\sqrt{3}\alpha C_A^2\zeta_3 + 2218104\sqrt{3}\alpha C_A^2 \\
&+134784\sqrt{3}\alpha C_A N_f\pi^2 T_F + 435456\sqrt{3}\alpha C_A N_f T_F\zeta_3 \\
&-808704\sqrt{3}\alpha C_A N_f T_F + 19776\sqrt{3}C_A^2\pi^4 \\
&+1118016\sqrt{3}C_A^2\pi^2 + 2921832\sqrt{3}C_A^2\zeta_3 \\
&-8567208\sqrt{3}C_A^2 - 494208\sqrt{3}C_A N_f\pi^2 T_F \\
&-559872\sqrt{3}C_A N_f T_F\zeta_3 + 6780672\sqrt{3}C_A N_f T_F \\
&+559872\sqrt{3}C_F N_f T_F - 1244160\sqrt{3}N_f^2 T_F^2 \\
&+405\ln(3)^2\alpha^4 C_A^2\pi - 3807\ln(3)^2\alpha^3 C_A^2\pi \\
&+10611\ln(3)^2\alpha^2 C_A^2\pi + 18063\ln(3)^2\alpha C_A^2\pi \\
&-10368\ln(3)^2\alpha C_A N_f\pi T_F - 79704\ln(3)^2 C_A^2\pi \\
&+31104\ln(3)^2 C_A N_f\pi T_F - 4860\ln(3)\alpha^4 C_A^2\pi \\
&+45684\ln(3)\alpha^3 C_A^2\pi - 127332\ln(3)\alpha^2 C_A^2\pi \\
&-216756\ln(3)\alpha C_A^2\pi + 124416\ln(3)\alpha C_A N_f\pi T_F \\
&+956448\ln(3)C_A^2\pi - 373248\ln(3)C_A N_f\pi T_F - 435\alpha^4 C_A^2\pi^3 \\
&+4089\alpha^3 C_A^2\pi^3 - 11397\alpha^2 C_A^2\pi^3 - 19401\alpha C_A^2\pi^3 \\
&+11136\alpha C_A N_f\pi^3 T_F + 85608 C_A^2\pi^3 \\
&-33408 C_A N_f\pi^3 T_F\big]\,\frac{a^3}{373248\sqrt{3}} \;+\; \mathcal{O}(a^4)
\end{aligned}
$$

$$
\begin{aligned}
\gamma_\psi^{\mathrm{MOMh}}(a,\alpha) \;=\;& \alpha C_F a \\
&+C_F\left[3\psi'\left(\tfrac{1}{3}\right)\alpha^3 C_A + 24\psi'\left(\tfrac{1}{3}\right)\alpha^2 C_A - 15\psi'\left(\tfrac{1}{3}\right)\alpha C_A\right. \\
&\quad -2\alpha^3 C_A\pi^2 - 16\alpha^2 C_A\pi^2 - 27\alpha^2 C_A + 10\alpha C_A\pi^2 + 54\alpha C_A \\
&\quad \left.+675 C_A - 162 C_F - 216 N_f T_F\right]\frac{a^2}{108} \\
&+C_F\left[126\sqrt{3}\psi'\left(\tfrac{1}{3}\right)^2\alpha^5 C_A^2 + 2016\sqrt{3}\psi'\left(\tfrac{1}{3}\right)^2\alpha^4 C_A^2\right. \\
&\quad +6804\sqrt{3}\psi'\left(\tfrac{1}{3}\right)^2\alpha^3 C_A^2 - 10080\sqrt{3}\psi'\left(\tfrac{1}{3}\right)^2\alpha^2 C_A^2 \\
&\quad +3150\sqrt{3}\psi'\left(\tfrac{1}{3}\right)^2\alpha C_A^2 - 168\sqrt{3}\psi'\left(\tfrac{1}{3}\right)\alpha^5 C_A^2\pi^2
\end{aligned}
$$

$$
\begin{aligned}
&-2688\sqrt{3}\psi'\left(\tfrac{1}{3}\right)\alpha^4 C_A^2\pi^2 + 3888\sqrt{3}\psi'\left(\tfrac{1}{3}\right)\alpha^4 C_A^2 \\
&-9072\sqrt{3}\psi'\left(\tfrac{1}{3}\right)\alpha^3 C_A^2\pi^2 - 65448\sqrt{3}\psi'\left(\tfrac{1}{3}\right)\alpha^3 C_A^2 \\
&+13440\sqrt{3}\psi'\left(\tfrac{1}{3}\right)\alpha^2 C_A^2\pi^2 + 71064\sqrt{3}\psi'\left(\tfrac{1}{3}\right)\alpha^2 C_A^2 \\
&-7776\sqrt{3}\psi'\left(\tfrac{1}{3}\right)\alpha^2 C_A C_F - 3456\sqrt{3}\psi'\left(\tfrac{1}{3}\right)\alpha^2 C_A N_f T_F \\
&-4200\sqrt{3}\psi'\left(\tfrac{1}{3}\right)\alpha C_A^2\pi^2 + 852768\sqrt{3}\psi'\left(\tfrac{1}{3}\right)\alpha C_A^2 \\
&-62208\sqrt{3}\psi'\left(\tfrac{1}{3}\right)\alpha C_A C_F - 347328\sqrt{3}\psi'\left(\tfrac{1}{3}\right)\alpha C_A N_f T_F \\
&-162000\sqrt{3}\psi'\left(\tfrac{1}{3}\right) C_A^2 + 38880\sqrt{3}\psi'\left(\tfrac{1}{3}\right) C_A C_F \\
&+51840\sqrt{3}\psi'\left(\tfrac{1}{3}\right) C_A N_f T_F + 27\sqrt{3}\psi'''\left(\tfrac{1}{3}\right)\alpha^4 C_A^2 \\
&-513\sqrt{3}\psi'''\left(\tfrac{1}{3}\right)\alpha^3 C_A^2 + 837\sqrt{3}\psi'''\left(\tfrac{1}{3}\right)\alpha^2 C_A^2 \\
&+2997\sqrt{3}\psi'''\left(\tfrac{1}{3}\right)\alpha C_A^2 + 58320\sqrt{3}s_2\left(\tfrac{\pi}{6}\right)\alpha^4 C_A^2 \\
&-373248\sqrt{3}s_2\left(\tfrac{\pi}{6}\right)\alpha^3 C_A^2 + 408240\sqrt{3}s_2\left(\tfrac{\pi}{6}\right)\alpha^2 C_A^2 \\
&+3825792\sqrt{3}s_2\left(\tfrac{\pi}{6}\right)\alpha C_A^2 - 1492992\sqrt{3}s_2\left(\tfrac{\pi}{6}\right)\alpha C_A N_f T_F \\
&-116640\sqrt{3}s_2\left(\tfrac{\pi}{2}\right)\alpha^4 C_A^2 + 746496\sqrt{3}s_2\left(\tfrac{\pi}{2}\right)\alpha^3 C_A^2 \\
&-816480\sqrt{3}s_2\left(\tfrac{\pi}{2}\right)\alpha^2 C_A^2 - 7651584\sqrt{3}s_2\left(\tfrac{\pi}{2}\right)\alpha C_A^2 \\
&+2985984\sqrt{3}s_2\left(\tfrac{\pi}{2}\right)\alpha C_A N_f T_F - 97200\sqrt{3}s_3\left(\tfrac{\pi}{6}\right)\alpha^4 C_A^2 \\
&+622080\sqrt{3}s_3\left(\tfrac{\pi}{6}\right)\alpha^3 C_A^2 - 680400\sqrt{3}s_3\left(\tfrac{\pi}{6}\right)\alpha^2 C_A^2 \\
&-6376320\sqrt{3}s_3\left(\tfrac{\pi}{6}\right)\alpha C_A^2 + 2488320\sqrt{3}s_3\left(\tfrac{\pi}{6}\right)\alpha C_A N_f T_F \\
&+77760\sqrt{3}s_3\left(\tfrac{\pi}{2}\right)\alpha^4 C_A^2 - 497664\sqrt{3}s_3\left(\tfrac{\pi}{2}\right)\alpha^3 C_A^2 \\
&+544320\sqrt{3}s_3\left(\tfrac{\pi}{2}\right)\alpha^2 C_A^2 + 5101056\sqrt{3}s_3\left(\tfrac{\pi}{2}\right)\alpha C_A^2 \\
&-1990656\sqrt{3}s_3\left(\tfrac{\pi}{2}\right)\alpha C_A N_f T_F + 56\sqrt{3}\alpha^5 C_A^2\pi^4 \\
&+824\sqrt{3}\alpha^4 C_A^2\pi^4 - 2592\sqrt{3}\alpha^4 C_A^2\pi^2 - 972\sqrt{3}\alpha^4 C_A^2\zeta_3 \\
&+4392\sqrt{3}\alpha^3 C_A^2\pi^4 + 43632\sqrt{3}\alpha^3 C_A^2\pi^2 + 33048\sqrt{3}\alpha^3 C_A^2\zeta_3 \\
&+48600\sqrt{3}\alpha^3 C_A^2 - 46656\sqrt{3}\alpha^3 C_A C_F - 6712\sqrt{3}\alpha^2 C_A^2\pi^4 \\
&-47376\sqrt{3}\alpha^2 C_A^2\pi^2 - 53460\sqrt{3}\alpha^2 C_A^2\zeta_3 - 268272\sqrt{3}\alpha^2 C_A^2 \\
&+5184\sqrt{3}\alpha^2 C_A C_F\pi^2 - 69984\sqrt{3}\alpha^2 C_A C_F \\
&+2304\sqrt{3}\alpha^2 C_A N_f\pi^2 T_F + 124416\sqrt{3}\alpha^2 C_A N_f T_F \\
&-6592\sqrt{3}\alpha C_A^2\pi^4 - 568512\sqrt{3}\alpha C_A^2\pi^2 \\
&-1809864\sqrt{3}\alpha C_A^2\zeta_3 - 660960\sqrt{3}\alpha C_A^2 \\
&+41472\sqrt{3}\alpha C_A C_F\pi^2 + 419904\sqrt{3}\alpha C_A C_F \\
&+231552\sqrt{3}\alpha C_A N_f\pi^2 T_F + 622080\sqrt{3}\alpha C_A N_f T_F\zeta_3 \\
&+202176\sqrt{3}\alpha C_A N_f T_F + 108000\sqrt{3}C_A^2\pi^2 \\
&-2857680\sqrt{3}C_A^2\zeta_3 + 6304392\sqrt{3}C_A^2 - 25920\sqrt{3}C_A C_F\pi^2
\end{aligned}
$$

$$
\begin{aligned}
&+1119744\sqrt{3}C_A C_F\zeta_3 - 2169504\sqrt{3}C_A C_F \\
&-34560\sqrt{3}C_A N_f\pi^2 T_F + 746496\sqrt{3}C_A N_f T_F\zeta_3 \\
&-3203712\sqrt{3}C_A N_f T_F + 139968\sqrt{3}C_F^2 \\
&-186624\sqrt{3}C_F N_f T_F + 248832\sqrt{3}N_f^2 T_F^2 \\
&+405\ln(3)^2\alpha^4 C_A^2\pi - 2592\ln(3)^2\alpha^3 C_A^2\pi \\
&+2835\ln(3)^2\alpha^2 C_A^2\pi + 26568\ln(3)^2\alpha C_A^2\pi \\
&-10368\ln(3)^2\alpha C_A N_f\pi T_F - 4860\ln(3)\alpha^4 C_A^2\pi \\
&+31104\ln(3)\alpha^3 C_A^2\pi - 34020\ln(3)\alpha^2 C_A^2\pi \\
&-318816\ln(3)\alpha C_A^2\pi + 124416\ln(3)\alpha C_A N_f\pi T_F \\
&-435\alpha^4 C_A^2\pi^3 + 2784\alpha^3 C_A^2\pi^3 - 3045\alpha^2 C_A^2\pi^3 \\
&-28536\alpha C_A^2\pi^3 + 11136\alpha C_A N_f\pi^3 T_F\big]\,\frac{a^3}{93312\sqrt{3}} \\
&+ \mathcal{O}(a^4)\;. \qquad (3.4.59)
\end{aligned}
$$

Looking closely at the results for the gluon and gauge parameter anomalous dimensions in both the $\overline{\rm MS}$ and MOMi schemes it becomes apparent that the following identity holds

$$
\gamma_\alpha(a,\alpha) \;=\; -\gamma_A(a,\alpha) \qquad (3.4.60)
$$

in all schemes for an arbitrary (linear) covariant gauge fixing. This relation comes from our convention when defining the renormalization constants in (2.1.55), most notably $\alpha_o = Z_\alpha^{-1} Z_A \alpha$ with $Z_\alpha = 1$ in this gauge. Therefore (3.4.60) is only valid in gauges where $Z_\alpha = 1$. We now present the results for the remaining MOMi schemes numerically. For the MOMg scheme the renormalization group functions are

$$
\begin{aligned}
\beta^{\rm MOMg}(a,\alpha) \;=\;& -\left[11.000000 - 0.666667 N_f\right]a^2 \\
& - \big[102.000000 + 19.654643\alpha - 0.271084\alpha^2 - 5.859139\alpha^3 \\
& \quad +1.125000\alpha^4 - \big[12.666667 + 2.015861\alpha + 0.437395\alpha^2 \\
& \quad -0.500000\alpha^3\big]\,N_f\big]\,a^3 \\
& - \big[1570.984380 + 658.070929\alpha + 269.223834\alpha^2 \\
& \quad +43.002961\alpha^3 - 99.279719\alpha^4 + 14.855025\alpha^5 + 5.334592\alpha^6 \\
& \quad -0.703125\alpha^7 + \big[0.565929 - 43.239367\alpha - 22.747196\alpha^2 \\
& \quad -19.870956\alpha^3 + 14.834757\alpha^4 + 0.976418\alpha^5
\end{aligned}
$$

$$
\begin{aligned}
& -0.281250\alpha^6\big] N_f - \big[67.089536 + 4.647961\alpha + 0.889805\alpha^2 \\
& -2.305695\alpha^3\big] N_f^2 + 2.658116 N_f^3\big] a^4 \ + \ \mathcal{O}(a^5) \\
\gamma_A^{\rm MOMg}(a,\alpha) &= [0.666667 N_f - 6.500000 + 1.500000\alpha] a \\
&+ \ \big[16.909511 - 41.643377\alpha + 6.153386\alpha^2 + 0.992070\alpha^3 \\
& -0.375000\alpha^4 - \big[12.093123 - 5.474404\alpha + 0.281302\alpha^2 \\
& +0.166667\alpha^3\big] N_f + 1.537130 N_f^2\big] a^2 \\
&- \ \big[1308.938674 - 647.926068\alpha + 376.230130\alpha^2 + 6.397113\alpha^3 \\
& -33.016247\alpha^4 + 7.325313\alpha^5 + 1.000873\alpha^6 - 0.164063\alpha^7 \\
& - \big[491.430950 - 302.353050\alpha + 52.302915\alpha^2 + 6.360434\alpha^3 \\
& -6.715315\alpha^4 - 0.128860\alpha^5 + 0.072917\alpha^6\big] N_f \\
& + \big[74.919017 - 29.399931\alpha + 1.415890\alpha^2 \\
& +1.344989\alpha^3\big] N_f^2 - 6.202269 N_f^3\big] a^3 \ + \ \mathcal{O}(a^4) \\
\gamma_\alpha^{\rm MOMg}(a,\alpha) &= [-0.666667 N_f + 6.500000 - 1.500000\alpha] a \\
&+ \ \big[-16.909511 + 41.643377\alpha - 6.153386\alpha^2 - 0.992070\alpha^3 \\
& +0.375000\alpha^4 + \big[12.093123 - 5.474404\alpha + 0.281302\alpha^2 \\
& +0.166667\alpha^3\big] N_f - 1.537130 N_f^2\big] a^2 \\
&+ \ \big[1308.938674 - 647.926068\alpha + 376.230130\alpha^2 + 6.397113\alpha^3 \\
& -33.016247\alpha^4 + 7.325313\alpha^5 + 1.000873\alpha^6 - 0.164063\alpha^7 \\
& - \big[491.430950 - 302.353050\alpha + 52.302915\alpha^2 + 6.360434\alpha^3 \\
& -6.715315\alpha^4 - 0.128860\alpha^5 + 0.072917\alpha^6\big] N_f \\
& + \big[74.919017 - 29.399931\alpha + 1.415890\alpha^2 \\
& +1.344989\alpha^3\big] N_f^2 - 6.202269 N_f^3\big] a^3 \ + \ \mathcal{O}(a^4) \\
\gamma_c^{\rm MOMg}(a,\alpha) &= [0.750000\alpha - 2.250000] a \\
&+ \ \big[8.795510 - 21.172897\alpha + 2.654739\alpha^2 + 1.371035\alpha^3 \\
& -0.187500\alpha^4 \ - \ [4.437815 - 1.729272\alpha] N_f\big] a^2 \\
&- \ \big[548.849239 - 436.672056\alpha + 199.293803\alpha^2 \\
& +32.708614\alpha^3 - 30.012394\alpha^4 + 1.430343\alpha^5 + 0.953562\alpha^6 \\
& -0.082031\alpha^7 - [157.466918 - 127.545756\alpha \\
& +20.052219\alpha^2 + 7.759276\alpha^3 - 1.513113\alpha^4\big] N_f \\
& + [19.974116 - 6.977553\alpha] N_f^2\big] a^3 \ + \ \mathcal{O}(a^4) \\
\gamma_\psi^{\rm MOMg}(a,\alpha) &= 1.333333\alpha a \\
&+ \ \big[22.333333 - 10.545541\alpha + 9.031722\alpha^2 + 1.437395\alpha^3
\end{aligned}
$$

$$
\begin{aligned}
& -0.333333\alpha^4 \; - \; [1.333333 - 3.074260\alpha]\, N_f \big]\, a^2 \\
- \; & \big[94.794329 - 204.199880\alpha + 218.840411\alpha^2 - 30.421666\alpha^3 \\
& -34.407386\alpha^4 + 6.315994\alpha^5 + 1.257721\alpha^6 - 0.145833\alpha^7 \\
& - \big[76.867272 - 80.560197\alpha + 53.071812\alpha^2 + 7.057668\alpha^3 \\
& -2.689978\alpha^4\big]\, N_f \; + \; [5.259632 - 12.404539\alpha]\, N_f^2\big]\, a^3 \\
& + \mathcal{O}(a^4)\ . \qquad (3.4.61)
\end{aligned}
$$

With the above presented numerically it is easier for one to see that at two loops the MOM and $\overline{\rm MS}$ results are equivalent in the Landau gauge, particularly in the case of the β-function. Finally for the MOMq scheme

$$
\begin{aligned}
\beta^{\rm MOMq}(a,\alpha) \; = \; & -\,[11.000000 - 0.666667 N_f] a^2 \\
& - \big[102.000000 + 15.237214\alpha - 1.383979\alpha^2 - 0.492070\alpha^3 \\
& \quad - \big[12.666667 + 1.562791\alpha + 0.218698\alpha^2\big]\, N_f\big]\, a^3 \\
& - \big[1843.652729 + 422.073185\alpha + 123.373496\alpha^2 \\
& \quad -19.513026\alpha^3 - 3.505519\alpha^4 - 0.096131\alpha^5 \\
& \quad - \big[588.654846 + 60.545481\alpha + 16.395570\alpha^2 + 0.928236\alpha^3 \\
& \qquad -0.000006\alpha^4\big]\, N_f \; + \; 22.587812 N_f^2\big]\, a^4 \; + \; \mathcal{O}(a^5) \\
\gamma_A^{\rm MOMq}(a,\alpha) \; = \; & [0.666667 N_f - 6.500000 + 1.500000\alpha] a \\
& - \big[46.639132 + 22.560876\alpha - 6.200129\alpha^2 + 0.878965\alpha^3 \\
& \quad - \big[9.411706 + 1.562791\alpha - 0.390651\alpha^2\big]\, N_f\big]\, a^2 \\
& - \big[2027.743714 + 333.308222\alpha + 184.238292\alpha^2 \\
& \quad -24.351972\alpha^3 + 12.671886\alpha^4 + 1.920079\alpha^5 \\
& \quad - \big[415.699015 + 49.405308\alpha + 9.700384\alpha^2 - 3.790855\alpha^3 \\
& \quad -0.478368\alpha^4\big]\, N_f + [11.178808 - 1.302171\alpha]\, N_f^2\big]\, a^3 \\
& + \mathcal{O}(a^4) \\
\gamma_\alpha^{\rm MOMq}(a,\alpha) \; = \; & [-0.666667 N_f + 6.500000 - 1.500000\alpha] a \\
& - \big[-46.639132 - 22.560876\alpha + 6.200129\alpha^2 - 0.878965\alpha^3 \\
& \quad + \big[9.411706 + 1.562791\alpha - 0.390651\alpha^2\big]\, N_f\big]\, a^2 \\
& + \big[2027.743714 + 333.308222\alpha + 184.238292\alpha^2 \\
& \quad -24.351972\alpha^3 + 12.671886\alpha^4 + 1.920079\alpha^5 \\
& \quad - \big[415.699015 + 49.405308\alpha + 9.700384\alpha^2 - 3.790855\alpha^3 \\
& \quad -0.478368\alpha^4\big]\, N_f + [11.178808 - 1.302171\alpha]\, N_f^2\big]\, a^3
\end{aligned}
$$

$$
\begin{aligned}
& + \mathcal{O}(a^4) \\
\gamma_c^{\mathrm{MOMq}}(a,\alpha) &= [0.750000\alpha - 2.250000]a \\
&- \left[13.202007 + 12.311251\alpha - 2.514088\alpha^2 - 0.685517\alpha^3 \right. \\
&\quad \left. -0.750000N_f\right] a^2 \\
&- \left[740.134165 + 1.866578\alpha + 100.645035\alpha^2 - 3.435592\alpha^3 \right. \\
&\quad -8.767800\alpha^4 - 1.096513\alpha^5 - [75.503272 + 4.118647\alpha \\
&\quad \left. +1.710977\alpha^2\right] N_f + 2.500000N_f^2\Big] a^3 \;+\; \mathcal{O}(a^4) \\
\gamma_\psi^{\mathrm{MOMq}}(a,\alpha) &= 1.333333\alpha a \\
&+ \left[22.333333 + 2.490078\alpha + 8.125582\alpha^2 + 1.218698\alpha^3 \right. \\
&\quad \left. -1.333333N_f\right] a^2 \\
&+ \left[341.898910 + 182.913289\alpha + 43.980106\alpha^2 + 74.928346\alpha^3 \right. \\
&\quad +21.435269\alpha^4 + 1.949356\alpha^5 - [52.191691 - 3.107628\alpha \\
&\quad \left. -2.166946\alpha^2\right] N_f \;+\; 0.888889N_f^2\Big] a^3 \;+\; \mathcal{O}(a^4) \;. \quad (3.4.62)
\end{aligned}
$$

The β-functions and anomalous dimensions calculated perturbatively in all schemes are also useful for non-perturbative approaches. In particular in lattice matching where high energy results can be mapped on to the low energy regime, improving measurements for the coupling constant.

3.5 Discussion

We close this chapter with some remarks on our computation. To recap we have considered the two loop renormalization of QCD fixed in an arbitrary (linear) covariant gauge. In particular we have focused on the structure of the ghost-gluon, triple-gluon and quark-gluon vertices of QCD at the symmetric subtraction point in the $\overline{\mathrm{MS}}$ and MOMi schemes. Independently reconstructing the results of [14] and [52] we have explicitly shown how the three loop renormalization group functions, including the β-functions for each MOMi scheme, can be constructed via the two loop results in the same scheme without the need to do an explicit three loop calculation. We also constructed the coupling constant mappings in each scheme and graphically presented the one and two loop truncated ghost-gluon vertex for various values of N_f for $SU(3)$. Graphically it could be said that the two loop results seem to converge quicker, whereas by looking at the numbers alone it is not so obvious to see what it happening. This is why results for higher loop orders are of importance, and the more multiloop results one can obtain the

more precise QCD becomes. However, to properly analyse these results in more depth and to gain a real understanding of the behaviour of the running coupling one needs to consider other techniques, such as the R-ratio which has been considered in [97].

Although largely the results presented in this chapter have been previously published in [14] we note that some results have been presented here for the first time. Notably the results of the renormalization constants themselves. Given the explicit forms of the renormalization group functions the underlying renormalization constants can be constructed. However, for the renormalization constants presented within this chapter we have explicitly calculated them from first principles and they are in exact agreement with [14]. We have made strong reference to earlier works that have been used when making checks on our results, ensuring our computational method is correct before extending to new gauges and/or loop orders where initial checks are harder to achieve. Although $\overline{\text{MS}}$ is currently the default scheme choice for QCD it is interesting to see how a physical scheme such as momentum subtraction can impact on results. The real differences (between the schemes) are only observed at three loops where the Landau gauge check is no longer valid. It would be interesting to see if this gauge dependence continues at higher loop orders or if at some point the results agree again with the $\overline{\text{MS}}$ results of the same loop order for $\alpha = 0$. It could be that of the three MOMi schemes one of the β-functions appears to be more convergent than the others. However this is not so straightforward to determine since the coupling constant runs at different rates in different schemes, so it is hard to see just from the numbers which β-function has better convergence. To appreciate this subtlety one would need to calculate something physical and compare the value at a particular momentum scale. For instance in [97] the R-ratio was computed in the Landau gauge in all MOMi schemes and also the mini-MOM scheme introduced in [98]. The mini-MOM scheme is defined such that the wave function renormalization is carried out in a MOM way, whilst the ghost-gluon vertex is treated differently from other schemes. Instead of computing it at the symmetric point, an asymmetric setup is used, where one external leg is nullified. The condition on the ghost-gluon vertex is that it is not renormalized in the Landau gauge. The motivation for the scheme is to preserve the non-renormalization of the ghost-gluon vertex. In our notation this corresponds to ensuring that the ghost-gluon vertex in the $\overline{\text{MS}}$ scheme is the

same as in the mini-MOM (mMOM) scheme, such that

$$Z_g^{(\mathrm{ccg})\,\overline{\mathrm{MS}}}\sqrt{Z_A^{\overline{\mathrm{MS}}}}Z_c^{\overline{\mathrm{MS}}} \;=\; Z_g^{(\mathrm{ccg})\,\mathrm{mMOM}}\sqrt{Z_A^{\mathrm{mMOM}}}Z_c^{\mathrm{mMOM}} \;. \qquad (3.5.63)$$

In [97] it was noted that the coefficients of the R-ratio appeared to be less convergent in one scheme compared to another. However when one plots the R-ratio's as a function of the centre of mass scale as in [97] the discrepancy between schemes is less than 0.5%.

Although for presentation purposes we chose to display most results numerically for $SU(3)$, leaving results in terms of $SU(N_c)$ variables and arbitrary α and N_f gives scope for others to easily compare results with our own, where analysis of these results can assist with things like Monte-Carlo simulations and further lattice matching. On completing this initial work in the arbitrary (linear) covariant gauge we are now in a position to extend and apply our algorithm to a more involved non-linear gauge fixing, which we visit in the next chapter.

Chapter 4

The Curci-Ferrari gauge

In this chapter we extend the work of the previous chapter, evaluating the two loop 3-point vertex functions of QCD in the Curci-Ferrari (CF) gauge at the symmetric subtraction point. Renormalizing each of the three vertices in their respective momentum subtraction (MOM) schemes, as well as in the $\overline{\text{MS}}$ scheme, we construct the two loop conversion functions for the wave function, coupling constant and gauge parameter renormalization constants for each MOMi scheme relative to the $\overline{\text{MS}}$ scheme. Using these conversion functions we are able to derive the three loop anomalous dimensions and β-functions for each MOMi scheme. These RG functions are new results which contribute to improving lattice matching. Although our method is the same, in contrast to the previous chapter we now consider a non-linear gauge fixing with a more complicated internal structure. This in turn introduces new field interactions, requiring additional Feynman rules, group algebra and master integrals.

4.1 Background

As a preliminary to studying the maximal abelian gauge it is useful to consider the Curci-Ferrari gauge, a non-linear covariant gauge fixing with similarities to, but extending that of the Landau gauge. The Curci-Ferrari gauge and its related model were introduced in [42]. The Curci-Ferrari model is an extension of QCD fixed in the Curci-Ferrari gauge, with a mass term for the gluon present in its formalism. Similar to QCD in its ultraviolet properties this model differs in the infrared. This renormalizable model of massive gluons was originally constructed as an alternative to the Higgs mechanism in understanding massive vector bosons. However the model has proved useful from a theoretical perspective in its non-linear gauge fixing term which introduces quartic ghost self interactions, [42, 99].

Since we are only interested in calculating in a massless regime the Curci-Ferrari gauge, which includes no direct mass term, will suffice. In addition to being an extension of our previous chapter, studying the Curci-Ferrari gauge is of importance as it may provide an insight into the closely related but much more complicated maximal abelian gauge, [100].

For background another motivation for considering the Curci-Ferrari gauge is that is has received renewed interest due to its relation to the ghost condensation problem through the presence of a four-ghost interaction term appearing in the Lagrangian, [100, 99]. The dimension two composite operator $\frac{1}{2}A^{A\ 2}_{\mu} - \alpha\bar{c}^{A}c^{A}$, which also appears in the maximal abelian gauge fixing, corresponds to the mass operator in a massive regime. It is these operators which may help in our understanding of confinement, [101]. A non-linear gauge fixing like Curci-Ferrari allows one to add a BRST invariant gluon mass to the Lagrangian, [102]. Although we do not concern ourselves with mass terms as this lies beyond the scope of our work, results for this gauge in a massless regime are still of interest.

We study the Curci-Ferrari gauge at two loops for two reasons. Firstly the gauge fixing is directly related to that of the MAG, where we treat this chapter as a preliminary calculation. Any results computed will be of interest when comparing with the MAG. Secondly, the Curci-Ferrari results at two loops for the MOMi schemes had not been determined prior to [67]. Analysis of this non-linear gauge fixing is presented here.

In this chapter, since it is self-contained we take the colour group $A \to a$, where for the Curci-Ferrari gauge the index a represents the full colour group, as is conventional and consistent with the textbook approach. With this in mind, we now move on to discuss the key properties of the Curci-Ferrari gauge. We begin by first stating the Lagrangian, which for the Curci-Ferrari gauge is, [42],

$$\begin{aligned} L^{\mathrm{CF}} &= -\frac{1}{4}G^{a}_{\mu\nu}G^{a\,\mu\nu} - \frac{1}{2\alpha}(\partial^{\mu}A^{a}_{\mu})^{2} - \bar{c}^{a}\partial^{\mu}D_{\mu}c^{a} + i\bar{\psi}^{iI}\not{D}\psi^{iI} \\ &\quad + \frac{g}{2}f^{abc}\partial^{\mu}A^{a}_{\mu}\bar{c}^{b}c^{c} + \frac{\alpha g^{2}}{8}f^{eab}f^{ecd}\bar{c}^{a}c^{b}\bar{c}^{c}c^{d} \,, \end{aligned} \tag{4.1.1}$$

where $D_{\mu} = \partial_{\mu} + igA^{a}_{\mu}$ is the covariant derivative and the the field strength tensor $\mathrm{G}^{a}_{\mu\nu} = \partial_{\mu}\mathrm{A}^{a}_{\nu} - \partial_{\nu}\mathrm{A}^{a}_{\mu} - gf^{abc}\mathrm{A}^{b}_{\mu}\mathrm{A}^{c}_{\nu}$ is defined in the same way as for the arbitrary (linear) covariant gauge. The coupling constant is denoted as g and α is the associated gauge parameter. Where the coupling constant and gauge parameter

are different to those considered in the previous chapter for the arbitrary (linear) covariant gauge. The massless quark is represented by ψ^{iI} and f^{abc} are the colour group structure constants whose generators are T^a. As before $c^a, \bar{c}^a$ represent the Faddeev-Popov ghosts. Our adjoint colour indices are denoted by a, b and c and run from $1 \leq a \leq N_A$, where N_A is the dimension of the adjoint representation of the colour group. Likewise our fundamental representation indices are i, j and k, running from $1 \leq i \leq N_F$ where N_F is the fundamental representation. The flavour indices are denoted by I with $1 \leq I \leq N_f$, where we choose to represent our results in terms of N_f for an arbitrary number of quarks. The Curci-Ferrari gauge fixed Lagrangian is not fully gauge invariant but it is invariant under the set of BRST transformations (2.1.36). Note the difference here to the arbitrary (linear) covariant gauge fixed Lagrangian is the addition of a quartic ghost interaction, which we commented on earlier, which is a special property of non-linear gauge fixings. Although the ghosts couple non-trivially, the addition of this interaction term does not spoil the renormalizability of the theory. These quartic ghost interactions show up in the ghost-gluon vertex in the Curci-Ferrari gauge and so we expect results in this vertex to differ from those computed in the same vertex in Chapter 3, [42]. It is indeed the case that the ghost-gluon vertex is structurally different. This becomes most apparent when we display the Λ parameters in section 4.6. The gauge parameter gets renormalized differently to that of the arbitrary (linear) covariant gauge, most notably because we now have $Z_\alpha \neq 1$ (which we see in the following section). When studying this gauge fixing we consider the same three vertex functions as before, namely

$$\langle A^a_\mu(p) A^b_\nu(q) A^c_\sigma(r) \rangle \quad , \quad \langle \psi^i(p) \bar{\psi}^j(q) A^c_\sigma(r) \rangle \quad \text{and} \quad \langle c^a(p) \bar{c}^b(q) A^c_\sigma(r) \rangle \ , \qquad (4.1.2)$$

with momentum conservation along $p + q + r = 0$. We compute all three vertices at the symmetric subtraction point, [91, 52]. Following the same technique in [14], discussed in Appendix B, we rewrite the Lorentz amplitudes as tensors multiplying scalar amplitudes. Although there are only six independent combinations of basis tensors for the triple-gluon vertex which we determined in our previous calculation for an arbitrary (linear) covariant gauge fixing (see equation (3.2.14)), we choose to include all possible tensors. Since the Green's functions remain unchanged, we apply the same tensor basis as before, where details are again given in Appendix B. Using the same method of projection we determine each scalar amplitude individually. By introducing a projection matrix, $\mathcal{M}^i_{kl}$, we project out each amplitude as before.

In terms of computational method, no further programs have been used other than those already discussed in section 2.3 for the 3-point vertex functions. In contrast to the arbitrary (linear) covariant gauge, if one were to determine the full renormalization of the Curci-Ferrari gauge several 4-point interactions would need to be considered. These are introduced via the quartic ghost and gluon terms in the Lagrangian. The MINCER algorithm would not be appropriate here as the only way one could apply MINCER to these 4-point functions would be to nullify two external legs, which would introduce spurious infrared divergences. In this thesis we only consider 2- and 3-point functions, with our focus on the 3-point vertices of QCD. All 3-point functions have been reduced using the Laporta algorithm in REDUZE, as would be the method for the 4-point functions if they were to be considered. It is only recently in [80, 103] that the 4-point vertices of QCD have been computed at one loop for the MOMgggg scheme. At two loops this is not yet possible since the master integrals are not known. The programs we have used in evaluating the QCD vertices in the Curci-Ferrari gauge are effectively the same as those considered for the arbitrary (linear) covariant gauge in chapter 3. This is with the exception of new Feynman rules, see Appendix C, to describe the ghost-gluon and quartic ghost interactions, and of course the number of diagrams constructed reflects this. The colour algebra however is the same, despite the tensor structure being different.

Equation (3.4.55) incorporates $\gamma_\alpha(a,\alpha)$, unlike in the linear covariant gauge, since γ_A and γ_α are not equivalent up to a minus sign as was the case before. Now

$$\begin{aligned} \gamma_A(a,\alpha) &= \beta(a,\alpha)\frac{\partial}{\partial a}\ln Z_A \;+\; \alpha\gamma_\alpha(a,\alpha)\frac{\partial}{\partial\alpha}\ln Z_A \\ \gamma_\alpha(a,\alpha) &= \left[\beta(a,\alpha)\frac{\partial}{\partial a}\ln Z_\alpha \;-\; \gamma_A(a,\alpha)\right]\left[1 \;-\; \alpha\frac{\partial}{\partial\alpha}\ln Z_\alpha\right]^{-1} \end{aligned} \tag{4.1.3}$$

where the β-function is α-dependent. Therefore the relation (3.4.60) no longer holds in this non-linear gauge fixing, instead being replaced by the definitions above.

Following the same structure as chapter 3 we present the majority of results numerically, with the exception of those for the ghost-gluon vertex, which we use for comparison with results for the same vertex in chapter 3. Note that all results within this chapter are the original and published in [67].

Our method of renormalization follows techniques of the previous section and has been discussed at length. We renormalize our Lagrangian using the standard QCD definitions of the renormalization constants, defined in (2.1.55). Since we are not restricting to the Landau gauge it is essential to renormalize our gauge parameter α and coupling constant g. We use dimensional regularization throughout in $d = 4 - 2\epsilon$ dimensions, where ϵ is the regularizing parameter.

4.2 $\overline{\text{MS}}$ scheme.

Since the technical details of the calculation have been discussed at length in chapters 2 and 3 we simply record our results for the Curci-Ferrari gauge, commenting on any interesting features. In this section we record our results in the basic reference scheme $\overline{\text{MS}}$. Similar to the arbitrary (linear) covariant gauge we have computed all diagrams to two loops, therefore all $\overline{\text{MS}}$ results will be of two loop order. We begin by presenting the results for the renormalization constants for the wave functions, gauge parameter and $\overline{\text{MS}}$ coupling constant. These are presented analytically as

$$
\begin{aligned}
Z_A(a,\alpha)\Big|_{\overline{\text{MS}}} &= 1 + \left[-\frac{4}{3} N_f T_F + C_A \left(\frac{13}{6} - \frac{\alpha}{2} \right) \right] \frac{a}{\epsilon} \\
&\quad + \left[\left(C_A^2 \left(-\frac{13}{8} - \frac{17}{24}\alpha + \frac{3}{16}\alpha^2 \right) + N_f T_F C_A \left(1 + \frac{2}{3}\alpha \right) \right) \frac{1}{\epsilon} \right. \\
&\quad \left. + C_A^2 \left(\frac{59}{16} - \frac{11}{16}\alpha - \frac{1}{16}\alpha^2 \right) - \frac{5}{2} N_f T_F C_A - 2 N_f T_F C_F \right] \frac{a^2}{\epsilon} \\
&\quad + \mathcal{O}(a^3) \\
Z_\alpha(a,\alpha)\Big|_{\overline{\text{MS}}} &= 1 - \frac{\alpha C_A a}{4\epsilon} + \left[C_A^2 \left(\frac{3\alpha}{16} + \frac{\alpha^2}{16} \right) \frac{1}{\epsilon} + C_A^2 \left(-\frac{5\alpha}{32} - \frac{\alpha^2}{32} \right) \right] \frac{a^2}{\epsilon} \\
&\quad + \mathcal{O}(a^3) \\
Z_c(a,\alpha)\Big|_{\overline{\text{MS}}} &= 1 + C_A \left(\frac{3}{4} - \frac{\alpha}{4} \right) \frac{a}{\epsilon} \\
&\quad + \left[\left(C_A^2 \left(-\frac{35}{32} + \frac{\alpha^2}{16} \right) + \frac{1}{2} N_f T_F C_A \right) \frac{1}{\epsilon} \right. \\
&\quad \left. + C_A^2 \left(\frac{95}{96} + \frac{\alpha}{32} - \frac{\alpha^2}{32} \right) - \frac{5}{12} N_f T_F C_A \right] \frac{a^2}{\epsilon} \; + \; \mathcal{O}(a^3) \\
Z_\psi(a,\alpha)\Big|_{\overline{\text{MS}}} &= 1 - \frac{\alpha C_F a}{\epsilon} \\
&\quad + \left[\left(C_F C_A \left(\frac{3\alpha}{4} + \frac{\alpha^2}{8} \right) + \frac{1}{2} C_F^2 \alpha^2 \right) \frac{1}{\epsilon} \right.
\end{aligned}
$$

$$
\begin{aligned}
& + C_F C_A \left(-\frac{25}{8} - \alpha \right) + \frac{3}{4} C_F^2 + N_f T_F C_F \Bigg] \frac{a^2}{\epsilon} \; + \; \mathcal{O}(a^3) \\
Z_g(a,\alpha) \Big|_{\overline{\mathrm{MS}}} \; &= \; 1 + \left[-\frac{11}{6} C_A + \frac{2}{3} T_F N_f \right] \frac{a}{\epsilon} \\
& + \left[2 \left(\frac{1}{3} T_F^2 N_f^2 - \frac{11}{6} C_A T_F N_f + \frac{121}{48} C_A^2 \right) \frac{1}{\epsilon} \right. \\
& \left. -2 \left(-\frac{5}{6} C_A T_F N_f + \frac{17}{12} C_A^2 - \frac{1}{2} C_F T_F N_f \right) \right] \frac{a^2}{\epsilon} \; + \; \mathcal{O}(a^3)
\end{aligned}
\tag{4.2.4}
$$

which we have determined using MINCER. As a check on our results we were able to compare with results in the Landau gauge, a gauge widely used by Landau and first referred to as the Landau gauge in [88]. In the above renormalization constants this corresponds to setting $\alpha = 0$. Taking this limit the renormalization constants determined in the $\overline{\mathrm{MS}}$ scheme for the Curci-Ferrari gauge should match on to those at the same Landau limit in the same scheme for the linear covariant gauge, (3.1.2) - (3.1.3). It is the case that we indeed see an exact match. Again it is understood that when variables are not labelled they correspond to the scheme defined on the object, in this case on the Z's, on the left hand side of the equation. Once the renormalization constants are fixed we can generate the amplitudes. We begin with the ghost-gluon vertex where the amplitudes at two loops are given explicitly as

$$
\begin{aligned}
\Sigma^{\mathrm{ccg}}_{(1)}(p,q) \Big|_{\overline{\mathrm{MS}}} \; &= \; - \Sigma^{\mathrm{ccg}}_{(2)}(p,q) \Big|_{\overline{\mathrm{MS}}} \\
&= \; -\frac{1}{2} + \left[6\psi'\left(\tfrac{1}{3}\right) \alpha - 15\psi'\left(\tfrac{1}{3}\right) - 4\alpha\pi^2 - 27\alpha + 10\pi^2 - 81 \right] \frac{C_A a}{216} \\
& + \Big[432\sqrt{3}\psi'\left(\tfrac{1}{3}\right) \alpha^3 C_A - 13716\sqrt{3}\psi'\left(\tfrac{1}{3}\right) \alpha^2 C_A \\
& \quad -3312\sqrt{3}\psi'\left(\tfrac{1}{3}\right) \alpha C_A + 2304\sqrt{3}\psi'\left(\tfrac{1}{3}\right) \alpha N_f T_F \\
& \quad +133296\sqrt{3}\psi'\left(\tfrac{1}{3}\right) C_A - 78528\sqrt{3}\psi'\left(\tfrac{1}{3}\right) N_f T_F \\
& \quad -18\sqrt{3}\psi'''\left(\tfrac{1}{3}\right) \alpha^2 C_A + 225\sqrt{3}\psi'''\left(\tfrac{1}{3}\right) \alpha C_A \\
& \quad +999\sqrt{3}\psi'''\left(\tfrac{1}{3}\right) C_A - 73872\sqrt{3}s_2\left(\tfrac{\pi}{6}\right) \alpha^2 C_A \\
& \quad +66096\sqrt{3}s_2\left(\tfrac{\pi}{6}\right) \alpha C_A + 1076976\sqrt{3}s_2\left(\tfrac{\pi}{6}\right) C_A \\
& \quad -497664\sqrt{3}s_2\left(\tfrac{\pi}{6}\right) N_f T_F + 147744\sqrt{3}s_2\left(\tfrac{\pi}{2}\right) \alpha^2 C_A \\
& \quad -132192\sqrt{3}s_2\left(\tfrac{\pi}{2}\right) \alpha C_A - 2153952\sqrt{3}s_2\left(\tfrac{\pi}{2}\right) C_A \\
& \quad +995328\sqrt{3}s_2\left(\tfrac{\pi}{2}\right) N_f T_F + 123120\sqrt{3}s_3\left(\tfrac{\pi}{6}\right) \alpha^2 C_A \\
& \quad -110160\sqrt{3}s_3\left(\tfrac{\pi}{6}\right) \alpha C_A - 1794960\sqrt{3}s_3\left(\tfrac{\pi}{6}\right) C_A
\end{aligned}
$$

$$
\begin{aligned}
&+829440\sqrt{3}s_3\left(\tfrac{\pi}{6}\right) N_f T_F - 98496\sqrt{3}s_3\left(\tfrac{\pi}{2}\right) \alpha^2 C_A \\
&+88128\sqrt{3}s_3\left(\tfrac{\pi}{2}\right) \alpha C_A + 1435968\sqrt{3}s_3\left(\tfrac{\pi}{2}\right) C_A \\
&-663552\sqrt{3}s_3\left(\tfrac{\pi}{2}\right) N_f T_F - 288\sqrt{3}\alpha^3 C_A\pi^2 - 1944\sqrt{3}\alpha^3 C_A \\
&+48\sqrt{3}\alpha^2 C_A\pi^4 + 9144\sqrt{3}\alpha^2 C_A\pi^2 + 6480\sqrt{3}\alpha^2 C_A\zeta_3 \\
&+3240\sqrt{3}\alpha^2 C_A - 600\sqrt{3}\alpha C_A\pi^4 + 2208\sqrt{3}\alpha C_A\pi^2 \\
&+28836\sqrt{3}\alpha C_A\zeta_3 - 101088\sqrt{3}\alpha C_A - 1536\sqrt{3}\alpha N_f\pi^2 T_F \\
&+10368\sqrt{3}\alpha N_f T_F - 2664\sqrt{3}C_A\pi^4 - 88864\sqrt{3}C_A\pi^2 \\
&-175608\sqrt{3}C_A\zeta_3 - 146448\sqrt{3}C_A + 52352\sqrt{3}N_f\pi^2 T_F \\
&+82944\sqrt{3}N_f T_F\zeta_3 + 36288\sqrt{3}N_f T_F - 513\ln(3)^2\alpha^2 C_A\pi \\
&+459\ln(3)^2\alpha C_A\pi + 7479\ln(3)^2 C_A\pi - 3456\ln(3)^2 N_f\pi T_F \\
&+6156\ln(3)\alpha^2 C_A\pi - 5508\ln(3)\alpha C_A\pi - 89748\ln(3)C_A\pi \\
&+41472\ln(3)N_f\pi T_F + 551\alpha^2 C_A\pi^3 - 493\alpha C_A\pi^3 - 8033 C_A\pi^3 \\
&+3712 N_f\pi^3 T_F\Big] \frac{C_A a^2}{62208\sqrt{3}} \;+\; \mathcal{O}(a^3) \;. \qquad (4.2.5)
\end{aligned}
$$

In comparison with the arbitrary (linear) covariant gauge the ghost-gluon vertex in the Curci-Ferrari gauge has only one independent amplitude. This is because the Feynman rule for this vertex is anti-symmetric. The emergence of this feature in our explicit computation is a non-trivial check on our analysis as we do not assume a priori that $\Sigma^{\rm ccg}_{(1)}(p,q)\Big|_{\overline{\rm MS}} = -\,\Sigma^{\rm ccg}_{(2)}(p,q)\Big|_{\overline{\rm MS}}$.

For the triple-gluon vertex the channel 1 amplitude in the $\overline{\rm MS}$ scheme is given analytically as

$$
\begin{aligned}
\Sigma^{\rm ggg}_{(1)}(p,q)\Big|_{\overline{\rm MS}} &= \Sigma^{\rm ggg}_{(2)}(p,q)\Big|_{\overline{\rm MS}} = -\frac{1}{2}\,\Sigma^{\rm ggg}_{(3)}(p,q)\Big|_{\overline{\rm MS}} = -\,\Sigma^{\rm ggg}_{(4)}(p,q)\Big|_{\overline{\rm MS}} \\
&= \frac{1}{2}\,\Sigma^{\rm ggg}_{(5)}(p,q)\Big|_{\overline{\rm MS}} = -\,\Sigma^{\rm ggg}_{(6)}(p,q)\Big|_{\overline{\rm MS}} \\
&= -1 \;-\; \Big[-36\psi'\left(\tfrac{1}{3}\right)\alpha^2 C_A + 162\psi'\left(\tfrac{1}{3}\right)\alpha C_A - 138\psi'\left(\tfrac{1}{3}\right) C_A \\
&\qquad +384\psi'\left(\tfrac{1}{3}\right) N_f T_F - 27\alpha^3 C_A + 24\alpha^2 C_A\pi^2 + 405\alpha^2 C_A \\
&\qquad -108\alpha C_A\pi^2 + 243\alpha C_A + 92 C_A\pi^2 + 243 C_A \\
&\qquad -256 N_f\pi^2 T_F - 1296 N_f T_F\Big]\frac{a}{648} \\
&\quad - \Big[1296\sqrt{3}\psi'\left(\tfrac{1}{3}\right)\alpha^4 C_A^2 - 10368\sqrt{3}\psi'\left(\tfrac{1}{3}\right)\alpha^3 C_A^2 \\
&\qquad -17112\sqrt{3}\psi'\left(\tfrac{1}{3}\right)\alpha^2 C_A^2 - 19200\sqrt{3}\psi'\left(\tfrac{1}{3}\right)\alpha^2 C_A N_f T_F \\
&\qquad -14328\sqrt{3}\psi'\left(\tfrac{1}{3}\right)\alpha C_A^2 - 4608\sqrt{3}\psi'\left(\tfrac{1}{3}\right)\alpha C_A N_f T_F
\end{aligned}
$$

$$
\begin{aligned}
&+308052\sqrt{3}\psi'\left(\tfrac{1}{3}\right) C_A^2 - 63360\sqrt{3}\psi'\left(\tfrac{1}{3}\right) C_A N_f T_F \\
&+55296\sqrt{3}\psi'\left(\tfrac{1}{3}\right) C_F N_f T_F + 18\sqrt{3}\psi'''\left(\tfrac{1}{3}\right) \alpha^3 C_A^2 \\
&+162\sqrt{3}\psi'''\left(\tfrac{1}{3}\right) \alpha^2 C_A^2 - 1296\sqrt{3}\psi'''\left(\tfrac{1}{3}\right) \alpha C_A^2 \\
&+3843\sqrt{3}\psi'''\left(\tfrac{1}{3}\right) C_A^2 - 2304\sqrt{3}\psi'''\left(\tfrac{1}{3}\right) C_A N_f T_F \\
&-31104\sqrt{3}s_2\left(\tfrac{\pi}{6}\right) \alpha^3 C_A^2 - 489888\sqrt{3}s_2\left(\tfrac{\pi}{6}\right) \alpha C_A^2 \\
&+2690496\sqrt{3}s_2\left(\tfrac{\pi}{6}\right) C_A^2 - 1244160\sqrt{3}s_2\left(\tfrac{\pi}{6}\right) C_A N_f T_F \\
&+62208\sqrt{3}s_2\left(\tfrac{\pi}{2}\right) \alpha^3 C_A^2 + 979776\sqrt{3}s_2\left(\tfrac{\pi}{2}\right) \alpha C_A^2 \\
&-5380992\sqrt{3}s_2\left(\tfrac{\pi}{2}\right) C_A^2 + 2488320\sqrt{3}s_2\left(\tfrac{\pi}{2}\right) C_A N_f T_F \\
&+51840\sqrt{3}s_3\left(\tfrac{\pi}{6}\right) \alpha^3 C_A^2 + 816480\sqrt{3}s_3\left(\tfrac{\pi}{6}\right) \alpha C_A^2 \\
&-4484160\sqrt{3}s_3\left(\tfrac{\pi}{6}\right) C_A^2 + 2073600\sqrt{3}s_3\left(\tfrac{\pi}{6}\right) C_A N_f T_F \\
&-41472\sqrt{3}s_3\left(\tfrac{\pi}{2}\right) \alpha^3 C_A^2 - 653184\sqrt{3}s_3\left(\tfrac{\pi}{2}\right) \alpha C_A^2 \\
&+3587328\sqrt{3}s_3\left(\tfrac{\pi}{2}\right) C_A^2 - 1658880\sqrt{3}s_3\left(\tfrac{\pi}{2}\right) C_A N_f T_F \\
&+972\sqrt{3}\alpha^5 C_A^2 - 864\sqrt{3}\alpha^4 C_A^2 \pi^2 - 7776\sqrt{3}\alpha^4 C_A^2 \\
&-48\sqrt{3}\alpha^3 C_A^2 \pi^4 + 6912\sqrt{3}\alpha^3 C_A^2 \pi^2 - 2592\sqrt{3}\alpha^3 C_A^2 \zeta_3 \\
&-4104\sqrt{3}\alpha^3 C_A^2 - 8640\sqrt{3}\alpha^3 C_A N_f T_F - 432\sqrt{3}\alpha^2 C_A^2 \pi^4 \\
&+11408\sqrt{3}\alpha^2 C_A^2 \pi^2 + 3888\sqrt{3}\alpha^2 C_A^2 \zeta_3 - 17280\sqrt{3}\alpha^2 C_A^2 \\
&+12800\sqrt{3}\alpha^2 C_A N_f \pi^2 T_F + 86400\sqrt{3}\alpha^2 C_A N_f T_F \\
&+3456\sqrt{3}\alpha C_A^2 \pi^4 + 9552\sqrt{3}\alpha C_A^2 \pi^2 + 167184\sqrt{3}\alpha C_A^2 \zeta_3 \\
&-84726\sqrt{3}\alpha C_A^2 + 3072\sqrt{3}\alpha C_A N_f \pi^2 T_F \\
&+36288\sqrt{3}\alpha C_A N_f T_F - 10248\sqrt{3} C_A^2 \pi^4 - 205368\sqrt{3} C_A^2 \pi^2 \\
&-447444\sqrt{3} C_A^2 \zeta_3 + 256338\sqrt{3} C_A^2 + 6144\sqrt{3} C_A N_f \pi^4 T_F \\
&+42240\sqrt{3} C_A N_f \pi^2 T_F - 41472\sqrt{3} C_A N_f T_F \zeta_3 \\
&-259632\sqrt{3} C_A N_f T_F - 36864\sqrt{3} C_F N_f \pi^2 T_F \\
&+497664\sqrt{3} C_F N_f T_F \zeta_3 - 590976\sqrt{3} C_F N_f T_F \\
&-216 \ln(3)^2 \alpha^3 C_A^2 \pi - 3402 \ln(3)^2 \alpha C_A^2 \pi \\
&+18684 \ln(3)^2 C_A^2 \pi - 8640 \ln(3)^2 C_A N_f \pi T_F \\
&+2592 \ln(3) \alpha^3 C_A^2 \pi + 40824 \ln(3) \alpha C_A^2 \pi \\
&-224208 \ln(3) C_A^2 \pi + 103680 \ln(3) C_A N_f \pi T_F \\
&+232\alpha^3 C_A^2 \pi^3 + 3654\alpha C_A^2 \pi^3 - 20068 C_A^2 \pi^3 \\
&+9280 C_A N_f \pi^3 T_F \Big] \frac{a^2}{31104\sqrt{3}} \; + \; \mathcal{O}(a^3). \qquad (4.2.6)
\end{aligned}
$$

The combination which emerges for the first six amplitudes is consistent with

other gauges, most noticeably this can be seen by comparing with the amplitudes in (3.2.14). This should be consistent since we are considering the same tensor basis and so this serves as a check on our computation. The remaining channels are presented numerically for $SU(3)$ as

$$\begin{aligned}
\Sigma^{\mathrm{ggg}}_{(7)}(p,q)\Big|_{\overline{\mathrm{MS}}} &= 2\,\Sigma^{\mathrm{ggg}}_{(9)}(p,q)\Big|_{\overline{\mathrm{MS}}} = -\,2\,\Sigma^{\mathrm{ggg}}_{(11)}(p,q)\Big|_{\overline{\mathrm{MS}}} = -\,\Sigma^{\mathrm{ggg}}_{(14)}(p,q)\Big|_{\overline{\mathrm{MS}}} \\
&= \left[0.057318\alpha^3 - 0.507930\alpha^2 - 3.328046\alpha - 1.092686N_f \right. \\
&\quad \left. +7.642693\right] a + \left[-0.128965\alpha^5 + 0.603663\alpha^4 + 0.191059\alpha^3 N_f \right. \\
&\quad +5.383015\alpha^3 + 0.574522\alpha^2 N_f + 3.920818\alpha^2 - 1.015302\alpha N_f \\
&\quad \left. -6.825370\alpha - 20.271008N_f + 124.046565\right] a^2 \;+\; \mathcal{O}(a^3) \\
\Sigma^{\mathrm{ggg}}_{(8)}(p,q)\Big|_{\overline{\mathrm{MS}}} &= -\;\Sigma^{\mathrm{ggg}}_{(13)}(p,q)\Big|_{\overline{\mathrm{MS}}} \\
&= \left[0.192682\alpha^3 - 0.570116\alpha^2 - 3.351838\alpha - 1.213010N_f \right. \\
&\quad \left. +7.954277\right] a + \left[-0.433535\alpha^5 + 0.134441\alpha^4 + 0.642274\alpha^3 N_f \right. \\
&\quad +5.205282\alpha^3 + 0.936332\alpha^2 N_f + 7.365924\alpha^2 + 0.015581\alpha N_f \\
&\quad \left. -4.947164\alpha - 23.589820N_f + 133.972477\right] a^2 \;+\; \mathcal{O}(a^3) \\
\Sigma^{\mathrm{ggg}}_{(10)}(p,q)\Big|_{\overline{\mathrm{MS}}} &= -\,\Sigma^{\mathrm{ggg}}_{(12)}(p,q)\Big|_{\overline{\mathrm{MS}}} \\
&= \left[-0.135364\alpha^3 + 0.062186\alpha^2 + 0.023791\alpha + 0.120324N_f \right. \\
&\quad \left. -0.311584\right] a + \left[0.304570\alpha^5 + 0.469222\alpha^4 - 0.451214\alpha^3 N_f \right. \\
&\quad +0.177733\alpha^3 - 0.361810\alpha^2 N_f - 3.445106\alpha^2 - 1.030883\alpha N_f \\
&\quad \left. -1.878205\alpha + 3.318812N_f - 9.925913\right] a^2 \;+\; \mathcal{O}(a^3)\;. \qquad (4.2.7)
\end{aligned}$$

Finally, for the quark-gluon vertex the amplitudes in the $\overline{\mathrm{MS}}$ scheme are

$$\begin{aligned}
\Sigma^{\mathrm{qqg}}_{(1)}(p,q)\Big|_{\overline{\mathrm{MS}}} &= 1 \;+\; \left[-0.457012\alpha^2 - 0.588760\alpha + 4.316221\right] a \\
&\quad + \left[0.342759\alpha^4 + 1.394721\alpha^3 - 0.507791\alpha^2 N_f - 1.842083\alpha^2 \right. \\
&\quad \left. -0.976628\alpha N_f - 2.548865\alpha - 12.136677N_f + 89.287677\right] a^2 \\
&\quad + \mathcal{O}(a^3) \\
\Sigma^{\mathrm{qqg}}_{(2)}(p,q)\Big|_{\overline{\mathrm{MS}}} &= \Sigma^{\mathrm{qqg}}_{(5)}(p,q)\Big|_{\overline{\mathrm{MS}}} \\
&= \left[-0.414023\alpha^2 - 2.305695\alpha + 2.598033\right] a + \left[0.310517\alpha^4 \right. \\
&\quad \left. +1.541598\alpha^3 - 0.460026\alpha^2 N_f - 2.574810\alpha^2 - 1.033946\alpha N_f \right. \\
&\quad \left. -19.509999\alpha - 6.271894N_f + 26.481250\right] a^2 \;+\; \mathcal{O}(a^3) \\
\Sigma^{\mathrm{qqg}}_{(3)}(p,q)\Big|_{\overline{\mathrm{MS}}} &= \Sigma^{\mathrm{qqg}}_{(4)}(p,q)\Big|_{\overline{\mathrm{MS}}} \\
&= \left[-0.500000\alpha^2 - 2.522631\alpha + 2.050269\right] a + \left[0.375000\alpha^4 \right.
\end{aligned}$$

$$
\begin{aligned}
& +1.247844\alpha^3 - 0.555556\alpha^2 N_f - 3.686459\alpha^2 - 0.919310\alpha N_f \\
& -22.991124\alpha - 4.871592 N_f + 12.735293 \big] a^2 \; + \; \mathcal{O}(a^3) \\
\Sigma^{\mathrm{qqg}}_{(6)}(p,q)\Big|_{\overline{\mathrm{MS}}} \; = \; & \big[-0.585977\alpha^2 - 2.343907\alpha - 4.362272 \big] a + \big[0.439483\alpha^4 \\
& +0.976628\alpha^3 - 0.651085\alpha^2 N_f - 0.499235\alpha^2 + 1.953256\alpha N_f \\
& -45.467503\alpha + 10.922850 N_f - 131.991115 \big] a^2 \; + \; \mathcal{O}(a^3)
\end{aligned}
\tag{4.2.8}
$$

where the one loop contribution to the amplitudes are identical to those computed in the arbitrary (linear) covariant gauge. As a check on the results for the other vertices we note that the relations between the amplitudes still hold even to higher loop orders, with these relations satisfied in all schemes. In Figure 4.1 we present plots of the one and two loop amplitudes for various values of N_f in terms of the partial coupling constants, $a_1(\mu, \Lambda)$ and $a_2(\mu, \Lambda)$. This was carried out in the previous chapter for the linear covariant gauge. Comparing to those graphs for the same values of N_f it is clear that the one and two loop Curci-Ferrari gauge results are much closer to eachother, particularly for the case when $N_f = 6$, than the one and two loop amplitudes in the linear covariant gauge. This could be as a result of the 4-point interactions introduced, specifically contributing to the ghost-gluon vertex, or due to the ghost-gluon vertex now being asymmetric, which would give better convergence. However, the reason why this gauge seems to converge quicker is not yet known for sure. Having presented all required results in the $\overline{\mathrm{MS}}$ scheme we now extend to the MOMi schemes.

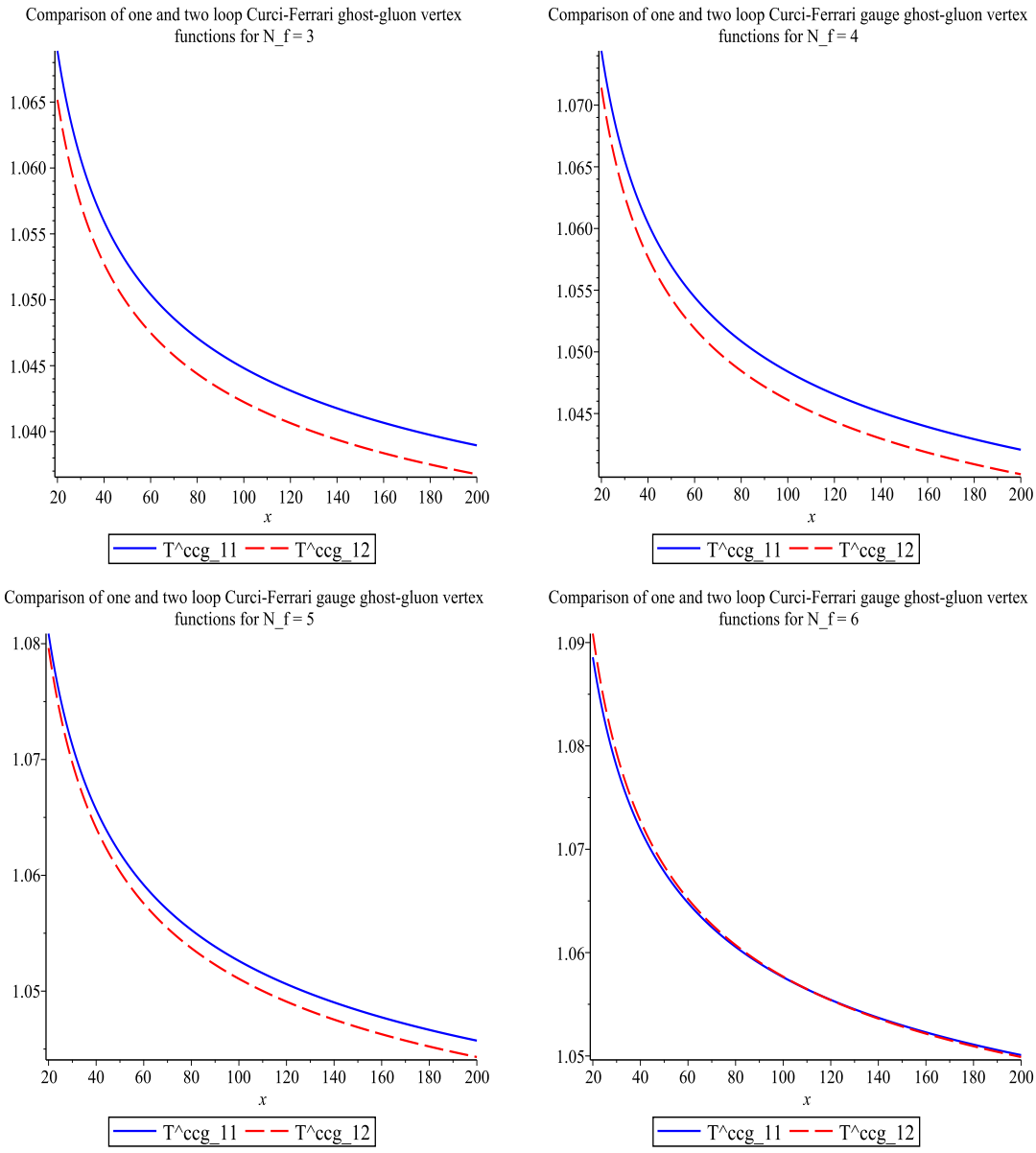

Figure 4.1: Comparison of one and two loop $\overline{\text{MS}}$ Curci-Ferrari gauge ghost-gluon vertex functions for different values of N_f.

4.3 MOMh scheme

So far all of our results have been determined in the $\overline{\text{MS}}$ scheme, where only the divergences are absorbed into the renormalization constants, along with a factor of $\ln(4\pi e^{-\gamma})$. For the MOMi schemes we recall from section 2.1.2 that as well as the divergences being absorbed into the renormalization constants, we now

require that there are no $\mathcal{O}(a)$ corrections after the renormalization constants are defined. Both the 2-point functions and 3-point vertex functions are defined in this way, where we renormalize the one loop 2-point functions first in each MOMi scheme followed by the one loop 3-point vertex functions. We then iterate this procedure to two loops. Presenting first the renormalization constants for the scheme corresponding to the ghost-gluon vertex we have

$$
\begin{aligned}
Z_g^{(\mathrm{ccg})}\big|_{\mathrm{MOMh}} \;=\; & 1 + \left[12\psi'\left(\tfrac{1}{3}\right) \alpha C_A - 30\psi'\left(\tfrac{1}{3}\right) C_A - 27\alpha^2 C_A - 8\alpha C_A \pi^2 - 108\alpha C_A \right. \\
& \quad + 20 C_A \pi^2 - 669 C_A + 240 N_f T_F \\
& \quad \left. + 36 \left(-11 C_A + 4 N_f T_F \right) \frac{1}{\epsilon} \right] \frac{a}{216} \\
& + \left[\left(121 C_A^2 - 88 C_A N_f T_F + 16 N_f^2 T_F^2 \right) \frac{1}{24\epsilon^2} \right. \\
& \quad + \left(288\sqrt{3}\psi'\left(\tfrac{1}{3}\right)^2 \alpha^2 C_A^2 - 1440\sqrt{3}\psi'\left(\tfrac{1}{3}\right)^2 \alpha C_A^2 \right. \\
& \qquad + 1800\sqrt{3}\psi'\left(\tfrac{1}{3}\right)^2 C_A^2 - 216\sqrt{3}\psi'\left(\tfrac{1}{3}\right) \alpha^3 C_A^2 \\
& \qquad - 384\sqrt{3}\psi'\left(\tfrac{1}{3}\right) \alpha^2 C_A^2 \pi^2 - 14040\sqrt{3}\psi'\left(\tfrac{1}{3}\right) \alpha^2 C_A^2 \\
& \qquad + 1920\sqrt{3}\psi'\left(\tfrac{1}{3}\right) \alpha C_A^2 \pi^2 - 14832\sqrt{3}\psi'\left(\tfrac{1}{3}\right) \alpha C_A^2 \\
& \qquad + 8064\sqrt{3}\psi'\left(\tfrac{1}{3}\right) \alpha C_A N_f T_F - 2400\sqrt{3}\psi'\left(\tfrac{1}{3}\right) C_A^2 \pi^2 \\
& \qquad + 203436\sqrt{3}\psi'\left(\tfrac{1}{3}\right) C_A^2 - 102528\sqrt{3}\psi'\left(\tfrac{1}{3}\right) C_A N_f T_F \\
& \qquad - 18\sqrt{3}\psi'''\left(\tfrac{1}{3}\right) \alpha^2 C_A^2 + 225\sqrt{3}\psi'''\left(\tfrac{1}{3}\right) \alpha C_A^2 \\
& \qquad + 999\sqrt{3}\psi'''\left(\tfrac{1}{3}\right) C_A^2 - 73872\sqrt{3} s_2\left(\tfrac{\pi}{6}\right) \alpha^2 C_A^2 \\
& \qquad + 66096\sqrt{3} s_2\left(\tfrac{\pi}{6}\right) \alpha C_A^2 + 1076976\sqrt{3} s_2\left(\tfrac{\pi}{6}\right) C_A^2 \\
& \qquad - 497664\sqrt{3} s_2\left(\tfrac{\pi}{6}\right) C_A N_f T_F + 147744\sqrt{3} s_2\left(\tfrac{\pi}{2}\right) \alpha^2 C_A^2 \\
& \qquad - 132192\sqrt{3} s_2\left(\tfrac{\pi}{2}\right) \alpha C_A^2 - 2153952\sqrt{3} s_2\left(\tfrac{\pi}{2}\right) C_A^2 \\
& \qquad + 995328\sqrt{3} s_2\left(\tfrac{\pi}{2}\right) C_A N_f T_F + 123120\sqrt{3} s_3\left(\tfrac{\pi}{6}\right) \alpha^2 C_A^2 \\
& \qquad - 110160\sqrt{3} s_3\left(\tfrac{\pi}{6}\right) \alpha C_A^2 - 1794960\sqrt{3} s_3\left(\tfrac{\pi}{6}\right) C_A^2 \\
& \qquad + 829440\sqrt{3} s_3\left(\tfrac{\pi}{6}\right) C_A N_f T_F - 98496\sqrt{3} s_3\left(\tfrac{\pi}{2}\right) \alpha^2 C_A^2 \\
& \qquad + 88128\sqrt{3} s_3\left(\tfrac{\pi}{2}\right) \alpha C_A^2 + 1435968\sqrt{3} s_3\left(\tfrac{\pi}{2}\right) C_A^2 \\
& \qquad - 663552\sqrt{3} s_3\left(\tfrac{\pi}{2}\right) C_A N_f T_F - 243\sqrt{3}\alpha^4 C_A^2 \\
& \qquad + 144\sqrt{3}\alpha^3 C_A^2 \pi^2 - 2916\sqrt{3}\alpha^3 C_A^2 + 176\sqrt{3}\alpha^2 C_A^2 \pi^4 \\
& \qquad + 9360\sqrt{3}\alpha^2 C_A^2 \pi^2 + 4536\sqrt{3}\alpha^2 C_A^2 \zeta_3 + 47790\sqrt{3}\alpha^2 C_A^2 \\
& \qquad - 12960\sqrt{3}\alpha^2 C_A N_f T_F - 1240\sqrt{3}\alpha C_A^2 \pi^4 + 9888\sqrt{3}\alpha C_A^2 \pi^2 \\
& \qquad - 13932\sqrt{3}\alpha C_A^2 \zeta_3 + 111132\sqrt{3}\alpha C_A^2 - 5376\sqrt{3}\alpha C_A N_f \pi^2 T_F \\
& \qquad - 41472\sqrt{3}\alpha C_A N_f T_F - 1864\sqrt{3} C_A^2 \pi^4 - 135624\sqrt{3} C_A^2 \pi^2
\end{aligned}
$$

$$
\begin{aligned}
&-99792\sqrt{3}C_A^2\zeta_3 - 133155\sqrt{3}C_A^2 + 68352\sqrt{3}C_AN_f\pi^2T_F \\
&+207360\sqrt{3}C_AN_fT_F\zeta_3 - 53280\sqrt{3}C_AN_fT_F \\
&-248832\sqrt{3}C_FN_fT_F\zeta_3 + 285120\sqrt{3}C_FN_fT_F \\
&+57600\sqrt{3}N_f^2T_F^2 - 513\ln(3)^2\alpha^2C_A^2\pi + 459\ln(3)^2\alpha C_A^2\pi \\
&+7479\ln(3)^2C_A^2\pi - 3456\ln(3)^2C_AN_f\pi T_F \\
&+6156\ln(3)\alpha^2C_A^2\pi - 5508\ln(3)\alpha C_A^2\pi - 89748\ln(3)C_A^2\pi \\
&+41472\ln(3)C_AN_f\pi T_F + 551\alpha^2C_A^2\pi^3 - 493\alpha C_A^2\pi^3 \\
&-8033C_A^2\pi^3 + 3712C_AN_f\pi^3T_F + 72\sqrt{3}\left(-132\psi'\left(\tfrac{1}{3}\right)\alpha C_A^2\right. \\
&+48\psi'\left(\tfrac{1}{3}\right)\alpha C_AN_fT_F + 330\psi'\left(\tfrac{1}{3}\right)C_A^2 - 120\psi'\left(\tfrac{1}{3}\right)C_AN_fT_F \\
&+297\alpha^2C_A^2 - 108\alpha^2C_AN_fT_F + 88\alpha C_A^2\pi^2 + 1188\alpha C_A^2 \\
&-32\alpha C_AN_f\pi^2T_F - 432\alpha C_AN_fT_F - 220C_A^2\pi^2 + 6135C_A^2 \\
&+80C_AN_f\pi^2T_F - 4596C_AN_fT_F + 432C_FN_fT_F \\
&\left.+960N_f^2T_F^2\right)\frac{1}{\epsilon}\Bigg)\frac{1}{31104\sqrt{3}}\Bigg]a^2 \;+\; \mathcal{O}(a^3) \qquad (4.3.9)
\end{aligned}
$$

analytically, followed by the renormalization constants for the wave functions and gauge parameter numerically for $SU(3)$

$$
\begin{aligned}
Z_A^{(\mathrm{ccg})}\Big|_{\mathrm{MOMh}} &= 1 + \Big[0.75\alpha^2 + 1.5\alpha - 1.111111N_f + 8.083333 \\
&\quad + (-1.5\alpha - 0.666667N_f + 6.5)\frac{1}{\epsilon}\Big]a \\
&\quad + \Bigg[\left(1.687500\alpha^2 + \alpha N_f - 6.375000\alpha + 1.5N_f - 14.625000\right)\frac{1}{\epsilon^2} \\
&\quad + 0.562500\alpha^4 + 3.691465\alpha^3 - 0.587169\alpha^2 + 0.364496\alpha N_f \\
&\quad - 3.503260\alpha - 21.027871N_f + 82.204984 + \big(-1.125000\alpha^3 \\
&\quad - 4.570430\alpha^2 + 1.885364\alpha N_f - 0.299975\alpha + 3.869923N_f \\
&\quad - 54.106746\big)\frac{1}{\epsilon}\Bigg]a^2 \;+\; \mathcal{O}(a^3) \\
Z_\alpha^{(\mathrm{ccg})}\Big|_{\mathrm{MOMh}} &= 1 + \left[-1.5\alpha - 0.75\frac{\alpha}{\epsilon}\right]a \\
&\quad + \Bigg[\alpha\left(0.562500\alpha + 1.687500\right)\frac{1}{\epsilon^2} + \alpha\left(-2.601680\alpha + 6.483018\right) \\
&\quad + \alpha\left(-0.035215\alpha + 8.666163\right)\frac{1}{\epsilon}\Bigg]a^2 \;+\; \mathcal{O}(a^3) \\
Z_c^{(\mathrm{ccg})}\Big|_{\mathrm{MOMh}} &= 1 + \left[3.0 + \left(-0.75\alpha + 2.25\right)\frac{1}{\epsilon}\right]a
\end{aligned}
$$

$$
\begin{aligned}
&+\left[\left(0.562500\alpha^2+0.75N_f-9.843750\right)\frac{1}{\epsilon^2}-1.968750\alpha^2\right.\\
&\quad -2.411572\alpha-2.604167N_f+16.396118+\left(-2.847715\alpha^2\right.\\
&\quad \left.\left.+3.990559\alpha+1.875000N_f-32.748489\right)\frac{1}{\epsilon}\right]a^2 \;+\; \mathcal{O}(a^3)\\
Z_{\psi}^{(\mathrm{ccg})}\Big|_{\mathrm{MOMh}} &= 1+\left[-1.333333\alpha-1.333333\frac{\alpha}{\epsilon}\right]a\\
&+\left[\alpha\left(1.388889\alpha+3.0\right)\frac{1}{\epsilon^2}-0.784827\alpha^2+6.331195\alpha\right.\\
&\quad +2.333333N_f-25.464206+\left(0.215173\alpha^2+13.906512\alpha\right.\\
&\quad \left.\left.+0.666667N_f-11.166667\right)\frac{1}{\epsilon}\right]a^2 \;+\; \mathcal{O}(a^3) \qquad (4.3.10)
\end{aligned}
$$

where all results for the above renormalization constants are functions of MOMi variables $(a_{\mathrm{MOMi}}, \alpha_{\mathrm{MOMi}})$. The amplitudes in the MOMh scheme were found to follow the relation given in [51] where

$$
\Sigma_{(1)}^{\mathrm{acc}}(p,q)\Big|_{\mathrm{MOMh}} \;=\; -\,\Sigma_{(2)}^{\mathrm{acc}}(p,q)\Big|_{\mathrm{MOMh}} \;=\; -\frac{1}{2}+\mathcal{O}(a^3)\;. \qquad (4.3.11)
$$

This is not the same as in the case of the arbitrary (linear) covariant gauge fixing where after renormalization in the MOMh scheme the two amplitudes are still independent of one another due to the nature of the ghost-gluon vertex in that gauge fixing. The fact that the amplitudes become linearly dependent is also partly due to the presence of the quartic ghost vertex that is introduced in both the Curci-Ferrari gauge and MAG, [14, 104].

Next we require the coupling constant and gauge parameter mappings between the $\overline{\mathrm{MS}}$ and MOMi schemes in the Curci-Ferrari gauge. Using (3.3.37) we can relate both the coupling constant and gauge parameter in one scheme to another. We have determined α_{MOMi} for each of the three vertices and found that for each vertex the result remains the same at two loops

$$
\begin{aligned}
\alpha_{\mathrm{MOMi}} &= \alpha+\left[-9\alpha^2C_A-36\alpha C_A-97C_A+80N_fT_F\right]\frac{\alpha a}{36}\\
&\quad +\left[18\alpha^4C_A^2+90\alpha^3C_A^2-36\alpha^2C_A^2\zeta_3+301\alpha^2C_A^2-320\alpha^2C_AN_fT_F\right.\\
&\quad -468\alpha C_A^2\zeta_3+284\alpha C_A^2-640\alpha C_AN_fT_F+864C_A^2\zeta_3-7143C_A^2\\
&\quad +2304C_AN_fT_F\zeta_3+4248C_AN_fT_F-4608C_FN_fT_F\zeta_3\\
&\quad \left.+5280C_FN_fT_F\right]\frac{\alpha a^2}{288} \;+\; \mathcal{O}(a^3) \qquad (4.3.12)
\end{aligned}
$$

where $\alpha_{\rm MOMi}$ is a function of $\overline{\rm MS}$ variables, $a_{\overline{\rm MS}}$ and $\alpha_{\overline{\rm MS}}$. This is consistent with the arbitrary (linear) covariant gauge where one gauge parameter mapping satisfies all three MOMi schemes. This is not the case however for the coupling constants, $a_{\rm MOMi}$, where that mapping is different for each of the three MOMi schemes. Therefore we present the results for this separately for each scheme. The analytic evaluation of the coupling constant mapping for the MOMh scheme is

$$
\begin{aligned}
a_{\rm MOMh} \;=\; & a + \left[-12\psi'\left(\tfrac{1}{3}\right)\alpha C_A + 30\psi'\left(\tfrac{1}{3}\right)C_A + 27\alpha^2 C_A + 8\alpha C_A\pi^2\right. \\
& \left. +108\alpha C_A - 20 C_A\pi^2 + 669 C_A - 240 N_f T_F\right]\frac{a^2}{108} \\
& + \Big[513\sqrt{3}\ln(3)^2\alpha^2 C_A^2\pi - 459\sqrt{3}\ln(3)^2\alpha C_A^2\pi \\
& -7479\sqrt{3}\ln(3)^2 C_A^2\pi + 3456\sqrt{3}\ln(3)^2 C_A N_f\pi T_F \\
& -6156\sqrt{3}\ln(3)\alpha^2 C_A^2\pi + 5508\sqrt{3}\ln(3)\alpha C_A^2\pi \\
& +89748\sqrt{3}\ln(3) C_A^2\pi - 41472\sqrt{3}\ln(3) C_A N_f\pi T_F \\
& -551\sqrt{3}\alpha^2 C_A^2\pi^3 + 493\sqrt{3}\alpha C_A^2\pi^3 + 8033\sqrt{3} C_A^2\pi^3 \\
& -3712\sqrt{3} C_A N_f\pi^3 T_F + 144\psi'\left(\tfrac{1}{3}\right)^2\alpha^2 C_A^2 - 720\psi'\left(\tfrac{1}{3}\right)^2\alpha C_A^2 \\
& +900\psi'\left(\tfrac{1}{3}\right)^2 C_A^2 - 2592\psi'\left(\tfrac{1}{3}\right)\alpha^3 C_A^2 - 192\psi'\left(\tfrac{1}{3}\right)\alpha^2 C_A^2\pi^2 \\
& +40500\psi'\left(\tfrac{1}{3}\right)\alpha^2 C_A^2 + 960\psi'\left(\tfrac{1}{3}\right)\alpha C_A^2\pi^2 - 8568\psi'\left(\tfrac{1}{3}\right)\alpha C_A^2 \\
& +4608\psi'\left(\tfrac{1}{3}\right)\alpha C_A N_f T_F - 1200\psi'\left(\tfrac{1}{3}\right) C_A^2\pi^2 \\
& -329328\psi'\left(\tfrac{1}{3}\right) C_A^2 + 206784\psi'\left(\tfrac{1}{3}\right) C_A N_f T_F \\
& +54\psi'''\left(\tfrac{1}{3}\right)\alpha^2 C_A^2 - 675\psi'''\left(\tfrac{1}{3}\right)\alpha C_A^2 - 2997\psi'''\left(\tfrac{1}{3}\right) C_A^2 \\
& +221616 s_2\left(\tfrac{\pi}{6}\right)\alpha^2 C_A^2 - 198288 s_2\left(\tfrac{\pi}{6}\right)\alpha C_A^2 \\
& -3230928 s_2\left(\tfrac{\pi}{6}\right) C_A^2 + 1492992 s_2\left(\tfrac{\pi}{6}\right) C_A N_f T_F \\
& -443232 s_2\left(\tfrac{\pi}{2}\right)\alpha^2 C_A^2 + 396576 s_2\left(\tfrac{\pi}{2}\right)\alpha C_A^2 \\
& +6461856 s_2\left(\tfrac{\pi}{2}\right) C_A^2 - 2985984 s_2\left(\tfrac{\pi}{2}\right) C_A N_f T_F \\
& -369360 s_3\left(\tfrac{\pi}{6}\right)\alpha^2 C_A^2 + 330480 s_3\left(\tfrac{\pi}{6}\right)\alpha C_A^2 \\
& +5384880 s_3\left(\tfrac{\pi}{6}\right) C_A^2 - 2488320 s_3\left(\tfrac{\pi}{6}\right) C_A N_f T_F \\
& +295488 s_3\left(\tfrac{\pi}{2}\right)\alpha^2 C_A^2 - 264384 s_3\left(\tfrac{\pi}{2}\right)\alpha C_A^2 \\
& -4307904 s_3\left(\tfrac{\pi}{2}\right) C_A^2 + 1990656 s_3\left(\tfrac{\pi}{2}\right) C_A N_f T_F \\
& +1728\alpha^3 C_A^2\pi^2 + 14580\alpha^3 C_A^2 - 80\alpha^2 C_A^2\pi^4 - 27000\alpha^2 C_A^2\pi^2 \\
& -13608\alpha^2 C_A^2\zeta_3 + 81648\alpha^2 C_A^2 + 1480\alpha C_A^2\pi^4 + 5712\alpha C_A^2\pi^2 \\
& +41796\alpha C_A^2\zeta_3 + 552420\alpha C_A^2 - 3072\alpha C_A N_f\pi^2 T_F
\end{aligned}
$$

$$
\begin{aligned}
&-134784\alpha C_A N_f T_F + 8392 C_A^2 \pi^4 + 219552 C_A^2 \pi^2 \\
&+299376 C_A^2 \zeta_3 + 3532392 C_A^2 - 137856 C_A N_f \pi^2 T_F \\
&-622080 C_A N_f T_F \zeta_3 - 2088000 C_A N_f T_F + 746496 C_F N_f T_F \zeta_3 \\
&-855360 C_F N_f T_F + 230400 N_f^2 T_F^2 \big] \frac{a^3}{46656} \; + \; \mathcal{O}(a^4) \; . \quad (4.3.13)
\end{aligned}
$$

Next we present the conversion functions at two loops, since these are used in (3.3.29) and (3.4.55) to determine the β-functions and anomalous dimensions in each MOMi scheme to the next loop order. The conversion function specific to the MOMh coupling constant is

$$
\begin{aligned}
C_g^{\rm MOMh}(a,\alpha) \;=\; & 1 + \big[12\psi'\left(\tfrac{1}{3}\right) \alpha C_A - 30\psi'\left(\tfrac{1}{3}\right) C_A - 27\alpha^2 C_A - 8\alpha C_A \pi^2 \\
& \quad -108\alpha C_A + 20 C_A \pi^2 - 669 C_A + 240 N_f T_F \big] \frac{a}{216} \\
& + \Big[288\sqrt{3}\psi'\left(\tfrac{1}{3}\right)^2 \alpha^2 C_A^2 - 1440\sqrt{3}\psi'\left(\tfrac{1}{3}\right)^2 \alpha C_A^2 \\
& \quad +1800\sqrt{3}\psi'\left(\tfrac{1}{3}\right)^2 C_A^2 + 648\sqrt{3}\psi'\left(\tfrac{1}{3}\right) \alpha^3 C_A^2 \\
& \quad -384\sqrt{3}\psi'\left(\tfrac{1}{3}\right) \alpha^2 C_A^2 \pi^2 - 43416\sqrt{3}\psi'\left(\tfrac{1}{3}\right) \alpha^2 C_A^2 \\
& \quad +1920\sqrt{3}\psi'\left(\tfrac{1}{3}\right) \alpha C_A^2 \pi^2 - 20160\sqrt{3}\psi'\left(\tfrac{1}{3}\right) \alpha C_A^2 \\
& \quad +12672\sqrt{3}\psi'\left(\tfrac{1}{3}\right) \alpha C_A N_f T_F - 2400\sqrt{3}\psi'\left(\tfrac{1}{3}\right) C_A^2 \pi^2 \\
& \quad +449748\sqrt{3}\psi'\left(\tfrac{1}{3}\right) C_A^2 - 249984\sqrt{3}\psi'\left(\tfrac{1}{3}\right) C_A N_f T_F \\
& \quad -54\sqrt{3}\psi'''\left(\tfrac{1}{3}\right) \alpha^2 C_A^2 + 675\sqrt{3}\psi'''\left(\tfrac{1}{3}\right) \alpha C_A^2 \\
& \quad +2997\sqrt{3}\psi'''\left(\tfrac{1}{3}\right) C_A^2 - 221616\sqrt{3} s_2\left(\tfrac{\pi}{6}\right) \alpha^2 C_A^2 \\
& \quad +198288\sqrt{3} s_2\left(\tfrac{\pi}{6}\right) \alpha C_A^2 + 3230928\sqrt{3} s_2\left(\tfrac{\pi}{6}\right) C_A^2 \\
& \quad -1492992\sqrt{3} s_2\left(\tfrac{\pi}{6}\right) C_A N_f T_F + 443232\sqrt{3} s_2\left(\tfrac{\pi}{2}\right) \alpha^2 C_A^2 \\
& \quad -396576\sqrt{3} s_2\left(\tfrac{\pi}{2}\right) \alpha C_A^2 - 6461856\sqrt{3} s_2\left(\tfrac{\pi}{2}\right) C_A^2 \\
& \quad +2985984\sqrt{3} s_2\left(\tfrac{\pi}{2}\right) C_A N_f T_F + 369360\sqrt{3} s_3\left(\tfrac{\pi}{6}\right) \alpha^2 C_A^2 \\
& \quad -330480\sqrt{3} s_3\left(\tfrac{\pi}{6}\right) \alpha C_A^2 - 5384880\sqrt{3} s_3\left(\tfrac{\pi}{6}\right) C_A^2 \\
& \quad +2488320\sqrt{3} s_3\left(\tfrac{\pi}{6}\right) C_A N_f T_F - 295488\sqrt{3} s_3\left(\tfrac{\pi}{2}\right) \alpha^2 C_A^2 \\
& \quad +264384\sqrt{3} s_3\left(\tfrac{\pi}{2}\right) \alpha C_A^2 + 4307904\sqrt{3} s_3\left(\tfrac{\pi}{2}\right) C_A^2 \\
& \quad -1990656\sqrt{3} s_3\left(\tfrac{\pi}{2}\right) C_A N_f T_F + 2187\sqrt{3}\alpha^4 C_A^2 \\
& \quad -432\sqrt{3}\alpha^3 C_A^2 \pi^2 + 2916\sqrt{3}\alpha^3 C_A^2 + 272\sqrt{3}\alpha^2 C_A^2 \pi^4 \\
& \quad +28944\sqrt{3}\alpha^2 C_A^2 \pi^2 + 13608\sqrt{3}\alpha^2 C_A^2 \zeta_3 + 61722\sqrt{3}\alpha^2 C_A^2 \\
& \quad -38880\sqrt{3}\alpha^2 C_A N_f T_F - 2440\sqrt{3}\alpha C_A^2 \pi^4 \\
& \quad +13440\sqrt{3}\alpha C_A^2 \pi^2 - 41796\sqrt{3}\alpha C_A^2 \zeta_3 - 118908\sqrt{3}\alpha C_A^2 \\
& \quad -8448\sqrt{3}\alpha C_A N_f \pi^2 T_F - 20736\sqrt{3}\alpha C_A N_f T_F
\end{aligned}
$$

$$
\begin{aligned}
&-7192\sqrt{3}C_A^2\pi^4 - 299832\sqrt{3}C_A^2\pi^2 - 299376\sqrt{3}C_A^2\zeta_3 \\
&-2189709\sqrt{3}C_A^2 + 166656\sqrt{3}C_AN_f\pi^2T_F \\
&+622080\sqrt{3}C_AN_fT_F\zeta_3 + 1124640\sqrt{3}C_AN_fT_F \\
&-746496\sqrt{3}C_FN_fT_F\zeta_3 + 855360\sqrt{3}C_FN_fT_F \\
&-57600\sqrt{3}N_f^2T_F^2 - 1539\ln(3)^2\alpha^2C_A^2\pi + 1377\ln(3)^2\alpha C_A^2\pi \\
&+22437\ln(3)^2C_A^2\pi - 10368\ln(3)^2C_AN_f\pi T_F \\
&+18468\ln(3)\alpha^2C_A^2\pi - 16524\ln(3)\alpha C_A^2\pi \\
&-269244\ln(3)C_A^2\pi + 124416\ln(3)C_AN_f\pi T_F \\
&+1653\alpha^2C_A^2\pi^3 - 1479\alpha C_A^2\pi^3 - 24099C_A^2\pi^3 \\
&+11136C_AN_f\pi^3T_F\big]\,\frac{a^2}{93312\sqrt{3}} \;+\; \mathcal{O}(a^3) \;. \qquad (4.3.14)
\end{aligned}
$$

Here a and α are the coupling constant and gauge parameter specific to the $\overline{\rm MS}$ scheme $\big(a_{\overline{\rm MS}}, \alpha_{\overline{\rm MS}}\big)$. We use this convention for the conversion functions throughout, denoted in equations (3.3.31). The following expressions for the conversion functions are found to be the same in all three MOMi schemes in the Curci-Ferrari gauge. This is a property which also appeared in the arbitrary (linear) covariant gauge. These are

$$
\begin{aligned}
C_A^{\rm MOMi}(a,\alpha) &= 1 + \big[9\alpha^2C_A + 18\alpha C_A + 97C_A - 80N_fT_F\big]\,\frac{a}{36} \\
&\quad + \big[162\alpha^3C_A^2 + 324\alpha^2C_A^2\zeta_3 + 1836\alpha^2C_A^2 + 5184\alpha C_A^2\zeta_3 \\
&\qquad +2817\alpha C_A^2 - 2880\alpha C_AN_fT_F - 7776C_A^2\zeta_3 + 83105C_A^2 \\
&\qquad -20736C_AN_fT_F\zeta_3 - 69272C_AN_fT_F + 41472C_FN_fT_F\zeta_3 \\
&\qquad -47520C_FN_fT_F + 12800N_f^2T_F^2\big]\,\frac{a^2}{2592} + \mathcal{O}(a^3) \\
C_\alpha^{\rm MOMi}(a,\alpha) &= 1 + \big[-9\alpha^2C_A - 36\alpha C_A - 97C_A + 80N_fT_F\big]\,\frac{a}{36} \\
&\quad + \big[18\alpha^4C_A^2 + 90\alpha^3C_A^2 - 36\alpha^2C_A^2\zeta_3 + 301\alpha^2C_A^2 \\
&\qquad -320\alpha^2C_AN_fT_F - 468\alpha C_A^2\zeta_3 + 284\alpha C_A^2 - 640\alpha C_AN_fT_F \\
&\qquad +864C_A^2\zeta_3 - 7143C_A^2 + 2304C_AN_fT_F\zeta_3 + 4248C_AN_fT_F \\
&\qquad -4608C_FN_fT_F\zeta_3 + 5280C_FN_fT_F\big]\,\frac{a^2}{288} + \mathcal{O}(a^3) \\
C_c^{\rm MOMi}(a,\alpha) &= 1 + C_Aa + \big[C_A^2(6\alpha^2 + 72\alpha\zeta_3 - 21\alpha - 180\zeta_3 + 1943) \\
&\qquad -760C_AN_fT_F\big]\,\frac{a^2}{192} \;+\; \mathcal{O}(a^3) \\
C_\psi^{\rm MOMi}(a,\alpha) &= 1 - \alpha C_Fa + \big[-2\alpha^2C_AC_F + 8\alpha^2C_F^2 + 24\alpha C_AC_F\zeta_3 - 52\alpha C_AC_F
\end{aligned}
$$

$$+24C_AC_F\zeta_3 - 82C_AC_F + 5C_F^2 + 28C_FN_fT_F\big]\,\frac{a^2}{8}$$
$$+\,\mathcal{O}(a^3)\;. \tag{4.3.15}$$

Note that the one loop contributions agree with those in the linear covariant gauge fixing (3.3.52). Now that we have recorded the conversion functions, coupling constant and gauge parameter mappings we can apply (3.3.29) and (3.4.55) in order to construct the β-functions and anomalous dimensions respectively to three loops for each of the three MOMi schemes. Following the procedure in Section 3 we first require the $\overline{\rm MS}$ renormalization group functions for the Curci-Ferrari gauge to the desired loop order, in our case the results need to be up to and including three loops. Since we have only computed the two loop $\overline{\rm MS}$ results directly the three loop results are extracted from [104]. Note that although the $\overline{\rm MS}$ results have already been determined for the anomalous dimensions, we extend [104] by providing a further analysis of the QCD vertices in the MOMi schemes. As well as providing new results for the $\overline{\rm MS}$ and MOMi amplitudes we use the results in [104] to construct the RG functions for each MOMi scheme. These of which are new to three loops. Additionally we have constructed the conversion functions, coupling constant mapping and gauge parameter mapping between the two schemes. These results are new and have been recorded in [67]. The $\overline{\rm MS}$ results for the anomalous dimensions in the Curci-Ferrari gauge are not the same as for the arbitrary (linear) covariant gauge setup past one loop order and so we present the results for the anomalous dimensions in this gauge below for completeness, [104]. Therefore, beginning with our anomalous dimensions in the $\overline{\rm MS}$ scheme we have, [104],

$$\begin{aligned}
\gamma_A^{\overline{\rm MS}}(a,\alpha) &= [3\alpha C_A - 13C_A + 8N_fT_F]\,\frac{a}{6} \\
&+ [\alpha^2C_A^2 + 11\alpha C_A^2 - 59C_A^2 + 40C_AN_fT_F + 32C_FN_fT_F]\frac{a^2}{8} \\
&+ [54\alpha^3C_A^3 + 909\alpha^2C_A^3 + 864\alpha C_A^3\zeta_3 + 6012\alpha C_A^3 - 2304\alpha C_A^2N_fT_F \\
&\quad +648C_A^3\zeta_3 - 39860C_A^3 - 20736C_A^2N_fT_F\zeta_3 + 58304C_A^2N_fT_F \\
&\quad +27648C_AC_FN_fT_F\zeta_3 + 320C_AC_FN_fT_F - 9728C_AN_f^2T_F^2 \\
&\quad -2304C_F^2N_fT_F - 5632C_FN_f^2T_F^2]\frac{a^3}{1152} \;+\; \mathcal{O}(a^4) \\
\gamma_c^{\overline{\rm MS}}(a,\alpha) &= C_A(\alpha-3)\frac{a}{4} + C_A[3\alpha^2C_A - 3\alpha C_A - 95C_A + 40N_fT_F]\frac{a^2}{48} \\
&+ C_A[162\alpha^3C_A^2 + 1485\alpha^2C_A^2 - 2592\alpha C_A^2\zeta_3 + 3672\alpha C_A^2 \\
&\quad -6048\alpha C_AN_fT_F - 1944C_A^2\zeta_3 - 63268C_A^2 + 62208C_AN_fT_F\zeta_3
\end{aligned}$$

$$
\begin{aligned}
&+6208C_A N_f T_F - 82944 C_F N_f T_F \zeta_3 + 77760 C_F N_f T_F \\
&+8960 N_f^2 T_F^2] \frac{a^3}{6912} \; + \; \mathcal{O}(a^4) \\
\gamma_\psi^{\overline{\rm MS}}(a,\alpha) &= \alpha C_F a + C_F \left[8\alpha C_A + 25 C_A - 6 C_F - 8 N_f T_F \right] \frac{a^2}{4} \\
&+ C_F \left[27\alpha^3 C_A^2 + 270 \alpha^2 C_A^2 + 216 \alpha C_A^2 \zeta_3 + 2367 \alpha C_A^2 \right. \\
&\quad -1224 \alpha C_A N_f T_F - 2484 C_A^2 \zeta_3 + 18310 C_A^2 + 3456 C_A C_F \zeta_3 \\
&\quad -10296 C_A C_F - 9184 C_A N_f T_F + 432 C_F^2 + 864 C_F N_f T_F \\
&\quad \left. +640 N_f^2 T_F^2 \right] \frac{a^3}{288} + \mathcal{O}(a^4) \\
\gamma_\alpha^{\overline{\rm MS}}(a,\alpha) &= \left[-3\alpha C_A + 26 C_A - 16 N_f T_F \right] \frac{a}{12} \\
&+ \left[-\alpha^2 C_A^2 - 17 \alpha C_A^2 + 118 C_A^2 - 80 C_A N_f T_F - 64 C_F N_f T_F \right] \frac{a^2}{16} \\
&+ \left[-27 \alpha^3 C_A^3 - 558 \alpha^2 C_A^3 - 864 \alpha C_A^3 \zeta_3 - 4203 \alpha C_A^3 + 1224 \alpha C_A^2 N_f T_F \right. \\
&\quad -648 C_A^3 \zeta_3 + 39860 C_A^3 + 20736 C_A^2 N_f T_F \zeta_3 - 58304 C_A^2 N_f T_F \\
&\quad -27648 C_A C_F N_f T_F \zeta_3 - 320 C_A C_F N_f T_F + 9728 C_A N_f^2 T_F^2 \\
&\quad \left. +2304 C_F^2 N_f T_F + 5632 C_F N_f^2 T_F^2 \right] \frac{a^3}{1152} + \mathcal{O}(a^4) \qquad (4.3.16)
\end{aligned}
$$

and the three loop β-function is, [1, 2, 92, 93, 94],

$$
\begin{aligned}
\beta^{\overline{\rm MS}}(a,\alpha) &= - \left[\frac{11}{3} C_A - \frac{4}{3} T_F N_f \right] a^2 \; - \; \left[\frac{34}{3} C_A^2 - 4 C_F T_F N_f - \frac{20}{3} C_A T_F N_f \right] a^3 \\
&+ \left[2830 C_A^2 T_F N_f - 2857 C_A^3 + 1230 C_A C_F T_F N_f - 316 C_A T_F^2 N_f^2 \right. \\
&\quad \left. - 108 C_F^2 T_F N_f - 264 C_F T_F^2 N_f^2 \right] \frac{a^4}{54} \; + \; \mathcal{O}(a^5) \qquad (4.3.17)
\end{aligned}
$$

which agrees with (3.4.56) since the $\overline{\rm MS}$ β-function is gauge independent to all known loop orders. Using (3.3.29) and (3.4.55) we construct the renormalization group equations for the MOMi schemes at three loops. For the MOMh scheme, the renormalization group functions are

$$
\begin{aligned}
\beta^{\rm MOMh}(a,\alpha) &= \left[-11 C_A + 4 N_f T_F \right] \frac{a^2}{3} \\
&+ \left[18 \psi'\left(\tfrac{1}{3}\right) \alpha^2 C_A^2 - 156 \psi'\left(\tfrac{1}{3}\right) \alpha C_A^2 + 96 \psi'\left(\tfrac{1}{3}\right) \alpha C_A N_f T_F \right. \\
&\quad -81 \alpha^3 C_A^2 - 12 \alpha^2 C_A^2 \pi^2 + 540 \alpha^2 C_A^2 - 432 \alpha^2 C_A N_f T_F \\
&\quad +104 \alpha C_A^2 \pi^2 + 1404 \alpha C_A^2 - 64 \alpha C_A N_f \pi^2 T_F - 864 \alpha C_A N_f T_F \\
&\quad \left. -7344 C_A^2 + 4320 C_A N_f T_F + 2592 C_F N_f T_F \right] \frac{a^3}{648} \\
&+ \Big[-3078 \sqrt{3} \ln(3)^2 \alpha^3 C_A^3 \pi + 5481 \sqrt{3} \ln(3)^2 \alpha^2 C_A^3 \pi
\end{aligned}
$$

$$
\begin{aligned}
&-8208\sqrt{3}\ln(3)^2\alpha^2C_A^2N_f\pi T_F + 8262\sqrt{3}\ln(3)^2\alpha C_A^3\pi \\
&+329076\sqrt{3}\ln(3)^2C_A^3\pi - 271728\sqrt{3}\ln(3)^2C_A^2N_f\pi T_F \\
&+55296\sqrt{3}\ln(3)^2C_AN_f^2\pi T_F^2 + 36936\sqrt{3}\ln(3)\alpha^3C_A^3\pi \\
&-65772\sqrt{3}\ln(3)\alpha^2C_A^3\pi + 98496\sqrt{3}\ln(3)\alpha^2C_A^2N_f\pi T_F \\
&-99144\sqrt{3}\ln(3)\alpha C_A^3\pi - 3948912\sqrt{3}\ln(3)C_A^3\pi \\
&+3260736\sqrt{3}\ln(3)C_A^2N_f\pi T_F - 663552\sqrt{3}\ln(3)C_AN_f^2\pi T_F^2 \\
&+3306\sqrt{3}\alpha^3C_A^3\pi^3 - 5887\sqrt{3}\alpha^2C_A^3\pi^3 + 8816\sqrt{3}\alpha^2C_A^2N_f\pi^3T_F \\
&-8874\sqrt{3}\alpha C_A^3\pi^3 - 353452\sqrt{3}C_A^3\pi^3 + 291856\sqrt{3}C_A^2N_f\pi^3T_F \\
&-59392\sqrt{3}C_AN_f^2\pi^3T_F^2 + 4320\psi'\left(\tfrac{1}{3}\right)^2\alpha^3C_A^3 \\
&-29232\psi'\left(\tfrac{1}{3}\right)^2\alpha^2C_A^3 + 16128\psi'\left(\tfrac{1}{3}\right)^2\alpha^2C_A^2N_fT_F \\
&-1440\psi'\left(\tfrac{1}{3}\right)^2\alpha C_A^3 - 23040\psi'\left(\tfrac{1}{3}\right)^2\alpha C_A^2N_fT_F \\
&+118800\psi'\left(\tfrac{1}{3}\right)^2C_A^3 - 43200\psi'\left(\tfrac{1}{3}\right)^2C_A^2N_fT_F \\
&-3888\psi'\left(\tfrac{1}{3}\right)\alpha^4C_A^3 - 5760\psi'\left(\tfrac{1}{3}\right)\alpha^3C_A^3\pi^2 \\
&-175608\psi'\left(\tfrac{1}{3}\right)\alpha^3C_A^3 - 41472\psi'\left(\tfrac{1}{3}\right)\alpha^3C_A^2N_fT_F \\
&+38976\psi'\left(\tfrac{1}{3}\right)\alpha^2C_A^3\pi^2 + 324648\psi'\left(\tfrac{1}{3}\right)\alpha^2C_A^3 \\
&-21504\psi'\left(\tfrac{1}{3}\right)\alpha^2C_A^2N_f\pi^2T_F - 668736\psi'\left(\tfrac{1}{3}\right)\alpha^2C_A^2N_fT_F \\
&+1920\psi'\left(\tfrac{1}{3}\right)\alpha C_A^3\pi^2 - 1564272\psi'\left(\tfrac{1}{3}\right)\alpha C_A^3 \\
&+30720\psi'\left(\tfrac{1}{3}\right)\alpha C_A^2N_f\pi^2T_F + 974592\psi'\left(\tfrac{1}{3}\right)\alpha C_A^2N_fT_F \\
&+497664\psi'\left(\tfrac{1}{3}\right)\alpha C_AC_FN_fT_F - 158400\psi'\left(\tfrac{1}{3}\right)C_A^3\pi^2 \\
&+23317632\psi'\left(\tfrac{1}{3}\right)C_A^3 + 57600\psi'\left(\tfrac{1}{3}\right)C_A^2N_f\pi^2T_F \\
&-20507904\psi'\left(\tfrac{1}{3}\right)C_A^2N_fT_F - 622080\psi'\left(\tfrac{1}{3}\right)C_AC_FN_fT_F \\
&+4230144\psi'\left(\tfrac{1}{3}\right)C_AN_f^2T_F^2 - 324\psi'''\left(\tfrac{1}{3}\right)\alpha^3C_A^3 \\
&+2457\psi'''\left(\tfrac{1}{3}\right)\alpha^2C_A^3 - 864\psi'''\left(\tfrac{1}{3}\right)\alpha^2C_A^2N_fT_F \\
&+12150\psi'''\left(\tfrac{1}{3}\right)\alpha C_A^3 + 131868\psi'''\left(\tfrac{1}{3}\right)C_A^3 \\
&-47952\psi'''\left(\tfrac{1}{3}\right)C_A^2N_fT_F - 1329696s_2\left(\tfrac{\pi}{6}\right)\alpha^3C_A^3 \\
&+2367792s_2\left(\tfrac{\pi}{6}\right)\alpha^2C_A^3 - 3545856s_2\left(\tfrac{\pi}{6}\right)\alpha^2C_A^2N_fT_F \\
&+3569184s_2\left(\tfrac{\pi}{6}\right)\alpha C_A^3 + 142160832s_2\left(\tfrac{\pi}{6}\right)C_A^3 \\
&-117386496s_2\left(\tfrac{\pi}{6}\right)C_A^2N_fT_F + 23887872s_2\left(\tfrac{\pi}{6}\right)C_AN_f^2T_F^2 \\
&+2659392s_2\left(\tfrac{\pi}{2}\right)\alpha^3C_A^3 - 4735584s_2\left(\tfrac{\pi}{2}\right)\alpha^2C_A^3 \\
&+7091712s_2\left(\tfrac{\pi}{2}\right)\alpha^2C_A^2N_fT_F - 7138368s_2\left(\tfrac{\pi}{2}\right)\alpha C_A^3 \\
&-284321664s_2\left(\tfrac{\pi}{2}\right)C_A^3 + 234772992s_2\left(\tfrac{\pi}{2}\right)C_A^2N_fT_F \\
&-47775744s_2\left(\tfrac{\pi}{2}\right)C_AN_f^2T_F^2 + 2216160s_3\left(\tfrac{\pi}{6}\right)\alpha^3C_A^3
\end{aligned}
$$

$$
\begin{aligned}
&-3946320 s_3\left(\tfrac{\pi}{6}\right) \alpha^2 C_A^3 + 5909760 s_3\left(\tfrac{\pi}{6}\right) \alpha^2 C_A^2 N_f T_F \\
&-5948640 s_3\left(\tfrac{\pi}{6}\right) \alpha C_A^3 - 236934720 s_3\left(\tfrac{\pi}{6}\right) C_A^3 \\
&+195644160 s_3\left(\tfrac{\pi}{6}\right) C_A^2 N_f T_F - 39813120 s_3\left(\tfrac{\pi}{6}\right) C_A N_f^2 T_F^2 \\
&-1772928 s_3\left(\tfrac{\pi}{2}\right) \alpha^3 C_A^3 + 3157056 s_3\left(\tfrac{\pi}{2}\right) \alpha^2 C_A^3 \\
&-4727808 s_3\left(\tfrac{\pi}{2}\right) \alpha^2 C_A^2 N_f T_F + 4758912 s_3\left(\tfrac{\pi}{2}\right) \alpha C_A^3 \\
&+189547776 s_3\left(\tfrac{\pi}{2}\right) C_A^3 - 156515328 s_3\left(\tfrac{\pi}{2}\right) C_A^2 N_f T_F \\
&+31850496 s_3\left(\tfrac{\pi}{2}\right) C_A N_f^2 T_F^2 + 2592 \alpha^4 C_A^3 \pi^2 - 137052 \alpha^4 C_A^3 \\
&+46656 \alpha^4 C_A^2 N_f T_F + 2784 \alpha^3 C_A^3 \pi^4 + 117072 \alpha^3 C_A^3 \pi^2 \\
&+81648 \alpha^3 C_A^3 \zeta_3 + 361584 \alpha^3 C_A^3 + 27648 \alpha^3 C_A^2 N_f \pi^2 T_F \\
&-93312 \alpha^3 C_A^2 N_f T_F - 19544 \alpha^2 C_A^3 \pi^4 - 216432 \alpha^2 C_A^3 \pi^2 \\
&-234252 \alpha^2 C_A^3 \zeta_3 + 1880820 \alpha^2 C_A^3 + 9472 \alpha^2 C_A^2 N_f \pi^4 T_F \\
&+445824 \alpha^2 C_A^2 N_f \pi^2 T_F + 217728 \alpha^2 C_A^2 N_f T_F \zeta_3 \\
&-1119744 \alpha^2 C_A^2 N_f T_F - 1679616 \alpha^2 C_A C_F N_f T_F \\
&-33040 \alpha C_A^3 \pi^4 + 1042848 \alpha C_A^3 \pi^2 - 752328 \alpha C_A^3 \zeta_3 \\
&+6689304 \alpha C_A^3 - 10240 \alpha C_A^2 N_f \pi^4 T_F \\
&-649728 \alpha C_A^2 N_f \pi^2 T_F - 5225472 \alpha C_A^2 N_f T_F \\
&-331776 \alpha C_A C_F N_f \pi^2 T_F - 4478976 \alpha C_A C_F N_f T_F \\
&-298848 C_A^3 \pi^4 - 15545088 C_A^3 \pi^2 - 13172544 C_A^3 \zeta_3 \\
&-66970800 C_A^3 + 108672 C_A^2 N_f \pi^4 T_F + 13671936 C_A^2 N_f \pi^2 T_F \\
&+32161536 C_A^2 N_f T_F \zeta_3 + 55349568 C_A^2 N_f T_F \\
&+414720 C_A C_F N_f \pi^2 T_F - 32845824 C_A C_F N_f T_F \zeta_3 \\
&+36516096 C_A C_F N_f T_F - 2820096 C_A N_f^2 \pi^2 T_F^2 \\
&-9953280 C_A N_f^2 T_F^2 \zeta_3 - 7838208 C_A N_f^2 T_F^2 \\
&-1119744 C_F^2 N_f T_F + 11943936 C_F N_f^2 T_F^2 \zeta_3 \\
&-11446272 C_F N_f^2 T_F^2 \big] \frac{a^4}{559872} \; + \; \mathcal{O}(a^5)
\end{aligned}
$$

$$
\begin{aligned}
\gamma_A^{\rm MOMh}(a,\alpha) \;=\; & \left[3\alpha C_A - 13 C_A + 8 N_f T_F\right] \frac{a}{6} \\
& + \big[36 \psi'\left(\tfrac{1}{3}\right) \alpha^2 C_A^2 - 246 \psi'\left(\tfrac{1}{3}\right) \alpha C_A^2 + 96 \psi'\left(\tfrac{1}{3}\right) \alpha C_A N_f T_F \\
&+390 \psi'\left(\tfrac{1}{3}\right) C_A^2 - 240 \psi'\left(\tfrac{1}{3}\right) C_A N_f T_F - 81 \alpha^3 C_A^2 - 24 \alpha^2 C_A^2 \pi^2 \\
&+459 \alpha^2 C_A^2 - 432 \alpha^2 C_A N_f T_F + 164 \alpha C_A^2 \pi^2 + 675 \alpha C_A^2 \\
&-64 \alpha C_A N_f \pi^2 T_F - 864 \alpha C_A N_f T_F - 260 C_A^2 \pi^2 - 2484 C_A^2 \\
&+160 C_A N_f \pi^2 T_F + 2376 C_A N_f T_F + 2592 C_F N_f T_F \big] \frac{a^2}{648}
\end{aligned}
$$

$$
\begin{aligned}
&+\Big[-1539\sqrt{3}\ln(3)^2\alpha^3C_A^3\pi+8046\sqrt{3}\ln(3)^2\alpha^2C_A^3\pi\\
&-4104\sqrt{3}\ln(3)^2\alpha^2C_A^2N_f\pi T_F+16470\sqrt{3}\ln(3)^2\alpha C_A^3\pi\\
&-6696\sqrt{3}\ln(3)^2\alpha C_A^2N_f\pi T_F-97227\sqrt{3}\ln(3)^2C_A^3\pi\\
&+104760\sqrt{3}\ln(3)^2C_A^2N_f\pi T_F-27648\sqrt{3}\ln(3)^2C_AN_f^2\pi T_F^2\\
&+18468\sqrt{3}\ln(3)\alpha^3C_A^3\pi-96552\sqrt{3}\ln(3)\alpha^2C_A^3\pi\\
&+49248\sqrt{3}\ln(3)\alpha^2C_A^2N_f\pi T_F-197640\sqrt{3}\ln(3)\alpha C_A^3\pi\\
&+80352\sqrt{3}\ln(3)\alpha C_A^2N_f\pi T_F+1166724\sqrt{3}\ln(3)C_A^3\pi\\
&-1257120\sqrt{3}\ln(3)C_A^2N_f\pi T_F+331776\sqrt{3}\ln(3)C_AN_f^2\pi T_F^2\\
&+1653\sqrt{3}\alpha^3C_A^3\pi^3-8642\sqrt{3}\alpha^2C_A^3\pi^3+4408\sqrt{3}\alpha^2C_A^2N_f\pi^3T_F\\
&-17690\sqrt{3}\alpha C_A^3\pi^3+7192\sqrt{3}\alpha C_A^2N_f\pi^3T_F+104429\sqrt{3}C_A^3\pi^3\\
&-112520\sqrt{3}C_A^2N_f\pi^3T_F+29696\sqrt{3}C_AN_f^2\pi^3T_F^2\\
&+3024\psi'\left(\tfrac{1}{3}\right)^2\alpha^3C_A^3-28224\psi'\left(\tfrac{1}{3}\right)^2\alpha^2C_A^3\\
&+8064\psi'\left(\tfrac{1}{3}\right)^2\alpha^2C_A^2N_fT_F+84420\psi'\left(\tfrac{1}{3}\right)^2\alpha C_A^3\\
&-40320\psi'\left(\tfrac{1}{3}\right)^2\alpha C_A^2N_fT_F-81900\psi'\left(\tfrac{1}{3}\right)^2C_A^3\\
&+50400\psi'\left(\tfrac{1}{3}\right)^2C_A^2N_fT_F-3888\psi'\left(\tfrac{1}{3}\right)\alpha^4C_A^3\\
&-4032\psi'\left(\tfrac{1}{3}\right)\alpha^3C_A^3\pi^2-70956\psi'\left(\tfrac{1}{3}\right)\alpha^3C_A^3\\
&-31104\psi'\left(\tfrac{1}{3}\right)\alpha^3C_A^2N_fT_F+37632\psi'\left(\tfrac{1}{3}\right)\alpha^2C_A^3\pi^2\\
&+416988\psi'\left(\tfrac{1}{3}\right)\alpha^2C_A^3-10752\psi'\left(\tfrac{1}{3}\right)\alpha^2C_A^2N_f\pi^2T_F\\
&-272160\psi'\left(\tfrac{1}{3}\right)\alpha^2C_A^2N_fT_F-112560\psi'\left(\tfrac{1}{3}\right)\alpha C_A^3\pi^2\\
&+1274184\psi'\left(\tfrac{1}{3}\right)\alpha C_A^3+53760\psi'\left(\tfrac{1}{3}\right)\alpha C_A^2N_f\pi^2T_F\\
&-573696\psi'\left(\tfrac{1}{3}\right)\alpha C_A^2N_fT_F+248832\psi'\left(\tfrac{1}{3}\right)\alpha C_AC_FN_fT_F\\
&+55296\psi'\left(\tfrac{1}{3}\right)\alpha C_AN_f^2T_F^2+109200\psi'\left(\tfrac{1}{3}\right)C_A^3\pi^2\\
&-5772384\psi'\left(\tfrac{1}{3}\right)C_A^3-67200\psi'\left(\tfrac{1}{3}\right)C_A^2N_f\pi^2T_F\\
&+6785856\psi'\left(\tfrac{1}{3}\right)C_A^2N_fT_F-622080\psi'\left(\tfrac{1}{3}\right)C_AC_FN_fT_F\\
&-2115072\psi'\left(\tfrac{1}{3}\right)C_AN_f^2T_F^2-162\psi'''\left(\tfrac{1}{3}\right)\alpha^3C_A^3\\
&+2727\psi'''\left(\tfrac{1}{3}\right)\alpha^2C_A^3-432\psi'''\left(\tfrac{1}{3}\right)\alpha^2C_A^2N_fT_F\\
&+216\psi'''\left(\tfrac{1}{3}\right)\alpha C_A^3+5400\psi'''\left(\tfrac{1}{3}\right)\alpha C_A^2N_fT_F-38961\psi'''\left(\tfrac{1}{3}\right)C_A^3\\
&+23976\psi'''\left(\tfrac{1}{3}\right)C_A^2N_fT_F-664848s_2\left(\tfrac{\pi}{6}\right)\alpha^3C_A^3\\
&+3475872s_2\left(\tfrac{\pi}{6}\right)\alpha^2C_A^3-1772928s_2\left(\tfrac{\pi}{6}\right)\alpha^2C_A^2N_fT_F\\
&+7115040s_2\left(\tfrac{\pi}{6}\right)\alpha C_A^3-2892672s_2\left(\tfrac{\pi}{6}\right)\alpha C_A^2N_fT_F\\
&-42002064s_2\left(\tfrac{\pi}{6}\right)C_A^3+45256320s_2\left(\tfrac{\pi}{6}\right)C_A^2N_fT_F\\
&-11943936s_2\left(\tfrac{\pi}{6}\right)C_AN_f^2T_F^2+1329696s_2\left(\tfrac{\pi}{2}\right)\alpha^3C_A^3
\end{aligned}
$$

$$
\begin{aligned}
&-6951744 s_2\left(\tfrac{\pi}{2}\right) \alpha^2 C_A^3 + 3545856 s_2\left(\tfrac{\pi}{2}\right) \alpha^2 C_A^2 N_f T_F \\
&-14230080 s_2\left(\tfrac{\pi}{2}\right) \alpha C_A^3 + 5785344 s_2\left(\tfrac{\pi}{2}\right) \alpha C_A^2 N_f T_F \\
&+84004128 s_2\left(\tfrac{\pi}{2}\right) C_A^3 - 90512640 s_2\left(\tfrac{\pi}{2}\right) C_A^2 N_f T_F \\
&+23887872 s_2\left(\tfrac{\pi}{2}\right) C_A N_f^2 T_F^2 + 1108080 s_3\left(\tfrac{\pi}{6}\right) \alpha^3 C_A^3 \\
&-5793120 s_3\left(\tfrac{\pi}{6}\right) \alpha^2 C_A^3 + 2954880 s_3\left(\tfrac{\pi}{6}\right) \alpha^2 C_A^2 N_f T_F \\
&-11858400 s_3\left(\tfrac{\pi}{6}\right) \alpha C_A^3 + 4821120 s_3\left(\tfrac{\pi}{6}\right) \alpha C_A^2 N_f T_F \\
&+70003440 s_3\left(\tfrac{\pi}{6}\right) C_A^3 - 75427200 s_3\left(\tfrac{\pi}{6}\right) C_A^2 N_f T_F \\
&+19906560 s_3\left(\tfrac{\pi}{6}\right) C_A N_f^2 T_F^2 - 886464 s_3\left(\tfrac{\pi}{2}\right) \alpha^3 C_A^3 \\
&+4634496 s_3\left(\tfrac{\pi}{2}\right) \alpha^2 C_A^3 - 2363904 s_3\left(\tfrac{\pi}{2}\right) \alpha^2 C_A^2 N_f T_F \\
&+9486720 s_3\left(\tfrac{\pi}{2}\right) \alpha C_A^3 - 3856896 s_3\left(\tfrac{\pi}{2}\right) \alpha C_A^2 N_f T_F \\
&-56002752 s_3\left(\tfrac{\pi}{2}\right) C_A^3 + 60341760 s_3\left(\tfrac{\pi}{2}\right) C_A^2 N_f T_F \\
&-15925248 s_3\left(\tfrac{\pi}{2}\right) C_A N_f^2 T_F^2 + 2592 \alpha^4 C_A^3 \pi^2 - 59778 \alpha^4 C_A^3 \\
&+23328 \alpha^4 C_A^2 N_f T_F + 1776 \alpha^3 C_A^3 \pi^4 + 47304 \alpha^3 C_A^3 \pi^2 \\
&+40824 \alpha^3 C_A^3 \zeta_3 + 209952 \alpha^3 C_A^3 + 20736 \alpha^3 C_A^2 N_f \pi^2 T_F \\
&-19816 \alpha^2 C_A^3 \pi^4 - 277992 \alpha^2 C_A^3 \pi^2 - 319788 \alpha^2 C_A^3 \zeta_3 \\
&-227448 \alpha^2 C_A^3 + 4736 \alpha^2 C_A^2 N_f \pi^4 T_F + 181440 \alpha^2 C_A^2 N_f \pi^2 T_F \\
&+108864 \alpha^2 C_A^2 N_f T_F \zeta_3 - 93312 \alpha^2 C_A^2 N_f T_F \\
&-839808 \alpha^2 C_A C_F N_f T_F + 36944 \alpha C_A^3 \pi^4 - 849456 \alpha C_A^3 \pi^2 \\
&-3457404 \alpha C_A^3 \zeta_3 + 2994732 \alpha C_A^3 \\
&-32320 \alpha C_A^2 N_f \pi^4 T_F + 382464 \alpha C_A^2 N_f \pi^2 T_F \\
&+1158624 \alpha C_A^2 N_f T_F \zeta_3 - 2947104 \alpha C_A^2 N_f T_F \\
&-165888 \alpha C_A C_F N_f \pi^2 T_F - 2239488 \alpha C_A C_F N_f T_F \\
&-36864 \alpha C_A N_f^2 \pi^2 T_F^2 + 248832 \alpha C_A N_f^2 T_F^2 + 67496 C_A^3 \pi^4 \\
&+3848256 C_A^3 \pi^2 + 10207944 C_A^3 \zeta_3 - 17386164 C_A^3 \\
&-41536 C_A^2 N_f \pi^4 T_F - 4523904 C_A^2 N_f \pi^2 T_F \\
&-1337472 C_A^2 N_f T_F \zeta_3 + 17153856 C_A^2 N_f T_F \\
&+414720 C_A C_F N_f \pi^2 T_F - 16422912 C_A C_F N_f T_F \zeta_3 \\
&+15738624 C_A C_F N_f T_F + 1410048 C_A N_f^2 \pi^2 T_F^2 \\
&-995328 C_A N_f^2 T_F^2 \zeta_3 - 2799360 C_A N_f^2 T_F^2 - 559872 C_F^2 N_f T_F \\
&+5971968 C_F N_f^2 T_F^2 \zeta_3 - 5723136 C_F N_f^2 T_F^2 \Big] \frac{a^3}{279936} \; + \; \mathcal{O}(a^4)
\end{aligned}
$$

$$
\gamma_\alpha^{\rm MOMh}(a,\alpha) \;=\; \left[-3\alpha C_A + 26 C_A - 16 N_f T_F\right] \frac{a}{12}
$$

$$
\begin{aligned}
&+\left[-36\psi'\left(\tfrac{1}{3}\right)\alpha^2C_A^2+402\psi'\left(\tfrac{1}{3}\right)\alpha C_A^2-192\psi'\left(\tfrac{1}{3}\right)\alpha C_AN_fT_F\right.\\
&-780\psi'\left(\tfrac{1}{3}\right)C_A^2+480\psi'\left(\tfrac{1}{3}\right)C_AN_fT_F+162\alpha^3C_A^2+24\alpha^2C_A^2\pi^2\\
&-675\alpha^2C_A^2+864\alpha^2C_AN_fT_F-268\alpha C_A^2\pi^2-1107\alpha C_A^2\\
&+128\alpha C_AN_f\pi^2T_F+1728\alpha C_AN_fT_F+520C_A^2\pi^2+4968C_A^2\\
&\left.-320C_AN_f\pi^2T_F-4752C_AN_fT_F-5184C_FN_fT_F\right]\frac{a^2}{1296}\\
&+\Big[1539\sqrt{3}\ln(3)^2\alpha^3C_A^3\pi-14715\sqrt{3}\ln(3)^2\alpha^2C_A^3\pi\\
&+8208\sqrt{3}\ln(3)^2\alpha^2C_A^2N_f\pi T_F-10503\sqrt{3}\ln(3)^2\alpha C_A^3\pi\\
&+3024\sqrt{3}\ln(3)^2\alpha C_A^2N_f\pi T_F+194454\sqrt{3}\ln(3)^2C_A^3\pi\\
&-209520\sqrt{3}\ln(3)^2C_A^2N_f\pi T_F+55296\sqrt{3}\ln(3)^2C_AN_f^2\pi T_F^2\\
&-18468\sqrt{3}\ln(3)\alpha^3C_A^3\pi+176580\sqrt{3}\ln(3)\alpha^2C_A^3\pi\\
&-98496\sqrt{3}\ln(3)\alpha^2C_A^2N_f\pi T_F+126036\sqrt{3}\ln(3)\alpha C_A^3\pi\\
&-36288\sqrt{3}\ln(3)\alpha C_A^2N_f\pi T_F-2333448\sqrt{3}\ln(3)C_A^3\pi\\
&+2514240\sqrt{3}\ln(3)C_A^2N_f\pi T_F-663552\sqrt{3}\ln(3)C_AN_f^2\pi T_F^2\\
&-1653\sqrt{3}\alpha^3C_A^3\pi^3+15805\sqrt{3}\alpha^2C_A^3\pi^3\\
&-8816\sqrt{3}\alpha^2C_A^2N_f\pi^3T_F+11281\sqrt{3}\alpha C_A^3\pi^3\\
&-3248\sqrt{3}\alpha C_A^2N_f\pi^3T_F-208858\sqrt{3}C_A^3\pi^3\\
&+225040\sqrt{3}C_A^2N_f\pi^3T_F-59392\sqrt{3}C_AN_f^2\pi^3T_F^2\\
&-3024\psi'\left(\tfrac{1}{3}\right)^2\alpha^3C_A^3+41328\psi'\left(\tfrac{1}{3}\right)^2\alpha^2C_A^3\\
&-16128\psi'\left(\tfrac{1}{3}\right)^2\alpha^2C_A^2N_fT_F-149940\psi'\left(\tfrac{1}{3}\right)^2\alpha C_A^3\\
&+80640\psi'\left(\tfrac{1}{3}\right)^2\alpha C_A^2N_fT_F+163800\psi'\left(\tfrac{1}{3}\right)^2C_A^3\\
&-100800\psi'\left(\tfrac{1}{3}\right)^2C_A^2N_fT_F+11664\psi'\left(\tfrac{1}{3}\right)\alpha^4C_A^3\\
&+4032\psi'\left(\tfrac{1}{3}\right)\alpha^3C_A^3\pi^2+47628\psi'\left(\tfrac{1}{3}\right)\alpha^3C_A^3\\
&+62208\psi'\left(\tfrac{1}{3}\right)\alpha^3C_A^2N_fT_F-55104\psi'\left(\tfrac{1}{3}\right)\alpha^2C_A^3\pi^2\\
&-916272\psi'\left(\tfrac{1}{3}\right)\alpha^2C_A^3+21504\psi'\left(\tfrac{1}{3}\right)\alpha^2C_A^2N_f\pi^2T_F\\
&+565056\psi'\left(\tfrac{1}{3}\right)\alpha^2C_A^2N_fT_F+199920\psi'\left(\tfrac{1}{3}\right)\alpha C_A^3\pi^2\\
&-1137024\psi'\left(\tfrac{1}{3}\right)\alpha C_A^3-107520\psi'\left(\tfrac{1}{3}\right)\alpha C_A^2N_f\pi^2T_F\\
&+354240\psi'\left(\tfrac{1}{3}\right)\alpha C_A^2N_fT_F-497664\psi'\left(\tfrac{1}{3}\right)\alpha C_AC_FN_fT_F\\
&-110592\psi'\left(\tfrac{1}{3}\right)\alpha C_AN_f^2T_F^2-218400\psi'\left(\tfrac{1}{3}\right)C_A^3\pi^2\\
&+11544768\psi'\left(\tfrac{1}{3}\right)C_A^3+134400\psi'\left(\tfrac{1}{3}\right)C_A^2N_f\pi^2T_F\\
&-13571712\psi'\left(\tfrac{1}{3}\right)C_A^2N_fT_F+1244160\psi'\left(\tfrac{1}{3}\right)C_AC_FN_fT_F\\
&+4230144\psi'\left(\tfrac{1}{3}\right)C_AN_f^2T_F^2+162\psi'''\left(\tfrac{1}{3}\right)\alpha^3C_A^3
\end{aligned}
$$

$$
\begin{aligned}
&-3429\psi'''\left(\tfrac{1}{3}\right)\alpha^2C_A^3+864\psi'''\left(\tfrac{1}{3}\right)\alpha^2C_A^2N_fT_F\\
&+8559\psi'''\left(\tfrac{1}{3}\right)\alpha C_A^3-10800\psi'''\left(\tfrac{1}{3}\right)\alpha C_A^2N_fT_F\\
&+77922\psi'''\left(\tfrac{1}{3}\right)C_A^3-47952\psi'''\left(\tfrac{1}{3}\right)C_A^2N_fT_F\\
&+664848s_2\left(\tfrac{\pi}{6}\right)\alpha^3C_A^3-6356880s_2\left(\tfrac{\pi}{6}\right)\alpha^2C_A^3\\
&+3545856s_2\left(\tfrac{\pi}{6}\right)\alpha^2C_A^2N_fT_F-4537296s_2\left(\tfrac{\pi}{6}\right)\alpha C_A^3\\
&+1306368s_2\left(\tfrac{\pi}{6}\right)\alpha C_A^2N_fT_F+84004128s_2\left(\tfrac{\pi}{6}\right)C_A^3\\
&-90512640s_2\left(\tfrac{\pi}{6}\right)C_A^2N_fT_F+23887872s_2\left(\tfrac{\pi}{6}\right)C_AN_f^2T_F^2\\
&-1329696s_2\left(\tfrac{\pi}{2}\right)\alpha^3C_A^3+12713760s_2\left(\tfrac{\pi}{2}\right)\alpha^2C_A^3\\
&-7091712s_2\left(\tfrac{\pi}{2}\right)\alpha^2C_A^2N_fT_F+9074592s_2\left(\tfrac{\pi}{2}\right)\alpha C_A^3\\
&-2612736s_2\left(\tfrac{\pi}{2}\right)\alpha C_A^2N_fT_F-168008256s_2\left(\tfrac{\pi}{2}\right)C_A^3\\
&+181025280s_2\left(\tfrac{\pi}{2}\right)C_A^2N_fT_F-47775744s_2\left(\tfrac{\pi}{2}\right)C_AN_f^2T_F^2\\
&-1108080s_3\left(\tfrac{\pi}{6}\right)\alpha^3C_A^3+10594800s_3\left(\tfrac{\pi}{6}\right)\alpha^2C_A^3\\
&-5909760s_3\left(\tfrac{\pi}{6}\right)\alpha^2C_A^2N_fT_F+7562160s_3\left(\tfrac{\pi}{6}\right)\alpha C_A^3\\
&-2177280s_3\left(\tfrac{\pi}{6}\right)\alpha C_A^2N_fT_F-140006880s_3\left(\tfrac{\pi}{6}\right)C_A^3\\
&+150854400s_3\left(\tfrac{\pi}{6}\right)C_A^2N_fT_F-39813120s_3\left(\tfrac{\pi}{6}\right)C_AN_f^2T_F^2\\
&+886464s_3\left(\tfrac{\pi}{2}\right)\alpha^3C_A^3-8475840s_3\left(\tfrac{\pi}{2}\right)\alpha^2C_A^3\\
&+4727808s_3\left(\tfrac{\pi}{2}\right)\alpha^2C_A^2N_fT_F-6049728s_3\left(\tfrac{\pi}{2}\right)\alpha C_A^3\\
&+1741824s_3\left(\tfrac{\pi}{2}\right)\alpha C_A^2N_fT_F+112005504s_3\left(\tfrac{\pi}{2}\right)C_A^3\\
&-120683520s_3\left(\tfrac{\pi}{2}\right)C_A^2N_fT_F+31850496s_3\left(\tfrac{\pi}{2}\right)C_AN_f^2T_F^2\\
&-7776\alpha^4C_A^3\pi^2+102060\alpha^4C_A^3-46656\alpha^4C_A^2N_fT_F\\
&-1776\alpha^3C_A^3\pi^4-31752\alpha^3C_A^3\pi^2-23328\alpha^3C_A^3\zeta_3\\
&-294516\alpha^3C_A^3-41472\alpha^3C_A^2N_f\pi^2T_F+27512\alpha^2C_A^3\pi^4\\
&+610848\alpha^2C_A^3\pi^2+689148\alpha^2C_A^3\zeta_3+174960\alpha^2C_A^3\\
&-9472\alpha^2C_A^2N_f\pi^4T_F-376704\alpha^2C_A^2N_f\pi^2T_F\\
&-217728\alpha^2C_A^2N_fT_F\zeta_3+279936\alpha^2C_A^2N_fT_F\\
&+1679616\alpha^2C_AC_FN_fT_F-89464\alpha C_A^3\pi^4+758016\alpha C_A^3\pi^2\\
&+4512024\alpha C_A^3\zeta_3-4114476\alpha C_A^3+64640\alpha C_A^2N_f\pi^4T_F\\
&-236160\alpha C_A^2N_f\pi^2T_F-1290816\alpha C_A^2N_fT_F\zeta_3\\
&+5101056\alpha C_A^2N_fT_F+331776\alpha C_AC_FN_f\pi^2T_F\\
&+4478976\alpha C_AC_FN_fT_F+73728\alpha C_AN_f^2\pi^2T_F^2\\
&-497664\alpha C_AN_f^2T_F^2-134992C_A^3\pi^4-7696512C_A^3\pi^2\\
&-20415888C_A^3\zeta_3+34772328C_A^3+83072C_A^2N_f\pi^4T_F
\end{aligned}
$$

$$
\begin{aligned}
&+9047808C_A^2N_f\pi^2T_F + 2674944C_A^2N_fT_F\zeta_3 \\
&-34307712C_A^2N_fT_F - 829440C_AC_FN_f\pi^2T_F \\
&+32845824C_AC_FN_fT_F\zeta_3 - 31477248C_AC_FN_fT_F \\
&-2820096C_AN_f^2\pi^2T_F^2 + 1990656C_AN_f^2T_F^2\zeta_3 \\
&+5598720C_AN_f^2T_F^2 + 1119744C_F^2N_fT_F - 11943936C_FN_f^2T_F^2\zeta_3 \\
&+11446272C_FN_f^2T_F^2\big]\,\frac{a^3}{559872} \;+\; \mathcal{O}(a^4)
\end{aligned}
$$

$$
\begin{aligned}
\gamma_c^{\rm MOMh}(a,\alpha) \;=\;& C_A\,[\alpha-3]\,\frac{a}{4} \\
&+C_A\,\big[12\psi'\left(\tfrac{1}{3}\right)\alpha^2C_A - 66\psi'\left(\tfrac{1}{3}\right)\alpha C_A + 90\psi'\left(\tfrac{1}{3}\right)C_A - 8\alpha^2C_A\pi^2 \\
&\quad +108\alpha^2C_A + 44\alpha C_A\pi^2 - 81\alpha C_A - 60C_A\pi^2 - 432C_A \\
&\quad +216N_fT_F\big]\,\frac{a^2}{432} \\
&+C_A\,\Big[-513\sqrt{3}\ln(3)^2\alpha^3C_A^2\pi + 1998\sqrt{3}\ln(3)^2\alpha^2C_A^2\pi \\
&\quad +6102\sqrt{3}\ln(3)^2\alpha C_A^2\pi - 3456\sqrt{3}\ln(3)^2\alpha C_AN_f\pi T_F \\
&\quad -22437\sqrt{3}\ln(3)^2C_A^2\pi + 10368\sqrt{3}\ln(3)^2C_AN_f\pi T_F \\
&\quad +6156\sqrt{3}\ln(3)\alpha^3C_A^2\pi - 23976\sqrt{3}\ln(3)\alpha^2C_A^2\pi \\
&\quad -73224\sqrt{3}\ln(3)\alpha C_A^2\pi + 41472\sqrt{3}\ln(3)\alpha C_AN_f\pi T_F \\
&\quad +269244\sqrt{3}\ln(3)C_A^2\pi - 124416\sqrt{3}\ln(3)C_AN_f\pi T_F \\
&\quad +551\sqrt{3}\alpha^3C_A^2\pi^3 - 2146\sqrt{3}\alpha^2C_A^2\pi^3 - 6554\sqrt{3}\alpha C_A^2\pi^3 \\
&\quad +3712\sqrt{3}\alpha C_AN_f\pi^3T_F + 24099\sqrt{3}C_A^2\pi^3 \\
&\quad -11136\sqrt{3}C_AN_f\pi^3T_F + 1008\psi'\left(\tfrac{1}{3}\right)^2\alpha^3C_A^2 \\
&\quad -8064\psi'\left(\tfrac{1}{3}\right)^2\alpha^2C_A^2 + 21420\psi'\left(\tfrac{1}{3}\right)^2\alpha C_A^2 \\
&\quad -18900\psi'\left(\tfrac{1}{3}\right)^2C_A^2 + 1296\psi'\left(\tfrac{1}{3}\right)\alpha^4C_A^2 \\
&\quad -1344\psi'\left(\tfrac{1}{3}\right)\alpha^3C_A^2\pi^2 - 32724\psi'\left(\tfrac{1}{3}\right)\alpha^3C_A^2 \\
&\quad +10752\psi'\left(\tfrac{1}{3}\right)\alpha^2C_A^2\pi^2 + 68148\psi'\left(\tfrac{1}{3}\right)\alpha^2C_A^2 \\
&\quad +6912\psi'\left(\tfrac{1}{3}\right)\alpha^2C_AN_fT_F - 28560\psi'\left(\tfrac{1}{3}\right)\alpha C_A^2\pi^2 \\
&\quad +515160\psi'\left(\tfrac{1}{3}\right)\alpha C_A^2 - 264384\psi'\left(\tfrac{1}{3}\right)\alpha C_AN_fT_F \\
&\quad +25200\psi'\left(\tfrac{1}{3}\right)C_A^2\pi^2 - 1365984\psi'\left(\tfrac{1}{3}\right)C_A^2 \\
&\quad +741312\psi'\left(\tfrac{1}{3}\right)C_AN_fT_F - 54\psi'''\left(\tfrac{1}{3}\right)\alpha^3C_A^2 \\
&\quad +837\psi'''\left(\tfrac{1}{3}\right)\alpha^2C_A^2 + 972\psi'''\left(\tfrac{1}{3}\right)\alpha C_A^2 - 8991\psi'''\left(\tfrac{1}{3}\right)C_A^2 \\
&\quad -221616s_2\left(\tfrac{\pi}{6}\right)\alpha^3C_A^2 + 863136s_2\left(\tfrac{\pi}{6}\right)\alpha^2C_A^2 \\
&\quad +2636064s_2\left(\tfrac{\pi}{6}\right)\alpha C_A^2 - 1492992s_2\left(\tfrac{\pi}{6}\right)\alpha C_AN_fT_F \\
&\quad -9692784s_2\left(\tfrac{\pi}{6}\right)C_A^2 + 4478976s_2\left(\tfrac{\pi}{6}\right)C_AN_fT_F
\end{aligned}
$$

$$
\begin{aligned}
&+443232 s_2\left(\tfrac{\pi}{2}\right) \alpha^3 C_A^2 - 1726272 s_2\left(\tfrac{\pi}{2}\right) \alpha^2 C_A^2 \\
&-5272128 s_2\left(\tfrac{\pi}{2}\right) \alpha C_A^2 + 2985984 s_2\left(\tfrac{\pi}{2}\right) \alpha C_A N_f T_F \\
&+19385568 s_2\left(\tfrac{\pi}{2}\right) C_A^2 - 8957952 s_2\left(\tfrac{\pi}{2}\right) C_A N_f T_F \\
&+369360 s_3\left(\tfrac{\pi}{6}\right) \alpha^3 C_A^2 - 1438560 s_3\left(\tfrac{\pi}{6}\right) \alpha^2 C_A^2 \\
&-4393440 s_3\left(\tfrac{\pi}{6}\right) \alpha C_A^2 + 2488320 s_3\left(\tfrac{\pi}{6}\right) \alpha C_A N_f T_F \\
&+16154640 s_3\left(\tfrac{\pi}{6}\right) C_A^2 - 7464960 s_3\left(\tfrac{\pi}{6}\right) C_A N_f T_F \\
&-295488 s_3\left(\tfrac{\pi}{2}\right) \alpha^3 C_A^2 + 1150848 s_3\left(\tfrac{\pi}{2}\right) \alpha^2 C_A^2 \\
&+3514752 s_3\left(\tfrac{\pi}{2}\right) \alpha C_A^2 - 1990656 s_3\left(\tfrac{\pi}{2}\right) \alpha C_A N_f T_F \\
&-12923712 s_3\left(\tfrac{\pi}{2}\right) C_A^2 + 5971968 s_3\left(\tfrac{\pi}{2}\right) C_A N_f T_F \\
&-864 \alpha^4 C_A^2 \pi^2 - 5832 \alpha^4 C_A^2 + 592 \alpha^3 C_A^2 \pi^4 + 21816 \alpha^3 C_A^2 \pi^2 \\
&+19440 \alpha^3 C_A^2 \zeta_3 + 73872 \alpha^3 C_A^2 - 5816 \alpha^2 C_A^2 \pi^4 \\
&-45432 \alpha^2 C_A^2 \pi^2 - 24300 \alpha^2 C_A^2 \zeta_3 - 109350 \alpha^2 C_A^2 \\
&-4608 \alpha^2 C_A N_f \pi^2 T_F - 15552 \alpha^2 C_A N_f T_F + 6928 \alpha C_A^2 \pi^4 \\
&-343440 \alpha C_A^2 \pi^2 - 745524 \alpha C_A^2 \zeta_3 + 977832 \alpha C_A^2 \\
&+176256 \alpha C_A N_f \pi^2 T_F + 342144 \alpha C_A N_f T_F \zeta_3 \\
&-381024 \alpha C_A N_f T_F + 15576 C_A^2 \pi^4 + 910656 C_A^2 \pi^2 \\
&+2128680 C_A^2 \zeta_3 - 4079484 C_A^2 - 494208 C_A N_f \pi^2 T_F \\
&-653184 C_A N_f T_F \zeta_3 + 3367008 C_A N_f T_F + 279936 C_F N_f T_F \\
&-622080 N_f^2 T_F^2 \Big] \frac{a^3}{186624} \; + \; \mathcal{O}(a^4)
\end{aligned}
$$

$$
\begin{aligned}
\gamma_\psi^{\rm MOMh}(a,\alpha) \;=\; & \alpha C_F a + C_F \left[12 \psi'\left(\tfrac{1}{3}\right) \alpha^2 C_A - 30 \psi'\left(\tfrac{1}{3}\right) \alpha C_A - 8 \alpha^2 C_A \pi^2 \right. \\
& \left. +27 \alpha^2 C_A + 20 \alpha C_A \pi^2 + 675 C_A - 162 C_F \right. \\
& \left. -216 N_f T_F \right] \frac{a^2}{108} \\
& + C_F \left[-513 \sqrt{3} \ln(3)^2 \alpha^3 C_A^2 \pi + 459 \sqrt{3} \ln(3)^2 \alpha^2 C_A^2 \pi \right. \\
& +7479 \sqrt{3} \ln(3)^2 \alpha C_A^2 \pi - 3456 \sqrt{3} \ln(3)^2 \alpha C_A N_f \pi T_F \\
& +6156 \sqrt{3} \ln(3) \alpha^3 C_A^2 \pi - 5508 \sqrt{3} \ln(3) \alpha^2 C_A^2 \pi \\
& -89748 \sqrt{3} \ln(3) \alpha C_A^2 \pi + 41472 \sqrt{3} \ln(3) \alpha C_A N_f \pi T_F \\
& +551 \sqrt{3} \alpha^3 C_A^2 \pi^3 - 493 \sqrt{3} \alpha^2 C_A^2 \pi^3 - 8033 \sqrt{3} \alpha C_A^2 \pi^3 \\
& +3712 \sqrt{3} \alpha C_A N_f \pi^3 T_F + 1008 \psi'\left(\tfrac{1}{3}\right)^2 \alpha^3 C_A^2 \\
& -5040 \psi'\left(\tfrac{1}{3}\right)^2 \alpha^2 C_A^2 + 6300 \psi'\left(\tfrac{1}{3}\right)^2 \alpha C_A^2 + 1296 \psi'\left(\tfrac{1}{3}\right) \alpha^4 C_A^2 \\
& -1344 \psi'\left(\tfrac{1}{3}\right) \alpha^3 C_A^2 \pi^2 - 36612 \psi'\left(\tfrac{1}{3}\right) \alpha^3 C_A^2 \\
& +6720 \psi'\left(\tfrac{1}{3}\right) \alpha^2 C_A^2 \pi^2 - 22248 \psi'\left(\tfrac{1}{3}\right) \alpha^2 C_A^2
\end{aligned}
$$

$$
\begin{aligned}
&+6912\psi'\left(\tfrac{1}{3}\right)\alpha^2 C_A N_f T_F - 8400\psi'\left(\tfrac{1}{3}\right)\alpha C_A^2\pi^2 \\
&+554688\psi'\left(\tfrac{1}{3}\right)\alpha C_A^2 - 15552\psi'\left(\tfrac{1}{3}\right)\alpha C_A C_F \\
&-285120\psi'\left(\tfrac{1}{3}\right)\alpha C_A N_f T_F - 162000\psi'\left(\tfrac{1}{3}\right) C_A^2 \\
&+38880\psi'\left(\tfrac{1}{3}\right) C_A C_F + 51840\psi'\left(\tfrac{1}{3}\right) C_A N_f T_F \\
&-54\psi'''\left(\tfrac{1}{3}\right)\alpha^3 C_A^2 + 675\psi'''\left(\tfrac{1}{3}\right)\alpha^2 C_A^2 + 2997\psi'''\left(\tfrac{1}{3}\right)\alpha C_A^2 \\
&-221616 s_2\left(\tfrac{\pi}{6}\right)\alpha^3 C_A^2 + 198288 s_2\left(\tfrac{\pi}{6}\right)\alpha^2 C_A^2 \\
&+3230928 s_2\left(\tfrac{\pi}{6}\right)\alpha C_A^2 - 1492992 s_2\left(\tfrac{\pi}{6}\right)\alpha C_A N_f T_F \\
&+443232 s_2\left(\tfrac{\pi}{2}\right)\alpha^3 C_A^2 - 396576 s_2\left(\tfrac{\pi}{2}\right)\alpha^2 C_A^2 \\
&-6461856 s_2\left(\tfrac{\pi}{2}\right)\alpha C_A^2 + 2985984 s_2\left(\tfrac{\pi}{2}\right)\alpha C_A N_f T_F \\
&+369360 s_3\left(\tfrac{\pi}{6}\right)\alpha^3 C_A^2 - 330480 s_3\left(\tfrac{\pi}{6}\right)\alpha^2 C_A^2 \\
&-5384880 s_3\left(\tfrac{\pi}{6}\right)\alpha C_A^2 + 2488320 s_3\left(\tfrac{\pi}{6}\right)\alpha C_A N_f T_F \\
&-295488 s_3\left(\tfrac{\pi}{2}\right)\alpha^3 C_A^2 + 264384 s_3\left(\tfrac{\pi}{2}\right)\alpha^2 C_A^2 \\
&+4307904 s_3\left(\tfrac{\pi}{2}\right)\alpha C_A^2 - 1990656 s_3\left(\tfrac{\pi}{2}\right)\alpha C_A N_f T_F \\
&-864\alpha^4 C_A^2\pi^2 - 5832\alpha^4 C_A^2 + 592\alpha^3 C_A^2\pi^4 \\
&+24408\alpha^3 C_A^2\pi^2 + 19440\alpha^3 C_A^2\zeta_3 + 33048\alpha^3 C_A^2 \\
&-11664\alpha^3 C_A C_F - 4040\alpha^2 C_A^2\pi^4 + 14832\alpha^2 C_A^2\pi^2 \\
&-972\alpha^2 C_A^2\zeta_3 - 207036\alpha^2 C_A^2 - 34992\alpha^2 C_A C_F \\
&-4608\alpha^2 C_A N_f\pi^2 T_F + 77760\alpha^2 C_A N_f T_F - 5192\alpha C_A^2\pi^4 \\
&-369792\alpha C_A^2\pi^2 - 1127520\alpha C_A^2\zeta_3 - 44712\alpha C_A^2 \\
&+10368\alpha C_A C_F\pi^2 + 139968\alpha C_A C_F + 190080\alpha C_A N_f\pi^2 T_F \\
&+435456\alpha C_A N_f T_F\zeta_3 - 15552\alpha C_A N_f T_F + 108000 C_A^2\pi^2 \\
&-1428840 C_A^2\zeta_3 + 2860596 C_A^2 - 25920 C_A C_F\pi^2 \\
&+559872 C_A C_F\zeta_3 - 1014768 C_A C_F - 34560 C_A N_f\pi^2 T_F \\
&+373248 C_A N_f T_F\zeta_3 - 1508544 C_A N_f T_F + 69984 C_F^2 \\
&-93312 C_F N_f T_F + 124416 N_f^2 T_F^2\big]\,\frac{a^3}{46656} + \mathcal{O}(a^4)\;. \qquad (4.3.18)
\end{aligned}
$$

Note the α dependence in the β-function after one loop is consistent with what we observed in our earlier calculation for the arbitrary (linear) covariant gauge in chapter 3. This is consistent with all mass dependent renormalization schemes.

The method used in constructing the β-functions and anomalous dimensions for each MOMi scheme at three loops is preferred to the direct calculation. Constructing the renormalization group functions using (3.3.29) and (3.4.55) relies

on performing only a direct two loop calculation, using the two loop MOM results and existing three loop $\overline{\rm MS}$ results from [104]. This is much faster, and therefore a preferred method over a direct three loop calculation, since the three loop master integrals are not known.

4.4 MOMg scheme.

Having recorded the results for the ghost-gluon vertex at length we briefly present the results for the triple-gluon vertex in numerical form for $SU(3)$. We present the results in the same order as in section 4.3. The renormalization constants in the MOMg scheme are given below, where we present the coupling constant renormalization constant analytically as

$$
\begin{aligned}
Z_g^{(\rm ggg)}\Big|_{\rm MOMg} &= 1 + \Big[-36\psi'\left(\tfrac{1}{3}\right)\alpha^2 C_A + 162\psi'\left(\tfrac{1}{3}\right)\alpha C_A - 138\psi'\left(\tfrac{1}{3}\right) C_A \\
&\quad +384\psi'\left(\tfrac{1}{3}\right) N_f T_F - 27\alpha^3 C_A + 24\alpha^2 C_A\pi^2 + 162\alpha^2 C_A \\
&\quad -108\alpha C_A\pi^2 - 243\alpha C_A + 92 C_A\pi^2 - 2376 C_A - 256 N_f\pi^2 T_F \\
&\quad +864 N_f T_F + 108\left(-11 C_A + 4 N_f T_F\right)\frac{1}{\epsilon}\Big]\frac{a}{648} \\
&\quad + \Bigg[\left(121 C_A^2 - 88 C_A N_f T_F + 16 N_f^2 T_F^2\right)\frac{1}{24\epsilon^2} \\
&\quad + \Big(2592\sqrt{3}\psi'\left(\tfrac{1}{3}\right)^2\alpha^4 C_A^2 - 23328\sqrt{3}\psi'\left(\tfrac{1}{3}\right)^2\alpha^3 C_A^2 \\
&\quad +72360\sqrt{3}\psi'\left(\tfrac{1}{3}\right)^2\alpha^2 C_A^2 - 55296\sqrt{3}\psi'\left(\tfrac{1}{3}\right)^2\alpha^2 C_A N_f T_F \\
&\quad -89424\sqrt{3}\psi'\left(\tfrac{1}{3}\right)^2\alpha C_A^2 + 248832\sqrt{3}\psi'\left(\tfrac{1}{3}\right)^2\alpha C_A N_f T_F \\
&\quad +38088\sqrt{3}\psi'\left(\tfrac{1}{3}\right)^2 C_A^2 - 211968\sqrt{3}\psi'\left(\tfrac{1}{3}\right)^2 C_A N_f T_F \\
&\quad +294912\sqrt{3}\psi'\left(\tfrac{1}{3}\right)^2 N_f^2 T_F^2 + 3888\sqrt{3}\psi'\left(\tfrac{1}{3}\right)\alpha^5 C_A^2 \\
&\quad -3456\sqrt{3}\psi'\left(\tfrac{1}{3}\right)\alpha^4 C_A^2\pi^2 - 42768\sqrt{3}\psi'\left(\tfrac{1}{3}\right)\alpha^4 C_A^2 \\
&\quad +31104\sqrt{3}\psi'\left(\tfrac{1}{3}\right)\alpha^3 C_A^2\pi^2 + 62532\sqrt{3}\psi'\left(\tfrac{1}{3}\right)\alpha^3 C_A^2 \\
&\quad -41472\sqrt{3}\psi'\left(\tfrac{1}{3}\right)\alpha^3 C_A N_f T_F - 96480\sqrt{3}\psi'\left(\tfrac{1}{3}\right)\alpha^2 C_A^2\pi^2 \\
&\quad -105300\sqrt{3}\psi'\left(\tfrac{1}{3}\right)\alpha^2 C_A^2 + 73728\sqrt{3}\psi'\left(\tfrac{1}{3}\right)\alpha^2 C_A N_f\pi^2 T_F \\
&\quad +134784\sqrt{3}\psi'\left(\tfrac{1}{3}\right)\alpha^2 C_A N_f T_F + 119232\sqrt{3}\psi'\left(\tfrac{1}{3}\right)\alpha C_A^2\pi^2 \\
&\quad -1107756\sqrt{3}\psi'\left(\tfrac{1}{3}\right)\alpha C_A^2 - 331776\sqrt{3}\psi'\left(\tfrac{1}{3}\right)\alpha C_A N_f\pi^2 T_F \\
&\quad -119232\sqrt{3}\psi'\left(\tfrac{1}{3}\right)\alpha C_A N_f T_F - 50784\sqrt{3}\psi'\left(\tfrac{1}{3}\right) C_A^2\pi^2 \\
&\quad +3843072\sqrt{3}\psi'\left(\tfrac{1}{3}\right) C_A^2 + 282624\sqrt{3}\psi'\left(\tfrac{1}{3}\right) C_A N_f\pi^2 T_F \\
&\quad -3827520\sqrt{3}\psi'\left(\tfrac{1}{3}\right) C_A N_f T_F + 497664\sqrt{3}\psi'\left(\tfrac{1}{3}\right) C_F N_f T_F
\end{aligned}
$$

$$
\begin{aligned}
&-393216\sqrt{3}\psi'\left(\tfrac{1}{3}\right) N_f^2\pi^2T_F^2 + 774144\sqrt{3}\psi'\left(\tfrac{1}{3}\right) N_f^2T_F^2 \\
&+162\sqrt{3}\psi'''\left(\tfrac{1}{3}\right) \alpha^3C_A^2 + 1458\sqrt{3}\psi'''\left(\tfrac{1}{3}\right) \alpha^2C_A^2 \\
&-11664\sqrt{3}\psi'''\left(\tfrac{1}{3}\right) \alpha C_A^2 + 34587\sqrt{3}\psi'''\left(\tfrac{1}{3}\right) C_A^2 \\
&-20736\sqrt{3}\psi'''\left(\tfrac{1}{3}\right) C_AN_fT_F - 279936\sqrt{3}s_2\left(\tfrac{\pi}{6}\right) \alpha^3C_A^2 \\
&-4408992\sqrt{3}s_2\left(\tfrac{\pi}{6}\right) \alpha C_A^2 + 24214464\sqrt{3}s_2\left(\tfrac{\pi}{6}\right) C_A^2 \\
&-11197440\sqrt{3}s_2\left(\tfrac{\pi}{6}\right) C_AN_fT_F + 559872\sqrt{3}s_2\left(\tfrac{\pi}{2}\right) \alpha^3C_A^2 \\
&+8817984\sqrt{3}s_2\left(\tfrac{\pi}{2}\right) \alpha C_A^2 - 48428928\sqrt{3}s_2\left(\tfrac{\pi}{2}\right) C_A^2 \\
&+22394880\sqrt{3}s_2\left(\tfrac{\pi}{2}\right) C_AN_fT_F + 466560\sqrt{3}s_3\left(\tfrac{\pi}{6}\right) \alpha^3C_A^2 \\
&+7348320\sqrt{3}s_3\left(\tfrac{\pi}{6}\right) \alpha C_A^2 - 40357440\sqrt{3}s_3\left(\tfrac{\pi}{6}\right) C_A^2 \\
&+18662400\sqrt{3}s_3\left(\tfrac{\pi}{6}\right) C_AN_fT_F - 373248\sqrt{3}s_3\left(\tfrac{\pi}{2}\right) \alpha^3C_A^2 \\
&-5878656\sqrt{3}s_3\left(\tfrac{\pi}{2}\right) \alpha C_A^2 + 32285952\sqrt{3}s_3\left(\tfrac{\pi}{2}\right) C_A^2 \\
&-14929920\sqrt{3}s_3\left(\tfrac{\pi}{2}\right) C_AN_fT_F + 1458\sqrt{3}\alpha^6C_A^2 \\
&-2592\sqrt{3}\alpha^5C_A^2\pi^2 - 21870\sqrt{3}\alpha^5C_A^2 + 1152\sqrt{3}\alpha^4C_A^2\pi^4 \\
&+28512\sqrt{3}\alpha^4C_A^2\pi^2 + 59049\sqrt{3}\alpha^4C_A^2 - 10800\sqrt{3}\alpha^3C_A^2\pi^4 \\
&-41688\sqrt{3}\alpha^3C_A^2\pi^2 - 23328\sqrt{3}\alpha^3C_A^2\zeta_3 + 152604\sqrt{3}\alpha^3C_A^2 \\
&+27648\sqrt{3}\alpha^3C_AN_f\pi^2T_F - 54432\sqrt{3}\alpha^3C_AN_fT_F \\
&+28272\sqrt{3}\alpha^2C_A^2\pi^4 + 70200\sqrt{3}\alpha^2C_A^2\pi^2 - 17496\sqrt{3}\alpha^2C_A^2\zeta_3 \\
&-944784\sqrt{3}\alpha^2C_A^2 - 24576\sqrt{3}\alpha^2C_AN_f\pi^4T_F \\
&-89856\sqrt{3}\alpha^2C_AN_f\pi^2T_F + 349920\sqrt{3}\alpha^2C_AN_fT_F \\
&-8640\sqrt{3}\alpha C_A^2\pi^4 + 738504\sqrt{3}\alpha C_A^2\pi^2 + 664848\sqrt{3}\alpha C_A^2\zeta_3 \\
&+1027890\sqrt{3}\alpha C_A^2 + 110592\sqrt{3}\alpha C_AN_f\pi^4T_F \\
&+79488\sqrt{3}\alpha C_AN_f\pi^2T_F - 349920\sqrt{3}\alpha C_AN_fT_F \\
&-75304\sqrt{3}C_A^2\pi^4 - 2562048\sqrt{3}C_A^2\pi^2 - 2767284\sqrt{3}C_A^2\zeta_3 \\
&-203067\sqrt{3}C_A^2 - 38912\sqrt{3}C_AN_f\pi^4T_F \\
&+2551680\sqrt{3}C_AN_f\pi^2T_F + 2985984\sqrt{3}C_AN_fT_F\zeta_3 \\
&-681696\sqrt{3}C_AN_fT_F - 331776\sqrt{3}C_FN_f\pi^2T_F \\
&-2239488\sqrt{3}C_FN_fT_F\zeta_3 + 2379456\sqrt{3}C_FN_fT_F \\
&+131072\sqrt{3}N_f^2\pi^4T_F^2 - 516096\sqrt{3}N_f^2\pi^2T_F^2 \\
&+767232\sqrt{3}N_f^2T_F^2 - 1944\ln(3)^2\alpha^3C_A^2\pi \\
&-30618\ln(3)^2\alpha C_A^2\pi + 168156\ln(3)^2C_A^2\pi \\
&-77760\ln(3)^2C_AN_f\pi T_F + 23328\ln(3)\alpha^3C_A^2\pi \\
&+367416\ln(3)\alpha C_A^2\pi - 2017872\ln(3)C_A^2\pi
\end{aligned}
$$

$$
\begin{aligned}
&+933120\ln(3)C_A N_f \pi T_F + 2088\alpha^3 C_A^2\pi^3 + 32886\alpha C_A^2\pi^3 \\
&-180612 C_A^2\pi^3 + 83520 C_A N_f \pi^3 T_F + 216\sqrt{3}\left(396\psi'\left(\tfrac{1}{3}\right)\alpha^2 C_A^2\right. \\
&-144\psi'\left(\tfrac{1}{3}\right)\alpha^2 C_A N_f T_F - 1782\psi'\left(\tfrac{1}{3}\right)\alpha C_A^2 \\
&+648\psi'\left(\tfrac{1}{3}\right)\alpha C_A N_f T_F + 1518\psi'\left(\tfrac{1}{3}\right) C_A^2 - 4776\psi'\left(\tfrac{1}{3}\right) C_A N_f T_F \\
&+1536\psi'\left(\tfrac{1}{3}\right) N_f^2 T_F^2 + 297\alpha^3 C_A^2 - 108\alpha^3 C_A N_f T_F \\
&-264\alpha^2 C_A^2\pi^2 - 1782\alpha^2 C_A^2 + 96\alpha^2 C_A N_f \pi^2 T_F \\
&+648\alpha^2 C_A N_f T_F + 1188\alpha C_A^2\pi^2 + 2673\alpha C_A^2 \\
&-432\alpha C_A N_f \pi^2 T_F - 972\alpha C_A N_f T_F - 1012 C_A^2\pi^2 + 22464 C_A^2 \\
&+3184 C_A N_f \pi^2 T_F - 16848 C_A N_f T_F + 1296 C_F N_f T_F \\
&\left.-1024 N_f^2\pi^2 T_F^2 + 3456 N_f^2 T_F^2\right)\frac{1}{\epsilon}\Bigg)\frac{1}{279936\sqrt{3}}\Bigg] a^2 \\
&+ \mathcal{O}(a^3)\ . \qquad (4.4.19)
\end{aligned}
$$

The renormalization constants for the wave functions are given numerically for $SU(3)$ as

$$
\begin{aligned}
Z_A^{(\mathrm{ggg})}\Big|_{\mathrm{MOMg}} &= 1 + \Big[0.75\alpha^2 + 1.5\alpha - 1.111111 N_f + 8.083333 \\
&\qquad + (-1.5\alpha - 0.666667 N_f + 6.5)\frac{1}{\epsilon}\Big] a \\
&\quad + \Bigg[\left(1.687500\alpha^2 + \alpha N_f - 6.375000\alpha + 1.5 N_f - 14.625000\right)\frac{1}{\epsilon^2} \\
&\quad -0.187500\alpha^5 + 0.996035\alpha^4 + 0.277778\alpha^3 N_f + 6.926580\alpha^3 \\
&\quad +0.531442\alpha^2 N_f + 11.670343\alpha^2 - 1.567892\alpha N_f \\
&\quad +28.246854\alpha - 2.561884 N_f^2 + 3.142356 N_f + 41.955873 \\
&\quad + \big(0.375000\alpha^4 + 0.166667\alpha^3 N_f - 4.367070\alpha^3 \\
&\quad -0.718698\alpha^2 N_f - 4.840885\alpha^2 - 4.807737\alpha N_f \\
&\quad +38.705877\alpha - 1.537130 N_f^2 + 22.176457 N_f \\
&\quad -86.472011\big)\frac{1}{\epsilon}\Bigg] a^2 \ + \ \mathcal{O}(a^3) \\
Z_\alpha^{(\mathrm{ggg})}\Big|_{\mathrm{MOMg}} &= 1 + \left[-1.5\alpha - 0.75\frac{\alpha}{\epsilon}\right] a \\
&\quad + \Bigg[\alpha\left(0.562500\alpha + 1.687500\right)\frac{1}{\epsilon^2} + \alpha\left(0.375000\alpha^3 - 1.617070\alpha^2\right. \\
&\quad -9.879437\alpha - 3.458543 N_f + 13.951925\big) + \alpha\big(0.187500\alpha^3 \\
&\quad -0.808535\alpha^2 - 3.674093\alpha - 1.729271 N_f
\end{aligned}
$$

$$
\begin{aligned}
&\quad +12.400617)\,\frac{1}{\epsilon}\Big]\,a^2 \;+\; \mathcal{O}(a^3) \\
Z_c^{(\mathrm{ggg})}\Big|_{\mathrm{MOMg}} &= 1+\left[3.0+(-0.75\alpha+2.25)\,\frac{1}{\epsilon}\right]a \\
&\quad +\Bigg[\left(0.562500\alpha^2+0.75N_f-9.843750\right)\frac{1}{\epsilon^2}-0.75\alpha^3 \\
&\quad +1.265389\alpha^2+12.143941\alpha+4.312919N_f+1.458303 \\
&\quad +\big(0.187500\alpha^4-1.371035\alpha^3-4.060989\alpha^2-1.729271\alpha N_f \\
&\quad +18.641647\alpha+7.062814N_f-43.951850\big)\,\frac{1}{\epsilon}\Bigg]\,a^2 \;+\; \mathcal{O}(a^3) \\
Z_\psi^{(\mathrm{ggg})}\Big|_{\mathrm{MOMg}} &= 1+\left[-1.333333\alpha-1.333333\alpha\frac{1}{\epsilon}\right]a \\
&\quad +\Bigg[\alpha\,(1.388889\alpha+3.0)\,\frac{1}{\epsilon^2}+0.333333\alpha^4-1.437395\alpha^3 \\
&\quad -7.253944\alpha^2-3.074260\alpha N_f+12.970224\alpha+2.333333N_f \\
&\quad -25.464206+\big(0.333333\alpha^4-1.437395\alpha^3-6.253944\alpha^2 \\
&\quad -3.074260\alpha N_f+20.545541\alpha+0.666667N_f \\
&\quad -11.166667\big)\,\frac{1}{\epsilon}\Bigg]\,a^2 \;+\; \mathcal{O}(a^3)\;. \qquad (4.4.20)
\end{aligned}
$$

We reiterate that when variables are not labelled it is understood that they correspond to the scheme defined on the function on the left hand side of the equation. Although the conversion functions for the wave functions are the same in all MOMi schemes, the conversion function for each vertex is different in each of the three cases. For the MOMg scheme this was found to be

$$
\begin{aligned}
C_g^{\mathrm{MOMg}}(a,\alpha) &= 1+\big[-0.125\alpha^3+0.164023\alpha^2+1.511896\alpha+1.708403N_f \\
&\quad -13.246244\big]\,a+\big[0.015625\alpha^6+0.099619\alpha^5-0.324659\alpha^4 \\
&\quad -0.635434\alpha^3N_f+1.563729\alpha^3-0.004743\alpha^2N_f \\
&\quad -6.557479\alpha^2+3.708634\alpha N_f-36.724780\alpha \\
&\quad +0.534266N_f^2+33.152725N_f-217.036863\big]\,a^2 \\
&\quad +\mathcal{O}(a^3) \qquad (4.4.21)
\end{aligned}
$$

where the conversion function is always defined in our convention to be a function of $\overline{\mathrm{MS}}$ variables. Using the above result for the coupling constant conversion function along with (4.3.15) and equation (3.3.37) we deduce that the coupling

constant mapping between the $\overline{\rm MS}$ and MOMg scheme is given by

$$\begin{aligned} a_{\rm MOMg} &= a + \big[0.25\alpha^3 - 0.328046\alpha^2 - 3.023791\alpha - 3.416806N_f \\ &\quad +26.492489\big]\, a^2 \\ &\quad + \big[0.015625\alpha^6 - 0.322256\alpha^5 - 0.403893\alpha^4 - 0.010434\alpha^3 N_f \\ &\quad +8.295142\alpha^3 + 1.690792\alpha^2 N_f + 6.936296\alpha^2 + 8.080297\alpha N_f \\ &\quad -46.712076\alpha + 7.687393N_f^2 - 202.085010N_f \\ &\quad +960.462701\big]\, a^3 \;+\; \mathcal{O}(a^4) \;. \end{aligned} \tag{4.4.22}$$

For completeness we display the expressions for the amplitudes in the MOMg scheme which are

$$\begin{aligned} \Sigma^{\rm ggg}_{(1)}(p,q)\Big|_{\rm MOMg} &= \Sigma^{\rm ggg}_{(2)}(p,q)\Big|_{\rm MOMg} \;=\; -\frac{1}{2}\,\Sigma^{\rm ggg}_{(3)}(p,q)\Big|_{\rm MOMg} \\ &= -\,\Sigma^{\rm ggg}_{(4)}(p,q)\Big|_{\rm MOMg} \;=\; \frac{1}{2}\,\Sigma^{\rm ggg}_{(5)}(p,q)\Big|_{\rm MOMg} \\ &= -\,\Sigma^{\rm ggg}_{(6)}(p,q)\Big|_{\rm MOMg} \;=\; -1 + \mathcal{O}(a^3) \\ \Sigma^{\rm ggg}_{(7)}(p,q)\Big|_{\rm MOMg} &= 2\,\Sigma^{\rm ggg}_{(9)}(p,q)\Big|_{\rm MOMg} \;=\; -2\,\Sigma^{\rm ggg}_{(11)}(p,q)\Big|_{\rm MOMg} \\ &= -\,\Sigma^{\rm ggg}_{(14)}(p,q)\Big|_{\rm MOMg} \\ &= \big[0.057318\alpha^3 - 0.507930\alpha^2 - 3.328046\alpha - 1.092686N_f \\ &\quad +7.642693\big]\, a + \big[-0.021494\alpha^6 + 0.283161\alpha^5 + 1.173228\alpha^4 \\ &\quad +0.607993\alpha^3 N_f - 12.047753\alpha^3 - 1.820392\alpha^2 N_f \\ &\quad -10.473322\alpha^2 - 16.242288\alpha N_f + 110.033630\alpha \\ &\quad -3.779101N_f^2 + 36.334708N_f - 86.996723\big]\, a^2 \;+\; \mathcal{O}(a^3) \\ \Sigma^{\rm ggg}_{(8)}(p,q)\Big|_{\rm MOMg} &= -\,\Sigma^{\rm ggg}_{(13)}(p,q)\Big|_{\rm MOMg} \\ &= \big[0.192682\alpha^3 - 0.570116\alpha^2 - 3.351838\alpha - 1.213010N_f \\ &\quad +7.954277\big]\, a + \big[-0.072256\alpha^6 + 0.525374\alpha^5 + 2.655909\alpha^4 \\ &\quad +1.121278\alpha^3 N_f - 13.649060\alpha^3 - 1.730035\alpha^2 N_f \\ &\quad -6.045336\alpha^2 - 16.083732\alpha N_f + 114.490800\alpha \\ &\quad -4.195246N_f^2 + 37.416111N_f - 85.674805\big]\, a^2 \;+\; \mathcal{O}(a^3) \\ \Sigma^{\rm ggg}_{(10)}(p,q)\Big|_{\rm MOMg} &= -\,\Sigma^{\rm ggg}_{(12)}(p,q)\Big|_{\rm MOMg} \\ &= \big[-0.135364\alpha^3 + 0.062186\alpha^2 + 0.023791\alpha + 0.120324N_f \\ &\quad -0.311584\big]\, a + \big[0.050762\alpha^6 - 0.242213\alpha^5 - 1.482681\alpha^4 \end{aligned}$$

$$
\begin{aligned}
&-0.513285\alpha^3 N_f + 1.601306\alpha^3 - 0.090357\alpha^2 N_f \\
&-4.427987\alpha^2 - 0.158555\alpha N_f - 4.457170\alpha \\
&+0.416145 N_f^2 - 1.081403 N_f - 1.321918\big]\, a^2 \;+\; \mathcal{O}(a^3)\;.
\end{aligned}
\tag{4.4.23}
$$

Notice here that the same relations are satisfied between the amplitudes as in the $\overline{\rm MS}$ scheme. The relation (3.2.13) also holds in the Curci-Ferrari gauge as well as the arbitrary (linear) covariant gauge. For the MOMg scheme we have

$$
\begin{aligned}
\beta^{\rm MOMg}(a,\alpha) &= [0.666667 N_f - 11.0]\, a^2 \\
&+ \big[-0.5625\alpha^4 - 0.5\alpha^3 N_f + 5.367070\alpha^3 + 0.437395\alpha^2 N_f \\
&\quad -1.996759\alpha^2 + 2.015861\alpha N_f - 19.654643\alpha + 12.666667 N_f \\
&\quad -102.0]\, a^3 + \big[0.351563\alpha^7 + 0.281250\alpha^6 N_f - 3.932921\alpha^6 \\
&\quad -0.976418\alpha^5 N_f - 0.940179\alpha^5 - 10.959442\alpha^4 N_f \\
&\quad +86.317268\alpha^4 - 2.305695\alpha^3 N_f^2 + 21.403554\alpha^3 N_f \\
&\quad -49.695719\alpha^3 + 0.889805\alpha^2 N_f^2 + 14.285994\alpha^2 N_f \\
&\quad -200.649724\alpha^2 + 4.647961\alpha N_f^2 + 43.239367\alpha N_f \\
&\quad -658.070943\alpha - 2.658115 N_f^3 + 67.089537 N_f^2 \\
&\quad -0.565953 N_f - 1570.984207]\, a^4 + \mathcal{O}(a^5) \\
\gamma_A^{\rm MOMg}(a,\alpha) &= [1.5\alpha + 0.666667 N_f - 6.5]\, a \\
&+ \big[-0.375\alpha^4 - 0.166667\alpha^3 N_f + 2.117070\alpha^3 - 0.281302\alpha^2 N_f \\
&\quad +8.403385\alpha^2 + 5.474404\alpha N_f - 41.643377\alpha + 1.537130 N_f^2 \\
&\quad -12.093123 N_f + 16.909511]\, a^2 + \big[0.164063\alpha^7 \\
&\quad +0.072917\alpha^6 N_f - 1.563373\alpha^6 - 0.128860\alpha^5 N_f \\
&\quad -5.550011\alpha^5 - 6.504338\alpha^4 N_f + 56.704696\alpha^4 \\
&\quad -1.344989\alpha^3 N_f^2 + 12.748297\alpha^3 N_f + 3.724481\alpha^3 \\
&\quad -1.415890\alpha^2 N_f^2 + 66.363813\alpha^2 N_f - 453.616596\alpha^2 \\
&\quad +29.399931\alpha N_f^2 - 302.353053\alpha N_f + 647.926112\alpha \\
&\quad +6.202269 N_f^3 - 74.919018 N_f^2 + 491.430969 N_f \\
&\quad -1308.938779]\, a^3 \;+\; \mathcal{O}(a^4) \\
\gamma_\alpha^{\rm MOMg}(a,\alpha) &= [-0.75\alpha - 0.666667 N_f + 6.5]\, a \\
&+ \big[0.187500\alpha^4 + 0.166667\alpha^3 N_f - 1.308535\alpha^3 + 0.281302\alpha^2 N_f \\
&\quad -2.198042\alpha^2 - 3.745132\alpha N_f + 37.399010\alpha - 1.537130 N_f^2
\end{aligned}
$$

$$
\begin{aligned}
&+12.093123N_f - 16.909511]\, a^2 + \big[-0.082031\alpha^7 \\
&-0.072917\alpha^6 N_f + 0.855905\alpha^6 + 0.128860\alpha^5 N_f \\
&+1.672113\alpha^5 + 4.991225\alpha^4 N_f - 34.418633\alpha^4 \\
&+1.344989\alpha^3 N_f^2 - 9.153359\alpha^3 N_f + 41.130432\alpha^3 \\
&+1.415890\alpha^2 N_f^2 - 30.831035\alpha^2 N_f + 320.119724\alpha^2 \\
&-22.422378\alpha N_f^2 + 265.150723\alpha N_f - 566.417010\alpha \\
&-6.202269N_f^3 + 74.919018N_f^2 - 491.430969N_f \\
&+1308.938779]\, a^3 \;+\; \mathcal{O}(a^4)
\end{aligned}
$$

$$
\begin{aligned}
\gamma_c^{\rm MOMg}(a,\alpha) &= [0.75\alpha - 2.25]\, a \\
&+ \big[-0.1875\alpha^4 + 1.371035\alpha^3 + 4.342239\alpha^2 + 1.729271\alpha N_f \\
&\quad -21.172897\alpha - 4.437814N_f + 8.795600]\, a^2 + \big[0.082031\alpha^7 \\
&\quad -0.953562\alpha^6 - 2.036744\alpha^5 - 1.513113\alpha^4 N_f \\
&\quad +34.288809\alpha^4 + 7.759276\alpha^3 N_f - 7.509981\alpha^3 \\
&\quad +27.833941\alpha^2 N_f - 246.255710\alpha^2 + 6.977553\alpha N_f^2 \\
&\quad -127.545757\alpha N_f + 436.672074\alpha - 19.974116N_f^2 \\
&\quad +157.466921N_f - 548.849275]\, a^3 \;+\; \mathcal{O}(a^4) \\
\gamma_\psi^{\rm MOMg}(a,\alpha) &= 1.333333a\alpha \\
&+ \big[-0.333333\alpha^4 + 1.437395\alpha^3 + 9.031722\alpha^2 + 3.074260\alpha N_f \\
&\quad -10.545541\alpha - 1.333333N_f + 22.333333]\, a^2 \\
&+ \big[0.145833\alpha^7 - 1.257721\alpha^6 - 5.894040\alpha^5 - 2.689978\alpha^4 N_f \\
&\quad +36.807483\alpha^4 + 7.057668\alpha^3 N_f + 34.428624\alpha^3 \\
&\quad +53.071812\alpha^2 N_f - 232.340415\alpha^2 + 12.404539\alpha N_f^2 \\
&\quad -80.560198\alpha N_f + 204.199902\alpha - 5.259632N_f^2 \\
&\quad +76.867272N_f - 94.794328]\, a^3 \;+\; \mathcal{O}(a^4)\ . \qquad (4.4.24)
\end{aligned}
$$

4.5 MOMq scheme.

As with the MOMh renormalization we now similarly present results for the MOMq scheme. Starting with the renormalization constants we have

$$
\begin{aligned}
Z_g^{(\rm qqg)}\Big|_{\rm MOMq} &= 1 + \big[-6\psi'\left(\tfrac{1}{3}\right)\alpha^2 C_A + 24\psi'\left(\tfrac{1}{3}\right)\alpha C_A + 96\psi'\left(\tfrac{1}{3}\right)\alpha C_F \\
&\quad +78\psi'\left(\tfrac{1}{3}\right) C_A - 48\psi'\left(\tfrac{1}{3}\right) C_F + 4\alpha^2 C_A\pi^2 + 27\alpha^2 C_A \\
&\quad -16\alpha C_A\pi^2 - 54\alpha C_A - 64\alpha C_F\pi^2 - 216\alpha C_F - 52C_A\pi^2
\end{aligned}
$$

$$
\begin{aligned}
&-993C_A + 32C_F\pi^2 + 432C_F + 240N_fT_F \\
&+36\left(-11C_A + 4N_fT_F\right)\frac{1}{\epsilon}\Bigg]\frac{a}{216} \\
&+\Bigg[\left(121C_A^2 - 88C_AN_fT_F + 16N_f^2T_F^2\right)\frac{1}{24\epsilon^2} \\
&\quad+\Big(72\sqrt{3}\psi'\left(\tfrac{1}{3}\right)^2\alpha^4C_A^2 - 576\sqrt{3}\psi'\left(\tfrac{1}{3}\right)^2\alpha^3C_A^2 \\
&\qquad-2304\sqrt{3}\psi'\left(\tfrac{1}{3}\right)^2\alpha^3C_AC_F - 720\sqrt{3}\psi'\left(\tfrac{1}{3}\right)^2\alpha^2C_A^2 \\
&\qquad+10368\sqrt{3}\psi'\left(\tfrac{1}{3}\right)^2\alpha^2C_AC_F + 18432\sqrt{3}\psi'\left(\tfrac{1}{3}\right)^2\alpha^2C_F^2 \\
&\qquad+7488\sqrt{3}\psi'\left(\tfrac{1}{3}\right)^2\alpha C_A^2 + 25344\sqrt{3}\psi'\left(\tfrac{1}{3}\right)^2\alpha C_AC_F \\
&\qquad-18432\sqrt{3}\psi'\left(\tfrac{1}{3}\right)^2\alpha C_F^2 + 19080\sqrt{3}\psi'\left(\tfrac{1}{3}\right)^2C_A^2 \\
&\qquad-35712\sqrt{3}\psi'\left(\tfrac{1}{3}\right)^2C_AC_F + 18432\sqrt{3}\psi'\left(\tfrac{1}{3}\right)^2C_F^2 \\
&\qquad-96\sqrt{3}\psi'\left(\tfrac{1}{3}\right)\alpha^4C_A^2\pi^2 - 972\sqrt{3}\psi'\left(\tfrac{1}{3}\right)\alpha^4C_A^2 \\
&\qquad+768\sqrt{3}\psi'\left(\tfrac{1}{3}\right)\alpha^3C_A^2\pi^2 + 2376\sqrt{3}\psi'\left(\tfrac{1}{3}\right)\alpha^3C_A^2 \\
&\qquad+3072\sqrt{3}\psi'\left(\tfrac{1}{3}\right)\alpha^3C_AC_F\pi^2 + 17280\sqrt{3}\psi'\left(\tfrac{1}{3}\right)\alpha^3C_AC_F \\
&\qquad+960\sqrt{3}\psi'\left(\tfrac{1}{3}\right)\alpha^2C_A^2\pi^2 + 28872\sqrt{3}\psi'\left(\tfrac{1}{3}\right)\alpha^2C_A^2 \\
&\qquad-13824\sqrt{3}\psi'\left(\tfrac{1}{3}\right)\alpha^2C_AC_F\pi^2 - 55296\sqrt{3}\psi'\left(\tfrac{1}{3}\right)\alpha^2C_AC_F \\
&\qquad-2880\sqrt{3}\psi'\left(\tfrac{1}{3}\right)\alpha^2C_AN_fT_F - 24576\sqrt{3}\psi'\left(\tfrac{1}{3}\right)\alpha^2C_F^2\pi^2 \\
&\qquad-82944\sqrt{3}\psi'\left(\tfrac{1}{3}\right)\alpha^2C_F^2 - 9984\sqrt{3}\psi'\left(\tfrac{1}{3}\right)\alpha C_A^2\pi^2 \\
&\qquad-65232\sqrt{3}\psi'\left(\tfrac{1}{3}\right)\alpha C_A^2 - 33792\sqrt{3}\psi'\left(\tfrac{1}{3}\right)\alpha C_AC_F\pi^2 \\
&\qquad-379872\sqrt{3}\psi'\left(\tfrac{1}{3}\right)\alpha C_AC_F + 17280\sqrt{3}\psi'\left(\tfrac{1}{3}\right)\alpha C_AN_fT_F \\
&\qquad+24576\sqrt{3}\psi'\left(\tfrac{1}{3}\right)\alpha C_F^2\pi^2 + 324864\sqrt{3}\psi'\left(\tfrac{1}{3}\right)\alpha C_F^2 \\
&\qquad+46080\sqrt{3}\psi'\left(\tfrac{1}{3}\right)\alpha C_FN_fT_F - 25440\sqrt{3}\psi'\left(\tfrac{1}{3}\right)C_A^2\pi^2 \\
&\qquad-127512\sqrt{3}\psi'\left(\tfrac{1}{3}\right)C_A^2 + 47616\sqrt{3}\psi'\left(\tfrac{1}{3}\right)C_AC_F\pi^2 \\
&\qquad+496224\sqrt{3}\psi'\left(\tfrac{1}{3}\right)C_AC_F - 44352\sqrt{3}\psi'\left(\tfrac{1}{3}\right)C_AN_fT_F \\
&\qquad-24576\sqrt{3}\psi'\left(\tfrac{1}{3}\right)C_F^2\pi^2 - 293760\sqrt{3}\psi'\left(\tfrac{1}{3}\right)C_F^2 \\
&\qquad-9216\sqrt{3}\psi'\left(\tfrac{1}{3}\right)C_FN_fT_F + 117\sqrt{3}\psi'''\left(\tfrac{1}{3}\right)\alpha^2C_A^2 \\
&\qquad-144\sqrt{3}\psi'''\left(\tfrac{1}{3}\right)\alpha^2C_AC_F - 198\sqrt{3}\psi'''\left(\tfrac{1}{3}\right)\alpha C_A^2 \\
&\qquad-720\sqrt{3}\psi'''\left(\tfrac{1}{3}\right)\alpha C_AC_F - 1152\sqrt{3}\psi'''\left(\tfrac{1}{3}\right)\alpha C_F^2 \\
&\qquad-414\sqrt{3}\psi'''\left(\tfrac{1}{3}\right)C_A^2 - 864\sqrt{3}\psi'''\left(\tfrac{1}{3}\right)C_AC_F \\
&\qquad+576\sqrt{3}\psi'''\left(\tfrac{1}{3}\right)C_AN_fT_F + 4608\sqrt{3}\psi'''\left(\tfrac{1}{3}\right)C_F^2 \\
&\qquad+77760\sqrt{3}s_2\left(\tfrac{\pi}{6}\right)\alpha^2C_A^2 - 124416\sqrt{3}s_2\left(\tfrac{\pi}{6}\right)\alpha^2C_AC_F \\
&\qquad+108864\sqrt{3}s_2\left(\tfrac{\pi}{6}\right)\alpha C_A^2 - 995328\sqrt{3}s_2\left(\tfrac{\pi}{6}\right)\alpha C_AC_F \\
&\qquad+497664\sqrt{3}s_2\left(\tfrac{\pi}{6}\right)\alpha C_F^2 - 443232\sqrt{3}s_2\left(\tfrac{\pi}{6}\right)C_A^2
\end{aligned}
$$

$$
\begin{aligned}
&+1306368\sqrt{3}s_2\left(\tfrac{\pi}{6}\right)C_AC_F - 124416\sqrt{3}s_2\left(\tfrac{\pi}{6}\right)C_AN_fT_F \\
&+248832\sqrt{3}s_2\left(\tfrac{\pi}{6}\right)C_F^2 - 155520\sqrt{3}s_2\left(\tfrac{\pi}{2}\right)\alpha^2C_A^2 \\
&+248832\sqrt{3}s_2\left(\tfrac{\pi}{2}\right)\alpha^2C_AC_F - 217728\sqrt{3}s_2\left(\tfrac{\pi}{2}\right)\alpha C_A^2 \\
&+1990656\sqrt{3}s_2\left(\tfrac{\pi}{2}\right)\alpha C_AC_F - 995328\sqrt{3}s_2\left(\tfrac{\pi}{2}\right)\alpha C_F^2 \\
&+886464\sqrt{3}s_2\left(\tfrac{\pi}{2}\right)C_A^2 - 2612736\sqrt{3}s_2\left(\tfrac{\pi}{2}\right)C_AC_F \\
&+248832\sqrt{3}s_2\left(\tfrac{\pi}{2}\right)C_AN_fT_F - 497664\sqrt{3}s_2\left(\tfrac{\pi}{2}\right)C_F^2 \\
&-129600\sqrt{3}s_3\left(\tfrac{\pi}{6}\right)\alpha^2C_A^2 + 207360\sqrt{3}s_3\left(\tfrac{\pi}{6}\right)\alpha^2C_AC_F \\
&-181440\sqrt{3}s_3\left(\tfrac{\pi}{6}\right)\alpha C_A^2 + 1658880\sqrt{3}s_3\left(\tfrac{\pi}{6}\right)\alpha C_AC_F \\
&-829440\sqrt{3}s_3\left(\tfrac{\pi}{6}\right)\alpha C_F^2 + 738720\sqrt{3}s_3\left(\tfrac{\pi}{6}\right)C_A^2 \\
&-2177280\sqrt{3}s_3\left(\tfrac{\pi}{6}\right)C_AC_F + 207360\sqrt{3}s_3\left(\tfrac{\pi}{6}\right)C_AN_fT_F \\
&-414720\sqrt{3}s_3\left(\tfrac{\pi}{6}\right)C_F^2 + 103680\sqrt{3}s_3\left(\tfrac{\pi}{2}\right)\alpha^2C_A^2 \\
&-165888\sqrt{3}s_3\left(\tfrac{\pi}{2}\right)\alpha^2C_AC_F + 145152\sqrt{3}s_3\left(\tfrac{\pi}{2}\right)\alpha C_A^2 \\
&-1327104\sqrt{3}s_3\left(\tfrac{\pi}{2}\right)\alpha C_AC_F + 663552\sqrt{3}s_3\left(\tfrac{\pi}{2}\right)\alpha C_F^2 \\
&-590976\sqrt{3}s_3\left(\tfrac{\pi}{2}\right)C_A^2 + 1741824\sqrt{3}s_3\left(\tfrac{\pi}{2}\right)C_AC_F \\
&-165888\sqrt{3}s_3\left(\tfrac{\pi}{2}\right)C_AN_fT_F + 331776\sqrt{3}s_3\left(\tfrac{\pi}{2}\right)C_F^2 \\
&+32\sqrt{3}\alpha^4C_A^2\pi^4 + 648\sqrt{3}\alpha^4C_A^2\pi^2 + 2673\sqrt{3}\alpha^4C_A^2 \\
&-256\sqrt{3}\alpha^3C_A^2\pi^4 - 1584\sqrt{3}\alpha^3C_A^2\pi^2 - 1024\sqrt{3}\alpha^3C_AC_F\pi^4 \\
&-11520\sqrt{3}\alpha^3C_AC_F\pi^2 - 27216\sqrt{3}\alpha^3C_AC_F \\
&-632\sqrt{3}\alpha^2C_A^2\pi^4 - 19248\sqrt{3}\alpha^2C_A^2\pi^2 - 5184\sqrt{3}\alpha^2C_A^2\zeta_3 \\
&-73710\sqrt{3}\alpha^2C_A^2 + 4992\sqrt{3}\alpha^2C_AC_F\pi^4 \\
&+36864\sqrt{3}\alpha^2C_AC_F\pi^2 + 20736\sqrt{3}\alpha^2C_AC_F\zeta_3 \\
&+38880\sqrt{3}\alpha^2C_AC_F + 1920\sqrt{3}\alpha^2C_AN_f\pi^2T_F \\
&+12960\sqrt{3}\alpha^2C_AN_fT_F + 8192\sqrt{3}\alpha^2C_F^2\pi^4 \\
&+55296\sqrt{3}\alpha^2C_F^2\pi^2 + 93312\sqrt{3}\alpha^2C_F^2 + 3856\sqrt{3}\alpha C_A^2\pi^4 \\
&+43488\sqrt{3}\alpha C_A^2\pi^2 + 20736\sqrt{3}\alpha C_A^2\zeta_3 + 136728\sqrt{3}\alpha C_A^2 \\
&+13184\sqrt{3}\alpha C_AC_F\pi^4 + 253248\sqrt{3}\alpha C_AC_F\pi^2 \\
&+10368\sqrt{3}\alpha C_AC_F\zeta_3 + 444528\sqrt{3}\alpha C_AC_F \\
&-11520\sqrt{3}\alpha C_AN_f\pi^2T_F - 25920\sqrt{3}\alpha C_AN_fT_F \\
&-5120\sqrt{3}\alpha C_F^2\pi^4 - 216576\sqrt{3}\alpha C_F^2\pi^2 + 41472\sqrt{3}\alpha C_F^2\zeta_3 \\
&-311040\sqrt{3}\alpha C_F^2 - 30720\sqrt{3}\alpha C_FN_f\pi^2T_F \\
&-103680\sqrt{3}\alpha C_FN_fT_F + 9584\sqrt{3}C_A^2\pi^4 + 85008\sqrt{3}C_A^2\pi^2 \\
&+109836\sqrt{3}C_A^2\zeta_3 + 115029\sqrt{3}C_A^2 - 13568\sqrt{3}C_AC_F\pi^4
\end{aligned}
$$

$$
\begin{aligned}
&-330816\sqrt{3}C_A C_F\pi^2 - 31104\sqrt{3}C_A C_F\zeta_3 \\
&-694656\sqrt{3}C_A C_F - 1536\sqrt{3}C_A N_f\pi^4 T_F \\
&+29568\sqrt{3}C_A N_f\pi^2 T_F + 145152\sqrt{3}C_A N_f T_F\zeta_3 \\
&-79200\sqrt{3}C_A N_f T_F - 4096\sqrt{3}C_F^2\pi^4 + 195840\sqrt{3}C_F^2\pi^2 \\
&-290304\sqrt{3}C_F^2\zeta_3 + 264384\sqrt{3}C_F^2 + 6144\sqrt{3}C_F N_f\pi^2 T_F \\
&-248832\sqrt{3}C_F N_f T_F\zeta_3 + 430272\sqrt{3}C_F N_f T_F \\
&+57600\sqrt{3}N_f^2 T_F^2 + 540\ln(3)^2\alpha^2 C_A^2\pi \\
&-864\ln(3)^2\alpha^2 C_A C_F\pi + 756\ln(3)^2\alpha C_A^2\pi \\
&-6912\ln(3)^2\alpha C_A C_F\pi + 3456\ln(3)^2\alpha C_F^2\pi \\
&-3078\ln(3)^2 C_A^2\pi + 9072\ln(3)^2 C_A C_F\pi \\
&-864\ln(3)^2 C_A N_f\pi T_F + 1728\ln(3)^2 C_F^2\pi \\
&-6480\ln(3)\alpha^2 C_A^2\pi + 10368\ln(3)\alpha^2 C_A C_F\pi \\
&-9072\ln(3)\alpha C_A^2\pi + 82944\ln(3)\alpha C_A C_F\pi \\
&-41472\ln(3)\alpha C_F^2\pi + 36936\ln(3)C_A^2\pi \\
&-108864\ln(3)C_A C_F\pi + 10368\ln(3)C_A N_f\pi T_F \\
&-20736\ln(3)C_F^2\pi - 580\alpha^2 C_A^2\pi^3 + 928\alpha^2 C_A C_F\pi^3 \\
&-812\alpha C_A^2\pi^3 + 7424\alpha C_A C_F\pi^3 - 3712\alpha C_F^2\pi^3 + 3306 C_A^2\pi^3 \\
&-9744 C_A C_F\pi^3 + 928 C_A N_f\pi^3 T_F - 1856 C_F^2\pi^3 \\
&+72\sqrt{3}\left(66\psi'\left(\tfrac{1}{3}\right)\alpha^2 C_A^2 - 24\psi'\left(\tfrac{1}{3}\right)\alpha^2 C_A N_f T_F\right. \\
&-264\psi'\left(\tfrac{1}{3}\right)\alpha C_A^2 - 1056\psi'\left(\tfrac{1}{3}\right)\alpha C_A C_F \\
&+96\psi'\left(\tfrac{1}{3}\right)\alpha C_A N_f T_F + 384\psi'\left(\tfrac{1}{3}\right)\alpha C_F N_f T_F \\
&-858\psi'\left(\tfrac{1}{3}\right) C_A^2 + 528\psi'\left(\tfrac{1}{3}\right) C_A C_F + 312\psi'\left(\tfrac{1}{3}\right) C_A N_f T_F \\
&-192\psi'\left(\tfrac{1}{3}\right) C_F N_f T_F - 44\alpha^2 C_A^2\pi^2 - 297\alpha^2 C_A^2 \\
&+16\alpha^2 C_A N_f\pi^2 T_F + 108\alpha^2 C_A N_f T_F + 176\alpha C_A^2\pi^2 \\
&+594\alpha C_A^2 + 704\alpha C_A C_F\pi^2 + 2376\alpha C_A C_F \\
&-64\alpha C_A N_f\pi^2 T_F - 216\alpha C_A N_f T_F - 256\alpha C_F N_f\pi^2 T_F \\
&-864\alpha C_F N_f T_F + 572 C_A^2\pi^2 + 9699 C_A^2 - 352 C_A C_F\pi^2 \\
&-4752 C_A C_F - 208 C_A N_f\pi^2 T_F - 5892 C_A N_f T_F \\
&+128 C_F N_f\pi^2 T_F + 2160 C_F N_f T_F \\
&\left.+960 N_f^2 T_F^2\right)\frac{1}{\epsilon}\Bigg)\frac{1}{31104\sqrt{3}}\Bigg]a^2 \;+\; \mathcal{O}(a^3)
\end{aligned}
\tag{4.5.25}
$$

analytically for the coupling constant renormalization constant and numerically for the wave function and gauge parameter renormalization constants in $SU(3)$ we have

$$
\begin{aligned}
Z_A^{(\mathrm{qqg})}\Big|_{\mathrm{MOMq}} &= 1 + \big[0.75\alpha^2 + 1.5\alpha - 1.111111N_f + 8.083333 \\
&\qquad + (-1.5\alpha - 0.666667N_f + 6.5)\,\frac{1}{\epsilon}\Big]\,a \\
&\quad + \Big[\big(1.687500\alpha^2 + \alpha N_f - 6.375000\alpha + 1.5N_f - 14.625000\big)\,\frac{1}{\epsilon^2} \\
&\qquad + 1.248017\alpha^4 + 8.191675\alpha^3 - 1.015581\alpha^2 N_f + 16.657617\alpha^2 \\
&\qquad - 4.271319\alpha N_f + 37.418456\alpha - 26.358363N_f + 120.984314 \\
&\qquad + \big(-2.496035\alpha^3 - 0.609349\alpha^2 N_f - 4.887629\alpha^2 \\
&\qquad\quad - 0.896125\alpha N_f + 19.623376\alpha + 0.671627N_f \\
&\qquad\quad - 22.923368\big)\,\frac{1}{\epsilon}\Big]\,a^2 \;+\; \mathcal{O}(a^3) \\
Z_\alpha^{(\mathrm{qqg})}\Big|_{\mathrm{MOMq}} &= 1 + \Big[-1.5\alpha - 0.75\frac{\alpha}{\epsilon}\Big]\,a + \Big[\alpha(0.562500\alpha + 1.687500)\frac{1}{\epsilon^2} \\
&\qquad + \alpha\left(-1.371035\alpha^2 - 8.860030\alpha - 0.713146\right) \\
&\qquad + \alpha(-0.685517\alpha^2 - 3.164390\alpha + 5.068081)\frac{1}{\epsilon}\Big]\,a^2 \;+\; \mathcal{O}(a^3) \\
Z_c^{(\mathrm{qqg})}\Big|_{\mathrm{MOMq}} &= 1 + \Big[3.0 + (-0.75\alpha + 2.25)\,\frac{1}{\epsilon}\Big]\,a \\
&\quad + \Big[\big(0.562500\alpha^2 + 0.75N_f - 9.843750\big)\,\frac{1}{\epsilon^2} + 0.773320\alpha^2 \\
&\qquad + 10.105127\alpha - 2.604167N_f + 30.788446 + \big(-0.685517\alpha^3 \\
&\qquad - 3.920338\alpha^2 + 9.780001\alpha + 1.875000N_f \\
&\qquad - 21.954243\big)\,\frac{1}{\epsilon}\Big]\,a^2 \;+\; \mathcal{O}(a^3) \\
Z_\psi^{(\mathrm{qqg})}\Big|_{\mathrm{MOMq}} &= 1 + \Big[-1.333333\alpha - 1.333333\frac{\alpha}{\epsilon}\Big]\,a + \Big[\alpha(1.388889\alpha + 3.0)\frac{1}{\epsilon^2} \\
&\qquad - 1.218698\alpha^3 - 6.347805\alpha^2 - 0.065396\alpha \\
&\qquad + 2.333333N_f - 25.464206 + \big(-1.218698\alpha^3 - 5.347805\alpha^2 \\
&\qquad + 7.509922\alpha + 0.666667N_f - 11.166667\big)\,\frac{1}{\epsilon}\Big]\,a^2 \;+\; \mathcal{O}(a^3)\ .
\end{aligned}
\tag{4.5.26}
$$

The amplitudes for the MOMq scheme at the symmetric point are

$$\begin{aligned}
\Sigma^{\mathrm{qqg}}_{(1)}(p,q)\Big|_{\mathrm{MOMq}} &= 1 + \mathcal{O}(a^3) \\
\Sigma^{\mathrm{qqg}}_{(2)}(p,q)\Big|_{\mathrm{MOMq}} &= \Sigma^{\mathrm{qqg}}_{(5)}(p,q)\Big|_{\mathrm{MOMq}} \\
&= \left[-0.414023\alpha^2 - 2.305695\alpha + 2.598033\right] a + \left[-0.567640\alpha^4\right. \\
&\quad -5.318037\alpha^3 - 12.626549\alpha^2 - 1.033946\alpha N_f \\
&\quad \left. +17.965565\alpha - 3.385190 N_f - 28.160578\right] a^2 \; + \; \mathcal{O}(a^3) \\
\Sigma^{\mathrm{qqg}}_{(3)}(p,q)\Big|_{\mathrm{MOMq}} &= \Sigma^{\mathrm{qqg}}_{(4)}(p,q)\Big|_{\mathrm{MOMq}} \\
&= \left[-0.5\alpha^2 - 2.522631\alpha + 2.050269\right] a + \left[-0.685517\alpha^4\right. \\
&\quad -6.677244\alpha^3 - 14.947140\alpha^2 - 0.919310\alpha N_f \\
&\quad \left. +15.686895\alpha - 2.593516 N_f - 30.385947\right] a^2 \; + \; \mathcal{O}(a^3) \\
\Sigma^{\mathrm{qqg}}_{(6)}(p,q)\Big|_{\mathrm{MOMq}} &= \left[-0.585977\alpha^2 - 2.343907\alpha - 4.362272\right] a + \left[-0.803395\alpha^4\right. \\
&\quad -7.471450\alpha^3 - 14.263665\alpha^2 + 1.953256\alpha N_f \\
&\quad \left. -27.911352\alpha + 6.075881 N_f - 40.243836\right] a^2 \; + \; \mathcal{O}(a^3) \; .
\end{aligned} \tag{4.5.27}$$

The emergence of the relations between various amplitudes is again a check on our computation. Like the previous two cases there are no $\mathcal{O}(a)$ corrections for the channel 1 amplitudes corresponding to the vertex Feynman rule. This is due to the definition of the MOMi schemes at the symmetric point. The MOMq coupling constant mapping is given numerically as

$$\begin{aligned}
a_{\mathrm{MOMq}} &= a + \left[-0.164023\alpha^2 - 2.344187\alpha - 1.111111 N_f + 16.715775\right] a^2 \\
&\quad + \left[0.208860\alpha^4 + 2.073303\alpha^3 + 0.237744\alpha^2 + 0.651396\alpha N_f\right. \\
&\quad \left. -43.057552\alpha + 1.234568 N_f^2 - 83.111217 N_f + 472.159094\right] a^3 \\
&\quad + \mathcal{O}(a^4)
\end{aligned} \tag{4.5.28}$$

with the conversion function corresponding to the quark-gluon vertex

$$\begin{aligned}
C_g^{\mathrm{MOMq}}(a,\alpha) &= 1 + \left[0.082012\alpha^2 + 1.172093\alpha + 0.555556 N_f - 8.357887\right] a \\
&\quad + [-0.094341\alpha^4 - 0.748276\alpha^3 + 0.136686\alpha^2 N_f - 0.114499\alpha^2 \\
&\quad +1.627791\alpha N_f - 7.859897\alpha - 0.154321 N_f^2 + 27.625796 N_f \\
&\quad -131.298127] a^2 \; + \; \mathcal{O}(a^3) \; .
\end{aligned} \tag{4.5.29}$$

Finally we record the renormalization group functions for the MOMq scheme in numerical form for $SU(3)$ starting with the β-function as

$$
\begin{aligned}
\beta^{\rm MOMq}(a,\alpha) &= [0.666667N_f - 11]a^2 \\
&+ [0.246035\alpha^3 + 0.218698\alpha^2 N_f - 0.374161\alpha^2 + 1.562791\alpha N_f \\
&\quad -15.237214\alpha + 12.666667N_f - 102]a^3 + [0.048066\alpha^5 \\
&\quad +0.000006\alpha^4 N_f + 2.147640\alpha^4 + 1.514213\alpha^3 N_f \\
&\quad +0.007428\alpha^3 + 16.598977\alpha^2 N_f - 123.345240\alpha^2 \\
&\quad +60.545481\alpha N_f - 422.073192\alpha - 22.587812N_f^2 \\
&\quad +588.654843N_f - 1843.652719]a^4 \; + \; \mathcal{O}(a^5) \\
\gamma_A^{\rm MOMq}(a,\alpha) &= [1.500000\alpha + 0.666667N_f - 6.500000]a \\
&+ [0.246035\alpha^3 - 0.390651\alpha^2 N_f + 8.450130\alpha^2 + 1.562791\alpha N_f \\
&\quad -22.560876\alpha + 9.411706N_f - 46.639132]a^2 \\
&+ [0.136474\alpha^5 - 0.478368\alpha^4 N_f + 8.765488\alpha^4 - 3.497867\alpha^3 N_f \\
&\quad +57.718718\alpha^3 + 11.368733\alpha^2 N_f - 197.964567\alpha^2 \\
&\quad +1.302171\alpha N_f^2 + 49.405307\alpha N_f - 333.308210\alpha \\
&\quad -11.178808N_f^2 + 415.699017N_f - 2027.743722]a^3 + \; \mathcal{O}(a^4) \\
\gamma_\alpha^{\rm MOMq}(a,\alpha) &= [-0.750000\alpha - 0.666667N_f + 6.500000]\, a \\
&+ [0.439483\alpha^3 + 0.390651\alpha^2 N_f - 2.754489\alpha^2 - 1.562791\alpha N_f \\
&\quad +25.649045\alpha - 9.411706N_f + 46.639132]a^2 + [0.960039\alpha^5 \\
&\quad +0.478368\alpha^4 N_f + 5.678015\alpha^4 + 3.497867\alpha^3 N_f \\
&\quad +1.538229\alpha^3 - 9.903791\alpha^2 N_f + 236.129260\alpha^2 \\
&\quad -1.302171\alpha N_f^2 - 48.345615\alpha N_f + 452.915078\alpha \\
&\quad +11.178808N_f^2 - 415.699015N_f + 2027.743714]a^3 \; + \; \mathcal{O}(a^4) \\
\gamma_c^{\rm MOMq}(a,\alpha) &= [0.750000\alpha - 2.250000]\, a \\
&+ [0.685517\alpha^3 + 4.201588\alpha^2 - 12.311251\alpha + 0.750000N_f \\
&\quad -13.202007]a^2 + [1.096513\alpha^5 + 12.182240\alpha^4 + 27.132851\alpha^3 \\
&\quad +1.7109768\alpha^2 N_f - 107.803424\alpha^2 + 4.118647\alpha N_f \\
&\quad -1.866574\alpha - 2.500000N_f^2 + 75.503272N_f - 740.134167]a^3 \\
&+ \mathcal{O}(a^4) \\
\gamma_\psi^{\rm MOMq}(a,\alpha) &= 1.333333\alpha a + [1.218698\alpha^3 + 8.125582\alpha^2 + 2.490078\alpha \\
&\quad -1.333333N_f + 22.333333]a^2 + [1.949356\alpha^5 + 22.021246\alpha^4
\end{aligned}
$$

$$
\begin{aligned}
&+74.901463\alpha^3 + 2.166946\alpha^2 N_f + 30.480104\alpha^2 \\
&+3.107628\alpha N_f + 182.913291\alpha + 0.888889 N_f^2 \\
&-52.191691 N_f + 341.898911]a^3 \; + \; \mathcal{O}(a^4) \qquad (4.5.30)
\end{aligned}
$$

where all of the above results for the renormalization group functions are functions of MOMq variables. This completes the summary of the results for all schemes and vertices.

4.6 Λ-parameters

In this section we repeat the analysis of the Λ-ratios, carried out in chapter 3 for the arbitrary (linear) covariant gauge (see (3.3.49)), for the Curci-Ferrari gauge. For each MOMi scheme we have

$$
\begin{aligned}
\Theta^{\mathrm{MOMh}}(\alpha, N_f) &= \frac{1}{108}\left[-12\psi'(\tfrac{1}{3})\alpha C_A + 30\psi'(\tfrac{1}{3})C_A + 27\alpha^2 C_A + 8\pi^2\alpha C_A \right. \\
&\quad \left. +108\alpha C_A - 20\pi^2 C_A + 669 C_A - 240 N_f T_F\right] \\
\Theta^{\mathrm{MOMg}}(\alpha, N_f) &= \frac{1}{324}\left[36\psi'(\tfrac{1}{3})\alpha^2 C_A - 162\psi'(\tfrac{1}{3})\alpha C_A + 138\psi'(\tfrac{1}{3})C_A \right. \\
&\quad -384\psi'(\tfrac{1}{3})N_f T_F + 27\alpha^3 C_A - 24\pi^2\alpha^2 C_A - 162\alpha^2 C_A \\
&\quad +108\pi^2\alpha C_A + 243\alpha C_A - 92\pi^2 C_A + 2376 C_A \\
&\quad \left. +256\pi^2 N_f T_F - 864 N_f T_F\right] \\
\Theta^{\mathrm{MOMq}}(\alpha, N_f) &= \frac{1}{108}\left[6\psi'(\tfrac{1}{3})\alpha^2 C_A - 24\psi'(\tfrac{1}{3})\alpha C_A - 96\psi'(\tfrac{1}{3})\alpha T_F \right. \\
&\quad -78\psi'(\tfrac{1}{3})C_A + 48\psi'(\tfrac{1}{3})C_F - 4\pi^2\alpha^2 C_A - 27\alpha^2 C_A \\
&\quad +16\pi^2\alpha C_A + 54\alpha C_A + 64\pi^2\alpha C_F + 216\alpha C_F + 52\pi^2 C_A \\
&\quad \left. +993 C_A - 32\pi^2 C_F - 432 C_F - 240 N_f T_F\right] \; . \qquad (4.6.31)
\end{aligned}
$$

The Λ-ratios are numerically evaluated for the same values of α and N_f considered in the previous chapter. These Λ-ratios are presented in Table 4.1. The values for the MOMg and MOMq schemes are equivalent to those of the linear covariant gauge fixing of [52], displayed in Table 3.3. This is because the coupling constant mapping is the same for both cases despite the fact that the ghost-gluon vertex is different. This does not affect the one loop vertices since the differences cancel out. However, this is not the case for the MOMh scheme since the quartic ghost vertex contributes to the mapping for all α and in the Landau gauge case the differences in the ghost-gluon vertex are significant. However, the same increase and decrease of the ratio with α and N_f is parallel to that for the standard linear

covariant gauge fixing results of [52], despite the difference in the Λ-paramters for the MOMh scheme. This variation between the Λ-ratio corresponding to the MOMh scheme can be seen via direct comparison of Tables 3.3 and 4.1.

α	N_f	MOMg	MOMh	MOMq
0	0	3.3341	2.6588	2.1379
0	1	3.0543	2.6837	2.1277
0	2	2.7644	2.7123	2.1163
0	3	2.4654	2.7456	2.1032
0	4	2.1587	2.7846	2.0881
0	5	1.8471	2.8312	2.0706
1	0	2.8957	2.9893	1.9075
1	3	2.0751	3.1684	1.8296
1	4	1.7921	3.2505	1.7964
1	5	1.5088	3.3496	1.7581
3	3	1.8392	5.4177	1.3110
3	4	1.5732	5.8018	1.2533
-2	4	2.5437	2.6772	2.6597

Table 4.1: Values of $\frac{\Lambda_{\mathrm{MOMi}}}{\Lambda_{\overline{\mathrm{MS}}}}$ for the Curci-Ferrari gauge in $SU(3)$.

4.7 Discussion.

We make several remarks about our computation. Firstly, to summarize the three loop renormalization group functions of QCD gauge fixed in the Curci-Ferrari gauge have been derived for the three momentum subtraction schemes introduced originally in [91, 52]. All results at two and three loops for the MOMi schemes within this chapter are new. Obtaining these results required renormalizing the 3-point vertices at the non-exceptional symmetric momentum configuration at two loops and then, using properties of the renormalization group equation we were able to deduce the three loop anomalous dimensions and β-functions. The explicit form of the vertex functions to two loops, not only in the MOMi schemes but also in the $\overline{\mathrm{MS}}$ scheme, are useful for both lattice and Schwinger-Dyson analyses of the vertices. The coupling constant and gauge parameter mappings were constructed along with the conversion functions for each MOMi scheme. We also explicitly computed the Λ-parameters which, when compared with those in the linear covariant gauge gave us numerical insight in to the differences in the ghost-gluon vertex structure between gauges. The MOMq and MOMg scheme Λ-parameters remain unchanged. With renewed interest in gluon confinement,

analysis carried out in this Curci-Ferrari gauge fixing is of interest. Originally introduced as a possible alternative to models of vector boson mass, the model of [42] fell out of fashion with the development of the Standard Model and its loss of unitarity when a mass term for the gluon is present. It regained interest primarily as lattice and Schwinger-Dyson studies appear to give evidence for a gluon propagator which freezes in the infrared limit to a non-zero value. See, for example, [105, 106, 107, 108, 109, 110, 111, 112, 95, 96, 113, 114] for some early evidence of this property. This non-zero freezing has been notionally termed a gluon mass but this is misleading as that would imply that the gluon has a fundamental propagator for all momenta with a non-zero pole in p^2. If that were the case the gluon would not be a confined quantum. Instead one viewpoint is that the freezing is believed to be related to the Gribov copy problem, [115], and recent models use the Curci-Ferrari model in this respect to study the gluon's infrared dynamics, [116, 117, 118, 119, 120]. For studies where the gluon mass running is necessary we have provided the corresponding anomalous dimensions for the MOMi schemes in the Curci-Ferrari gauge. The results determined in this chapter are new and can be used as the foundations for future calculations in this gauge. The analysis of QCD gauge fixed in the Curci-Ferrari gauge provides a basis for studying the more involved maximal abelian gauge. The Curci-Ferrari gauge is strongly related to the MAG, which becomes apparent in the following chapter where the MAG is studied in the same schemes at one loop.

Chapter 5

The Maximal Abelian gauge

5.1 Introduction

The maximal abelian gauge (MAG) is interesting as it is thought that the low energy beheviour of QCD may be best described using an effective abelian theory, an idea first proposed by 't Hooft, [18, 19, 21, 20, 22]. It is thought that confinement may be best explained by the condensation of abelian monopoles originating from the diagonal elements of the colour group, [79], which is a Lie group, and that at low energies the behaviour of the diagonal and off-diagonal gluons may differ. Abelian monopoles are believed to dominate the infrared dynamics and for this analysis one has to have a way of making contact with the diagonal sector directly, [51]. It is for this reason that the maximal abelian gauge, [19, 21, 20, 121, 122], is appealing, as one of its underlying properties is to split the colour group into its diagonal and off-diagonal parts. The gluons corresponding to the diagonal parts are named diagonal, while those which are not part of this abelian subgroup are termed off-diagonal, [79, 51]. So in choosing the MAG, anyone focusing on this supposition will find results calculated in this gauge useful. Various lattice studies of the infrared support the hypothesis that the confinement mechanism is driven by abelian monopoles [18, 20, 19, 21, 22]. The off-diagonal gluons become massive leaving the abelian gluons as the relevant degrees of freedom in this regime. Therefore, simulations are carried out in this gauge where the gluon and ghost propagators are measured as well as the vertex functions. The results we obtain will assist with further study in these areas.

In a recent lattice study, [123], the effect of the diagonal gluons on the inter-quark static potential was investigated. Within the theoretical setup it was possible to identify the contributions made by the diagonal gluons to the potential. Within

the study it was claimed that excluding these contributions forced the linearly rising potential to collapse, indicating that the abelian sector was effectively responsible for quark confinement. The data was determined on the fine lattice, where the authors concluded that in studying this maximally abelian projection they had found that confinement is entirely kept in the abelian sector of QCD in the MAG. Although this and other similar research is interesting in studying the confinement mechanism, this lies beyond the scope of perturbation theory. The property of the MAG we are interested in here is its structure and relationship with other gauges. In particular the Landau gauge and the (non-linear) covariant Curci-Ferrari gauge. To assist with accurate lattice measurements, results need to match the ultraviolet behaviour, which we can compute in perturbation theory. This is where our motivation lies. In this chapter we provide the one loop analysis of QCD in the maximal abelian gauge at the symmetric subtraction point. This allows for the MAG to be studied both in the $\overline{\text{MS}}$ and MOMi schemes. The latter being the preferred scheme since it is a mass dependent renormalization scheme, meaning it is physical. With the one loop results computed the β-function and anomalous dimensions can be constructed, as in the previous chapters, to two loops for all MOMi schemes. In addition, we comment on the relationship between the MAG and the Curci-Ferrari gauge which we explored in the previous chapter.

5.2 Preliminaries

Having discussed the general background and formulation of the Lagrangian in Chapter 2 we use this section to point out the essential features of the MAG, which fundamentally differ from the previous gauges studied. To begin with let us discuss the structure of the colour group. The basic idea behind the maximal abelian gauge is to remove as many non-abelian degrees of freedom as possible by partially fixing the gauge, leaving the theory with a residual abelian gauge symmetry which is then gauge fixed separately. In the MAG it is usual to do this by decomposing the gauge field into its diagonal (or photonic) and off-diagonal parts

$$\begin{aligned} A_\mu &= A^A_\mu \mathrm{T}^A \\ \Rightarrow \quad A_\mu &= A^a_\mu \mathrm{T}^a + A^i_\mu \mathrm{T}^i \end{aligned} \tag{5.2.1}$$

where we have split the group generators into two sets, where i denotes the diagonal (centre or photonic) group elements and a denotes the off-diagonal group elements. The Faddeev-Popov ghost fields are also split in this manner. The index i labels the $(N_c - 1)$ generators T^i of the Cartan subalgebra of $SU(N_c)$. For example, consider the gauge group $SU(2)$ where, using the formula $N^2 - 1$ there are three generators. In this case $a = 1, 2$ would denote the off-diagonal generators with $i = 3$ being the only diagonal generator of $SU(2)$. The dimensions of these elements are $1 \leq i \leq N_A^d$ and $1 \leq a \leq N_a^o$ respectively. For an $SU(N_c)$ gauge group the diagonal components are $N_A^d = (N_c - 1)$ dimensional and the off-diagonal components are $N_A^o = (N_c^2 - 1) - (N_c - 1) = N_c(N_c - 1)$ dimensional such that the total number of generators is given by $N_A^o + N_A^d = N_A$, [79, 51]. Before constructing the Lagrangian we must first discuss the new group theory needed as a result of splitting the colour group. To determine the new identities we can rewrite the Jacobi identity, (2.1.7), using the symmetries of the structure constants (2.1.4). Firstly the structure constants are derived as

$$f^{aij} \;=\; 0 \;=\; f^{ijk} \,. \tag{5.2.2}$$

There are two new identities we must derive for the MAG, these are

$$f^{abi}f^{bjc} + f^{abj}f^{bci} \;=\; 0 \,, \tag{5.2.3}$$

$$f^{abc}f^{bdi} + f^{abd}f^{bic} + f^{abi}f^{bcd} \;=\; 0 \,. \tag{5.2.4}$$

For the first identity we can write (2.1.7) as

$$f^{Pai}f^{Pcj} + f^{Pac}f^{Pij} + f^{Paj}f^{Pic} \;=\; 0 \tag{5.2.5}$$

where the middle term drops out as a result of applying (2.1.6) to the diagonal counterparts

$$\begin{aligned} [T^i, T^j] = 0 \;\;&\Rightarrow\;\; if^{ijA}T^A \;=\; if^{ija}T^a + if^{ijk}T^k \\ &\Rightarrow\;\; if^{ija}T^a \;=\; 0 \end{aligned} \tag{5.2.6}$$

which in turn implies

$$f^{pai}f^{pcj} + f^{paj}f^{pic} \;=\; 0\,. \tag{5.2.7}$$

Another important property of (2.1.6) is

$$[T^a, T^j] \;=\; if^{ajc}T^c\,. \tag{5.2.8}$$

Now for the second identity, going back to our Jacobi identity, let $D = i$ and $A, B, C = a, b, c$ respectively, then (2.1.7) becomes

$$f^{Pab}f^{Pci} + f^{Pac}f^{Pib} + f^{Pai}f^{Pbc} \;=\; 0\,. \tag{5.2.9}$$

The only choice we have for P is to set it to be off-diagonal, otherwise we will have f^{Aij} in each term resulting in a trivial solution coming from (5.2.2). The second identity becomes

$$f^{pab}f^{pci} + f^{pac}f^{pib} + f^{pai}f^{pbc} \;=\; 0\,. \tag{5.2.10}$$

We also have the condition $f^{icd}f^{bcd} = 0$ which is a result of the Lie algebra (2.1.6),

$$\begin{aligned} f^{ACD}f^{BCD} &= C_A\delta^{AB} \\ f^{icd}f^{bcd} &= C_A\delta^{ib} \end{aligned} \tag{5.2.11}$$

where

$$C_A\delta^{ab} \;=\; f^{acd}f^{bcd} \;+\; 2f^{acj}f^{bcj} \tag{5.2.12}$$

and $\delta^{ib} = 0$ where

$$\delta^{AB} = \begin{pmatrix} \delta^{ij} & 0 \\ 0 & \delta^{ab} \end{pmatrix}.$$

Several other useful relations have been established using the Jacobi identity and the properties of the Lie algebra provided in chapter 2 which are detailed below. Written in terms of the dimension of the diagonal and off-diagonal elements by taking a contraction of (5.2.12) we have

$$f^{iab}f^{iab} \;=\; N_A^d C_A \quad , \quad f^{abc}f^{abc} \;=\; \left[N_A^o - 2N_A^d\right] C_A \tag{5.2.13}$$

where we recall N_A^d is the dimension of the diagonal and N_A^o is the dimension of the off-diagonal. Hence we have the following

$$f^{acj}f^{bcj} \;=\; \frac{N_A^d}{N_A^o}C_A\delta^{ab} \quad , \quad f^{acd}f^{bcd} \;=\; \frac{\left[N_A^o - 2N_A^d\right]C_A\delta^{ab}}{N_A^o} \tag{5.2.14}$$

which we extend using the Jacobi identity to establish the following useful relations

$$\begin{aligned} f^{apq}f^{bpr}f^{cqr} &= \frac{[N_A^o - 3N_A^d]}{2N_A^o}C_A f^{abc} \quad , \quad f^{apq}f^{bpi}f^{cqi} = \frac{N_A^d}{2N_A^o}C_A f^{abc} \\ f^{ipq}f^{bpr}f^{cqr} &= \frac{[N_A^o - 2N_A^d]}{2N_A^o}C_A f^{ibc} \quad , \quad f^{ipq}f^{bpj}f^{cqj} = \frac{N_A^d}{N_A^o}C_A f^{ibc} \end{aligned} \tag{5.2.15}$$

where p, q are off-diagonal indices here and are not the same p, q defined for the momentum. For the group generators, in addition to the relations discussed in chapter 3 we have

$$\mathrm{Tr}\left(T^aT^b\right) \;=\; T_F\delta^{ab} \quad , \quad \mathrm{Tr}\left(T^aT^i\right) \;=\; 0 \quad , \quad \mathrm{Tr}\left(T^iT^j\right) \;=\; T_F\delta^{ij} \tag{5.2.16}$$

as well as

$$T^iT^i \;=\; \frac{T_F}{N_F}N_A^d\mathbb{I} \quad , \quad T^aT^a \;=\; \left[C_F \;-\; \frac{T_F}{N_F}N_A^d\right]\mathbb{I} \tag{5.2.17}$$

where N_F is the dimension of the fundamental representation. N_F is defined by

$$N_F \;=\; \frac{\left[N_A^o + N_A^d\right]T_F}{C_F} \tag{5.2.18}$$

which will be used to simplify the algebra from the quark sector. These basic results and others have been coded within a FORM module and applied prior to the integrals being mapped to the basic topologies.

As $SU(3)$ is a non-abelian theory we can form a subgroup within $SU(3)$ made up of only abelian parts i.e. diagonal (centre) pieces. This can be demonstrated via the field strength tensor (2.1.30) which, due to this separation of diagonal and off-diagonal components decomposes to become

$$G_{\mu\nu} \;=\; G_{\mu\nu}^A T^A \;=\; G_{\mu\nu}^a T^a + G_{\mu\nu}^i T^i \tag{5.2.19}$$

with diagonal and off-diagonal parts given respectively as

$$G_{\mu\nu}^i \;=\; \partial_\mu A_\nu^i - \partial_\nu A_\mu^i + g f^{abi}A_\mu^a A_\nu^b \tag{5.2.20}$$

$$G^a_{\mu\nu} \;=\; D^{ab}_\mu A^b_\nu - D^{ab}_\nu A^b_\mu + g f^{abc} A^b_\mu A^c_\nu \,. \tag{5.2.21}$$

The covariant derivative is redefined as

$$D^{ab}_\mu \;\equiv\; \partial_\mu \delta^{ab} - g f^{abi} A^i_\mu \,. \tag{5.2.22}$$

Notice how the structure constants can contain a mix of both diagonal and off-diagonal components. We use the definition of the maximal abelian gauge to split the indices A into two sectors, diagonal, a, and off-diagonal, i, [79, 51], so in essence it is split into an abelian part and the rest of the algebra. Thus, taking the above into consideration, the Lagrangian contains two field strength tensors, one for each sector

$$\mathcal{L}^{\text{MAG}} = -\frac{1}{4}\mathrm{G}^a_{\mu\nu}\mathrm{G}^{a\,\mu\nu} - \frac{1}{4}\mathrm{G}^i_{\mu\nu}\mathrm{G}^{i\,\mu\nu} + i\bar{\psi}\gamma_\mu \mathrm{D}^\mu \psi + L^{\text{MAG}}_{\text{GF}} \tag{5.2.23}$$

where $L^{\text{MAG}}_{\text{GF}}$ is the gauge fixing term specific to the MAG, already presented in (2.1.52). It is useful, where possible, to write down the gauge fixing terms of the Lagrangian in terms of interpolating parameters. This serves many purposes. An interpolating gauge allows one to simultaneously calculate results for multiple gauge fixings whilst at the same time be able to compare results between the gauges by taking specific limits of these interpolating parameters. In [41] the authors present an interpolating gauge which connects the MAG to the Landau gauge. In this context we can rewrite $L^{\text{MAG}}_{\text{GF}}$ in the form

$$L^{\text{MAG}}_{\text{GF}} \;=\; \delta\bar{\delta}\left[\frac{1}{2}A^a_\mu A^{a\,\mu} \;+\; \frac{1}{2}\alpha\bar{c}^a c^a \;+\; \frac{1}{2}\zeta A^i_\mu A^{i\,\mu}\right] \;+\; (1-\zeta)\delta\left[\bar{c}^i \partial^\mu A^i_\mu\right] \tag{5.2.24}$$

where ζ is our interpolating parameter and α is the arbitrary gauge parameter. There is also a gauge parameter, α_p associated with the diagonal gluons which appears only in the quadratic term of the Lagrangian, see (5.2.27). It is necessary in order to construct the diagonal gluon propagator and is set to zero thereafter. Note here that we have chosen to neglect α_p in (5.2.24) since this gauge parameter neither appears in the Landau gauge nor (modified) MAG. The Landau gauge corresponds to $\alpha = 0$ and $\zeta = 1$, whereas the MAG corresponds to setting $\zeta = 0$ and $\alpha \neq 0$. Setting $\alpha = 0$ corresponds to the *true* (unmodified) MAG, however setting $\alpha = 0$ from the beginning results in the gauge being unrenormalizable, [40]. This is due to a factor of $\frac{1}{\alpha}$ appearing in the Feynman rule that directly affects one of our gluon diagrams, resulting in a zero-divisor when $\alpha = 0$. Therefore we keep α arbitrary until the very end, upon which a graphical analysis of our results

for the amplitudes can be made in the $\overline{\rm MS}$ scheme. The other reason we keep α and ζ arbitrary is so that checks can be made against results in the Landau gauge via interpolation. The objects $\delta, \bar{\delta}$ are BRST and anti-BRST transforms and the Lagrangian is fixed in a BRST-invariant way, as discussed in section 2.1.1. The BRST and anti-BRST transformations for the MAG are, [79],

$$\begin{aligned}
\delta A^a_\mu &= -\left(\partial_\mu c^a + g f^{ajc} A^j_\mu c^c + g f^{abc} A^b_\mu c^c + g f^{abk} A^b_\mu c^k\right) \\
\delta c^a &= g f^{abk} c^b c^k + \frac{1}{2} f^{abc} c^b c^c \quad , \quad \delta \bar{c}^a = b^a \quad , \quad \delta A^i_\mu = -\left(\partial_\mu c^i + g f^{ibc} A^b_\mu c^c\right) \\
\delta b^a &= 0 \quad , \quad \delta c^i = \frac{1}{2} g f^{ibc} c^b c^c \quad , \quad \delta \bar{c}^i = b^i \quad , \quad \delta b^i = 0
\end{aligned} \tag{5.2.25}$$

and

$$\begin{aligned}
\bar{\delta} A^a_\mu &= -\left(\partial_\mu c^a + g f^{ajc} A^j_\mu c^c + g f^{abc} A^b_\mu c^c + g f^{abk} A^b_\mu c^k\right) \\
\bar{\delta} c^a &= -b^a + g f^{abc} c^b \bar{c}^c + g f^{abk} c^b \bar{c}^k + g f^{abk} \bar{c}^b c^k \\
\bar{\delta} \bar{c}^a &= g f^{abk} \bar{c}^b \bar{c}^k + \frac{1}{2} g f^{abc} \bar{c}^b \bar{c}^c \quad , \quad \bar{\delta} b^a = -g f^{abc} b^b \bar{c}^c - g f^{abk} b^b \bar{c}^k + g f^{abk} \bar{c}^b b^k \ , \\
\bar{\delta} A^i_\mu &= -\left(\partial_\mu \bar{c}^i + g f^{ibc} A^b_\mu \bar{c}^c\right) \quad , \quad \bar{\delta} c^i = -b^i + g f^{ibc} c^b \bar{c}^c \\
\bar{\delta} \bar{c}^i &= \frac{1}{2} g f^{ibc} \bar{c}^b \bar{c}^c \quad , \quad \bar{\delta} b^i = -g f^{ibc} b^b \bar{c}^c \ .
\end{aligned} \tag{5.2.26}$$

Note that the b^i field re-introduces α_p which we set to zero throughout, apart from where it contributes to the quadratic term in the final Lagrangian since this allows us to derive the Feynman rule for the photonic gluon propagator. Therefore the MAG gauge fixed Lagrangian, generated by a FORM procedure so as to avoid errors, is

$$\begin{aligned}
L^{\rm MAG}_{\rm GF} &= -\frac{1}{2\alpha}\left(\partial^\mu A^a_\mu\right)^2 - \frac{1}{2\alpha_p}\left(\partial^\mu A^i_\mu\right)^2 + \bar{c}^a \partial^\mu \partial_\mu c^a + \bar{c}^i \partial^\mu \partial_\mu c^i \\
&\quad + g\left[(1-\zeta) f^{abk} A^a_\mu \bar{c}^k \partial^\mu c^b - \zeta f^{abk} A^a_\mu \partial^\mu c^b \bar{c}^k - f^{abc} A^a_\mu \bar{c}^b \partial^\mu c^c - \zeta f^{abk} A^a_\mu \bar{c}^b \partial^\mu c^k \right. \\
&\qquad - \frac{(1-\zeta)}{\alpha} f^{abk} \partial^\mu A^a_\mu A^b_\nu A^{k\,\nu} - f^{abk} \partial^\mu A^a_\mu c^b \bar{c}^k - \frac{1}{2} f^{abc} \partial^\mu A^a_\mu \bar{c}^b c^c \\
&\qquad \left. - (2-\zeta) f^{abk} A^k_\mu \bar{c}^a \partial^\mu \bar{c}^b - f^{abk} \partial^\mu A^k_\mu \bar{c}^b c^c \right] \\
&\quad + g^2 \left[(1-\zeta) f^{acbd}_d A^a_\mu A^{b\,\mu} \bar{c}^c c^d - \frac{(1-\zeta)^2}{2\alpha} f^{akbl}_o A^a_\mu A^{b\,\mu} A^k_\nu A^{l\,\nu} \right. \\
&\qquad + (1-\zeta) f^{adcj}_o A^a_\mu A^{j\,\mu} \bar{c}^c c^d - \frac{(1-\zeta)}{2} f^{ajcd}_o A^a_\mu A^{j\,\mu} \bar{c}^c c^d \\
&\qquad + (1-\zeta) f^{ajcl}_o A^a_\mu A^{j\,\mu} \bar{c}^c c^l + (1-\zeta) f^{alcj}_o A^a_\mu A^{j\,\mu} \bar{c}^c c^l \\
&\qquad \left. - (1-\zeta) f^{cjdi}_o A^i_\mu A^{j\,\mu} \bar{c}^c c^d - \frac{\alpha}{4} f^{abcd}_d \bar{c}^a \bar{c}^b c^c c^d - \frac{\alpha}{8} f^{abcd}_o \bar{c}^a \bar{c}^b c^c c^d \right.
\end{aligned}$$

$$+\frac{\alpha}{8}f_o^{acbd}\bar{c}^a\bar{c}^b c^c c^d - \frac{\alpha}{4}f_o^{abcl}\bar{c}^a\bar{c}^b c^c c^l + \frac{\alpha}{4}f_o^{acbl}\bar{c}^a\bar{c}^b c^c c^l$$
$$-\frac{\alpha}{4}f_o^{albc}\bar{c}^a\bar{c}^b c^c c^l + \frac{\alpha}{2}f_o^{akbl}\bar{c}^a\bar{c}^b c^k c^l \Big] \tag{5.2.27}$$

where it is understood that α_p, which is distinct from α, is set to zero after our renormalization, [79, 51]. This means that the diagonal gluons are fixed in the Landau gauge. Note here that we have introduced the shorthand notation

$$f_d^{ABCD} = f^{iAB}f^{iCD} \quad , \quad f_o^{ABCD} = f^{eAB}f^{eCD} \tag{5.2.28}$$

for the diagonal and off-diagonal quartic interaction terms respectively, where

$$f^{ABCD} + f^{ACDB} + f^{ADBC} = 0 \, . \tag{5.2.29}$$

This Lagrangian is fully renormalizable and the Feynman rules generated from it are given in Appendix C where in addition to the quartic ghost interaction which we encountered in the Curci-Ferrari gauge, the MAG includes quartic ghost-gluon interactions. In addition to the standard QCD definitions of the renormalization constants (2.1.55) we have the definitions for the photonic fields, interpolating parameter and gauge parameter, α_p, specific to the MAG. The renormalization procedure is repeated with the full set of renormalization constants defined by

$$\begin{aligned}
A^{a\,\mu}_{\rm o} &= \sqrt{Z_A}\, A^{a\,\mu} \quad , \quad A^{i\,\mu}_{\rm o} = \sqrt{Z_{A^i}}\, A^{i\,\mu} \quad , \quad c^a_{\rm o} = \sqrt{Z_c}\, c^a \quad , \quad \bar{c}^a_{\rm o} = \sqrt{Z_c}\, \bar{c}^a \, , \\
c^i_{\rm o} &= \sqrt{Z_{c^i}}\, c^i \quad , \quad \bar{c}^i_{\rm o} = \sqrt{Z_{\bar{c}^i}}\bar{c}^i \quad , \quad \psi_{\rm o} = \sqrt{Z_\psi}\psi \quad , \quad g_{\rm o} = \mu^\epsilon Z_g\, g \, , \\
\alpha_{\rm o} &= Z_\alpha^{-1} Z_A\, \alpha \quad , \quad \alpha_{p_{\rm o}} = Z_{\alpha^i}^{-1} Z_{A^i}\, \alpha_p \quad , \quad \zeta_{\rm o} = Z_\zeta \zeta
\end{aligned} \tag{5.2.30}$$

where the index i on objects in the subscript is to indicate the diagonal sector and is not summed over. By splitting the Lie algebra into its diagonal and off-diagonal components the Slavnov-Taylor identities, that we would usually apply to our calculations to ensure that the renormalization constants are correct, differ slightly from those of the linear and Curci-Ferrari gauges. A derivation of the Slavnov-Taylor identities for the MAG using algebraic renormalization is given in [40, 41]. The idea underlying this procedure for constructing the relations between the renormalization constants is as follows. Briefly the authors of [40, 41] begin by writing down the complete action (Σ) in terms of external sources introduced to couple to the BRST-invariant fields. Under the condition that the action remains BRST invariant a Ward identity emerges. Generalizing this Ward identity to all orders of perturbation theory is achieved by assuming that the same Ward identity

satisfied by the action (Σ) will also apply to a perturbed action ($\Sigma + \Sigma^{\text{counterterms}}$), where $\Sigma^{\text{counterterms}}$ is a complete set of the most general invariant counterterms that can be added to the classical action (Σ). This, in essence forces certain conditions on both sides of the equation

$$\Sigma(g, \alpha, \phi, \dots) \; + \; \Sigma^{\text{counterterms}} \; = \; \Sigma(g_0, \alpha_0, \phi_0, \dots) \tag{5.2.31}$$

with the fields $\phi \in (A^a, A^i, c^a, \bar{c}^a, c^i, \bar{c}^i, b^a, b^i)$. This in turn gives us the corresponding relationships between the bare and renormalized fields, gauge parameter and coupling constant. Observing what we had (5.2.30) with what we now have for the photonic (diagonal) gluon and photonic ghost we see that the following Slavnov-Taylor identities emerge, [40, 41],

$$Z_{\bar{c}^i} Z_{c^i} \;=\; 1 \tag{5.2.32}$$

$$Z_{A^i}^{\frac{1}{2}} Z_g \;=\; 1 \tag{5.2.33}$$

where Z_{A^i} is the renormalization constant for the photonic gluon and Z_{c^i} and $Z_{\bar{c}^i}$ are the renormalization constants for the photonic ghost and anti-ghost. The second of our Slavnov-Taylor identities, (5.2.33), is similar to that arising in the background field gauge, [124, 125], which one would expect since the background field method is to split the gauge field into the background field and the quantum field. Similar to how the MAG is split into its diagonal and off-diagonal parts, the diagonal gluons play a similar role to the background gluons of the background field gauge. The Slavnov-Taylor identity (5.2.33) in the MAG gives rise to the relationship between γ_{A^i} and the β-function. Again, this strongly correlates with the background field method where the relationship $\beta^{\text{BFG}}(\mu) = g(\mu)\gamma_B^{\text{BFG}}(\alpha)$ holds, where $\gamma_B(\alpha)$ is the anomalous dimension for the background gluon field B, [124, 125]. In the MAG a similar identity is true

$$\beta_{\text{MOMi}}(a, \mu) = a_{\text{MOMi}}(\mu)\gamma_{A^i}^{\text{MOMi}}(a, \alpha) \tag{5.2.34}$$

in our convention for the coupling constant. Notice that if we look at the $\mathcal{O}(g)$ pieces in the Lagrangian alone we can pick out the 9 vertices, which, when choosing $\zeta = 0$ cancel down to just 6 vertices

$$\begin{aligned} L_{\text{GF}}^{\text{MAG}} \;=\; & -\frac{1}{2\alpha}\left(\partial^\mu A_\mu^a\right)^2 - \frac{1}{2\alpha_p}\left(\partial^\mu A_\mu^i\right)^2 + \bar{c}^a \partial^\mu \partial_\mu c^a + \bar{c}^i \partial^\mu \partial_\mu c^i \\ & + g\left[f^{abk} A_\mu^a \bar{c}^k \partial^\mu c^b - f^{abc} A_\mu^a \bar{c}^b \partial^\mu c^c \right. \end{aligned}$$

$$- \frac{1}{\alpha} f^{abk} \partial^\mu A^a_\mu A^b_\nu A^{k\,\nu} - f^{abk} \partial^\mu A^a_\mu c^b \bar{c}^k - \frac{1}{2} f^{abc} \partial^\mu A^a_\mu \bar{c}^b c^c$$
$$- 2 f^{abk} A^k_\mu \bar{c}^a \partial^\mu \bar{c}^b - f^{abk} \partial^\mu A^k_\mu \bar{c}^b c^c \big] \qquad (5.2.35)$$

where the sixth comes from the $i\bar{\psi}\gamma_\mu \mathrm{D}^\mu \psi$ piece in the full Lagrangian. This means that there are potentially 6 MOMi schemes, each based on one of the vertices.

The off-diagonal sector of the MAG corresponds to QCD fixed in the Curci-Ferrari gauge, [126], except that in the Curci-Ferrari gauge the off-diagonal sector corresponds to the full colour group. This can be seen by removing the diagonal parts from L^{MAG}, where the resulting Lagrangian is simply that fixed in the Curci-Ferrari gauge, (4.1.1). Clearly both Lagrangians (4.1.1) and (5.2.35) include quartic ghost interactions. Again, we reiterate from the previous chapter that whilst ordinarily an abelian gauge theory does not have coupled ghosts this statement only applies to the case where the gauge fixing is linear. For instance in the 't Hooft-Veltman gauge in QED, [127], there are interacting Faddeev-Popov ghosts. The situation is the same with the Curci-Ferrari gauge and here with the MAG that the non-linear gauge fixings produce interacting ghost terms. The ghost terms coupling in this non-trivial way does not spoil renormalization.

Taking the naive view that there could possibly be more MOMi schemes for the MAG due to its construction, we initially computed all the one loop diagrams for all possible combinations of the vertex, as shown in Table 5.1, where only eight of the vertices produced tree diagrams. It was not until we began our renormalization procedure that we realised there was a contradiction in defining the renormalization constants; they did not satisfy the Slavnov-Taylor identities (5.2.32) and (5.2.33). The Slavnov-Taylor identities render the vertices involving diagonal gluons effectively trivial. Applying the Slavnov-Taylor identities to the MOMi scheme vertices we see that the condition $Z_{A^i} Z_g^2 = 1$ implies that there are no photonic vertices. We can see this specifically in the $A^i \bar{\psi} \psi$ vertex as it contains the factor $\sqrt{Z_{A^i}} Z_g Z_\psi$ and as $\sqrt{Z_{A^i}} Z_g = 1$, this implies that we must fix both Z_{A^i} and Z_g. However, we already have Z_{A^i} set from our 2-point calculations and so we cannot change this for each different vertex structure as we would end up with several different values for Z_{A^i}, which is not correct. So our possible 6 MOMi schemes collapse down to the three we are familiar with; the MOMh, MOMg, and MOMq schemes. No new MOMi schemes other than those for the ghost-gluon, triple-gluon and quark-gluon vertex functions are introduced via a MAG gauge fixing.

Green's Function	Number of one loop diagrams
$A^a_\mu \bar{c}^i c^b$	5
$A^a_\mu A^b_\nu A^c_\sigma$	23
$A^a_\mu A^b_\nu A^i_\sigma$	18
$A^a_\mu \psi\bar{\psi}$	5
$A^i_\mu \psi\bar{\psi}$	3
$A^a_\mu \bar{c}^b c^d$	16
$A^a_\mu \bar{c}^b c^i$	9
$A^i_\mu \bar{c}^a c^b$	11
$A^i_\mu A^j_\nu A^k_\sigma$	11
$A^a_\mu A^i_\nu A^j_\sigma$	11
$A^a_\mu \bar{c}^i c^j$	2
$A^i_\mu \bar{c}^j c^a$	3
$A^i_\mu \bar{c}^a c^j$	5
$A^i_\mu \bar{c}^j c^k$	3
Total:	125

Table 5.1: Number of 3-point vertex diagrams calculated in the MAG for all possible vertices

5.3 $\overline{\rm MS}$ scheme

Since we only consider the MAG at one loop due to the complexity of the gauge fixing we present all results within this chapter analytically, since at one-loop order the results are more compact than those calculated in the arbitrary (linear) covariant gauge and the Curci-Ferrari gauge at two and three loops. We begin by reporting our renormalization constants in the $\overline{\rm MS}$ scheme. These are

$$
\begin{aligned}
Z_g(\alpha,\zeta,\alpha_p)\Big|_{\overline{\rm MS}} &= 1 + \left[C_A\left(-\frac{11}{6}\right) + \frac{2}{3}T_F N_f\right]\frac{a}{\epsilon} \;+\; \mathcal{O}(a^2) \\
Z_A(\alpha,\zeta,\alpha_p)\Big|_{\overline{\rm MS}} &= 1 + \left[C_A\left(-\frac{\alpha}{2} + \frac{13}{6} + \frac{\alpha N^d_A}{2N^o_A} + \frac{\alpha_p \zeta N^d_A}{2N^o_A} - \frac{\alpha_p N^d_A}{N^o_A} + \frac{3\zeta N^d_A}{2N^o_A}\right.\right. \\
&\qquad \left.\left. -\frac{3N^d_A}{2N^o_A}\right) - \frac{4}{3}N_f T_F\right]\frac{a}{\epsilon} \;+\; \mathcal{O}(a^2) \\
Z_{A^i}(\alpha,\zeta,\alpha_p)\Big|_{\overline{\rm MS}} &= 1 + \left[-\frac{4}{3}N_f T_F + C_A\left(\frac{11}{3} - \frac{\alpha_p\zeta}{2} - \frac{3\zeta}{2}\right)\right]\frac{a}{\epsilon} \;+\; \mathcal{O}(a^2) \\
Z_\alpha(\alpha,\zeta,\alpha_p)\Big|_{\overline{\rm MS}} &= 1 + \left[C_A\left(\frac{3N^d_A}{\alpha N^o_A}(\zeta-1) - \frac{3\alpha\zeta N^d_A}{2N^o_A} + \frac{\alpha N^d_A}{N^o_A} - \frac{\alpha}{4} + \frac{\alpha_p\zeta N^d_A}{2N^o_A}\right.\right. \\
&\qquad \left.\left. + \frac{\alpha_p\zeta^2 N^d_A}{2N^o_A} - \frac{\alpha_p N^d_A}{N^o_A} - \frac{3\zeta N^d_A}{N^o_A} + \frac{3\zeta^2 N^d_A}{2N^o_A} + \frac{3N^d_A}{2N^o_A}\right)\right]\frac{a}{\epsilon} \\
&\quad + \mathcal{O}(a^2)
\end{aligned}
$$

$$
\begin{aligned}
Z_{\alpha_p}(\alpha,\zeta,\alpha_p)\Big|_{\overline{\rm MS}} &= 1 \;+\; \mathcal{O}(a^2) \\
Z_c(\alpha,\zeta,\alpha_p)\Big|_{\overline{\rm MS}} &= 1 + \left[\frac{C_A}{4}\left(3-\alpha-\frac{3\alpha\zeta N_A^d}{N_A^o}+\frac{2\alpha N_A^d}{N_A^o}+\frac{4\alpha_p\zeta N_A^d}{N_A^o}-\frac{\alpha_p\zeta^2 N_A^d}{N_A^o}\right.\right. \\
&\qquad \left.\left. -\frac{4\alpha_p N_A^d}{N_A^o}-\frac{9\zeta N_A^d}{N_A^o}+\frac{3\zeta^2 N_A^d}{N_A^o}+\frac{6N_A^d}{N_A^o}\right)\right]\frac{a}{\epsilon} \;+\; \mathcal{O}(a^2) \\
Z_{c^i}^{\overline{\rm MS}}(\alpha,\zeta,\alpha_p) &= 1 + \left[C_A\zeta\left(\frac{\alpha}{4}+\frac{3}{4}\right)\right]\frac{a}{\epsilon} \;+\; \mathcal{O}(a^2) \\
Z_{\psi}(\alpha,\zeta,\alpha_p)\Big|_{\overline{\rm MS}} &= 1 + \left[-\alpha C_F + T_F\left(-\frac{\alpha N_A^o}{N_c}+\frac{\alpha_p N_A^o}{N_c}\right)\right]\frac{a}{\epsilon} \;+\; \mathcal{O}(a^2)\;. \qquad (5.3.36)
\end{aligned}
$$

where we have displayed results in terms of the gauge parameters α and α_p for demonstration purposes. Here c^i is the label for the photonic ghost, A^i the photonic gluon, A^a the off-diagonal gluon, c^a the off-diagonal ghost and ψ the quark. With the conditions, $\alpha \neq 0$, $\alpha_p = 0$ and $\zeta = 0$, as we discussed earlier the renormalization constants for the (modified) MAG are given by

$$
\begin{aligned}
Z_g(\alpha,0,0)\Big|_{\overline{\rm MS}} &= 1 + \left[-\frac{11}{6}C_A+\frac{2}{3}T_F N_f\right]\frac{a}{\epsilon} \;+\; \mathcal{O}(a^2) \\
Z_A(\alpha,0,0)\Big|_{\overline{\rm MS}} &= 1 + \left[C_A\left(-\frac{\alpha}{2}+\frac{13}{6}+\frac{\alpha N_A^d}{2N_A^o}-\frac{3N_A^d}{2N_A^o}\right)-\frac{4}{3}N_f T_F\right]\frac{a}{\epsilon} \;+\; \mathcal{O}(a^2) \\
Z_{A^i}(\alpha,0,0)\Big|_{\overline{\rm MS}} &= 1 + \left[-\frac{4}{3}N_f T_F+\frac{11}{3}C_A\right]\frac{a}{\epsilon} \;+\; \mathcal{O}(a^2) \\
Z_{\alpha}(\alpha,0,0)\Big|_{\overline{\rm MS}} &= 1 + \left[C_A\left(\frac{3N_A^d}{\alpha N_A^o}+\frac{\alpha N_A^d}{N_A^o}-\frac{\alpha}{4}+\frac{3N_A^d}{2N_A^o}\right)\right]\frac{a}{\epsilon} \;+\; \mathcal{O}(a^2) \\
Z_{\alpha_p}(\alpha,0,0)\Big|_{\overline{\rm MS}} &= 1 \;+\; \mathcal{O}(a^2) \\
Z_c(\alpha,0,0)\Big|_{\overline{\rm MS}} &= 1 + \left[\frac{C_A}{4}\left(3-\alpha+\frac{2\alpha N_A^d}{N_A^o}+\frac{6N_A^d}{N_A^o}\right)\right]\frac{a}{\epsilon} \;+\; \mathcal{O}(a^2) \\
Z_{c^i}(\alpha,0,0)\Big|_{\overline{\rm MS}} &= 1 \;+\; \mathcal{O}(a^2) \\
Z_{\psi}(\alpha,0,0)\Big|_{\overline{\rm MS}} &= 1 + \left[-\alpha C_F-\frac{\alpha N_A^o}{N_c}T_F\right]\frac{a}{\epsilon} \;+\; \mathcal{O}(a^2)\;. \qquad (5.3.37)
\end{aligned}
$$

From these we can see that the Slavnov-Taylor identity (5.2.33) holds. For example, in the $\overline{\rm MS}$ scheme we have the following

$$
Z_{A^i} Z_g^2 = 1\;. \qquad (5.3.38)
$$

This is the same as saying $z_{A_1^i} = -2z_{g1}$. For $\overline{\text{MS}}$ we have above

$$\begin{aligned} z_{A_1^i}(\alpha_p,\zeta)\Big|_{\overline{\text{MS}}} &= -\frac{4}{3}N_f T_F + C_A\left(\frac{11}{3} - \frac{\alpha_p\zeta}{2} - \frac{3\zeta}{2}\right) \\ z_{g_1}(\alpha_p,\zeta)\Big|_{\overline{\text{MS}}} &= -\frac{11}{6}C_A + \frac{2}{3}T_F N_f \end{aligned} \tag{5.3.39}$$

which, when setting the MAG conditions $\zeta = 0, \alpha_p = 0$, gives

$$\begin{aligned} z_{A_1^i}(\alpha,0,0)\Big|_{\overline{\text{MS}}} &= -\frac{4}{3}N_f T_F + \frac{11}{3}C_A \\ z_{g_1}(\alpha,0,0)\Big|_{\overline{\text{MS}}} &= -\frac{11}{6}C_A + \frac{2}{3}T_F N_f \end{aligned} \tag{5.3.40}$$

which implies $z_{A_1^i} = -2z_{g1}$. This means that the Slavnov-Taylor identity holds in $\overline{\text{MS}}$, which we need in order to preserve gauge invariance. The reason for introducing the interpolating parameter ζ into our Lagrangian (5.2.27) was so that a comparison of results can be made in the Landau gauge. Specifically, when taking the Landau limit the renormalization constant for the off-diagonal gluon should equal that of the diagonal gluon and likewise for the diagonal and off-diagonal ghosts. Setting $\alpha_p = 0$, $\zeta = 1$ and $\alpha = 0$ we can make a Landau gauge check between these renormalization constants

$$\begin{aligned} Z_g(0,1,0)\Big|_{\overline{\text{MS}}} &= 1 + \left[-\frac{11}{6}C_A + \frac{2}{3}T_F N_f\right]\frac{a}{\epsilon} + \mathcal{O}(a^2) \\ Z_A(0,1,0)\Big|_{\overline{\text{MS}}} &= 1 + \left[\frac{13}{6}C_A - \frac{4}{3}N_f T_F\right]\frac{a}{\epsilon} + \mathcal{O}(a^2) \\ Z_{A^i}(0,1,0)\Big|_{\overline{\text{MS}}} &= 1 + \left[-\frac{4}{3}N_f T_F + \frac{13}{6}C_A\right]\frac{a}{\epsilon} + \mathcal{O}(a^2) \\ Z_\alpha(0,1,0)\Big|_{\overline{\text{MS}}} &= 1 + \mathcal{O}(a^2) \\ Z_{\alpha_p}(0,1,0)\Big|_{\overline{\text{MS}}} &= 1 + \mathcal{O}(a^2) \\ Z_c(0,1,0)\Big|_{\overline{\text{MS}}} &= 1 + \left[\frac{3C_A}{4}\right]\frac{a}{\epsilon} + \mathcal{O}(a^2) \\ Z_{c_i}(0,1,0)\Big|_{\overline{\text{MS}}} &= 1 + \left[\frac{3}{4}C_A\right]\frac{a}{\epsilon} + \mathcal{O}(a^2) \\ Z_\psi(0,1,0)\Big|_{\overline{\text{MS}}} &= 1 + \mathcal{O}(a^2)\ . \end{aligned} \tag{5.3.41}$$

Because of the $(\zeta - 1)$ term complementing the factor of $\frac{1}{\alpha}$ in Z_α we are able to take the Landau limit, where $\alpha \to 0$. Using this check we can see that the MAG renormalization constants in the Landau gauge agree with those in the arbitrary

(linear) covariant gauge in the same limit for the $\overline{\rm MS}$ scheme. Also that the off-diagonal and diagonal counterparts match on to each other. The interpolating parameters have allowed us to check the correctness of both the renormalization constants and our programming. Now that we have made this check on our results the interpolating parameters have served their purpose and are no longer needed, therefore we record all future results in the traditional (modified) MAG with

$$\zeta \;=\; \alpha_p \;=\; 0 \;, \quad \alpha \;\neq\; 0 \;. \tag{5.3.42}$$

Essentially the diagonal gluons, corresponding to the subgroup of generators which totally commute, are fixed in the Landau gauge, [67]. Our results for the renormalization constants will be used to determine the renormalization group functions as well as the conversion functions later on. As a preliminary to the MOMi scheme computations we first record the results for the amplitudes in the $\overline{\rm MS}$ scheme, since this is the basic reference scheme. Indeed to deduce the two loop MOMi scheme renormalization group functions using the conversion functions, the two loop $\overline{\rm MS}$ results are necessary. Therefore, for completeness we note that these are, [14, 21],

$$\begin{aligned}
\gamma_A^{\overline{\rm MS}}(a,\alpha) \;&=\; \frac{1}{6N_A^o}\left[N_A^o\left((3\alpha-13)C_A+8T_FN_f\right)+N_A^d(-3\alpha+9)C_A\right]a \\
&\quad+\frac{1}{48N_A^{o2}}\left[N_A^{o2}\left((6\alpha^2+66\alpha-354)C_A^2+240C_AT_FN_f+192C_FT_FN_f\right)\right. \\
&\qquad\qquad+\;N_A^oN_A^d\left((3\alpha^2+210\alpha+331)C_A^2-80C_AT_FN_f\right) \\
&\qquad\qquad\left.+\;N_A^{d2}\left(15\alpha^2-6\alpha-33\right)C_A^2\right]a^2 \;+\; \mathcal{O}(a^3) \\
\gamma_{A^i}^{\overline{\rm MS}}(a) \;&=\; \frac{1}{3}\left[4T_FN_f-11C_A\right]a \\
&\quad+\;\frac{1}{3}\left[-\;34C_A^2+20C_AT_FN_f+12C_FT_FN_f\right]a^2 \;+\; \mathcal{O}(a^3) \\
\gamma_\alpha^{\overline{\rm MS}}(a,\alpha) \;&=\; \frac{1}{12\alpha N_A^o}\left[N_A^o\left((-\;3\alpha^2+26\alpha)C_A-16\alpha T_FN_f\right)\right. \\
&\qquad\qquad\left.+N_A^d(-\;6\alpha^2-36\alpha-36)C_A\right]a \\
&\quad+\;\frac{1}{48\alpha N_A^{o2}}\left[N_A^{o2}\left((-\;3\alpha^3-51\alpha^2+354\alpha)C_A^2-240\alpha C_AT_FN_f\right.\right. \\
&\qquad\qquad\left.-192\alpha C_FT_FN_f\right) \\
&\qquad\qquad+\;N_A^oN_A^d\left((-\;27\alpha^3-339\alpha^2-647\alpha-928)C_A^2\right. \\
&\qquad\qquad\qquad\left.+\;(160\alpha+512)C_AT_FN_f\right) \\
&\qquad\qquad\left.+\;N_A^{d2}(-\;30\alpha^3-366\alpha^2+294\alpha+2016)C_A^2\right]a^2
\end{aligned}$$

$$
\begin{aligned}
& + \mathcal{O}(a^3) \\
\gamma_c^{\overline{\rm MS}}(a,\alpha) &= \frac{1}{4N_A^o}\left[N_A^o(\alpha-3)C_A + N_A^d(-2\alpha-6)C_A\right] a \\
&+ \frac{1}{96N_A^{o2}}\left[N_A^{o2}\left((6\alpha^2-6\alpha-190)C_A^2 + 80C_AT_FN_f\right)\right. \\
&\qquad + N_A^oN_A^d\left((-42\alpha^2-126\alpha-347)C_A^2 + 160C_AT_FN_f\right) \\
&\qquad \left. + N_A^{d2}(12\alpha^2-588\alpha+510)C_A^2\right] a^2 \; + \; \mathcal{O}(a^3) \\
\gamma_{c^i}^{\overline{\rm MS}}(a,\alpha) &= \frac{1}{4N_A^o}\left[N_A^o(-\alpha-3)C_A + N_A^d(-2\alpha-6)C_A\right] a \\
&+ \frac{1}{96N_A^{o2}}\left[N_A^{o2}\left((-6\alpha^2-66\alpha-190)C_A^2 + 80C_AT_FN_f\right)\right. \\
&\qquad + N_A^oN_A^d\left((-54\alpha^2-354\alpha-323)C_A^2 + 160C_AT_FN_f\right) \\
&\qquad \left. + N_A^{d2}(-60\alpha^2-372\alpha+510)C_A^2\right] a^2 \; + \; \mathcal{O}(a^3) \\
\gamma_\psi^{\overline{\rm MS}}(a,\alpha) &= \frac{\alpha N_A^oT_F}{N_F}a \\
&+ \frac{1}{4N_F}\left[(-\alpha^2+22\alpha+23)C_AC_FN_F + (\alpha^2-14\alpha+2)N_A^oC_AT_F\right. \\
&\qquad \left. - 6C_F^2N_F - 8C_FN_fT_FN_F\right] a^2 \; + \; \mathcal{O}(a^3) \; . \qquad (5.3.43)
\end{aligned}
$$

Though the three loop results are also available, [21]. Next, the full one loop amplitudes for each of the three vertex functions computed in $\overline{\rm MS}$ are

$$
\begin{aligned}
\Sigma_{(1)}^{\rm ccg}(p,q)\Big|_{\overline{\rm MS}} &= -\; \Sigma_{(2)}^{\rm ccg}(p,q)\Big|_{\overline{\rm MS}} \\
&= -\frac{1}{2} - \left[18\psi'(\tfrac{1}{3})\alpha N_A^d - 6\psi'(\tfrac{1}{3})\alpha N_A^o - 33\psi'(\tfrac{1}{3})N_A^d + 15\psi'(\tfrac{1}{3})N_A^o\right. \\
&\qquad -12\alpha N_A^d\pi^2 - 27\alpha N_A^d + 4\alpha N_A^o\pi^2 + 27\alpha N_A^o + 22N_A^d\pi^2 \\
&\qquad \left. +27N_A^d - 10N_A^o\pi^2 + 81N_A^o\right]\frac{C_Aa}{216N_A^o} \; + \; \mathcal{O}(a^2) \qquad (5.3.44)
\end{aligned}
$$

for the ghost-gluon vertex. For the triple gluon vertex the amplitudes are

$$
\begin{aligned}
\Sigma_{(1)}^{\rm ggg}(p,q)\Big|_{\overline{\rm MS}} &= \Sigma_{(2)}^{\rm ggg}(p,q)\Big|_{\overline{\rm MS}} \; = \; -\frac{1}{2}\,\Sigma_{(3)}^{\rm ggg}(p,q)\Big|_{\overline{\rm MS}} \; = \; -\; \Sigma_{(4)}^{\rm ggg}(p,q)\Big|_{\overline{\rm MS}} \\
&= \frac{1}{2}\,\Sigma_{(5)}^{\rm ggg}(p,q)\Big|_{\overline{\rm MS}} \; = \; -\; \Sigma_{(6)}^{\rm ggg}(p,q)\Big|_{\overline{\rm MS}} \\
&= -1 + \left[-72\psi'(\tfrac{1}{3})\alpha^2C_AN_A^d + 36\psi'(\tfrac{1}{3})\alpha^2C_AN_A^o + 90\psi'(\tfrac{1}{3})\alpha C_AN_A^d\right. \\
&\qquad -162\psi'(\tfrac{1}{3})\alpha C_AN_A^o - 702\psi'(\tfrac{1}{3})C_AN_A^d + 138\psi'(\tfrac{1}{3})C_AN_A^o \\
&\qquad -384\psi'(\tfrac{1}{3})N_fN_A^oT_F - 81\alpha^3C_AN_A^d + 27\alpha^3C_AN_A^o \\
&\qquad +48\pi^2\alpha^2C_AN_A^d + 810\alpha^2C_AN_A^d - 24\pi^2\alpha^2C_AN_A^o \\
&\qquad \left. -405\alpha^2C_AN_A^o - 60\pi^2\alpha C_AN_A^d + 243\alpha C_AN_A^d\right.
\end{aligned}
$$

$$
\begin{aligned}
&+108\pi^2\alpha C_A N_A^o - 243\alpha C_A N_A^o + 468\pi^2 C_A N_A^d \\
&+2916 C_A N_A^d - 92\pi^2 C_A N_A^o - 243 C_A N_A^o + 256\pi^2 N_f N_A^o T_F \\
&+1296 N_f N_A^o T_F] \, \frac{a}{648 N_A^o} \; + \; \mathcal{O}(a^2)
\end{aligned}
$$

$$
\begin{aligned}
\Sigma^{\rm ggg}_{(7)}(p,q)\Big|_{\overline{\rm MS}} &= 2\,\Sigma^{\rm ggg}_{(9)}(p,q)\Big|_{\overline{\rm MS}} \;=\; -\,2\,\Sigma^{\rm ggg}_{(11)}(p,q)\Big|_{\overline{\rm MS}} \;=\; -\,\Sigma^{\rm ggg}_{(14)}(p,q)\Big|_{\overline{\rm MS}} \\
&= -\big[108\psi'(\tfrac{1}{3})\alpha^5 C_A N_A^d - 36\psi'(\tfrac{1}{3})\alpha^5 C_A N_A^o - 324\psi'(\tfrac{1}{3})\alpha^4 C_A N_A^d \\
&\quad +162\psi'(\tfrac{1}{3})\alpha^4 C_A N_A^o + 324\psi'(\tfrac{1}{3})\alpha^3 C_A N_A^d - 108\psi'(\tfrac{1}{3})\alpha^3 C_A N_A^o \\
&\quad +1296\psi'(\tfrac{1}{3})\alpha^2 C_A N_A^d - 456\psi'(\tfrac{1}{3})\alpha^2 C_A N_A^o \\
&\quad +768\psi'(\tfrac{1}{3})\alpha^2 N_f N_A^o T_F + 216\psi'(\tfrac{1}{3})\alpha C_A N_A^d + 270\psi'(\tfrac{1}{3}) C_A N_A^d \\
&\quad -72\pi^2\alpha^5 C_A N_A^d - 324\alpha^5 C_A N_A^d + 24\pi^2\alpha^5 C_A N_A^o \\
&\quad +108\alpha^5 C_A N_A^o + 216\pi^2\alpha^4 C_A N_A^d + 810\alpha^4 C_A N_A^d \\
&\quad -108\pi^2\alpha^4 C_A N_A^o - 405\alpha^4 C_A N_A^o - 216\pi^2\alpha^3 C_A N_A^d \\
&\quad -1377\alpha^3 C_A N_A^d + 72\pi^2\alpha^3 C_A N_A^o + 1458\alpha^3 C_A N_A^o \\
&\quad -864\pi^2\alpha^2 C_A N_A^d + 891\alpha^2 C_A N_A^d + 304\pi^2\alpha^2 C_A N_A^o \\
&\quad -873\alpha^2 C_A N_A^o - 512\pi^2\alpha^2 N_f N_A^o T_F - 576\alpha^2 N_f N_A^o T_F \\
&\quad -144\pi^2\alpha C_A N_A^d - 243\alpha C_A N_A^d - 180\pi^2 C_A N_A^d \\
&\quad +243 C_A N_A^d] \, \frac{a}{972\alpha^2 N_A^o} \; + \; \mathcal{O}(a^2)
\end{aligned}
$$

$$
\begin{aligned}
\Sigma^{\rm ggg}_{(8)}(p,q)\Big|_{\overline{\rm MS}} &= -\;\Sigma^{\rm ggg}_{(13)}(p,q)\Big|_{\overline{\rm MS}} \\
&= \big[108\psi'(\tfrac{1}{3})\alpha^5 C_A N_A^d - 36\psi'(\tfrac{1}{3})\alpha^5 C_A N_A^o - 540\psi'(\tfrac{1}{3})\alpha^4 C_A N_A^d \\
&\quad +270\psi'(\tfrac{1}{3})\alpha^4 C_A N_A^o + 270\psi'(\tfrac{1}{3})\alpha^3 C_A N_A^d - 378\psi'(\tfrac{1}{3})\alpha^3 C_A N_A^o \\
&\quad -1242\psi'(\tfrac{1}{3})\alpha^2 C_A N_A^d + 390\psi'(\tfrac{1}{3})\alpha^2 C_A N_A^o \\
&\quad -384\psi'(\tfrac{1}{3})\alpha^2 N_f N_A^o T_F - 216\psi'(\tfrac{1}{3})\alpha C_A N_A^d - 270\psi'(\tfrac{1}{3}) C_A N_A^d \\
&\quad -72\pi^2\alpha^5 C_A N_A^d - 567\alpha^5 C_A N_A^d + 24\pi^2\alpha^5 C_A N_A^o + 189\alpha^5 C_A N_A^o \\
&\quad +360\pi^2\alpha^4 C_A N_A^d + 2268\alpha^4 C_A N_A^d - 180\pi^2\alpha^4 C_A N_A^o \\
&\quad -1134\alpha^4 C_A N_A^o - 180\pi^2\alpha^3 C_A N_A^d - 648\alpha^3 C_A N_A^d \\
&\quad +252\pi^2\alpha^3 C_A N_A^o + 243\alpha^3 C_A N_A^o + 828\pi^2\alpha^2 C_A N_A^d \\
&\quad -1053\alpha^2 C_A N_A^d - 260\pi^2\alpha^2 C_A N_A^o + 1206\alpha^2 C_A N_A^o \\
&\quad +256\pi^2\alpha^2 N_f N_A^o T_F - 1008\alpha^2 N_f N_A^o T_F + 144\pi^2\alpha C_A N_A^d \\
&\quad +243\alpha C_A N_A^d + 180\pi^2 C_A N_A^d - 243 C_A N_A^d] \, \frac{a}{972\alpha^2 N_A^o} \; + \; \mathcal{O}(a^2)
\end{aligned}
$$

$$
\begin{aligned}
\Sigma^{\rm ggg}_{(10)}(p,q)\Big|_{\overline{\rm MS}} &= -\;\Sigma^{\rm ggg}_{(12)}(p,q)\Big|_{\overline{\rm MS}} \\
&= \big[-216\psi'(\tfrac{1}{3})\alpha^3 C_A N_A^d + 72\psi'(\tfrac{1}{3})\alpha^3 C_A N_A^o + 864\psi'(\tfrac{1}{3})\alpha^2 C_A N_A^d
\end{aligned}
$$

$$
\begin{aligned}
&-432\psi'(\tfrac{1}{3})\alpha^2 C_A N_A^o - 594\psi'(\tfrac{1}{3})\alpha C_A N_A^d + 486\psi'(\tfrac{1}{3})\alpha C_A N_A^o \\
&-54\psi'(\tfrac{1}{3}) C_A N_A^d + 66\psi'(\tfrac{1}{3}) C_A N_A^o - 384\psi'(\tfrac{1}{3}) N_f N_A^o T_F \\
&+144\pi^2\alpha^3 C_A N_A^d + 891\alpha^3 C_A N_A^d - 48\pi^2\alpha^3 C_A N_A^o - 297\alpha^3 C_A N_A^o \\
&-576\pi^2\alpha^2 C_A N_A^d - 3078\alpha^2 C_A N_A^d + 288\pi^2\alpha^2 C_A N_A^o \\
&+1539\alpha^2 C_A N_A^o + 396\pi^2\alpha C_A N_A^d + 2025\alpha C_A N_A^d \\
&-324\pi^2\alpha C_A N_A^o - 1701\alpha C_A N_A^o + 36\pi^2 C_A N_A^d + 162 C_A N_A^d \\
&-44\pi^2 C_A N_A^o - 333 C_A N_A^o + 256\pi^2 N_f N_A^o T_F \\
&+1584 N_f N_A^o T_F] \frac{a}{972 N_A^o} \;+\; \mathcal{O}(a^2)
\end{aligned}
\tag{5.3.45}
$$

and those for the quark-gluon vertex are

$$
\begin{aligned}
\Sigma^{\mathrm{qqg}}_{(1)}(p,q)\Big|_{\overline{\mathrm{MS}}} &= 1 - \big[6\psi'(\tfrac{1}{3})\alpha^2 C_A N_F N_A^d - 3\psi'(\tfrac{1}{3})\alpha^2 C_A N_F N_A^o \\
&\quad -12\psi'(\tfrac{1}{3})\alpha C_A N_F N_A^d + 12\psi'(\tfrac{1}{3})\alpha C_A N_F N_A^o \\
&\quad +48\psi'(\tfrac{1}{3})\alpha N_A^{o2} T_F + 30\psi'(\tfrac{1}{3}) C_A N_F N_A^d \\
&\quad +39\psi'(\tfrac{1}{3}) C_A N_F N_A^o - 24\psi'(\tfrac{1}{3}) C_F N_F N_A^o - 4\pi^2\alpha^2 C_A N_F N_A^d \\
&\quad -54\alpha^2 C_A N_F N_A^d + 2\pi^2\alpha^2 C_A N_F N_A^o + 27\alpha^2 C_A N_F N_A^o \\
&\quad +8\pi^2\alpha C_A N_F N_A^d - 8\pi^2\alpha C_A N_F N_A^o - 32\pi^2\alpha N_A^{o2} T_F \\
&\quad -216\alpha N_A^{o2} T_F - 20\pi^2 C_A N_F N_A^d - 162 C_A N_F N_A^d \\
&\quad -26\pi^2 C_A N_F N_A^o - 351 C_A N_F N_A^o + 16\pi^2 C_F N_F N_A^o \\
&\quad +216 C_F N_F N_A^o] \frac{a}{108 N_F N_A^o} \;+\; \mathcal{O}(a^2) \\
\Sigma^{\mathrm{qqg}}_{(2)}(p,q)\Big|_{\overline{\mathrm{MS}}} &= \Sigma^{\mathrm{qqg}}_{(5)}(p,q)\Big|_{\overline{\mathrm{MS}}} \\
&= -\big[6\psi'(\tfrac{1}{3})\alpha^2 C_A N_F N_A^d - 3\psi'(\tfrac{1}{3})\alpha^2 C_A N_F N_A^o + 24\psi'(\tfrac{1}{3})\alpha N_A^{o2} T_F \\
&\quad +6\psi'(\tfrac{1}{3}) C_A N_F N_A^d + 15\psi'(\tfrac{1}{3}) C_A N_F N_A^o - 24\psi'(\tfrac{1}{3}) C_F N_F N_A^o \\
&\quad -4\pi^2\alpha^2 C_A N_F N_A^d - 36\alpha^2 C_A N_F N_A^d + 2\pi^2\alpha^2 C_A N_F N_A^o \\
&\quad +18\alpha^2 C_A N_F N_A^o - 36\alpha C_A N_F N_A^d + 36\alpha C_A N_F N_A^o \\
&\quad -16\pi^2\alpha N_A^{o2} T_F - 72\alpha N_A^{o2} T_F - 4\pi^2 C_A N_F N_A^d + 36 C_A N_F N_A^d \\
&\quad -10\pi^2 C_A N_F N_A^o - 126 C_A N_F N_A^o + 16\pi^2 C_F N_F N_A^o \\
&\quad +144 C_F N_F N_A^o] \frac{a}{54 N_F N_A^o} \;+\; \mathcal{O}(a^2) \\
\Sigma^{\mathrm{qqg}}_{(3)}(p,q)\Big|_{\overline{\mathrm{MS}}} &= \Sigma^{\mathrm{qqg}}_{(4)}(p,q)\Big|_{\overline{\mathrm{MS}}} \\
&= -\big[6\psi'(\tfrac{1}{3})\alpha C_A N_F N_A^d - 6\psi'(\tfrac{1}{3})\alpha C_A N_F N_A^o + 24\psi'(\tfrac{1}{3})\alpha N_A^{o2} T_F \\
&\quad +6\psi'(\tfrac{1}{3}) C_A N_F N_A^d + 6\psi'(\tfrac{1}{3}) C_A N_F N_A^o - 18\alpha^2 C_A N_F N_A^d
\end{aligned}
$$

$$
\begin{aligned}
&+9\alpha^2 C_A N_F N_A^o - 4\pi^2 \alpha C_A N_F N_A^d - 45\alpha C_A N_F N_A^d \\
&+4\pi^2 \alpha C_A N_F N_A^o + 45\alpha C_A N_F N_A^o - 16\pi^2 \alpha N_A^{o2} T_F - 36\alpha N_A^{o2} T_F \\
&-4\pi^2 C_A N_F N_A^d + 45 C_A N_F N_A^d - 4\pi^2 C_A N_F N_A^o \\
&-90 C_A N_F N_A^o + 72 C_F N_F N_A^o] \, \frac{a}{54 N_F N_A^o} \; + \; \mathcal{O}(a^2)
\end{aligned}
$$

$$
\begin{aligned}
\Sigma^{\mathrm{qqg}}_{(6)}(p,q)\Big|_{\overline{\mathrm{MS}}} \;=\; & \big[6\psi'(\tfrac{1}{3})\alpha^2 C_A N_A^d - 3\psi'(\tfrac{1}{3})\alpha^2 C_A N_A^o + 12\psi'(\tfrac{1}{3})\alpha C_A N_A^d \\
&-12\psi'(\tfrac{1}{3})\alpha C_A N_A^o + 6\psi'(\tfrac{1}{3}) C_A N_A^d - 33\psi'(\tfrac{1}{3}) C_A N_A^o \\
&+24\psi'(\tfrac{1}{3}) C_F N_A^o - 4\pi^2\alpha^2 C_A N_A^d + 2\pi^2\alpha^2 C_A N_A^o - 8\pi^2 \alpha C_A N_A^d \\
&+8\pi^2 \alpha C_A N_A^o - 4\pi^2 C_A N_A^d + 22\pi^2 C_A N_A^o - 16\pi^2 C_F N_A^o] \, \frac{a}{54 N_A^o} \\
&+ \mathcal{O}(a^2) \; . \qquad (5.3.46)
\end{aligned}
$$

Again, one minor check on the expressions is that the correct symmetry structure for each vertex emerged. In other words the relations between the various amplitudes for the triple off-diagonal gluon vertex, for instance, are consistent with expectations based on [117]. At this point, instead of making checks against the Landau gauge we can cross check directly with the Curci-Ferrari gauge $\overline{\mathrm{MS}}$ results for the amplitudes by taking the limit $N_A^d \to 0$. Essentially by removing the diagonal pieces the off-diagonal results in the MAG map on to the results for the full colour group in the Curci-Ferrari gauge. We have verified the results in the Curci-Ferrari scheme via this check which holds in all MOMi schemes unlike the Landau check which is no longer applicable here.

Defining the renormalization constants as before we display the results for the MOMi schemes. We note that at one loop the renormalization constants are the same in all three MOM schemes. This is not true for higher orders, as we have seen in the two previous gauges considered. This property is unique to one loop. The renormalization constants given analytically for arbitrary α are

$$
\begin{aligned}
Z_A(a,\alpha)\Big|_{\mathrm{MOMi}} \;=\; & 1 + \left[C_A \left(\frac{13}{6} + \frac{\alpha N_A^d}{2N_A^o} - \frac{\alpha}{2} - \frac{3N_A^d}{2N_A^o} \right) - \frac{4}{3} N_f T_F \right. \\
& \left. + \epsilon \left[-\frac{20}{9} N_f T_F + C_A \left(\frac{97}{36} - \frac{\alpha N_A^d}{2N_A^o} + \frac{\alpha}{2} - \frac{\alpha^2 N_A^d}{2N_A^o} \right. \right. \right. \\
& \left. \left. \left. + \frac{\alpha^2}{4} - 3\frac{N_A^d}{N_A^o} \right) \right] \right] \frac{a}{\epsilon} \; + \; \mathcal{O}(a^2) \\
Z_{A^i}(a,\alpha)\Big|_{\mathrm{MOMi}} \;=\; & 1 + \left[\frac{4}{3} N_f T_F + \frac{11}{3} C_A + \epsilon \left[-\frac{20}{9} N_f T_F + C_A \left(\frac{205}{36} + \frac{3\alpha}{2} \right. \right. \right.
\end{aligned}
$$

$$
\begin{aligned}
& + \frac{\alpha^2}{4}\Bigg)\Bigg]\Bigg]\frac{a}{\epsilon} \; + \; \mathcal{O}(a^2) \\
Z_\alpha(a,\alpha)\Big|_{\text{MOMi}} &= 1 + \Bigg[C_A\left(+\frac{3N_A^d}{\alpha N_A^o} + \alpha\frac{N_A^d}{N_A^o} - \frac{\alpha}{4} + \frac{3N_A^d}{2N_A^o}\right) \\
& \quad + \epsilon\left[C_A\left(\frac{5N_A^d}{2\alpha N_A^o} + \alpha\frac{N_A^d}{N_A^o} - \frac{\alpha}{2} + \frac{7N_A^d}{2N_A^o}\right)\right]\Bigg]\frac{a}{\epsilon} \; + \; \mathcal{O}(a^2) \\
Z_{\alpha_p}(a,\alpha)\Big|_{\text{MOMi}} &= 1 \; + \; \mathcal{O}(a^2) \\
Z_c(a,\alpha)\Big|_{\text{MOMi}} &= 1 + \left[C_A\left(\frac{3}{4} + \frac{\alpha N_A^d}{2N_A^o} - \frac{\alpha}{4} + \frac{3N_A^d}{2N_A^o}\right) + C_A\epsilon\left(1 + 2\frac{N_A^d}{N_A^o}\right)\right]\frac{a}{\epsilon} \\
& \quad + \mathcal{O}(a^2) \\
Z_{c^i}(a,\alpha)\Big|_{\text{MOMi}} &= 1 \; + \; \mathcal{O}(a^2) \\
Z_\psi(a,\alpha)\Big|_{\text{MOMi}} &= 1 + \left[-\frac{\alpha N_A^o}{N_c}T_F\,(1+\epsilon)\right]\frac{a}{\epsilon} \; + \; \mathcal{O}(a^2)
\end{aligned}
\tag{5.3.47}
$$

where the MAG condition (5.3.42) is assumed. Now, recall that the MOMi schemes are based upon the 3-point vertices of the Lagrangian. In this scheme the renormalization constants contain both the divergent and finite parts (as we have seen above for the 2-point functions). Because the MOM scheme is physical the coupling constant renormalization constants for each MOMi scheme are dependent on that particular vertex. We define the coupling constant renormalization constants as before, labelled by MOMh for the scheme corresponding to the ghost-gluon vertex, MOMg for the triple-gluon vertex and MOMq for the quark-gluon vertex coupling constant. These are presented below as

$$
\begin{aligned}
Z_g^{(\text{ccg})}(a,\alpha)\Big|_{\text{MOMh}} &= 1 + \Bigg[-\frac{11}{6}C_A + \frac{2}{3}T_F N_f + \epsilon\Bigg(C_A\Bigg(-\frac{205}{72} - \frac{2}{27}\alpha\pi^2 - \frac{3}{4}\alpha \\
& \quad - \frac{1}{108}\alpha^2\pi^2 - \frac{1}{8}\alpha^2 + \frac{5}{108}\pi^2 - \frac{5}{72}\psi'\left(\frac{1}{3}\right) \\
& \quad + \frac{1}{9}\psi'\left(\frac{1}{3}\right)\alpha + \frac{1}{72}\psi'\left(\frac{1}{3}\right)\alpha^2\Bigg) + T_F N_f\left(\frac{10}{9}\right)\Bigg)\Bigg]\frac{a}{\epsilon} \\
& \quad + \mathcal{O}(a^2) \\
Z_g^{(\text{ggg})}(a,\alpha)\Big|_{\text{MOMg}} &= 1 + \Bigg[-\frac{11}{6}C_A + \frac{2}{3}T_F N_f + \epsilon\Bigg(C_A\Bigg(-\frac{11}{3} - \frac{1}{6}\alpha\pi^2 - \frac{3}{8}\alpha \\
& \quad + \frac{1}{27}\alpha^2\pi^2 + \frac{1}{4}\alpha^2 - \frac{1}{24}\alpha^3 + \frac{23}{162}\pi^2 - \frac{23}{108}\psi'\left(\frac{1}{3}\right) \\
& \quad + \frac{1}{4}\psi'\left(\frac{1}{3}\right)\alpha - \frac{1}{18}\psi'\left(\frac{1}{3}\right)\alpha^2\Bigg) + T_F N_f\left(\frac{4}{3} - \frac{32}{81}\pi^2 \right. \\
& \quad \left. + \frac{16}{27}\psi'\left(\frac{1}{3}\right)\right)\Bigg)\Bigg]\frac{a}{\epsilon} \; + \; \mathcal{O}(a^2)
\end{aligned}
$$

$$
\begin{aligned}
Z_g^{(\mathrm{qqg})}(a,\alpha)\Big|_{\mathrm{MOMq}} &= 1 + \left[-\frac{11}{6} C_A + \frac{2}{3} T_F N_f - \epsilon \left(C_F \left(-2 + \frac{8}{27} \alpha \pi^2 + \alpha \right. \right. \right. \\
&\quad \left. - \frac{4}{27} \pi^2 + \frac{2}{9} \psi'\left(\frac{1}{3}\right) - \frac{4}{9} \psi'\left(\frac{1}{3}\right) \alpha \right) + C_A \left(\frac{331}{72} \right. \\
&\quad + \frac{2}{27} \alpha \pi^2 + \frac{1}{4} \alpha - \frac{1}{54} \alpha^2 \pi^2 - \frac{1}{8} \alpha^2 + \frac{13}{54} \pi^2 - \frac{13}{36} \psi'\left(\frac{1}{3}\right) \\
&\quad \left. \left. \left. - \frac{1}{9} \psi'\left(\frac{1}{3}\right) \alpha + \frac{1}{36} \psi'\left(\frac{1}{3}\right) \alpha^2 \right) + T_F N_f \left(-\frac{10}{9} \right) \right) \right] \frac{a}{\epsilon} \\
&\quad + \mathcal{O}(a^2) \; . \qquad (5.3.48)
\end{aligned}
$$

5.4 MOMh scheme

Having discussed the structure of the 3-point vertices in the $\overline{\mathrm{MS}}$ scheme at one loop in detail we can now renormalize in each of the MOMi schemes defined by the same vertices. We define the MOMi schemes in the MAG in the same way as we have done in chapters 3 and 4, by ensuring that after renormalization there are no $\mathcal{O}(a)$ corrections to the Lorentz channels containing the divergences in ϵ. In other words, taking the MOMg scheme for example, for the first six amplitudes there are no $\mathcal{O}(a)$ parts at the symmetric point but the remaining eight amplitudes can have $\mathcal{O}(a)$ contributions. In this section we present the results for the MOMh scheme only. Given this and the nature of the MOMh scheme the amplitudes are effectively trivial since

$$
\Sigma_{(1)}^{\mathrm{ccg}}(p,q)\Big|_{\mathrm{MOMh}} = - \Sigma_{(2)}^{\mathrm{ccg}}(p,q)\Big|_{\mathrm{MOMh}} = -\frac{1}{2} + \mathcal{O}(a^2) \; . \qquad (5.4.49)
$$

This is because of the anti-symmetric property of the original ghost-gluon vertex and the definition of the MOMh scheme. Next we require the mappings of the parameters between schemes. For this we apply the same fomulae as for the arbitrary linear and Curci-Ferrari gauge analyses, see (3.3.35) and (3.3.37). The coupling constant mapping is unique for each vertex, given for the ghost-gluon vertex by

$$
\begin{aligned}
a_{\mathrm{MOMh}} &= a + \left[36\psi'\left(\tfrac{1}{3}\right) \alpha C_A N_A^d - 12\psi'\left(\tfrac{1}{3}\right) \alpha C_A N_A^o - 66\psi'\left(\tfrac{1}{3}\right) C_A N_A^d \right. \\
&\quad + 30\psi'\left(\tfrac{1}{3}\right) C_A N_A^o - 54\alpha^2 C_A N_A^d + 27\alpha^2 C_A N_A^o - 24\alpha C_A N_A^d \pi^2 \\
&\quad - 108\alpha C_A N_A^d + 8\alpha C_A N_A^o \pi^2 + 108\alpha C_A N_A^o + 44 C_A N_A^d \pi^2 \\
&\quad \left. + 162 C_A N_A^d - 20 C_A N_A^o \pi^2 + 669 C_A N_A^o - 240 N_f N_A^o T_F \right] \frac{a^2}{108 N_A^o} \\
&\quad + \mathcal{O}(a^3) \qquad (5.4.50)
\end{aligned}
$$

and the gauge parameter maps between schemes as

$$\begin{aligned}\alpha_{\rm MOMi} &= \alpha + \big[18\alpha^3 C_A N_A^d - 9\alpha^3 C_A N_A^o + 54\alpha^2 C_A N_A^d - 36\alpha^2 C_A N_A^o \\ &\quad +234\alpha C_A N_A^d - 97\alpha C_A N_A^o + 80\alpha N_f N_A^o T_F + 90 C_A N_A^d\big] \frac{a}{36 N_A^o} \\ &\quad + \mathcal{O}(a^2) \; . \end{aligned} \tag{5.4.51}$$

Given the nature of the one loop 2-point functions it transpires that the gauge parameter mapping is the same for all schemes. At one loop this is assumed since the effect the scheme choice makes on the renormalization of the gauge parameter does not occur until two loops. This agrees with our previous work, however in the Curci-Ferrari gauge this exact similarity between MOMi schemes also holds at two loops. It would be interesting to see at what loop order, if any, the gauge parameter mapping varies between MOMi schemes. The same comment applies to the conversion functions for the field renormalizations which are given by

$$\begin{aligned} C_A^{\rm MOMi}(a,\alpha) &= 1 + \big[-18\alpha^2 C_A N_A^d + 9\alpha^2 C_A N_A^o - 18\alpha C_A N_A^d + 18\alpha C_A N_A^o \\ &\quad -108 C_A N_A^d + 97 C_A N_A^o - 80 N_f N_A^o T_F\big] \frac{a}{36 N_A^o} \; + \; \mathcal{O}(a^2) \\ C_\alpha^{\rm MOMi}(a,\alpha) &= 1 \; + \; \mathcal{O}(a^2) \\ C_c^{\rm MOMi}(a,\alpha) &= 1 + C_A \left[2N_A^d + N_A^o\right] \frac{a}{N_A^o} \; + \; \mathcal{O}(a^2) \\ C_\psi^{\rm MOMi}(a,\alpha) &= 1 - \frac{\alpha N_A^o T_F a}{N_F} \; + \; \mathcal{O}(a^2) \end{aligned} \tag{5.4.52}$$

at one loop. The coupling constant conversion function is different for each scheme by the nature of its construction. For the MOMh scheme this is

$$\begin{aligned} C_g^{\rm MOMh}(a,\alpha) &= 1 + \big[-36\psi'\left(\tfrac{1}{3}\right) \alpha C_A N_A^d + 12\psi'\left(\tfrac{1}{3}\right) \alpha C_A N_A^o + 66\psi'\left(\tfrac{1}{3}\right) C_A N_A^d \\ &\quad -30\psi'\left(\tfrac{1}{3}\right) C_A N_A^o + 54\alpha^2 C_A N_A^d - 27\alpha^2 C_A N_A^o \\ &\quad +24\alpha C_A N_A^d \pi^2 + 108\alpha C_A N_A^d - 8\alpha C_A N_A^o \pi^2 - 108\alpha C_A N_A^o \\ &\quad -44 C_A N_A^d \pi^2 - 162 C_A N_A^d + 20 C_A N_A^o \pi^2 - 669 C_A N_A^o \\ &\quad +240 N_f N_A^o T_F] \frac{a}{216 N_A^o} \; + \; \mathcal{O}(a^2) \; . \end{aligned} \tag{5.4.53}$$

Having determined the conversion functions it is straightforward to apply the renormalization group formalism (3.3.29) and (3.4.55) to construct the two loop MOMh renormalization group functions. In the MOMh scheme these are

$$\beta^{\rm MOMh}(a,\alpha) \;=\; [-11 C_A + 4 N_f T_F] \frac{a^2}{3}$$

$$
\begin{aligned}
&+\Big[-108\psi'\left(\tfrac{1}{3}\right)\alpha^2 C_A^2 N_A^{d\,2} - 18\psi'\left(\tfrac{1}{3}\right)\alpha^2 C_A^2 N_A^d N_A^o \\
&+18\psi'\left(\tfrac{1}{3}\right)\alpha^2 C_A^2 N_A^{o\,2} - 648\psi'\left(\tfrac{1}{3}\right)\alpha C_A^2 N_A^{d\,2} \\
&+684\psi'\left(\tfrac{1}{3}\right)\alpha C_A^2 N_A^d N_A^o - 156\psi'\left(\tfrac{1}{3}\right)\alpha C_A^2 N_A^{o\,2} \\
&-288\psi'\left(\tfrac{1}{3}\right)\alpha C_A N_A^d N_f N_A^o T_F + 96\psi'\left(\tfrac{1}{3}\right)\alpha C_A N_f N_A^{o\,2} T_F \\
&-648\psi'\left(\tfrac{1}{3}\right) C_A^2 N_A^{d\,2} + 216\psi'\left(\tfrac{1}{3}\right) C_A^2 N_A^d N_A^o + 324\alpha^3 C_A^2 N_A^{d\,2} \\
&-81\alpha^3 C_A^2 N_A^{o\,2} + 72\alpha^2 C_A^2 N_A^{d\,2}\pi^2 + 2268\alpha^2 C_A^2 N_A^{d\,2} \\
&+12\alpha^2 C_A^2 N_A^d N_A^o \pi^2 - 2538\alpha^2 C_A^2 N_A^d N_A^o - 12\alpha^2 C_A^2 N_A^{o\,2}\pi^2 \\
&+540\alpha^2 C_A^2 N_A^{o\,2} + 864\alpha^2 C_A N_A^d N_f N_A^o T_F - 432\alpha^2 C_A N_f N_A^{o\,2} T_F \\
&+432\alpha C_A^2 N_A^{d\,2}\pi^2 + 3888\alpha C_A^2 N_A^{d\,2} - 456\alpha C_A^2 N_A^d N_A^o \pi^2 \\
&-4320\alpha C_A^2 N_A^d N_A^o + 104\alpha C_A^2 N_A^{o\,2}\pi^2 + 1404\alpha C_A^2 N_A^{o\,2} \\
&+192\alpha C_A N_A^d N_f N_A^o \pi^2 T_F + 864\alpha C_A N_A^d N_f N_A^o T_F \\
&-64\alpha C_A N_f N_A^{o\,2}\pi^2 T_F - 864\alpha C_A N_f N_A^{o\,2} T_F + 432 C_A^2 N_A^{d\,2}\pi^2 \\
&+1944 C_A^2 N_A^{d\,2} - 144 C_A^2 N_A^d N_A^o \pi^2 - 1944 C_A^2 N_A^d N_A^o \\
&-7344 C_A^2 N_A^{o\,2} + 4320 C_A N_f N_A^{o\,2} T_F \\
&+2592 C_F N_f N_A^{o\,2} T_F\Big]\frac{a^3}{648 N_A^{o\,2}} \;+\; \mathcal{O}(a^4)
\end{aligned}
$$

$$
\begin{aligned}
\gamma_A^{\rm MOMh}(a,\alpha) \;=\; &\left[-3\alpha C_A N_A^d + 3\alpha C_A N_A^o + 9 C_A N_A^d - 13 C_A N_A^o + 8 N_f N_A^o T_F\right]\frac{a}{6 N_A^o} \\
&+\Big[216\psi'\left(\tfrac{1}{3}\right)\alpha^2 C_A^2 N_A^{d\,2} - 288\psi'\left(\tfrac{1}{3}\right)\alpha^2 C_A^2 N_A^d N_A^o \\
&+72\psi'\left(\tfrac{1}{3}\right)\alpha^2 C_A^2 N_A^{o\,2} - 1044\psi'\left(\tfrac{1}{3}\right)\alpha C_A^2 N_A^{d\,2} \\
&+1728\psi'\left(\tfrac{1}{3}\right)\alpha C_A^2 N_A^d N_A^o - 492\psi'\left(\tfrac{1}{3}\right)\alpha C_A^2 N_A^{o\,2} \\
&-576\psi'\left(\tfrac{1}{3}\right)\alpha C_A N_A^d N_f N_A^o T_F + 192\psi'\left(\tfrac{1}{3}\right)\alpha C_A N_f N_A^{o\,2} T_F \\
&+1188\psi'\left(\tfrac{1}{3}\right) C_A^2 N_A^{d\,2} - 2256\psi'\left(\tfrac{1}{3}\right) C_A^2 N_A^d N_A^o \\
&+780\psi'\left(\tfrac{1}{3}\right) C_A^2 N_A^{o\,2} + 1056\psi'\left(\tfrac{1}{3}\right) C_A N_A^d N_f N_A^o T_F \\
&-480\psi'\left(\tfrac{1}{3}\right) C_A N_f N_A^{o\,2} T_F + 648\alpha^3 C_A^2 N_A^{d\,2} - 162\alpha^3 C_A^2 N_A^{o\,2} \\
&-144\alpha^2 C_A^2 N_A^{d\,2}\pi^2 + 5913\alpha^2 C_A^2 N_A^{d\,2} + 192\alpha^2 C_A^2 N_A^d N_A^o \pi^2 \\
&-4671\alpha^2 C_A^2 N_A^d N_A^o - 48\alpha^2 C_A^2 N_A^{o\,2}\pi^2 + 918\alpha^2 C_A^2 N_A^{o\,2} \\
&+1728\alpha^2 C_A N_A^d N_f N_A^o T_F - 864\alpha^2 C_A N_f N_A^{o\,2} T_F \\
&+696\alpha C_A^2 N_A^{d\,2}\pi^2 + 12798\alpha C_A^2 N_A^{d\,2} - 1152\alpha C_A^2 N_A^d N_A^o \pi^2 \\
&-4914\alpha C_A^2 N_A^d N_A^o + 328\alpha C_A^2 N_A^{o\,2}\pi^2 + 1350\alpha C_A^2 N_A^{o\,2} \\
&+384\alpha C_A N_A^d N_f N_A^o \pi^2 T_F + 1728\alpha C_A N_A^d N_f N_A^o T_F \\
&-128\alpha C_A N_f N_A^{o\,2}\pi^2 T_F - 1728\alpha C_A N_f N_A^{o\,2} T_F - 792 C_A^2 N_A^{d\,2}\pi^2
\end{aligned}
$$

$$
\begin{aligned}
&-243C_A^2N_A^{d\,2} + 1504C_A^2N_A^dN_A^o\pi^2 + 11799C_A^2N_A^dN_A^o \\
&-520C_A^2N_A^{o\,2}\pi^2 - 4968C_A^2N_A^{o\,2} - 704C_AN_A^dN_fN_A^o\pi^2T_F \\
&-5616C_AN_A^dN_fN_A^oT_F + 320C_AN_fN_A^{o\,2}\pi^2T_F \\
&+4752C_AN_fN_A^{o\,2}T_F + 5184C_FN_fN_A^{o\,2}T_F \Big] \frac{a^2}{1296N_A^{o\,2}} \\
&+ \mathcal{O}(a^3)
\end{aligned}
$$

$$
\begin{aligned}
\gamma_\alpha^{\rm MOMh}(a,\alpha) &= \big[-6\alpha^2C_AN_A^d - 3\alpha^2C_AN_A^o - 36\alpha C_AN_A^d + 26\alpha C_AN_A^o \\
&\quad -16\alpha N_fN_A^oT_F - 36C_AN_A^d\big] \frac{a}{12\alpha N_A^o} \\
&+ \Big[216\psi'\left(\tfrac{1}{3}\right)\alpha^3C_A^2N_A^{d\,2} + 36\psi'\left(\tfrac{1}{3}\right)\alpha^3C_A^2N_A^dN_A^o \\
&\quad -36\psi'\left(\tfrac{1}{3}\right)\alpha^3C_A^2N_A^{o\,2} + 900\psi'\left(\tfrac{1}{3}\right)\alpha^2C_A^2N_A^{d\,2} \\
&\quad -1386\psi'\left(\tfrac{1}{3}\right)\alpha^2C_A^2N_A^dN_A^o + 402\psi'\left(\tfrac{1}{3}\right)\alpha^2C_A^2N_A^{o\,2} \\
&\quad +576\psi'\left(\tfrac{1}{3}\right)\alpha^2C_AN_A^dN_fN_A^oT_F - 192\psi'\left(\tfrac{1}{3}\right)\alpha^2C_AN_fN_A^{o\,2}T_F \\
&\quad -1080\psi'\left(\tfrac{1}{3}\right)\alpha C_A^2N_A^{d\,2} + 2364\psi'\left(\tfrac{1}{3}\right)\alpha C_A^2N_A^dN_A^o \\
&\quad -780\psi'\left(\tfrac{1}{3}\right)\alpha C_A^2N_A^{o\,2} - 1056\psi'\left(\tfrac{1}{3}\right)\alpha C_AN_A^dN_fN_A^oT_F \\
&\quad +480\psi'\left(\tfrac{1}{3}\right)\alpha C_AN_fN_A^{o\,2}T_F - 2376\psi'\left(\tfrac{1}{3}\right)C_A^2N_A^{d\,2} \\
&\quad +1080\psi'\left(\tfrac{1}{3}\right)C_A^2N_A^dN_A^o - 648\alpha^4C_A^2N_A^{d\,2} + 162\alpha^4C_A^2N_A^{o\,2} \\
&\quad -144\alpha^3C_A^2N_A^{d\,2}\pi^2 - 7290\alpha^3C_A^2N_A^{d\,2} - 24\alpha^3C_A^2N_A^dN_A^o\pi^2 \\
&\quad +4347\alpha^3C_A^2N_A^dN_A^o + 24\alpha^3C_A^2N_A^{o\,2}\pi^2 - 675\alpha^3C_A^2N_A^{o\,2} \\
&\quad -1728\alpha^3C_AN_A^dN_fN_A^oT_F + 864\alpha^3C_AN_fN_A^{o\,2}T_F \\
&\quad -600\alpha^2C_A^2N_A^{d\,2}\pi^2 - 22194\alpha^2C_A^2N_A^{d\,2} + 924\alpha^2C_A^2N_A^dN_A^o\pi^2 \\
&\quad +7263\alpha^2C_A^2N_A^dN_A^o - 268\alpha^2C_A^2N_A^{o\,2}\pi^2 - 1107\alpha^2C_A^2N_A^{o\,2} \\
&\quad -384\alpha^2C_AN_A^dN_fN_A^o\pi^2T_F - 1728\alpha^2C_AN_A^dN_fN_A^oT_F \\
&\quad +128\alpha^2C_AN_fN_A^{o\,2}\pi^2T_F + 1728\alpha^2C_AN_fN_A^{o\,2}T_F \\
&\quad +720\alpha C_A^2N_A^{d\,2}\pi^2 + 1458\alpha C_A^2N_A^{d\,2} - 1576\alpha C_A^2N_A^dN_A^o\pi^2 \\
&\quad -15201\alpha C_A^2N_A^dN_A^o + 520\alpha C_A^2N_A^{o\,2}\pi^2 + 4968\alpha C_A^2N_A^{o\,2} \\
&\quad +704\alpha C_AN_A^dN_fN_A^o\pi^2T_F + 9504\alpha C_AN_A^dN_fN_A^oT_F \\
&\quad -320\alpha C_AN_fN_A^{o\,2}\pi^2T_F - 4752\alpha C_AN_fN_A^{o\,2}T_F \\
&\quad -5184\alpha C_FN_fN_A^{o\,2}T_F + 1584C_A^2N_A^{d\,2}\pi^2 + 44712C_A^2N_A^{d\,2} \\
&\quad -720C_A^2N_A^dN_A^o\pi^2 - 9396C_A^2N_A^dN_A^o \\
&\quad +5184C_AN_A^dN_fN_A^oT_F\big] \frac{a^2}{1296\alpha N_A^{o\,2}} \;+\; \mathcal{O}(a^3)
\end{aligned}
$$

$$
\gamma_c^{\rm MOMh}(a,\alpha) = C_A\left[-2\alpha N_A^d + \alpha N_A^o - 6N_A^d - 3N_A^o\right]\frac{a}{4N_A^o}
$$

$$
\begin{aligned}
&+C_A\Big[144\psi'\left(\tfrac{1}{3}\right)\alpha^2 C_A N_A^{d^2} - 120\psi'\left(\tfrac{1}{3}\right)\alpha^2 C_A N_A^d N_A^o \\
&\quad +24\psi'\left(\tfrac{1}{3}\right)\alpha^2 C_A N_A^{o^2} + 168\psi'\left(\tfrac{1}{3}\right)\alpha C_A N_A^{d^2} \\
&\quad +324\psi'\left(\tfrac{1}{3}\right)\alpha C_A N_A^d N_A^o - 132\psi'\left(\tfrac{1}{3}\right)\alpha C_A N_A^{o^2} \\
&\quad -792\psi'\left(\tfrac{1}{3}\right) C_A N_A^{d^2} - 36\psi'\left(\tfrac{1}{3}\right) C_A N_A^d N_A^o \\
&\quad +180\psi'\left(\tfrac{1}{3}\right) C_A N_A^{o^2} - 96\alpha^2 C_A N_A^{d^2}\pi^2 - 324\alpha^2 C_A N_A^{d^2} \\
&\quad +80\alpha^2 C_A N_A^d N_A^o\pi^2 - 486\alpha^2 C_A N_A^d N_A^o - 16\alpha^2 C_A N_A^{o^2}\pi^2 \\
&\quad +216\alpha^2 C_A N_A^{o^2} - 112\alpha C_A N_A^{d^2}\pi^2 - 3132\alpha C_A N_A^{d^2} \\
&\quad -216\alpha C_A N_A^d N_A^o\pi^2 - 702\alpha C_A N_A^d N_A^o + 88\alpha C_A N_A^{o^2}\pi^2 \\
&\quad -162\alpha C_A N_A^{o^2} + 528 C_A N_A^{d^2}\pi^2 + 7614 C_A N_A^{d^2} \\
&\quad +24 C_A N_A^d N_A^o\pi^2 - 999 C_A N_A^d N_A^o - 120 C_A N_A^{o^2}\pi^2 \\
&\quad -864 C_A N_A^{o^2} + 864 N_A^d N_f N_A^o T_F + 432 N_f N_A^{o^2} T_F\Big]\frac{a^2}{864 N_A^{o^2}} \\
&+ \mathcal{O}(a^3)
\end{aligned}
$$

$$
\begin{aligned}
\gamma_\psi^{\rm MOMh}(a,\alpha) &= \frac{\alpha N_A^o T_F a}{N_F} \\
&+\Big[-36\psi'\left(\tfrac{1}{3}\right)\alpha^2 C_A C_F N_F + 48\psi'\left(\tfrac{1}{3}\right)\alpha^2 C_A N_A^o T_F \\
&\quad +66\psi'\left(\tfrac{1}{3}\right)\alpha C_A C_F N_F - 96\psi'\left(\tfrac{1}{3}\right)\alpha C_A N_A^o T_F \\
&\quad +24\alpha^2 C_A C_F N_F\pi^2 - 27\alpha^2 C_A C_F N_F - 32\alpha^2 C_A N_A^o\pi^2 T_F \\
&\quad +54\alpha^2 C_A N_A^o T_F - 44\alpha C_A C_F N_F\pi^2 + 54\alpha C_A C_F N_F \\
&\quad +64\alpha C_A N_A^o\pi^2 T_F - 54\alpha C_A N_A^o T_F + 675 C_A C_F N_F - 162 C_F^2 N_F \\
&\quad -216 C_F N_F N_f T_F\Big]\frac{a^2}{108 N_F} \;+\; \mathcal{O}(a^3) \qquad (5.4.54)
\end{aligned}
$$

which agree with the explicit direct two loop computation carried out recently in [67]. We have chosen to present the quark anomalous dimension in terms of N_F, where N_F was defined in (5.2.18). This is simply for presentation purposes where the results in this format are more compact.

5.5 MOMg scheme.

Having recorded the results for the ghost-gluon vertex at length we briefly present the results for the triple-gluon vertex in the same order as the previous section. Starting with the amplitudes in the MOMg scheme. The explicit forms of the associated amplitudes are

$$
\Sigma_{(1)}^{\rm ggg}(p,q)\Big|_{\rm MOMg} \;=\; \Sigma_{(2)}^{\rm ggg}(p,q)\Big|_{\rm MOMg} \;=\; -\frac{1}{2}\,\Sigma_{(3)}^{\rm ggg}(p,q)\Big|_{\rm MOMg}
$$

$$
\begin{aligned}
&= - \left. \Sigma^{ggg}_{(4)}(p,q) \right|_{\rm MOMg} = \frac{1}{2} \left. \Sigma^{ggg}_{(5)}(p,q) \right|_{\rm MOMg} \\
&= - \left. \Sigma^{ggg}_{(6)}(p,q) \right|_{\rm MOMg} = -1 + \mathcal{O}(a^2) \\
\left. \Sigma^{ggg}_{(7)}(p,q) \right|_{\rm MOMg} &= 2 \left. \Sigma^{ggg}_{(9)}(p,q) \right|_{\rm MOMg} = -2 \left. \Sigma^{ggg}_{(11)}(p,q) \right|_{\rm MOMg} \\
&= - \left. \Sigma^{ggg}_{(14)}(p,q) \right|_{\rm MOMg} \\
&= \big[-108\psi'(\tfrac{1}{3})\alpha^5 C_A N_A^d + 36\psi'(\tfrac{1}{3})\alpha^5 C_A N_A^o + 324\psi'(\tfrac{1}{3})\alpha^4 C_A N_A^d \\
&\quad -162\psi'(\tfrac{1}{3})\alpha^4 C_A N_A^o - 324\psi'(\tfrac{1}{3})\alpha^3 C_A N_A^d \\
&\quad +108\psi'(\tfrac{1}{3})\alpha^3 C_A N_A^o - 1296\psi'(\tfrac{1}{3})\alpha^2 C_A N_A^d \\
&\quad +456\psi'(\tfrac{1}{3})\alpha^2 C_A N_A^o - 768\psi'(\tfrac{1}{3})\alpha^2 N_f N_A^o T_F \\
&\quad -216\psi'(\tfrac{1}{3})\alpha C_A N_A^d - 270\psi'(\tfrac{1}{3}) C_A N_A^d + 72\pi^2\alpha^5 C_A N_A^d \\
&\quad +324\alpha^5 C_A N_A^d - 24\pi^2\alpha^5 C_A N_A^o - 108\alpha^5 C_A N_A^o \\
&\quad -216\pi^2\alpha^4 C_A N_A^d - 810\alpha^4 C_A N_A^d + 108\pi^2\alpha^4 C_A N_A^o \\
&\quad +405\alpha^4 C_A N_A^o + 216\pi^2\alpha^3 C_A N_A^d + 1377\alpha^3 C_A N_A^d \\
&\quad -72\pi^2\alpha^3 C_A N_A^o - 1458\alpha^3 C_A N_A^o + 864\pi^2\alpha^2 C_A N_A^d \\
&\quad -891\alpha^2 C_A N_A^d - 304\pi^2\alpha^2 C_A N_A^o + 873\alpha^2 C_A N_A^o \\
&\quad +512\pi^2\alpha^2 N_f N_A^o T_F + 576\alpha^2 N_f N_A^o T_F + 144\pi^2\alpha C_A N_A^d \\
&\quad +243\alpha C_A N_A^d + 180\pi^2 C_A N_A^d - 243 C_A N_A^d \big] \frac{a}{972\alpha^2 N_A^o} \\
&\quad + \mathcal{O}(a^2) \\
\left. \Sigma^{ggg}_{(8)}(p,q) \right|_{\rm MOMg} &= - \left. \Sigma^{ggg}_{(13)}(p,q) \right|_{\rm MOMg} \\
&= \big[108\psi'(\tfrac{1}{3})\alpha^5 C_A N_A^d - 36\psi'(\tfrac{1}{3})\alpha^5 C_A N_A^o - 540\psi'(\tfrac{1}{3})\alpha^4 C_A N_A^d \\
&\quad +270\psi'(\tfrac{1}{3})\alpha^4 C_A N_A^o + 270\psi'(\tfrac{1}{3})\alpha^3 C_A N_A^d \\
&\quad -378\psi'(\tfrac{1}{3})\alpha^3 C_A N_A^o - 1242\psi'(\tfrac{1}{3})\alpha^2 C_A N_A^d \\
&\quad +390\psi'(\tfrac{1}{3})\alpha^2 C_A N_A^o - 384\psi'(\tfrac{1}{3})\alpha^2 N_f N_A^o T_F \\
&\quad -216\psi'(\tfrac{1}{3})\alpha C_A N_A^d - 270\psi'(\tfrac{1}{3}) C_A N_A^d - 72\pi^2\alpha^5 C_A N_A^d \\
&\quad -567\alpha^5 C_A N_A^d + 24\pi^2\alpha^5 C_A N_A^o + 189\alpha^5 C_A N_A^o \\
&\quad +360\pi^2\alpha^4 C_A N_A^d + 2268\alpha^4 C_A N_A^d - 180\pi^2\alpha^4 C_A N_A^o \\
&\quad -1134\alpha^4 C_A N_A^o - 180\pi^2\alpha^3 C_A N_A^d - 648\alpha^3 C_A N_A^d \\
&\quad +252\pi^2\alpha^3 C_A N_A^o + 243\alpha^3 C_A N_A^o + 828\pi^2\alpha^2 C_A N_A^d \\
&\quad -1053\alpha^2 C_A N_A^d - 260\pi^2\alpha^2 C_A N_A^o + 1206\alpha^2 C_A N_A^o \\
&\quad +256\pi^2\alpha^2 N_f N_A^o T_F - 1008\alpha^2 N_f N_A^o T_F + 144\pi^2\alpha C_A N_A^d \\
&\quad +243\alpha C_A N_A^d + 180\pi^2 C_A N_A^d - 243 C_A N_A^d \big] \frac{a}{972\alpha^2 N_A^o}
\end{aligned}
$$

$$
\begin{aligned}
& + \mathcal{O}(a^2) \\
\Sigma^{ggg}_{(10)}(p,q)\Big|_{\rm MOMg} &= - \Sigma^{ggg}_{(12)}(p,q)\Big|_{\rm MOMg} \\
&= \big[-216\psi'(\tfrac{1}{3})\alpha^3 C_A N_A^d + 72\psi'(\tfrac{1}{3})\alpha^3 C_A N_A^o + 864\psi'(\tfrac{1}{3})\alpha^2 C_A N_A^d \\
&\quad -432\psi'(\tfrac{1}{3})\alpha^2 C_A N_A^o - 594\psi'(\tfrac{1}{3})\alpha C_A N_A^d + 486\psi'(\tfrac{1}{3})\alpha C_A N_A^o \\
&\quad -54\psi'(\tfrac{1}{3}) C_A N_A^d + 66\psi'(\tfrac{1}{3}) C_A N_A^o - 384\psi'(\tfrac{1}{3}) N_f N_A^o T_F \\
&\quad +144\pi^2\alpha^3 C_A N_A^d + 891\alpha^3 C_A N_A^d - 48\pi^2\alpha^3 C_A N_A^o \\
&\quad -297\alpha^3 C_A N_A^o - 576\pi^2\alpha^2 C_A N_A^d - 3078\alpha^2 C_A N_A^d \\
&\quad +288\pi^2\alpha^2 C_A N_A^o + 1539\alpha^2 C_A N_A^o + 396\pi^2\alpha C_A N_A^d \\
&\quad +2025\alpha C_A N_A^d - 324\pi^2\alpha C_A N_A^o - 1701\alpha C_A N_A^o + 36\pi^2 C_A N_A^d \\
&\quad +162 C_A N_A^d - 44\pi^2 C_A N_A^o - 333 C_A N_A^o + 256\pi^2 N_f N_A^o T_F \\
&\quad +1584 N_f N_A^o T_F] \frac{a}{972 N_A^o} \\
&\quad + \mathcal{O}(a^2) \; . \qquad (5.5.55)
\end{aligned}
$$

Again we observe that the same symmetries emerge as in the $\overline{\rm MS}$ case which is a minor check on the computation. These symmetries are consistent with those in the Curci-Ferrari gauge, where the limit $N_A^d \to 0$ gives us the Curci-Ferrari amplitudes.

The coupling constant mapping between the MOMg and $\overline{\rm MS}$ schemes is

$$
\begin{aligned}
a_{\rm MOMg} &= a + \big[-72\psi'(\tfrac{1}{3})\alpha^2 C_A N_A^d + 36\psi'(\tfrac{1}{3})\alpha^2 C_A N_A^o + 90\psi'(\tfrac{1}{3})\alpha C_A N_A^d \\
&\quad -162\psi'(\tfrac{1}{3})\alpha C_A N_A^o - 702\psi'(\tfrac{1}{3}) C_A N_A^d + 138\psi'(\tfrac{1}{3}) C_A N_A^o \\
&\quad -384\psi'(\tfrac{1}{3}) N_f N_A^o T_F - 81\alpha^3 C_A N_A^d + 27\alpha^3 C_A N_A^o + 48\pi^2\alpha^2 C_A N_A^d \\
&\quad +324\alpha^2 C_A N_A^d - 24\pi^2\alpha^2 C_A N_A^o - 162\alpha^2 C_A N_A^o - 60\pi^2\alpha C_A N_A^d \\
&\quad -243\alpha C_A N_A^d + 108\pi^2\alpha C_A N_A^o + 243\alpha C_A N_A^o + 468\pi^2 C_A N_A^d \\
&\quad -92\pi^2 C_A N_A^o + 2376 C_A N_A^o + 256\pi^2 N_f N_A^o T_F \\
&\quad -864 N_f N_A^o T_F] \frac{a^2}{324 N_A^o} \; + \; \mathcal{O}(a^3) \qquad (5.5.56)
\end{aligned}
$$

where we reiterate that the gauge parameter mapping (5.4.51) is the same in all schemes. In order to construct the two loop renormalization group functions we need only record the conversion function for the coupling constants. In the MOMg scheme this is

$$
C_g^{\rm MOMg}(a,\alpha) = 1 + \big[72\psi'(\tfrac{1}{3})\alpha^2 C_A N_A^d - 36\psi'(\tfrac{1}{3})\alpha^2 C_A N_A^o - 90\psi'(\tfrac{1}{3})\alpha C_A N_A^d
$$

$$
\begin{aligned}
&+162\psi'(\tfrac{1}{3})\alpha C_A N_A^o + 702\psi'(\tfrac{1}{3})C_A N_A^d - 138\psi'(\tfrac{1}{3})C_A N_A^o \\
&+384\psi'(\tfrac{1}{3})N_f N_A^o T_F + 81\alpha^3 C_A N_A^d - 27\alpha^3 C_A N_A^o \\
&-48\alpha^2 C_A N_A^d \pi^2 - 324\alpha^2 C_A N_A^d + 24\alpha^2 C_A N_A^o \pi^2 \\
&+162\alpha^2 C_A N_A^o + 60\alpha C_A N_A^d \pi^2 + 243\alpha C_A N_A^d \\
&-108\alpha C_A N_A^o \pi^2 - 243\alpha C_A N_A^o - 468 C_A N_A^d \pi^2 + 92 C_A N_A^o \pi^2 \\
&-2376 C_A N_A^o - 256 N_f N_A^o \pi^2 T_F + 864 N_f N_A^o T_F \Big] \frac{a}{648 N_A^o} \\
&+ \mathcal{O}(a^2) \; . \qquad (5.5.57)
\end{aligned}
$$

For the other conversion functions we do not label them with a scheme but note that like $C_g^{\rm MOMh}(a,\alpha)$ and $C_g^{\rm MOMg}(a,\alpha)$ the variables on the left hand side are the $\overline{\rm MS}$ ones, where a mapping is made from MOMi $\to \overline{\rm MS}$ as is our convention. For the β-function we find

$$
\begin{aligned}
\beta^{\rm MOMg}(a,\alpha) \;=\; & [-11C_A + 4N_f T_F]\frac{a^2}{3} \\
&+\Big[288\psi'(\tfrac{1}{3})\alpha^3 C_A^2 N_A^{d^2} - 72\psi'(\tfrac{1}{3})\alpha^3 C_A^2 N_A^{o^2} + 1548\psi'(\tfrac{1}{3})\alpha^2 C_A^2 N_A^{d^2} \\
&-1878\psi'(\tfrac{1}{3})\alpha^2 C_A^2 N_A^d N_A^o + 786\psi'(\tfrac{1}{3})\alpha^2 C_A^2 N_A^{o^2} \\
&+768\psi'(\tfrac{1}{3})\alpha^2 C_A N_A^d N_f N_A^o T_F - 384\psi'(\tfrac{1}{3})\alpha^2 C_A N_f N_A^{o^2} T_F \\
&+648\psi'(\tfrac{1}{3})\alpha C_A^2 N_A^{d^2} + 1860\psi'(\tfrac{1}{3})\alpha C_A^2 N_A^d N_A^o \\
&-1404\psi'(\tfrac{1}{3})\alpha C_A^2 N_A^{o^2} - 480\psi'(\tfrac{1}{3})\alpha C_A N_A^d N_f N_A^o T_F \\
&+864\psi'(\tfrac{1}{3})\alpha C_A N_f N_A^{o^2} T_F - 1080\psi'(\tfrac{1}{3})C_A^2 N_A^{d^2} \\
&+1944\psi'(\tfrac{1}{3})C_A^2 N_A^d N_A^o + 486\alpha^4 C_A^2 N_A^{d^2} + 81\alpha^4 C_A^2 N_A^d N_A^o \\
&-81\alpha^4 C_A^2 N_A^{o^2} - 192\pi^2\alpha^3 C_A^2 N_A^{d^2} + 1620\alpha^3 C_A^2 N_A^{d^2} \\
&-3078\alpha^3 C_A^2 N_A^d N_A^o + 48\pi^2\alpha^3 C_A^2 N_A^{o^2} + 1026\alpha^3 C_A^2 N_A^{o^2} \\
&+1296\alpha^3 C_A N_A^d N_f N_A^o T_F - 432\alpha^3 C_A N_f N_A^{o^2} T_F \\
&-1032\pi^2\alpha^2 C_A^2 N_A^{d^2} - 4374\alpha^2 C_A^2 N_A^{d^2} + 1252\pi^2\alpha^2 C_A^2 N_A^d N_A^o \\
&+8289\alpha^2 C_A^2 N_A^d N_A^o - 524\pi^2\alpha^2 C_A^2 N_A^{o^2} - 3051\alpha^2 C_A^2 N_A^{o^2} \\
&-512\pi^2\alpha^2 C_A N_A^d N_f N_A^o T_F - 3456\alpha^2 C_A N_A^d N_f N_A^o T_F \\
&+256\pi^2\alpha^2 C_A N_f N_A^{o^2} T_F + 1728\alpha^2 C_A N_f N_A^{o^2} T_F \\
&-432\pi^2\alpha C_A^2 N_A^{d^2} - 4860\alpha C_A^2 N_A^{d^2} - 1240\pi^2\alpha C_A^2 N_A^d N_A^o \\
&-1134\alpha C_A^2 N_A^d N_A^o + 936\pi^2\alpha C_A^2 N_A^{o^2} + 2106\alpha C_A^2 N_A^{o^2} \\
&+320\pi^2\alpha C_A N_A^d N_f N_A^o T_F + 1296\alpha C_A N_A^d N_f N_A^o T_F \\
&-576\pi^2\alpha C_A N_f N_A^{o^2} T_F - 1296\alpha C_A N_f N_A^{o^2} T_F + 720\pi^2 C_A^2 N_A^{d^2}
\end{aligned}
$$

$$
\begin{aligned}
&+2916C_A^2N_A^{d\,2} - 1296\pi^2C_A^2N_A^dN_A^o - 2916C_A^2N_A^dN_A^o \\
&-14688C_A^2N_A^{o\,2} + 8640C_AN_fN_A^{o\,2}T_F \\
&+5184C_FN_fN_A^{o\,2}T_F\Big]\,\frac{a^3}{1296N_A^{o\,2}} \;+\; \mathcal{O}(a^4)
\end{aligned}
\tag{5.5.58}
$$

and the anomalous dimensions for the fields at two loops in the MOMg scheme are

$$
\begin{aligned}
\gamma_A^{\rm MOMg}(a,\alpha) \;=\; & [-\,3\alpha C_AN_A^d + 3\alpha C_AN_A^o + 9C_AN_A^d - 13C_AN_A^o + 8N_fN_A^oT_F]\frac{a}{6N_A^o} \\
&+\Big[-\,432\psi'(\tfrac{1}{3})\alpha^3C_A^2N_A^{d\,2} + 648\psi'(\tfrac{1}{3})\alpha^3C_A^2N_A^dN_A^o \\
&-216\psi'(\tfrac{1}{3})\alpha^3C_A^2N_A^{o\,2} + 1836\psi'(\tfrac{1}{3})\alpha^2C_A^2N_A^{d\,2} \\
&-4032\psi'(\tfrac{1}{3})\alpha^2C_A^2N_A^dN_A^o + 1908\psi'(\tfrac{1}{3})\alpha^2C_A^2N_A^{o\,2} \\
&+1152\psi'(\tfrac{1}{3})\alpha^2C_AN_A^dN_fN_A^oT_F - 576\psi'(\tfrac{1}{3})\alpha^2C_AN_fN_A^{o\,2}T_F \\
&-5832\psi'(\tfrac{1}{3})\alpha C_A^2N_A^{d\,2} + 10296\psi'(\tfrac{1}{3})\alpha C_A^2N_A^dN_A^o \\
&-5040\psi'(\tfrac{1}{3})\alpha C_A^2N_A^{o\,2} - 3744\psi'(\tfrac{1}{3})\alpha C_AN_A^dN_fN_A^oT_F \\
&+4896\psi'(\tfrac{1}{3})\alpha C_AN_fN_A^{o\,2}T_F + 12636\psi'(\tfrac{1}{3})C_A^2N_A^{d\,2} \\
&-20736\psi'(\tfrac{1}{3})C_A^2N_A^dN_A^o + 3588\psi'(\tfrac{1}{3})C_A^2N_A^{o\,2} \\
&+18144\psi'(\tfrac{1}{3})C_AN_A^dN_fN_A^oT_F - 12192\psi'(\tfrac{1}{3})C_AN_fN_A^{o\,2}T_F \\
&+6144\psi'(\tfrac{1}{3})N_f^2N_A^{o\,2}T_F^2 - 486\alpha^4C_A^2N_A^{d\,2} + 648\alpha^4C_A^2N_A^dN_A^o \\
&-162\alpha^4C_A^2N_A^{o\,2} + 288\pi^2\alpha^3C_A^2N_A^{d\,2} + 6318\alpha^3C_A^2N_A^{d\,2} \\
&-432\pi^2\alpha^3C_A^2N_A^dN_A^o - 6966\alpha^3C_A^2N_A^dN_A^o + 144\pi^2\alpha^3C_A^2N_A^{o\,2} \\
&+1674\alpha^3C_A^2N_A^{o\,2} + 1296\alpha^3C_AN_A^dN_fN_A^oT_F \\
&-432\alpha^3C_AN_fN_A^{o\,2}T_F - 1224\pi^2\alpha^2C_A^2N_A^{d\,2} + 9477\alpha^2C_A^2N_A^{d\,2} \\
&+2688\pi^2\alpha^2C_A^2N_A^dN_A^o + 2025\alpha^2C_A^2N_A^dN_A^o - 1272\pi^2\alpha^2C_A^2N_A^{o\,2} \\
&-3078\alpha^2C_A^2N_A^{o\,2} - 768\pi^2\alpha^2C_AN_A^dN_fN_A^oT_F \\
&-2592\alpha^2C_AN_A^dN_fN_A^oT_F + 384\pi^2\alpha^2C_AN_fN_A^{o\,2}T_F \\
&+1296\alpha^2C_AN_fN_A^{o\,2}T_F + 3888\pi^2\alpha C_A^2N_A^{d\,2} \\
&+34020\alpha C_A^2N_A^{d\,2} - 6864\pi^2\alpha C_A^2N_A^dN_A^o - 6048\alpha C_A^2N_A^dN_A^o \\
&+3360\pi^2\alpha C_A^2N_A^{o\,2} - 270\alpha C_A^2N_A^{o\,2} + 2496\pi^2\alpha C_AN_A^dN_fN_A^oT_F \\
&+3024\alpha C_AN_A^dN_fN_A^oT_F - 3264\pi^2\alpha C_AN_fN_A^{o\,2}T_F \\
&-3024\alpha C_AN_fN_A^{o\,2}T_F - 8424\pi^2C_A^2N_A^{d\,2} + 8019C_A^2N_A^{d\,2} \\
&+13824\pi^2C_A^2N_A^dN_A^o + 16119C_A^2N_A^dN_A^o - 2392\pi^2C_A^2N_A^{o\,2} \\
&-5310C_A^2N_A^{o\,2} - 12096\pi^2C_AN_A^dN_fN_A^oT_F - 6480C_AN_A^dN_fN_A^oT_F
\end{aligned}
$$

$$
\begin{aligned}
&+8128\pi^2 C_A N_f N_A^{o2} T_F + 4608 C_A N_f N_A^{o2} T_F \\
&+15552 C_F N_f N_A^{o2} T_F - 4096\pi^2 N_f^2 N_A^{o2} T_F^2 \\
&+2304 N_f^2 N_A^{o2} T_F^2 \big] \frac{a^2}{3888 N_A^{o2}} \; + \; \mathcal{O}(a^3) \\
\gamma_\alpha^{\rm MOMg}(a,\alpha) \;=\; & \big[- 6\alpha^2 C_A N_A^d - 3\alpha^2 C_A N_A^o - 36\alpha C_A N_A^d + 26\alpha C_A N_A^o \\
&-16\alpha N_f N_A^o T_F - 36 C_A N_A^d \big] \frac{a}{12\alpha N_A^o} \\
&+ \Big[- 432\psi'(\tfrac{1}{3})\alpha^4 C_A^2 N_A^{d^2} + 108\psi'(\tfrac{1}{3})\alpha^4 C_A^2 N_A^{o2} \\
&-2052\psi'(\tfrac{1}{3})\alpha^3 C_A^2 N_A^{d^2} + 2466\psi'(\tfrac{1}{3})\alpha^3 C_A^2 N_A^d N_A^o \\
&-1422\psi'(\tfrac{1}{3})\alpha^3 C_A^2 N_A^{o2} - 1152\psi'(\tfrac{1}{3})\alpha^3 C_A N_A^d N_f N_A^o T_F \\
&+576\psi'(\tfrac{1}{3})\alpha^3 C_A N_f N_A^{o2} T_F - 3564\psi'(\tfrac{1}{3})\alpha^2 C_A^2 N_A^{d^2} \\
&-8154\psi'(\tfrac{1}{3})\alpha^2 C_A^2 N_A^d N_A^o + 4626\psi'(\tfrac{1}{3})\alpha^2 C_A^2 N_A^{o2} \\
&-864\psi'(\tfrac{1}{3})\alpha^2 C_A N_A^d N_f N_A^o T_F - 3744\psi'(\tfrac{1}{3})\alpha^2 C_A N_f N_A^{o2} T_F \\
&-22032\psi'(\tfrac{1}{3})\alpha C_A^2 N_A^{d^2} + 17388\psi'(\tfrac{1}{3})\alpha C_A^2 N_A^d N_A^o \\
&-3588\psi'(\tfrac{1}{3})\alpha C_A^2 N_A^{o2} - 25056\psi'(\tfrac{1}{3})\alpha C_A N_A^d N_f N_A^o T_F \\
&+12192\psi'(\tfrac{1}{3})\alpha C_A N_f N_A^{o2} T_F - 6144\psi'(\tfrac{1}{3})\alpha N_f^2 N_A^{o2} T_F^2 \\
&-25272\psi'(\tfrac{1}{3}) C_A^2 N_A^{d^2} + 4968\psi'(\tfrac{1}{3}) C_A^2 N_A^d N_A^o \\
&-13824\psi'(\tfrac{1}{3}) C_A N_A^d N_f N_A^o T_F - 486\alpha^5 C_A^2 N_A^{d^2} \\
&-81\alpha^5 C_A^2 N_A^d N_A^o + 81\alpha^5 C_A^2 N_A^{o2} + 288\pi^2\alpha^4 C_A^2 N_A^{d^2} \\
&-1944\alpha^4 C_A^2 N_A^{d^2} + 3078\alpha^4 C_A^2 N_A^d N_A^o - 72\pi^2\alpha^4 C_A^2 N_A^{o2} \\
&-945\alpha^4 C_A^2 N_A^{o2} - 1296\alpha^4 C_A N_A^d N_f N_A^o T_F \\
&+432\alpha^4 C_A N_f N_A^{o2} T_F + 1368\pi^2\alpha^3 C_A^2 N_A^{d^2} \\
&-6804\alpha^3 C_A^2 N_A^{d^2} - 1644\pi^2\alpha^3 C_A^2 N_A^d N_A^o - 7614\alpha^3 C_A^2 N_A^d N_A^o \\
&+948\pi^2\alpha^3 C_A^2 N_A^{o2} + 4050\alpha^3 C_A^2 N_A^{o2} + 768\pi^2\alpha^3 C_A N_A^d N_f N_A^o T_F \\
&+2592\alpha^3 C_A N_A^d N_f N_A^o T_F - 384\pi^2\alpha^3 C_A N_f N_A^{o2} T_F \\
&-1296\alpha^3 C_A N_f N_A^{o2} T_F + 2376\pi^2\alpha^2 C_A^2 N_A^{d^2} - 49086\alpha^2 C_A^2 N_A^{d^2} \\
&+5436\pi^2\alpha^2 C_A^2 N_A^d N_A^o + 8775\alpha^2 C_A^2 N_A^d N_A^o - 3084\pi^2\alpha^2 C_A^2 N_A^{o2} \\
&-108\alpha^2 C_A^2 N_A^{o2} + 576\pi^2\alpha^2 C_A N_A^d N_f N_A^o T_F \\
&-4752\alpha^2 C_A N_A^d N_f N_A^o T_F + 2496\pi^2\alpha^2 C_A N_f N_A^{o2} T_F \\
&+3456\alpha^2 C_A N_f N_A^{o2} T_F + 14688\pi^2\alpha C_A^2 N_A^{d^2} \\
&-10206\alpha C_A^2 N_A^{d^2} - 11592\pi^2\alpha C_A^2 N_A^d N_A^o - 22599\alpha C_A^2 N_A^d N_A^o \\
&+2392\pi^2\alpha C_A^2 N_A^{o2} + 5310\alpha C_A^2 N_A^{o2} + 16704\pi^2\alpha C_A N_A^d N_f N_A^o T_F \\
&+15552\alpha C_A N_A^d N_f N_A^o T_F - 8128\pi^2\alpha C_A N_f N_A^{o2} T_F
\end{aligned}
$$

$$
\begin{aligned}
&-4608\alpha C_A N_f N_A^{o2} T_F - 15552\alpha C_F N_f N_A^{o2} T_F \\
&+4096\pi^2 \alpha N_f^2 N_A^{o2} T_F^2 - 2304\alpha N_f^2 N_A^{o2} T_F^2 + 16848\pi^2 C_A^2 N_A^{d2} \\
&+116640 C_A^2 N_A^{d2} - 3312\pi^2 C_A^2 N_A^d N_A^o - 14904 C_A^2 N_A^d N_A^o \\
&+9216\pi^2 C_A N_A^d N_f N_A^o T_F + 10368 C_A N_A^d N_f N_A^o T_F \big] \frac{a^2}{3888\alpha N_A^{o2}} \\
&+ \mathcal{O}(a^3)
\end{aligned}
$$

$$
\begin{aligned}
\gamma_c^{\rm MOMg}(a,\alpha) &= \big[-2\alpha N_A^d + \alpha N_A^o - 6N_A^d - 3N_A^o \big] \frac{C_A a}{4N_A^o} \\
&+\Big[-288\psi'(\tfrac{1}{3})\alpha^3 C_A N_A^{d2} + 288\psi'(\tfrac{1}{3})\alpha^3 C_A N_A^d N_A^o \\
&-72\psi'(\tfrac{1}{3})\alpha^3 C_A N_A^{o2} - 504\psi'(\tfrac{1}{3})\alpha^2 C_A N_A^{d2} \\
&-828\psi'(\tfrac{1}{3})\alpha^2 C_A N_A^d N_A^o + 540\psi'(\tfrac{1}{3})\alpha^2 C_A N_A^{o2} \\
&-1728\psi'(\tfrac{1}{3})\alpha C_A N_A^{d2} + 552\psi'(\tfrac{1}{3})\alpha C_A N_A^d N_A^o \\
&-1248\psi'(\tfrac{1}{3})\alpha C_A N_A^{o2} - 1536\psi'(\tfrac{1}{3})\alpha N_A^d N_f N_A^o T_F \\
&+768\psi'(\tfrac{1}{3})\alpha N_f N_A^{o2} T_F - 8424\psi'(\tfrac{1}{3}) C_A N_A^{d2} \\
&-2556\psi'(\tfrac{1}{3}) C_A N_A^d N_A^o + 828\psi'(\tfrac{1}{3}) C_A N_A^{o2} - 324\alpha^4 C_A N_A^{d2} \\
&-4608\psi'(\tfrac{1}{3}) N_A^d N_f N_A^o T_F - 2304\psi'(\tfrac{1}{3}) N_f N_A^{o2} T_F \\
&+270\alpha^4 C_A N_A^d N_A^o - 54\alpha^4 C_A N_A^{o2} + 192\pi^2\alpha^3 C_A N_A^{d2} \\
&+972\alpha^3 C_A N_A^{d2} - 192\pi^2\alpha^3 C_A N_A^d N_A^o - 2106\alpha^3 C_A N_A^d N_A^o \\
&+48\pi^2\alpha^3 C_A N_A^{o2} + 648\alpha^3 C_A N_A^{o2} + 336\pi^2\alpha^2 C_A N_A^{d2} \\
&+5184\alpha^2 C_A N_A^{d2} + 552\pi^2\alpha^2 C_A N_A^d N_A^o - 1944\alpha^2 C_A N_A^d N_A^o \\
&-360\pi^2\alpha^2 C_A N_A^{o2} - 648\alpha^2 C_A N_A^{o2} + 1152\pi^2\alpha C_A N_A^{d2} \\
&-10368\alpha C_A N_A^{d2} - 368\pi^2\alpha C_A N_A^d N_A^o - 144\alpha C_A N_A^d N_A^o \\
&+832\pi^2\alpha C_A N_A^{o2} - 1710\alpha C_A N_A^{o2} + 1024\pi^2\alpha N_A^d N_f N_A^o T_F \\
&-576\alpha N_A^d N_f N_A^o T_F - 512\pi^2\alpha N_f N_A^{o2} T_F + 288\alpha N_f N_A^{o2} T_F \\
&+5616\pi^2 C_A N_A^{d2} + 17010 C_A N_A^{d2} + 1704\pi^2 C_A N_A^d N_A^o \\
&-1485 C_A N_A^d N_A^o - 552\pi^2 C_A N_A^{o2} - 378 C_A N_A^{o2} \\
&+3072\pi^2 N_A^d N_f N_A^o T_F + 864 N_A^d N_f N_A^o T_F + 1536\pi^2 N_f N_A^{o2} T_F \\
&+432 N_f N_A^{o2} T_F \big] \frac{C_A a^2}{2592 N_A^{o2}} \; + \; \mathcal{O}(a^3)
\end{aligned}
$$

$$
\begin{aligned}
\gamma_\psi^{\rm MOMg}(a,\alpha) &= \frac{\alpha N_A^o T_F a}{N_F} \\
&+ \big[72\psi'(\tfrac{1}{3})\alpha^3 C_A C_F N_F - 108\psi'(\tfrac{1}{3})\alpha^3 C_A N_A^o T_F \\
&-90\psi'(\tfrac{1}{3})\alpha^2 C_A C_F N_F + 252\psi'(\tfrac{1}{3})\alpha^2 C_A N_A^o T_F \\
&+702\psi'(\tfrac{1}{3})\alpha C_A C_F N_F - 840\psi'(\tfrac{1}{3})\alpha C_A N_A^o T_F
\end{aligned}
$$

$$
\begin{aligned}
&+384\psi'(\tfrac{1}{3})\alpha N_f N_A^o T_F^2 + 81\alpha^4 C_A C_F N_F - 108\alpha^4 C_A N_A^o T_F \\
&-48\pi^2\alpha^3 C_A C_F N_F - 486\alpha^3 C_A C_F N_F + 72\pi^2\alpha^3 C_A N_A^o T_F \\
&+729\alpha^3 C_A N_A^o T_F + 60\pi^2\alpha^2 C_A C_F N_F - 162\alpha^2 C_A C_F N_F \\
&-168\pi^2\alpha^2 C_A N_A^o T_F + 324\alpha^2 C_A N_A^o T_F - 468\pi^2\alpha C_A C_F N_F \\
&+648\alpha C_A C_F N_F + 560\pi^2\alpha C_A N_A^o T_F - 1017\alpha C_A N_A^o T_F \\
&-256\pi^2\alpha N_f N_A^o T_F^2 + 144\alpha N_f N_A^o T_F^2 + 2025 C_A C_F N_F \\
&-486 C_F^2 N_F - 648 C_F N_F N_f T_F \big] \frac{a^2}{324 N_F} \; + \; \mathcal{O}(a^3) \; . \qquad (5.5.59)
\end{aligned}
$$

5.6 MOMq scheme.

In this section we simply present our results, where our method of determining the results in this scheme is the same as in the previous two sections. For the MOMq scheme we also give the results analytically. Starting with the amplitudes we have

$$
\begin{aligned}
\Sigma^{\rm qqg}_{(1)}(p,q)\Big|_{\rm MOMq} &= 1 \; + \; \mathcal{O}(a^2) \\
\Sigma^{\rm qqg}_{(2)}(p,q)\Big|_{\rm MOMq} &= \Sigma^{\rm qqg}_{(5)}(p,q)\Big|_{\rm MOMq} \\
&= \big[-6\psi'\big(\tfrac{1}{3}\big)\, \alpha^2 C_A N_F N_A^d + 3\psi'\big(\tfrac{1}{3}\big)\, \alpha^2 C_A N_F N_A^o \\
&\quad -24\psi'\big(\tfrac{1}{3}\big)\, \alpha N_A^{o2} T_F - 6\psi'\big(\tfrac{1}{3}\big)\, C_A N_F N_A^d \\
&\quad -15\psi'\big(\tfrac{1}{3}\big)\, C_A N_F N_A^o + 24\psi'\big(\tfrac{1}{3}\big)\, C_F N_F N_A^o \\
&\quad +4\alpha^2 C_A N_F N_A^d \pi^2 + 36\alpha^2 C_A N_F N_A^d - 2\alpha^2 C_A N_F N_A^o \pi^2 \\
&\quad -18\alpha^2 C_A N_F N_A^o + 36\alpha C_A N_F N_A^d - 36\alpha C_A N_F N_A^o \\
&\quad +16\alpha N_A^{o2}\pi^2 T_F + 72\alpha N_A^{o2} T_F + 4 C_A N_F N_A^d \pi^2 \\
&\quad -36 C_A N_F N_A^d + 10 C_A N_F N_A^o \pi^2 + 126 C_A N_F N_A^o \\
&\quad -16 C_F N_F N_A^o \pi^2 - 144 C_F N_F N_A^o \big] \frac{a}{54 N_F N_A^o} \; + \; \mathcal{O}(a^2) \\
\Sigma^{\rm qqg}_{(3)}(p,q)\Big|_{\rm MOMq} &= \Sigma^{\rm qqg}_{(4)}(p,q)\Big|_{\rm MOMq} \\
&= \big[-6\psi'\big(\tfrac{1}{3}\big)\, \alpha C_A N_F N_A^d + 6\psi'\big(\tfrac{1}{3}\big)\, \alpha C_A N_F N_A^o \\
&\quad -24\psi'\big(\tfrac{1}{3}\big)\, \alpha N_A^{o2} T_F - 6\psi'\big(\tfrac{1}{3}\big)\, C_A N_F N_A^d - 6\psi'\big(\tfrac{1}{3}\big)\, C_A N_F N_A^o \\
&\quad +18\alpha^2 C_A N_F N_A^d - 9\alpha^2 C_A N_F N_A^o + 4\alpha C_A N_F N_A^d \pi^2 \\
&\quad +45\alpha C_A N_F N_A^d - 4\alpha C_A N_F N_A^o \pi^2 - 45\alpha C_A N_F N_A^o \\
&\quad +16\alpha N_A^{o2}\pi^2 T_F + 36\alpha N_A^{o2} T_F + 4 C_A N_F N_A^d \pi^2 - 45 C_A N_F N_A^d \\
&\quad +4 C_A N_F N_A^o \pi^2 + 90 C_A N_F N_A^o - 72 C_F N_F N_A^o \big] \frac{a}{54 N_F N_A^o}
\end{aligned}
$$

$$
\begin{aligned}
&+ \mathcal{O}(a^2) \\
\Sigma^{\mathrm{qqg}}_{(6)}(p,q)\Big|_{\mathrm{MOMq}} &= \big[6\psi'\big(\tfrac{1}{3}\big)\,\alpha^2 C_A N_A^d - 3\psi'\big(\tfrac{1}{3}\big)\,\alpha^2 C_A N_A^o + 12\psi'\big(\tfrac{1}{3}\big)\,\alpha C_A N_A^d \\
&\quad -12\psi'\big(\tfrac{1}{3}\big)\,\alpha C_A N_A^o + 6\psi'\big(\tfrac{1}{3}\big)\,C_A N_A^d - 33\psi'\big(\tfrac{1}{3}\big)\,C_A N_A^o \\
&\quad +24\psi'\big(\tfrac{1}{3}\big)\,C_F N_A^o - 4\alpha^2 C_A N_A^d \pi^2 + 2\alpha^2 C_A N_A^o \pi^2 \\
&\quad -8\alpha C_A N_A^d \pi^2 + 8\alpha C_A N_A^o \pi^2 - 4 C_A N_A^d \pi^2 + 22 C_A N_A^o \pi^2 \\
&\quad -16 C_F N_A^o \pi^2\big]\,\frac{a}{54 N_A^o} \;+\; \mathcal{O}(a^2)\;. \qquad (5.6.60)
\end{aligned}
$$

The coupling constant mapping is

$$
\begin{aligned}
a_{\mathrm{MOMq}} &= a + \big[-12\psi'\big(\tfrac{1}{3}\big)\,\alpha^2 C_A N_F N_A^d + 6\psi'\big(\tfrac{1}{3}\big)\,\alpha^2 C_A N_F N_A^o \\
&\quad +24\psi'\big(\tfrac{1}{3}\big)\,\alpha C_A N_F N_A^d - 24\psi'\big(\tfrac{1}{3}\big)\,\alpha C_A N_F N_A^o - 96\psi'\big(\tfrac{1}{3}\big)\,\alpha N_A^{o\,2} T_F \\
&\quad -60\psi'\big(\tfrac{1}{3}\big)\,C_A N_F N_A^d - 78\psi'\big(\tfrac{1}{3}\big)\,C_A N_F N_A^o + 48\psi'\big(\tfrac{1}{3}\big)\,C_F N_F N_A^o \\
&\quad +8\alpha^2 C_A N_F N_A^d \pi^2 + 54\alpha^2 C_A N_F N_A^d - 4\alpha^2 C_A N_F N_A^o \pi^2 \\
&\quad -27\alpha^2 C_A N_F N_A^o - 16\alpha C_A N_F N_A^d \pi^2 - 54\alpha C_A N_F N_A^d \\
&\quad +16\alpha C_A N_F N_A^o \pi^2 + 54\alpha C_A N_F N_A^o + 64\alpha N_A^{o\,2} \pi^2 T_F + 216\alpha N_A^{o\,2} T_F \\
&\quad +40 C_A N_F N_A^d \pi^2 + 52 C_A N_F N_A^o \pi^2 + 993 C_A N_F N_A^o \\
&\quad -32 C_F N_F N_A^o \pi^2 - 432 C_F N_F N_A^o - 240 N_F N_f N_A^o T_F\big]\,\frac{a^2}{108 N_F N_A^o} \\
&\quad + \mathcal{O}(a^3)\;. \qquad (5.6.61)
\end{aligned}
$$

The associated coupling constant conversion function is

$$
\begin{aligned}
C_g^{\mathrm{MOMq}}(a,\alpha) &= 1 + \big[12\psi'\big(\tfrac{1}{3}\big)\,\alpha^2 C_A N_F N_A^d - 6\psi'\big(\tfrac{1}{3}\big)\,\alpha^2 C_A N_F N_A^o \\
&\quad -24\psi'\big(\tfrac{1}{3}\big)\,\alpha C_A N_F N_A^d + 24\psi'\big(\tfrac{1}{3}\big)\,\alpha C_A N_F N_A^o \\
&\quad +96\psi'\big(\tfrac{1}{3}\big)\,\alpha N_A^{o\,2} T_F + 60\psi'\big(\tfrac{1}{3}\big)\,C_A N_F N_A^d \\
&\quad +78\psi'\big(\tfrac{1}{3}\big)\,C_A N_F N_A^o - 48\psi'\big(\tfrac{1}{3}\big)\,C_F N_F N_A^o \\
&\quad -8\alpha^2 C_A N_F N_A^d \pi^2 - 54\alpha^2 C_A N_F N_A^d + 4\alpha^2 C_A N_F N_A^o \pi^2 \\
&\quad +27\alpha^2 C_A N_F N_A^o + 16\alpha C_A N_F N_A^d \pi^2 + 54\alpha C_A N_F N_A^d \\
&\quad -16\alpha C_A N_F N_A^o \pi^2 - 54\alpha C_A N_F N_A^o - 64\alpha N_A^{o\,2} \pi^2 T_F \\
&\quad -216\alpha N_A^{o\,2} T_F - 40 C_A N_F N_A^d \pi^2 - 52 C_A N_F N_A^o \pi^2 \\
&\quad -993 C_A N_F N_A^o + 32 C_F N_F N_A^o \pi^2 + 432 C_F N_F N_A^o \\
&\quad +240 N_F N_f N_A^o T_F]\,\frac{a}{216 N_F N_A^o} \;+\; \mathcal{O}(a^2) \qquad (5.6.62)
\end{aligned}
$$

from which we deduce that the two loop renormalization group functions are

$$
\begin{aligned}
\beta^{\mathrm{MOMq}}(a,\alpha) &= \left[-11C_A + 4N_f T_F\right]\frac{a^2}{3} \\
&+ \Big[72\psi'\left(\tfrac{1}{3}\right)\alpha^3 C_A^2 N_F N_A^{d\,2} - 18\psi'\left(\tfrac{1}{3}\right)\alpha^3 C_A^2 N_F N_A^{o\,2} \\
&\quad +360\psi'\left(\tfrac{1}{3}\right)\alpha^2 C_A^2 N_F N_A^{d\,2} - 492\psi'\left(\tfrac{1}{3}\right)\alpha^2 C_A^2 N_F N_A^d N_A^o \\
&\quad +192\psi'\left(\tfrac{1}{3}\right)\alpha^2 C_A^2 N_F N_A^{o\,2} + 288\psi'\left(\tfrac{1}{3}\right)\alpha^2 C_A C_F N_F^2 N_f N_A^o \\
&\quad -96\psi'\left(\tfrac{1}{3}\right)\alpha^2 C_A N_F N_A^d N_f N_A^o T_F - 384\psi'\left(\tfrac{1}{3}\right)\alpha^2 C_A N_F N_f N_A^{o\,2} T_F \\
&\quad +288\psi'\left(\tfrac{1}{3}\right)\alpha^2 C_A N_A^d N_A^{o\,2} T_F + 144\psi'\left(\tfrac{1}{3}\right)\alpha^2 C_A N_A^{o\,3} T_F \\
&\quad +528\psi'\left(\tfrac{1}{3}\right)\alpha C_A^2 N_F N_A^d N_A^o - 312\psi'\left(\tfrac{1}{3}\right)\alpha C_A^2 N_F N_A^{o\,2} \\
&\quad -576\psi'\left(\tfrac{1}{3}\right)\alpha C_A C_F N_F^2 N_f N_A^o + 384\psi'\left(\tfrac{1}{3}\right)\alpha C_A N_F N_A^d N_f N_A^o T_F \\
&\quad +768\psi'\left(\tfrac{1}{3}\right)\alpha C_A N_F N_f N_A^{o\,2} T_F + 1728\psi'\left(\tfrac{1}{3}\right)\alpha C_A N_A^d N_A^{o\,2} T_F \\
&\quad -1248\psi'\left(\tfrac{1}{3}\right)\alpha C_A N_A^{o\,3} T_F + 768\psi'\left(\tfrac{1}{3}\right)\alpha N_f N_A^{o\,3} T_F^2 \\
&\quad -432\psi'\left(\tfrac{1}{3}\right) C_A^2 N_F N_A^{d\,2} + 432\psi'\left(\tfrac{1}{3}\right) C_A^2 N_F N_A^d N_A^o \\
&\quad +1440\psi'\left(\tfrac{1}{3}\right) C_A C_F N_F^2 N_f N_A^o - 1440\psi'\left(\tfrac{1}{3}\right) C_A N_F N_A^d N_f N_A^o T_F \\
&\quad -1440\psi'\left(\tfrac{1}{3}\right) C_A N_F N_f N_A^{o\,2} T_F + 1728\psi'\left(\tfrac{1}{3}\right) C_A N_A^d N_A^{o\,2} T_F \\
&\quad -48\alpha^3 C_A^2 N_F N_A^{d\,2}\pi^2 - 324\alpha^3 C_A^2 N_F N_A^{d\,2} + 12\alpha^3 C_A^2 N_F N_A^{o\,2}\pi^2 \\
&\quad +81\alpha^3 C_A^2 N_F N_A^{o\,2} - 240\alpha^2 C_A^2 N_F N_A^{d\,2}\pi^2 - 1782\alpha^2 C_A^2 N_F N_A^{d\,2} \\
&\quad +328\alpha^2 C_A^2 N_F N_A^d N_A^o\pi^2 + 2295\alpha^2 C_A^2 N_F N_A^d N_A^o \\
&\quad -128\alpha^2 C_A^2 N_F N_A^{o\,2}\pi^2 - 783\alpha^2 C_A^2 N_F N_A^{o\,2} \\
&\quad -192\alpha^2 C_A C_F N_F^2 N_f N_A^o\pi^2 - 1296\alpha^2 C_A C_F N_F^2 N_f N_A^o \\
&\quad +64\alpha^2 C_A N_F N_A^d N_f N_A^o\pi^2 T_F + 432\alpha^2 C_A N_F N_A^d N_f N_A^o T_F \\
&\quad +256\alpha^2 C_A N_F N_f N_A^{o\,2}\pi^2 T_F + 1728\alpha^2 C_A N_F N_f N_A^{o\,2} T_F \\
&\quad -192\alpha^2 C_A N_A^d N_A^{o\,2}\pi^2 T_F - 648\alpha^2 C_A N_A^d N_A^{o\,2} T_F \\
&\quad -96\alpha^2 C_A N_A^{o\,3}\pi^2 T_F - 324\alpha^2 C_A N_A^{o\,3} T_F - 972\alpha C_A^2 N_F N_A^{d\,2} \\
&\quad -352\alpha C_A^2 N_F N_A^d N_A^o\pi^2 - 702\alpha C_A^2 N_F N_A^d N_A^o \\
&\quad +208\alpha C_A^2 N_F N_A^{o\,2}\pi^2 + 702\alpha C_A^2 N_F N_A^{o\,2} \\
&\quad +384\alpha C_A C_F N_F^2 N_f N_A^o\pi^2 + 1296\alpha C_A C_F N_F^2 N_f N_A^o \\
&\quad -256\alpha C_A N_F N_A^d N_f N_A^o\pi^2 T_F - 864\alpha C_A N_F N_A^d N_f N_A^o T_F \\
&\quad -512\alpha C_A N_F N_f N_A^{o\,2}\pi^2 T_F - 1728\alpha C_A N_F N_f N_A^{o\,2} T_F \\
&\quad -1152\alpha C_A N_A^d N_A^{o\,2}\pi^2 T_F - 3888\alpha C_A N_A^d N_A^{o\,2} T_F \\
&\quad +832\alpha C_A N_A^{o\,3}\pi^2 T_F + 2808\alpha C_A N_A^{o\,3} T_F \\
&\quad -512\alpha N_f N_A^{o\,3}\pi^2 T_F^2 - 1728\alpha N_f N_A^{o\,3} T_F^2 + 288 C_A^2 N_F N_A^{d\,2}\pi^2
\end{aligned}
$$

$$
\begin{aligned}
&+972C_A^2N_FN_A^{d2} - 288C_A^2N_FN_A^dN_A^o\pi^2 - 972C_A^2N_FN_A^dN_A^o \\
&-7344C_A^2N_FN_A^{o2} - 960C_AC_F^2N_fN_A^o\pi^2 \\
&+960C_AN_FN_A^dN_fN_A^o\pi^2T_F + 960C_AN_FN_fN_A^{o2}\pi^2T_F \\
&+4320C_AN_FN_fN_A^{o2}T_F - 1152C_AN_A^dN_A^{o2}\pi^2T_F \\
&-3888C_AN_A^dN_A^{o2}T_F + 2592C_FN_FN_fN_A^{o2}T_F\big]\,\frac{a^3}{648N_FN_A^{o2}} \\
&+\mathcal{O}(a^4)
\end{aligned}
$$

$$
\begin{aligned}
\gamma_A^{\mathrm{MOMq}}(a,\alpha) \;=\;& \big[-3\alpha C_AN_A^d + 3\alpha C_AN_A^o + 9C_AN_A^d - 13C_AN_A^o + 8N_fN_A^oT_F\big]\,\frac{a}{6N_A^o} \\
&+\Big[-72\psi'\left(\tfrac{1}{3}\right)\alpha^3C_A^2N_FN_A^{d2} + 108\psi'\left(\tfrac{1}{3}\right)\alpha^3C_A^2N_FN_A^dN_A^o \\
&-36\psi'\left(\tfrac{1}{3}\right)\alpha^3C_A^2N_FN_A^{o2} + 360\psi'\left(\tfrac{1}{3}\right)\alpha^2C_A^2N_FN_A^{d2} \\
&-708\psi'\left(\tfrac{1}{3}\right)\alpha^2C_A^2N_FN_A^dN_A^o + 300\psi'\left(\tfrac{1}{3}\right)\alpha^2C_A^2N_FN_A^{o2} \\
&+192\psi'\left(\tfrac{1}{3}\right)\alpha^2C_AN_FN_A^dN_fN_A^oT_F - 96\psi'\left(\tfrac{1}{3}\right)\alpha^2C_AN_FN_fN_A^{o2}T_F \\
&-576\psi'\left(\tfrac{1}{3}\right)\alpha^2C_AN_A^dN_A^{o2}T_F + 576\psi'\left(\tfrac{1}{3}\right)\alpha^2C_AN_A^{o3}T_F \\
&-792\psi'\left(\tfrac{1}{3}\right)\alpha C_A^2N_FN_A^{d2} + 948\psi'\left(\tfrac{1}{3}\right)\alpha C_A^2N_FN_A^dN_A^o \\
&-156\psi'\left(\tfrac{1}{3}\right)\alpha C_A^2N_FN_A^{o2} + 288\psi'\left(\tfrac{1}{3}\right)\alpha C_AC_FN_FN_A^dN_A^o \\
&-288\psi'\left(\tfrac{1}{3}\right)\alpha C_AC_FN_FN_A^{o2} - 384\psi'\left(\tfrac{1}{3}\right)\alpha C_AN_FN_A^dN_fN_A^oT_F \\
&+384\psi'\left(\tfrac{1}{3}\right)\alpha C_AN_FN_fN_A^{o2}T_F + 1728\psi'\left(\tfrac{1}{3}\right)\alpha C_AN_A^dN_A^{o2}T_F \\
&-2496\psi'\left(\tfrac{1}{3}\right)\alpha C_AN_A^{o3}T_F + 1536\psi'\left(\tfrac{1}{3}\right)\alpha N_fN_A^{o3}T_F^2 \\
&+1080\psi'\left(\tfrac{1}{3}\right)C_A^2N_FN_A^{d2} - 156\psi'\left(\tfrac{1}{3}\right)C_A^2N_FN_A^dN_A^o \\
&-2028\psi'\left(\tfrac{1}{3}\right)C_A^2N_FN_A^{o2} - 864\psi'\left(\tfrac{1}{3}\right)C_AC_FN_FN_A^dN_A^o \\
&+1248\psi'\left(\tfrac{1}{3}\right)C_AC_FN_FN_A^{o2} + 960\psi'\left(\tfrac{1}{3}\right)C_AN_FN_A^dN_fN_A^oT_F \\
&+1248\psi'\left(\tfrac{1}{3}\right)C_AN_FN_fN_A^{o2}T_F - 768\psi'\left(\tfrac{1}{3}\right)C_FN_FN_fN_A^{o2}T_F \\
&+48\alpha^3C_A^2N_FN_A^{d2}\pi^2 + 1296\alpha^3C_A^2N_FN_A^{d2} \\
&-72\alpha^3C_A^2N_FN_A^dN_A^o\pi^2 - 972\alpha^3C_A^2N_FN_A^dN_A^o \\
&+24\alpha^3C_A^2N_FN_A^{o2}\pi^2 + 162\alpha^3C_A^2N_FN_A^{o2} \\
&-240\alpha^2C_A^2N_FN_A^{d2}\pi^2 + 4293\alpha^2C_A^2N_FN_A^{d2} \\
&+472\alpha^2C_A^2N_FN_A^dN_A^o\pi^2 - 1539\alpha^2C_A^2N_FN_A^dN_A^o \\
&-200\alpha^2C_A^2N_FN_A^{o2}\pi^2 - 162\alpha^2C_A^2N_FN_A^{o2} \\
&-128\alpha^2C_AN_FN_A^dN_fN_A^o\pi^2T_F + 64\alpha^2C_AN_FN_fN_A^{o2}\pi^2T_F \\
&+384\alpha^2C_AN_A^dN_A^{o2}\pi^2T_F + 1296\alpha^2C_AN_A^dN_A^{o2}T_F \\
&-384\alpha^2C_AN_A^{o3}\pi^2T_F - 1296\alpha^2C_AN_A^{o3}T_F \\
&+528\alpha C_A^2N_FN_A^{d2}\pi^2 + 10854\alpha C_A^2N_FN_A^{d2}
\end{aligned}
$$

$$
\begin{aligned}
&-632\alpha C_A^2 N_F N_A^d N_A^o \pi^2 + 378\alpha C_A^2 N_F N_A^d N_A^o \\
&+104\alpha C_A^2 N_F N_A^{o2} \pi^2 - 1998\alpha C_A^2 N_F N_A^{o2} \\
&-192\alpha C_A C_F N_F N_A^d N_A^o \pi^2 - 2592\alpha C_A C_F N_F N_A^d N_A^o \\
&+192\alpha C_A C_F N_F N_A^{o2} \pi^2 + 2592\alpha C_A C_F N_F N_A^{o2} \\
&+256\alpha C_A N_F N_A^d N_f N_A^o \pi^2 T_F + 864\alpha C_A N_F N_A^d N_f N_A^o T_F \\
&-256\alpha C_A N_F N_f N_A^{o2} \pi^2 T_F - 864\alpha C_A N_F N_f N_A^{o2} T_F \\
&-1152\alpha C_A N_A^d N_A^{o2} \pi^2 T_F - 3888\alpha C_A N_A^d N_A^{o2} T_F \\
&+1664\alpha C_A N_A^{o3} \pi^2 T_F + 5616\alpha C_A N_A^{o3} T_F \\
&-1024\alpha N_f N_A^{o3} \pi^2 T_F^2 - 3456\alpha N_f N_A^{o3} T_F^2 - 720 C_A^2 N_F N_A^{d2} \pi^2 \\
&+2673 C_A^2 N_F N_A^{d2} + 104 C_A^2 N_F N_A^d N_A^o \pi^2 + 1755 C_A^2 N_F N_A^d N_A^o \\
&+1352 C_A^2 N_F N_A^{o2} \pi^2 + 3456 C_A^2 N_F N_A^{o2} + 576 C_A C_F N_F N_A^d N_A^o \pi^2 \\
&+7776 C_A C_F N_F N_A^d N_A^o - 832 C_A C_F N_F N_A^{o2} \pi^2 \\
&-11232 C_A C_F N_F N_A^{o2} - 640 C_A N_F N_A^d N_f N_A^o \pi^2 T_F \\
&-3024 C_A N_F N_A^d N_f N_A^o T_F - 832 C_A N_F N_f N_A^{o2} \pi^2 T_F \\
&-432 C_A N_F N_f N_A^{o2} T_F + 512 C_F N_F N_f N_A^{o2} \pi^2 T_F \\
&+12096 C_F N_F N_f N_A^{o2} T_F \big] \frac{a^2}{1296 N_F N_A^{o2}} \; + \; \mathcal{O}(a^3)
\end{aligned}
$$

$$
\begin{aligned}
\gamma_\alpha^{\rm MOMq}(a,\alpha) \;=\; & \big[-6\alpha^2 C_A N_A^d - 3\alpha^2 C_A N_A^o - 36\alpha C_A N_A^d + 26\alpha C_A N_A^o \\
& -16\alpha N_f N_A^o T_F - 36 C_A N_A^d \big] \frac{a}{12\alpha N_A^o} \\
& + \Big[-72\psi'\left(\tfrac{1}{3}\right) \alpha^4 C_A^2 N_F N_A^{d2} + 18\psi'\left(\tfrac{1}{3}\right) \alpha^4 C_A^2 N_F N_A^{o2} \\
& -288\psi'\left(\tfrac{1}{3}\right) \alpha^3 C_A^2 N_F N_A^{d2} + 456\psi'\left(\tfrac{1}{3}\right) \alpha^3 C_A^2 N_F N_A^d N_A^o \\
& -228\psi'\left(\tfrac{1}{3}\right) \alpha^3 C_A^2 N_F N_A^{o2} - 192\psi'\left(\tfrac{1}{3}\right) \alpha^3 C_A N_F N_A^d N_f N_A^o T_F \\
& +96\psi'\left(\tfrac{1}{3}\right) \alpha^3 C_A N_F N_f N_A^{o2} T_F - 576\psi'\left(\tfrac{1}{3}\right) \alpha^3 C_A N_A^d N_A^{o2} T_F \\
& -288\psi'\left(\tfrac{1}{3}\right) \alpha^3 C_A N_A^{o3} T_F + 72\psi'\left(\tfrac{1}{3}\right) \alpha^2 C_A^2 N_F N_A^{d2} \\
& -1920\psi'\left(\tfrac{1}{3}\right) \alpha^2 C_A^2 N_F N_A^d N_A^o + 390\psi'\left(\tfrac{1}{3}\right) \alpha^2 C_A^2 N_F N_A^{o2} \\
& +288\psi'\left(\tfrac{1}{3}\right) \alpha^2 C_A C_F N_F N_A^d N_A^o + 144\psi'\left(\tfrac{1}{3}\right) \alpha^2 C_A C_F N_F N_A^{o2} \\
& +384\psi'\left(\tfrac{1}{3}\right) \alpha^2 C_A N_F N_A^d N_f N_A^o T_F \\
& -384\psi'\left(\tfrac{1}{3}\right) \alpha^2 C_A N_F N_f N_A^{o2} T_F - 3456\psi'\left(\tfrac{1}{3}\right) \alpha^2 C_A N_A^d N_A^{o2} T_F \\
& +2496\psi'\left(\tfrac{1}{3}\right) \alpha^2 C_A N_A^{o3} T_F - 1536\psi'\left(\tfrac{1}{3}\right) \alpha^2 N_f N_A^{o3} T_F^2 \\
& -1296\psi'\left(\tfrac{1}{3}\right) \alpha C_A^2 N_F N_A^{d2} - 2112\psi'\left(\tfrac{1}{3}\right) \alpha C_A^2 N_F N_A^d N_A^o \\
& +2028\psi'\left(\tfrac{1}{3}\right) \alpha C_A^2 N_F N_A^{o2} + 1728\psi'\left(\tfrac{1}{3}\right) \alpha C_A C_F N_F N_A^d N_A^o \\
& -1248\psi'\left(\tfrac{1}{3}\right) \alpha C_A C_F N_F N_A^{o2} - 960\psi'\left(\tfrac{1}{3}\right) \alpha C_A N_F N_A^d N_f N_A^o T_F
\end{aligned}
$$

$$
\begin{aligned}
&-1248\psi'\left(\tfrac{1}{3}\right)\alpha C_A N_F N_f N_A^{o2} T_F - 3456\psi'\left(\tfrac{1}{3}\right)\alpha C_A N_A^d N_A^{o2} T_F \\
&+768\psi'\left(\tfrac{1}{3}\right)\alpha C_F N_F N_f N_A^{o2} T_F - 2160\psi'\left(\tfrac{1}{3}\right) C_A^2 N_F N_A^{d2} \\
&-2808\psi'\left(\tfrac{1}{3}\right) C_A^2 N_F N_A^d N_A^o + 1728\psi'\left(\tfrac{1}{3}\right) C_A C_F N_F N_A^d N_A^o \\
&+48\alpha^4 C_A^2 N_F N_A^{d2}\pi^2 - 12\alpha^4 C_A^2 N_F N_A^{o2}\pi^2 \\
&+192\alpha^3 C_A^2 N_F N_A^{d2}\pi^2 - 3078\alpha^3 C_A^2 N_F N_A^{d2} \\
&-304\alpha^3 C_A^2 N_F N_A^d N_A^o\pi^2 - 567\alpha^3 C_A^2 N_F N_A^d N_A^o \\
&+152\alpha^3 C_A^2 N_F N_A^{o2}\pi^2 + 567\alpha^3 C_A^2 N_F N_A^{o2} \\
&+128\alpha^3 C_A N_F N_A^d N_f N_A^o\pi^2 T_F - 64\alpha^3 C_A N_F N_f N_A^{o2}\pi^2 T_F \\
&+384\alpha^3 C_A N_A^d N_A^{o2}\pi^2 T_F + 1296\alpha^3 C_A N_A^d N_A^{o2} T_F \\
&+192\alpha^3 C_A N_A^{o3}\pi^2 T_F + 648\alpha^3 C_A N_A^{o3} T_F \\
&-48\alpha^2 C_A^2 N_F N_A^{d2}\pi^2 - 17334\alpha^2 C_A^2 N_F N_A^{d2} \\
&+1280\alpha^2 C_A^2 N_F N_A^d N_A^o\pi^2 + 3429\alpha^2 C_A^2 N_F N_A^d N_A^o \\
&-260\alpha^2 C_A^2 N_F N_A^{o2}\pi^2 + 1269\alpha^2 C_A^2 N_F N_A^{o2} \\
&-192\alpha^2 C_A C_F N_F N_A^d N_A^o\pi^2 - 2592\alpha^2 C_A C_F N_F N_A^d N_A^o \\
&-96\alpha^2 C_A C_F N_F N_A^{o2}\pi^2 - 1296\alpha^2 C_A C_F N_F N_A^{o2} \\
&-256\alpha^2 C_A N_F N_A^d N_f N_A^o\pi^2 T_F - 864\alpha^2 C_A N_F N_A^d N_f N_A^o T_F \\
&+256\alpha^2 C_A N_F N_f N_A^{o2}\pi^2 T_F + 864\alpha^2 C_A N_F N_f N_A^{o2} T_F \\
&+2304\alpha^2 C_A N_A^d N_A^{o2}\pi^2 T_F + 7776\alpha^2 C_A N_A^d N_A^{o2} T_F \\
&-1664\alpha^2 C_A N_A^{o3}\pi^2 T_F - 5616\alpha^2 C_A N_A^{o3} T_F \\
&+1024\alpha^2 N_f N_A^{o3}\pi^2 T_F^2 + 3456\alpha^2 N_f N_A^{o3} T_F^2 \\
&+864\alpha C_A^2 N_F N_A^{d2}\pi^2 - 2430\alpha C_A^2 N_F N_A^{d2} \\
&+1408\alpha C_A^2 N_F N_A^d N_A^o\pi^2 - 1269\alpha C_A^2 N_F N_A^d N_A^o \\
&-1352\alpha C_A^2 N_F N_A^{o2}\pi^2 - 3456\alpha C_A^2 N_F N_A^{o2} \\
&-1152\alpha C_A C_F N_F N_A^d N_A^o\pi^2 - 15552\alpha C_A C_F N_F N_A^d N_A^o \\
&+832\alpha C_A C_F N_F N_A^{o2}\pi^2 + 11232\alpha C_A C_F N_F N_A^{o2} \\
&+640\alpha C_A N_F N_A^d N_f N_A^o\pi^2 T_F + 6912\alpha C_A N_F N_A^d N_f N_A^o T_F \\
&+832\alpha C_A N_F N_f N_A^{o2}\pi^2 T_F + 432\alpha C_A N_F N_f N_A^{o2} T_F \\
&+2304\alpha C_A N_A^d N_A^{o2}\pi^2 T_F + 7776\alpha C_A N_A^d N_A^{o2} T_F \\
&-512\alpha C_F N_F N_f N_A^{o2}\pi^2 T_F - 12096\alpha C_F N_F N_f N_A^{o2} T_F \\
&+1440 C_A^2 N_F N_A^{d2}\pi^2 + 38880 C_A^2 N_F N_A^{d2} + 1872 C_A^2 N_F N_A^d N_A^o\pi^2 \\
&+2268 C_A^2 N_F N_A^d N_A^o - 1152 C_A C_F N_F N_A^d N_A^o\pi^2 \\
&-15552 C_A C_F N_F N_A^d N_A^o
\end{aligned}
$$

$$
\begin{aligned}
&+5184 C_A N_F N_A^d N_f N_A^o T_F \Big] \frac{a^2}{1296 \alpha N_F N_A^{o2}} \; + \; \mathcal{O}(a^3) \\
\gamma_c^{\rm MOMq}(a,\alpha) \;=\; & C_A \left[-2\alpha N_A^d + \alpha N_A^o - 6 N_A^d - 3 N_A^o \right] \frac{a}{4 N_A^o} \\
& + C_A \Big[-48 \psi'\left(\tfrac{1}{3}\right) \alpha^3 C_A N_F N_A^{d2} + 48 \psi'\left(\tfrac{1}{3}\right) \alpha^3 C_A N_F N_A^d N_A^o \\
& -12 \psi'\left(\tfrac{1}{3}\right) \alpha^3 C_A N_F N_A^{o2} - 48 \psi'\left(\tfrac{1}{3}\right) \alpha^2 C_A N_F N_A^{d2} \\
& -144 \psi'\left(\tfrac{1}{3}\right) \alpha^2 C_A N_F N_A^d N_A^o + 84 \psi'\left(\tfrac{1}{3}\right) \alpha^2 C_A N_F N_A^{o2} \\
& -384 \psi'\left(\tfrac{1}{3}\right) \alpha^2 N_A^d N_A^{o2} T_F + 192 \psi'\left(\tfrac{1}{3}\right) \alpha^2 N_A^{o3} T_F \\
& +48 \psi'\left(\tfrac{1}{3}\right) \alpha C_A N_F N_A^{d2} - 336 \psi'\left(\tfrac{1}{3}\right) \alpha C_A N_F N_A^d N_A^o \\
& +12 \psi'\left(\tfrac{1}{3}\right) \alpha C_A N_F N_A^{o2} + 192 \psi'\left(\tfrac{1}{3}\right) \alpha C_F N_F N_A^d N_A^o \\
& -96 \psi'\left(\tfrac{1}{3}\right) \alpha C_F N_F N_A^{o2} - 1152 \psi'\left(\tfrac{1}{3}\right) \alpha N_A^d N_A^{o2} T_F \\
& -576 \psi'\left(\tfrac{1}{3}\right) \alpha N_A^{o3} T_F - 720 \psi'\left(\tfrac{1}{3}\right) C_A N_F N_A^{d2} \\
& -1296 \psi'\left(\tfrac{1}{3}\right) C_A N_F N_A^d N_A^o - 468 \psi'\left(\tfrac{1}{3}\right) C_A N_F N_A^{o2} \\
& +576 \psi'\left(\tfrac{1}{3}\right) C_F N_F N_A^d N_A^o + 288 \psi'\left(\tfrac{1}{3}\right) C_F N_F N_A^{o2} \\
& +32 \alpha^3 C_A N_F N_A^{d2} \pi^2 + 432 \alpha^3 C_A N_F N_A^{d2} \\
& -32 \alpha^3 C_A N_F N_A^d N_A^o \pi^2 - 432 \alpha^3 C_A N_F N_A^d N_A^o \\
& +8 \alpha^3 C_A N_F N_A^{o2} \pi^2 + 108 \alpha^3 C_A N_F N_A^{o2} \\
& +32 \alpha^2 C_A N_F N_A^{d2} \pi^2 + 1188 \alpha^2 C_A N_F N_A^{d2} \\
& +96 \alpha^2 C_A N_F N_A^d N_A^o \pi^2 - 810 \alpha^2 C_A N_F N_A^d N_A^o \\
& -56 \alpha^2 C_A N_F N_A^{o2} \pi^2 + 256 \alpha^2 N_A^d N_A^{o2} \pi^2 T_F \\
& +864 \alpha^2 N_A^d N_A^{o2} T_F - 128 \alpha^2 N_A^{o3} \pi^2 T_F \\
& -432 \alpha^2 N_A^{o3} T_F - 32 \alpha C_A N_F N_A^{d2} \pi^2 - 3132 \alpha C_A N_F N_A^{d2} \\
& +224 \alpha C_A N_F N_A^d N_A^o \pi^2 + 594 \alpha C_A N_F N_A^d N_A^o \\
& -8 \alpha C_A N_F N_A^{o2} \pi^2 - 1134 \alpha C_A N_F N_A^{o2} \\
& -128 \alpha C_F N_F N_A^d N_A^o \pi^2 - 1728 \alpha C_F N_F N_A^d N_A^o \\
& +64 \alpha C_F N_F N_A^{o2} \pi^2 + 864 \alpha C_F N_F N_A^{o2} + 768 \alpha N_A^d N_A^{o2} \pi^2 T_F \\
& +2592 \alpha N_A^d N_A^{o2} T_F + 384 \alpha N_A^{o3} \pi^2 T_F + 1296 \alpha N_A^{o3} T_F \\
& +480 C_A N_F N_A^{d2} \pi^2 + 5670 C_A N_F N_A^{d2} + 864 C_A N_F N_A^d N_A^o \pi^2 \\
& +1917 C_A N_F N_A^d N_A^o + 312 C_A N_F N_A^{o2} \pi^2 + 1080 C_A N_F N_A^{o2} \\
& -384 C_F N_F N_A^d N_A^o \pi^2 - 5184 C_F N_F N_A^d N_A^o - 192 C_F N_F N_A^{o2} \pi^2 \\
& -2592 C_F N_F N_A^{o2} + 864 N_F N_A^d N_f N_A^o T_F \\
& +432 N_F N_f N_A^{o2} T_F \Big] \frac{a^2}{864 N_F N_A^{o2}} \; + \; \mathcal{O}(a^3)
\end{aligned}
$$

$$
\begin{aligned}
\gamma_\psi^{\mathrm{MOMq}}(a,\alpha) &= \frac{\alpha N_A^o T_F a}{N_F} \\
&+ \left[12\psi'\left(\tfrac{1}{3}\right)\alpha^3 C_A C_F N_F^2 - 18\psi'\left(\tfrac{1}{3}\right)\alpha^3 C_A N_F N_A^o T_F \right. \\
&\quad -24\psi'\left(\tfrac{1}{3}\right)\alpha^2 C_A C_F N_F^2 + 48\psi'\left(\tfrac{1}{3}\right)\alpha^2 C_A N_F N_A^o T_F \\
&\quad +96\psi'\left(\tfrac{1}{3}\right)\alpha^2 N_A^{o2} T_F^2 + 60\psi'\left(\tfrac{1}{3}\right)\alpha C_A C_F N_F^2 \\
&\quad +18\psi'\left(\tfrac{1}{3}\right)\alpha C_A N_F N_A^o T_F - 48\psi'\left(\tfrac{1}{3}\right)\alpha C_F N_F N_A^o T_F \\
&\quad -8\alpha^3 C_A C_F N_F^2 \pi^2 - 108\alpha^3 C_A C_F N_F^2 + 12\alpha^3 C_A N_F N_A^o \pi^2 T_F \\
&\quad +162\alpha^3 C_A N_F N_A^o T_F + 16\alpha^2 C_A C_F N_F^2 \pi^2 - 81\alpha^2 C_A C_F N_F^2 \\
&\quad -32\alpha^2 C_A N_F N_A^o \pi^2 T_F + 162\alpha^2 C_A N_F N_A^o T_F - 64\alpha^2 N_A^{o2} \pi^2 T_F^2 \\
&\quad -216\alpha^2 N_A^{o2} T_F^2 - 40\alpha C_A C_F N_F^2 \pi^2 + 216\alpha C_A C_F N_F^2 \\
&\quad -12\alpha C_A N_F N_A^o \pi^2 T_F - 540\alpha C_A N_F N_A^o T_F + 32\alpha C_F N_F N_A^o \pi^2 T_F \\
&\quad +432\alpha C_F N_F N_A^o T_F + 675 C_A C_F N_F^2 - 162 C_F^2 N_F^2 \\
&\quad \left. -216 C_F N_F^2 N_f T_F \right] \frac{a^2}{108 N_F^2} \; + \; \mathcal{O}(a^3) \; . \qquad (5.6.63)
\end{aligned}
$$

Unlike in the MOMh scheme the quark anomalous dimension in the MOMq scheme is cubic in the gauge parameter. This is also the case for the Curci-Ferrari gauge for the same anomalous dimension. However in the arbitrary linear covariant gauge fixing no differences in the power of the gauge parameter are observed. The results for the renormalization group functions have been verified in all MOMi schemes by taking the Curci-Ferrari limit, $N_A^d \to 0$. In this limit *all* known results in the MAG in *all* schemes considered here agree with those of the Curci-Ferrari gauge in the same schemes at the same loop order for a full colour group.

5.7 Λ-ratios

For completeness we use this section to present the numerical analysis of the Λ-ratios for comparison with those of the linear covariant and Curci-Ferrari gauges as well as for applications to computations in different schemes. Using the coupling constant mappings we can construct the Λ-ratios as defined in chapter 3. For each of the three MOMi schemes we have

$$
\begin{aligned}
\Theta^{\mathrm{MOMg}}(\alpha, N_f) &= \frac{1}{324 N_A^o} \left[-72\psi'(\tfrac{1}{3})\alpha^2 C_A N_A^d + 36\psi'(\tfrac{1}{3})\alpha^2 C_A N_A^o \right. \\
&\qquad +90\psi'(\tfrac{1}{3})\alpha C_A N_A^d - 162\psi'(\tfrac{1}{3})\alpha C_A N_A^o \\
&\qquad \left. -702\psi'(\tfrac{1}{3}) C_A N_A^d + 138\psi'(\tfrac{1}{3}) C_A N_A^o \right.
\end{aligned}
$$

$$
\begin{aligned}
&-384\psi'(\tfrac{1}{3})N_f N_A^o T_F - 81\alpha^3 C_A N_A^d + 27\alpha^3 C_A N_A^o \\
&+48\pi^2\alpha^2 C_A N_A^d + 324\alpha^2 C_A N_A^d - 24\pi^2\alpha^2 C_A N_A^o \\
&-162\alpha^2 C_A N_A^o - 60\pi^2\alpha C_A N_A^d - 243\alpha C_A N_A^d \\
&+108\pi^2\alpha C_A N_A^o + 243\alpha C_A N_A^o + 468\pi^2 C_A N_A^d \\
&-92\pi^2 C_A N_A^o + 2376 C_A N_A^o + 256\pi^2 N_f N_A^o T_F \\
&-864 N_f N_A^o T_F] \\
\Theta^{\mathrm{MOMh}}(\alpha, N_f) &= \frac{1}{108 N_A^o} \left[36\psi'(\tfrac{1}{3})\alpha C_A N_A^d - 12\psi'(\tfrac{1}{3})\alpha C_A N_A^o - 66\psi'(\tfrac{1}{3}) C_A N_A^d \right. \\
&+30\psi'(\tfrac{1}{3}) C_A N_A^o - 54\alpha^2 C_A N_A^d + 27\alpha^2 C_A N_A^o \\
&-24\pi^2\alpha C_A N_A^d - 108\alpha C_A N_A^d + 8\pi^2\alpha C_A N_A^o \\
&+108\alpha C_A N_A^o + 44\pi^2 C_A N_A^d + 162 C_A N_A^d \\
&\left. -20\pi^2 C_A N_A^o + 669 C_A N_A^o - 240 N_f N_A^o T_F \right] \\
\Theta^{\mathrm{MOMq}}(\alpha, N_f) &= \frac{1}{108 N_F N_A^o} \left[-12\psi'(\tfrac{1}{3})\alpha^2 C_A N_F N_A^d + 6\psi'(\tfrac{1}{3})\alpha^2 C_A N_F N_A^o \right. \\
&+24\psi'(\tfrac{1}{3})\alpha C_A N_F N_A^d - 24\psi'(\tfrac{1}{3})\alpha C_A N_F N_A^o \\
&-96\psi'(\tfrac{1}{3})\alpha N_A^{o2} T_F - 60\psi'(\tfrac{1}{3}) C_A N_F N_A^d \\
&-78\psi'(\tfrac{1}{3}) C_A N_F N_A^o + 48\psi'(\tfrac{1}{3}) C_F N_F N_A^o \\
&+8\pi^2\alpha^2 C_A N_F N_A^d + 54\alpha^2 C_A N_F N_A^d \\
&-4\pi^2\alpha^2 C_A N_F N_A^o - 27\alpha^2 C_A N_F N_A^o \\
&-16\pi^2\alpha C_A N_F N_A^d - 54\alpha C_A N_F N_A^d \\
&+16\pi^2\alpha C_A N_F N_A^o + 54\alpha C_A N_F N_A^o + 64\pi^2\alpha N_A^{o2} T_F \\
&+216\alpha N_A^{o2} T_F + 40\pi^2 C_A N_F N_A^d + 52\pi^2 C_A N_F N_A^o \\
&+993 C_A N_F N_A^o - 32\pi^2 C_F N_F N_A^o - 432 C_F N_F N_A^o \\
&\left. -240 N_F N_f N_A^o T_F \right] \; . \qquad (5.7.64)
\end{aligned}
$$

In Table 5.2 we record our results for the Λ-ratios numerically for the same choice of N_f and α given in both previous analyses for the arbitrary (linear) covariant and Curci-Ferrari gauges for $SU(3)$ in chapters 3 and 4 respectively. Interestingly for certain choices of α and N_f the ratio for the MOMg scheme in the MAG is less than unity. This does not happen for the other two gauges considered, nor does it happen in the MAG for the other two MOM schemes.

Although unrelated to the Λ-parameters we now plot the truncated channel 1 amplitude for the MAG ghost-gluon vertex in the $\overline{\mathrm{MS}}$ scheme. This is plotted as a function of the partial coupling constant $a_1(\mu, \Lambda)$ where only the one loop

α	N_f	MOMg	MOMh	MOMq
0	0	2.3583	2.5816	1.9562
0	1	2.1127	2.6008	1.9359
0	2	1.8642	2.6228	1.9129
0	3	1.6167	2.6484	1.8869
0	4	1.3668	2.6784	1.8572
0	5	1.1239	2.7140	1.8229
1	0	2.0664	2.8596	1.8073
1	3	1.3739	3.0010	1.7128
1	4	1.1480	3.0655	1.6729
1	5	0.9298	3.1429	1.6271
3	3	0.9591	4.1883	1.3858
3	4	0.7787	4.3939	1.3308
-2	4	1.8624	2.2372	2.2445

Table 5.2: Values of $\frac{\Lambda_{\mathrm{MOMi}}}{\Lambda_{\overline{\mathrm{MS}}}}$ for the MAG in $SU(3)$.

coupling is required since we have only computed the amplitudes for the MAG at one loop. This means however that no comparison can be made with a two loop result, as was the case with the other gauges considered in the previous chapters. Therefore we have plotted both the one loop Curci-Ferrari and one loop MAG amplitudes on the same plots for visual comparison of the gauges. These should be equivalent when taking the limit $N_A^d \to 0$. This can be seen in Figure 5.1. For large N_c it should be the case that we start to see the two results overlapping. This is indeed true and is displayed in Figure 5.2 for $SU(100)$.

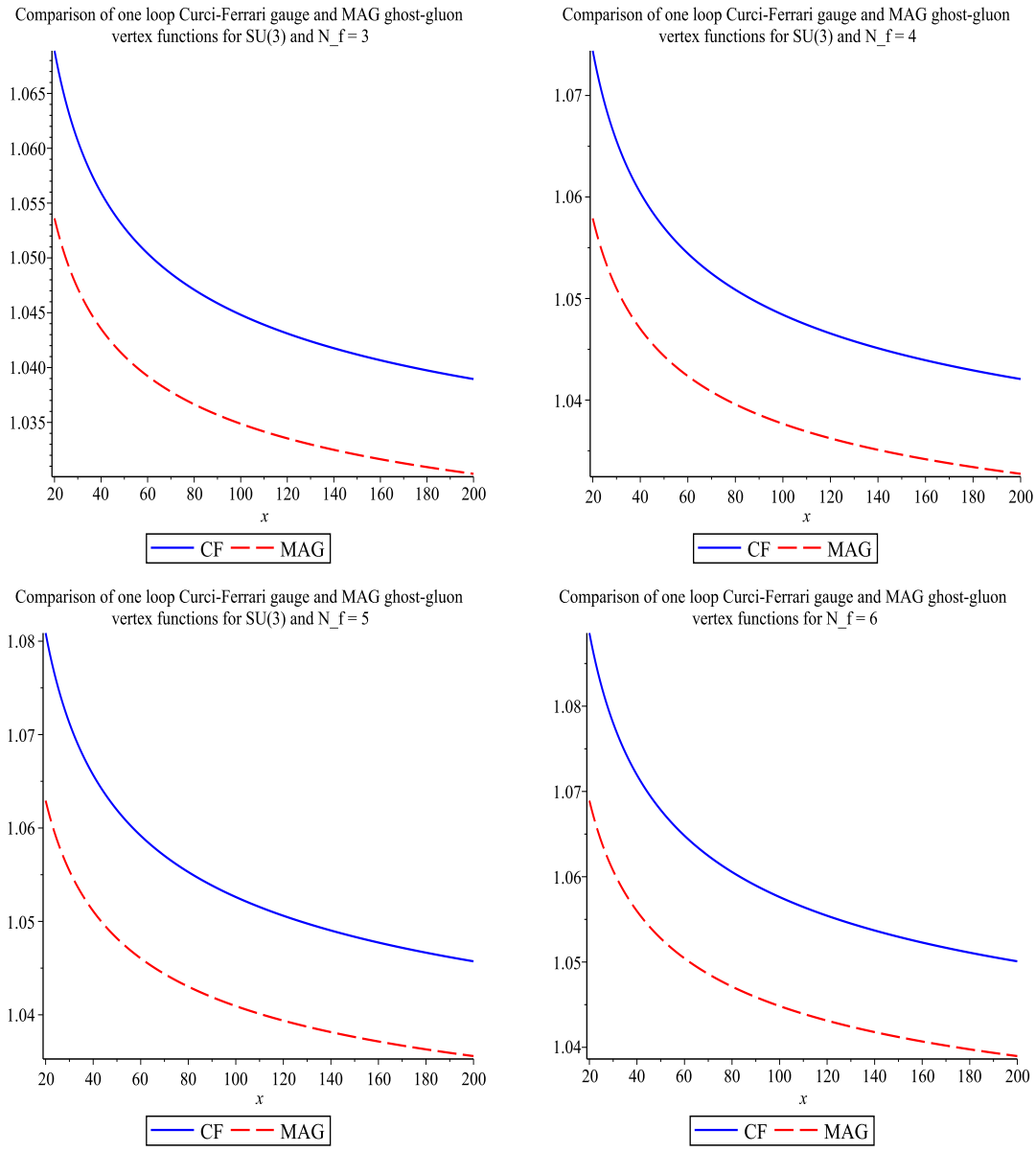

Figure 5.1: Comparison of one loop $\overline{\text{MS}}$ Curci-Ferrari and MAG ghost-gluon vertex functions in $SU(3)$ for different values of N_f.

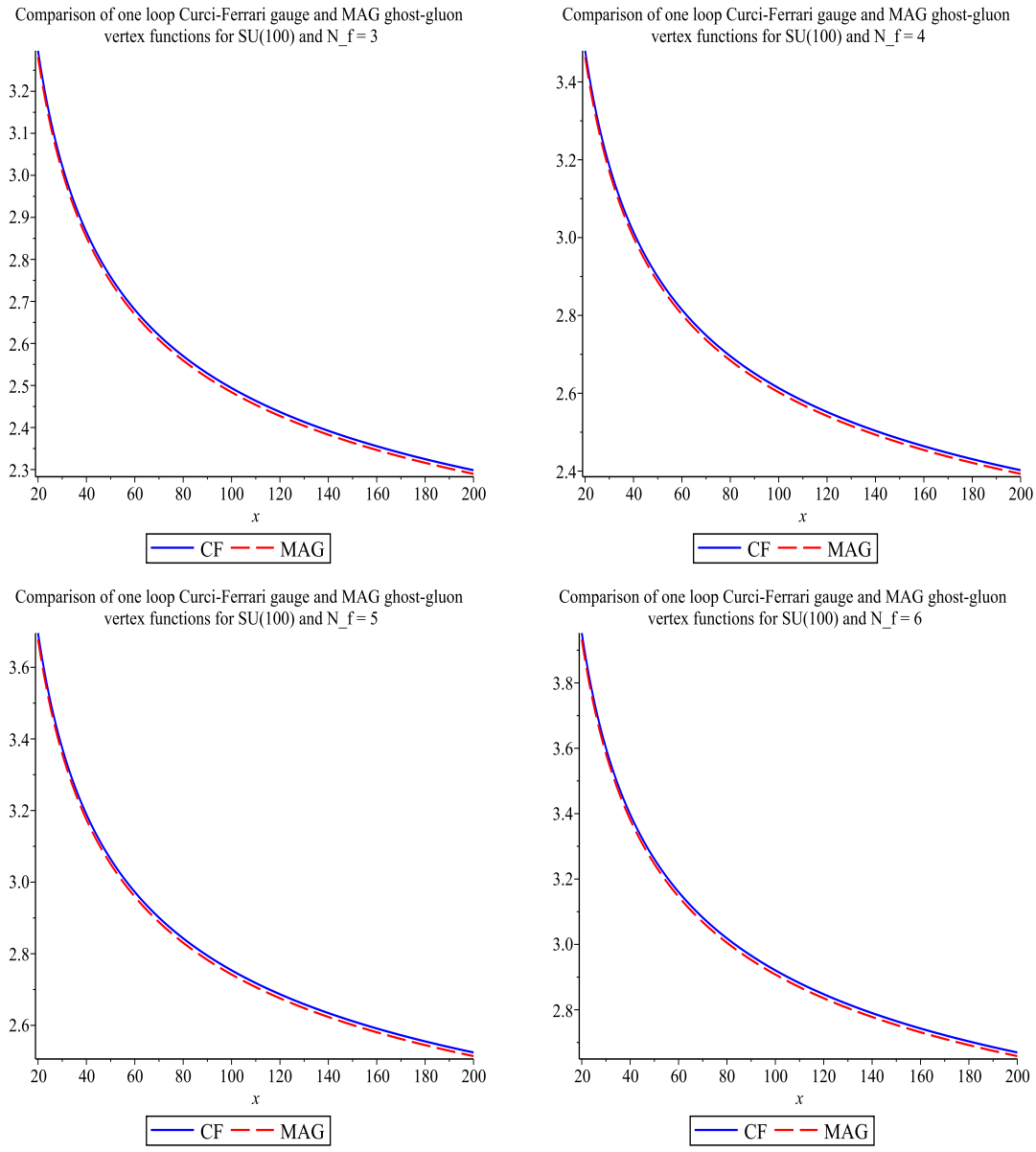

Figure 5.2: Comparison of one loop $\overline{\text{MS}}$ Curci-Ferrari and MAG ghost-gluon vertex functions for large $SU(N_c)$ for different values of N_f.

5.8 Discussion

We make some comments on our analysis. First, we have provided all the information on the 3-point vertex functions relevant for the definition of the MOMi schemes for the maximal abelian gauge. This is an analysis parallel to that of [52] for QCD fixed in the canonical linear covariant gauge, which we considered

in chapter 3. It is also a parallel analysis of QCD fixed in the Curci-Ferrari gauge considered in chapter 4. Our motivation for studying the MAG was to provide data in relation to future lattice analyses of the vertex functions in the infrared in order to have precision matching at high energy. Moreover, the explicit values of the amplitudes in both the $\overline{\rm MS}$ and MOMi schemes will be useful for assisting overlap with Schwinger-Dyson studies. Several features which were observed in [79] are present here. One is the relation to the Curci-Ferrari gauge. In order to have confidence in our results it is important to indicate the checks we have carried out on our work. We have checked all our expressions with the independent evaluation of the same quantities in the Curci-Ferrari gauge, where this gauge fixing is synonymous with the off-diagonal sector of the MAG, in the limit where the diagonal gluons are omitted. Specifically, by substituting

$$\frac{N_A^d}{N_A^o} \to 0 \quad \& \quad N_A^o = N_A \tag{5.8.65}$$

in all the RG functions, amplitudes, renormalization constants, conversion functions and mappings for the MAG we get the direct result for the same RG functions, amplitudes, renormalization constants, conversion functions and mappings in the Curci-Ferrari gauge. This provides a highly non-trivial check on our analysis. We note here that it is possible to present results in the MAG in terms of N_c for $SU(N_c)$ by fixing the Casimirs, i.e. $C_A = N_c$, $C_F = \frac{(N_c^2-1)}{2N_c}$. However, it is not evident how the Curci-Ferrari limit is taken if the parameters N_A^d and N_A^o are not present, [51]. Given properties of the renormalization group equation the one loop conversion functions for relating parameters in the MOMi schemes to those of the $\overline{\rm MS}$ scheme have allowed us to compute the two loop renormalization group functions in each of the three MOMi schemes. These have direct parallels with those of [79] since they are based on the triple-gluon, ghost-gluon and quark-gluon vertices. Though an essential difference here is that with the split nature of the colour group in the MAG, it is the vertices with the off-diagonal gluons which are relevant. This is due in part to the fact that there are Slavnov-Taylor identities which ensure that the structure of the vertices with diagonal gluons are predetermined. Indeed this is not unrelated to the fact these gluons are similar to the background fields of the background field gauge of [37, 128, 129, 130, 131, 132] with the off-diagonal gluons corresponding to the quantum fluctuations. Whether this scenario is significant in the picture of abelian monopoles underlying a picture of colour confinement would be interesting to investigate.

Chapter 6

Summary and conclusions

In Part 1 of this thesis we have studied the renormalization of QCD at the symmetric subtraction point for various linear and non-linear gauges. We applied the renormalization group method to determine the next loop order anomalous dimensions and β-functions at one higher loop for the momentum subtraction schemes of [52]. Specifically we obtained the three loop MOMi scheme results for both the arbitrary linear covariant and Curci-Ferrari gauges and the two loop MAG MOMi results. All results computed in the non-linear gauges are new with results for the one loop MAG published in [51], and the Curci-Ferrari analysis at three loops published in [67]. We have discussed how our motivation for studying the QCD vertices in various gauge fixings and schemes lies in providing data to assist in future developments within the field. These developments could lie in the structure of the nucleons, where the main computing tools for studying this area are lattice gauge theory and Schwinger-Dyson methods. Both of which complement each other. In particular, providing the full off-shell massless vertex functions for each of the three distinct QCD vertices is important in order to have precision matching at high energy.

The amplitudes and RG functions were determined in all three gauges; the arbitrary (linear) covariant, Curci-Ferrari and maximal abelian gauges. Where the former two gauges were computed explicitly at two loops in order to determine the three loop MOMi scheme RG functions. Due to the technical difficulty of the MAG gauge fixing we studied this at the one loop level, where the two loop MOMi scheme RG functions were constructed. Although we have only presented the MOMh, MOMg and MOMq results for each of the ghost-gluon, triple-gluon and quark-gluon vertices respectively we comment that it is possible to carry out, for example, the MOMg renormalization on the ghost-gluon and quark-gluon ver-

tices also. The results presented in this thesis allow one carry out this extension if needed. As a remark on our computational setup, the symmetry of the subtraction point heavily simplified the structure of the basic Feynman graphs. This symmetry about all three external legs resulted in a smaller set of master integrals.

Throughout Part 1 of this thesis we have focused heavily on the MAG. The MAG provides us with direct access to examining the separately treated diagonal and off-diagonal gluons. Results in this gauge will assist in abelian monopole studies where one requires a way of separating out the Abelian part of the group. No direct access to an abelian projection was available through any of the other gauges we studied. However a strong link between the MAG and Curci-Ferrari gauge was observed. If one simply omits an interaction with the diagonal field the results for the MAG directly correspond with results in the Curci-Ferrari gauge, [102].

As an extension to our work the next step would be to consider the 4-point vertices of QCD. Having completed the 3-point analysis at two loops the natural progression would be to consider the 4-point functions, in particular those of the Curci-Ferrari gauge and the MAG. The 4-point analysis has been considered recently for the arbitrary (linear) covariant gauge in [103] at one loop where a two loop explicit calculation is not yet possible. This is due the the master integrals which to date are not yet known. A calculation at this level would be extremely difficult, however it would be interesting to see the influence these quartic vertices have on our results, since in our work we only considered the 2- and 3-point functions. Studying the renormalization of these 4-point vertices in a momentum subtraction scheme would introduce new MOMi schemes, as is the case for the quartic-gluon vertex of [103] with the MOMgggg scheme. It would be interesting to study these other MOMi schemes and their corresponding β-functions.

Alternatively the same computation could be repeated in all gauges to the next loop order. This would require doing a three loop calculation explicitly, which would require the three loop master integrals.

In principle we could consider another setup, for example the asymmetric point with an interpolating parameter to map between this setup and the symmetric subtraction point. In the second part of this thesis we do exactly this, where we consider an operator insertion through the top leg of our Green's function $\langle \psi \bar{\psi} \rangle$.

Part II

Renormalization of the Quark Vertex in an Interpolating Momentum Subtraction (IMOM) Setup

Chapter 7

Operator Renormalization

7.1 Background

A strong motivation of this thesis has been to provide results via perturbation theory which can be used to map on to the non-perturbative or low energy regime, where perturbation theory is not applicable. Whilst lattice computations concentrate on the low energy regime the resulting matrix elements must still match the high energy behaviour computed perturbatively. These matrix elements can involve various operators, with the aim being to achieve a good approximation to the physics of hadrons. The matrix elements give us the moments of the operators related to the structure functions, where the moments are the number of free indices on each operator. Incorporating operators in the form of the scalar, vector, tensor and deep inelastic scattering (DIS) operators may give us a more physical description of the low energy regime. Contributing to the structure functions, the matrix elements for each operator help one to measure the distribution of quarks within the nucleon. As mentioned in chapter 2 the lattice uses the $\overline{\text{MS}}$ scheme as well as other schemes which are physical in their definition. Although the lattice does not use the $\overline{\text{MS}}$ scheme directly, a conversion to $\overline{\text{MS}}$ is needed in order to make calculations on the lattice useful to the outside world. To perform any calculations in perturbation theory which are useful in lattice matching, knowledge of these matrix elements in the same schemes, whether $\overline{\text{MS}}$ or a scheme preferred by the lattice such as MOM or a regularization invariant (RI) scheme [134, 135], is required. The RI scheme is a physical scheme similar to the MOM scheme which was analysed in the previous chapters. Physical schemes such as MOMi serve as useful intermediate schemes which can be implemented both on the lattice and in continuum perturbation theory. The scheme we consider in this chapter is a modification on the RI scheme called RI$'$. The RI$'$ scheme is a preferred scheme

of the lattice, however with more results available in $\overline{\mathrm{MS}}$, in order to improve lattice matching the conversion functions between these two schemes are necessary. We discuss the definitions of the regularization invariant schemes and the renormalization procedure in the following section.

In this chapter we determine the two loop amplitudes for various flavour non-singlet operator insertions in to a massless quark two-point function at both the symmetric subtraction point and at a more general point which is asymmetric with interpolating parameter ω. We consider only flavour non-singlet operators since the current lattice interest concentrates on these. For the scalar (or mass) operator we renormalize in two schemes; $\overline{\mathrm{MS}}$ and RI$'$. The results for the renormalization constants and amplitudes are presented at two loops, as well as the scalar conversion function for comparison with [133]. We reproduce the conversion function for the scalar in the RI$'$ scheme since this was the scheme used in [133]. Once these checks have been carried out and the results for the scalar conversion function have been confirmed we continue this chapter by producing new and original results for the vector current, tensor operator and DIS operators for $\overline{\mathrm{MS}}$ only. The motivation and reasoning behind this is developed in the next section. We make the important note that throughout our work we consider only massless quarks.

7.2 Setup differences

We now turn to the setup for the particular Green's function we are interested in. Rather than study the ghost-gluon, triple-gluon and quark-gluon vertices of QCD as before we now solely focus on the Green's function

$$\langle \psi(p) \mathcal{O}^u_{\mu_1 \ldots \mu_{n_u}}(-p-q) \bar{\psi}(q) \rangle \tag{7.2.1}$$

as illustrated in Figure 7.1, where $\mathcal{O}^u$ is the operator of interest and $\bar{\psi}, \psi$ are massless quarks. Here p and q are independent external momenta flowing in through each quark leg, similar to earlier. Our convention is that the operators are inserted through the top leg, indicated by a circle containing a cross in our diagram, with momenta incoming there too. We consider a non-exceptional momentum configuration throughout. The operators we will be considering, which

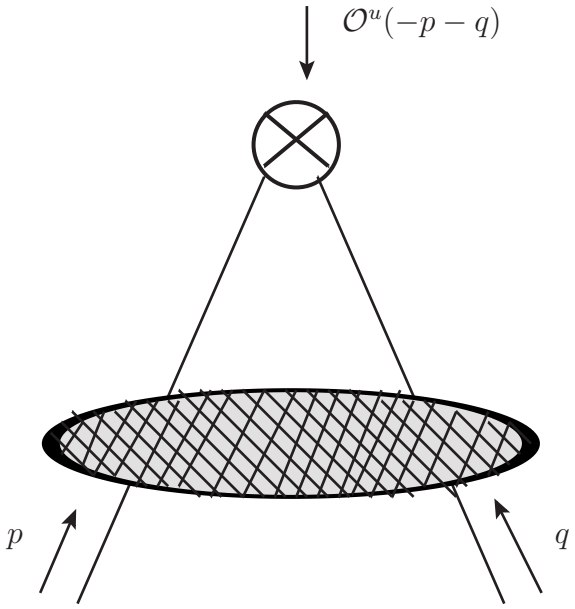

Figure 7.1: Momentum flow for the Green's function $\langle\psi(p)\mathcal{O}^u_{\mu_1\ldots\mu_{n_u}}(-p-q)\bar{\psi}(q)\rangle$.

are gauge invariant, are

$$\begin{aligned} S &= \bar{\psi}\psi \\ V &= \bar{\psi}\gamma^\mu\psi \\ T &= \bar{\psi}\sigma^{\mu\nu}\psi \\ W_2 &= \mathcal{S}\bar{\psi}\gamma^\mu \mathrm{D}^\nu\psi \\ \partial W_2 &= \mathcal{S}\partial^\mu(\bar{\psi}\gamma^\nu\psi) \end{aligned} \tag{7.2.2}$$

where S, V and T are the scalar (or mass), vector and tensor operators respectively and W_2 and its total derivative ∂W_2 are twist-2 Wilson operators for moment $n = 2$. Twist is defined such that

$$\text{twist} \;=\; \text{dimension} - \text{spin}\;. \tag{7.2.3}$$

In the tensor operator $\sigma^{\mu\nu}$ is given by $\sigma^{\mu\nu} = \frac{1}{2}\left[\gamma^\mu, \gamma^\nu\right]$. We note that all derivatives (ordinary and covariant) act to the right and $\mathcal{S}$ means that the free Lorentz indices are totally symmetrized and traceless. We consider all operators in both a symmetric momentum subtraction setup, which we label as SMOM to differentiate the momentum setup from the MOM *scheme*. The asymmetric setup or interpolating momentum subtraction setup is labelled IMOM. All computations are

done for an arbitrary (linear) covariant gauge. Computing results in the former configuration enables us to make checks against original work, [59, 134, 135, 137], whilst ensuring our programming is consistent.

In the SMOM configuration the momentum is defined at the symmetric subtraction point with

$$p^2 \;=\; q^2 \;=\; r^2 \;=\; (p+q)^2 \;=\; -\mu^2 \tag{7.2.4}$$

which as before implies

$$pq \;=\; \tfrac{1}{2}\mu^2 \tag{7.2.5}$$

with μ previously defined in section 2.1.2.

Ultimately, upon reproducing the results of [134, 137] for the renormalization constants and amplitudes of the scalar, vector, tensor and DIS operators, we aim to produce new results for the Green's function of the same operators in an IMOM configuration. In this setup we choose our interpolating parameter, ω, to be situated at the operator insertion, see Figure 7.1. This way the operator can be tuned. Considered at an asymmetric point the momenta now satisfy

$$p^2 \;=\; q^2 \;=\; -\mu^2 \;\;,\;\; r^2 \;=\; (p+q)^2 \;=\; -\omega\mu^2 \tag{7.2.6}$$

where the squared momenta of two external quark legs are the same whilst the third is proportional to the other two. This implies

$$pq \;=\; \left[1-\frac{\omega}{2}\right]\mu^2 \;\;,\;\; pr \;=\; qr \;=\; \frac{\omega}{2}\mu^2 \;. \tag{7.2.7}$$

This is a much more desired setup than a SMOM configuration as there is more flexibility with results in this setup, meaning improved precision measurements on the lattice. In particular a zero-momentum quark is difficult to incorporate on the lattice. By taking $\omega = 1$ in our results we will be able to check with earlier work at the symmetric point, and we make reference to these checks throughout. Introducing an interpolating parameter has implications. For instance, in chapers 2 - 5 of this thesis our master integral reduction was greatly simplified due to the symmetries which came with considering the Green's functions at the symmetric subtraction point. These symmetries are no longer applicable for obvious reasons.

With this in mind we present in Figure 7.2 the basic one and two loop topologies encountered in our calculation for an IMOM configuration, where we note that away from the symmetric point we have two additional ladder topologies. This

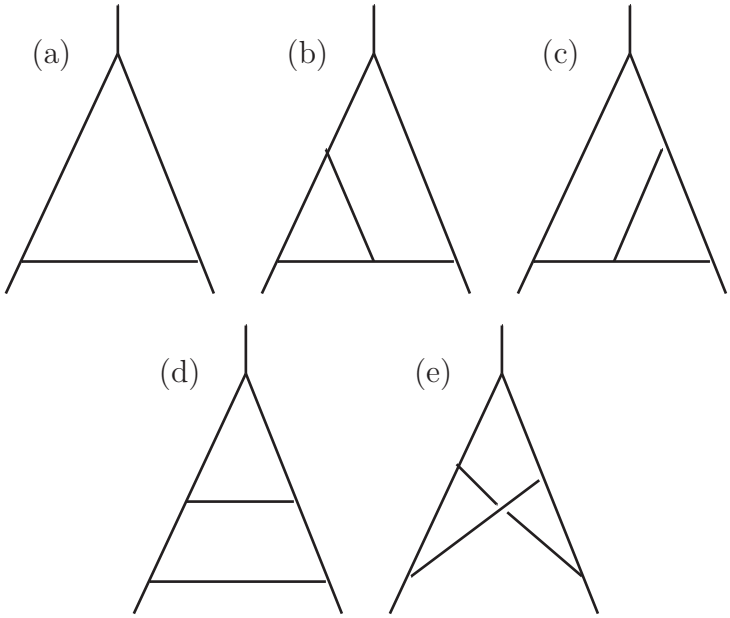

Figure 7.2: Basic topologies for the IMOM setup, where it is understood that (b) and (c) are no longer contained within (d), and (b) and (c) are symmetric about p and q, where p and q are defined as the incoming momenta on the two lower legs.

loss of symmetry along with the new structures appearing in the Green's function gives rise to more involved master integrals.

Since the background to the SMOM setup (or momentum subtraction setup at a symmetric subtraction point, where the two descriptions are synonomous) has been considered at length in chapter 2, in the remainder of this section we focus solely on the IMOM setup. Prior to this however let us first make some important remarks on earlier work that has been carried out for the set of RI schemes in a SMOM configuration. As we have said previously, the lattice have their own set of preferred schemes, with RI and RI$'$ being two of them. These schemes were originally defined in lattice computations [134, 135] and developed up to four loops for the Landau gauge [59] and arbitrary (linear) covariant gauge [137]. All computations prior to the development of the RI$'$/SMOM renormalization scheme in [138] were considered at an exceptional point, where essentially the operator insertion was at zero momentum, [139]. This scheme has been applied

to the scalar, vector and tensor operators at one and two loops [138, 133] and also to low moment operators used in deep inelastic scattering to three loops, [75, 140]. An introduction to the notation of the RI′/SMOM and RI′/IMOM schemes are given in section 7.3. We note that all calculations performed in this chapter are considered at a non-exceptional momentum configuration and the above references along with [133, 137] will be used when comparing results in a SMOM setup for $\overline{\text{MS}}$ and RI′ schemes.

The Green's function (7.2.1) requires a new tensor basis since the tensor basis used in the previous chapters is only applicable to the Green's functions for the ghost-gluon, triple-gluon and quark-gluon vertices respectively. Following the same technique as discussed in Appendix B we decompose the Green's function in to a set of scalar amplitudes multiplying a basis of Lorentz tensors

$$\langle \psi(p) \mathcal{O}^u_{\mu_1 \ldots \mu_{n_u}}(-p-q) \bar{\psi}(q) \rangle \Big|_\omega \;=\; \sum_{k=1}^{n_u} \mathcal{P}^u_{(k)\ \mu_1 \ldots \mu_{n_u}}(p,q) \Sigma^{\mathcal{O}^u}_{(k)}(p,q) \qquad (7.2.8)$$

where u is the operator label (7.2.2) and we have introduced the shorthand notation

$$\Big|_\omega \;\equiv\; \Big|_{p^2=q^2=-\mu^2,\ r^2=-\omega\mu^2} \qquad (7.2.9)$$

to denote the IMOM configuration. The explicit tensors for each operator insertion are given in Appendix B along with their respective projection matrices, which differ for each operator level. The number of tensors in each tensor basis for all operators are presented in Table 7.1.

Operator	S	V	T	W_2	∂W_2
Number of basis tensors	2	6	8	10	10

Table 7.1: Number of projectors for each operator insertion.

7.3 Renormalization

In the analyses of the operators in a SMOM and IMOM setup we use the same renormalization techniques as described in chapter 2 with dimensional regularization in $d = 4 - 2\epsilon$ dimensions. Another calculation using a similar setup to ours has been carried out first by Gorbahn and Jäger in [133]. We make ref-

erence to this calculation where checks are made against their results for the scalar (or mass) conversion function in a regularization invariant (RI) renormalization scheme. The authors of [133] also introduced the more general kniematic setup with interpolating parameter ω. Therefore in order to make contact with this work we first reproduce the results of [133, 137] in this new renormalization scheme. In part this is used as a check for the extension discussed here.

In this section we discuss the details surrounding renormalization of the Lagrangian in the RI and RI′ schemes. There are several ways in which the schemes are defined [134, 135, 137, 139]. In our work, which compliments that of [137, 139], we choose to renormalize using a modified regularization invariant (RI′) scheme. There are so many different ways to define an RI′ scheme for an operator insertion with tensor indices. It is appropriate at this point to clarify the different nomenclatures in the literature with that which we use in [141]. RI and RI′ are both defined with respect to the quark two-point wave function renormalization. As with the modification on the MS scheme resulting in a new definition of the scheme, namely $\overline{\text{MS}}$, RI′ is a modification of the RI scheme. Their differences lie in which part of the Green's function is renormalized. Determining both the RI and RI′ schemes requires the renormalization of the Lagrangian to get the wave function renormalization of the external legs first. These are the two-point functions for the ghost, gluon and quark wave functions. The difference between the two schemes is as follows. The RI′ scheme definition of [142, 134, 135] is to renormalize the quark wave function such that

$$\lim_{\epsilon\to 0}\left[Z_\psi^{\text{RI}'}\Sigma_\psi(p)\right]\Big|_{p^2=\mu^2} \;=\; \not{p} \tag{7.3.10}$$

where $\Sigma_\psi(p)$ is the bare (massless) quark two-point function and Z_ψ is the related renormalization constant for the quark. The RI scheme acts on a different part of the Green's function, [139], which is

$$\lim_{\epsilon\to 0}\left[\frac{1}{4d}\text{tr}\left(Z_\psi^{\text{RI}}\gamma_\mu\frac{\partial}{\partial p^\mu}\Sigma_\psi(p)\right)\right]\Big|_{p^2=\mu^2} \;=\; 1\;. \tag{7.3.11}$$

From the above it can be seen that the RI scheme is more involved. Due to the presence of the derivatives it is much more difficult and costly to implement this scheme on the lattice compared with (7.3.10). This cost refers to the computer time needed, which greatly increases with the addition of derivatives within operators, since a derivative in a vertex increases the degree of divergence. It is for

this reason the RI′ scheme is the preferred mass dependent scheme for the lattice when considering an operator insertion.

The renormalization constants for the wave functions in both the RI and RI′ schemes are defined such that the poles in ϵ are absorbed in to the wave function renormalization constants along with the finite pieces. This is similar to the MOM scheme definition. Throughout the literature the usual definition of the RI′ scheme is to not renormalize the gauge parameter, where the relation $Z_\alpha^{\overline{\rm MS}} = Z_\alpha^{\rm RI'}$ holds between the two schemes. However we define our gauge parameter, α, to be renormalized. The renormalization of this parameter is the same as that for the wave functions, where both the poles and finite parts are absorbed in to the renormalization constants. It is because of our convention for the renormalization of α that we cannot compare directly with available results, [141]. Therefore when comparing with [133] we do so in the Landau gauge, since in this limit the way in which α is defined can be neglected. In other words we only find agreement when $\alpha = 0$.

It is also the case that the coupling constants are the same in both the RI′ and $\overline{\rm MS}$ schemes, and this is known up to five loops, [59, 137],

$$a_{\rm RI'} \;=\; a_{\overline{\rm MS}} + \mathcal{O}(a^5_{\overline{\rm MS}}) \;. \tag{7.3.12}$$

This relation also holds between the $\overline{\rm MS}$ and RI′ schemes and so when we construct the conversion function for the scalar operator there will be no need to produce a coupling constant mapping between the two schemes first, at least not to the loop order we require. Contrary to the wave function renormalization, the coupling constant renormalization constant is renormalized in an $\overline{\rm MS}$ way where only the poles in ϵ are absorbed in to the renormalization constant. This is the setup for the Lagrangian which defines the basic wave function coupling constant and gauge parameter renormalization constants for the external legs of any Green's function, for example with an operator renormalization.

On the lattice the above RI′ scheme is commonly referred to as RI′/MOM. This should not be confused with applying a MOMi scheme renormalization to the vertex. For this reason we choose not to adopt this choice of labelling since the notation could be ambiguous and we do not want the reader to confuse the MOM scheme with a "MOM" configuration. Another definition of the RI′

scheme applied to the operator renormalization which we can use is RI′/SMOM. This identifies that the *operator renormalization* is considered at the completely symmetric point. This is the notation we will use in this chapter to distinguish the modified regularization invariant scheme applied to the quark wave function with operator renormalization considered at the symmetric subtraction point in the $\overline{\text{MS}}$ scheme (RI′/SMOM). When moving to the asymmetric setup we will use RI′/IMOM to indicate that we have introduced an interpolating parameter. However, the method of renormalizing the 2-point wave functions in an RI′ way and the operators in an $\overline{\text{MS}}$ way remains the same as defined for the SMOM configuration. The details may be different but the method remains unchanged.

In [133] we note that where the authors define an RI/SMOM scheme with interpolating parameter ω this is synonomous to our definition of RI′/IMOM. Although [133] use the RI/SMOM labelling they have specified that the vertex is not symmetric, with an external leg tuned differently to the other two. Their choice of labelling could be misleading, which is why we have introduced the label RI′/IMOM when specifically considering an asymmetric setup for the vertex with an interpolating parameter. It is hoped that further development in this area will encorouge others to adopt the same standard notation so that there is no confusion surrounding schemes and momentum configurations used.

With the ambiguity in defining regularization invariant schemes we reiterate that all checks with other authors carried out in this chapter are performed in the Landau limit. This is because we have used a different definition of the arbitrary gauge parameter α as mentioned before, and so it is only for the limit $\alpha \to 0$ that our results can be compared with [133] for example. Once checks against [133] have been made, confirming our results and computational method and programs are correct, all further renormalization will be carried out for the mass independent $\overline{\text{MS}}$ scheme. Although RI′ has been described in the literature as being a preferred scheme of the lattice, it is more convenient for lattice theorists at this time, who are interested in using our data, to have results presented for arbitrary α in the standard reference scheme; $\overline{\text{MS}}$. The $\overline{\text{MS}}$ results can then be transformed to any scheme of their choice via conversion functions and mappings. As we have already mentioned, the RI′/SMOM and RI′/IMOM schemes can be defined in a number of ways. This definition depends on the choice of the tensor basis. If a different tensor basis is used and the renormalization carried out on a projection which does not directly correspond to the Feynman rule

then renormalization constants computed in this scheme will not match those defined in what is thought to be the same scheme. In this thesis, when working with mass-dependent renormalization schemes, we have chosen to always use the channel 1 projection to define the renormalization constants for the operator in the RI′/SMOM and RI′/IMOM schemes. This means that we absorb the finite pieces in the channel 1 projection, leaving this part of the amplitude with no $\mathcal{O}(a)$ corrections after renormalization. It can be seen straight away that if one were to choose a different tensor basis to that of ours and define the renormalization such that the channel with the divergence, for example, was left with no $\mathcal{O}(a)$ corrections, the results for the renormalization constants would not match on to our own results for the same objects. This is why we only present the amplitudes for the vector, tensor and DIS operators in the $\overline{\text{MS}}$ scheme. If we were to define the amplitudes in the RI′/SMOM or RI′/IMOM schemes using a particular tensor basis and projection this may not be the most efficient choice for numerical lattice calculations. It is for this reason that most RI′ computations on the lattice are usually considered in the Landau gauge, [135, 136]. Another reason for choosing to represent results in terms of $\overline{\text{MS}}$ variables is that this scheme still remains the cheapest to run on the lattice. The results for $\overline{\text{MS}}$ in an interpolating momentum subtraction configuration have not been determined before it was carried out in [141] for operator insertions above the most basic level; the scalar (or mass). The five operators we consider are the scalar, vector and tensor operators and the Wilson DIS operators W_2 and ∂W_2. The details surrounding each of these individual operator insertions are discussed in the subsequent sections.

In our vertex setup there are 3 one loop diagrams and 37 two loop diagrams. This is consistent for all operator insertions considered. These have been computed using QGRAF. We note that no additional computer packages have been used in this chapter other than those detailed in chapter 2 which we use throughout. We do note however that there are new master integrals which are ω-dependent that we need to compute. These are detailed in Appendix C. Also the new projection matrices depend on this interpolating parameter ω.

7.4 Scalar (Mass) operator

On discussing our renormalization procedure we now move on to presenting results for each operator insertion. We begin with the scalar operator, $\bar{\psi}\psi$. The first step in our process is to renormalize in an $\overline{\text{MS}}$ way. Since we have already established

the $\overline{\rm MS}$ renormalization constants for an arbitrary (linear) covariant gauge in Part 1 of this thesis it is simply a matter of plugging these in to the amplitudes. In addition to the renormalization constants defined in (3.1.2) and (3.1.3) we introduce a renormalization constant specific to the operator, $Z^u_{\mathcal{O}}$, where $u \in \{S, V, T, W_2, \partial W_2\}$. This operator renormalization constant is defined as

$$Z^u_{\mathcal{O}}(a) = 1 + \frac{z^u_{\mathcal{O}_1}}{\epsilon} a + \left(\frac{z^u_{\mathcal{O}_{22}}}{\epsilon^2} + \frac{z^u_{\mathcal{O}_{21}}}{\epsilon} \right) a^2 + \mathcal{O}(a^3) \tag{7.4.13}$$

where a is the coupling constant defined for any scheme. This operator renormalization multiplies the entire Green's function.

Our initial aim is to reproduce the scalar conversion function. In order to do this one has to renormalize in two schemes, where we have chosen $\overline{\rm MS}$ and RI$'$. Let us first renormalize the Green's function using an $\overline{\rm MS}$ prescription. By inserting the $\overline{\rm MS}$ renormalization constants of (3.1.2) and (3.1.3) in to the amplitudes at two loops we are able to set the corresponding operator renormalization constant $Z^u_{\mathcal{O}}$ which we do in an $\overline{\rm MS}$ way. Our results for the renormalization constants in the $\overline{\rm MS}$ scheme for the wave functions are the same as (3.1.2) in chapter 3. For the operator renormalization constant we find

$$\begin{aligned} Z^S_{\mathcal{O}}(a,\alpha)\Big|_{\overline{\rm MS}} &= 1 - \frac{3C_F a}{\epsilon} + \left[\frac{5}{3} C_F T_F N_f - \frac{97}{12} C_F C_A - \frac{3}{4} C_F^2 \right. \\ &\quad \left. + \left(2C_F T_F N_f + \frac{11}{2} C_F C_A + \frac{9}{2} C_F^2 \right) \frac{1}{\epsilon} \right] \frac{a^2}{\epsilon} + \mathcal{O}(a^3) \end{aligned} \tag{7.4.14}$$

which is independent of the gauge parameter α.

Once the renormalization constants have been verified, we remove the $\overline{\rm MS}$ wave function and coupling constant renormalization constants but keep $Z_{\mathcal{O}}$ set for the scalar. Following an iterative procedure we are able to determine the RI$'$ wave function and coupling constant renormalization constants which we find are given by

$$\begin{aligned} Z^S_A(a,\alpha)\Big|_{\rm RI'} &= 1 + \left[C_A \left(\frac{13}{6} - \frac{\alpha}{2} \right) - \frac{4}{3} T_F N_f \right. \\ &\quad \left. + \epsilon \left(-\frac{20}{9} N_f T_F + C_A \left(\frac{97}{36} + \frac{\alpha}{2} + \frac{\alpha^2}{4} \right) \right) \right] \frac{a}{\epsilon} + \mathcal{O}(a^2) \\ Z^S_\alpha(a,\alpha)\Big|_{\rm RI'} &= 1 + \mathcal{O}(a^2) \end{aligned}$$

$$
\begin{aligned}
Z_g^S(a,\alpha)\Big|_{\mathrm{RI}'} &= 1 + \left[-\frac{11}{6} C_A + \frac{2}{3} T_F N_f \right] \frac{a}{\epsilon} \; + \; \mathcal{O}(a^2) \\
Z_\psi^S(a,\alpha)\Big|_{\mathrm{RI}'} &= 1 - [1+\epsilon] \frac{C_F \alpha a}{\epsilon} + \left[\left[C_F C_A \left(\frac{3\alpha}{4} + \frac{\alpha^2}{4} \right) + \frac{1}{2} C_F^2 \alpha^2 \right] \frac{1}{\epsilon^2} \right. \\
&\quad + \left[C_F C_A \left(-\frac{25}{8} - \frac{133\alpha}{36} - \frac{5\alpha^2}{8} - \frac{\alpha^3}{4} \right) \right. \\
&\quad + T_F N_f C_F \left(1 + \frac{20}{9} \alpha \right) + C_F^2 \left(\frac{3}{4} + \alpha^2 \right) \\
&\quad + \epsilon \left(N_f T_F C_F \left(\frac{7}{2} + \frac{20}{9} \alpha \right) + C_F C_A \left(-\frac{41}{4} + 3\zeta_3 \alpha + 3\zeta_3 \right. \right. \\
&\quad \left. \left. \left. - \frac{331}{36} \alpha - \frac{13}{8} \alpha^2 - \frac{1}{4} \alpha^3 \right) + C_F^2 \left(\frac{5}{8} + \alpha^2 \right) \right) \right] \frac{1}{\epsilon} \Bigg] a^2 \\
&\quad + \mathcal{O}(a^3)
\end{aligned}
\tag{7.4.15}
$$

where it can be seen that the wave function renormalization constants have been renormalized such that the poles in ϵ and the finite pieces are absorbed in to the renormalization constants, resulting in no $\mathcal{O}(a)$ pieces remaining in the channel 1 amplitude. These results agree with those of [137]. The coupling constant renormalization however is carried out in an $\overline{\mathrm{MS}}$ way, where only the divergences are absorbed in to the definition of the renormalization constant. Note that the label on the renormalization constant defines the labelling of the parameters a and α, in other words $Z_\psi^S(a,\alpha)\big|_{\mathrm{RI}'} \equiv Z_\psi^S(a_{\mathrm{RI}'}, \alpha_{\mathrm{RI}'})$. Also here RI′ is shorthand for the RI′/IMOM scheme where it cannot be written out fully when presented within results due to lack of space.

The next step in our iterative procedure is to remove the $\overline{\mathrm{MS}}$ values for the operator renormalization constant. This can now be set for the scalar in the RI′/IMOM scheme where the operator is renormalized in the same way as the wave functions; absorbing both the $\frac{1}{\epsilon}$ pieces and finite parts in to the operator renormalization constant. The renormalization constant for the scalar (or mass) operator is

$$
\begin{aligned}
Z_{\mathcal{O}}^S(a,\alpha)\Big|_{\mathrm{RI}'} &= 1 + \left[-3C_F + \epsilon C_F \left(-4 - \alpha + \frac{3}{2} \Phi_1(1,\omega)\, \omega + \frac{1}{2} \Phi_1(1,\omega)\, \alpha\omega \right) \right] \frac{a}{\epsilon} \\
&\quad + \left[\left(-2C_F T_F N_f + \frac{11}{2} C_F C_A + \frac{9}{2} C_F^2 \right) \frac{1}{\epsilon^2} + \left(\frac{5}{3} C_F T_F N_f \right. \right. \\
&\quad \left. - \frac{97}{12} C_F C_A + C_F^2 \left(\frac{45}{4} + 3\alpha - \frac{9}{2} \Phi_1(1,\omega)\, \omega - \frac{3}{2} \Phi_1(1,\omega)\, \alpha\omega \right) \right. \\
&\quad \left. + \epsilon C_F T_F N_f \left(\frac{83}{6} + \frac{20}{9} \alpha - \frac{10}{3} \Phi_1(1,\omega)\, \omega - \frac{10}{9} \Phi_1(1,\omega)\, \alpha\omega \right) \right.
\end{aligned}
$$

$$
\begin{aligned}
&+\epsilon C_F C_A \left(-\frac{1285}{24} + 12\zeta_3 - \frac{223}{36}\alpha - \frac{5}{4}\alpha^2 - \frac{1}{4}\alpha^3 \right. \\
&+\frac{1}{2}\Omega_2\left(\frac{1}{\omega},\frac{1}{\omega}\right) - \Omega_2(\omega,1) - \frac{1}{2}\ln(\omega)\Phi_1(1,\omega)\,\omega - \Phi_2\left(\frac{1}{\omega},\frac{1}{\omega}\right) \\
&+\Phi_2(1,\omega)\,\omega + \frac{385}{24}\Phi_1(1,\omega)\,\omega + \frac{223}{72}\Phi_1(1,\omega)\,\alpha\omega \\
&+\frac{5}{8}\Phi_1(1,\omega)\,\alpha^2\omega + \frac{1}{8}\Phi_1(1,\omega)\,\alpha^3\omega - \Phi_1(1,\omega)^2\,\omega \\
&\left.+\frac{1}{2}\Phi_1(1,\omega)^2\,\omega^2\right) + \epsilon C_F^2 \left(+\frac{19}{8} + 4\alpha + \alpha^2 - \Omega_2\left(\frac{1}{\omega},\frac{1}{\omega}\right) \right. \\
&+2\Omega_2(\omega,1) - \frac{5}{2}\ln(\omega)\Phi_1(1,\omega)\,\omega - \frac{3}{2}\ln(\omega)\Phi_1(1,\omega)\,\alpha\omega \\
&-\Phi_2\left(\frac{1}{\omega},\frac{1}{\omega}\right) - \Phi_2\left(\frac{1}{\omega},\frac{1}{\omega}\right)\alpha - 7\Phi_1(1,\omega)\,\omega - 2\Phi_1(1,\omega)\,\alpha\omega \\
&-\Phi_1(1,\omega)\,\alpha^2\omega + 2\Phi_1(1,\omega)^2\,\omega + \frac{5}{4}\Phi_1(1,\omega)^2\,\omega^2 \\
&\left.\left.+\frac{3}{2}\Phi_1(1,\omega)^2\,\alpha\omega^2 + \frac{1}{4}\Phi_1(1,\omega)^2\,\alpha^2\omega^2\right)\right)\frac{1}{\epsilon}\Bigg]\,a^2 \;+\; \mathcal{O}(a^3)\;.
\end{aligned}
\tag{7.4.16}
$$

where again $Z_{\mathcal{O}}^{S}(a,\alpha)\big|_{\mathrm{RI}'} \equiv Z_{\mathcal{O}}^{S}(a_{\mathrm{RI}'},\alpha_{\mathrm{RI}'})$ and RI′ defined on the operator renormalization constant is shorthand for RI′/IMOM. This is assumed throughout, unless otherwise specified. Note that all results presented so far have been for the IMOM setup with interpolating parameter ω. However it is only at this point where the ω dependence becomes apparent. There are several functions of ω which appear here. These come directly from the master integrals given explicitly in Appendix C.

With the renormalization constants determined we present the amplitudes in each scheme. For the scalar operator there are only two channels coming from the tensor basis

$$
\Sigma_{(k)\,\sigma}^{S}(p,q)\,\Big|_{\omega} \;=\; \sum_{k=1}^{2} \mathcal{P}_{(k)\,\sigma}^{S}(p,q)\Sigma_{(k)\,\sigma}^{S}(p,q)\;. \tag{7.4.17}
$$

Throughout this chapter we present the results for only one or two amplitudes per operator and scheme considered. Despite applying the full tensor basis to construct all amplitudes for each scheme, we choose to display a small set of results in this chapter due to restrictions on the space available. The channel 1

amplitude for the scalar (or mass) in the $\overline{\rm MS}$ scheme is

$$\begin{aligned}
\Sigma^{\rm S}_{(1)}(p,q)\Big|_{\overline{\rm MS}} &= -1 + C_F \left[\Phi_1\left(\frac{1}{\omega},\frac{1}{\omega}\right) \alpha + 3\Phi_1\left(\frac{1}{\omega},\frac{1}{\omega}\right) - 4\alpha - 8 \right] \frac{a}{2} \\
&+C_F \left[-36\ln(\omega)\Phi_1\left(\frac{1}{\omega},\frac{1}{\omega}\right) \alpha C_F\omega - 12\ln(\omega)\Phi_1\left(\frac{1}{\omega},\frac{1}{\omega}\right) C_A\omega \right. \\
&-60\ln(\omega)\Phi_1\left(\frac{1}{\omega},\frac{1}{\omega}\right) C_F\omega + 12\Omega_2\left(\frac{1}{\omega},\frac{1}{\omega}\right) C_A\omega \\
&-24\Omega_2\left(\frac{1}{\omega},\frac{1}{\omega}\right) C_F\omega - 24\Omega_2(1,\omega)\, C_A\omega + 48\Omega_2(1,\omega)\, C_F\omega \\
&+12\Phi_1\left(\frac{1}{\omega},\frac{1}{\omega}\right)^2 C_A\omega - 24\Phi_1\left(\frac{1}{\omega},\frac{1}{\omega}\right)^2 C_A \\
&-24\Phi_1\left(\frac{1}{\omega},\frac{1}{\omega}\right)^2 C_F\omega + 48\Phi_1\left(\frac{1}{\omega},\frac{1}{\omega}\right)^2 C_F \\
&+9\Phi_1\left(\frac{1}{\omega},\frac{1}{\omega}\right) \alpha^2 C_A\omega + 12\Phi_1\left(\frac{1}{\omega},\frac{1}{\omega}\right) \alpha^2 C_F\omega \\
&+42\Phi_1\left(\frac{1}{\omega},\frac{1}{\omega}\right) \alpha C_A\omega + 156\Phi_1\left(\frac{1}{\omega},\frac{1}{\omega}\right) \alpha C_F\omega \\
&+385\Phi_1\left(\frac{1}{\omega},\frac{1}{\omega}\right) C_A\omega + 120\Phi_1\left(\frac{1}{\omega},\frac{1}{\omega}\right) C_F\omega \\
&-80\Phi_1\left(\frac{1}{\omega},\frac{1}{\omega}\right) N_f\omega T_F - 24\Phi_2\left(\frac{1}{\omega},\frac{1}{\omega}\right) \alpha C_F\omega \\
&-24\Phi_2\left(\frac{1}{\omega},\frac{1}{\omega}\right) C_A\omega - 24\Phi_2\left(\frac{1}{\omega},\frac{1}{\omega}\right) C_F\omega \\
&+24\Phi_2(1,\omega)\, C_A\omega^2 - 45\alpha^2 C_A\omega - 24\alpha^2 C_F\omega + 72\alpha C_A\omega\zeta_3 \\
&-240\alpha C_A\omega - 192\alpha C_F\omega + 360 C_A\omega\zeta_3 - 1531 C_A\omega \\
&\left. -312 C_F\omega + 416 N_f\omega T_F \right] \frac{a^2}{24\omega} \; + \; \mathcal{O}(a^3) \; . \qquad (7.4.18)
\end{aligned}$$

In order to make contact with the known results of [139] we take the SMOM limit by setting $\omega = 1$. This gives us the channel 1 amplitude for the scalar operator at the symmetric subtraction point as

$$\begin{aligned}
\Sigma^{\rm S}_{(1)}(p,q)\Big|_{\omega=1} &= -1 + C_F \left[3\psi'\left(\tfrac{1}{3}\right) \alpha + 9\psi'\left(\tfrac{1}{3}\right) - 2\alpha\pi^2 - 18\alpha - 6\pi^2 - 36 \right] \frac{a}{9} \\
&+C_F \left[-144\sqrt{3}\psi'\left(\tfrac{1}{3}\right)^2 C_A + 288\sqrt{3}\psi'\left(\tfrac{1}{3}\right)^2 C_F \right. \\
&+162\sqrt{3}\psi'\left(\tfrac{1}{3}\right) \alpha^2 C_A + 216\sqrt{3}\psi'\left(\tfrac{1}{3}\right) \alpha^2 C_F \\
&+756\sqrt{3}\psi'\left(\tfrac{1}{3}\right) \alpha C_A + 2808\sqrt{3}\psi'\left(\tfrac{1}{3}\right) \alpha C_F \\
&+192\sqrt{3}\psi'\left(\tfrac{1}{3}\right) C_A\pi^2 + 8226\sqrt{3}\psi'\left(\tfrac{1}{3}\right) C_A \\
&\left. -384\sqrt{3}\psi'\left(\tfrac{1}{3}\right) C_F\pi^2 - 432\sqrt{3}\psi'\left(\tfrac{1}{3}\right) C_F \right.
\end{aligned}$$

$$
\begin{aligned}
&-1440\sqrt{3}\psi'\left(\tfrac{1}{3}\right) N_f T_F - 18\sqrt{3}\psi'''\left(\tfrac{1}{3}\right) \alpha C_F \\
&-18\sqrt{3}\psi'''\left(\tfrac{1}{3}\right) C_F + 7776\sqrt{3}s_2\left(\tfrac{\pi}{6}\right) C_A \\
&-15552\sqrt{3}s_2\left(\tfrac{\pi}{6}\right) C_F - 15552\sqrt{3}s_2\left(\tfrac{\pi}{2}\right) C_A \\
&+31104\sqrt{3}s_2\left(\tfrac{\pi}{2}\right) C_F - 12960\sqrt{3}s_3\left(\tfrac{\pi}{6}\right) C_A \\
&+25920\sqrt{3}s_3\left(\tfrac{\pi}{6}\right) C_F + 10368\sqrt{3}s_3\left(\tfrac{\pi}{2}\right) C_A \\
&-20736\sqrt{3}s_3\left(\tfrac{\pi}{2}\right) C_F - 108\sqrt{3}\alpha^2 C_A\pi^2 - 1215\sqrt{3}\alpha^2 C_A \\
&-144\sqrt{3}\alpha^2 C_F\pi^2 - 648\sqrt{3}\alpha^2 C_F - 504\sqrt{3}\alpha C_A\pi^2 \\
&+1944\sqrt{3}\alpha C_A\zeta_3 - 6480\sqrt{3}\alpha C_A + 48\sqrt{3}\alpha C_F\pi^4 \\
&-1872\sqrt{3}\alpha C_F\pi^2 - 5184\sqrt{3}\alpha C_F - 64\sqrt{3}C_A\pi^4 \\
&-5484\sqrt{3}C_A\pi^2 + 8424\sqrt{3}C_A\zeta_3 - 41337\sqrt{3}C_A \\
&+176\sqrt{3}C_F\pi^4 + 288\sqrt{3}C_F\pi^2 + 2592\sqrt{3}C_F\zeta_3 \\
&-8424\sqrt{3}C_F + 960\sqrt{3}N_f\pi^2 T_F + 11232\sqrt{3}N_f T_F \\
&+54\ln(3)^2 C_A\pi - 108\ln(3)^2 C_F\pi - 648\ln(3)C_A\pi \\
&+1296\ln(3)C_F\pi - 58C_A\pi^3 + 116C_F\pi^3\Big] \frac{a^2}{648\sqrt{3}} \\
&+ \mathcal{O}(a^3)
\end{aligned}
\tag{7.4.19}
$$

which agrees exactly with the results of [139]. In order to obtain this result the following identities have been applied, [62, 63, 64, 149],

$$
\begin{aligned}
\Psi_1(\omega,1) &= \Psi_1(1,\omega) = \frac{1}{\omega}\left[\Psi_1\left(\frac{1}{\omega},\frac{1}{\omega}\right) - \ln(\omega)\Phi_1\left(\frac{1}{\omega},\frac{1}{\omega}\right)\right] \\
\Phi_1(\omega,1) &= \Phi_1(1,\omega) = \frac{1}{\omega}\Phi_1\left(\frac{1}{\omega},\frac{1}{\omega}\right) \\
\Phi_1\left(\frac{1}{\omega},\frac{1}{\omega}\right) &= \omega[\Phi_1(1,\omega)\ln(\omega) + \Phi_1(1,\omega)] \\
\Psi_2(\omega,1) &= \Psi_2(1,\omega) \\
\Phi_2(\omega,1) &= \Phi_2(1,\omega) \\
\Omega_2(1,\omega) &= \Omega_2(\omega,1)
\end{aligned}
\tag{7.4.20}
$$

which arise from the various underlying master integrals and have been evaluated explicitly in terms of polylogarithm functions in [62, 63, 64, 149]. The above identities are based on the asymmetric properties of the Green's function in an IMOM configuration. Note that although Ψ_1 does not appear explicitly it is needed in the ϵ expansion. Generalising to the SMOM limit we need only consider,

[62, 136, 151, 103]

$$
\begin{aligned}
\Phi_1(1,1) &= -\frac{2}{3}\pi^2 - \frac{2}{3}\psi'\left(\tfrac{1}{3}\right) \\
\Psi_1(1,1) &= 12 s_3\left(\tfrac{\pi}{6}\right) - \frac{35}{108\sqrt{3}}\pi^3 - \frac{\ln^2(3)}{4\sqrt{3}} \\
\Phi_2(1,1) &= -\frac{2}{27}\pi^4 + \frac{1}{36}\psi'''\left(\tfrac{1}{3}\right) \\
\Omega_2(1,1) &= 4\left[\frac{2}{3}\pi^2 + \zeta_3 - 6 s_2\left(\tfrac{\pi}{6}\right) + 12 s_2\left(\tfrac{\pi}{2}\right) + 10 s_3\left(\tfrac{\pi}{6}\right) - 8 s_3\left(\tfrac{\pi}{2}\right) - \psi'\left(\tfrac{1}{3}\right)\right. \\
&\quad \left. + \frac{29}{648\sqrt{3}}\pi^3 + \frac{1}{2\sqrt{3}}\ln(3)\pi - \frac{1}{24\sqrt{3}}\ln(3)^2\pi\right] . \qquad (7.4.21)
\end{aligned}
$$

Next we present the amplitudes for the RI′/IMOM scheme, these are

$$
\begin{aligned}
\Sigma^{\rm S}_{(1)}(p,q)\Big|_{\rm RI'} &= -1 + \mathcal{O}(a^3) \\
\Sigma^{\rm S}_{(2)}(p,q)\Big|_{\rm RI'} &= C_F\left[-2\ln(\omega)\alpha\omega + 2\ln(\omega)\omega + \Phi_1\left(\frac{1}{\omega},\frac{1}{\omega}\right)\alpha\omega\right. \\
&\quad \left. -2\Phi_1\left(\frac{1}{\omega},\frac{1}{\omega}\right)\alpha - \Phi_1\left(\frac{1}{\omega},\frac{1}{\omega}\right)\omega + 2\Phi_1\left(\frac{1}{\omega},\frac{1}{\omega}\right)\right]\frac{a}{\omega(\omega-4)} \\
&\quad + C_F\left[36\ln(\omega)^2\alpha C_A\omega^2 + 72\ln(\omega)^2\alpha C_F\omega^2\right. \\
&\quad -36\ln(\omega)^2 C_A\omega^2 - 72\ln(\omega)^2 C_F\omega^2 \\
&\quad -36\ln(\omega)\Phi_1\left(\frac{1}{\omega},\frac{1}{\omega}\right)\alpha^2 C_F\omega^2 - 18\ln(\omega)\Phi_1\left(\frac{1}{\omega},\frac{1}{\omega}\right)\alpha C_A\omega^2 \\
&\quad +36\ln(\omega)\Phi_1\left(\frac{1}{\omega},\frac{1}{\omega}\right)\alpha C_A\omega - 108\ln(\omega)\Phi_1\left(\frac{1}{\omega},\frac{1}{\omega}\right)\alpha C_F\omega^2 \\
&\quad +72\ln(\omega)\Phi_1\left(\frac{1}{\omega},\frac{1}{\omega}\right)\alpha C_F\omega + 18\ln(\omega)\Phi_1\left(\frac{1}{\omega},\frac{1}{\omega}\right) C_A\omega^2 \\
&\quad -36\ln(\omega)\Phi_1\left(\frac{1}{\omega},\frac{1}{\omega}\right) C_A\omega + 144\ln(\omega)\Phi_1\left(\frac{1}{\omega},\frac{1}{\omega}\right) C_F\omega^2 \\
&\quad -72\ln(\omega)\Phi_1\left(\frac{1}{\omega},\frac{1}{\omega}\right) C_F\omega - 18\ln(\omega)\alpha^3 C_A\omega^2 \\
&\quad -54\ln(\omega)\alpha^2 C_A\omega^2 - 338\ln(\omega)\alpha C_A\omega^2 + 160\ln(\omega)\alpha N_f\omega^2 T_F \\
&\quad -142\ln(\omega) C_A\omega^2 - 64\ln(\omega) N_f\omega^2 T_F - 36\Omega_2\left(\frac{1}{\omega},\frac{1}{\omega}\right)\alpha C_A\omega^2 \\
&\quad +36\Omega_2\left(\frac{1}{\omega},\frac{1}{\omega}\right)\alpha C_A\omega + 252\Omega_2\left(\frac{1}{\omega},\frac{1}{\omega}\right) C_A\omega^2 \\
&\quad -324\Omega_2\left(\frac{1}{\omega},\frac{1}{\omega}\right) C_A\omega - 144\Omega_2\left(\frac{1}{\omega},\frac{1}{\omega}\right) C_F\omega^2 \\
&\quad -36\Omega_2(1,\omega)\,\alpha C_A\omega^2 + 144\Omega_2(1,\omega)\,\alpha C_F\omega^2 \\
&\quad \left. +252\Omega_2(1,\omega)\, C_A\omega^2 - 720\Omega_2(1,\omega)\, C_F\omega^2\right.
\end{aligned}
$$

$$
\begin{aligned}
&+18\Phi_1\left(\frac{1}{\omega},\frac{1}{\omega}\right)^2 \alpha^2 C_F\omega^2 - 36\Phi_1\left(\frac{1}{\omega},\frac{1}{\omega}\right)^2 \alpha^2 C_F\omega \\
&+36\Phi_1\left(\frac{1}{\omega},\frac{1}{\omega}\right)^2 \alpha C_F\omega^2 - 72\Phi_1\left(\frac{1}{\omega},\frac{1}{\omega}\right)^2 \alpha C_F\omega \\
&-36\Phi_1\left(\frac{1}{\omega},\frac{1}{\omega}\right)^2 C_A\omega^2 + 144\Phi_1\left(\frac{1}{\omega},\frac{1}{\omega}\right)^2 C_A\omega \\
&+18\Phi_1\left(\frac{1}{\omega},\frac{1}{\omega}\right)^2 C_F\omega^2 - 180\Phi_1\left(\frac{1}{\omega},\frac{1}{\omega}\right)^2 C_F\omega \\
&+9\Phi_1\left(\frac{1}{\omega},\frac{1}{\omega}\right) \alpha^3 C_A\omega^2 - 18\Phi_1\left(\frac{1}{\omega},\frac{1}{\omega}\right) \alpha^3 C_A\omega \\
&+27\Phi_1\left(\frac{1}{\omega},\frac{1}{\omega}\right) \alpha^2 C_A\omega^2 - 54\Phi_1\left(\frac{1}{\omega},\frac{1}{\omega}\right) \alpha^2 C_A\omega \\
&+133\Phi_1\left(\frac{1}{\omega},\frac{1}{\omega}\right) \alpha C_A\omega^2 - 194\Phi_1\left(\frac{1}{\omega},\frac{1}{\omega}\right) \alpha C_A\omega \\
&-36\Phi_1\left(\frac{1}{\omega},\frac{1}{\omega}\right) \alpha C_F\omega^2 + 144\Phi_1\left(\frac{1}{\omega},\frac{1}{\omega}\right) \alpha C_F\omega \\
&-80\Phi_1\left(\frac{1}{\omega},\frac{1}{\omega}\right) \alpha N_f\omega^2 T_F + 160\Phi_1\left(\frac{1}{\omega},\frac{1}{\omega}\right) \alpha N_f\omega T_F \\
&+251\Phi_1\left(\frac{1}{\omega},\frac{1}{\omega}\right) C_A\omega^2 - 862\Phi_1\left(\frac{1}{\omega},\frac{1}{\omega}\right) C_A\omega \\
&+36\Phi_1\left(\frac{1}{\omega},\frac{1}{\omega}\right) C_F\omega^2 - 144\Phi_1\left(\frac{1}{\omega},\frac{1}{\omega}\right) C_F\omega \\
&+32\Phi_1\left(\frac{1}{\omega},\frac{1}{\omega}\right) N_f\omega^2 T_F - 64\Phi_1\left(\frac{1}{\omega},\frac{1}{\omega}\right) N_f\omega T_F \\
&-72\Phi_2\left(\frac{1}{\omega},\frac{1}{\omega}\right) \alpha C_A - 72\Phi_2\left(\frac{1}{\omega},\frac{1}{\omega}\right) \alpha C_F\omega^2 \\
&+144\Phi_2\left(\frac{1}{\omega},\frac{1}{\omega}\right) \alpha C_F\omega + 216\Phi_2\left(\frac{1}{\omega},\frac{1}{\omega}\right) C_A\omega^2 \\
&-576\Phi_2\left(\frac{1}{\omega},\frac{1}{\omega}\right) C_A\omega + 648\Phi_2\left(\frac{1}{\omega},\frac{1}{\omega}\right) C_A \\
&-72\Phi_2\left(\frac{1}{\omega},\frac{1}{\omega}\right) C_F\omega^2 + 144\Phi_2\left(\frac{1}{\omega},\frac{1}{\omega}\right) C_F\omega \\
&-360\Phi_2(1,\omega)\, C_A\omega^3 + 576\Phi_2(1,\omega)\, C_F\omega^3 + 216\alpha C_A\omega^2\zeta_3 \\
&-864\alpha C_F\omega^2\zeta_3 + 648 C_A\omega^2\zeta_3 + 864 C_F\omega^2\zeta_3\big]\, \frac{a^2}{36\omega^2(\omega-4)} \\
&+ \mathcal{O}(a^3) \; . \qquad (7.4.22)
\end{aligned}
$$

We have checked that our results agree exactly with the results of [137, 139] for both the $\overline{\rm MS}$ and RI$'$/SMOM schemes. Note that between the two amplitudes for the scalar it was found that no relations exist; the two channels are independent

of each other.

From the above results for the renormalization constants and amplitudes we are able to construct the conversion function for the scalar. Since the mapping of the coupling constant is not required we simply define the gauge parameter mapping, where we have used the same techniques to determine it as was defined in chapter 3. This is

$$\begin{aligned}\alpha_{\mathrm{RI}'} &= \alpha + \left[-9\alpha^2 C_A - 18\alpha C_A - 97 C_A + 80 N_f T_F\right] \frac{\alpha a}{36} \\ &+ \left[18\alpha^4 C_A^2 - 18\alpha^3 C_A^2 + 190\alpha^2 C_A^2 - 320\alpha^2 C_A N_f T_F - 576\alpha C_A^2 \zeta_3 \right. \\ &\quad +463\alpha C_A^2 - 320\alpha C_A N_f T_F + 864 C_A^2 \zeta_3 - 7143 C_A^2 + 2304 C_A N_f T_F \zeta_3 \\ &\quad \left. +4248 C_A N_f T_F - 4608 C_F N_f T_F \zeta_3 + 5280 C_F N_f T_F\right] \frac{\alpha a^2}{288} \; + \; \mathcal{O}(a^3)\end{aligned} \tag{7.4.23}$$

which is in direct agreement with [137, 139], where the result for the gauge parameter mapping is the same for both the SMOM and IMOM setups for RI′. This is as expected since this mapping only uses the wave function renormalization constants in its construction. It is only in the operator renormalization constant where we see the ω dependence emerging. The three loop result for the gauge parameter mapping is also available in [137]. We are now able to construct the conversion function using the definition

$$C_S^{\mathrm{RI}'/\mathrm{IMOM}}(a_{\overline{\mathrm{MS}}}, \alpha_{\overline{\mathrm{MS}}}) = \left. \frac{Z_S^{\mathrm{RI}'}}{Z_S^{\overline{\mathrm{MS}}}} \right|_{\mathrm{RI}'/\mathrm{IMOM} \to \overline{\mathrm{MS}}} \tag{7.4.24}$$

where it is our convention to always have the conversion functions in terms of $\overline{\mathrm{MS}}$ scheme parameters. In other words the conversion function is a funcion of $(a_{\overline{\mathrm{MS}}}, \alpha_{\overline{\mathrm{MS}}})$ where $a = g^2/(16\pi^2)$. The conversion function for the scalar operator is

$$\begin{aligned}C_S^{\mathrm{RI}'/\mathrm{IMOM}} &= 1 + C_F \left[\Phi_1\left(\frac{1}{\omega}, \frac{1}{\omega}\right) \alpha + 3\Phi_1\left(\frac{1}{\omega}, \frac{1}{\omega}\right) - 2\alpha - 8\right] \frac{a}{2} \\ &+ C_F \left[-36 \ln(\omega) \Phi_1\left(\frac{1}{\omega}, \frac{1}{\omega}\right) \alpha C_F \omega - 12 \ln(\omega) \Phi_1\left(\frac{1}{\omega}, \frac{1}{\omega}\right) C_A \omega \right. \\ &\quad -60 \ln(\omega) \Phi_1\left(\frac{1}{\omega}, \frac{1}{\omega}\right) C_F \omega + 12 \Omega_2\left(\frac{1}{\omega}, \frac{1}{\omega}\right) C_A \omega \\ &\quad \left. -24 \Omega_2\left(\frac{1}{\omega}, \frac{1}{\omega}\right) C_F \omega - 24 \Omega_2(1, \omega) C_A \omega\right.\end{aligned}$$

$$
\begin{aligned}
&+48\Omega_2(1,\omega)\,C_F\omega + 6\Phi_1\left(\frac{1}{\omega},\frac{1}{\omega}\right)^2\alpha^2 C_F\omega \\
&+36\Phi_1\left(\frac{1}{\omega},\frac{1}{\omega}\right)^2\alpha C_F\omega + 12\Phi_1\left(\frac{1}{\omega},\frac{1}{\omega}\right)^2 C_A\omega \\
&-24\Phi_1\left(\frac{1}{\omega},\frac{1}{\omega}\right)^2 C_A + 30\Phi_1\left(\frac{1}{\omega},\frac{1}{\omega}\right)^2 C_F\omega \\
&+48\Phi_1\left(\frac{1}{\omega},\frac{1}{\omega}\right)^2 C_F + 9\Phi_1\left(\frac{1}{\omega},\frac{1}{\omega}\right)\alpha^2 C_A\omega \\
&-24\Phi_1\left(\frac{1}{\omega},\frac{1}{\omega}\right)\alpha^2 C_F\omega + 42\Phi_1\left(\frac{1}{\omega},\frac{1}{\omega}\right)\alpha C_A\omega \\
&-48\Phi_1\left(\frac{1}{\omega},\frac{1}{\omega}\right)\alpha C_F\omega + 385\Phi_1\left(\frac{1}{\omega},\frac{1}{\omega}\right) C_A\omega \\
&-168\Phi_1\left(\frac{1}{\omega},\frac{1}{\omega}\right) C_F\omega - 80\Phi_1\left(\frac{1}{\omega},\frac{1}{\omega}\right) N_f\omega T_F \\
&-24\Phi_2\left(\frac{1}{\omega},\frac{1}{\omega}\right)\alpha C_F\omega - 24\Phi_2\left(\frac{1}{\omega},\frac{1}{\omega}\right) C_A\omega \\
&-24\Phi_2\left(\frac{1}{\omega},\frac{1}{\omega}\right) C_F\omega + 24\Phi_2(1,\omega)\,C_A\omega^2 - 18\alpha^2 C_A\omega \\
&+24\alpha^2 C_F\omega - 84\alpha C_A\omega + 96\alpha C_F\omega + 288 C_A\omega\zeta_3 - 1285 C_A\omega \\
&+57 C_F\omega + 332 N_f\omega T_F]\,\frac{a^2}{24\omega} \;+\; \mathcal{O}(a^3)
\end{aligned}
\tag{7.4.25}
$$

where in the Landau limit $\alpha = 0$ we are able to make checks against other work. This is fine since lattice simulations are usually carried out in the Landau gauge, [75]. The result

$$
\begin{aligned}
C_S^{\mathrm{RI}'/\mathrm{IMOM}}(a,0) \;=\;& 1 + C_F\left[3\Phi_1\left(\frac{1}{\omega},\frac{1}{\omega}\right) - 8\right]\frac{a}{2} \\
&+C_F\left[-12\ln(\omega)\,\Phi_1\left(\frac{1}{\omega},\frac{1}{\omega}\right) C_A\omega\right. \\
&\quad -60\ln(\omega)\,\Phi_1\left(\frac{1}{\omega},\frac{1}{\omega}\right) C_F\omega + 12\Omega_2\left(\frac{1}{\omega},\frac{1}{\omega}\right) C_A\omega \\
&\quad -24\Omega_2\left(\frac{1}{\omega},\frac{1}{\omega}\right) C_F\omega - 24\Omega_2(1,\omega)\,C_A\omega \\
&\quad +48\Omega_2(1,\omega)\,C_F\omega + 12\Phi_1\left(\frac{1}{\omega},\frac{1}{\omega}\right)^2 C_A\omega \\
&\quad -24\Phi_1\left(\frac{1}{\omega},\frac{1}{\omega}\right)^2 C_A + 30\Phi_1\left(\frac{1}{\omega},\frac{1}{\omega}\right)^2 C_F\omega \\
&\quad +48\Phi_1\left(\frac{1}{\omega},\frac{1}{\omega}\right)^2 C_F + 385\Phi_1\left(\frac{1}{\omega},\frac{1}{\omega}\right) C_A\omega
\end{aligned}
$$

$$
\begin{aligned}
&-168\Phi_1\left(\frac{1}{\omega},\frac{1}{\omega}\right) C_F\omega - 80\Phi_1\left(\frac{1}{\omega},\frac{1}{\omega}\right) N_f\omega T_F \\
&-24\Phi_2\left(\frac{1}{\omega},\frac{1}{\omega}\right) C_A\omega - 24\Phi_2\left(\frac{1}{\omega},\frac{1}{\omega}\right) C_F\omega \\
&+24\Phi_2(1,\omega)\, C_A\omega^2 + 288 C_A\omega\zeta_3 - 1285 C_A\omega \\
&+57 C_F\omega + 332 N_f\omega T_F] \,\frac{a^2}{24\omega} \;+\; \mathcal{O}(a^3)
\end{aligned}
\tag{7.4.26}
$$

is in exact agreement with [133] in this limit, where we have chosen the Casimirs to be

$$
C_A \;=\; N_c \;\;,\;\; C_F \;=\; \frac{(N_c^2-1)}{2N_c} \;\;,\;\; T_F \;=\; \frac{1}{2} \tag{7.4.27}
$$

in order to match the convention of the published result in [133]. Note that in all of our above results for the conversion function the parameter α is mapped to the $\overline{\rm MS}$ scheme. As would also be the case with the coupling constant a if $a_{\rm RI'}$ and $a_{\overline{\rm MS}}$ were not equivalent up to the loop order required.

The anomalous dimension for the scalar operator in the $\overline{\rm MS}$ scheme at two loops is

$$
\gamma_S^{\overline{\rm MS}}(a,\alpha) \;=\; 3C_F a + \left[C_F\left(97C_A + 9C_F - 20N_f T_F\right)\right]\frac{a^2}{6} \;+\; \mathcal{O}(a^3) \tag{7.4.28}
$$

where there is no dependence on the gauge parameter. The anomalous dimension for the scalar operator in this scheme is gauge independent. This result has been confirmed with [139] and is in exact agreement with [75]. We note that this anomalous dimension for the $\overline{\rm MS}$ scheme has been constructed using the formula

$$
\gamma_S \;=\; \beta(a,\alpha)\frac{\partial}{\partial a}\ln Z_S \;+\; \alpha\gamma_\alpha(a,\alpha)\frac{\partial}{\partial a}\ln Z_S \tag{7.4.29}
$$

which is a variation on the formula we have used to determine the anomalous dimensions throughout, where γ_α and γ_A have been determined using (4.1.3). Although we have constructed the conversion function and confirmed our results with [133], which was the main reason for computing in the RI$'$/IMOM scheme, we present the anomalous dimension for the scalar in the RI$'$/IMOM scheme for completeness. For this we needed to adjust (3.4.55) to the following

$$
\gamma_S^{\rm RI'/IMOM} \;=\; -\left[\gamma_S^{\overline{\rm MS}}(a) + \beta^{\overline{\rm MS}}(a)\,\frac{\partial}{\partial a_{\overline{\rm MS}}}\ln C_S^{\rm RI'/IMOM}\left(a,\alpha_{\overline{\rm MS}}\right)\right.
$$

$$+\alpha_{\overline{\mathrm{MS}}}\gamma_{\alpha}^{\overline{\mathrm{MS}}}\left(a,\alpha_{\overline{\mathrm{MS}}}\right)\frac{\partial}{\partial\alpha_{\overline{\mathrm{MS}}}}\ln C_{S}^{\mathrm{RI}'/\mathrm{IMOM}}\left(a,\alpha_{\overline{\mathrm{MS}}}\right)\Bigg]_{\overline{\mathrm{MS}}\to\mathrm{RI}'/\mathrm{IMOM}} \tag{7.4.30}$$

where we have not labelled the coupling constant a with a scheme dependence since the $\overline{\mathrm{MS}}$ coupling is equivalent to the RI′/IMOM coupling constant up to five loops, [137]. We also partly do this due to lack of space when presenting the equation fully. In comparison to (3.4.55) a minus sign is introduced. This is as a result of the renormalization of the mass not being computed directly. With all operators, if one were to deduce the RI′/IMOM anomalous dimensions the same way in which we have done for the mass, the above formula would always carry a minus sign. We have chosen this convention to match with other work, [133, 137, 139]. If we were to carry out the full massive calculation then we would not need to manually include this sign in the formula since the correct convention for the sign of the anomalous dimensions would naturally be projected out. For completeness the mass anomalous dimension for the RI′/IMOM scheme is given as

$$\begin{aligned}\gamma_{S}^{\mathrm{RI}'/\mathrm{IMOM}} &= 3C_{F}a+C_{F}\left[-3\Phi_{1}\left(\frac{1}{\omega},\frac{1}{\omega}\right)\alpha^{2}C_{A}-9\Phi_{1}\left(\frac{1}{\omega},\frac{1}{\omega}\right)\alpha C_{A}\right.\\ &\quad -66\Phi_{1}\left(\frac{1}{\omega},\frac{1}{\omega}\right)C_{A}+24\Phi_{1}\left(\frac{1}{\omega},\frac{1}{\omega}\right)N_{f}T_{F}+6\alpha^{2}C_{A}\\ &\quad \left.+18\alpha C_{A}+370C_{A}+18C_{F}-104N_{f}T_{F}\right]\frac{a^{2}}{12}\;+\;\mathcal{O}(a^{3})\;.\end{aligned} \tag{7.4.31}$$

where we have used the identities (7.4.20) to rearrange (7.4.31) in to the same form as [133] in order to make comparing results easier. Our result agrees with the same results in [75, 138, 133, 139] for the scalar anomalous dimension when $\omega = 1$.

7.5 Vector operator

We now move on to the vector current. As in the case of the scalar operator, we have a quark 2-point function where the operator is inserted through the top leg with momenta incoming. We now replace the scalar with the vector current $\bar{\psi}\gamma_{\mu}\psi$. This operator is strongly related to the DIS operator ∂W_2. Analysing the vector operator helps us to build a bigger picture of what is happening inside the nucleus and is a preliminary computation to that of ∂W_2.

Using the $\overline{\rm MS}$ renormalization constants defined in chapter 3 we determine the operator renormalization constant. For the vector operator this is found to be

$$Z^V_{\mathcal{O}}(a,\alpha)\Big|_{\overline{\rm MS}} \;=\; 1 \;+\; \mathcal{O}(a^3) \tag{7.5.32}$$

With this, we construct the amplitudes for the $\overline{\rm MS}$ scheme in an IMOM configuration setup where the amplitudes are defined by

$$\Sigma^V_{(k)\,\sigma}(p,q)\;\Big|_{\omega} \;=\; \sum_{k=1}^{6} \mathcal{P}^V_{(k)\,\sigma}(p,q)\Sigma^V_{(k)\,\sigma}(p,q)\;. \tag{7.5.33}$$

where $\mathcal{P}^V_{(k)\,\sigma}(p,q)$ are the tensors for the vector operator defined in Appendix C. We have computed all six amplitudes but choose to display only one here. The channel 1 amplitude, corresponding to the tree-level vertex, in the $\overline{\rm MS}$ scheme is

$$\begin{aligned}
\Sigma^{\rm V}_{(1)}(p,q)\Big|_{\overline{\rm MS}} \;=\;& -1 + C_F\left[\ln(\omega)\alpha\omega^2 - 2\ln(\omega)\alpha\omega - 2\ln(\omega)\omega^2 + 4\ln(\omega)\omega\right.\\
&\quad -2\Phi_1\left(\frac{1}{\omega},\frac{1}{\omega}\right)\alpha + \Phi_1\left(\frac{1}{\omega},\frac{1}{\omega}\right)\omega^2 - 4\Phi_1\left(\frac{1}{\omega},\frac{1}{\omega}\right)\omega\\
&\quad \left.+4\Phi_1\left(\frac{1}{\omega},\frac{1}{\omega}\right) - 2\alpha\omega^2 + 8\alpha\omega + 2\omega^2 - 8\omega\right]\frac{a}{\omega(\omega-4)}\\
&+C_F\left[-180\ln(\omega)^2 C_A\omega^2 + 432\ln(\omega)^2 C_F\omega^2\right.\\
&\quad +18\ln(\omega)\Phi_1\left(\frac{1}{\omega},\frac{1}{\omega}\right)C_A\omega^2 + 108\ln(\omega)\Phi_1\left(\frac{1}{\omega},\frac{1}{\omega}\right)C_A\omega\\
&\quad -432\ln(\omega)\Phi_1\left(\frac{1}{\omega},\frac{1}{\omega}\right)C_F\omega + 54\ln(\omega)\alpha^2 C_A\omega^2\\
&\quad -108\ln(\omega)\alpha^2 C_A\omega + 72\ln(\omega)\alpha^2 C_F\omega^2 - 144\ln(\omega)\alpha^2 C_F\omega\\
&\quad +252\ln(\omega)\alpha C_A\omega^2 - 504\ln(\omega)\alpha C_A\omega - 288\ln(\omega)\alpha C_F\omega^2\\
&\quad +576\ln(\omega)\alpha C_F\omega - 1414\ln(\omega)C_A\omega^2 + 2828\ln(\omega)C_A\omega\\
&\quad +252\ln(\omega)C_F\omega^2 - 504\ln(\omega)C_F\omega + 464\ln(\omega)N_f\omega^2 T_F\\
&\quad -928\ln(\omega)N_f\omega T_F + 18\Omega_2\left(\frac{1}{\omega},\frac{1}{\omega}\right)\alpha C_A\omega^2\\
&\quad -36\Omega_2\left(\frac{1}{\omega},\frac{1}{\omega}\right)\alpha C_A\omega - 126\Omega_2\left(\frac{1}{\omega},\frac{1}{\omega}\right)C_A\omega^2\\
&\quad +288\Omega_2\left(\frac{1}{\omega},\frac{1}{\omega}\right)C_A\omega + 72\Omega_2\left(\frac{1}{\omega},\frac{1}{\omega}\right)C_F\omega^2\\
&\quad -144\Omega_2\left(\frac{1}{\omega},\frac{1}{\omega}\right)C_F\omega + 36\Omega_2(1,\omega)\,\alpha C_A\omega^2\\
&\quad -72\Omega_2(1,\omega)\,\alpha C_A\omega - 144\Omega_2(1,\omega)\,\alpha C_F\omega^2
\end{aligned}$$

$$
\begin{aligned}
&+288\Omega_2(1,\omega)\,\alpha C_F\omega - 288\Omega_2(1,\omega)\,C_A\omega^2 \\
&+216\Omega_2(1,\omega)\,C_A\omega + 720\Omega_2(1,\omega)\,C_F\omega^2 \\
&-576\Omega_2(1,\omega)\,C_F\omega + 36\Phi_1\left(\frac{1}{\omega},\frac{1}{\omega}\right)^2 C_A\omega^2 \\
&-216\Phi_1\left(\frac{1}{\omega},\frac{1}{\omega}\right)^2 C_A\omega + 288\Phi_1\left(\frac{1}{\omega},\frac{1}{\omega}\right)^2 C_A \\
&-72\Phi_1\left(\frac{1}{\omega},\frac{1}{\omega}\right)^2 C_F\omega^2 + 432\Phi_1\left(\frac{1}{\omega},\frac{1}{\omega}\right)^2 C_F\omega \\
&-576\Phi_1\left(\frac{1}{\omega},\frac{1}{\omega}\right)^2 C_F - 108\Phi_1\left(\frac{1}{\omega},\frac{1}{\omega}\right)\alpha^2 C_A \\
&-144\Phi_1\left(\frac{1}{\omega},\frac{1}{\omega}\right)\alpha^2 C_F - 504\Phi_1\left(\frac{1}{\omega},\frac{1}{\omega}\right)\alpha C_A \\
&+288\Phi_1\left(\frac{1}{\omega},\frac{1}{\omega}\right)\alpha C_F\omega^2 - 1152\Phi_1\left(\frac{1}{\omega},\frac{1}{\omega}\right)\alpha C_F\omega \\
&+576\Phi_1\left(\frac{1}{\omega},\frac{1}{\omega}\right)\alpha C_F + 920\Phi_1\left(\frac{1}{\omega},\frac{1}{\omega}\right) C_A\omega^2 \\
&-3680\Phi_1\left(\frac{1}{\omega},\frac{1}{\omega}\right) C_A\omega + 2828\Phi_1\left(\frac{1}{\omega},\frac{1}{\omega}\right) C_A \\
&-1044\Phi_1\left(\frac{1}{\omega},\frac{1}{\omega}\right) C_F\omega^2 + 4176\Phi_1\left(\frac{1}{\omega},\frac{1}{\omega}\right) C_F\omega \\
&-504\Phi_1\left(\frac{1}{\omega},\frac{1}{\omega}\right) C_F - 208\Phi_1\left(\frac{1}{\omega},\frac{1}{\omega}\right) N_f\omega^2 T_F \\
&+832\Phi_1\left(\frac{1}{\omega},\frac{1}{\omega}\right) N_f\omega T_F - 928\Phi_1\left(\frac{1}{\omega},\frac{1}{\omega}\right) N_f T_F \\
&+288\Phi_2\left(\frac{1}{\omega},\frac{1}{\omega}\right)\alpha C_F - 144\Phi_2\left(\frac{1}{\omega},\frac{1}{\omega}\right) C_A\omega^2 \\
&+648\Phi_2\left(\frac{1}{\omega},\frac{1}{\omega}\right) C_A\omega - 648\Phi_2\left(\frac{1}{\omega},\frac{1}{\omega}\right) C_A \\
&-288\Phi_2\left(\frac{1}{\omega},\frac{1}{\omega}\right) C_F + 216\Phi_2(1,\omega)\,C_A\omega^3 \\
&-288\Phi_2(1,\omega)\,C_F\omega^3 - 576\Phi_2(1,\omega)\,C_F\omega^2 - 135\alpha^2 C_A\omega^2 \\
&+540\alpha^2 C_A\omega - 72\alpha^2 C_F\omega^2 + 288\alpha^2 C_F\omega - 720\alpha C_A\omega^2 \\
&-432\alpha C_A\omega\zeta_3 + 2880\alpha C_A\omega + 864\alpha C_F\omega^2\zeta_3 + 288\alpha C_F\omega^2 \\
&-1728\alpha C_F\omega\zeta_3 - 1152\alpha C_F\omega + 216 C_A\omega^2\zeta_3 + 676 C_A\omega^2 \\
&-432 C_A\omega\zeta_3 - 2704 C_A\omega - 1728 C_F\omega^2\zeta_3 - 207 C_F\omega^2 \\
&+3456 C_F\omega\zeta_3 + 828 C_F\omega - 212 N_f\omega^2 T_F \\
&+848 N_f\omega T_F]\,\frac{a^2}{72\omega(\omega-4)} \;+\; \mathcal{O}(a^3)
\end{aligned}
\tag{7.5.34}
$$

whereby taking the limit $\omega \to 1$ this becomes

$$\begin{aligned}
\Sigma^{\rm V}_{(1)}(p,q)\Big|_{\omega=1} &= -1 + 2C_F\left[6\psi'\left(\tfrac{1}{3}\right)\alpha - 3\psi'\left(\tfrac{1}{3}\right) - 4\alpha\pi^2 - 27\alpha + 2\pi^2 + 27\right]\frac{a}{27} \\
&+C_F\Big[-432\sqrt{3}\psi'\left(\tfrac{1}{3}\right)^2 C_A + 864\sqrt{3}\psi'\left(\tfrac{1}{3}\right)^2 C_F \\
&\quad +648\sqrt{3}\psi'\left(\tfrac{1}{3}\right)\alpha^2 C_A + 864\sqrt{3}\psi'\left(\tfrac{1}{3}\right)\alpha^2 C_F \\
&\quad +1080\sqrt{3}\psi'\left(\tfrac{1}{3}\right)\alpha C_A + 6912\sqrt{3}\psi'\left(\tfrac{1}{3}\right)\alpha C_F \\
&\quad +576\sqrt{3}\psi'\left(\tfrac{1}{3}\right) C_A\pi^2 + 2832\sqrt{3}\psi'\left(\tfrac{1}{3}\right) C_A \\
&\quad -1152\sqrt{3}\psi'\left(\tfrac{1}{3}\right) C_F\pi^2 - 13176\sqrt{3}\psi'\left(\tfrac{1}{3}\right) C_F \\
&\quad +1824\sqrt{3}\psi'\left(\tfrac{1}{3}\right) N_f T_F - 72\sqrt{3}\psi'''\left(\tfrac{1}{3}\right)\alpha C_F \\
&\quad -18\sqrt{3}\psi'''\left(\tfrac{1}{3}\right) C_A + 288\sqrt{3}\psi'''\left(\tfrac{1}{3}\right) C_F \\
&\quad -11664\sqrt{3}s_2\left(\tfrac{\pi}{6}\right)\alpha C_A + 31104\sqrt{3}s_2\left(\tfrac{\pi}{6}\right)\alpha C_F \\
&\quad +19440\sqrt{3}s_2\left(\tfrac{\pi}{6}\right) C_A + 15552\sqrt{3}s_2\left(\tfrac{\pi}{6}\right) C_F \\
&\quad +23328\sqrt{3}s_2\left(\tfrac{\pi}{2}\right)\alpha C_A - 62208\sqrt{3}s_2\left(\tfrac{\pi}{2}\right)\alpha C_F \\
&\quad -38880\sqrt{3}s_2\left(\tfrac{\pi}{2}\right) C_A - 31104\sqrt{3}s_2\left(\tfrac{\pi}{2}\right) C_F \\
&\quad +19440\sqrt{3}s_3\left(\tfrac{\pi}{6}\right)\alpha C_A - 51840\sqrt{3}s_3\left(\tfrac{\pi}{6}\right)\alpha C_F \\
&\quad -32400\sqrt{3}s_3\left(\tfrac{\pi}{6}\right) C_A - 25920\sqrt{3}s_3\left(\tfrac{\pi}{6}\right) C_F \\
&\quad -15552\sqrt{3}s_3\left(\tfrac{\pi}{2}\right)\alpha C_A + 41472\sqrt{3}s_3\left(\tfrac{\pi}{2}\right)\alpha C_F \\
&\quad +25920\sqrt{3}s_3\left(\tfrac{\pi}{2}\right) C_A + 20736\sqrt{3}s_3\left(\tfrac{\pi}{2}\right) C_F \\
&\quad -432\sqrt{3}\alpha^2 C_A\pi^2 - 3645\sqrt{3}\alpha^2 C_A - 576\sqrt{3}\alpha^2 C_F\pi^2 \\
&\quad -1944\sqrt{3}\alpha^2 C_F - 720\sqrt{3}\alpha C_A\pi^2 + 5832\sqrt{3}\alpha C_A\zeta_3 \\
&\quad -19440\sqrt{3}\alpha C_A + 192\sqrt{3}\alpha C_F\pi^4 - 4608\sqrt{3}\alpha C_F\pi^2 \\
&\quad +2592\sqrt{3}\alpha C_F\zeta_3 + 7776\sqrt{3}\alpha C_F - 144\sqrt{3}C_A\pi^4 \\
&\quad -1888\sqrt{3}C_A\pi^2 - 1296\sqrt{3}C_A\zeta_3 + 18252\sqrt{3}C_A \\
&\quad -384\sqrt{3}C_F\pi^4 + 8784\sqrt{3}C_F\pi^2 - 18144\sqrt{3}C_F\zeta_3 \\
&\quad -5589\sqrt{3}C_F - 1216\sqrt{3}N_f\pi^2 T_F - 5724\sqrt{3}N_f T_F \\
&\quad -81\ln(3)^2\alpha C_A\pi + 216\ln(3)^2\alpha C_F\pi + 135\ln(3)^2 C_A\pi \\
&\quad +108\ln(3)^2 C_F\pi + 972\ln(3)\alpha C_A\pi - 2592\ln(3)\alpha C_F\pi \\
&\quad -1620\ln(3) C_A\pi - 1296\ln(3) C_F\pi + 87\alpha C_A\pi^3 \\
&\quad -232\alpha C_F\pi^3 - 145 C_A\pi^3 - 116 C_F\pi^3\Big]\frac{a^2}{1944\sqrt{3}} \\
&+ \mathcal{O}(a^3)
\end{aligned} \tag{7.5.35}$$

which exactly matches the SMOM result of [137, 139].

Of the six $\overline{\rm MS}$ amplitudes computed it was found that, when taking the limit $\omega = 1$, the following relations hold. These are

$$\Sigma^{\rm V}_{(2)}(p,q)\Big|_{\omega=1} \;=\; \Sigma^{\rm V}_{(5)}(p,q)\Big|_{\omega=1} \quad , \quad \Sigma^{\rm V}_{(3)}(p,q)\Big|_{\omega=1} \;=\; \Sigma^{\rm V}_{(4)}(p,q)\Big|_{\omega=1} \tag{7.5.36}$$

where the above relations are consistent with those of the quark-gluon vertex in Part 1 of this thesis and must be satisfied in the $\overline{\rm MS}$ scheme. These relations are symmetric under the interchange of p and q in the external legs, where this property emerges naturally and acts as a useful check on our calculation.

Since the vector current is a physical operator its renormalization is trivial in all schemes, this implies that its anomalous dimension is zero, i.e. $\gamma^{\nu}(a) = 0$. If the anomalous dimension of a physical operator vanishes in one scheme it vanishes in all other schemes. This is consistent with our result, where the vector current anomalous dimension is zero in [137].

This concludes our analysis of the vector operator, where we have produced results for a new configuration in the $\overline{\rm MS}$ scheme. It is not necessary to compute these results in any other scheme since at this moment in time the Landau gauge is preferred by lattice theorists over any other scheme, [135, 136].

7.6 Tensor operator

Next we record the results for the tensor operator $\bar{\psi}\sigma^{\mu\nu}\psi$. Using the $\overline{\rm MS}$ renormalization constants defined in chapter 3 we determine the operator renormalization constant. For the tensor operator this is found to be

$$Z^{T}_{\mathcal{O}}(a,\alpha)\Big|_{\overline{\rm MS}} \;=\; 1 \;+\; \mathcal{O}(a^3) \;. \tag{7.6.37}$$

With this, we construct the amplitudes for the $\overline{\rm MS}$ scheme for an IMOM configuration setup where the amplitudes are defined by

$$\Sigma^{T}_{(k)\,\sigma}(p,q) \;\Big|_{\omega} \;=\; \sum_{k=1}^{8} \mathcal{P}^{T}_{(k)\,\sigma}(p,q)\Sigma^{T}_{(k)\,\sigma}(p,q) \;. \tag{7.6.38}$$

We have computed all eight amplitudes but, similarly to the vector current, choose to display only one here. As with the vector operator we present the channel 1

amplitude in the $\overline{\rm MS}$ scheme. There is no need to compute the same set of results for the RI$'$ scheme since the $\overline{\rm MS}$ results are adequate. The channel 1 amplitude is given by

$$
\begin{aligned}
\Sigma^{\rm T}_{(1)}(p,q)\Big|_{\overline{\rm MS}} \;=\; & -1 + C_F \left[4\ln(\omega)\alpha\omega^2 - 8\ln(\omega)\alpha\omega - 4\ln(\omega)\omega^2 + 8\ln(\omega)\omega \right. \\
& -\Phi_1\left(\frac{1}{\omega},\frac{1}{\omega}\right)\alpha\omega^2 + 4\Phi_1\left(\frac{1}{\omega},\frac{1}{\omega}\right)\alpha\omega - 8\Phi_1\left(\frac{1}{\omega},\frac{1}{\omega}\right)\alpha \\
& +\Phi_1\left(\frac{1}{\omega},\frac{1}{\omega}\right)\omega^2 - 4\Phi_1\left(\frac{1}{\omega},\frac{1}{\omega}\right)\omega + 8\Phi_1\left(\frac{1}{\omega},\frac{1}{\omega}\right) \\
& \left. -4\alpha\omega^2 + 16\alpha\omega + 4\omega^2 - 16\omega \right] \frac{a}{2\omega(\omega-4)} \\
& + C_F \left[432\ln(\omega)^2\alpha C_F\omega^3 - 864\ln(\omega)^2\alpha C_F\omega^2 - 216\ln(\omega)^2 C_A\omega^3 \right. \\
& +432\ln(\omega)^2 C_F\omega^3 + 864\ln(\omega)^2 C_F\omega^2 \\
& -108\ln(\omega)\Phi_1\left(\frac{1}{\omega},\frac{1}{\omega}\right)\alpha C_F\omega^3 \\
& +432\ln(\omega)\Phi_1\left(\frac{1}{\omega},\frac{1}{\omega}\right)\alpha C_F\omega^2 \\
& -864\ln(\omega)\Phi_1\left(\frac{1}{\omega},\frac{1}{\omega}\right)\alpha C_F\omega \\
& +216\ln(\omega)\Phi_1\left(\frac{1}{\omega},\frac{1}{\omega}\right) C_A\omega^2 + 108\ln(\omega)\Phi_1\left(\frac{1}{\omega},\frac{1}{\omega}\right) C_F\omega^3 \\
& -1296\ln(\omega)\Phi_1\left(\frac{1}{\omega},\frac{1}{\omega}\right) C_F\omega^2 + 864\ln(\omega)\Phi_1\left(\frac{1}{\omega},\frac{1}{\omega}\right) C_F\omega \\
& +324\ln(\omega)\alpha^2 C_A\omega^3 - 648\ln(\omega)\alpha^2 C_A\omega^2 \\
& +432\ln(\omega)\alpha^2 C_F\omega^3 - 864\ln(\omega)\alpha^2 C_F\omega^2 \\
& +1512\ln(\omega)\alpha C_A\omega^3 - 3024\ln(\omega)\alpha C_A\omega^2 \\
& -1728\ln(\omega)\alpha C_F\omega^3 + 3456\ln(\omega)\alpha C_F\omega^2 - 2460\ln(\omega) C_A\omega^3 \\
& +4920\ln(\omega) C_A\omega^2 + 1296\ln(\omega) C_F\omega^3 - 2592\ln(\omega) C_F\omega^2 \\
& +960\ln(\omega) N_f\omega^3 T_F - 1920\ln(\omega) N_f\omega^2 T_F \\
& +108\Omega_2\left(\frac{1}{\omega},\frac{1}{\omega}\right)\alpha C_A\omega^3 - 216\Omega_2\left(\frac{1}{\omega},\frac{1}{\omega}\right)\alpha C_A\omega^2 \\
& -1008\Omega_2\left(\frac{1}{\omega},\frac{1}{\omega}\right) C_A\omega^3 + 3168\Omega_2\left(\frac{1}{\omega},\frac{1}{\omega}\right) C_A\omega^2 \\
& -2592\Omega_2\left(\frac{1}{\omega},\frac{1}{\omega}\right) C_A\omega + 936\Omega_2\left(\frac{1}{\omega},\frac{1}{\omega}\right) C_F\omega^3 \\
& -2880\Omega_2\left(\frac{1}{\omega},\frac{1}{\omega}\right) C_F\omega^2 + 1728\Omega_2\left(\frac{1}{\omega},\frac{1}{\omega}\right) C_F\omega \\
& +216\Omega_2(1,\omega)\,\alpha C_A\omega^3 - 432\Omega_2(1,\omega)\,\alpha C_A\omega^2
\end{aligned}
$$

$$
\begin{aligned}
&-864\Omega_2(1,\omega)\,\alpha C_F\omega^3 + 1728\Omega_2(1,\omega)\,\alpha C_F\omega^2 \\
&-1368\Omega_2(1,\omega)\,C_A\omega^3 + 2448\Omega_2(1,\omega)\,C_A\omega^2 \\
&+3600\Omega_2(1,\omega)\,C_F\omega^3 - 5760\Omega_2(1,\omega)\,C_F\omega^2 \\
&+108\Phi_1\left(\frac{1}{\omega},\frac{1}{\omega}\right)^2 C_A\omega^3 - 648\Phi_1\left(\frac{1}{\omega},\frac{1}{\omega}\right)^2 C_A\omega^2 \\
&+864\Phi_1\left(\frac{1}{\omega},\frac{1}{\omega}\right)^2 C_A\omega - 216\Phi_1\left(\frac{1}{\omega},\frac{1}{\omega}\right)^2 C_F\omega^3 \\
&+1296\Phi_1\left(\frac{1}{\omega},\frac{1}{\omega}\right)^2 C_F\omega^2 - 1728\Phi_1\left(\frac{1}{\omega},\frac{1}{\omega}\right)^2 C_F\omega \\
&-81\Phi_1\left(\frac{1}{\omega},\frac{1}{\omega}\right)\alpha^2 C_A\omega^3 + 324\Phi_1\left(\frac{1}{\omega},\frac{1}{\omega}\right)\alpha^2 C_A\omega^2 \\
&-648\Phi_1\left(\frac{1}{\omega},\frac{1}{\omega}\right)\alpha^2 C_A\omega - 108\Phi_1\left(\frac{1}{\omega},\frac{1}{\omega}\right)\alpha^2 C_F\omega^3 \\
&+432\Phi_1\left(\frac{1}{\omega},\frac{1}{\omega}\right)\alpha^2 C_F\omega^2 - 864\Phi_1\left(\frac{1}{\omega},\frac{1}{\omega}\right)\alpha^2 C_F\omega \\
&-378\Phi_1\left(\frac{1}{\omega},\frac{1}{\omega}\right)\alpha C_A\omega^3 + 1512\Phi_1\left(\frac{1}{\omega},\frac{1}{\omega}\right)\alpha C_A\omega^2 \\
&-3024\Phi_1\left(\frac{1}{\omega},\frac{1}{\omega}\right)\alpha C_A\omega + 972\Phi_1\left(\frac{1}{\omega},\frac{1}{\omega}\right)\alpha C_F\omega^3 \\
&-3456\Phi_1\left(\frac{1}{\omega},\frac{1}{\omega}\right)\alpha C_F\omega^2 + 1728\Phi_1\left(\frac{1}{\omega},\frac{1}{\omega}\right)\alpha C_F\omega \\
&-33\Phi_1\left(\frac{1}{\omega},\frac{1}{\omega}\right) C_A\omega^3 + 1428\Phi_1\left(\frac{1}{\omega},\frac{1}{\omega}\right) C_A\omega^2 \\
&-264\Phi_1\left(\frac{1}{\omega},\frac{1}{\omega}\right) C_A\omega - 1728\Phi_1\left(\frac{1}{\omega},\frac{1}{\omega}\right) C_F\omega^3 \\
&+5616\Phi_1\left(\frac{1}{\omega},\frac{1}{\omega}\right) C_F\omega^2 + 2592\Phi_1\left(\frac{1}{\omega},\frac{1}{\omega}\right) C_F\omega \\
&-240\Phi_1\left(\frac{1}{\omega},\frac{1}{\omega}\right) N_f\omega^3 T_F + 960\Phi_1\left(\frac{1}{\omega},\frac{1}{\omega}\right) N_f\omega^2 T_F \\
&-1920\Phi_1\left(\frac{1}{\omega},\frac{1}{\omega}\right) N_f\omega T_F + 216\Phi_2\left(\frac{1}{\omega},\frac{1}{\omega}\right)\alpha C_F\omega^3 \\
&-864\Phi_2\left(\frac{1}{\omega},\frac{1}{\omega}\right)\alpha C_F\omega^2 + 1728\Phi_2\left(\frac{1}{\omega},\frac{1}{\omega}\right)\alpha C_F\omega \\
&-648\Phi_2\left(\frac{1}{\omega},\frac{1}{\omega}\right) C_A\omega^3 + 3024\Phi_2\left(\frac{1}{\omega},\frac{1}{\omega}\right) C_A\omega^2 \\
&-6480\Phi_2\left(\frac{1}{\omega},\frac{1}{\omega}\right) C_A\omega + 5184\Phi_2\left(\frac{1}{\omega},\frac{1}{\omega}\right) C_A \\
&+216\Phi_2\left(\frac{1}{\omega},\frac{1}{\omega}\right) C_F\omega^3 - 864\Phi_2\left(\frac{1}{\omega},\frac{1}{\omega}\right) C_F\omega^2
\end{aligned}
$$

$$
\begin{aligned}
&+1728\Phi_2\left(\frac{1}{\omega},\frac{1}{\omega}\right)C_F\omega - 3456\Phi_2\left(\frac{1}{\omega},\frac{1}{\omega}\right)C_F \\
&+1080\Phi_2(1,\omega)\,C_A\omega^4 - 864\Phi_2(1,\omega)\,C_A\omega^3 \\
&-1728\Phi_2(1,\omega)\,C_F\omega^4 - 405\alpha^2C_A\omega^3 + 1620\alpha^2C_A\omega^2 \\
&-216\alpha^2C_F\omega^3 + 864\alpha^2C_F\omega^2 - 648\alpha C_A\omega^3\zeta_3 - 2160\alpha C_A\omega^3 \\
&+8640\alpha C_A\omega^2 + 5184\alpha C_F\omega^3\zeta_3 + 864\alpha C_F\omega^3 \\
&-10368\alpha C_F\omega^2\zeta_3 - 3456\alpha C_F\omega^2 - 1944C_A\omega^3\zeta_3 \\
&+7097C_A\omega^3 + 5184C_A\omega^2\zeta_3 - 28388C_A\omega^2 \\
&-5184C_F\omega^3\zeta_3 - 5688C_F\omega^3 + 10368C_F\omega^2\zeta_3 \\
&+22752C_F\omega^2 - 1456N_f\omega^3T_F \\
&+5824N_f\omega^2T_F\big]\,\frac{a^2}{216\omega^2(\omega-4)} \;+\; \mathcal{O}(a^3)
\end{aligned}
\tag{7.6.39}
$$

for the asymmetric configuration, where ω is the interpolating parameter. Taking the SMOM limit and applying the identities (7.4.21) we see that the same result at the symmetric point is

$$
\begin{aligned}
\Sigma^{\mathrm{T}}_{(1)}(p,q)\Big|_{\omega=1} \;=\; & -1 + C_F\big[15\psi'\left(\tfrac{1}{3}\right)\alpha - 15\psi'\left(\tfrac{1}{3}\right) - 10\alpha\pi^2 - 54\alpha + 10\pi^2 + 54\big]\,\frac{a}{27} \\
& + C_F\Big[-432\sqrt{3}\psi'\left(\tfrac{1}{3}\right)^2 C_A + 864\sqrt{3}\psi'\left(\tfrac{1}{3}\right)^2 C_F \\
& +810\sqrt{3}\psi'\left(\tfrac{1}{3}\right)\alpha^2C_A + 1080\sqrt{3}\psi'\left(\tfrac{1}{3}\right)\alpha^2C_F \\
& -108\sqrt{3}\psi'\left(\tfrac{1}{3}\right)\alpha C_A + 11880\sqrt{3}\psi'\left(\tfrac{1}{3}\right)\alpha C_F \\
& +576\sqrt{3}\psi'\left(\tfrac{1}{3}\right)C_A\pi^2 + 5514\sqrt{3}\psi'\left(\tfrac{1}{3}\right)C_A \\
& -1152\sqrt{3}\psi'\left(\tfrac{1}{3}\right)C_F\pi^2 - 41472\sqrt{3}\psi'\left(\tfrac{1}{3}\right)C_F \\
& +2400\sqrt{3}\psi'\left(\tfrac{1}{3}\right)N_fT_F - 90\sqrt{3}\psi'''\left(\tfrac{1}{3}\right)\alpha C_F \\
& -108\sqrt{3}\psi'''\left(\tfrac{1}{3}\right)C_A + 342\sqrt{3}\psi'''\left(\tfrac{1}{3}\right)C_F \\
& -23328\sqrt{3}s_2\left(\tfrac{\pi}{6}\right)\alpha C_A + 62208\sqrt{3}s_2\left(\tfrac{\pi}{6}\right)\alpha C_F \\
& +46656\sqrt{3}s_2\left(\tfrac{\pi}{6}\right)C_A - 171072\sqrt{3}s_2\left(\tfrac{\pi}{6}\right)C_F \\
& +46656\sqrt{3}s_2\left(\tfrac{\pi}{2}\right)\alpha C_A - 124416\sqrt{3}s_2\left(\tfrac{\pi}{2}\right)\alpha C_F \\
& -93312\sqrt{3}s_2\left(\tfrac{\pi}{2}\right)C_A + 342144\sqrt{3}s_2\left(\tfrac{\pi}{2}\right)C_F \\
& +38880\sqrt{3}s_3\left(\tfrac{\pi}{6}\right)\alpha C_A - 103680\sqrt{3}s_3\left(\tfrac{\pi}{6}\right)\alpha C_F \\
& -77760\sqrt{3}s_3\left(\tfrac{\pi}{6}\right)C_A + 285120\sqrt{3}s_3\left(\tfrac{\pi}{6}\right)C_F \\
& -31104\sqrt{3}s_3\left(\tfrac{\pi}{2}\right)\alpha C_A + 82944\sqrt{3}s_3\left(\tfrac{\pi}{2}\right)\alpha C_F \\
& +62208\sqrt{3}s_3\left(\tfrac{\pi}{2}\right)C_A - 228096\sqrt{3}s_3\left(\tfrac{\pi}{2}\right)C_F \\
& -540\sqrt{3}\alpha^2C_A\pi^2 - 3645\sqrt{3}\alpha^2C_A - 720\sqrt{3}\alpha^2C_F\pi^2
\end{aligned}
$$

$$
\begin{aligned}
&-1944\sqrt{3}\alpha^2 C_F + 72\sqrt{3}\alpha C_A\pi^2 + 5832\sqrt{3}\alpha C_A\zeta_3 \\
&-19440\sqrt{3}\alpha C_A + 240\sqrt{3}\alpha C_F\pi^4 - 7920\sqrt{3}\alpha C_F\pi^2 \\
&+5184\sqrt{3}\alpha C_F\zeta_3 + 7776\sqrt{3}\alpha C_F + 96\sqrt{3}C_A\pi^4 \\
&-3676\sqrt{3}C_A\pi^2 - 17496\sqrt{3}C_A\zeta_3 + 63873\sqrt{3}C_A \\
&-528\sqrt{3}C_F\pi^4 + 27648\sqrt{3}C_F\pi^2 + 12960\sqrt{3}C_F\zeta_3 \\
&-51192\sqrt{3}C_F - 1600\sqrt{3}N_f\pi^2 T_F - 13104\sqrt{3}N_f T_F \\
&-162\ln(3)^2\alpha C_A\pi + 432\ln(3)^2\alpha C_F\pi + 324\ln(3)^2 C_A\pi \\
&-1188\ln(3)^2 C_F\pi + 1944\ln(3)\alpha C_A\pi - 5184\ln(3)\alpha C_F\pi \\
&-3888\ln(3)C_A\pi + 14256\ln(3)C_F\pi + 174\alpha C_A\pi^3 \\
&-464\alpha C_F\pi^3 - 348 C_A\pi^3 + 1276 C_F\pi^3\big]\,\frac{a^2}{1944\sqrt{3}} \\
&+ \mathcal{O}(a^3)\;. \qquad (7.6.40)
\end{aligned}
$$

On inspection it was found that the following relationships must be satisfied between the amplitudes at two loops

$$
\Sigma^{\rm T}_{(3)}(p,q)\Big|_{\omega=1} \;=\; \Sigma^{\rm T}_{(6)}(p,q)\Big|_{\omega=1} \quad,\quad \Sigma^{\rm T}_{(4)}(p,q)\Big|_{\omega=1} \;=\; \Sigma^{\rm T}_{(5)}(p,q)\Big|_{\omega=1} \qquad (7.6.41)
$$

when $\omega = 1$. We have checked that these amplitudes satisfy the relationships at two loops in the $\overline{\rm MS}$ scheme, [141].

7.7 W_2 and ∂W_2 operators

Finally we record our results for the DIS operators (or Wilson operators) $\mathcal{S}\bar{\psi}\gamma^\mu {\rm D}^\nu\psi$ and $\mathcal{S}\partial^\mu(\bar{\psi}\gamma^\nu\psi)$. Due to the way in which the tensor basis has been defined we note that the channel 2 amplitude for the DIS operator W_2 is the channel corresponding to the Feynman rule, i.e. the tree level vertex. Therefore we present the channel 2 amplitude as

$$
\begin{aligned}
\Sigma^{W_2}_{(2)}(p,q)\Big|_{\overline{\rm MS}} \;=\;& -1 + C_F\left[18\ln(\omega)\alpha\omega^3 - 90\ln(\omega)\alpha\omega^2 + 180\ln(\omega)\alpha\omega\right. \\
&-51\ln(\omega)\omega^3 + 240\ln(\omega)\omega^2 - 324\ln(\omega)\omega - 72\Phi_1\left(\frac{1}{\omega},\frac{1}{\omega}\right)\alpha\omega \\
&+180\Phi_1\left(\frac{1}{\omega},\frac{1}{\omega}\right)\alpha + 18\Phi_1\left(\frac{1}{\omega},\frac{1}{\omega}\right)\omega^3 - 126\Phi_1\left(\frac{1}{\omega},\frac{1}{\omega}\right)\omega^2 \\
&\left.+342\Phi_1\left(\frac{1}{\omega},\frac{1}{\omega}\right)\omega - 324\Phi_1\left(\frac{1}{\omega},\frac{1}{\omega}\right) - 36\alpha\omega^3 + 270\alpha\omega^2\right.
\end{aligned}
$$

$$
\begin{aligned}
&-504\alpha\omega + 79\omega^3 - 602\omega^2 + 1144\omega\big]\,\frac{a}{18\omega(\omega-4)^2}\\
&+C_F\,\big[81\ln(\omega)^2\alpha C_A\omega^4 - 324\ln(\omega)^2\alpha C_A\omega^3 + 972\ln(\omega)^2\alpha C_A\omega^2\\
&+540\ln(\omega)^2\alpha C_F\omega^4 - 2160\ln(\omega)^2\alpha C_F\omega^3 + 6480\ln(\omega)^2\alpha C_F\omega^2\\
&-2349\ln(\omega)^2 C_A\omega^4 - 972\ln(\omega)^2 C_A\omega^3 - 4860\ln(\omega)^2 C_A\omega^2\\
&+2340\ln(\omega)^2 C_F\omega^4 + 16560\ln(\omega)^2 C_F\omega^3 - 5616\ln(\omega)^2 C_F\omega^2\\
&-486\ln(\omega)\Phi_1\left(\frac{1}{\omega},\frac{1}{\omega}\right)\alpha C_A\omega^2 + 972\ln(\omega)\Phi_1\left(\frac{1}{\omega},\frac{1}{\omega}\right)\alpha C_A\omega\\
&-3240\ln(\omega)\Phi_1\left(\frac{1}{\omega},\frac{1}{\omega}\right)\alpha C_F\omega^2 + 6480\ln(\omega)\Phi_1\left(\frac{1}{\omega},\frac{1}{\omega}\right)\alpha C_F\omega\\
&+162\ln(\omega)\Phi_1\left(\frac{1}{\omega},\frac{1}{\omega}\right) C_A\omega^4 + 3888\ln(\omega)\Phi_1\left(\frac{1}{\omega},\frac{1}{\omega}\right) C_A\omega^3\\
&-5346\ln(\omega)\Phi_1\left(\frac{1}{\omega},\frac{1}{\omega}\right) C_A\omega^2 - 4860\ln(\omega)\Phi_1\left(\frac{1}{\omega},\frac{1}{\omega}\right) C_A\omega\\
&+864\ln(\omega)\Phi_1\left(\frac{1}{\omega},\frac{1}{\omega}\right) C_F\omega^4 - 17496\ln(\omega)\Phi_1\left(\frac{1}{\omega},\frac{1}{\omega}\right) C_F\omega^3\\
&+33048\ln(\omega)\Phi_1\left(\frac{1}{\omega},\frac{1}{\omega}\right) C_F\omega^2 - 5616\ln(\omega)\Phi_1\left(\frac{1}{\omega},\frac{1}{\omega}\right) C_F\omega\\
&+567\ln(\omega)\alpha^2 C_A\omega^4 - 2754\ln(\omega)\alpha^2 C_A\omega^3 + 5832\ln(\omega)\alpha^2 C_A\omega^2\\
&+486\ln(\omega)\alpha^2 C_F\omega^4 - 2592\ln(\omega)\alpha^2 C_F\omega^3 + 4536\ln(\omega)\alpha^2 C_F\omega^2\\
&+2430\ln(\omega)\alpha C_A\omega^4 - 12312\ln(\omega)\alpha C_A\omega^3 + 25920\ln(\omega)\alpha C_A\omega^2\\
&-6030\ln(\omega)\alpha C_F\omega^4 + 25632\ln(\omega)\alpha C_F\omega^3 - 47304\ln(\omega)\alpha C_F\omega^2\\
&-19881\ln(\omega) C_A\omega^4 + 97434\ln(\omega) C_A\omega^3 - 123696\ln(\omega) C_A\omega^2\\
&+11934\ln(\omega) C_F\omega^4 - 59436\ln(\omega) C_F\omega^3 + 65808\ln(\omega) C_F\omega^2\\
&+6624\ln(\omega) N_f\omega^4 T_F - 30672\ln(\omega) N_f\omega^3 T_F\\
&+40032\ln(\omega) N_f\omega^2 T_F + 162\Omega_2\left(\frac{1}{\omega},\frac{1}{\omega}\right)\alpha C_A\omega^4\\
&-729\Omega_2\left(\frac{1}{\omega},\frac{1}{\omega}\right)\alpha C_A\omega^3 + 648\Omega_2\left(\frac{1}{\omega},\frac{1}{\omega}\right)\alpha C_A\omega^2\\
&+1620\Omega_2\left(\frac{1}{\omega},\frac{1}{\omega}\right)\alpha C_A\omega - 1674\Omega_2\left(\frac{1}{\omega},\frac{1}{\omega}\right) C_A\omega^4\\
&+7911\Omega_2\left(\frac{1}{\omega},\frac{1}{\omega}\right) C_A\omega^3 - 6156\Omega_2\left(\frac{1}{\omega},\frac{1}{\omega}\right) C_A\omega^2\\
&-8100\Omega_2\left(\frac{1}{\omega},\frac{1}{\omega}\right) C_A\omega + 1728\Omega_2\left(\frac{1}{\omega},\frac{1}{\omega}\right) C_F\omega^4\\
&-9072\Omega_2\left(\frac{1}{\omega},\frac{1}{\omega}\right) C_F\omega^3 + 7344\Omega_2\left(\frac{1}{\omega},\frac{1}{\omega}\right) C_F\omega^2\\
&+7776\Omega_2\left(\frac{1}{\omega},\frac{1}{\omega}\right) C_F\omega + 324\Omega_2(1,\omega)\,\alpha C_A\omega^4
\end{aligned}
$$

$$
\begin{aligned}
&-1620\Omega_2(1,\omega)\,\alpha C_A\omega^3 + 3240\Omega_2(1,\omega)\,\alpha C_A\omega^2 \\
&-1296\Omega_2(1,\omega)\,\alpha C_F\omega^4 + 6480\Omega_2(1,\omega)\,\alpha C_F\omega^3 \\
&-12960\Omega_2(1,\omega)\,\alpha C_F\omega^2 - 3672\Omega_2(1,\omega)\,C_A\omega^4 \\
&+7236\Omega_2(1,\omega)\,C_A\omega^3 - 8424\Omega_2(1,\omega)\,C_A\omega^2 \\
&+8640\Omega_2(1,\omega)\,C_F\omega^4 - 16416\Omega_2(1,\omega)\,C_F\omega^3 \\
&+23328\Omega_2(1,\omega)\,C_F\omega^2 + 324\Phi_1\left(\frac{1}{\omega},\frac{1}{\omega}\right)^2 C_A\omega^4 \\
&-2916\Phi_1\left(\frac{1}{\omega},\frac{1}{\omega}\right)^2 C_A\omega^3 + 7776\Phi_1\left(\frac{1}{\omega},\frac{1}{\omega}\right)^2 C_A\omega^2 \\
&-5184\Phi_1\left(\frac{1}{\omega},\frac{1}{\omega}\right)^2 C_A\omega - 648\Phi_1\left(\frac{1}{\omega},\frac{1}{\omega}\right)^2 C_F\omega^4 \\
&+5832\Phi_1\left(\frac{1}{\omega},\frac{1}{\omega}\right)^2 C_F\omega^3 - 15552\Phi_1\left(\frac{1}{\omega},\frac{1}{\omega}\right)^2 C_F\omega^2 \\
&+10368\Phi_1\left(\frac{1}{\omega},\frac{1}{\omega}\right)^2 C_F\omega - 2430\Phi_1\left(\frac{1}{\omega},\frac{1}{\omega}\right)\alpha^2 C_A\omega^2 \\
&+5832\Phi_1\left(\frac{1}{\omega},\frac{1}{\omega}\right)\alpha^2 C_A\omega - 1620\Phi_1\left(\frac{1}{\omega},\frac{1}{\omega}\right)\alpha^2 C_F\omega^2 \\
&+4536\Phi_1\left(\frac{1}{\omega},\frac{1}{\omega}\right)\alpha^2 C_F\omega - 81\Phi_1\left(\frac{1}{\omega},\frac{1}{\omega}\right)\alpha C_A\omega^4 \\
&+972\Phi_1\left(\frac{1}{\omega},\frac{1}{\omega}\right)\alpha C_A\omega^3 - 14256\Phi_1\left(\frac{1}{\omega},\frac{1}{\omega}\right)\alpha C_A\omega^2 \\
&+31104\Phi_1\left(\frac{1}{\omega},\frac{1}{\omega}\right)\alpha C_A\omega + 2916\Phi_1\left(\frac{1}{\omega},\frac{1}{\omega}\right)\alpha C_F\omega^4 \\
&-19008\Phi_1\left(\frac{1}{\omega},\frac{1}{\omega}\right)\alpha C_F\omega^3 + 48276\Phi_1\left(\frac{1}{\omega},\frac{1}{\omega}\right)\alpha C_F\omega^2 \\
&-34344\Phi_1\left(\frac{1}{\omega},\frac{1}{\omega}\right)\alpha C_F\omega + 9918\Phi_1\left(\frac{1}{\omega},\frac{1}{\omega}\right) C_A\omega^4 \\
&-64548\Phi_1\left(\frac{1}{\omega},\frac{1}{\omega}\right) C_A\omega^3 + 149922\Phi_1\left(\frac{1}{\omega},\frac{1}{\omega}\right) C_A\omega^2 \\
&-149616\Phi_1\left(\frac{1}{\omega},\frac{1}{\omega}\right) C_A\omega - 12222\Phi_1\left(\frac{1}{\omega},\frac{1}{\omega}\right) C_F\omega^4 \\
&+65808\Phi_1\left(\frac{1}{\omega},\frac{1}{\omega}\right) C_F\omega^3 - 89964\Phi_1\left(\frac{1}{\omega},\frac{1}{\omega}\right) C_F\omega^2 \\
&+70128\Phi_1\left(\frac{1}{\omega},\frac{1}{\omega}\right) C_F\omega - 2232\Phi_1\left(\frac{1}{\omega},\frac{1}{\omega}\right) N_f\omega^4 T_F \\
&+15264\Phi_1\left(\frac{1}{\omega},\frac{1}{\omega}\right) N_f\omega^3 T_F - 41184\Phi_1\left(\frac{1}{\omega},\frac{1}{\omega}\right) N_f\omega^2 T_F \\
&+40032\Phi_1\left(\frac{1}{\omega},\frac{1}{\omega}\right) N_f\omega T_F - 324\Phi_2\left(\frac{1}{\omega},\frac{1}{\omega}\right)\alpha C_A\omega^2
\end{aligned}
$$

$$
\begin{aligned}
&+1620\Phi_2\left(\frac{1}{\omega},\frac{1}{\omega}\right)\alpha C_A\omega - 3240\Phi_2\left(\frac{1}{\omega},\frac{1}{\omega}\right)\alpha C_A \\
&+5184\Phi_2\left(\frac{1}{\omega},\frac{1}{\omega}\right)\alpha C_F\omega^2 - 12960\Phi_2\left(\frac{1}{\omega},\frac{1}{\omega}\right)\alpha C_F\omega \\
&-1296\Phi_2\left(\frac{1}{\omega},\frac{1}{\omega}\right)C_A\omega^4 + 9720\Phi_2\left(\frac{1}{\omega},\frac{1}{\omega}\right)C_A\omega^3 \\
&-23004\Phi_2\left(\frac{1}{\omega},\frac{1}{\omega}\right)C_A\omega^2 + 10692\Phi_2\left(\frac{1}{\omega},\frac{1}{\omega}\right)C_A\omega \\
&+16200\Phi_2\left(\frac{1}{\omega},\frac{1}{\omega}\right)C_A - 6480\Phi_2\left(\frac{1}{\omega},\frac{1}{\omega}\right)C_F\omega^2 \\
&+18144\Phi_2\left(\frac{1}{\omega},\frac{1}{\omega}\right)C_F\omega - 15552\Phi_2\left(\frac{1}{\omega},\frac{1}{\omega}\right)C_F \\
&+1944\Phi_2(1,\omega)\,C_A\omega^5 + 1296\Phi_2(1,\omega)\,C_A\omega^4 \\
&-2592\Phi_2(1,\omega)\,C_F\omega^5 - 12960\Phi_2(1,\omega)\,C_F\omega^4 \\
&+10368\Phi_2(1,\omega)\,C_F\omega^3 - 1296\alpha^2C_A\omega^4 + 9720\alpha^2C_A\omega^3 \\
&-18144\alpha^2C_A\omega^2 - 486\alpha^2C_F\omega^4 + 3564\alpha^2C_F\omega^3 - 6480\alpha^2C_F\omega^2 \\
&-6642\alpha C_A\omega^4 - 5832\alpha C_A\omega^3\zeta_3 + 50544\alpha C_A\omega^3 \\
&+11664\alpha C_A\omega^2\zeta_3 - 95904\alpha C_A\omega^2 + 7776\alpha C_F\omega^4\zeta_3 \\
&+5526\alpha C_F\omega^4 - 38880\alpha C_F\omega^3\zeta_3 - 37332\alpha C_F\omega^3 \\
&+77760\alpha C_F\omega^2\zeta_3 + 60912\alpha C_F\omega^2 + 648C_A\omega^4\zeta_3 + 24337C_A\omega^4 \\
&+8424C_A\omega^3\zeta_3 - 186020C_A\omega^3 - 32400C_A\omega^2\zeta_3 + 354688C_A\omega^2 \\
&-22032C_F\omega^4\zeta_3 - 10861C_F\omega^4 + 103680C_F\omega^3\zeta_3 + 83720C_F\omega^3 \\
&-139968C_F\omega^2\zeta_3 - 161104C_F\omega^2 - 9044N_f\omega^4T_F \\
&+68464N_f\omega^3T_F - 129152N_f\omega^2T_F\big]\,\frac{a^2}{648\omega^2(\omega-4)^2} \\
&+\mathcal{O}(a^3)
\end{aligned}
\tag{7.7.42}
$$

in the $\overline{\rm MS}$ scheme evaluated at the IMOM configuration. For the DIS operators the amplitudes are the only results we provide, which are sufficient for lattice manipulations.

For the operator ∂W_2 the channel 1 and 2 amplitudes are related such that

$$
\begin{aligned}
\Sigma^{\partial W_2}_{(1)}(p,q)\Big|_{\overline{\rm MS}} &= \Sigma^{\partial W_2}_{(2)}(p,q)\Big|_{\overline{\rm MS}} \\
&= -1 + C_F\left[\ln(\omega)\alpha\omega^2 - 2\ln(\omega)\alpha\omega - 2\ln(\omega)\omega^2 + 4\ln(\omega)\omega\right. \\
&\quad \left. -2\Phi_1\left(\frac{1}{\omega},\frac{1}{\omega}\right)\alpha + \Phi_1\left(\frac{1}{\omega},\frac{1}{\omega}\right)\omega^2 - 4\Phi_1\left(\frac{1}{\omega},\frac{1}{\omega}\right)\omega\right.
\end{aligned}
$$

$$
\begin{aligned}
&+4\Phi_1\left(\frac{1}{\omega},\frac{1}{\omega}\right)-2\alpha\omega^2+8\alpha\omega+2\omega^2-8\omega\Big]\frac{a}{\omega(\omega-4)}\\
&+C_F\left[-180\ln(\omega)^2C_A\omega^2+432\ln(\omega)^2C_F\omega^2\right.\\
&+18\ln(\omega)\Phi_1\left(\frac{1}{\omega},\frac{1}{\omega}\right)C_A\omega^2+108\ln(\omega)\Phi_1\left(\frac{1}{\omega},\frac{1}{\omega}\right)C_A\omega\\
&-432\ln(\omega)\Phi_1\left(\frac{1}{\omega},\frac{1}{\omega}\right)C_F\omega+54\ln(\omega)\alpha^2C_A\omega^2\\
&-108\ln(\omega)\alpha^2C_A\omega+72\ln(\omega)\alpha^2C_F\omega^2-144\ln(\omega)\alpha^2C_F\omega\\
&+252\ln(\omega)\alpha C_A\omega^2-504\ln(\omega)\alpha C_A\omega-288\ln(\omega)\alpha C_F\omega^2\\
&+576\ln(\omega)\alpha C_F\omega-1414\ln(\omega)C_A\omega^2+2828\ln(\omega)C_A\omega\\
&+252\ln(\omega)C_F\omega^2-504\ln(\omega)C_F\omega+464\ln(\omega)N_f\omega^2T_F\\
&-928\ln(\omega)N_f\omega T_F+18\Omega_2\left(\frac{1}{\omega},\frac{1}{\omega}\right)\alpha C_A\omega^2\\
&-36\Omega_2\left(\frac{1}{\omega},\frac{1}{\omega}\right)\alpha C_A\omega-126\Omega_2\left(\frac{1}{\omega},\frac{1}{\omega}\right)C_A\omega^2\\
&+288\Omega_2\left(\frac{1}{\omega},\frac{1}{\omega}\right)C_A\omega+72\Omega_2\left(\frac{1}{\omega},\frac{1}{\omega}\right)C_F\omega^2\\
&-144\Omega_2\left(\frac{1}{\omega},\frac{1}{\omega}\right)C_F\omega+36\Omega_2(1,\omega)\,\alpha C_A\omega^2\\
&-72\Omega_2(1,\omega)\,\alpha C_A\omega-144\Omega_2(1,\omega)\,\alpha C_F\omega^2\\
&+288\Omega_2(1,\omega)\,\alpha C_F\omega-288\Omega_2(1,\omega)\,C_A\omega^2\\
&+216\Omega_2(1,\omega)\,C_A\omega+720\Omega_2(1,\omega)\,C_F\omega^2-576\Omega_2(1,\omega)\,C_F\omega\\
&+36\Phi_1\left(\frac{1}{\omega},\frac{1}{\omega}\right)^2C_A\omega^2-216\Phi_1\left(\frac{1}{\omega},\frac{1}{\omega}\right)^2C_A\omega\\
&+288\Phi_1\left(\frac{1}{\omega},\frac{1}{\omega}\right)^2C_A-72\Phi_1\left(\frac{1}{\omega},\frac{1}{\omega}\right)^2C_F\omega^2\\
&+432\Phi_1\left(\frac{1}{\omega},\frac{1}{\omega}\right)^2C_F\omega-576\Phi_1\left(\frac{1}{\omega},\frac{1}{\omega}\right)^2C_F\\
&-108\Phi_1\left(\frac{1}{\omega},\frac{1}{\omega}\right)\alpha^2C_A-144\Phi_1\left(\frac{1}{\omega},\frac{1}{\omega}\right)\alpha^2C_F\\
&-504\Phi_1\left(\frac{1}{\omega},\frac{1}{\omega}\right)\alpha C_A+288\Phi_1\left(\frac{1}{\omega},\frac{1}{\omega}\right)\alpha C_F\omega^2\\
&-1152\Phi_1\left(\frac{1}{\omega},\frac{1}{\omega}\right)\alpha C_F\omega+576\Phi_1\left(\frac{1}{\omega},\frac{1}{\omega}\right)\alpha C_F\\
&+920\Phi_1\left(\frac{1}{\omega},\frac{1}{\omega}\right)C_A\omega^2-3680\Phi_1\left(\frac{1}{\omega},\frac{1}{\omega}\right)C_A\omega\\
&+2828\Phi_1\left(\frac{1}{\omega},\frac{1}{\omega}\right)C_A-1044\Phi_1\left(\frac{1}{\omega},\frac{1}{\omega}\right)C_F\omega^2
\end{aligned}
$$

$$
\begin{aligned}
&+4176\Phi_1\left(\frac{1}{\omega},\frac{1}{\omega}\right) C_F\omega - 504\Phi_1\left(\frac{1}{\omega},\frac{1}{\omega}\right) C_F \\
&-208\Phi_1\left(\frac{1}{\omega},\frac{1}{\omega}\right) N_f\omega^2 T_F + 832\Phi_1\left(\frac{1}{\omega},\frac{1}{\omega}\right) N_f\omega T_F \\
&-928\Phi_1\left(\frac{1}{\omega},\frac{1}{\omega}\right) N_f T_F + 288\Phi_2\left(\frac{1}{\omega},\frac{1}{\omega}\right) \alpha C_F \\
&-144\Phi_2\left(\frac{1}{\omega},\frac{1}{\omega}\right) C_A\omega^2 + 648\Phi_2\left(\frac{1}{\omega},\frac{1}{\omega}\right) C_A\omega \\
&-648\Phi_2\left(\frac{1}{\omega},\frac{1}{\omega}\right) C_A - 288\Phi_2\left(\frac{1}{\omega},\frac{1}{\omega}\right) C_F \\
&+216\Phi_2(1,\omega)\, C_A\omega^3 - 288\Phi_2(1,\omega)\, C_F\omega^3 - 576\Phi_2(1,\omega)\, C_F\omega^2 \\
&-135\alpha^2 C_A\omega^2 + 540\alpha^2 C_A\omega - 72\alpha^2 C_F\omega^2 + 288\alpha^2 C_F\omega \\
&-720\alpha C_A\omega^2 - 432\alpha C_A\omega\zeta_3 + 2880\alpha C_A\omega + 864\alpha C_F\omega^2\zeta_3 \\
&+288\alpha C_F\omega^2 - 1728\alpha C_F\omega\zeta_3 - 1152\alpha C_F\omega + 216 C_A\omega^2\zeta_3 \\
&+676 C_A\omega^2 - 432 C_A\omega\zeta_3 - 2704 C_A\omega - 1728 C_F\omega^2\zeta_3 \\
&-207 C_F\omega^2 + 3456 C_F\omega\zeta_3 + 828 C_F\omega - 212 N_f\omega^2 T_F \\
&+848 N_f\omega T_F]\, \frac{a^2}{72\omega(\omega-4)} \;+\; \mathcal{O}(a^3) \;. \qquad (7.7.43)
\end{aligned}
$$

Other relations between the amplitudes were found as

$$
\begin{aligned}
\Sigma^{\partial W_2}_{(3)}(p,q)\Big|_{\omega=1} &= \Sigma^{\partial W_2}_{(8)}(p,q)\Big|_{\omega=1} \quad , \quad \Sigma^{\partial W_2}_{(4)}(p,q)\Big|_{\omega=1} = \Sigma^{\partial W_2}_{(7)}(p,q)\Big|_{\omega=1} \\
\Sigma^{\partial W_2}_{(5)}(p,q)\Big|_{\omega=1} &= \Sigma^{\partial W_2}_{(6)}(p,q)\Big|_{\omega=1} \quad , \quad \Sigma^{\partial W_2}_{(9)}(p,q)\Big|_{\omega=1} = \Sigma^{\partial W_2}_{(10)}(p,q)\Big|_{\omega=1}
\end{aligned} \qquad (7.7.44)
$$

This completes our analysis of the operator insertion in to a quark 2-point function at the asymmetric point.

7.8 Discussion

We have evaluated the flavour non-singlet Green's function $\langle\psi(p)\mathcal{O}^u_{\mu_1\ldots\mu_{n_u}}(-p-q)\bar{\psi}(q)\rangle$ in the chiral limit, [59]. Developing the work of [137] we have considered, in addition to the scalar, vector and tensor operators, the twist-2 Wilson operators W_2 and ∂W_2. By reproducing the results of [133] for the mass conversion function and verifying this result in the Landau gauge we have been able to check that our programming works before building up to more complicated operators, such as the DIS operators. In this chapter we do not concern ourselves with the

analysis of schemes for the operators, where we only considered the RI′ scheme in order to compare with [133]. This is completely separate to Part 1 of this thesis where scheme analysis was our main focus.

On confirming our result for the mass conversion function, where we note that this was only verified in the Landau gauge since our convention for the definition of α differs to that of [133], we then returned to the $\overline{\text{MS}}$ scheme where all further operator analysis was carried out. For the vector, tensor and DIS operators we are only interested in the amplitudes, where the conversion functions and RG functions are not necessary. We define the amplitudes in the $\overline{\text{MS}}$ scheme since there is no flexibility in how one defines this scheme. We discussed at the start of the chapter that there are several ways to define a regularization invariant renormalization scheme. By sticking with $\overline{\text{MS}}$ this saves the lattice a lot of work. This is also the cheapest scheme to run in simulations. With no scheme or gauge analysis we reiterate that in this chapter we have simply produced wanted results which others will develop.

In this calculation we have considered an asymmetric point. This brought with it new master integrals which we have defined in Appendix C in terms of the various functions arising as a result of the asymmetry in the graph. This configuration setup is easier to simulate on the lattice since the symmetric point has relatively noisier signals, [51].

We close with a few remarks. Firstly the amplitudes for the mass, vector, tensor and DIS operators have been computed at two loops in the $\overline{\text{MS}}$ scheme. This data will contribute to improving the measurement of Green's functions relevant for deep inelastic scattering. In order to develop our understanding of the QCD vertex functions our next step could be to apply this asymmetric point renormalization to those gauges we heavily analysed in chapters 3 - 5. Studying these non-linear gauges in this new configuration setup would provide more results for Schwinger-Dyson analyses. There are also more complicated operators such as $\mathcal{S}\bar{\psi}\gamma_\mu\mathcal{D}^\nu\mathcal{D}^\sigma\psi$ which one could potentially study in this setup. Again, assisting in lattice research.

Appendix A

Gauge Fixing and BRST Symmetry

As discussed in Chapter 2 it is necessary to first fix a gauge, where the gauge fixing terms satisfy a symmetry, before any calculations can be carried out using the Lagrangian for that theory. Since the addition of these gauge fixing terms breaks gauge invariance we require another symmetry which restores as much of this gauge symmetry as possible. It was Becci, Rouet, Stora, [33, 34] and Tyutin, [35] who independently noticed that by choosing a Landau gauge fixing which transforms as

$$\begin{aligned} \delta A_\mu^A &= (D_\mu \Lambda)^A && \text{(A.0.1)} \\ \delta c^A &= \frac{g}{2} f^{ABC} c^B \Lambda^C && \text{(A.0.2)} \\ \delta \bar{c}^A &= b^A && \text{(A.0.3)} \\ \delta b^A &= 0 && \text{(A.0.4)} \end{aligned}$$

where δ is the BRST transform that anticommutes with the ghost and anti-ghost fields c^A, $\bar{c}^A$, one can determine the gauge fixing terms. The authors of [33, 34, 35] proposed that by setting

$$\Lambda^a = -c^a \lambda \qquad \text{(A.0.5)}$$

where λ is some Grassmann constant required in order to make Λ^a non-Grassmann, the following identities must hold in order to render the QCD Lagrangian gauge invariant

$$\begin{aligned} \delta A_\mu^a &= -\frac{1}{g} \left(\mathrm{D}_\mu c\right)^a \lambda \\ \delta c^a &= -\frac{1}{2} f^{abc} c^b c^c \lambda \end{aligned}$$

$$\delta\bar{c}^a = -\frac{1}{\alpha g}\left(\partial^\mu A^a_\mu\right)\lambda \tag{A.0.6}$$

where the quarks and anti-quarks also transform in a BRST way as

$$\delta\psi^{iI} = igc^A\left(T^A\right)_{IJ}\psi^{iJ} \tag{A.0.7}$$
$$\delta\bar{\psi}^{iI} = -igc^A\left(T^A\right)_{IJ}\bar{\psi}^{iJ}\ . \tag{A.0.8}$$

Generalizing this to all gauges we define our BRST transformations as

$$\delta A^a_\mu = -\left(\mathrm{D}_\mu c\right)^a \tag{A.0.9}$$
$$\delta c^a = -\frac{g}{2}f^{abc}c^b c^c \tag{A.0.10}$$
$$\delta\bar{c}^a = b^a \tag{A.0.11}$$
$$\delta b^a = 0 \tag{A.0.12}$$

where we will take this as our consistent set of transformations for subsequent manipulations.

We will now explicitly show that the QCD Lagrangian is indeed invariant under the BRST transformations. Neglecting the quark contribution, since its gauge invariant term means that this is trivially BRST-invariant, and splitting (2.1.44) into its gluon and ghost counterparts, we can show that both gauge-fixed terms are invariant under the above transformations. Applying the BRST transforms to each of the gauge fixing terms we have

$$\begin{aligned}
\delta\mathcal{L}_{\mathrm{gf}} &= \delta\left[-\frac{1}{2\alpha}\left(\partial^\mu A_\mu\right)\left(\partial^\nu A_\nu\right)\right] \\
&= -\frac{1}{2\alpha}\left(\partial^\mu \delta A_\mu\right)\left(\partial^\nu A_\nu\right) - \frac{1}{2\alpha}\left(\partial^\mu A_\mu\right)\left(\partial^\nu \delta A_\nu\right) \\
&= -\frac{1}{2\alpha}\partial^\mu\left(-\mathrm{D}_\mu c\right)^a\left(\partial^\nu A_\nu\right) - \frac{1}{2\alpha}\left(\partial^\mu A_\mu\right)\partial^\nu\left(-\mathrm{D}_\nu c\right)^a \\
&= \frac{1}{2\alpha}\partial^\nu\left(\mathrm{D}_\nu c\right)^a\left(\partial^\mu A_\mu\right) + \frac{1}{2\alpha}\left(\partial^\mu A_\mu\right)\partial^\nu\left(\mathrm{D}_\nu c\right)^a \\
&= \frac{1}{\alpha}\left(\partial^\mu A_\mu\right)\partial^\nu\left(\mathrm{D}_\nu c\right)^a
\end{aligned} \tag{A.0.13}$$

and

$$\begin{aligned}
\delta\mathcal{L}_{\mathrm{ghost}} &= \delta\left[-\bar{c}^a\partial^\mu \mathrm{D}_\mu c^a\right] \\
&= -\left(\delta\bar{c}^a\right)\partial^\mu \mathrm{D}_\mu c^a - \bar{c}^a\partial^\mu\left(\delta\left(\mathrm{D}_\mu c\right)^a\right)\ .
\end{aligned} \tag{A.0.14}$$

The second piece of (A.0.14) is tedious to evaluate, and so we tackle this piece separately

$$\begin{aligned}
\delta\left(\mathrm{D}_\mu c\right)^a &= \delta\left(\partial^\mu c^a - g f^{abc} A^b_\mu c^c\right) \\
&= \delta\left(\partial^\mu c^a\right) - g f^{abc}\left(\delta A^b_\mu\right) c^c - g f^{abc} A^b_\mu \left(\delta c^c\right) \\
&= -\frac{g}{2} f^{abc}\partial^\mu\left(c^b c^c\right) + g f^{abc}\left(\mathrm{D}_\mu c\right)^b c^c + \frac{g^2}{2} f^{abc} f^{cde} A^b_\mu c^d c^e \\
&= -\frac{g}{2} f^{abc}\left(\partial^\mu c^b c^c\right) + g f^{abc}\left(\partial_\mu c^b\right) c^c - g^2 f^{abc} f^{bde} A^d_\mu c^e c^c \\
&\quad + \frac{g^2}{2} f^{abc} f^{cde} A^b_\mu c^d c^e \ . \qquad \text{(A.0.15)}
\end{aligned}$$

By rearranging and interchanging indices the first two terms drop out, leaving

$$\delta\left(\mathrm{D}_\mu c\right)^a = -g^2 f^{abc} f^{bde} A^d_\mu c^e c^c + \frac{g^2}{2} f^{abc} f^{cde} A^b_\mu c^d c^e \ . \qquad \text{(A.0.16)}$$

Applying the following generalization of the Jacobi identity (2.1.7)

$$f_4^{abcd} = -f_4^{adbc} - f_4^{acdb} \qquad \text{(A.0.17)}$$

where f_4^{abcd} is shorthand notation for $f_4^{abcd} = f^{abe} f^{ecd}$, (A.0.16) becomes

$$\begin{aligned}
\delta\left(\mathrm{D}_\mu c\right)^a &= g^2 f_4^{aebd} A^b_\mu c^d c^e + \frac{g^2}{2} f_4^{abde} A^b_\mu c^d c^e \\
&= g^2 f_4^{aebd} A^b_\mu c^d c^e + \frac{g^2}{2}\left(-f_4^{aebd} A^b_\mu c^d c^e - f_4^{adeb} A^b_\mu c^d c^e\right) \\
&= \frac{g^2}{2} f_4^{aebd} A^b_\mu c^d c^e - \frac{g}{2} f_4^{aedb} A^b_\mu c^e c^d \\
&= 0 \qquad \text{(A.0.18)}
\end{aligned}$$

leaving us with

$$\begin{aligned}
\delta\mathcal{L}_{\text{ghost}} &= \delta\left[-\bar{c}^a \partial^\mu \mathrm{D}_\mu c^a\right] \\
&= -\left(\delta\bar{c}^a\right)\partial^\mu \mathrm{D}_\mu c^a - \bar{c}^a \partial^\mu\left(\delta\left(\mathrm{D}_\mu c\right)^a\right) \\
&= -b^a \partial^\mu \mathrm{D}_\mu c^a \qquad \text{(A.0.19)}
\end{aligned}$$

and

$$\delta\mathcal{L}_{\text{GF}} = \frac{1}{\alpha}\left(\partial^\mu A_\mu\right)\partial^\nu\left(\mathrm{D}_\nu c\right)^a - b^a \partial^\mu \mathrm{D}_\mu c^a \qquad \text{(A.0.20)}$$

which implies that

$$b^a \;=\; -\frac{1}{\alpha}\left(\partial^\mu A^a_\mu\right) \;. \tag{A.0.21}$$

This agrees with the definition (A.0.6) for an arbitrary (linear) covariant gauge in QCD given by the authors of [33] and [35], up to a factor of the coupling constant which we defined differently in the general definitions (A.0.9) - (A.0.12).

Above we have shown an example of how the fields transform under BRST symmetry and how one would determine the Nakanishi-Lautrup (b) field, which is dependent on the type of gauge fixing. We now move on to the Curci-Ferrari gauge. Briefly the complete set of BRST transformations for the Curci-Ferrari gauge fixing are

$$\delta A^a_\mu \;=\; -\mathrm{D}_\mu c^a \tag{A.0.22}$$

$$\delta c^a \;=\; -\frac{g}{2} f^{abc} c^b c^c \tag{A.0.23}$$

$$\delta \bar{c}^a \;=\; \frac{1}{\alpha}\partial^\mu A^a_\mu - \frac{g}{2}\left(1-\zeta\right) f^{abc}\bar{c}^b c^c \tag{A.0.24}$$

where ζ is again our interpolating parameter where this time $\zeta = 1$ takes us to the covariant BRST transformation (A.0.6). In addition to the above we also have the transform of ψ and $\bar{\psi}$. These transform as before in (A.0.7).

Using a BRST approach to fixing the gauge is the easiest way in determining *all* of the gauge fixing terms in the theory. The original terms of the Lagrangian are naturally BRST-invariant by definition. An important property of the BRST and anti-BRST transformations is that they remain nilpotent, that is to say that

$$\delta^2 \;=\; 0 \tag{A.0.25}$$

must hold for all fields. This also ensures that the gauge fixed theory is unitary. If a BRST invariant gluon mass, m, is included in the theory, such as for computations in the Curci-Ferrari model, then $\delta^2 \propto m^2$. Performing a second BRST transform on each of (A.0.22) we will prove this for the Curci-Ferrari case, starting with the gluon field

$$\begin{aligned}
\delta\left[\delta A^a_\mu\right] \;&=\; \delta\left[-\partial_\mu c^a + g f^{abc} A^b_\mu c^c\right] \\
&=\; -\partial_\mu\left(\delta c^a\right) + g f^{abc}(\delta A^b_\mu) c^c + g f^{abc} A^b_\mu\left(\delta c^c\right)
\end{aligned}$$

$$
\begin{aligned}
&= \frac{g}{2} f^{abc} \partial_\mu c^b c^c - g f^{abc} \left(\partial_\mu c^b + g f^{bde} A^d_\mu c^e \right) c^c - \frac{g^2}{2} f^{abc} f^{cde} A^b_\mu c^d c^e \\
&= \frac{g}{2} f^{abc} (\partial_\mu c^b) c^c + \frac{g}{2} f^{abc} c^b (\partial_\mu c^c) - g f^{abc} (\partial_\mu c^b) c^c - g^2 f^{abc} f^{bde} A^d_\mu c^e c^c \\
&\quad - \frac{g^2}{2} f^{abc} f^{cde} A^b_\mu c^d c^e \\
&= -g^2 f^{abc} f^{bde} A^d_\mu c^e c^c - \frac{g^2}{2} f^{abc} f^{cde} A^b_\mu c^d c^e \\
&= -g^2 f_4^{acde} A^d_\mu c^e c^c - \frac{g^2}{2} f_4^{adec} A^d_\mu c^e c^c \\
&= -\frac{g^2}{2} f_4^{acde} A^d_\mu c^e c^c + \frac{g^2}{2} f_4^{aecd} A^d_\mu c^e c^c \\
&= 0
\end{aligned}
\tag{A.0.26}
$$

and by performing another BRST transform on the ghost field we have

$$
\begin{aligned}
\delta \left[\delta c^a \right] &= \delta \left[-\frac{g}{2} f^{abc} c^b c^c \right] \\
&= -\frac{g}{2} f^{abc} \left(\delta c^b c^c - c^b \delta c^c \right) \\
&= -g f^{abc} \delta c^b c^c \\
&= \frac{g^2}{2} f^{abc} f^{bde} c^d c^e c^c \\
&= -\frac{g^2}{2} \left(f^{abd} f^{bec} + f^{abe} f^{bcd} \right) c^d c^e c^c \\
&= -\frac{g^2}{2} f^{abd} f^{bec} \left(c^d c^e c^c + c^c c^d c^e \right) \\
&= -g^2 f^{abd} f^{bec} c^d c^e c^c \\
&= -g^2 f^{abc} f^{bde} c^d c^e c^c \\
&= \frac{g^2}{2} f^{abc} f^{bde} c^d c^e c^c \\
&= -g^2 f^{abc} f^{bde} c^c c^e c^c \\
&= 0
\end{aligned}
\tag{A.0.27}
$$

where we apply the Jacobi identity in step 7. Finally the BRST transform on the anti-ghost is

$$
\begin{aligned}
\delta \left[\delta \bar{c}^a \right] &= \delta \left[b^a \right] \\
&= 0
\end{aligned}
\tag{A.0.28}
$$

where the transform on the Nakanishi-Lautrup field is zero by definition. Therefore we have proven that $\delta^2 = 0$. This can also be proven for the MAG BRST

and anti-BRST tranformations given by

$$\begin{aligned}
\delta A^a_\mu &= -\left(\partial_\mu c^a + g f^{ajc} A^j_\mu c^c + g f^{abc} A^b_\mu c^c + g f^{abk} A^b_\mu c^k\right) \\
\delta c^a &= g f^{abk} c^b c^k + \frac{1}{2} f^{abc} c^b c^c \quad , \quad \delta \bar{c}^a = b^a \quad , \quad \delta A^i_\mu = -\left(\partial_\mu c^i + g f^{ibc} A^b_\mu c^c\right) \\
\delta b^a &= 0 \quad , \quad \delta c^i = \frac{1}{2} g f^{ibc} c^b c^c \quad , \quad \delta \bar{c}^i = b^i \quad , \quad \delta b^i = 0
\end{aligned} \tag{A.0.29}$$

and

$$\begin{aligned}
\bar{\delta} A^a_\mu &= -\left(\partial_\mu c^a + g f^{ajc} A^j_\mu c^c + g f^{abc} A^b_\mu c^c + g f^{abk} A^b_\mu c^k\right) \\
\bar{\delta} c^a &= -b^a + g f^{abc} c^b \bar{c}^c + g f^{abk} c^b \bar{c}^k + g f^{abk} \bar{c}^b c^k \\
\bar{\delta} \bar{c}^a &= g f^{abk} \bar{c}^b \bar{c}^k + \frac{1}{2} g f^{abc} \bar{c}^b \bar{c}^c \quad , \quad \bar{\delta} b^a = -g f^{abc} b^b \bar{c}^c - g f^{abk} b^b \bar{c}^k + g f^{abk} \bar{c}^b b^k \ , \\
\bar{\delta} A^i_\mu &= -\left(\partial_\mu \bar{c}^i + g f^{ibc} A^b_\mu \bar{c}^c\right) \quad , \quad \bar{\delta} c^i = -b^i + g f^{ibc} c^b \bar{c}^c \quad , \quad \bar{\delta} \bar{c}^i = \frac{1}{2} g f^{ibc} \bar{c}^b \bar{c}^c \ , \\
\bar{\delta} b^i &= -g f^{ibc} b^b \bar{c}^c \ .
\end{aligned} \tag{A.0.30}$$

Note that this property of nilpotency can be seen when we apply the BRST transform to $\mathrm{D}_\mu c^a$, which is ultimately zero, as we have proven in (A.0.18).

Since their discovery the BRST identities have helped in the study of Yang-Mills theories, rendering the problem of renormalization considerably simpler, [143, 144].

Appendix B

Tensor Basis

In this Appendix we record the explicit form of the tensors that are used in the decomposition of each 3-point vertex into scalar amplitudes. In chapter 2 we showed that we can decompose the Lorentz amplitudes into scalar amplitudes as

$$\begin{aligned}
\Sigma^{\rm ggg}_{\mu\nu\sigma}(p,q)|_{p^2=q^2=-\mu^2} &= \sum_{k=1}^{14} \mathcal{P}^{\rm ggg}_{(k)\mu\nu\sigma}(p,q)\Sigma^{\rm ggg}_{(k)}(p,q) \\
\left(\Sigma^{\rm qqg}_{\sigma}(p,q)\right)_{\alpha}^{\ \beta}|_{p^2=q^2=-\mu^2} &= \sum_{k=1}^{6} \left(\mathcal{P}^{\rm qqg}_{(k)\sigma}(p,q)\right)_{\alpha}^{\ \beta}\Sigma^{\rm qqg}_{(k)}(p,q) \\
\Sigma^{\rm ccg}_{\sigma}(p,q)|_{p^2=q^2=-\mu^2} &= \sum_{k=1}^{2} \mathcal{P}^{\rm ccg}_{(k)\sigma}(p,q)\Sigma^{\rm ccg}_{(k)}(p,q)\ . \qquad \text{(B.0.1)}
\end{aligned}$$

where $\mathcal{P}^{V}_{(k)\ \mu_1\ldots\nu_n}(p,q)$ are the basic tensors for each vertex, V, and $\Sigma^{V}_{(k)}(p,q)$ are the scalar amplitudes. The tensors are chosen as follows. Since the colour group structure has already been factored out we are left with three free Lorentz indices to play with for the triple gluon vertex. The only combinations of tensors which can be made out of these three Lorentz indices are of the form

$$\eta_{**}X_{*} \ \text{ and } \ \frac{1}{\mu^2}\left[X_{*}X_{*}X_{*}\right] \qquad \text{(B.0.2)}$$

where $X \in \{p,q\}$ and $* \in \{\mu,\nu,\sigma\}$. The factor μ^2 is included for dimensionality purposes. In the case of the quark-gluon vertex the basis of Lorentz tensors can also be built from the γ-matrices in addition to p,q and the metric. With these constraints applied the full set of basic tensors at the symmetric point for the triple-gluon vertex is

$$\mathcal{P}^{\rm ggg}_{(1)\mu\nu\sigma}(p,q) \ = \ \eta_{\mu\nu}p_{\sigma} \ \ , \ \ \mathcal{P}^{\rm ggg}_{(2)\mu\nu\sigma}(p,q) \ = \ \eta_{\nu\sigma}p_{\mu} \ \ , \ \ \mathcal{P}^{\rm ggg}_{(3)\mu\nu\sigma}(p,q) \ = \ \eta_{\sigma\mu}p_{\nu}$$

$$
\begin{aligned}
\mathcal{P}^{\rm ggg}_{(4)\mu\nu\sigma}(p,q) &= \eta_{\mu\nu}q_\sigma \quad , \quad \mathcal{P}^{\rm ggg}_{(5)\mu\nu\sigma}(p,q) = \eta_{\nu\sigma}q_\mu \quad , \quad \mathcal{P}^{\rm ggg}_{(6)\mu\nu\sigma}(p,q) = \eta_{\sigma\mu}q_\nu \\
\mathcal{P}^{\rm ggg}_{(7)\mu\nu\sigma}(p,q) &= \frac{1}{\mu^2}p_\mu p_\nu p_\sigma \quad , \quad \mathcal{P}^{\rm ggg}_{(8)\mu\nu\sigma}(p,q) = \frac{1}{\mu^2}p_\mu p_\nu q_\sigma \\
\mathcal{P}^{\rm ggg}_{(9)\mu\nu\sigma}(p,q) &= \frac{1}{\mu^2}p_\mu q_\nu p_\sigma \quad , \quad \mathcal{P}^{\rm ggg}_{(10)\mu\nu\sigma}(p,q) = \frac{1}{\mu^2}q_\mu p_\nu p_\sigma \\
\mathcal{P}^{\rm ggg}_{(11)\mu\nu\sigma}(p,q) &= \frac{1}{\mu^2}p_\mu q_\nu q_\sigma \quad , \quad \mathcal{P}^{\rm ggg}_{(12)\mu\nu\sigma}(p,q) = \frac{1}{\mu^2}q_\mu p_\nu q_\sigma \\
\mathcal{P}^{\rm ggg}_{(13)\mu\nu\sigma}(p,q) &= \frac{1}{\mu^2}q_\mu q_\nu p_\sigma \quad , \quad \mathcal{P}^{\rm ggg}_{(14)\mu\nu\sigma}(p,q) = \frac{1}{\mu^2}q_\mu q_\nu q_\sigma \ . \qquad \text{(B.0.3)}
\end{aligned}
$$

The first six tensors all appear in the Feynman rule for the triple-gluon vertex $\langle A^a_\mu(p)A^b_\nu(q)A^c_\sigma(r)\rangle$, where $r=-p-q$. Although other authors choose to compute only with one or two channels, we consider all possible channels (for the triple-gluon vertex this is 14) since a combination of these channels assists in lattice studies where they have the freedom to select only the channels they are interested in. Measurements can be made on the lattice in various directions to extract specific data. Another reason for considering all channels is to get the full picture and gain a deeper understanding of each vertex whilst checking that the symmetries between channels still hold at higher loop order. Once we have our tensor basis we would now like to project out the scalar amplitudes for each individual channel, k. Since an integration by parts routine can only be applied to scalar integrals it is important we rewrite (2.1.65) making $\Sigma^i_{(k)}(p,q)$ the subject. We begin by defining the matrix

$$
\mathcal{N}^V_{kl} = \mathcal{P}^V_{(k)\mu_1\ldots\mu_{n_V}}(p,q)\mathcal{P}^{V\mu_1\ldots\mu_{n_V}}_{(l)}(p,q)\Big|_{p^2=q^2=-\mu^2} \qquad \text{(B.0.4)}
$$

where k and l distinguish the projection tensors. The matrix $\mathcal{N}^V_{kl}$ is symmetric in k and l. We can write

$$
\begin{aligned}
\Sigma^{\rm ggg}_{\mu\nu\sigma}(p,q) &= \Sigma^{\rm ggg}_{(j)}(p,q)\mathcal{P}^{\rm ggg}_{(j)\ \mu\nu\sigma}(p,q) \\
\mathcal{P}^{\rm ggg\ \mu\nu\sigma}_{(l)}(p,q)\Sigma^{\rm ggg}_{\mu\nu\sigma}(p,q) &= \Sigma^{\rm ggg}_{(j)}(p,q)\mathcal{P}^{\rm ggg\ \mu\nu\sigma}_{(l)}(p,q)\mathcal{P}^{\rm ggg}_{(j)\ \mu\nu\sigma}(p,q) \\
\mathcal{P}^{\rm ggg\ \mu\nu\sigma}_{(l)}(p,q)\Sigma^{\rm ggg}_{\mu\nu\sigma}(p,q) &= \Sigma^{\rm ggg}_{(j)}(p,q)\mathcal{N}^{\rm ggg}_{lj} \qquad \text{(B.0.5)}
\end{aligned}
$$

Multiplying by $\mathcal{M}^{\rm ggg}_{kl}$ which is defined to be the inverse of $\mathcal{N}^{\rm ggg}_{kl}$ we have

$$
\begin{aligned}
\mathcal{P}^{\rm ggg\ \mu\nu\sigma}_{(l)}(p,q)\Sigma^{\rm ggg}_{\mu\nu\sigma}(p,q)\mathcal{M}^{\rm ggg}_{kl} &= \Sigma^{\rm ggg}_{(j)}(p,q)\mathcal{N}^{\rm ggg}_{lj}\mathcal{M}^{\rm ggg}_{kl} \\
\mathcal{P}^{\rm ggg\ \mu\nu\sigma}_{(l)}(p,q)\Sigma^{\rm ggg}_{\mu\nu\sigma}(p,q)\mathcal{M}^{\rm ggg}_{kl} &= \Sigma^{\rm ggg}_{(j)}(p,q)\delta_{jk} \\
\mathcal{M}^{\rm ggg}_{kl}\mathcal{P}^{\rm ggg\ \mu\nu\sigma}_{(l)}(p,q)\Sigma^{\rm ggg}_{\mu\nu\sigma}(p,q) &= \Sigma^{\rm ggg}_{(k)}(p,q)\ . \qquad \text{(B.0.6)}
\end{aligned}
$$

Since there are 14 basis tensors for the triple-gluon vertex the projection matrix $\mathcal{M}^{ggg}_{kl}$ is a 14×14 matrix which allows one to project out the amplitudes $\Sigma^{ggg}_{(k)}(p,q)$. For the associated projection matrix we partition it into submatrices for ease of presentation. With the general form

$$\mathcal{M}^{ggg} = -\frac{1}{27(d-2)}\begin{pmatrix} \mathcal{M}^{ggg}_{11} & \mathcal{M}^{ggg}_{12} & \mathcal{M}^{ggg}_{13} \\ \mathcal{M}^{ggg}_{21} & \mathcal{M}^{ggg}_{22} & \mathcal{M}^{ggg}_{23} \\ \mathcal{M}^{ggg}_{31} & \mathcal{M}^{ggg}_{32} & \mathcal{M}^{ggg}_{33} \end{pmatrix}$$

then each of the submatrices are

$$\mathcal{M}^{ggg}_{11} = \begin{pmatrix} 36 & 0 & 0 & 18 & 0 & 0 \\ 0 & 36 & 0 & 0 & 18 & 0 \\ 0 & 0 & 36 & 0 & 0 & 18 \\ 18 & 0 & 0 & 36 & 0 & 0 \\ 0 & 18 & 0 & 0 & 36 & 0 \\ 0 & 0 & 18 & 0 & 0 & 36 \end{pmatrix}, \quad \mathcal{M}^{ggg}_{12} = \begin{pmatrix} 48 & 24 & 24 & 24 \\ 48 & 24 & 24 & 24 \\ 48 & 24 & 24 & 24 \\ 24 & 48 & 12 & 12 \\ 24 & 12 & 12 & 48 \\ 24 & 12 & 48 & 12 \end{pmatrix}$$

$$\mathcal{M}^{ggg}_{13} = \begin{pmatrix} 12 & 12 & 48 & 24 \\ 48 & 12 & 12 & 24 \\ 12 & 48 & 12 & 24 \\ 24 & 24 & 24 & 48 \\ 24 & 24 & 24 & 48 \\ 24 & 24 & 24 & 48 \end{pmatrix}, \quad \mathcal{M}^{ggg}_{21} = \begin{pmatrix} 48 & 48 & 48 & 24 & 24 & 24 \\ 24 & 24 & 24 & 48 & 12 & 12 \\ 24 & 24 & 24 & 12 & 12 & 48 \\ 24 & 24 & 24 & 12 & 48 & 12 \end{pmatrix}$$

$$\mathcal{M}^{ggg}_{22} = \begin{pmatrix} 64(d+1) & 32(d+1) & 32(d+1) & 32(d+1) \\ 32(d+1) & 32(2d-1) & 16(d+1) & 16(d+1) \\ 32(d+1) & 16(d+1) & 32(2d-1) & 16(d+1) \\ 32(d+1) & 16(d+1) & 16(d+1) & 32(2d-1) \end{pmatrix}$$

$$\mathcal{M}^{ggg}_{23} = \begin{pmatrix} 16(d+4) & 16(d+4) & 16(d+4) & 8(d+10) \\ 8(4d+1) & 8(4d+1) & 8(d+4) & 16(d+4) \\ 8(4d+1) & 8(d+4) & 8(4d+1) & 16(d+4) \\ 8(d+4) & 8(4d+1) & 8(4d+1) & 16(d+4) \end{pmatrix}$$

$$\mathcal{M}^{ggg}_{31} = \begin{pmatrix} 12 & 48 & 12 & 24 & 24 & 24 \\ 12 & 12 & 48 & 24 & 24 & 24 \\ 48 & 12 & 12 & 24 & 24 & 24 \\ 24 & 24 & 24 & 48 & 48 & 48 \end{pmatrix}$$

$$
\begin{aligned}
\mathcal{M}_{32}^{\mathrm{ggg}} &= \begin{pmatrix} 16(d+4) & 8(4d+1) & 8(4d+1) & 8(d+4) \\ 16(d+4) & 8(4d+1) & 8(d+4) & 8(4d+1) \\ 16(d+4) & 8(d+4) & 8(4d+1) & 8(4d+1) \\ 8(d+10) & 16(d+4) & 16(d+4) & 16(d+4) \end{pmatrix} \\
\mathcal{M}_{33}^{\mathrm{ggg}} &= \begin{pmatrix} 32(2d-1) & 16(d+1) & 16(d+1) & 32(d+1) \\ 16(d+1) & 32(2d-1) & 16(d+1) & 32(d+1) \\ 16(d+1) & 16(d+1) & 32(2d-1) & 32(d+1) \\ 32(d+1) & 32(d+1) & 32(d+1) & 64(d+1) \end{pmatrix} .
\end{aligned} \tag{B.0.7}
$$

Similarly for the ghost-gluon vertex the tensor basis have the form X_σ where $X \in \{p, q\}$ and σ is the only free Lorentz index,

$$
\mathcal{P}_{(1)\sigma}^{\mathrm{ccg}}(p,q) \;=\; p_\sigma \quad , \quad \mathcal{P}_{(2)\sigma}^{\mathrm{ccg}}(p,q) \;=\; q_\sigma \; . \tag{B.0.8}
$$

The projection matrix for the two tensors is

$$
\mathcal{M}^{\mathrm{ccg}} \;=\; -\,\frac{1}{3}\begin{pmatrix} 4 & 2 \\ 2 & 4 \end{pmatrix} \; . \tag{B.0.9}
$$

Likewise for the quark-gluon vertex where the number of independent tensors one can build from two independent external momenta and the generalized γ-matrices are

$$
\begin{aligned}
\mathcal{P}_{(1)\sigma}^{\mathrm{qqg}}(p,q) &= \gamma_\sigma \quad , \quad \mathcal{P}_{(2)\sigma}^{\mathrm{qqg}}(p,q) \;=\; \frac{p_\sigma \not{p}}{\mu^2} \quad , \quad \mathcal{P}_{(3)\sigma}^{\mathrm{qqg}}(p,q) \;=\; \frac{p_\sigma \not{q}}{\mu^2} \; , \\
\mathcal{P}_{(4)\sigma}^{\mathrm{qqg}}(p,q) &= \frac{q_\sigma \not{p}}{\mu^2} \quad , \quad \mathcal{P}_{(5)\sigma}^{\mathrm{qqg}}(p,q) \;=\; \frac{q_\sigma \not{q}}{\mu^2} \quad , \quad \mathcal{P}_{(6)\sigma}^{\mathrm{qqg}}(p,q) \;=\; \frac{1}{\mu^2}\Gamma_{(3)\,\sigma pq} \; .
\end{aligned} \tag{B.0.10}
$$

where $\Gamma_{(3)\,\sigma pq}$ is shorthand for $\Gamma_{(3)\,\mu\nu\sigma}p^\mu q^\nu$. This choice of tensors leads to the projection matrix

$$
\mathcal{M}^{\mathrm{qqg}} \;=\; \frac{1}{36(d-2)}\begin{pmatrix} 9 & 12 & 6 & 6 & 12 & 0 \\ 12 & 16(d-1) & 8(d-1) & 8(d-1) & 4(d+2) & 0 \\ 6 & 8(d-1) & 4(4d-7) & 4(d-1) & 8(d-1) & 0 \\ 6 & 8(d-1) & 4(d-1) & 4(4d-7) & 8(d-1) & 0 \\ 12 & 4(d+2) & 8(d-1) & 8(d-1) & 16(d-1) & 0 \\ 0 & 0 & 0 & 0 & 0 & -12 \end{pmatrix} . \tag{B.0.11}
$$

We have used the convention that when a momenta is contracted with a Lorentz index then that momentum appears instead of the index in the tensor. We note that these forms are specific to the symmetric point only. At another external momentum configuration the elements in each $\mathcal{M}^V$ would be different. For the quark-gluon vertex we use the generalized γ-matrices $\Gamma^{\mu_1\ldots\mu_n}_{(n)}$ which are defined by

$$\Gamma^{\mu_1\ldots\mu_n}_{(n)} \;=\; \gamma^{[\mu_1}\ldots\gamma^{\mu_n]} \tag{B.0.12}$$

where the factor of $1/n!$ is understood and n is an integer with $n \geq 0$. These generalized matrices were introduced in [61, 145, 148] and are totally antisymmetric in the Lorentz indices. These generalized matrices span spinor space in d-dimensions and the underlying algebra necessary for loop calculations has been developed in [61]. The trace operation is isotropic with respect the basis since, [146, 147],

$$\mathrm{tr}\left(\Gamma^{\mu_1\ldots\mu_m}_{(m)}\Gamma^{\nu_1\ldots\nu_n}_{(n)}\right) \;\propto\; \delta_{mn}I^{\mu_1\ldots\mu_m\nu_1\ldots\nu_n} \;. \tag{B.0.13}$$

It is also possible to write products of the original γ-matrices as a finite sum over $\Gamma^{\mu_1\ldots\mu_n}_{(n)}$. This can be achieved recursively by applying the relations, [146, 147, 148]

$$\Gamma^{\mu_1\ldots\mu_n}_{(n)}\gamma^{\nu} \;=\; \Gamma^{\mu_1\ldots\mu_n\nu}_{(n+1)} \;+\; \sum_{r=1}^{n}(-1)^{n-r}\,\eta^{\mu_r\nu}\,\Gamma^{\mu_1\ldots\mu_{r-1}\mu_{r+1}\ldots\mu_n}_{(n-1)} \tag{B.0.14}$$

$$\gamma^{\nu}\Gamma^{\mu_1\ldots\mu_n}_{(n)} \;=\; \Gamma^{\nu\mu_1\ldots\mu_n}_{(n+1)} \;+\; \sum_{r=1}^{n}(-1)^{r-1}\,\eta^{\mu_r\nu}\,\Gamma^{\mu_1\ldots\mu_{r-1}\mu_{r+1}\ldots\mu_n}_{(n-1)} \tag{B.0.15}$$

where $\eta_{\mu\nu}$ is the metric. Restricting to four dimensions, for example, one would have

$$\begin{aligned}\Gamma^{\mu\nu}_{(2)}\Big|_{d=4} \;&=\; \sigma^{\mu\nu} \quad , \quad \Gamma^{\mu\nu\sigma\rho}_{(4)}\Big|_{d=4} \;=\; \epsilon^{\mu\nu\sigma\rho}\gamma^5 \\ \Gamma^{\mu_1\ldots\mu_n}_{(n)}\Big|_{d=4} \;&=\; 0 \;\text{ for } n \geq 5\end{aligned} \tag{B.0.16}$$

where $\epsilon^{\mu\nu\sigma\rho}$ is the totally antisymmetric pseudotensor in four dimensions. We reiterate that γ^5 exists in strictly four dimensions and defines chirality. Notationally we will use γ^μ and $\Gamma^{\mu}_{(1)}$ synonymously in d-dimensions.

In particular in d-dimensions we require

$$\begin{aligned}\Gamma^{\mu\nu}_{(2)} \;&=\; \frac{1}{2}\left(\gamma^\mu\gamma^\nu - \gamma^\nu\gamma^\mu\right) \\ \Gamma^{\mu\nu\sigma}_{(3)} \;&=\; \gamma^\mu\gamma^\nu\gamma^\sigma - \eta^{\mu\nu}\gamma^\sigma + \eta^{\mu\sigma}\gamma^\nu - \eta^{\nu\sigma}\gamma^\mu\end{aligned}$$

$$\Gamma^{\mu\nu\sigma\rho}_{(4)} = \gamma^\mu\gamma^\nu\gamma^\sigma\gamma^\rho - \eta^{\mu\nu}\gamma^\sigma\gamma^\rho + \eta^{\mu\sigma}\gamma^\nu\gamma^\rho - \eta^{\nu\sigma}\gamma^\mu\gamma^\rho - \eta^{\mu\rho}\left(\gamma^\nu\gamma^\sigma - \eta^{\nu\sigma}\right) + \eta^{\nu\rho}\left(\gamma^\mu\gamma^\sigma - \eta^{\mu\sigma}\right) - \eta^{\sigma\rho}\left(\gamma^\mu\gamma^\nu - \eta^{\mu\nu}\right) \quad \text{(B.0.17)}$$

in order to compute the vector and tensor operators. This is also the case for the DIS operators.

The tensor basis and projection matrices are the same for all three schemes considered in Part 1 of this thesis. Again, this is because the same three vertices are considered in all gauge fixings. For the operator insertions the tensor basis is different.

B.1 Operator Tensor Basis

In this section of the appendix we record in succession the basis of projection tensors used for each operator level. The projection matrix $\mathcal{M}^u_{kl}$ is defined as before but now in terms of operators, $\mathcal{O}^u$, such that

$$\Sigma^{\mathcal{O}^u}_{(k)}(p,q) = \mathcal{M}^u_{kl}\mathcal{P}^{u\ \mu_1\ldots\mu_{n_u}}_{(l)}(p,q)\left(\langle\psi(p)\mathcal{O}^u_{\mu_1\ldots\mu_{n_u}}(-p-q)\bar{\psi}(q)\rangle\right)\Big|_\omega \quad \text{(B.1.18)}$$

with $u \in \{S, V, T, W_2, \partial W_2\}$.

When presenting our tensor basis for each operator in the following sections we will do so for an IMOM configuration with arbitrary ω. It is understood that to obtain the SMOM tensor basis the limit $\omega \to 1$ is taken.

B.1.1 Scalar (Mass)

For the scalar we define a tensor basis of two projections

$$\mathcal{P}^S_{(1)}(p,q) = \Gamma_{(0)} \quad , \quad \mathcal{P}^S_{(2)}(p,q) = \frac{1}{\mu^2}\Gamma^{pq}_{(2)} \quad \text{(B.1.19)}$$

with projection matrix

$$\mathcal{M}^S = \frac{1}{4\omega[\omega-4]}\begin{pmatrix} \omega[\omega-4] & 0 \\ 0 & 4 \end{pmatrix} . \quad \text{(B.1.20)}$$

By setting $\omega = 1$ the above reduces to the projection matrix for a SMOM configuration

$$\mathcal{M}^S \;=\; \frac{1}{12}\begin{pmatrix} 3 & 0 \\ 0 & -4 \end{pmatrix} . \tag{B.1.21}$$

with the tensor basis remaining unchanged.

B.1.2 Vector

The tensor basis for the vector current involves six independent tensors, these are

$$\begin{aligned} \mathcal{P}^V_{(1)\mu}(p,q) &= \gamma_\mu \quad , \quad \mathcal{P}^V_{(2)\mu}(p,q) = \frac{p^\mu \not{p}}{\mu^2} \quad , \quad \mathcal{P}^V_{(3)\mu}(p,q) = \frac{p_\mu \not{q}}{\mu^2} \, , \\ \mathcal{P}^V_{(4)\mu}(p,q) &= \frac{q_\mu \not{p}}{\mu^2} \quad , \quad \mathcal{P}^V_{(5)\mu}(p,q) = \frac{q_\mu \not{q}}{\mu^2} \quad , \quad \mathcal{P}^V_{(6)\mu}(p,q) = \frac{1}{\mu^2}\Gamma_{(3)\,\mu pq} \end{aligned} \tag{B.1.22}$$

with the projection matrix

$$\mathcal{M}^V \;=\; \frac{1}{4(d-2)\omega^2[\omega-4]^2}\tilde{\mathcal{M}}^V \, . \tag{B.1.23}$$

Each component of $\tilde{\mathcal{M}}^V$ is given as

$$\begin{aligned} \tilde{\mathcal{M}}^V_{11} &= [\omega-4]^2\omega^2 \;\;,\;\; \tilde{\mathcal{M}}^V_{12} = -4[\omega-4]\omega \;\;,\;\; \tilde{\mathcal{M}}^V_{13} = 2[\omega-2][\omega-4]\omega \\ \tilde{\mathcal{M}}^V_{14} &= 2[\omega-2][\omega-4]\omega \;\;,\;\; \tilde{\mathcal{M}}^V_{15} = -4[\omega-4]\omega \;\;,\;\; \tilde{\mathcal{M}}^V_{16} = 0 \\ \tilde{\mathcal{M}}^V_{22} &= 16[d-1] \;\;,\;\; \tilde{\mathcal{M}}^V_{23} = -8[d-1][\omega-2] \;\;,\;\; \tilde{\mathcal{M}}^V_{24} = -8[d-1][\omega-2] \\ \tilde{\mathcal{M}}^V_{25} &= -4[2[\omega^2-4\omega+2]-[\omega-2]^2 d] \;\;,\;\; \tilde{\mathcal{M}}^V_{26} = 0 \\ \tilde{\mathcal{M}}^V_{33} &= 4[\omega^2-4\omega-4+4d] \;\;,\;\; \tilde{\mathcal{M}}^V_{34} = 4[d-1][\omega-2]^2 \\ \tilde{\mathcal{M}}^V_{35} &= -8[d-1][\omega-2] \;\;,\;\; \tilde{\mathcal{M}}^V_{36} = 0 \;\;,\;\; \tilde{\mathcal{M}}^V_{44} = 4[\omega^2-4\omega-4+4d] \\ \tilde{\mathcal{M}}^V_{45} &= -8[d-1][\omega-2] \;\;,\;\; \tilde{\mathcal{M}}^V_{46} = 0 \;\;,\;\; \tilde{\mathcal{M}}^V_{55} = 16[d-1] \\ \tilde{\mathcal{M}}^V_{56} &= 0 \;\;,\;\; \tilde{\mathcal{M}}^V_{66} = 4[\omega-4]\omega \end{aligned} \tag{B.1.24}$$

where we take the convention $\mathcal{M}_{\text{row column}}$.

B.1.3 Tensor

For the tensor operator there are eight independent tensors making up the tensor basis

$$\begin{aligned}
\mathcal{P}^T_{(1)\mu\nu}(p,q) &= \Gamma_{(2)\,\mu\nu} \quad , \quad \mathcal{P}^T_{(2)\mu\nu}(p,q) = \frac{1}{\mu^2}\left[p_\mu q_\nu - p_\nu q_\mu\right]\Gamma_{(0)} \ , \\
\mathcal{P}^T_{(3)\mu\nu}(p,q) &= \frac{1}{\mu^2}\left[\Gamma_{(2)\,\mu p} p_\nu - \Gamma_{(2)\,\nu p} p_\mu\right] \ , \\
\mathcal{P}^T_{(4)\mu\nu}(p,q) &= \frac{1}{\mu^2}\left[\Gamma_{(2)\,\mu p} q_\nu - \Gamma_{(2)\,\nu p} q_\mu\right] \ , \\
\mathcal{P}^T_{(5)\mu\nu}(p,q) &= \frac{1}{\mu^2}\left[\Gamma_{(2)\,\mu q} p_\nu - \Gamma_{(2)\,\nu q} p_\mu\right] \ , \\
\mathcal{P}^T_{(6)\mu\nu}(p,q) &= \frac{1}{\mu^2}\left[\Gamma_{(2)\,\mu q} q_\nu - \Gamma_{(2)\,\nu q} q_\mu\right] \ , \\
\mathcal{P}^T_{(7)\mu\nu}(p,q) &= \frac{1}{\mu^4}\left[\Gamma_{(2)\,pq} p_\mu q_\nu - \Gamma_{(2)\,pq} p_\nu q_\mu\right] \quad , \quad \mathcal{P}^T_{(8)\mu\nu}(p,q) = \frac{1}{\mu^2}\Gamma_{(4)\,\mu\nu pq} \ .
\end{aligned} \tag{B.1.25}$$

The corresponding projection matrix is

$$\mathcal{M}^T = \frac{1}{4(d-2)(d-3)\omega^2[\omega-4]^2}\tilde{\mathcal{M}}^T \tag{B.1.26}$$

where the components of $\tilde{\mathcal{M}}^T$ are displayed below

$$\begin{aligned}
\tilde{\mathcal{M}}^T_{11} &= -[\omega-4]^2\omega^2 \ , \ \tilde{\mathcal{M}}^T_{12} = 0 \ , \ \tilde{\mathcal{M}}^T_{13} = 4[\omega-4]\omega \\
\tilde{\mathcal{M}}^T_{14} &= -2[\omega-2][\omega-4]\omega \ , \ \tilde{\mathcal{M}}^T_{15} = -2[\omega-2][\omega-4]\omega \\
\tilde{\mathcal{M}}^T_{16} &= 4[\omega-4]\omega \ , \ \tilde{\mathcal{M}}^T_{17} = 4[\omega-4]\omega \ , \ \tilde{\mathcal{M}}^T_{18} = 0 \\
\tilde{\mathcal{M}}^T_{22} &= -2[d-2][d-3][\omega-4]\omega \ , \ \tilde{\mathcal{M}}^T_{23} = 0 \ , \ \tilde{\mathcal{M}}^T_{24} = 0 \ , \ \tilde{\mathcal{M}}^T_{25} = 0 \\
\tilde{\mathcal{M}}^T_{26} &= 0 \ , \ \tilde{\mathcal{M}}^T_{27} = 0 \ , \ \tilde{\mathcal{M}}^T_{28} = 0 \ , \ \tilde{\mathcal{M}}^T_{33} = -8[d-1] \\
\tilde{\mathcal{M}}^T_{34} &= 4[d-1][\omega-2] \ , \ \tilde{\mathcal{M}}^T_{35} = 4[d-1][\omega-2] \\
\tilde{\mathcal{M}}^T_{36} &= -2[d\omega^2 - 4d\omega + 4d - 3\omega^2 + 12\omega - 4] \ , \ \tilde{\mathcal{M}}^T_{37} = -8[d-1] \\
\tilde{\mathcal{M}}^T_{38} &= 0 \ , \ \tilde{\mathcal{M}}^T_{44} = -4[2d + \omega^2 - 4\omega - 2] \ , \ \tilde{\mathcal{M}}^T_{45} = -2[d-1][\omega-2]^2 \\
\tilde{\mathcal{M}}^T_{46} &= 4[d-1][\omega-2] \ , \ \tilde{\mathcal{M}}^T_{47} = 4[d-1][\omega-2] \ , \ \tilde{\mathcal{M}}^T_{48} = 0 \\
\tilde{\mathcal{M}}^T_{55} &= -4[2d + \omega^2 - 4\omega - 2] \ , \ \tilde{\mathcal{M}}^T_{56} = 4[d-1][\omega-2] \\
\tilde{\mathcal{M}}^T_{57} &= 4[d-1][\omega-2] \ , \ \tilde{\mathcal{M}}^T_{58} = 0 \ , \ \tilde{\mathcal{M}}^T_{66} = -8[d-1] \\
\tilde{\mathcal{M}}^T_{67} &= -8[d-1] \ , \ \tilde{\mathcal{M}}^T_{68} = 0 \ , \ \tilde{\mathcal{M}}^T_{77} = -8[d-1][d-2] \\
\tilde{\mathcal{M}}^T_{78} &= 0 \ , \ \tilde{\mathcal{M}}^T_{88} = -4[\omega-4]\omega \ .
\end{aligned} \tag{B.1.27}$$

B.1.4 W_2 and ∂W_2

We choose our tensor basis for the DIS operators to be symmetric and traceless. We want our results to be in terms of symmetric traceless projections since the operator is also defined to be symmetric and traceless. This is achieved by enforcing the following conditions on to our projections

$$\mathcal{P}^{u}_{(l)\ \mu\nu}(p,q)\eta^{\mu\nu} \ = \ 0 \quad , \quad \mathcal{P}^{u}_{(l)\ \mu\nu}(p,q) \ \equiv \ \mathcal{P}^{u}_{(l)\ \nu\mu}(p,q) \ . \tag{B.1.28}$$

It turns out that by comparing with the tensor basis for the same operators in the SMOM setup, [150], there are only two projections which do not already satisfy the traceless condition in (B.1.28), these are

$$\begin{aligned}
\mathcal{P}^{W_2}_{(4)\mu\nu}(p,q) &= \not{p}\left[\frac{1}{\mu^2}p_\mu q_\nu + \frac{1}{\mu^2}q_\mu p_\nu - \frac{1}{d}\eta_{\mu\nu}\right] \\
\mathcal{P}^{W_2}_{(7)\mu\nu}(p,q) &= \not{q}\left[\frac{1}{\mu^2}p_\mu q_\nu + \frac{1}{\mu^2}q_\mu p_\nu - \frac{1}{d}\eta_{\mu\nu}\right]
\end{aligned} \tag{B.1.29}$$

for the SMOM setup. Therefore these are the only two in the IMOM tensor basis below that carry a factor of ω. This is as a result of pq appearing in requiring the tracelessness condition. Since the Lorentz indices on the Green's functions are the same for both operators W_2 and ∂W_2 they both share the same tensor basis. The tensor basis is

$$\begin{aligned}
\mathcal{P}^{W_2}_{(1)\mu\nu}(p,q) &= \gamma_\mu p_\nu + \gamma_\nu p_\mu - \frac{2}{d}\not{p}\eta_{\mu\nu} \quad , \quad \mathcal{P}^{W_2}_{(2)\mu\nu}(p,q) \ = \ \gamma_\mu q_\nu + \gamma_\nu q_\mu - \frac{2}{d}\not{q}\eta_{\mu\nu} \\
\mathcal{P}^{W_2}_{(3)\mu\nu}(p,q) &= \not{p}\left[\frac{1}{\mu^2}p_\mu p_\nu + \frac{1}{d}\eta_{\mu\nu}\right] \\
\mathcal{P}^{W_2}_{(4)\mu\nu}(p,q) &= \not{p}\left[\frac{1}{\mu^2}p_\mu q_\nu + \frac{1}{\mu^2}q_\mu p_\nu - \frac{(2-\omega)}{d}\eta_{\mu\nu}\right] \\
\mathcal{P}^{W_2}_{(5)\mu\nu}(p,q) &= \not{p}\left[\frac{1}{\mu^2}q_\mu q_\nu + \frac{1}{d}\eta_{\mu\nu}\right] \quad , \quad \mathcal{P}^{W_2}_{(6)\mu\nu}(p,q) \ = \ \not{q}\left[\frac{1}{\mu^2}p_\mu p_\nu + \frac{1}{d}\eta_{\mu\nu}\right] \\
\mathcal{P}^{W_2}_{(7)\mu\nu}(p,q) &= \not{q}\left[\frac{1}{\mu^2}p_\mu q_\nu + \frac{1}{\mu^2}q_\mu p_\nu - \frac{(2-\omega)}{d}\eta_{\mu\nu}\right] \ , \\
\mathcal{P}^{W_2}_{(8)\mu\nu}(p,q) &= \not{q}\left[\frac{1}{\mu^2}q_\mu q_\nu + \frac{1}{d}\eta_{\mu\nu}\right] \\
\mathcal{P}^{W_2}_{(9)\mu\nu}(p,q) &= \frac{1}{\mu^2}\left[\Gamma_{(3)\,\mu pq}p_\nu + \Gamma_{(3)\,\nu pq}p_\mu\right] \\
\mathcal{P}^{W_2}_{(10)\mu\nu}(p,q) &= \frac{1}{\mu^2}\left[\Gamma_{(3)\,\mu pq}q_\nu + \Gamma_{(3)\,\nu pq}q_\mu\right] \ .
\end{aligned} \tag{B.1.30}$$

The projection matrix for W_2 and ∂W_2 is

$$\mathcal{M}^{W_2} \;=\; \frac{1}{4(d-2)^2\omega^3[\omega-4]^3}\tilde{\mathcal{M}}^{W_2} \tag{B.1.31}$$

where the entries for the matrix $\tilde{\mathcal{M}}^{W_2}$ are

$$\begin{aligned}
\tilde{\mathcal{M}}^{W_2}_{11} &= 2[d-2][\omega-4]^2\omega^2 \;\;,\;\; \tilde{\mathcal{M}}^{W_2}_{12} \;=\; -[d-2][\omega-2][\omega-4]^2\omega^2 \\
\tilde{\mathcal{M}}^{W_2}_{13} &= -16[d-2][\omega-4]\omega \;\;,\;\; \tilde{\mathcal{M}}^{W_2}_{14} \;=\; 8[d-2][\omega-2][\omega-4]\omega \\
\tilde{\mathcal{M}}^{W_2}_{15} &= -4[d-2][\omega-2]^2[\omega-4]\omega \;\;,\;\; \tilde{\mathcal{M}}^{W_2}_{16} \;=\; 8[d-2][\omega-2][\omega-4]\omega \\
\tilde{\mathcal{M}}^{W_2}_{17} &= -2[d-2][\omega^2-4\omega+8][\omega-4]\omega \;\;,\;\; \tilde{\mathcal{M}}^{W_2}_{18} \;=\; 8[d-2][\omega-2][\omega-4]\omega \\
\tilde{\mathcal{M}}^{W_2}_{19} &= 0 \;\;,\;\; \tilde{\mathcal{M}}^{W_2}_{110} \;=\; 0 \;\;,\;\; \tilde{\mathcal{M}}^{W_2}_{22} \;=\; 2[d-2][\omega-4]^2\omega^2 \\
\tilde{\mathcal{M}}^{W_2}_{23} &= 8[d-2][\omega-2][\omega-4]\omega \;\;,\;\; \tilde{\mathcal{M}}^{W_2}_{24} \;=\; -2[d-2][\omega^2-4\omega+8][\omega-4]\omega \\
\tilde{\mathcal{M}}^{W_2}_{25} &= 8[d-2][\omega-2][\omega-4]\omega \;\;,\;\; \tilde{\mathcal{M}}^{W_2}_{26} \;=\; -4[d-2][\omega-2]^2[\omega-4]\omega \\
\tilde{\mathcal{M}}^{W_2}_{27} &= 8[d-2][\omega-2][\omega-4]\omega\tilde{\mathcal{M}}^{W_2}_{28} \;=\; -16[d-2][\omega-4]\omega \\
\tilde{\mathcal{M}}^{W_2}_{29} &= 0 \;\;,\;\; \tilde{\mathcal{M}}^{W_2}_{210} \;=\; 0 \;\;,\;\; \tilde{\mathcal{M}}^{W_2}_{33} \;=\; 64[d+1][d-2] \\
\tilde{\mathcal{M}}^{W_2}_{34} &= -32[d+1][d-2][\omega-2] \;\;,\;\; \tilde{\mathcal{M}}^{W_2}_{35} \;=\; 16[d\omega^2-4d\omega+4d+4][d-2] \\
\tilde{\mathcal{M}}^{W_2}_{36} &= -32[d+1][d-2][\omega-2] \;\;,\;\; \tilde{\mathcal{M}}^{W_2}_{37} \;=\; 16[d\omega^2-4d\omega+4d+4][d-2] \\
\tilde{\mathcal{M}}^{W_2}_{38} &= -8[d\omega^2-4d\omega+4d-2\omega^2+8\omega+4][d-2][\omega-2] \;\;,\;\; \tilde{\mathcal{M}}^{W_2}_{39} \;=\; 0 \\
\tilde{\mathcal{M}}^{W_2}_{310} &= 0 \;\;,\;\; \tilde{\mathcal{M}}^{W_2}_{44} \;=\; 8[d\omega^2-4d\omega+8d+3\omega^2-12\omega+8][d-2] \\
\tilde{\mathcal{M}}^{W_2}_{45} &= -8[4d+\omega^2-4\omega+4][d-2][\omega-2] \\
\tilde{\mathcal{M}}^{W_2}_{46} &= 16[d+1][d-2][\omega-2]^2 \\
\tilde{\mathcal{M}}^{W_2}_{47} &= -4[d+1][d-2][\omega^2-4\omega+8][\omega-2] \\
\tilde{\mathcal{M}}^{W_2}_{48} &= 16[d\omega^2-4d\omega+4d+4][d-2] \;\;,\;\; \tilde{\mathcal{M}}^{W_2}_{49} \;=\; 0 \;\;,\;\; \tilde{\mathcal{M}}^{W_2}_{410} \;=\; 0 \\
\tilde{\mathcal{M}}^{W_2}_{55} &= 32[2d+\omega^2-4\omega+2][d-2] \\
\tilde{\mathcal{M}}^{W_2}_{56} &= -8[d\omega^2-4d\omega+4d+4][d-2][\omega-2] \\
\tilde{\mathcal{M}}^{W_2}_{57} &= 16[d+1][d-2][\omega-2]^2 \\
\tilde{\mathcal{M}}^{W_2}_{58} &= -32[d+1][d-2][\omega-2] \;\;,\;\; \tilde{\mathcal{M}}^{W_2}_{59} \;=\; 0 \;\;,\;\; \tilde{\mathcal{M}}^{W_2}_{510} \;=\; 0 \\
\tilde{\mathcal{M}}^{W_2}_{66} &= 32[2d+\omega^2-4\omega+2][d-2] \\
\tilde{\mathcal{M}}^{W_2}_{67} &= -8[4d+\omega^2-4\omega+4][d-2][\omega-2] \\
\tilde{\mathcal{M}}^{W_2}_{68} &= 16[d\omega^2-4d\omega+4d+4][d-2] \;\;,\;\; \tilde{\mathcal{M}}^{W_2}_{69} \;=\; 0 \;\;,\;\; \tilde{\mathcal{M}}^{W_2}_{610} \;=\; 0 \\
\tilde{\mathcal{M}}^{W_2}_{77} &= 8[d\omega^2-4d\omega+8d+3\omega^2-12\omega+8][d-2] \\
\tilde{\mathcal{M}}^{W_2}_{78} &= -32[d+1][d-2][\omega-2] \;\;,\;\; \tilde{\mathcal{M}}^{W_2}_{79} \;=\; 0 \;\;,\;\; \tilde{\mathcal{M}}^{W_2}_{710} \;=\; 0 \\
\tilde{\mathcal{M}}^{W_2}_{88} &= 64[d+1][d-2] \;\;,\;\; \tilde{\mathcal{M}}^{W_2}_{89} \;=\; 0 \;\;,\;\; \tilde{\mathcal{M}}^{W_2}_{810} \;=\; 0
\end{aligned}$$

$$\tilde{\mathcal{M}}^{W_2}_{99} = 8[d-2][\omega-4]\omega \ , \ \tilde{\mathcal{M}}^{W_2}_{910} = -4[d-2][\omega-2][\omega-4]\omega$$
$$\tilde{\mathcal{M}}^{W_2}_{1010} = 8[d-2][\omega-4]\omega \ . \qquad \text{(B.1.32)}$$

Appendix C

Feynman rules

In this appendix we record the Feynman rules used within this thesis.

C.1 Linear gauge Feynman rules

For the linear covariant gauge at the symmetric subtraction point we have

$$\begin{aligned}
\langle A^a_\mu(p)A^b_\nu(-p)\rangle &= -\frac{\delta^{ab}}{p^2}\left[\eta_{\mu\nu}-(1-\alpha)\frac{p_\mu p_\nu}{p^2}\right] \\
\langle c^a(p)\bar{c}^b(-p)\rangle &= -\frac{\delta^{ab}}{p^2} \\
\langle \psi(p)\bar{\psi}(-p)\rangle &= \frac{\not{p}}{p^2} \\
\langle A^a_\mu(p_1)\bar{c}^b(p_2)c^c(p_3)\rangle &= -igf^{abc}p_{2\,\mu} \\
\langle A^a_\mu(p_1)\bar{\psi}(p_2)\psi(p_3)\rangle &= gT^a\gamma_\mu \\
\langle A^a_\mu(p_1)A^b_\nu(p_2)A^c_\sigma(p_3)\rangle &= igf^{abc}\left(\eta_{\nu\sigma}(p_2-p_3)_\mu+\eta_{\sigma\mu}(p_3-p_1)_\nu\right. \\
&\qquad \left.+\eta_{\mu\nu}(p_1-p_2)_\sigma\right)\ . \qquad \text{(C.1.1)}
\end{aligned}$$

C.2 MAG and Curci-Ferrari Feynman rules

For the maximal abelian gauge fixing the propagators are

$$\begin{aligned}
\langle A^A_\mu(p)A^B_\nu(-p)\rangle &= -\frac{\delta^{AB}}{p^2}\left[\eta_{\mu\nu}-(1-\alpha)\frac{p_\mu p_\nu}{p^2}\right] \\
\langle c^A(p)\bar{c}^B(-p)\rangle &= -\frac{\delta^{AB}}{p^2} \\
\langle \psi(p)\bar{\psi}(-p)\rangle &= \frac{\not{p}}{p^2}\ . \qquad \text{(C.2.2)}
\end{aligned}$$

where p is the momentum and the indices A, B can be either diagonal or offdiagonal but not a combination of the two. In the case of the diagonal (or photonic) gluon propagator the arbitrary gauge parameter α is replaced by the photonic gauge parameter α_p. The non-zero 3- and 4-point vertices are, [41, 79],

$$
\begin{aligned}
\langle A^A_\mu(p_1)\bar{\psi}(p_2)\psi(p_3)\rangle &= gT^A\gamma_\mu \\
\langle A^a_\mu(p_1)\bar{c}^b(p_2)c^c(p_3)\rangle &= -igf^{abc}\left(-\frac{1}{2}p_1 - p_3\right)_\mu \\
\langle A^a_\mu(p_1)\bar{c}^b(p_2)c^k(p_3)\rangle &= -igf^{abk}\left(-\zeta p_3\right)_\mu \\
\langle A^a_\mu(p_1)\bar{c}^j(p_2)c^c(p_3)\rangle &= -igf^{acj}\left(p_1 + p_3\right)_\mu \\
\langle A^i_\mu(p_1)\bar{c}^b(p_2)c^c(p_3)\rangle &= -igf^{bci}\left(-p_1 - 2p_3 + p_3\zeta\right)_\mu \\
\langle A^a_\mu(p_1)A^b_\nu(p_2)A^c_\sigma(p_3)\rangle &= igf^{abc}\left(\eta_{\nu\sigma}(p_2 - p_3)_\mu + \eta_{\sigma\mu}(p_3 - p_1)_\nu\right. \\
&\qquad \left. +\eta_{\mu\nu}(p_1 - p_2)_\sigma\right) \\
\langle A^a_\mu(p_1)A^b_\nu(p_2)A^c_\sigma(p_3)A^d_\rho(p_4)\rangle &= -g^2\left[f_d^{abcd}\left(-\eta_{\mu\sigma}\eta_{\nu\rho} + \eta_{\mu\rho}\eta_{\nu\sigma}\right)\right. \\
&\qquad +f_d^{acbd}\left(-\eta_{\mu\nu}\eta_{\sigma\rho} + \eta_{\mu\rho}\eta_{\nu\sigma}\right) \\
&\qquad +f_d^{adbc}\left(-\eta_{\mu\nu}\eta_{\sigma\rho} + \eta_{\mu\sigma}\eta_{\nu\rho}\right) \\
&\qquad +f_o^{abcd}\left(-\eta_{\mu\sigma}\eta_{\nu\rho} + \eta_{\mu\rho}\eta_{\nu\sigma}\right) \\
&\qquad +f_o^{acbd}\left(-\eta_{\mu\nu}\eta_{\sigma\rho} + \eta_{\mu\rho}\eta_{\nu\sigma}\right) \\
&\qquad \left.+f_o^{adbc}\left(-\eta_{\mu\nu}\eta_{\sigma\rho} + \eta_{\mu\sigma}\eta_{\nu\rho}\right)\right] \\
\langle A^a_\mu(p_1)A^b_\nu(p_2)A^c_\sigma(p_3)A^l_\rho(p_4)\rangle &= -g^2\left(f_o^{abcl}\left(-\eta_{\mu\sigma}\eta_{\nu\rho} + \eta_{\mu\rho}\eta_{\nu\sigma}\right)\right. \\
&\qquad +f_o^{acbl}\left(-\eta_{\mu\nu}\eta_{\sigma\rho} + \eta_{\mu\rho}\eta_{\nu\sigma}\right) \\
&\qquad \left.+f_o^{albc}\left(-\eta_{\mu\nu}\eta_{\sigma\rho} + \eta_{\mu\sigma}\eta_{\nu\rho}\right)\right) \\
\langle A^a_\mu(p_1)A^b_\nu(p_2)A^k_\sigma(p_3)A^l_\rho(p_4)\rangle &= -g^2\left(f_o^{akbl}\left(-\eta_{\mu\nu}\eta_{\sigma\rho} + \frac{\zeta(2-\zeta)}{2\alpha}\eta_{\mu\sigma}\eta_{\nu\rho}\right.\right. \\
&\qquad \left. -\frac{1}{2\alpha}\eta_{\mu\sigma}\eta_{\nu\rho} + \eta_{\mu\rho}\eta_{\nu\sigma}\right) \\
&\qquad +f_o^{albk}\left(-\eta_{\mu\nu}\eta_{\sigma\rho} + \eta_{\mu\sigma}\eta_{\nu\rho}\right. \\
&\qquad \left. +\frac{\zeta(2-\zeta)}{2\alpha}\eta_{\mu\rho}\eta_{\nu\sigma} - \frac{1}{2\alpha}\eta_{\mu\rho}\eta_{\nu\sigma}\right) \\
&\qquad +f_o^{bkal}\left(\frac{\zeta(2-\zeta)}{2\alpha}\eta_{\mu\rho}\eta_{\nu\sigma} - \frac{1}{2\alpha}\eta_{\mu\rho}\eta_{\nu\sigma}\right) \\
&\qquad \left.+f_o^{blak}\left(\frac{\zeta(2-\zeta)}{2\alpha}\eta_{\mu\sigma}\eta_{\nu\rho} - \frac{1}{2\alpha}\eta_{\mu\sigma}\eta_{\nu\rho}\right)\right) \\
\langle A^a_\mu(p_1)A^b_\nu(p_2)\bar{c}^c(p_3)c^d(p_4)\rangle &= -g^2\left(f_d^{acbd}\left(-\eta_{\mu\nu} + \zeta\eta_{\mu\nu}\right) + f_d^{bcad}\left(-\eta_{\mu\nu} + \zeta\eta_{\mu\nu}\right)\right) \\
\langle A^a_\mu(p_1)A^j_\nu(p_2)\bar{c}^c(p_3)c^d(p_4)\rangle &= -g^2\left(f_o^{adcj}\left(-\eta_{\mu\nu} + \zeta\eta_{\mu\nu}\right)\right.
\end{aligned}
$$

$$
\begin{aligned}
& \qquad\qquad\qquad\qquad + f_o^{ajcd}\left(\frac{1}{2}\eta_{\mu\nu} - \frac{\zeta}{2}\eta_{\mu\nu}\zeta\right)\Big) \\
\langle A^a_\mu(p_1)A^j_\nu(p_2)\bar{c}^c(p_3)c^l(p_4)\rangle &= -\, g^2\left(f_o^{ajcl}\left(\eta_{\mu\nu} - \zeta\eta_{\mu\nu}\right) + f_o^{alcj}\left(-\zeta\eta_{\mu\nu} + \eta_{\mu\nu}\right)\right) \\
\langle A^i_\mu(p_1)A^j_\nu(p_2)\bar{c}^c(p_3)c^d(p_4)\rangle &= -\, g^2\left(f_o^{cidj}\left(\eta_{\mu\nu} - \zeta\eta_{\mu\nu}\right) + f_o^{cjdi}\left(\zeta\eta_{\mu\nu} - \eta_{\mu\nu}\right)\right) \\
\langle \bar{c}^a(p_1)c^b(p_2)\bar{c}^c(p_3)c^d(p_4)\rangle &= -\, g^2\left(\alpha f_d^{acbd} - \frac{\alpha}{4}f_o^{abcd} + \frac{\alpha}{2}f_o^{acbd} - \frac{\alpha}{4}f_o^{adbc}\right) \\
\langle \bar{c}^a(p_1)c^b(p_2)\bar{c}^c(p_3)c^l(p_4)\rangle &= -\, g^2\left(-\frac{\alpha}{2}f_o^{abcl} + \frac{\alpha}{2}f_o^{acbl} - \frac{\alpha}{2}f_o^{albc}\right) \\
\langle \bar{c}^a(p_1)c^j(p_2)\bar{c}^c(p_3)c^l(p_4)\rangle &= -\, g^2\left(-\alpha f_o^{ajcl} + \alpha f_o^{alcj}\right) \qquad \text{(C.2.3)}
\end{aligned}
$$

where we choose the momentum flow for each vertex to be incoming*. This set of Feynman rules has been generated from the full MAG Lagrangian, using a FORM routine. We have not used any simplification coming from the Jacobi identity when displaying the above rules, however it can be seen that applying the Jacobi identity results in several of the above rules to be trivially zero. Note that we have chosen not to present any of the Feynman rules which are trivially zero. By neglecting all diagonal elements and taking the limit $f_d \to 0$ the above Feynman rules for the MAG reduce to the full set of Feynman rules for the Curci-Ferrari gauge. Therefore the only contributing Feynman rules to the Curci-Ferrari gauge are

$$
\begin{aligned}
\langle A^a_\mu(p_1)\bar{\psi}(p_2)\psi(p_3)\rangle &= gT^a\gamma_\mu \\
\langle A^a_\mu(p_1)\bar{c}^b(p_2)c^c(p_3)\rangle &= -\, igf^{abc}\left(-\frac{1}{2}p_1 - p_3\right)_\mu \\
\langle A^a_\mu(p_1)A^b_\nu(p_2)A^c_\sigma(p_3)\rangle &= igf^{abc}\left(\eta_{\nu\sigma}(p_2-p_3)_\mu + \eta_{\sigma\mu}(p_3-p_1)_\nu\right. \\
&\qquad \left. + \eta_{\mu\nu}(p_1-p_2)_\sigma\right) \\
\langle A^a_\mu(p_1)A^b_\nu(p_2)A^c_\sigma(p_3)A^d_\rho(p_4)\rangle &= -\, g^2\left[f^{abcd}\left(-\eta_{\mu\sigma}\eta_{\nu\rho} + \eta_{\mu\rho}\eta_{\nu\sigma}\right)\right. \\
&\qquad + f^{acbd}\left(-\eta_{\mu\nu}\eta_{\sigma\rho} + \eta_{\mu\rho}\eta_{\nu\sigma}\right) \\
&\qquad \left. + f^{adbc}\left(-\eta_{\mu\nu}\eta_{\sigma\rho} + \eta_{\mu\sigma}\eta_{\nu\rho}\right)\right] \\
\langle \bar{c}^a(p_1)c^b(p_2)\bar{c}^c(p_3)c^d(p_4)\rangle &= -\, g^2\left(-\frac{\alpha}{4}f^{abcd} + \frac{\alpha}{2}f^{acbd} - \frac{\alpha}{4}f^{adbc}\right) \quad \text{(C.2.4)}
\end{aligned}
$$

in addition to those defined for the propagators in (C.2.2) where for the Curci-Ferrari gauge the indices a, b, c, d represent the full colour group. In the limit where we go to the off-diagonal sector we note that $f_o^{abcd} \to f^{abcd}$, where now f^{abcd} in the case of the Curci-Ferrari gauge represents the colour group structure constant for a full colour group.

*Note this corrects several typographical errors in [79].

C.3 One loop Feynman integral solutions

In this section we display several integrals encountered when considering the one loop renormalization of QCD. We first recall the essential integrals needed in deducing the 2-point functions. Defining

$$\mathrm{I}_1(\alpha,\beta,\gamma) \;=\; \int_k \frac{\mathrm{d}^d k}{(2\pi)^d}\frac{1}{(k^2)^\alpha((k-p)^2)^\beta((k+q)^2)^\gamma} \tag{C.3.5}$$

the corresponding 2-point integrals are

$$\mathrm{I}_1(1,1,0) \;=\; \frac{\Gamma(2-\frac{d}{2})\Gamma(\frac{d}{2}-1)\Gamma(\frac{d}{2}-1)(p^2)^{\frac{d}{2}-2}}{(4\pi)^{\frac{d}{2}}\Gamma(d-2)} \tag{C.3.6}$$

$$\mathrm{I}_1(2,1,0) \;=\; \frac{\Gamma(3-\frac{d}{2})\Gamma(\frac{d}{2}-2)\Gamma(\frac{d}{2}-1)(p^2)^{\frac{d}{2}-3}}{(4\pi)^{\frac{d}{2}}\Gamma(d-3)} \tag{C.3.7}$$

$$\mathrm{I}_1(2,2,0) \;=\; \frac{\Gamma(4-\frac{d}{2})\Gamma(\frac{d}{2}-2)\Gamma(\frac{d}{2}-2)(p^2)^{\frac{d}{2}-4}}{(4\pi)^{\frac{d}{2}}\Gamma(d-4)}\;. \tag{C.3.8}$$

Followed by the 3-point integrals

$$\mathrm{I}_1(2,1,1) \;=\; \frac{\Gamma(3-\frac{d}{2})\Gamma(\frac{d}{2}-2)\Gamma(\frac{d}{2}-1)(p^2)^{\frac{d}{2}-4}}{(4\pi)^{\frac{d}{2}}\Gamma(d-3)} - \frac{(d-4)}{2p^2}\mathrm{I}_1(1,1,1) \tag{C.3.9}$$

$$\mathrm{I}_1(2,2,1) \;=\; \frac{1}{4(p^2)^2}(8-d)\,\mathrm{I}_1(2,1,1)$$

$$\mathrm{I}_1(1,1,-1) \;=\; \frac{\Gamma(2-\frac{d}{2})\Gamma(\frac{d}{2}-1)}{(4\pi)^{\frac{d}{2}}(p^2)^{2-\frac{d}{2}}}\left[2pq\frac{\Gamma(\frac{d}{2})}{\Gamma(d-1)}+q^2\frac{\Gamma(\frac{d}{2}-1)}{\Gamma(d-2)}\right] \tag{C.3.10}$$

$$\begin{aligned}\mathrm{I}_1(2,1,-1) \;=\;& \frac{\Gamma(3-\frac{d}{2})\Gamma(\frac{d}{2}-1)}{(4\pi)^{\frac{d}{2}}(p^2)^{3-\frac{d}{2}}}\left[2pq\frac{\Gamma(\frac{d}{2}-1)}{\Gamma(d-2)}+q^2\frac{\Gamma(\frac{d}{2}-2)}{\Gamma(d-3)}\right]\\ &+\frac{\Gamma(2-\frac{d}{2})\Gamma(\frac{d}{2}-1)\Gamma(\frac{d}{2}-1)(p^2)^{\frac{d}{2}-2}}{(4\pi)^{\frac{d}{2}}\Gamma(d-2)}\end{aligned} \tag{C.3.11}$$

$$\begin{aligned}\mathrm{I}_1(2,1,-2) \;=\;& \left[2q^2+\frac{2q^2}{(d-1)}-\frac{4(pq)^2\left(1-\frac{d}{2}\right)}{(d-1)p^2}\right]\mathrm{I}_1(1,1,0)\\ &+\left[(q^2)^2-\frac{p^2q^2}{(d-1)}+\frac{d(pq)^2}{(d-1)}\right]I_1(2,1,0)\\ &+4pq\frac{\Gamma(2-\frac{d}{2})\Gamma(\frac{d}{2}-1)\Gamma(\frac{d}{2})(p^2)^{\frac{d}{2}-2}}{(4\pi)^{\frac{d}{2}}\Gamma(d-1)}\\ &+4pq(q^2)\frac{\Gamma(3-\frac{d}{2})\Gamma(\frac{d}{2}-1)\Gamma(\frac{d}{2}-1)(p^2)^{\frac{d}{2}-3}}{(4\pi)^{\frac{d}{2}}\Gamma(d-2)}\end{aligned} \tag{C.3.12}$$

$$
\begin{aligned}
\mathrm{I}_1(2,2,-2) &= \left[\frac{2q^2}{(d-1)p^2} - \frac{2d(pq)^2}{(d-1)(p^2)^2}\right]\mathrm{I}_1(1,1,0) \\
&+ \left[2q^2 + \frac{4q^2}{(d-1)} - \frac{4(pq)^2}{(d-1)p^2}\right]\mathrm{I}_1(2,1,0) \\
&+ \left[(q^2)^2 - \frac{p^2q^2 - d(pq)^2}{(d-1)}\right]\mathrm{I}_1(2,2,0) \\
&+ 4pq\frac{\Gamma(3-\frac{d}{2})\Gamma(\frac{d}{2}-2)\Gamma(\frac{d}{2})(p^2)^{\frac{d}{2}-3}}{(4\pi)^{\frac{d}{2}}\Gamma(d-2)} \\
&+ 4pq(q^2)\frac{\Gamma(4-\frac{d}{2})\Gamma(\frac{d}{2}-2)\Gamma(\frac{d}{2}-1)(p^2)^{\frac{d}{2}-4}}{(4\pi)^{\frac{d}{2}}\Gamma(d-3)}
\end{aligned}
\tag{C.3.13}
$$

where $\mathrm{I}_1(1,1,1)$ is the only master integral for the 3-point function at one loop. This is evaluated in [63, 64] as

$$
\mathrm{I}_1(1,1,1) = -\frac{1}{\mu}\left[\Phi_1(x,y) + \Psi_1(x,y)\varepsilon + \left[\frac{\zeta_2}{2}\Phi_1(x,y) + \chi_1(x,y)\right]\varepsilon^2 + \mathcal{O}(\varepsilon^3)\right] \tag{C.3.14}
$$

where $\Phi_1(x,y)$ involves $\mathrm{Li}_2(z)$ and $\Psi_1(x,y)$ involves $\mathrm{Li}_3(z)$, [151], where both polylogarithms were defined in (2.1.73) and (2.1.74). The function $\chi_1(x,y)$ is not known, where this is not important since it always appears with a similar term $\chi_3(x,y)$ coming from the two loop master such that

$$
\chi_3(x,y) - \chi_1(x,y) = \Phi_2(x,y) - \frac{1}{2}\ln(xy)\Psi_1(x,y) + \frac{1}{4}\left[\ln^2(x) + \ln^2(y)\right]\Phi_1(x,y) \tag{C.3.15}
$$

where this combination of harmonic polylogarithms has already been defined in (2.1.76) as

$$
\chi_3(1,1) - \chi_1(1,1) = \frac{1}{36}\psi'''\left(\tfrac{1}{3}\right) - \frac{2\pi^4}{27} \tag{C.3.16}
$$

for $x = y = 1$ defined at the completely symmetric point.

C.4 Master integral derivation

Returning to section 2.2 where we defined a general definition of a one loop integral containing three propagators by

$$
\mathrm{I}_1(\alpha,\beta,\gamma) = \int_k \frac{\mathrm{d}^d k}{(2\pi)^d}\frac{1}{(k^2)^\alpha((k-p)^2)^\beta((k+q)^2)^\gamma} \tag{C.4.17}
$$

where α, β, γ take any integer value, represented diagramatically in Figure 2.2 with internal loop momenta k. Using Feynman parametrization we can rewrite the above as, [53],

$$\begin{aligned} \mathrm{I}_1(\alpha,\beta,\gamma) &= \int_k \frac{\Gamma(\alpha+\beta+\gamma)}{\Gamma(\alpha)\Gamma(\beta)\Gamma(\gamma)} \\ &\quad \times \int_0^1 \mathrm{d}x \int_0^1 \mathrm{d}y \int_0^1 \mathrm{d}z \frac{x^{\alpha-1}y^{\beta-1}z^{\gamma-1}\delta(1-x-y-z)}{[k^2x+(k-p)^2y+(k+q)^2z]^{\alpha+\beta+\gamma}} \ . \end{aligned} \tag{C.4.18}$$

Rearranging the denominator by completing the square the integral becomes

$$\begin{aligned} \mathrm{I}_1(\alpha,\beta,\gamma) &= \int_k \frac{\Gamma(\alpha+\beta+\gamma)}{\Gamma(\alpha)\Gamma(\beta)\Gamma(\gamma)} \\ &\quad \times \int_0^1 \mathrm{d}x \int_0^1 \mathrm{d}y \int_0^1 \mathrm{d}z \frac{x^{\alpha-1}y^{\beta-1}z^{\gamma-1}\delta(1-x-y-z)}{[(k')^2+xyp^2+xq^2z+yzr^2]^{\alpha+\beta+\gamma}} \ . \end{aligned} \tag{C.4.19}$$

where $k' = k - yp + zq$ and $x + y + z = 1$. Then integrating with respect to k' using

$$\int \frac{1}{(k^2+m^2)^\alpha} = \frac{\Gamma(\alpha-\frac{d}{2})}{\Gamma(\alpha)}(m^2)^{\alpha-\frac{d}{2}} \tag{C.4.20}$$

where we let $xyp^2 + xq^2z + yzr^2 = m^2$ then $\mathrm{I}_1(\alpha,\beta,\gamma)$ becomes

$$\begin{aligned} \mathrm{I}_1(\alpha,\beta,\gamma) &= \frac{\Gamma\left(\alpha+\beta+\gamma-\frac{d}{2}\right)}{\Gamma(\alpha)\Gamma(\beta)\Gamma(\gamma)} \\ &\quad \times \int_0^1 \mathrm{d}x \int_0^1 \mathrm{d}y \int_0^1 \mathrm{d}z \frac{x^{\alpha-1}y^{\beta-1}z^{\gamma-1}\delta(1-x-y-z)}{[xyp^2+xq^2z+yzr^2]^{\alpha+\beta+\gamma-\frac{d}{2}}} \ . \end{aligned} \tag{C.4.21}$$

Now let $D = xyp^2 + xq^2z + yzr^2$ and without loss of generality we can set $r^2 = 1$ since this is a common factor which appears in our integrals as $(p_3^2)^{1+\epsilon}$ and so we can factor this out, giving

$$\begin{aligned} \mathrm{I}_1(\alpha,\beta,\gamma) &= \frac{\Gamma\left(\alpha+\beta+\gamma-\frac{d}{2}\right)}{\Gamma(\alpha)\Gamma(\beta)\Gamma(\gamma)} \\ &\quad \times \int_0^1 \mathrm{d}x \int_0^1 \mathrm{d}y \int_0^1 \mathrm{d}z \frac{x^{\alpha-1}y^{\beta-1}z^{\gamma-1}\delta(1-x-y-z)}{D^{\alpha+\beta+\gamma-\frac{d}{2}}} \ . \end{aligned} \tag{C.4.22}$$

Taking the simplest case for α, β and γ we have

$$\begin{aligned} \mathrm{I}_1(1,1,1) &= \frac{\Gamma\left(3-\frac{d}{2}\right)}{\Gamma(1)\Gamma(1)\Gamma(1)} \int_0^1 \mathrm{d}x \int_0^1 \mathrm{d}y \int_0^1 \mathrm{d}z \frac{1}{D^{3-\frac{d}{2}}} \\ &= \Gamma(1+\epsilon) \int_{x,y,z} \frac{1}{D} \left[1 - \epsilon \ln D + \frac{\epsilon^2}{2} \ln^2 D\right] . \end{aligned} \tag{C.4.23}$$

applying $\Gamma(1+\epsilon) = \frac{\epsilon^2}{2}\zeta_2$ we can rewrite the above as

$$\mathrm{I}_1(1,1,1) = \int_{x,y,z} \frac{1}{D} \left[1 - \epsilon \ln D + \frac{\epsilon^2}{2} \ln^2 D + \zeta_2\right] . \tag{C.4.24}$$

Now by uniqueness, [62],

$$\mathrm{I}_1(1,1,1) = (p_1^2)^{-\epsilon} (P_2^2)^{-\epsilon} \mathrm{I}_1(d-3,1,1) \tag{C.4.25}$$

Then $\mathrm{I}_1(d-3,1,1)$ becomes

$$\mathrm{I}_1(d-3,1,1) = \int_{x,y,z} \frac{1}{D} \left[1 + \epsilon\left(\ln D - 2\ln X\right) + \frac{\epsilon^2}{2}\left(\ln D - 3\ln X\right)^2\right] \frac{\Gamma(1-\epsilon)}{\Gamma(1-2\epsilon)} \tag{C.4.26}$$

with $\frac{\Gamma(1-\epsilon)}{\Gamma(1-2\epsilon)} = -\frac{3}{2}\epsilon^2\zeta_2$. By comparing both (C.4.24) and (C.4.26) we get the following relationships between the integrals

$$\int \frac{(\ln X - \ln D)}{D} = -\frac{1}{2} \int \frac{\ln(p^2 q^2)}{D} \tag{C.4.27}$$

and

$$\int \frac{1}{D} \ln X (\ln D - \ln X) = \int \frac{1}{D} \left[-\zeta_2 - \frac{1}{2}\ln(p^2q^2)(\ln D - 2\ln X) + \frac{1}{4}\ln^2(p^2q^2)\right] \tag{C.4.28}$$

From [62] it follows that the integrals can be written in the form

$$\begin{aligned} \mathrm{I}_1(1,1,1) &= \Gamma(1+\epsilon)\left[\Phi_1 + \epsilon\Psi_1 + \epsilon^2\chi_1\right] \\ \mathrm{I}_1\left(3-\frac{d}{2},1,1\right) &= \Gamma(1+\epsilon)\left[\Phi_1 + \epsilon\left(\Psi_1 - \frac{1}{2}\ln(p^2q^2)\Phi_1\right) + \epsilon^2\chi_3\right] \end{aligned} \tag{C.4.29}$$

where numerically these can be evaluated to, [62],

$$\begin{aligned}
\Phi_1(1,1) &= \frac{2}{3}\pi^2 - \frac{2}{3}\psi'\left(\tfrac{1}{3}\right) \\
\Psi_1(1,1) &= 12 s_3\left(\tfrac{\pi}{6}\right) - \frac{35\pi^3}{108\sqrt{3}} - \frac{\ln^2(3)\pi}{4\sqrt{3}} \\
\chi_1 &= -\mathcal{H}^{(2)}_{31} - \frac{\pi^2}{12}\Phi_1(1,1)
\end{aligned} \tag{C.4.30}$$

at the symmetric subtraction point. This is enough to enable us to take the SMOM limit for all results computed at the asymmetric point.

The general expression for $\Phi_1(x,y)$ includes the usual dilogarithm function $\mathrm{Li}_2(z)$ via, [64, 149, 103],

$$\begin{aligned}
\Phi_1(x,y) &= \frac{1}{\lambda}\left[2\mathrm{Li}_2(-\rho x) + 2\mathrm{Li}_2(-\rho y) + \ln\left(\frac{y}{x}\right)\ln\left(\frac{(1+\rho y)}{(1+\rho x)}\right)\right. \\
&\qquad \left. + \ln(\rho x)\ln(\rho y) + \frac{\pi^2}{3}\right]
\end{aligned} \tag{C.4.31}$$

where

$$\lambda(x,y) = \sqrt{\Delta_G} \quad , \quad \rho(x,y) = \frac{2}{[1-x-y+\lambda(x,y)]} \tag{C.4.32}$$

and

$$\Delta_G(x,y) = x^2 - 2xy + y^2 - 2x - 2y + 1 \tag{C.4.33}$$

is the Gram determinant. When one evaluates these functions from (C.4.31) the dilogarithms involve the Clausen function, $\mathrm{Cl}_2(\theta)$, since the argument of the dilogarithm is complex.

Bibliography

[1] D.J. Gross & F.J. Wilczek, Phys. Rev. Lett. **30** (1973), 1343.

[2] H.D. Politzer, Phys. Rev. Lett. **30** (1973), 1346.

[3] G. 't Hooft & M.J.G. Veltman, *Proceedings of the Marseille conference* (1972), 1.

[4] W. Marciano & H. Pagels, Phys. Rep. **36** (1978), 137.

[5] O.W. Greenberg, Am. J. Phys. **50** (1982), 1074.

[6] M. Gell-Mann & Y. Ne'eman, *The Eightfold Way* (New York, Benjamin, 1964).

[7] F. Close, M. Martin & C. Sutton, *The Particle Odyssey* (Oxford University Press, Oxford, 2002).

[8] F. Abe et al. (CDF Collaboration), Phys. Rev. Lett. **74** (1995), 2626.

[9] S. Abachi et al. (D0 collaboration), Phys. Rev. Lett. **74**, (1995), 2632.

[10] D.P. Barber *et al.* Phys. Rev. Lett. **43** (1979), 830.

[11] V. Gogokhia & G.G. Barnaföldi, *The Mass Gap and its Applications* (World Scientific, Hungary, 2013).

[12] A. Pickering, *Constructing Quarks*, (University of Chicago Press, 1984).

[13] V.G. Bornyakov, M.N. Chernodub, F.V. Gubarev, S.M. Morozov & M.I. Polikarpov, Phys. Lett. **B559** (2003), 214.

[14] J. A. Gracey, Phys. Rev. **D84** (2011), 085011.

[15] E.G. Eichtein & F.L. Feinberg, Phys. Rev. **D10** (1974), 3254.

[16] M. Baker & C. Lee, Phys Rev **D15** (1977), 2201.

[17] U. Bar-Gadda, Nucl. Phys. **B163** (1980), 312.

[18] Y. Nambu, Phys. Rev. **D10** (1975), 4262.

[19] G. 't Hooft, High Energy Physics EPS Int. Conference, Palermo 1975, ed. A. Zichichi

[20] S. Mandelstam, Phys. Rep. **23** (1976), 245.

[21] G. 't Hooft, Nucl. Phys. **B190** (1981), 455.

[22] Z. F. Ezawa & A. Iwazaki, Phys. Rev. **D25** (1982), 2681.

[23] A.J. Macfarlane, A. Sudbery & P.H. Weisz, Commun. Math. Phys. **11** (1968), 77.

[24] P.Z. Skands, arXiv:1207.2389v1 [Hep-ph], (2012).

[25] O.W. Greenberg, Phys. Rev. Lett. **13** (1964), 598.

[26] D. Griffiths, *Introduction to elementary particles*, (Wiley, 2008).

[27] J.A. Gracey, Nucl. Phys. **B696** (2004), 295.

[28] L.D. Faddeev & V.N. Popov, Phys. Lett. **B25** (1967), 29.

[29] R. Parthasarathy, J. Phys. **A21** (1988), 4593.

[30] L.H. Ryder, *Quantum Field Theory*, (Cambridge University Press, 1996).

[31] A.A. Slavnov, Theor. Math. Phys. **10** (1972), 99.

[32] J.C. Taylor, Nucl. Phys. **B33** (1971), 436.

[33] C. Becchi, A. Rouet & A. Stora, Phys. Lett. **B52** (1974), 344.

[34] C. Becchi, A. Rouet & A. Stora, Commun. Math. Phys. **42** (1975), 127.

[35] I.V. Tyutin, Lebedev Institute preprint, Report No. FIAN-39 (1975) *unpublished*.

[36] B.S. DeWitt, Phys, Rev. Lett. **12** (1964), 742.

[37] B.S. DeWitt, Phys. Rev. **162** (1967), 1195.

[38] R.P. Feynman, Acta. Phys. Polonica **24** (1963), 697.

[39] R. Browne, *Thesis: Investigations into dimension two operators and dynamically generated gluon mass in QCD* (2005).

[40] D. Dudal, J.A. Gracey, V.E.R. Lemes, M.S. Sarandy, R.F. Sobreiro, S.P. Sorella & H.Verschelde, Phys. Rev. **D70** (2004), 114038.

[41] D. Dudal, J.A. Gracey, V.E.R. Lemes, M.S. Sarandy, R.F. Sobreiro, S.P. Sorella, R. Thibes & H. Verschelde, arXiv:0505037v1 [Hep-th], (2005).

[42] G. Curci & R. Ferrari, Nuovo Cim. **A32** (1976), 151.

[43] G. Curci & R. Ferrari, Nuovo Cim. **A32** (1976), 151.

[44] T. Teubner, *The Standard Model - Lecture Notes* (The University of Liverpool, 2009).

[45] G. 't Hooft & Veltman, Nucl. Phys. **B44** (1972), 189.

[46] C.G. Bollini & J.J. Giambiagi, Phys. Lett. **B40** (1972), 566.

[47] C.G. Bollini & J.J. Giambiagi, Nuovo. Cim. **B12** (1972), 20.

[48] P. Ramond, *Field Theory. A Modern Primer* (Addison-Wesley, Redwood City, CA, 1981)

[49] Smilga, *Lectures on QCD*, (World Scientific Publishing, London, 2001).

[50] F.J. Yndurain, *The Theory of Quark and Gluon Interactions*, (Springer, 1999).

[51] J.M. Bell & J.A. Gracey, Phys. Rev. **D88** (2013), 085027.

[52] W. Celmaster & R.J. Gonsalves, Phys. Rev. **D20** (1979), 1420.

[53] A. Grozin, *Lectures on QED and QCD*, arXiv:hep-ph/0508242 (2005).

[54] G. t' Hooft, *50 years of Yang-Mills Theory* (World Scientific, London, 2005).

[55] G. 't Hooft, Nucl. Phys. **B61** (1973), 455.

[56] W.A. Bardeen, A.J. Buras, D.W. Duke & T. Muta, Phys.Rev. D18 (1978), 3998.

[57] P. Pascual & R. Tarrach, *QCD: Renormalization for the Practitioner*, (Springer-Verlag, 1984).

[58] K.G. Chetyrkin & T. Seidensticker, Phys. Lett. **B495** (2000), 74.

[59] K.G. Chetyrkin & A. Retey, Nucl. Phys. **B583** (2000), 3.

[60] S. Laporta, Int. J. Mod. Phys. **A15** (2000), 5087.

[61] A. Bondi, G. Curci, G. Paffuti & P. Rossi, Ann. Phys. **199** (1990), 268.

[62] A.I. Davydychev, J. Phys. **A25** (1992), 5587.

[63] N.I. Usyukina & A.I. Davydychev, Phys. Atom. Nucl. **56** (1993), 1553.

[64] N.I. Usyukina & A.I. Davydychev, Phys. Lett. **B332** (1994), 159.

[65] T.G. Birthwright, E.W.N. Glover & P. Marquard, JHEP **0409** (2004), 042.

[66] S. Hollands, Fields Institute Communications, Volume **50** (2007), 131.

[67] J.M. Bell & J.A. Gracey, Phys. Rev. **D92** (2015), 125001.

[68] C. Studerus, Comput. Phys. Commun. **181** (2010), 1293.

[69] P. Nogueira, J. Comput. Phys. **105** (1993), 279.

[70] J.A.M. Vermaseren, math-ph/0010025.

[71] M. Tentyukov & J.A.M. Vermaseren, Comput. Phys. Commun. **181** (2010), 1419.

[72] S.G. Gorishny, S.A. Larin, L.R. Surguladze & F.K. Tkachov, Comput. Phys. Commun. **55** (1989), 381.

[73] S.A. Larin & J.A.M. Vermaseren, Phys. Lett. **B303** (1993), 334.

[74] C.W. Bauer, A. Frink & R. Kreckel, J. Symb. Comput, **33** (2002). 1.

[75] L.G. Almeida & C. Sturm, Phys. Rev. **D82** (2010), 054017.

[76] A.C. Hearn, *R*educe: A user oriented interactive system for algebraic simplification (1967), C670826-1.

[77] J.A.M. Vermaseren, Comp. Phys. Comm. **83** (1994), 45.

[78] D. Binosi & L. Theussl, Comp. Phys. Comm. **161** (2004), 76.

[79] J.A. Gracey, JHEP 0504 (2005), 059.

[80] P. Pascual & R. Tarrach, Nucl. Phys. **B174** (1980) 123.

[81] W.E. Caswell, Phys. Rev. Lett. **33** (1974), 244.

[82] D.R.T. Jones, Nucl. Phys. **B75** (1974), 531.

[83] O.V. Tarasov, A.A. Vladimirov & A.Yu. Zharkov, Phys. Lett. **B93**, (1980),429.

[84] M. Gell-Mann & F.E. Low, Phys. Rev. **95**, (1954), 1300.

[85] C.G. Callan, Jr. Phys. Rev. **D2** (1970), 1541.

[86] K. Symanzik, Commun. Math. Phys. **18** (1970), 227.

[87] K.G. Wilson, Rev. Mod. Phys. **47** (1975), 773.

[88] B. Zumino, J. Math. Phys. **1** (1960), 1.

[89] J.C. Collins, *Renormalization* (Cambridge University Press, Cambridge 1984).

[90] E. Braaten & J.P. Leveille, Phys. Rev. **D24** (1981), 1369.

[91] W. Celmaster & R.J. Gonsalves, Phys. Rev. Lett. **42** (1979), 1435.

[92] W.E. Caswell, Phys. Rev. Lett. **33** (1974), 244.

[93] D.R.T. Jones, Nucl. Phys. **B75** (1974), 531.

[94] O.V. Tarasov, A.A. Vladimirov & A.Yu. Zharkov, Phys. Lett. **B93** (1980), 429.

[95] Ph. Boucaud, J.P. Leroy, A.L. Yaounac, J. Micheli, O. Pène & J. Rodríguez-Quintero, JHEP **0806** (2008), 099.

[96] A.C. Aguilar, D. Binosi & J. Papavassiliou, Phys. Rev. **D78** (2008), 025010.

[97] J.A.Gracey, Phys. Rev. **D90** (2014), 094026.

[98] L. von Smekal, K. Maltman & A. Sternbeck, Phys. Lett. **B681** (2009), 336.

[99] R.E Browne & J.A.Gracey, Phys. Lett. **b540** (2002), 68.

[100] A.R. Fazio, V.E.R. Lemes, M.S. Sarandy & S.P. Sorella, Phys. Rev. **D64** (2001), 085003.

[101] Ph. Boucaud, J.P. Leroy, A.L. Yaounac, J. Micheli, O. Pène & J. Rodríguez-Quintero, Phys. Rev. **D63** (2001), 114003.

[102] K.I. Kondo, Phys. Lett. **B514** (2001), 335.

[103] J.A. Gracey, Phys.Rev. **D90** (2014), 025011.

[104] J.A. Gracey, Phys. Lett. **B552** (2003), 101.

[105] J.M. Cornwall, Phys. Rev. **D26** (1982), 1453.

[106] J.M. Cornwall & A. Soni, Phys. Lett. **B120** (1983), 431.

[107] A. Cucchieri & T. Mendes, PoS LAT2007 (2007), 297.

[108] I.L. Bogolubsky, E.M. Ilgenfritz, M. Müller-Preussker & A. Sternbeck, PoS LAT2007 (2007), 290.

[109] A. Maas, Phys. Rev. **D75** (2007), 116004.

[110] A. Sternbeck, L. von Smekal, D.B. Leinweber & A.G. Williams, PoS LAT2007 (2007), 304.

[111] A. Cucchieri & T. Mendes, Phys. Rev. Lett. **100** (2008), 241601.

[112] A. Cucchieri & T. Mendes, Phys. Rev. **D78** (2008), 094503.

[113] C.S. Fischer, A. Maas & J.M. Pawlowski, Annals Phys. **324** (2009), 2408.

[114] O. Oliveira & P.J. Silva, Phys. Rev. **D79** (2009), 031501.

[115] V.N. Gribov, Nucl. Phys. **B139** (1978), 1.

[116] M. Tissier & N. Wschebor, Phys. Rev. **D82** (2010), 101701.

[117] M. Tissier & N. Wschebor, Phys. Rev. **D84** (2011), 045018.

[118] J. Serreau & M. Tissier, Phys. Lett. **B712** (2012), 97.

[119] J. Serreau, M. Tissier & A. Tresmontant, Phys. Rev. **D89** (2014), 125019.

[120] M. Pelaez, M. Tissier & N. Wschebor, Phys. Rev. **D88** (2013), 125003.

[121] A.S. Kronfeld, G. Schierholz & U.J. Wiese, Nucl. Phys. **B293** (1987), 461.

[122] A.S. Kronfeld, M.L. Laursen, G. Schierholz & U.J. Wiese, Phys. Lett. **B198** (1987), 516.

[123] N. Sakumichi & H. Suganuma, Phys. Rev. **D90** (2014), 111501.

[124] L.F. Abbott, Acta Phys. Polon. **B13** (1982), 33.

[125] L.F. Abbott, Nucl. Phys. **B185** (1981), 189.

[126] J.A. Gracey, Fields Institute Communications, Volume **50** (2007), 107.

[127] G. 't Hooft & M. Veltman, *"Diagrammar"*, CERN-73-09.

[128] G. 't Hooft, Acta Universitatis Wratislaviensis **368** (1976), 345, Proceedings of the 1975 Winter School of Theoretical Physics held in Karpacz.

[129] B.S. DeWitt, in Proceedings of Quantum Gravity II, eds C. Isham, R. Penrose & S. Sciama, (Oxford, 1980), 449.

[130] D.G. Boulware, Phys. Rev. **D23** (1981), 389.

[131] L.F. Abbott, Nucl. Phys. **B185** (1981), 189.

[132] D.M. Capper & A. MacLean, Nucl. Phys. **B203** (1982), 413.

[133] M. Gorbahn & S. Jäger, Phys. Rev. **D82** (2010), 114001.

[134] G. Martinelli, C. Pittori, C.T. Sachrajda, M. Testa & A. Vladikas, Nucl. Phys. **B445** (1995), 81.

[135] E. Franco & V. Lubicz, Nucl. Phys. **B531** (1998), 641.

[136] L.G. Almeida & C. Sturm, Phys. Rev. **D82** (2010), 054017.

[137] J.A. Gracey, Nucl. Phys. **B662** (2003), 247.

[138] C. Sturm, Y. Aoki, N.H. Christ, T. Izubuchi, C.T.C. Sachrajda & A. Soni, Phys. Rev. **D80** (2009), 014501.

[139] J.A. Gracey, Eur. Phys. J. **C71** (2011), 71.

[140] J.A. Gracey, arXiv:1009.3895 v2 [hep-ph].

[141] J.M. Bell & J.A. Gracey, Phys. Rev. **D93** (2016), 065031.

[142] S. Moch, J.A.M. Vermaseren & A. Vogt, Phys. Lett **B606** (2005), 123.

[143] J. Zinn-Justin, Bonn Lectures 1974, in: *Lecture Notes in Physics* (Springer, 1975) Vol. 37.

[144] H. Kluberg-Stern & J.B. Zuber, Phys. Rev. **D12** (1975), 3159.

[145] A.D. Kennedy, J. Math. Phys. **22** (1981), 1330.

[146] A.N. Vasil'ev, M.I. Vyazovskii, S.É. Derkachov & N.A. Kivel, Theor. Math. Phys. **107** (1996), 441.

[147] A.N. Vasil'ev, M.I. Vyazovskii, S.É. Derkachov & N.A. Kivel, Theor. Math. Phys. **107** (1996), 710.

[148] A.N. Vasil'ev, S.É. Derkachov & N.A. Kivel, Theor. Math. Phys. **103** (1995), 487.

[149] N.I. Usyukina & A.I. Davydychev, Phys. Lett. **B305** (1993), 136.

[150] J.A. Gracey, Phys. Rev. **D83** (2011), 054024.

[151] J.A. Gracey, Proceedings of Science (2014), POS(LL2014)061.